John Dolson

Understanding Oil and Gas Shows and Seals in the Search for Hydrocarbons

Springer

Understanding Oil and Gas Shows and Seals in the Search for Hydrocarbons

John Dolson

Understanding Oil and Gas Shows and Seals in the Search for Hydrocarbons

Springer

John Dolson
DSP Geosciences and Associates
Coconut Grove, FL, USA

ISBN 978-3-319-29708-8 ISBN 978-3-319-29710-1 (eBook)
DOI 10.1007/978-3-319-29710-1

Library of Congress Control Number: 2016933331

Printed on acid-free paper

This Springer imprint is published by Springer Nature
The registered company is Springer International Publishing AG Switzerland

This book is dedicated to my daughter, Kristin, who legitimately claims 'I owe her one', since the last book was dedicated to her brother right before she was born. This book would also not have been possible without the help of my wife, Debbie, who has persevered over the years with my passion for geology, teaching, public service, and a roving expatriate lifestyle. My son, Josh, and his wife Noemi, have introduced to the world to a new grandson (Conrad), who just might think about becoming a geologist someday. I would hope that years from now, he might still have some use for this book, just as I did as a young boy from a textbook my grandfather coauthored, A Study of the Physical World.

Preface

This book is meant for the young geoscientist, but can also serve as a useful reminder for many experienced geoscientists of the need for carefully thinking about hydrocarbon shows in a migration and trap context. The science of petroleum exploration and production evolves at a rapid pace, but some fundamentals will always remain that must be adhered to. Finding oil and gas has never been easy and never risk-free. The techniques and examples in this book should help reinforce the most fundamental need of any petroleum geologist—the ability to understand hydrocarbon shows quantitatively and turn that knowledge into drillable prospects.

This book has evolved over a lifetime of chasing oil and gas prospects around the world, first in the Denver Basin of Colorado and later in Egypt, Russia, and India, along with many other basins. Like many young geoscientists, I spent years honing my ability to make stratigraphic and structural maps, but often neglecting to build them in such a way that I could explain where the oil and gas shows were. As I became more experienced, and learned the value of understanding the petrophysical properties of rocks, my ability to find oil and gas increased. Along the way, I have had many successes and a number of regrettable, and avoidable failures. Fortunately, when we learn from the failures, it makes us better explorers later on.

The book is an outgrowth of courses taught years ago by Larry Meckel and Tim Schowalter, and championed by Dan Hartmann. My introduction to hydrodynamics was from discussions and workshops with Eric Dahlberg, who has published one of the best summary textbooks in the industry. Since the early 1990s I have been teaching workshops on shows and seals and have always found it interesting how even attendees with 25–30 years of experience leave the class with a renewed sense of appreciation for thinking quantitatively about basic test and show data.

In recent years, a common complaint I hear from senior management in all companies is a sense of frustration that many basic principles are not being used by many of their younger staff. A fixation on 3D seismic imaging or computer models far too often moves ahead of the basic task of actually looking at well logs, reports, sample and core data to see where the hydrocarbons have migrated and been trapped. This kind of work, often less glamorous than a 3D seismic display or computer graphic, remains essential to make sense out of those beautiful computer

images. Ironically, when I hear that complaint, I can hear my early bosses telling me the same thing: 'you need to pay more attention to the shows data'. Some things, I think, simply don't change and only firm insistence by technical and managerial leaders that shows information is incorporated in every analysis will cause that situation to change.

This is an exciting business to work in. The opportunities to travel and interact with many fine people grappling with difficult problems are always stimulating. I hope that for those reading this book it might cut the critical learning curve to finding oil and gas by many years.

I wish I had been exposed to materials like this the first day on the job, rather than learning it piecemeal over a decade or more.

Coconut Grove, FL John Dolson

Acknowledgements

I am deeply grateful for the help of many teachers and colleagues. Dan Hartmann, Larry Meckel, Tim Schowalter, and Eric Dahlberg have had a profound impact on my professional career by teaching me many of the fundamentals covered in this book. Like many great oil finders, they are generous with their ideas and shared learnings and have helped review and edit this book. Frank Ethridge, in addition to being an enormous influence on me and many others while taking courses from him at CSU, has helped edit these chapters and provided excellent advice. Gary Massie (formerly BP) has been very helpful by giving me the chance to rewrite and permission to use figures and course materials from the BP-Chevron Drilling Consortium course, "Geology and Geophysics for Drillers, Engineers and Geotechs," a course I have taught now for several years.

Don Hall, Mohamed Said, and Maniesh Singh need particular recognition for agreeing to coauthor key chapters on fluid inclusion technology, geochemistry, and log analysis. Paul Farrimond, while not a coauthor, did extensive review of Chap. 8.

Zhiyong He not only has provided ideas for this book and extensive edits but also has given me access to his petroleum systems software (Trinity 3D), a superb visualization and modeling package. Using Trinity over the last 15 years has helped me put oil and gas shows in a burial and 3D migration model context while making it much easier to quickly visualize how migration might work and oil and gas deposits be detected.

Cairn Energy India has also been very helpful in providing figures for this book. During my over 8 years of consulting with Cairn Energy, working more or less quarterly, I've enjoyed working with talented staff who continue to pay close attention to detailed analysis of hydrocarbon shows. That attention to detail has paid off many times with new discoveries. A special thanks at Cairn goes to Pinak Mohapatra for his continued support and Kaushal Pander for contributing an excellent case history (Chap. 3) on a new play in the Barmer Basin. Stuart Burley and David Ginger (formerly with Cairn) also supported numerous shows and seals workshops as part of the formal training program. Delonex Energy (London), a group I am part of, has also provided help with some figures.

I am also thankful for the 35+ years I have had with the American Association of Petroleum Geologists and the Rocky Mountain Association of Petroleum Geologists. Through these fine institutions I've been able to meet and interact with many great explorers and fellow civic-minded people who want to give something back to their profession. Both organizations have been generous in permissions to reprint some of their published figures in this book.

Lastly, none of this would have been possible without additional editorial reviews and help from Jeff Corrigan, Bernd Herold, Phil Heppard, Martin Traugott, George Pemberton, and Lorna Blaisse. Max Tenaglia has critiqued much of this book through the eyes of a young geoscientist. Lastly, thanks to the many students and younger staff I've had an opportunity to work with globally for helping me continue to find ways to make some of the more difficult technical topics covered perhaps a bit easier to understand.

Contents

About the Author

John C. Dolson, Director, DSP Geosciences and Associates, LLC and Senior Geological Advisor, Delonex Energy (London). He has 35+ year's oil and gas exploration both domestic and international. He has served as Vice President of the American Association of Petroleum Geologists (2006/2007), and was Senior Geological Advisor for TNK-BP (Russia), Amoco/BP before starting DSP Geosciences in 2008. Dolson has supervised hundreds of geoscientists and has been responsible for prospect generation as well as training and development, with 15 years spent living abroad (Egypt, London, and Moscow). He has served as an adjunct faculty member at the University of Miami (Fla), Colorado State University, Royal Holloway University (London) and geological advisor to Moscow State University and Tyumen State University (Russia). He has an extensive publications list including several landmark papers for AAPG dealing with stratigraphic traps and regional petroleum potential assessment and has authored books on Black Canyon of the Gunnison National Monument in 1982 and on unconformity analysis with the Rock Mountain Association of Geologists in 1994.

Chapter 1
Introduction to the Oil Industry and Oil Show Evaluation: A Personal Retrospective

Contents

Abstract Searching for oil and gas has never been easy. Each generation faces its own challenges, after building on the knowledge of those who came earlier. Mentors to younger staff play a big role in helping to shorten the time it takes to learn to look for hydrocarbons effectively. There is a language of petroleum exploration and it must be learned early. The hardest part, however, remains the ability to think creatively and break paradigms and thus develop new plays which can sustain a company or the industry over a long period.

J. Dolson, *Understanding Oil and Gas Shows and Seals in the Search for Hydrocarbons*, DOI 10.1007/978-3-319-29710-1_1

Breaking paradigms requires the ability to critically analyze data objectively, but then think of it differently, in term how oil and gas molecules might respond to changes in temperature, pressure and reservoirs over time as they migrate from the source rock to the trap. New ideas also require the ability to work with other people, to understand and accept differences of opinion, but most of all, the ability to see information which doesn't readily fit into the readily accepted ideas of others.

1.1 Introduction and Vocabulary of Oil and Gas

For thousands of years people have searched for oil and gas deposits to light their homes, provide warmth, energy for transportation, and a multitude of derivative products including plastics, vinyl and other things we too frequently take for granted.

Today, the world consumes over 90 million barrels of oil daily, and that number is only projected to grow in the future. While the world continues to search for alternatives to fossil fuels, a long period of transition lies ahead where the skills of millions of scientists will still be needed to find and develop these resources that are so much a part of our daily lives.

This book is designed for the entry level geoscientist or student, but perhaps can serve as a refresher for more experienced explorers. It is the outgrowth of over three decades of learning and teaching how to find oil and gas using existing information from wells, some of which have been abandoned as barren when in fact, they are within an oil field. I've included many personal experiences and learnings from both failures and successes. For that reason, I have tried to keep the format somewhat less technical where possible and, instead, to share the reality of what goes on in a real workplace in teams of geoscientists. I have been fortunate to work and live globally and across many cultures and languages. The fundamentals covered in this book have carried me well through all those experiences, so many examples are from international settings. The technical language of geology and oil and gas is universal and common, despite the country or dialect. An outstanding reference for beginners in oil and gas exploration is that of (Hyne 2012). An excellent source of oil field terms is available online (Schlumberger 2015) and can be downloaded to phones and computers for quick reference.

Chapter 2 lays out the basic technical concepts key to understanding shows. Later chapters cover more detail on how data is captured and analyzed, including modern techniques with fluid inclusions, mud gasses and petroleum systems modeling software. To understand this book, however, there are many basic terms which define a language of oil and gas. Some of these fundamental terms and concepts used in this chapter are in Table 1.1. Conversions and other definitions are included in the appendices.

Table 1.1 Common terms used in this chapter

Term	Abbreviation	Definition
2D seismic	2D	Reflection acoustic seismic imaging using single lines of seismic, usually shot on land or in difficult areas. 2D seismic was an industry standard for nearly a century, and is still used in basin level reconnaissance, but has been supplanted by 3D seismic in recent decades.
3D seismic	3D	Densely spaced lines of seismic that can be processed and visualized to model structure, stratigraphy and reservoir properties of rock from acoustic variations in three dimensions. 3D seismic has been used heavily since the 1990s and many new wells are not drilled without acquiring a 3D seismic grid first, especially where the wells are deep and very expensive. Much more accurate facies and structural maps can be made with 3D seismic than with 2D.
4D seismic	4D	3D seismic shot from the same location over different intervals of time. The various data sets can show a change in fluid saturations with time, such as the impact of a water flood on swept oil in a reservoir.
Acreage		The land area held under contract by a company through agreement with mineral holders or governments. In the US, the measure is often in acres. Internationally, it may be in square kilometers.
API gravity	API	A unit of measure (American Petroleum Institute) that provides an easy way to define the density of oil. This is covered in detail in Chap. 2. Heavy oils (like tars or asphaltenes) have low API numbers under 20. 20–40 API is considered mid-range oil and above 40, the oils are considered light oils. Generally, operators prefer to find the lighter oils
Appraisal wells		Wells drilled after an exploratory discovery that define the limits of the pool.
Barrels of oil or water	BO, BW, BOPD, BWPD	A barrel of oil is about 42 gallons. The term arose from the size of wooden barrels used to haul oil from the earliest oil fields. A common measure of flow is in barrels of oil or water per day (BOPD, BWPD).
BCF	BCF	Billions of cubic feet of gas. In the US, a BCF of gas is often a significant find. Internationally, or in remote regions, it might be too small to be commercial.
Buoyancy pressure	Pb	The pressure differential in a trap between the hydrocarbon and water. The difference (Pb) is due to density differences. The higher the buoyancy pressure, the greater the hydrocarbons saturation at any position in the trap if rock type stays constant. This is covered more in Chaps. 4, 5 and 6.
Column height		The total vertical height from the top of the trap to the free water level. Column height is usually expressed in feet or meters. A trap with the top at 3000 m and the free water level, or spill point, at 3500 m has a column height of 500 m.

(continued)

Table 1.1 (continued)

Term	Abbreviation	Definition
Conventional exploration		Exploration for oil and gas in 'conventional or common' reservoirs, like sandstones and limestones that occur in structural, stratigraphic or combination traps.
Development wells		Infill wells in a pool designed to drain the accumulation most economically.
Dry hole	D&A, P&A	A well which is declared barren of hydrocarbons or containing uneconomic oil and gas saturations and is subsequently abandoned. Often referred to as a P&A well (plugged and abandoned). Dry holes do not necessarily mean the area has no potential. How to evaluate and post-appraise dry holes to find new location or pools drilled through and missed by the operator are the subject of much of this book.
Exploratory well		Generally a well testing a new concept, pool or play.
Farm-out		A business arrangement made when a company decides it needs financial or technical help to drill a well. The lease is 'farmed out' to other companies who buy into the well and development costs, but give the originator of the idea and land owners percentage royalties or bonus payments for the right to participate in the drilling.
Free water level	FWL	The point in a trap where the buoyancy pressure (Pb) = 0. This is always at the very base of the trap and is often different from the OWC. The FWL is controlled by the geometry of the trap and the seal or, capacity of the weakest seal, in addition, potentially to the amount of oil that trap receives during migration.
Gas-oil-ratio	GOR	The ratio of gas to oil measured in standard cubic ft gas per barrel of crude oil. Dry gas as a GOR limit >60,000, gas condensates, wet gas <60,000, volatile oil 1465, and black oil <320 (Whitson 1992).
Giant field		Generally (in US terms) a field with greater than 100 million barrels oil equivalent (MMBOE) recoverable. This equates to about 600 billion cubic feet (BCF) in terms of gas.
Hydraulic fracturing		A process of injecting fluids into a reservoir under high pressure. The process fractures the rock around the wellbore, enhancing productivity.
Leases		Mineral leases are held by landowners or oil companies and are necessary to have in order to get access to the land to drill the well. In the USA, lease-holders are generally awarded royalty interest in a well, usually varying from 8 to 25 % of the income from the well. Internationally, governments hold leases and may take as much as 80 % of the income in taxes.

(continued)

Table 1.1 (continued)

Term	Abbreviation	Definition
Matrix		The solid part of a rock. Porosity is the measurement of the void spaces between the rock grains themselves, which make up the rock matrix.
MMBO	MMBO	Millions of barrels of oil. A barrel of oil (BO) is roughly 42 gallons. The barrel unit was defined in the 1800s in the United States as that size barrel ended up being the standard size for transporting oil. BBO is short for billions of barrels.
MMBOE	MMBOE	Millions of barrels of oil equivalent. Makes a conversion from gas to equivalent volume of oil, usually at 5.8 or 6 MMBO/BCF.
MMCF	MMCF	Millions of cubic feet of gas. 1 MMCF is roughly equivalent to 178,000 BO. SCF = 1 standard ft^3 of gas. BCF = Billions of ft^3 and TCF trillions of ft^3.
Oil or gas in place	OIP, GIP	Oil or gas total volume in a pool. This is not the total recoverable, but the amount calculated to be in the trap. Recoverable volumes are a function of economics and the limitations on technology to extract hydrocarbons late in the life of a field due to low temperature, pressure or other factors.
Oil-water contact	OWC	The point where the hydrocarbon saturation (So) is 0 %. Conversely, the point where the water saturation (Sw) = 100 %. Oil-water contacts can vary considerably within a trap due to changes in rock type (Chaps. 2, 5 and 6).
Permeability	Kmd	A physical measure of the rate at which a rock can flow fluids. Permeability is a function of pressure drops, cross-sectional area, rock properties and fluid viscosity (Chap. 2). Kmd = permeability in millidarcy units.
Petroleum system		An aggregate of mature source rock, migration pathways, reservoirs, traps and seals that allows a hydrocarbon accumulation to exit.
Petrophysics		The quantitative study of rock properties such as water saturation, porosity, permeability and well log analysis.
Plays		Aggregates of prospects containing the same general type of trap. For example, the 'salt dome' play or the 'Marcellus gas play'.
Pool		An informal term used to describe oil or gas in a trap.
Porosity		The percentage of a rock occupied by pore systems, and not the matrix of the rock. Porosity is measured in % of total rock volume (Chap. 2).
Primary recovery		Production that can be achieved without secondary or tertiary recovery techniques like water recovery, CO_2 injection or other techniques designed to get at more difficult oil at lower pressures after production.

(continued)

Table 1.1 (continued)

Term	Abbreviation	Definition
Prospects		Recommended drill locations for any well.
Recoverable reserves		What can ultimately be produced from a field to some economic limit. Reserves are 'moving targets' that vary with oil price and technological advances.
Relative permeability	Kro, Krw	In any two phase fluid system (oil/water or gas/water) the percentage of fluid recovered of hydrocarbon versus water is a function of the fluid and rock properties themselves (Chaps. 2 and 5). Some rocks will flow 100 % oil at 80 % SW, and others only at 20 % Sw. Relative permeability has to be measured in a laboratory. Kro = percent permeable to oil; Krw = percent permeable to water.
Reservoir rock		Any rock capable of holding hydrocarbons. Porosity, either fracture or matrix, must be present.
Royalty interest		A type of ownership of an oil and gas lease where the lease-holder receives a negotiated percentage of profits from a well in exchange for granting permission to drill. A royalty interest owner does not incur any costs for drilling and developing the field.
Scout ticket		A written report, often only one page, of a well history or results. Industry 'scouts' were people hired by oil companies to find out what other companies were finding. The scout ticket, for many years, was the best way to get detailed information on many wells. Within companies, many well reports were also referred to as scout tickets.
Seals		Any rock capable of sealing hydrocarbons. Seal quality varies substantially, not just with lithology, but by the type of fluid in the system (oil or gas). Gas is generally more difficult to seal than oil.
Seismic inversion		The quantitative method of analyzing acoustic waves in seismic and finding equations to convert the time information into attempts to model and predict things like lithology, porosity and fluid content.
Source rock		Rock with initial total organic carbon % (TOC) capable of generating oil and gas when buried and mature through time and temperature.
TCF	TCF	Trillions of cubic feet of gas. A TCF of gas is considered a giant gas field.
Tight hole		A well where the drilling information is kept highly confidential by the company operating the well. This is a normal practice when drilling an important new well with new ideas or technology. The operator does not want other people to figure out what they are doing to find the oil or what others have missed or failed to envision.

(continued)

Table 1.1 (continued)

Term	Abbreviation	Definition
Unconventional exploration		A loosely defined term for exploration for oil and gas in reservoirs long-thought to unproductive. This includes gas from coal and oil and gas from shales and extremely tight carbonate source rocks. Unconventional shale plays hold the bulk of the world's future petroleum resources, and require hydraulic fracturing and horizontal wells to tap effectively.
Water saturation	Sw	The percentage of water in a porosity system (Chap. 2). Hydrocarbon saturation (So) = 1-Sw, also measured in percentage. An Sw of 30 %, then, has an So of 70 % with the remaining pore space occupied by water.
Well log		Plots and measures of various electrical or physical readings such as borehole size, made to understand rocks and fluids in a well. Chapter 2 provides an introduction and Chap. 6 deals with this topic in more detail.
Wildcat well		US oil industry term for exploratory tests, usually located more than 1 mile from the nearest pool.
Working interest	W.I. %	A type of ownership of an oil and gas lease where the owners participate in all operating and well expenses, and then are entitled to a negotiated percentage of profits.

1.2 The Art of Exploration

The search for oil is relentless, and what once began as a task of finding it seeping at the surface and then collecting it has evolved into a highly technical task that is a mix of science, rapidly advancing technology and an art. In 1972, Michel T. Halbouty invoked Wallace Pratt (1885–1985) in a quote from 40 years earlier that 'oil is found in the minds of men' (Halbouty 1972). Halbouty's essay warned that finding oil was first and foremost the art of using first principles rather than increasingly relying simply on computers and 'black box' software to arrive at an answer. That quote long ago has been expanded to 'in the minds of men and women' as today's workforce is highly diverse in both culture and gender, but his warning is just as relevant today.

Computing technology, software and diverse disciplines are vital to finding new oil and being able to rapidly evaluate any area. But nothing replaces the human mind and insight in the hunt for new oil. Despite all our technology and efforts, we still fail more than succeed and new ideas and techniques are continually needed to find new oil pools.

Fig. 1.1 Hand dug oil well located over a seep, mid-nineteenth century, Baku, Azerbaijan. Photo courtesy SOCAR oil company, Baku. Reprinted by permission of the Oil and Gas Journal from their cover photo (Narimanov and Palaz 1995)

1.2.1 A History of Drilling and Exploration

Chinese oil wells in 347 A.D. were drilled up to 800 ft (209 m) deep with bamboo spikes. Hand dug wells were common in Baku, Azerbaijan up to 35 m, essentially mined by workers lowered on ropes into open shafts (Fig. 1.1). Azerbaijan has been called the 'land of fire' as many gas caps over shallow fields leak to the surface that have been perpetually on fire at outcrops for thousands of years. It is thus no surprise that much of early drilling technology was developed in this part of the world, where giant fields lay close to the surface and oozed oil.

With oil bubbling to the surface or eternal fires marking traps, the concept of 'why is it there?' was not necessary to understand. The emphasis was on finding the seep and drilling wells to try to tap it. But shallow wells and bamboo pipes soon proved insufficient for tapping deeper and deeper oil pools, so early drilling rigs were developed and the hunt became more difficult.

By 1848, engineers in Baku had developed the first mechanical oil rig, followed in 1859 by the famous Drake well in Pennsylvania (Fig. 1.2).

These early wells were drilled with 'post-hole digger' technology, without modern rotary drill bits. The rocks were more or less pounded into fragments and lifted to the surface, limiting drill depth. Also, being drilled without mud or water in the hole, they were susceptible to blowouts when pockets of higher pressure oil, gas or water entered the hole. Successful wells frequently blew out and deaths and maiming on rigs were a common occurrence. Rock cuttings and oil show descriptions were very limited.

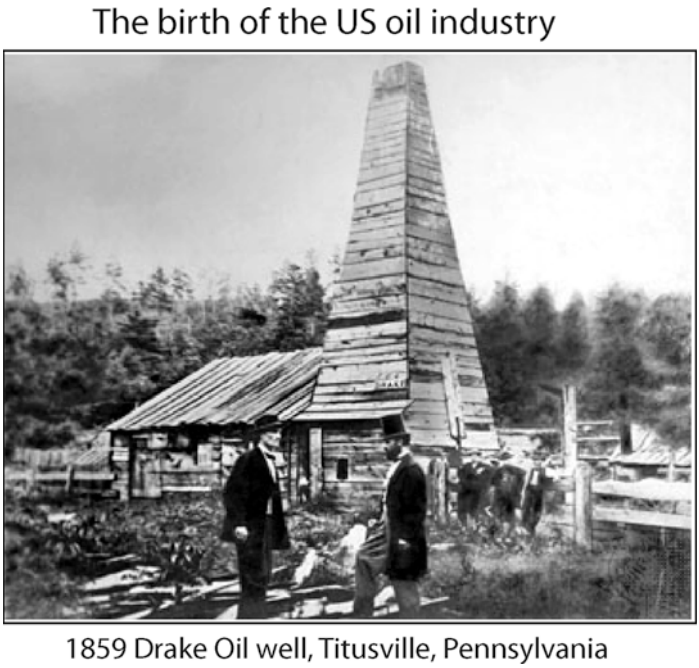

Fig. 1.2 1859 Drake Oil well, Pennsylvania. Although touted in the west as the first true oil well, the Drake well post-dated the first mechanical rig by 11 years, a rig developed in the oil fields of Baku, Azerbaijan. Source credit: http://www.britannica.com/biography/Edwin-Laurentine-Drake

Surprisingly, drilling a deeper well near a seep often does not result in finding any oil. This is due to the complex geology and migration pathways oil takes to the surface. Sometimes, years of effort have been spent trying to tap seeps with no commercial result. In an example from Oil Bay, Alaska (Fig. 1.3), seeps were reported as early as 1886, but, due to the remote location and lack of roads, attempts to develop the seeps started 10 years later in 1896. However, it took another 6 years to get proper equipment to the site. Thus, the first wells weren't drilled until 1902 (Detterman and Hartsock 1966; Director 2014), and these were very shallow. Deeper drilling required more equipment, and that didn't arrive until shipped by boat in 1936, when a surface anticline with only minor oil and gas shows was tested unsuccessfully. By 1956, two relatively deep tests (to 3400+m) were completed based on careful surface mapping of the Fitz Creek anticline. These wells, although they encountered enough gas to keep the lights on in a bunkhouse for a few days, were unsuccessful and abandoned. The area has not been tested again since, but the prolific Cook Inlet fields 90 miles (144 km) to the northeast, were discovered with seismic in the late 1950s and 1960s (Magoon 1994). The oil and gas shows encountered in the Oil Bay area were one of the reason the Cook Inlet area was eventually explored. Seeps are still major targets of study and exploration in many remote regions of the world, particularly in areas with unstable or hostile governments

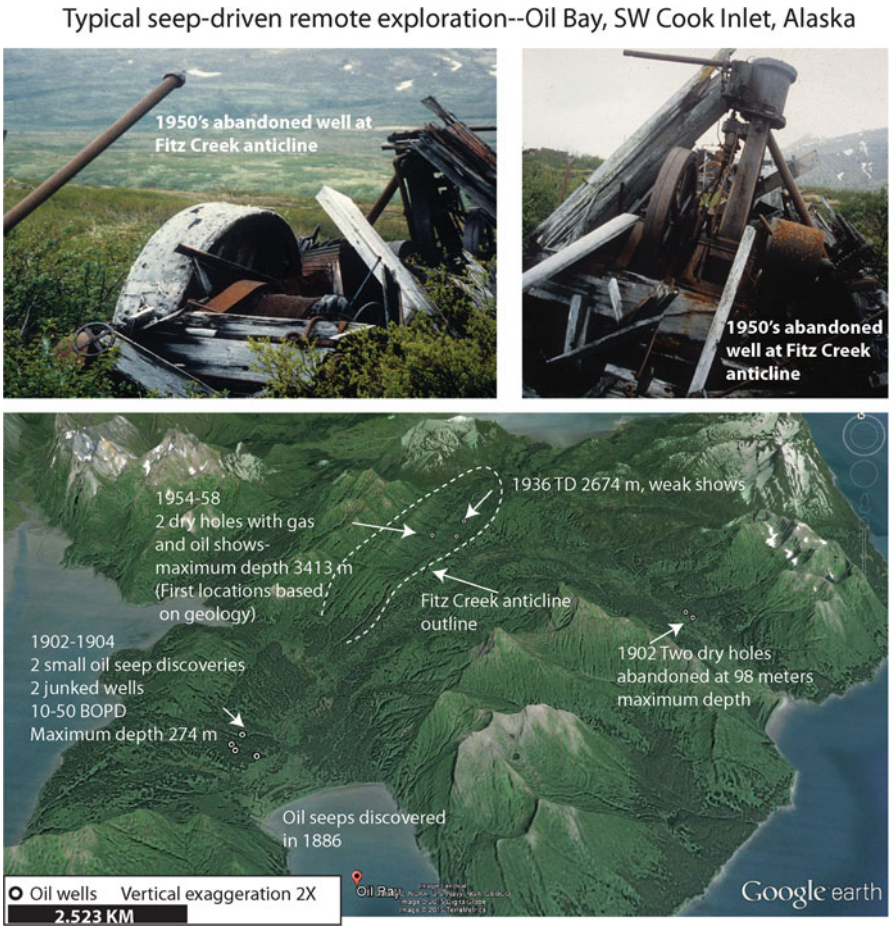

Fig. 1.3 A typical early exploration pattern, Oil Bay, southwestern Cook Inlet, Alaska. Early, very shallow wells were drilled at seep locations. Later, deeper wells tested surface anticlines, without the aid of seismic. Each generation of explorers faces its own challenges, in this case, difficult access and hostile arctic weather

where there has been no exploration for decades. But today, many more extensive studies are performed on the geology near the seeps in an attempt to best locate a rig to trap the deeper pools, if there are any.

1.2.2 Generational Challenges and Evolving Technology

Finding oil and gas has never been easy. Each generation of explorers faces its own difficulties. In the Oil Bay example, it was very difficult surface access. The deep wells drilled in the 1950s required an airstrip to get equipment in, and the location was staked without 2D seismic, on field mapping alone, under difficult terrain and

climate with virtually no prior work on the geology of the region. While surface mapping and seep detection is still required in many parts of the world, most big fields today are found with advanced technology and very sophisticated drilling systems, often in areas where there are no surface seeps at all. Technology moves at an astonishing pace, and failure to keep up with constant learning means being left behind.

Drilling and evaluation techniques have become more and more sophisticated, but still rely on an interpreter's experience and wisdom to use the information gathered to find new fields. Over time, as more modern drill bits were developed, mud systems were used to reduce heat from bit friction and to control pressures and prevent loss of life and property, causing show and sample description to become more difficult and involve more detail. Oil often became more difficult to recognize in cuttings, as the mud in the drill string frequently suppressed oil and gas shows in the rocks around the wellbores. Understanding these oil shows on a rig is the subject of Chap. 3. Chapters 4 and 5 cover the concepts of fluid flow, pressure analysis and rock property petrophysics in detail, information which is essential to understand what the shows mean.

One of the most important innovations in shows assessment was development of the wireline log (Chaps. 3 and 6), which uses electrical or other properties to detect lithology and fluid content. In 1912, Conrad Schlumberger, running experiments in a bathtub filled with various rocks, recognized that electrical conductivity could be used to tell some rock types apart. His research led, in 1927, to development of the first wireline log (Wikipedia 2014) to recognize oil and gas from a tool run down the wellbore. By the 1930s the newly formed Schlumberger Well Surveying Corporation was firmly established and wireline well logging has advanced tremendously in the last 80 years. Today's logging suites offer a wide variety of tools and an entire science of log interpretation has evolved to the point that petrophysical staff are generally embedded in every company to monitor wells and make recommendations for perforations, testing and development. Chapter 6 provides an introduction to 'quick look' techniques with well logs that provide additional insight to where oil and gas is located.

Today, Class EE drill ships (Fig. 1.4) are essentially small floating cities that can drill in extremely deep water and to depths exceeding 30,000 ft (10,000 m). Oil rig and drilling technology continues to evolve, but, through all that innovation, there lies a basic need to understand the oil and gas shows in wells and what they mean for well safety, well completion and exploration and development.

1.2.3 Some Personal Experiences in Learning About Seals and Shows

Within a few hours on the job with Amoco Production Company in Denver, Colorado in 1980, I was given a large map of the Denver Basin and asked to make a 'shows map' of all the wells on the map (and there were thousands). I meticulously poured through thousands of scout reports kept in three ring binders, posting symbols for oil shows, gas shows, oil recovery, gas recovery, pertinent pressures, mud recovery, tight wells, etc. until I had my wall plastered into a colorful mosaic of plastic

Fig. 1.4 Class EE drill ship. Modern rigs operate like small cities, with crew cabins, helicopter pads, entertainment centers and multiple laboratories. Photo courtesy of BP/Chevron Drilling Consortium course notes, by permission

stickers. Patterns were evident. There were areas where largely water was recovered with no shows, areas of mixed oil and gas shows and toward the basin center, decreasing volumes of water and increasing gas shows with few oil shows.

The map was a sight to behold, but the detailed significance of those shows eluded me. I was quizzed almost daily on that map, and chastised when I didn't know what a recent well had tested. I found out my immediate supervisor was actually reading daily well reports before I got them and then coming in and quizzing me on those wells and goading me to stay on top of activity I wasn't even aware of. We soon learned to get in earlier than him and quiz him before he quizzed us.

He espoused a simple philosophy of exploration summed up as "first you drill the structural high, then you drill the flank, then you drill the low and after that you farm it out" (sell the mineral rights to another company for an override and ask someone else to take the risk). The idea was simply to get higher on the trap and once found, work your way downdip with other wells. I used to laugh at this strategy until getting to Russia in 2004 and having a Russian colleague tell me: "We had rules in the Soviet past. You must drill four wells on every prospect until abandoning it. First a well at the top, then two on the flanks and one in the syncline". That wisdom and approach was more global than I had thought!

Another early tip I found equally befuddling and useless was: "there are only two kinds of rocks, throwing rocks and reservoir rocks". This was a comment made after I had come back from repeated trips to a core warehouse to look at depositional facies to aid my mapping in the Denver Basin. I was being asked why I spent so

much time looking at cores instead of getting after well locations in the basin from looking at well logs in the office. "How many bucks per barrel did you get from that *Ophiomorpha* trace fossil you found in the cores?" was another common taunt from my supervisor.

Ironically, in the middle of this goading was a grain of truth. When looking at those cores, I was focused completely on sedimentary structures and facies, something I had a good academic background in. I'd re-work my well log correlations daily with knowledge gained from those cores, but I seldom looked at the rock properties or paid much attention to the oil and gas shows and what they were telling me about the trap. I got better and better at making maps of ancient depositional systems based on the core data, but not much better at finding oil! It was years before I learned to quantitatively add the oil and gas show information to my workflow and begin to really reduce risk properly by understanding water saturations and show information.

When I refer to 'quantitatively adding the oil and gas show' to my interpretation, it means to be able to predict why those oil shows are there. Are they residual traces of oil left along a migration pathway, or are they shows within a proven trap? If in a proven trap, then how many meters above the base of the trap? Are the dry holes with reported shows really dry, or did the operator miss something and leave producible oil in the ground for me to find and exploit? Do my structure and facies maps explain the shows data? Where should I drill based on the best map? Quantifying shows is the essence of this book.

I was fortunate to start out in a basin where wells were cheap, costing as little at $150,000 per well and taking only about 5 days to drill. In contrast, the last well I drilled for BP, in 2003, found a giant field in the deep water Nile Delta but cost $79 million to drill and was over budget. Last year, BP made another deep discovery in the Nile Delta where the well cost exceeded $300 million dollars. These expensive plays are not a good place to be working for a young geoscientist, as it takes too long to learn how to drill wells (many years). It is best to be in an active drilling area, thrust into the heat of an exploration and development program and learning to properly design, drill and monitor wells.

We had a vast block of expiring lease acreage in the Denver Basin and most of the new-hires were tasked to evaluate deals with other companies to drill expiring acreage as rapidly as possible before we lost the mineral rights. Risk assessment wasn't part of the game. We were using money from other companies in a process known as 'farming out' and retaining an interest. For the most part, we came up with ideas for others to test, but we also put Amoco's money to risk in prospects we thought were the best, and those were always close to, or extensions of, known pools.

Looking back, the experience I got in that first year of recommending 50 wells and seeing the results weekly was incredibly valuable, but also 'blind-sided' me to a better process. The learning curve was so steep from day 1 that there was little time to learn all the things I needed to know to become an effective explorer without burning a lot of money with bad decisions. After the Denver Basin experience, I spent a year monitoring and participating with many others in recommending over 100 new wells in the Anadarko Basin, again with outside funding and a large team of Amoco geoscientists and engineers. Unlike the Denver Basin, these were deep and expensive tight gas sand wells. The basin was quite forgiving, being prolific and

a place where nearly blind luck could find you a pool of gas. In fact, the 'play' was based on a statistical assumption that 60 % of the wells would find something and perhaps 30 % of those would be economic. So geological insight pre-drill was not as highly valued as it should have been, not just because someone else was spending the money, but also because there was historical precedent for that statistical drilling technique working in that area. Consequently, for the next 2 years, the center of every block was targeted with a well. This was a great place to put inexperienced new-hires who could get involved in operations and well recommendations with few real consequences if mistakes were made.

But, as in the Denver Basin, very little teaching was done on the job to really get us to understand the significance of the rock properties and the oil and gas shows. The emphasis was on operations and well recommendations. Amoco, like many companies today, had a superb formal training program, with 5–7 weeks per year in Tulsa, Oklahoma and field trips and other courses to understand the tools and technology of the trade. Amoco's year-long petrophysical school in Tulsa was another bright spot. For those fortunate to go through that program, the principles outlined in this book were covered in detail and provided a lifetime of invaluable tools.

I have always felt an opportunity on the job was missed by not focusing early on the shows and reservoir properties in the context of traps and migration. Much of that, frankly, was considered 'academic' and the emphasis was placed on simply identifying where the shows were and then moving updip to try to find the trap. That was often the absolute wrong direction to go.

In the end, the statistical approach worked, money was made, and my personal learnings were invaluable, but less than they might have been with better mentoring. As a teacher today, one of the things I ask any young geoscientist to do is to generate a map that fully explains the oil and gas shows and reservoir properties in an area, including the geometry of the seals, individual traps and lateral and vertical migration from the source rock. Often, this is easier said than done.

While many companies place a heavy emphasis on early training and a steady progression of responsibilities with younger staff, others, through lack of manpower or loss of experience through attrition or retirement, are forced into using inexperienced staff to make expensive recommendations. These companies inevitably suffer a poor track record and lost income.

I am hopeful this book will help those young explorers avoid many of the mistakes that I and others made early in our careers by not understanding the principles of hydrocarbon show, petrophysics, seal and migration analysis.

1.2.4 The Art of Exploration: Plays Versus Prospects and Getting Proper Experience Early

There is an art to exploration and it needs to be learned early. It starts with really understanding the basin drilling history, its regional stratigraphic and structural framework and, very early on, getting familiar with the rocks and oil and gas shows

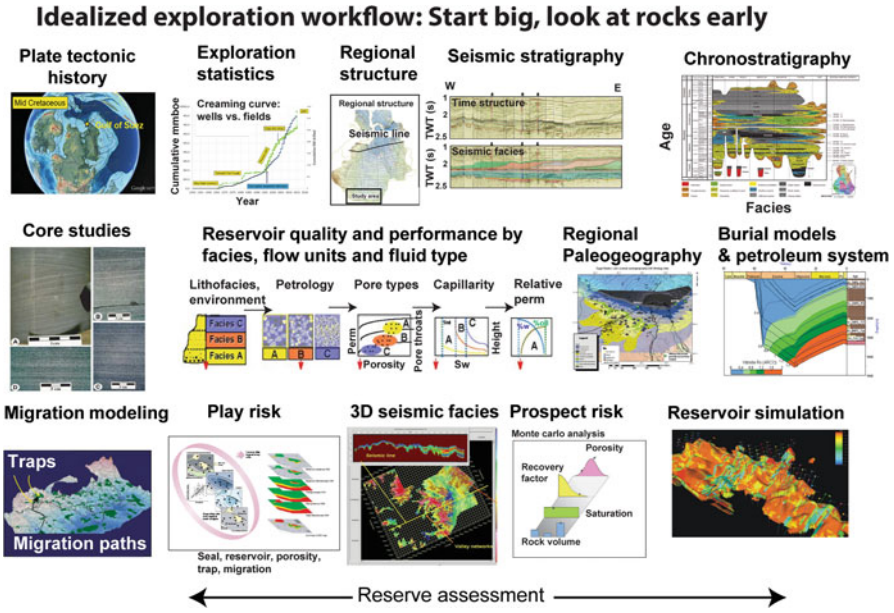

Fig. 1.5 Idealized exploration workflow. Understanding rock properties and oil and gas shows should occur, ideally, early in the interpretive process. Regional work should always be done first, and then modified later with details

(Fig. 1.5). Companies that follow a similar work-flow in exploration are generally very successful. Sophisticated computing tools allow increasingly rapid data integration, but nothing replaces the human insight simply gained from thinking about how all the bits and pieces of vast quantity of information available to evaluate a basin or prospect relate to one another.

1.2.5 Creaming Curves and New Plays Versus Prospects: Challenging the 'Peak oil' Paradigm

Successful exploration companies also learn early on to identify and pursue 'plays', not 'prospects'. Prospects involve the concept for why and where to drill a single well. Plays are trends which will eventually contain hundreds, if not thousands, of prospects. The term is common in the oil patch. "I'm getting into the Marcellus play; I think there is a play to me made in the Utica Shale; I am convinced there is a new, deeper play in that old basin that hasn't been made".

Prospects are fairly easy to generate, as they rely on proven strategies and existing tools. New plays, however, require 'out of the box' thinking and a break from traditional ways of viewing oil and gas entrapment based on historic industry activity.

New plays are particularly difficult to find in mature exploration areas, where thousands of skilled geoscientists have exploited the known trends fairly efficiently.

In a great play, you understand the petroleum system from top to bottom, or at least learn to live with the uncertainty and have a plan to drill a well to get the data you need to 'figure out the play'. Focusing strictly on prospects, however, means eventually spending a lot of money to look for increasingly smaller accumulations in known trends. Prospects are critical to evaluate properly and to keep failure rates low, but will give a much lower return on investment than being the first well in a basin to open up a new play. That new play may transform a company or industry fortune, eventually taking thousands of wells and decades of drilling to fully evaluate.

In 2015, 120 miles (192 km) offshore in Egypt, ENI astonished the petroleum industry with a 30 TCF (trillion cubic feet) gas discovery in a Miocene reef (ENI 2015). Shell had held the acreage for over a decade but dropped the acreage without testing the anomaly. Multiple companies turned down the opportunity to participate in the deep water well (4757 ft. or 1450 m water depth), but ENI focused on the new play and new potential and ended up the winner. One of the biases in place was the fact that no carbonate reefs existed anywhere in the Nile Delta or onshore Egypt, so how could the feature on seismic be a reef? This anomaly, even shown on a schematic cross section by Dolson et al. (2001) as having reef-like reflectivity, was deemed too risky. It took 'out of the box' thinking for ENI to test the well and win the prize.

In many companies, if the well is not testing a new play, it isn't even called an 'exploration' well and might be designated an appraisal well. Once a field is found, the infill wells are termed development wells. In all cases, the fundamentals covered in this book are necessary to optimize each location.

The oil and gas industry has long been focused on developing methods to determine how much oil and gas is left in basins or how well an industry or company is doing finding it (Arps et al. 1971; Arringdon 1960). One of the most influential papers was that of Hubbert (1967), who predicted that US 'peak oil' would be reached in the 1970s and then begin a steady decline. Actual US production until the last decade tracked Hubbert's curve almost precisely, leading many to declare that 'peak oil' had been reached and the world would soon run out of oil

However, within the last decade, that decline curve has been obliterated. The reason for the turn-around was the development of unconventional shale plays. These plays involve hydraulic fracturing of the oil and gas remaining in shales and source rocks. As of this writing, US oil and gas daily production on an oil equivalent basis, is at a 50 year high. How long this will last is still unknown, but the change in reserve base and production has been remarkable. While the debate over peak oil continues to rage (Gold 2014; Patterson 2015), one thing is certain; new discoveries take new ideas and big changes mean new plays.

The breakthrough with horizontal drilling and invalidation of a 40 year USA peak oil paradigm was made possible because the oil industry focused on new plays, not prospects. The focus was on new technology to access reservoirs once thought impossible to produce. Higher oil and gas prices and global demand encourage development of expensive new techniques. This is why companies try so hard to find the 'next big play' and not just the next interesting prospect.

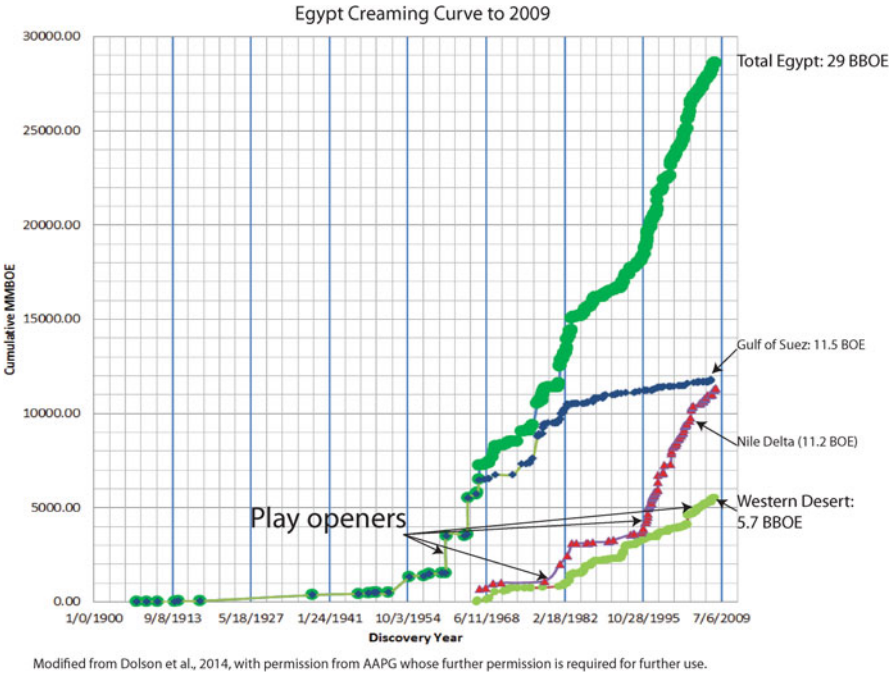

Fig. 1.6 Creaming curves measure cumulative oil found against time. Sharp jumps followed by steep upward trends indicate successful play opening wildcats (Dolson et al. 2014a). Some of the jumps related to new terms or oil and gas prices. The sharp jump shown in 1995 was due to Egypt's government awarding gas rights to companies in the offshore Nile Delta. But the play opener in 1965 in the Gulf of Suez was due to finding sub-salt pays in Amoco's giant El Morgan Field

The reason for emphasis on 'play opening wildcats' can best be shown with creaming curves. Oil and gas field sizes and discovery rates by time provide quantitative ways to compare companies and basins economically. There are a number of good resources for understanding statistical approaches to play and prospect evaluation (Klett et al. 2011; Rice 1986; Rose 2001, 2012; Steinmetz 1992). Perhaps one of the simplest methods of illustrating play versus prospect impact is by examining a creaming curve (Fig. 1.6).

Creaming curves plot cumulative reserve growth against time. Often, the footage or number of drilled wells is also included. The curves can be made for any given basin, company or play type. In Fig. 1.6, play openers are shown as sharp jumps in the finding rate, often followed by dramatic increases in volumes found.

For instance, the oil prolific Gulf of Suez had its first successful offshore sub-salt well discovery in the early 1960s and that play concept was pursued aggressively and successfully with large reserve additions until about 1989, when finding rates dropped off. The drop in finding rate was due to successful drilling of virtually all salt-related offshore closures and tilted fault blocks that could easily be found with 2D seismic. In the early 1990s most companies shot extensive 3D seismic surveys

in an attempt to find more difficult and smaller traps, but with the same play concept (Dolson et al. 1997). The result has been only incremental reserve additions since 1990 versus the heady play opening period from 1965 to 1989, when most of the oil was found.

Likewise, in the mid-1990s, Egypt's government granted gas rights offshore in the Nile Delta, which, up until that time, had its only significant reserves in a Miocene stratigraphic trap fairway called the 'Abu Madi Channel' (Dolson et al. 2000, 2001, 2004, 2005). Access to gas rights opened up a prolific Pliocene play—dominated by direct hydrocarbon indicators (DHI's) recognizable on seismic, giving the industry nearly a 90 % success finding rate. Finding rates are still high, but not in the Pliocene play which has more or less been 'played out'. Current large reserve growth is from deeper Oligocene targets in a new play opened up in 2003 with the discovery of the Raven Field (Dolson et al. 2014a) and extension of that play to the northeast into offshore Israel and the Levant Basin (Belopolsky et al. 2012; Lie et al. 2011; Peace 2011; Roberts and Peace 2007; Schenk et al. 2012; Stieglitz et al. 2011). The 2015 ENI Zohr Miocene reef discovery (ENI 2015), mentioned earlier, has now caused the creaming curve to spike again, with a brand new play developed that other companies missed.

1.2.6 Looking at Rocks, Dealing with People and Your Learning Curve

There is no replacement for looking at rocks early on, as they are the only piece of information we have that is incontrovertible. Everything else is derived. Seismic is shot and processed in time and then modeled to calculate depth and rock properties and hence, it has limitations of accuracy and resolution. Well logs are based largely on electrical measurements in a wellbore, and then the lithologies and saturations are modeled, again leaving room for error or just approximation. Petroleum migration is modeled with software, not directly observed in rocks. I live by the credo that 'those who see the most rocks win'. If you do your homework right, and understand the rocks and the fluids early, you can go on to understand and build petroleum migration models and well locations that have a better chance of being correct.

I know very few geoscientists who understand all aspects of all the available exploration technologies enough to call themselves 'experts'. In fact, the best oil finders I know have developed a keen appreciation for what other people's insight brings to a prospect. Finding oil is usually a team experience and learning to share observations and ideas and challenge each other is a large part of a successful exploration effort. For those who develop the 'language of oil and gas' and make an effort to understand the diverse disciplines and people involved, all is possible.

Dry holes or uneconomic wells are a humbling experience, and remind you that oil and gas exploration is not an academic exercise. In universities, I have seen horrible conflicts between professors, where success is measured by the number of citations you accumulate through papers and where peer reviews are intense and

sometimes involve personally nasty attacks. One of my academic colleagues explained it this way: “Nasty conflict amongst academics can be intense because there is so little at stake”. Nasty conflict doesn’t work well in the oil business. The stakes are high, and seeking out differences of opinion is not only welcomed, but essential. And, as you progress in your career, prior bad encounters with people you differ with unprofessionally will come back to haunt you, as it is a small world out there and people have long memories!

In a college or university, you can begin teaching immediately and have an immediate positive impact which grows substantially with time as you learn more and more and hone your skills. In the oil business, it takes many years of rigorous training and practical experience to be able to add great value to a company. That time period can be shortened somewhat for those who have studied at universities with strong petroleum geoscience curricula, but nothing substitutes for experience. Great companies don’t hire based on where you have studied or how many petroleum courses you have gone through. Great companies hire great scientists, engineers or mathematicians and chemists, and then train them. What companies want are independent thinkers and world-class problem solvers. Some of the best seismic processing geophysicists I know are mathematicians, some of the best geologists never had a course in petroleum and a lot of chemical engineers or chemists have become top notch logging specialists or petroleum systems analysts.

Nothing, however, substitutes for drilling wells early and being exposed to the proper concepts and training. Drilling wells early and learning well operations can cut a normal 8 year learning curve substantially. Many major oil companies rotate new hires through 2–3 years of training under mentor programs where you experience rank exploration, drilling operations, perhaps petroleum systems modeling, a stint with the petrophysics team or even wellbore design or seismic processing. That kind of training provides huge benefit to the company and for the new hire, feels a bit like ‘drinking water through a fire hose’. Great companies also push their junior staff into professional societies like the American Association of Petroleum Geologists (AAPG), Society of Professional Engineers (SPE), Society of Exploration Geophysicists (SEG) and others, championing multi-discipline learning and access to many world-class professionals outside of the company.

In the heady days of the late 1970s and early 1980s, when oil had spiked from $3 per barrel up to the unheard of price of $40 per barrel, many talented staff in the ‘majors’ simply quit and went to work for independents where they were given royalty interests in wells or large bonuses for their prospects. That left the majors full of highly inexperienced staff rapidly promoted into management vacancies without adequate training and experience developing plays and evaluating wells. Attrition was bad enough that when I walked into Amoco’s Southern Division my first week in August, 1980, someone had a sign on the door saying “will the last person quitting Southern Division please turn out the lights”.

In 1986, when the price crashed back to $9 per barrel, the industry, and Amoco, shed 25 % or its staff. Unfortunately, many of these staff were the ‘old wise men’ who were approaching retirement, so tremendous experience again walked out the door. Other staff that lost positions were those thrown into rank exploration projects

who had never drilled wells, and didn't really understand how to do so. A lot of really good people lost their jobs simply because they had been in the wrong projects at the wrong time, with the wrong idea of how to train and develop.

The results were disastrous. In the late 1980s Amoco assessed its performance and announced that over one billion dollars had been spent globally on exploration with no economic value added. On the safety front, Red Adair, perhaps the father of modern well firefighting, announced in a 1987 AAPG convention luncheon (paraphrased) that "I have never been so busy putting out fires and blowouts in my career. It is shameful the way companies have forced into retirement all that experience in proper well management". So the problems weren't limited to exploration.

We had to refocus and relearn as a company and as an industry, how to explore carefully and systematically. Promotions were frequently halted for people without a track record of drilling success, and slowed dramatically across the board. Unfortunately, training programs were cut back to save money, university donations and support were scuttled, and a long period of chaos ensued as we built back up expertise and proper exploration processes. Amoco was not unique. This was common across the industry and continues today. In 2015, as of this writing, similar scale layoffs are occurring with another spectacular drop in oil price. History is repeating itself.

1.2.7 Break from Paradigms: Believe in Yourself and Your Data

It was in that context of loss of mentoring experience that I was taught quickly, and sloppily, to 'go updip young man', when looking at a good show. I did that a number of times updip of tight wells with oil shows and ran into sealing facies and earned a dry hole. Years later, I came to understand that often you need to go downdip of a tight oil show as that is in a 'waste zone' in the updip part of the trap. The key is to look for better rock downdip, and that requires a lot of work mapping facies correctly and then using the show and petrophysical information to understand the trap. I wish someone had told me that then, instead of getting exposed to that concept much later largely through literature and personal interaction with truly great explorers. I am confident I left a lot of oil in the ground in the Denver Basin with a large number of 'dumb wells' that should never have been drilled had the right questions been asked.

At one point, my supervisor asked me where I should look in the basin for the next big oil field. He also warned me that with the tens of thousands of wells already drilled, it was a statistically 'mature' basin and had very little left to find. He pulled out a creaming curve and showed me that the 'basin was statistically dead'.

I showed him a township (a 36 mi^2 block of land) south of Denver. I pointed out that there were only five or six wells within it and most had interesting oil and gas shows. I argued that the petroleum system must be working and there should be a field in there somewhere. He promptly told me that "the industry has many more

clever employees than a first year geoscientist, so that is the worst place to look, as the industry has dismissed it, knowing it is no good. I will drink all of the oil you find in that area."

What I was being exposed to was the concept of a paradigm—an idea entrenched in someone's mind that prevented him from thinking 'out of the box' and finding new oil. As a follow-up on that conversation, I pulled a map of oil and gas leases out and pointed out that the area I looked at was under a city and had a new suburb in it, which might be the reason it wasn't drilled. I didn't think industry evaluation had anything to do with it, but rather, it was surface access and inability to get a drill location easily.

My boss reminded me again of how much oil he would drink after drilling my dry holes. We 'farmed out' the block to another company in return for an over-riding interest in anything found. On their fourth well, they discovered a small field. The next morning, in our well review, the drilling foreman arrived with a jar filled with Kahlua liquor but labeled 'oil discovery'. He offered it up to my supervisor, who had to drink the 'oil' from the newly named Harvey Wallbanger Field (named after a popular 1970s cocktail).

Learning to question paradigms was a great lesson to for me. The paradigm of why that township was not drilled was conclusively disproven.

Today, the Denver Basin, once considered a driller's graveyard, has undergone a renaissance of drilling for unconventional resources in the Niobrara shale, Thermopolis Shale, Codell Sandstone and other more difficult reservoirs. So paradigms continue to be broken there and the basin continues to churn out that 'new oil in an old area', but with 'new ideas and new technology'.

1.2.8 Pay Attention to the Fluids and the Key Well Concept

I also learned early on to pay attention to key details regarding fluids in rocks. Finding oil and gas in the Denver Basin had inappropriately inflated my sense of self-worth, and as I moved to deep gas exploration in the Anadarko Basin in Oklahoma, I 'got sloppy', brushing over critical data. I had a well recommendation located between two producers in a Pennsylvanian age sandstone called the Atoka Sand. It had a remarkably linear isopach (thickness) trend paralleling structure, as it was a shoreface or shallow marine sandstone that the more experienced 'old timers' called a 'strike parallel sand'.

The drilling success in that trend was so high that wells were spotted simply on trend with the strike of the structural contours and the producing wells. Seismic was only peripherally used. My well proposal fell between two producers with exactly the same well log profiles, porosities and similar saturations, at the same structural level. I was certain my location could not fail. At the recommendation time, my exploration supervisor asked me a simple question. "The two wells flanking your prospect have different GORs and API gravities. Does that bother you?" I brushed off the observation and replied that this was simple trend drilling and everything

would work out well. I drilled the first 'duster' in that trend, drilling a shale filled tidal channel seal that had compartmentalized the offshore sands. The difference in fluid phase should have warned me unequivocally that there was a barrier somewhere between these wells, and I found it! This was a lesson learned the hard way, but after millions of dollars were spent.

I hate dry holes, but they are difficult to avoid. Over the next few years, I was given projects involving regional basin analysis, extensive field work and a chance to test a couple of rank wildcats in the Cook Inlet Basin of Alaska. Like many young geoscientists, I took a hard look at my future in light of both my failures and successes. That introspective look caused me work harder to understand to petrophysical rock and fluid analysis more quickly, and develop better ways to integrate, visualize and understand subsurface data. I needed help, however, and was fortunate enough to have been given superb supervision of several large integrated core-based petrophysical projects dealing with both carbonates and clastics, by truly world-class experts.

I learned about the key well concept the hard way. Dan Hartmann told me repeatedly that I could learn most of what I needed to know from only one or two key wells in any basin. These wells needed to have rocks to look at (either cuttings or core) and good well log suites and test information. Studying these in detail, he assured me, would reveal most of the things that make a petroleum system work. Skeptical, our team proceeded to scour all of the available data instead of just focusing on one or two key wells. That work added months to our analysis.

In two separate projects over 1 year, we collectively examined 10,000 ft (3200 m) of core and another 10,000 ft of cuttings. Both data sets provided critical rock information and quantitative assessment of potential source rocks. We moved our analysis and data to some of the first geological workstations available to the Industry and went to work trying to carefully map out and understand the shows in the context of traps and migration. It was humbling to find out, under supervision of much more experienced staff, how little I really knew about rocks and how their rock properties controlled water saturation. My prior efforts to understand facies and deposition environments in the context of core-based sequence stratigraphy, had, unfortunately, left much of that analysis out.

What surprised me more, however, was discovering that Dan had been right about the key well concept and we could have saved a lot of time early on by focusing on key wells. We had several wells with complete information, including long cores, and those wells gave us 90 % of what we needed to know. It would have been best to have concentrated on those wells first and asked the right questions early. Months could have been shaved off the project cycle time from start to finish.

I was forced to think quantitatively about the difference between residual oils (like those in a 'swept' oil field or along migration pathways or paleo-oil accumulations that have been lost due to later uplift) and 'continuous phase' shows that are actually within a viable trap. I was re-introduced to the difference between oil-water contacts and the 'base of the trap' at the free-water level. I learned to appreciate that oil-water contacts can vary significantly across a field just by a change in rock type.

Eventually, our workstation-generated maps, underpinned with rock and fluid details, explained migration and entrapment well enough to make economic deci-

sions. One case resulted in a decision to stop work and abandon the area and another to farm-out a prospect considered high risk that was subsequently confirmed with a dry hole. My immersion with rocks and fluids over that 2 year period was perhaps the best technical decision I have made in my lifetime.

1.2.9 The Value of Teams, Peer Assists and Risk Assessment

I transferred to Houston in 1991 and started working on international projects, initially in Russia, Azerbaijan and Kazakhstan. These projects, while great for learning new cultures and understanding how vastly different the Soviet exploration and development practices were, did little to advance my knowledge of oil and gas shows.

However, I relocated, family in tow, to Egypt in 1994 for 8 ½ years as a geological advisor to the Gulf of Suez Petroleum Company (GUPCO, an Amoco-Egyptian partnership). This long-term assignment involved extensive drilling and was a great place to learn to apply show and seal analysis.

There was a prominent banner hanging in our Cairo office at GUPCO: "The map is wrong. It is always wrong. It is never right. The question is, 'how wrong is it?'" Clearly, the staff had the right attitude, and this is good advice to remember for any explorer. Every map ever made has built in assumptions, biases and limits. Making good maps is best done by interacting with others with different views and approaches. Ultimately, you need to assess just how wrong that map might be. When that happens, you find more oil and disappoint fewer people.

By example, from 1990 to 1993, GUPCO had suffered through a string of 32 exploration dry holes at the 'end of the creaming curve', with no discoveries. In addition, development wells were finding only about 60 % of what the staff predicted. Peer reviews were almost never held. Risk assessment was not done. Data was badly organized or sometimes lost completely.

Changes needed to be made. We were given a 3-year window by management to fix things, or, as management clearly stated, 'turn off the lights and go home'. We acquired 3D seismic to image new, more difficult traps and also trained staff in how to use geological workstations (new tools at the time) to better visualize, process and integrate subsurface data. The entire company moved toward multi-discipline, integrated teams of geophysicists, geologists, data managers, engineers and log analysts. Just as importantly, perhaps, we instituted comprehensive peer reviews and quantitative risk assessment.

The initial transition was difficult, but within a few years, we had gone from a legacy of 32 consecutive dry holes to a 75 % success rate and reserves found within 10 % of what was predicted. In 1997, our exploration team received Amoco's highest award for 'Technology Excellence in Exploration' and the quantitative results were hundreds of millions of new barrels added and developed while decline rates in older fields dramatically slowed or reversed (Hughes et al. 1997).

The 128 Egyptian staff I worked with and learned from, and scores of expats, remain close friends to this day and all of us look back on that period with pride, as the Gulf of Suez was another basin considered 'written off'. Despite all the success,

however, there were some preventable failures, and many of these are discussed in this book as case studies.

In the end, it was learning to look at every map skeptically, envision other ways to draw it, to quantify risk and then being able to withstand criticism and suggestions from peers that proved the real key to success.

1.2.10 The Need to Get It Right Needs to Be Balanced by a Need for Speed

Properly assessing risk and getting your maps through peer reviews takes time, but there is always pressure to do work faster and smarter. Time is, after all, money. An explorer's ability to do projects thoroughly but quickly is an important skill. A mantra at BP was "we want 80 % of the solution in 20 % of the time". At GUPCO we had the daily reminder from management that "we have a need for speed". So learning to ask the right questions early on with a few key wells and then filling in details later is an essential part of your job. Having said that, there is always a need to dive into key detail to get at answers, especially as you approach a well recommendation that might costs hundreds of millions of dollars.

Robert M. Sneider (1929–2005), a former AAPG President and renowned oil finder, once told me his company had a process of screening opportunities to buy old fields. The process took two people 1 day in a deal room to make a decision on whether or not to proceed with a four person review for another 4 days. Four basic questions were asked. (1) Did they use core and seismic based sequence stratigraphy to understand the reservoirs? (2) How good was the log analysis and did they tie that to core and cuttings? (3) How carefully did they look at the pressure history? (4) Was there by-passed pay on the logs, particularly in 'laminated' sands and shales which had low resistivity?

He also told me they had a list of companies they didn't bother with, because they did all those things well, and there was likely little left of value in the fields. But he had another list of companies that did those things badly. He focused on those companies. He bought and more than doubled production in scores of fields with that simple approach.

Much of what he focused on we touch on in this book. He believed in that 'need for speed'. But his teams always asked the right questions early and studied the oil and gas shows carefully, in the context of rock properties, and made the right decisions.

1.2.11 Looking for the NULF (Nasty, Ugly, Little Fact) to Break Paradigms

Despite the 'need for speed', critical details count. One of my favorite quotes is that of Thomas Huxley (Fig. 1.7):

> The great tragedy of science—the slaying of a beautiful hypothesis by an ugly fact.

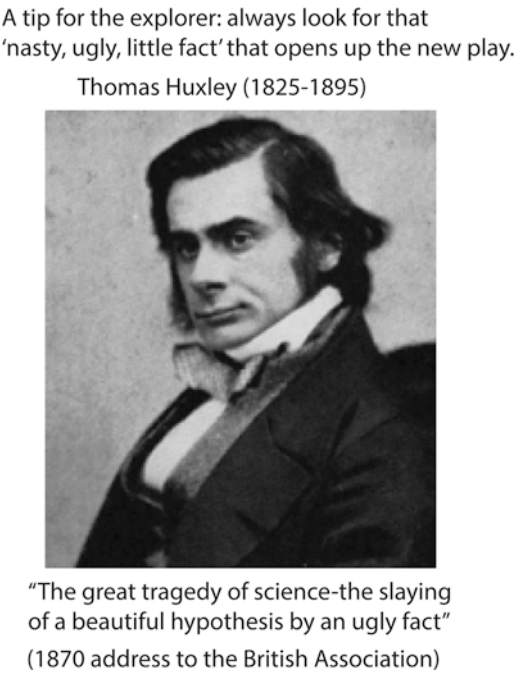

Fig. 1.7 Thomas Huxley (1825–1895). Photo from Wikiquote (2015)

I use the expression NULF (nasty, ugly, little fact) to characterize those pieces of information which often break a paradigm wide open. An astute explorer seeks out the NULFs when looking to open a new play.

Numerous examples in this book deal with a number of discoveries made with quantitative show assessment, often near or at old dry holes or producers that had been 'written off' by others. Paradigms negated by NULFs are ubiquitous in science, and particularly in the oil industry.

Here are some examples:

1. "You can't produce oil and gas from shales". That was the paradigm up until the 1990s when horizontal drilling and multi-stage hydraulic fracturing proved the paradigm wrong. What was the NULF? Oil and gas had been successfully produced from fractured shales for centuries in many shallow fields, and often by accident if vertical wellbores when oil and gas unexpectedly flowed from a fractured shale or limestone during drilling. In addition, George Mitchell had pioneered horizontal drilling in the Barnett Shale in Texas as far back as 1980.
2. "The Oligocene in the Nile Delta won't work because there is no source rock in the Oligocene". This was a common perception in Egypt through the 1990s (Dolson et al. 2002, 2004). The NULF's? Oil and gas shows were found in fluid inclusions and logs in a key deep offshore dry hole and one well was productive from the Oligocene. Subsequent drilling since 2003 has proven that Oligocene source rocks are responsible for many of the lower Miocene-Oligocene giant fields now discovered in the Nile Delta (Dolson et al. 2014a).

3. "You'll never get commercial gas out of coal". As hard as it might be to believe now, in the mid 1980s the perception existed that gas from coal was never going to amount for much. The NULF? Reports of gas explosions in coal mines showed the potential to trap methane from coal. Some early calculations showed large potential volumes available. The first coal gas completion attempted by Amoco in the late 1980s failed economically due to high water recovery. The company was going to 'write off the concept' but persistent engineers and geoscientists asked for a second well so they could try different completion techniques to produce the water until gas free production occurred. As is often said, "the rest is history" and 20 TCF of reserves were booked before other companies had thought of the right approach. (Coal gas technology is well covered in EIA 2007; Schwochow and Nuccio 2002; and Flores 2014).
4. "East African rifts won't work". This was a paradigm from many major oil companies until the giant field discoveries of the Lake Albert rift in Uganda in 2004 (Cloke 2009). The NULF? There were over 50 oil and gas seeps around Lake Albert and numerous hydrocarbon shows in other rifts. One major company interpreted this as proof there were no seals in the basin and therefore, no traps. Others saw it as proof of a working petroleum system with unexplored traps. Interestingly, the first well drilled by Tullow and Heritage discovered CO_2 and was abandoned. It took a second well to unlock the Kingfisher discovery. Persistence pays.

In all these cases, looking at the oil and gas shows was pivotal to unlocking the play. The issue was how to think about them differently, and not just in a negative light.

1.2.12 Pay Attention to Tight Rocks with Oil and Gas Shows

For the last several years I have been an adjunct professor at the University of Miami, teaching petroleum geology to graduate students, as well as to many geologists through AAPG workshops and consulting trips. This continuous exposure to new geoscientists and new plays continues to show me how much I 'really don't know that I thought I knew'. But it has also shown me that a common technical language exists, regardless of country.

In 2004, I moved to TNK-BP in Moscow, Russia as a Senior Geological Advisor for Exploration. The experience was reinvigorating, not just from having to learn some Russian, but trying to understand the Russian approach to exploration and a brand new suite of resistivity-based logging tools and exploration processes I had not used before. I had the chance to interact with hundreds of Russian geoscientists within TNK-BP and other companies, as well as universities. Despite a lot of common ground, however, there were large gaps in approaches, primarily in how to deal with sequence stratigraphy, petroleum systems analysis and oil and gas show evaluation.

Our Russian staff cut countless kilometers of cores for routine porosity, permeability and rock property information, but seldom visited the core warehouses to physically describe the cores or to think about the oil shows quantitatively. Capillary pressure data (Chap. 5) was never used in exploration to determine how high into a trap an oil show might be above the free water level. Low or minuscule rates of oil recoveries in tight rock were looked upon negatively and not as an indicator of a trap that could be much larger and more prolific than what was drilled. These conceptual gaps exist in many western companies today.

Consequently, in all our training, we placed an emphasis on oil shows, stratigraphy, petroleum migration and petrophysics. In the process, we uncovered over three billion barrels of oil in complex Jurassic age stratigraphic traps set up by low structural dip and multiple seals in incised valley deposits (Dolson et al. 2014b). All of the wells we looked at had been drilled on small structural closures, generally with no more than 15 m or so of structural relief (traps are defined at length in Chap. 2). The oil shows indicated the traps were, in fact, not structural traps, but part of a huge stratigraphic accumulation.

1.2.13 You Never Have Enough Data, But Perseverance Pays Off

Over my 35 years of experience, I have been struck with how different companies and individuals approach risk. Some suffer from 'paralysis by analysis', agonizing over what data they lack, more than what they have, and moving too slowly to make a decision to take a risk. Others make plays, opening them up early and dominating acreage positions. These latter companies create great wealth and more often than not, share an ability to persist through early failures.

Successful companies, if faced with early and negative results, use that knowledge, if they still believe in the play, to figure out what to do next that is different. Failure to do that often means abandoning a good idea too early. This has been shown over and over again in exploration, with winners and losers created yearly from companies looking at the same data, but with different views and stamina.

I have been especially fortunate to have spent 6 years as a rotational consultant with Cairn Energy India, one of the few companies in the world that I know have discovered two new hydrocarbon basins in the last 15 years (the Barmer Basin Rift and offshore Sri Lanka). The Cairn story in the Barmer Basin, however, is remarkable in that they started with so little information and managed to find an entirely new basin (Dolson et al. 2015).

In the early 1990s the basin was only speculative, buried underneath a featureless desert with no surface expression and no oil and gas shows. Gravity and magnetic data suggested an extension of the prolific Cambay Rift northwards, and seismic processed in 1998 led to drilling of the first well. The discovery, by a partnership between Shell Oil Company, the government of India (ONGC) and

Cairn Energy, was an economic disappointment, but flowed 2000 barrels of oil per day (BOPD) from a thin, silty sandstone. Gas in poor reservoir quality volcanics was also found. Shell and ONGC dropped their partnership in 2000, giving full control to Cairn Energy (then a tiny independent operated out of Edinburg, Scotland), which went on to discover the giant Mangala Field on their 14th exploratory well.

Perseverance paved the way to success. Rather than viewing the earlier results negatively, Cairn saw potential in a new basin. The tested oil on the initial well showed that a working petroleum system existed, but they had to figure out where to find quality reservoirs. Where Shell and ONGC had tested only a few trap types with three wells in a relatively small area, Cairn decided to test the rest of the basin. As part of their drilling campaign, they were diligent in choosing (1) a variety of trap types to test and (2) collecting as much information as possible to advance their basin understanding. After 13 disappointing wells (but collectively having found about 200 MMBOIP, but not enough economically), and on the verge of exiting the play, they drilled the giant Mangala Field with the 14th well, in 2004. Unlike the earlier wells, Mangala had multi-darcy high quality reservoirs. The oil was waxy at the surface and required a heated pipeline to produce, but was clearly economic. The company grew from 18 employees to more than 2000, and from 13,000 barrels of oil per day (BOPD) to over 250,000 BOPD, a remarkable achievement.

They have been diligent on data collection, assembling some of the best subsurface data sets on oil and gas shows, cores, fluid inclusions, apatite fission track, organic geochemistry, radiometric age data and 2 and 3D seismic. These data underpin their petroleum systems understanding, helping constrain and model three dimensional migration of hydrocarbons and quantify seal and reservoir from seismic inversion. Cairn continues to learn and capture new information, with an eye to the future, but building firmly on the past. Every well brings some surprises, despite the extensive subsurface database. But usually, some of those outcomes have already been discussed pre-drill as part of a comprehensive risk assessment.

In the end, however, it was their ability to take a small amount of information and see the big picture that separated them as a company from those who exited the basin too early, with too little insight and too little information. Perseverance paid off.

1.3 Some Background on Seismic

A full discussion of seismic is far beyond the scope of this book, but some basic concepts need to be understood. The first and most important concept is that seismic data is acquired by generating sound waves at the surface by 'thumping' either water or land with vibrator trucks, dynamite or any source which can generate waves (Fig. 1.8). The best source of details on seismic acquisition and processing is that of (Yilmaz 2008a, b). Easily the best volume for overall interpretive workflows of 3D seismic is that of Brown (2011).

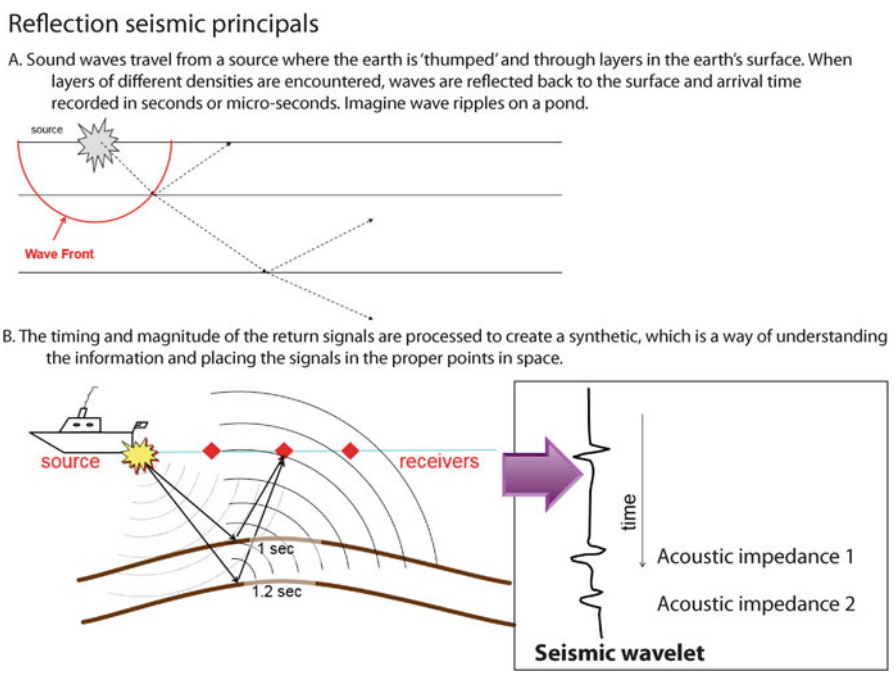

Fig. 1.8 Reflection seismic. It is shot in time and processed in depth. The seismic wavelet shown is the primary visualization tool to map the reflective boundaries. The wavelets are recording changes in velocity at the interface of different rock types which have different velocities. Modified from BP-Chevron drilling consortium course notes, by permission

As the sound waves travel through the crust, they encounter rocks of different densities and velocities, speeding up or slowing down as they pass through them. The changes in velocity and density at the boundaries are termed 'acoustic impedance'. The reflective energy at the boundaries goes back to the surface where its arrival time is captured with receivers and then processed by computers into its restored position in time and space for the reflected wave. The processing is complicated, and often involves super computers and can take months to deliver an interpretive volume.

What is critical about seismic is that it is virtually the only tool that allows relationships between wells to be visualized directly. For instance, are there faults between or in the wells? Are the facies changing laterally? Where are the reservoirs and where are the seals? In some cases, you can even detect oil or gas versus water, thus finding hydrocarbons directly, a process termed DHI (Direct Hydrocarbon Indicators). DHI's are wonderful to have, as they can greatly reduce risk, but many seismic features thought to be DHI's may turn out to be caused by rock changes, and not fluids.

Being able to see changes in velocities at boundaries is the key to interpreting reflectivity. Acoustic impedance contrasts are necessary in order to visualize reservoir layers and faults. If porous sandstones, for instance, have the same velocity

and density as the surrounding shales, the sands will be invisible on the seismic. Where the velocities and densities are different at the boundaries, there will be a change in character that shows up on a seismic wavelet (Fig. 1.8). The higher the impedance contrast, the larger the reflectivity and amplitude. Wavelet analysis is the key to understanding seal and reservoir variation in detail. Amplitude strength, along with other attributes, can be a key how much data can be extracted from seismic.

Factors that affect impedance (and thus amplitude) include:

1. Rock type
2. Compaction
3. Porosity
4. Cementation
5. Fluid type (water, oil or gas)
6. Geopressure
7. Depth of burial

There are three main types of seismic (Fig. 1.9).

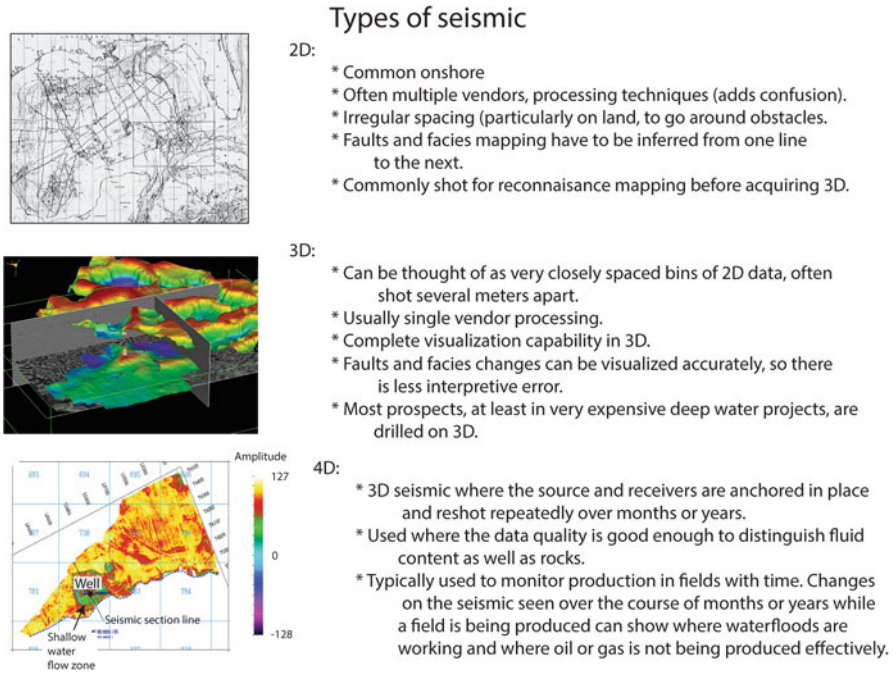

Fig. 1.9 Seismic types. 2D seismic is primarily used in large regional surveys and 3D seismic at smaller scales requiring more detail. 4D seismic is only run over currently producing fields where changes in fluid properties an also be imaged by changes in acoustic impedance with time as oil and gas is produced. Modified from BP-Chevron Drilling Consortium course notes, by permission

The oldest reflection seismic methods involved 2D acquisition on land, and was developed in the 1930s. By the 1980s, 3D seismic was being experimentally tested. In contrast to 2D seismic, which is usually fairly widely spaced and irregular (particularly on land) line orientations, 3D seismic is shot with receivers that are very close together. The resultant 'seismic cubes' contain enough data to visualize reflectivity in three dimensions. The seismic can be sliced vertically, like in a 2D section, or looked through from top to bottom, as in peeling back layers in maps at different depths. The result is a much more detailed look at how faults connect up, are linked (or not) in three dimensions and how facies changes between wells.

When it is possible to resolve fluid differences as well as rocks, from the travel time information alone, 4D surveys are shot. These kinds of surveys are acquired by leaving the recording instruments anchored at the same location (often on the sea floor) and reshooting the 3D seismic every 6 months or so. It is used over producing fields to track changes in fluid saturation as the fields are produced. Some really good papers help explain the concept and utility (Calvert et al. 2014; Marten et al. 2002; McClay et al. 2005; Riviere et al. 2010).

Seismic can be visualized in many ways. There are far too many display types to list here, but Fig. 1.10 gives an example of a few. Each type of display brings out

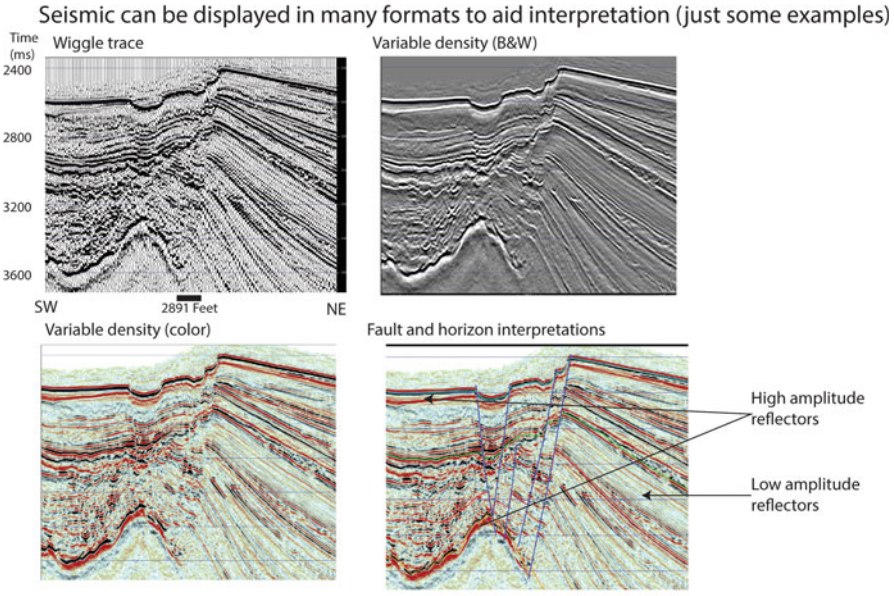

Fig. 1.10 Different ways to view seismic. Interpreting seismic can be somewhat addictive, with many ways to process and visualize data and multiple levels to map and interpret. Adapted from BP-Chevron Drilling Consortium course notes, by permission

different features. Many interpreters have their own preferred color scales or imaging tools. Regardless of the displays used, horizons of similar character are picked and carried around from line to line, or in a 3D volume to determine their geometry. Faults are picked, as are unconformities and even seismic facies changes. Seismic amplitude is also important, as high amplitude reflectors indicate a sharp change in velocity.

With rocks, we talk about the 'coarse grained, poorly sorted' facies and then relate it to a depositional system, like a braided channel or debris flow. The same is done with seismic, with terms like 'smooth parallel reflectivity' or 'chaotic reflectivity'. These patterns are caused by changes in depositional systems which can then be tied back to wells and cores for construction of seismic facies maps. These in turn, can be further modeled quantitatively, often in a process called 'seismic inversion' which is just someone deriving the mathematical relationships between the acoustic properties of the wavelets and things like fluid saturation, lithology or porosity.

Much of this book deals with modeling migration with seals. Seal geometries are controlled by faults and facies changes, like from a porous reservoir to a sealing shale. Having high quality 3D seismic to guide building those maps away from wellbores is essential to develop high resolution migration models.

It is also important to recognize the limits of seismic resolution.

Seismic resolution at a reservoir scale is difficult to achieve, as it requires very high frequency data not normally used in acquisition. Seismic energy also diminishes with depth, so the deeper you are looking, the lower the frequency. The resolution of a seismic wavelet is generally controlled by both wavelength frequency and velocity. When ¼ of the velocity divided by frequency is reached, that is the seismic limit.

In the diagram in Fig. 1.11, the resolution is 30 m. Think of that as about three stories high and you are looking for a reservoir one story in height or less. The seismic images will give a gross approximately of several layers of reservoirs and seals, but not just one. In the Gulf of Suez, our deep seismic reflectivity was reduced to 10 Hz frequency, which meant we could resolve reservoirs that were even 600 ft (157 m) thick. It also caused us to miss a large number of substantial faults that remained invisible.

Another issue is time to depth conversion. Seismic is shot in time, and then processed and modeled in depth. Many things show up on time sections that do not represent the true geometries in depth. An example is shown on Fig. 1.12, where there is velocity pull up due to a fast layer of salt in the shallow section. Salt velocities are faster than surrounding rocks, so sound waves speed up through salt, arriving faster at the surface than through other lithologies. Depth processing is done to convert the time data to its proper subsurface depth, and the shifts can be substantial.

In addition, on Fig. 1.12 are processing artifacts that produce reflectors that aren't showing real geology, just the way the sound waves are moving around. They must also be removed from the final interpretations. Another complication can

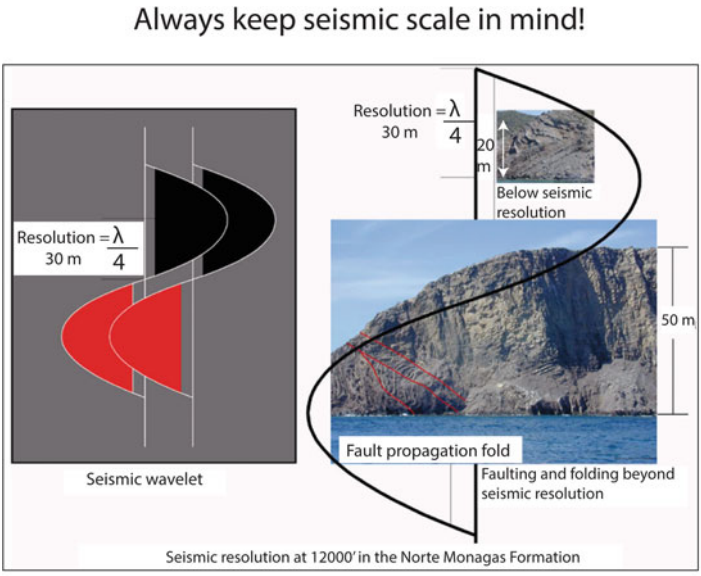

Fig. 1.11 Seismic wavelet resolution. It is easy to overestimate from a seismic image what it is really resolving. Scale of resolution is always something to bear in mind. Figure modified from BP-Chevron Drilling Consortium course notes, by permission

arise from what software or processes contractors use to convert or even prep the raw seismic data to depth or time. Different interpreters and different software can give different depth conversions.

When things go well, however, the results can be spectacular. Analyzing wavelet level detail can reveal depositional facies and faults with high accuracy (Fig. 1.13).

These images show geometries from 3D seismic that actually look like modern depositional systems (Posamentier 2006a, b). Figure 1.13a, for instance, is a Cretaceous fluvial reservoir from seismic, while Fig. 1.13b is an aerial photo of a similar depositional system on the earth's surface today. Likewise, ancient deep water channels and Miocene and Devonian reef and shelf edges are clear on Fig. 1.13c–e.

When I consult with younger geophysical staff, I am frequently presented with seismic amplitude maps that have no discernable geometry to them. If the geometry isn't clear, or resembling a modern depositional system, then the imaging is not very good and has limited predictability. I often get 'push back' that 'the math says that bright amplitude should be a sand'. On further discussion, we find out that the interval from which the amplitude was extracted was 500 m thick and the target is no

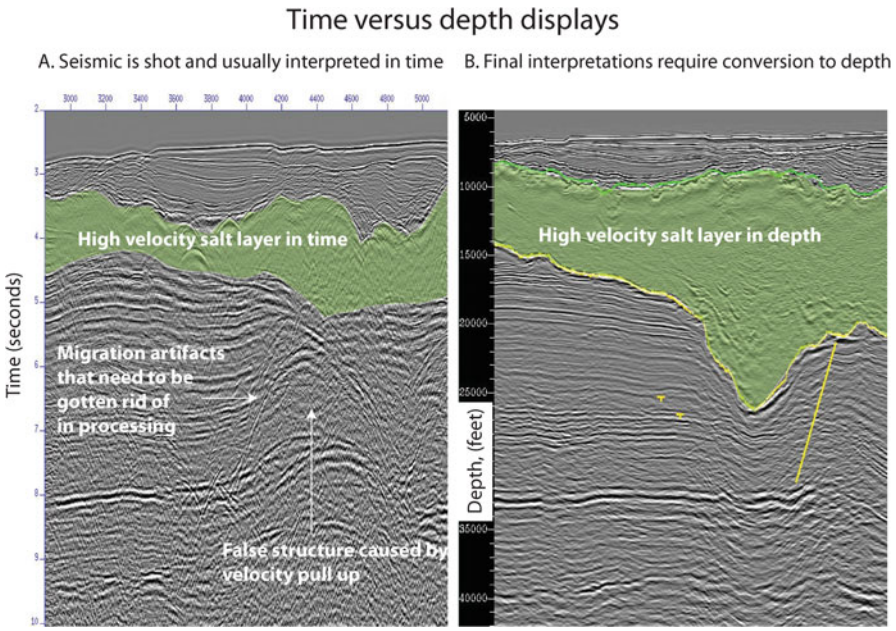

Fig. 1.12 Time versus depth. A depth model is only as good as the amount of time and energy spent converting the time data. Again, resolution and accuracy have to be taken into account. Modified from BP-Chevron Drilling Consortium course notes, by permission

more than 25 m thick. Hence, the amplitude map is showing 20 layers of different reservoir and seal combinations smeared into one. Hence, the geology disappears on the imaging. It comes back down to resolution.

Throughout the book, seismic images will be used to help explain how to look at reservoirs, seals and traps. Seismic can also be used to model geo-pressure, a topic touched on in Chap. 4. The reader doesn't need to be a geophysicist to understand the subsequent chapters. It is important, however to remember a few key things:

1. Seismic is shot in time and processed in depth.
2. Seismic resolution is limited by velocity and frequency. Always be aware of scale and limits.
3. 3D data is necessary to accurately define facies relationships between wells or fault linkages, while 2D data requires interpolation between lines.
4. Seismic can be used to identify fluids (DHI's) as well as lithology.
5. Seismic inversion refers to the process of modeling the seismic velocities such that output is in terms of things like porosity, net to gross, seal capacity, pressure or other variables. Resolution of the wavelet and the information it contains is the key to accuracy.

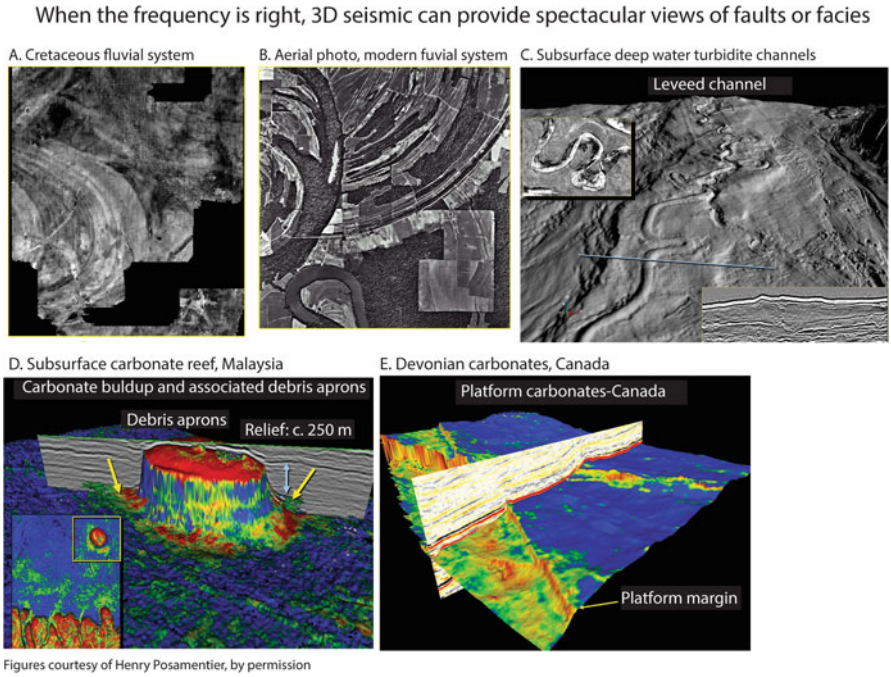

Fig. 1.13 Facies visualization from high resolution 3D seismic. When high quality data is interpreted at a wavelet scale using 3D seismic, stunning and highly predictive geometries of both faults and facies can result. Figure courtesy of Henry Posamentier from unpublished AAPG Distinguished lecture tour (Posamentier 2006a, b)

1.4 New Tools: Advances in Migration Modeling and Shows Calibration

Two major technologies have been rapidly changing our ability to understand subsurface oil and gas shows; seismic imaging and petroleum systems modeling. As mentioned, advances in seismic technology, from both acquisition, processing and software standpoints have been astonishing in the last 20 years. These advances are having a profound ability to reduce risk. Contrary to when I started in the Industry in 1979, a 20 % success rate is no longer considered 'good'. Companies routinely drill at a 50 % success rate or higher.

A laudable goal would be a zero percent failure rate, but that target is probably still far into the future. I believe much of future exploration success will come from the marriage of seismic and petroleum systems modeling software, coupled with sound reasoning and grounded in understanding where the hydrocarbon shows are. Our ability to increasingly quantify lithology, porosity, saturation, fracture systems and other attributes from seismic at a reservoir scale means we can now do a much better job of quantifying seals and trap geometries.

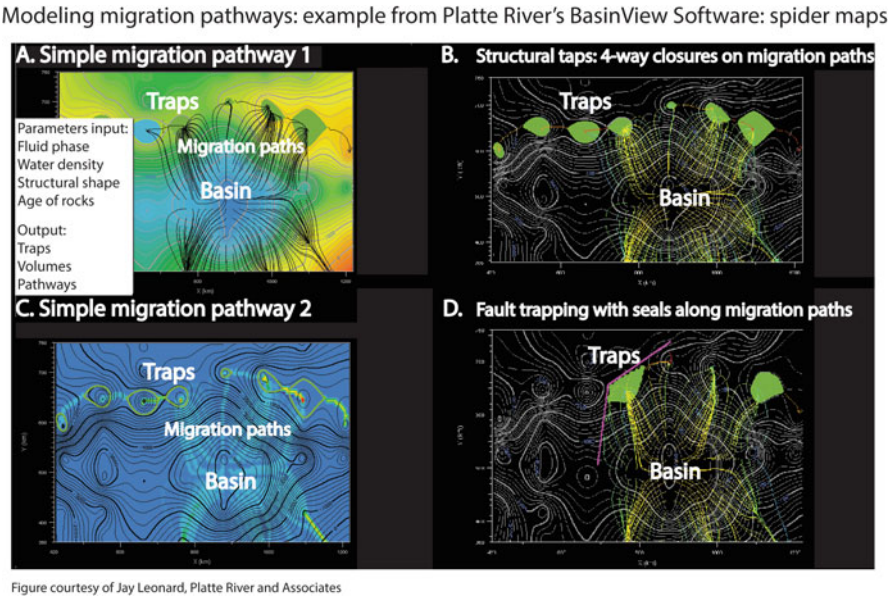

Fig. 1.14 Spider maps modeling flow of hydrocarbons from a mature source rock kitchen to traps flanking the kitchen. Software has become increasingly sophisticated, incorporating subsurface pressure, time and temperature controls on maturation, hydrodynamics and multiple seals and trapping geometry predictions. All models, however, need calibration to shows data to validate the accuracy of the model. Figure provided by Jay Leonard, Platte River Associates, Boulder, Colorado

The petroleum systems software is becoming steadily more capable of modeling hydrodynamic flow, pressures and migration using seals from faults and facies changes. But in the end, the oil shows information is perhaps one of the few ways to validate a model. Modeling hydrocarbon migration can be done not just in a three dimensional volume, but as a function of time, temperature and pressure. Despite these advances, however, validating a model requires a quantitative understanding of known oil and gas shows.

1.4.1 Spider Maps to 3D Models

One of the primary goals of quantitative shows assessment should be the ability to ground-truth a petroleum system migration and trap model. Early concepts of fluid flow and migration (Gussow 1953; Hubbert 1953) have advanced substantially in the last 60 years. Standard analysis relies on 'spider maps' which attempt to predict the migration of petroleum from a mature source rock in the 'kitchen' to traps (Fig. 1.14). My first exposure to spider maps (sometimes called 'hairy dog' maps) was using ZMAP+ software in the early 1980s. The software would trace lines perpendicular to structural contours to mark potential migration pathways. The assumption was that oil and gas would flow perpendicular to structural grains if left

Table 1.2 Some common Petroleum systems software packages which can model migration

Trinity 3D	www.zetaware.com	2 and 3D migration modeling with 1D burial history packages and kinetics packages (Genesis/Kinex). Superb editing tools for grids and maps.
Petromod	http://www.software.slb.com/products/foundation/Pages/petromod.aspx	Schlumberger product with very sophistical 3D modeling capability.
TemisFlow	http://www.beicip.com/petroleum-system-assessment	BeicipFranlab 3D modeling package.
Permedia	http://www.permedia.ca/	Halliburton petroleum systems modeling solution formerly called M-path.
Basinmod	http://platte.com/software/basinmod-2012.html	2 and 3D migration and burial history modeling from Platte River Associates, Inc.
MIGRI	http://www.migris.no/software/migri	Basic migration modeling tools.

unimpeded. These early models only considered simple fluid flow and were incapable of displaying traps along migration pathways due to fault or facies seals. They also could not incorporate subsurface pressure information or water flow, additional limiting factors. Figure 1.14 is a snapshot of some of the basic concepts of spider mapping. Throughout this book, there are examples of much more sophisticated modeling runs utilizing 3D migration with seals and hydrodynamic flow which alter migration pathways and trapping significantly.

There are many superb petroleum systems modeling software packages available today (Table 1.2). Examples in this book focus on Trinity tools (http://www.zetaware.com), as that is the tool I use and find easiest to display shows databases in 2D and 3D cross-sections and layers. It also has the advantage of powerful grid editing and spreadsheet visualization tools which allow quick modification to maps and ability to test a multitude of different reservoir and seal combinations in a migration model.

I firmly believe every exploring geoscientist needs to increasingly understand how to run these kinds of software tools and put their shows database in a migration context.

However, this book isn't about software; it is about fundamentals of rocks, petrophysics, pressure, geochemical rock to oil correlations, water flow and hydrocarbon migration. It is about the basic tools we need to understand if these sophisticated models, which produce splendid graphics, are useful or wrong. One of my favorite quotes that is also posted conspicuously on Zhiyong He's Trinity webpage (www.zetaware.com), is that of George Box, a prominent twentieth century statistician:

> All models are wrong, some models are useful.

While we are a long way from building migration models in three dimensions which use enough layers and details to get a perfect answer, many tools now exist to test ideas about migration in time and space. The following examples give a glimpse

into some of the things that can be done with migration and seal modeling, but it is good to remember the quote above and the other key concept that;

> The map is wrong, it is always wrong, the question is how wrong is it?

I have seen hundreds of petroleum systems models, some virtually drawn by hand in the 1980s but now nearly routinely developed using computer software. Along the way, I have had a chance to drill hundreds of wells and find out just how wrong my maps could be. That learning has been invaluable, as the temptation to believe a computer generated graphic is huge, especially when you are the one who generated it. They can look great, but can be horribly wrong.

To build a model, data inputs need to include accurate maps of things like structural and fault geometry, facies models with seal capacity and reservoir properties. Also required is a knowledge of the source rock, its age, geochemical properties and thermal maturation history. Timing of oil and gas migration can be modeled, but not often proven, so there are ranges of inaccuracies in any model. Despite this, many models do a good job of explaining known accumulations. But all models need calibration to oil and gas shows data from wells or perhaps even seismic. When most or all of the known distributions of oil and gas can be explained with a model, further locations to drill wells or develop the next play may become obvious. Chapter 5 provides a good case history in the four corners area of Colorado and Utah.

I firmly believe that the best software packages allow quick iterations where grids, faults, facies maps and other data can be modified rapidly and then the model re-run. Testing multiple models often shows that there are a few solutions which give similar answers but with different inputs. When you understand the risks in how bad or good your models might be, you are well positioned to make economic decisions based on this.

1.4.2 Some Examples of Model Development and Visualization

Figure 1.15 illustrates a simplified vertical and lateral migration model using Trinity software. Different colors mean different model accumulations at different levels. On the map at left, a large number of potential traps show up as tan and green colored polygons. The colors vary by the level each trap is modeled for. These traps are visible on the structural cross section A-A' and also in a 3D view. Modeling of these accumulations involves a simple adjustment of top-seal capacity at each level and then using simple 3D migration scenarios to pick where the largest number of stacked accumulations will occur. It is a highly simplified model, and cannot possibly accurately describe the complexity of seal capacity at each level and has not taken into account how faults or facies changes might also impact the model. However, it does a good job of building a basic, quick understanding of how migration might work in an area and what might make a prospect fail before drilling. The model can only be validated by looking at where oil and gas shows are in existing well control.

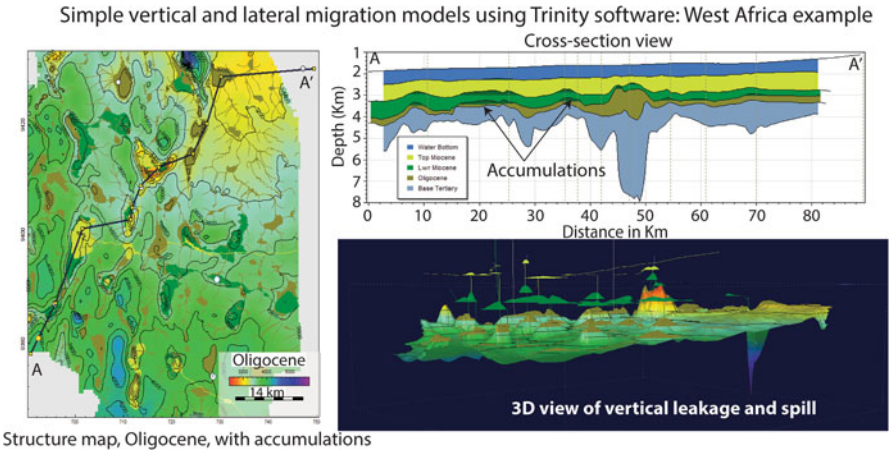

Fig. 1.15 Simplified vertical migration models using Trinity software. Example from West Africa. Top seals at four levels above a source rock have been varied in seal capacity (defined in meters of column height) to assess how oil might migrate vertically. The different colored polygons on the structure map are showing accumulations at different levels. A 3D model (*lower right*) shows multiple traps from vertical leakage and spill as top seal capacity is exceeded by structural closure

Calibrating these models usually requires analysis of the oil and gas shows in wells and where they fall on a cross-section or map in a migration model (Fig. 1.16). The model was developed from a Trinity 3D migration scenario utilizing fault seal capacity and multiple structural levels in Egypt. What is important about the model is not just what it got right, but what it got wrong. It successfully predicted an accumulation in FMT 4 in Well 5. It also predicted a dry test with residual oil in FMT 8 in Well 2 and a successful pool in FMT 8 in Well 4. However, it also predicted accumulations that aren't present in wells 2 and 3 and also in well 5, at FMT 6. By varying other parameters in the model, perhaps those dry levels could be explained. Even when explained by the model, the model may not be predictive away from this area, but if the model is clearly wrong, then using it elsewhere is dangerous.

It is unusual to get the perfect match between a model and wells. To do so requires robust and very accurate structural and stratigraphic maps and enough detail to more or less simulate migration in earth models that are much simpler than reality. Further complications come from limits on detailed understanding of rock properties vertically and laterally from seismic models versus sparse well control. The process of seismic inversion is a complex one and beyond the scope of this book, but involves finding algorithms which can convert seismic velocity data to meaningful rock property and fluid data to simulate and predict both rock facies and traps. Inversion models, as discussed, are only as accurate as the frequency of the seismic data and the processing techniques used. Ultimately, the goal of any interpreter is to be able to accurately describe fluids and rocks in three-dimensional

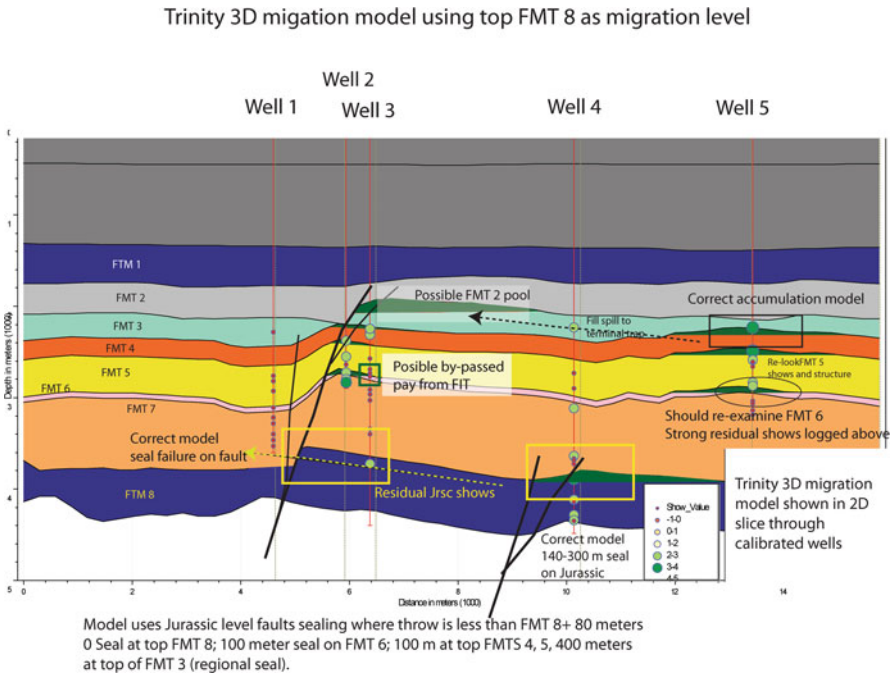

Fig. 1.16 A structural cross-section through a 3D migration simulation using Trinity software. Shows are posted on wells to calibrate the migration model. See text for discussion

space and to be able to simulate how hydrocarbons move vertically and laterally into traps, including through time.

I think of it as analogous to understanding the complexity of the human body with increasing resolution from rapidly evolving imaging technology. Despite advances, we are still a long way to reaching a molecular scale understanding of the human body in order to prevent or cure disease. Understanding cubic kilometers of rock variations is a similar challenge and hence, all petroleum systems migration models remain gross approximations of reality with inherent error built in, simply because we don't have all the tools and resolution necessary to fully model earth changes at the scale migration and charge take place.

An example is shown in Fig. 1.17, where a seismic line in depth (meters) has been converted in Trinity by using a simple scaler from the amplitude variations the original seismic (top) converted to reservoir/seal pairs (middle). Vertical migration from a deep source rock is simulated in the lowest diagram. This 'quick look' at migration is not a sophisticated 3D seismic inversion model which accurately estimates seal capacity from rock velocity, but rather, a simple model that arbitrarily scales the amplitudes. The resultant migration model illustrates conceptually the complexity in two dimensions of oil migrating from a source rock through many potential traps and up to the sea floor. In some areas, low relief structures do not

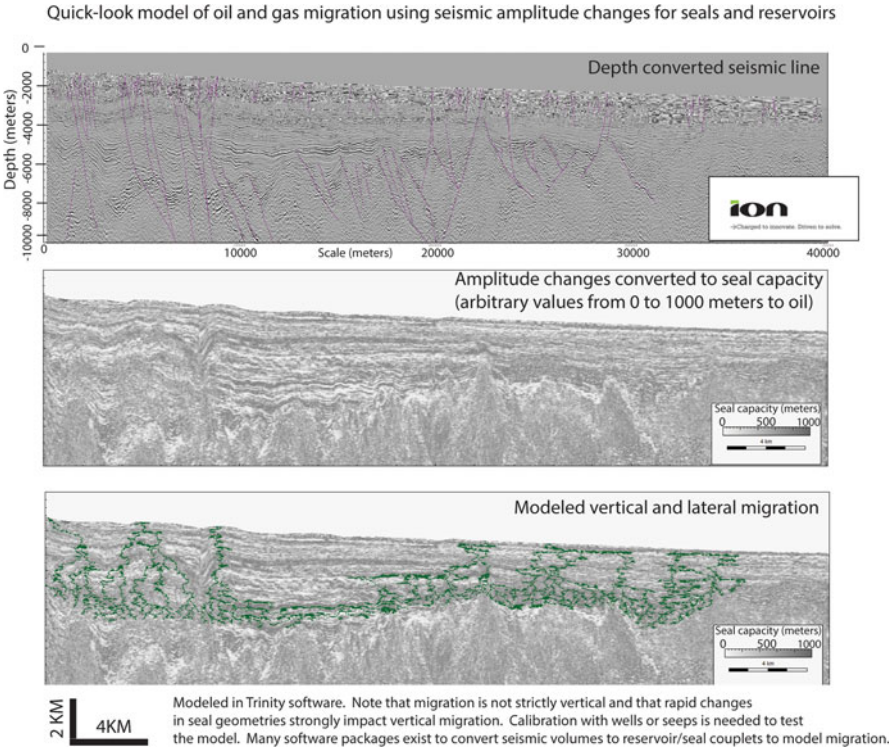

Fig. 1.17 Simplified model of vertical and lateral migration from a seismic depth section. Full 3D volume migration models incorporating seismic attributes are difficult to build, but when built, still require calibration to known accumulations and shows. *Top*: Depth seismic image. *Middle*: Seismic image arbitrarily converted to seals and reservoirs from amplitude differences. *Bottom*: Oil migration simulated from a source rock to the surface. Seismic section provided by Ion Geophysical, used with permission

allow strong vertical migration and oil accumulates and spills laterally and then vertically where the right kind of structure, faulting and reservoir/seal juxtapositions allow vertical migration.

The model can only be calibrated with studies of sea-floor seeps or from wells. Properly modeling the reservoir and seal capacities from seismic at all levels from surface to depth of your objective in three dimensions over a large area is virtually impossible at a reservoir scale.

It is good to remember this when calibrating shows data to any petroleum systems model. The earth is generally much more complex than we can interpret accurately with the tools we have today, but the tools get better with ever advancing technology. As in medical technology, the envelope of ability to interpret and predict is constantly moving and getting better.

1.5 Summary

Even with all the rapidly advancing ability to model migration and entrapment, some things won't change. Oil and gas shows in wells, surface seeps, and geochemical information will remain critical to understanding and calibrating migration and trap models. The core concepts of extracting information from oil and gas shows and rocks will remain the same. In an age of increasing emphasis on software manipulation, particularly with 3D seismic and petroleum systems software, using basic principles to understand the limits of these tools, as well as the potential, is key. A great computer graphic and 3D display can be dreadfully inaccurate but, like a master painting, be a wonder to behold. Hence, flaws in the models are often overlooked when the model looks so beautiful.

The principles laid out in this book will be refined and will evolve in the future, but the basic concepts should remain firm. Once you get accustomed to thinking about oil and gas shows as a dynamic process of generation, migration and entrapment, you are part way to discovery. When you learn to evaluate rock properties that control water saturation, water cut, fluid phases, pressure and fluid flow, breaking old paradigms and finding new oil will become easier.

The oil industry today faces tremendous challenges, and, as it was when I entered the workforce in 1979. Once again, it is undergoing a massive transfer of knowledge from retirees to the next generation of oil finders. The 'Great Crew Change', as it is frequently called, is upon us. So too, are rapidly advancing technologies, increasing reliance on computer models, changes in drilling technology and rapidly shifting global geo-politics. I have been exploring for oil and gas for 36 years, and the tools I use today I wouldn't have dreamed of when I started. My learning curve remains steep and I am confident that newcomers to this business, reading this book today, will look back in 36 years and say "I wish I'd known then what I know now".

I hope this book will help any newcomer to oil and gas exploration 'get up to speed' quickly on these critical techniques for show, seal and migration evaluation in the search for new traps.

References

Arps JJ, Mortada M, Smith AE (1971) Relationship between proved reserves and exploration effort. J Pet Technol 23:671–675

Arringdon JR (1960) Predicting the size of crude reserves is key to evaluating exploration programs. Oil Gas J 58:130–134

Belopolsky A, Tari G, Craig J, Illife J (eds) (2012) New and emerging plays in the eastern Mediterranean: an introduction, vol 18. Petroleum Geoscience, The Geological Society of London, London, 372 p

Brown AR (2011) Interpretation of three-dimensional seismic data, 7th edn. v. AAPG Memori 42/SEG Investigations no. 9. American Association of Petroleum Geologists, 315 p

Calvert MA, Roende HH, Herbert IH, Zaske J, Hickman P, Micksch U (2014) The impact of quick 4D seismic survey and processing over the Halfdan Field, Danish North Sea. First Break 32:43–50

Cloke I (2009) The Albert Rift, Uganda: a history of successful exploration, IRC-Egyptian Petroleum Exploration Society (EPEX), Cairo, Egypt, AAPG Search and Discovery Article #10192

Detterman RL, Hartsock JK (1966) Geology of the Iniskin-Tuxedni region, Alaska, United States. Geological Survey Professional Paper 512, p 78, 6 sheets

Director (2014) Chapter six: oil and gas exploration, development, production, and transportation, Southwest Cook Inlet oil and gas exploration license: Director's written finding. Alaska Department of Natural Resources, p 19. http://dog.dnr.alaska.gov/leasing/Documents%5CBIF%5CExploration_Licenses%5CSW_CookInlet%5CSWCI_Ch6.pdf

Dolson J, Burley SD, Sunder VR, Kothari V, Naidu B, Whiteley NP, Farrimond P, Taylor A, Direen N, Ananthakrishnan B (2015) The discovery of the Barmer Basin, Rajasthan, India, and its petroleum geology. Am Assoc Pet Geol Bull 99:433–465

Dolson JC, Atta M, Blanchard D, Sehim A, Villinski J, Loutit T, Romine K (2014a) Egypt's future petroleum resources: a revised look in the 21st century. In: Marlow L, Kendall C, Yose L (eds) Petroleum systems of the Tethyan region, Memoir 106. American Association of Petroleum Geologists, Tulsa, OK, pp 143–178

Dolson JC, Boucher PJ, Dodd T, Ismail J (2002) The petroleum potential of the emerging Mediterranean offshore gas plays, Egypt. Oil Gas J:32–37

Dolson JC, Boucher PJ, Siok J, Heppard PD (2004) Key challenges to realizing full potential in an emerging giant gas province: Nile Delta/Mediterranean offshore, deep water, Egypt. Petroleum Geology: North-West Europe and Global Perspectives—Proceedings of the 6th petroleum geology conference, pp 607–624

Dolson JC, Boucher PJ, Siok J, Heppard PD (2005) Key challenges to realizing full potential in an emerging giant gas province: Nile Delta/Mediterranean offshore, deep water, Egypt. 6th Petroleum geology conference, p 607–624

Dolson JC, Pemberton SG, Hafizov S, Bratkova V, Volfovich E, Averyanova I (2014b) Giant incised vally fill and shoreface ravinement traps, Urna, Ust-Teguss and Tyamkinskoe Field areas, southern West Sibertian Basin, Russia, American Association of Petroleum Geologists Annual Convention, Houston, Texas, Search and Discovery Article #1838534, p 33

Dolson JC, Shann MV, Matbouly S, Harwood C, Rashed R, Hammouda H (2001) The petroleum potential of Egypt. In: Downey MW, Threet JC, Morgan WA (eds) Petroleum provinces of the 21st century, Memoir 74. American Association of Petroleum Geologists, Tulsa, OK, pp 453–482

Dolson JC, Shann MV, Matbouly SI, Hammouda H, Rashed RM (2000) Egypt in the twenty-first century: petroleum potential in offshore trends. GeoArabia 6:211–229

Dolson JC, Steer B, Garing J, Osborne G, Gad A, Amr H (1997) 3D seismic and workstation technology brings technical revolution to the Gulf of Suez Petroleum Company. Lead Edge 16:1809–1817

EIA (2007) US coalbed methane: past, present and future. Energy Information Administration Office of Oil and Gas, Washington, D.C., p. 1

ENI (2015) ENI discovers a supergiant gas field in the Egyptian offshore, the largest ever found in the Mediterranean Sea. http://www.eni.com/en_IT/media/press-releases/2015/08/Eni_discovers_supergiant_gas_field_in_Egyptian_offshore_the_largest_ever_found_in_Mediterranean_Sea.shtml. ENI, p 1

Flores RM (ed) (2014) Coal and coal bed gas: fueling the future. Elsevier, Waltham, MA, 697 p

Gold R (2014) Why peak-oil predictions haven't come true. Wall Street J, Sept 29 2014

Gussow WC (1953) Differential trapping of hydrocarbons. Alberta Soc Pet Geol News Bull 1:4–5

Halbouty MT (1972) Oil is found in the minds of men. Gulf Coast Assoc Geol Soc 22:33–37

Hubbert MK (1953) Entrapment of petroleum under hydrodynamic conditions. Am Assoc Pet Geol Bull 37:1954–2026

Hubbert MK (1967) Degree of advancement of petroleum exploration in the United States. Am Assoc Pet Geol Bull 51:2207–2227

Hughes SC, Ahmed H, Raheem TA (1997) Exploiting the mature South El Morgan Kareem reservior for yet more oil: a case study on multi-discipline reservoir management, Middle East Oil Show and Conference, Bahrain, Society of Petroleum Engineers

Hyne NJ (2012) Nontechnical guide to petroleum geology, exploration, drilling and production, 3rd edn. PennWell Corporation, Tulsa, OK, 698 p

Klett TR, Attanasai ED, Charpentier RR, Cook TA, Freeman PA, Gautier DL, Le PA, Ryder RT, Schenk CJ, Tennyson ME, Verma MK (2011) New U S. Geological Survey method for the assessment of reserve growth. World Petroleum Research Project. United States Geological Survey, Reston, VI, p 11

Lie O, Skiple C, Lowrey C (2011) New insights into the Levantine Basin, GeoExPro. Geopublishing Ltd., London, pp 24–27

Magoon LB (1994) Tuxedni-Hemlock(!) petroleum system in Cook Inlet, Alaska, U.S.A. In: Magoon LG, Dows WG (eds) The petroleum system-from source to trap. American Association of Petroleum Geologists, Tulsa, OK, pp 359–370

Marten RF, Keggin JA, Watts GF (2002) The future of 4D in the Nile Delta (abs.). International Petroleum Conference and Exhibition, p A56

McClay KR, Dooley T, Whitehouse PS, Anadon-Ruiz S (2005) 4D analogue models of extensional fault systems in asymmetric rifts: 3D visualizations and comparisons with natural examples. In: Dore AG, Viking BA (eds) Petroleum geology: North-West Europe and global perspectives—proceedings of the 6th petroleum geology conference. Geological Society of London, London, pp 1543–1556

Narimanov AA, Palaz I (1995) Oil history, potential converge in Azerbaijan. Oil Gas J 93:4

Patterson R (2015) Why peak oil is finally here. In OILPRICE.com (ed). http://oilprice.com/Energy/Crude-Oil/Why-Peak-Oil-Is-Finally-Here.html

Peace D (2011) Eastern Mediterranean: the Hot New Exploration Region, GeoExPro. Geopublishing Ltd., London, pp 36–41

Posamentier HW (2006a) Imaging elements of depositional systems from shelf to deep basin using 3D seismic data: implications for exploration and development, AAPG Dean A. McGee Funded Distinguished Lecture

Posamentier HW (2006b) Stratigraphy, sedimentology and geomorphology of deep-water deposits based on analysis of 3D seismic data: reducing the rick of lithology prediction, AAPG Dean A. McGee Funded Distinguished Lecture

Rice DD (ed) (1986) Risk analysis and management of petroleum exploration ventures: AAPG studies in geology #21. American Association of Petroleum Geologists, Tulsa, OK, 265 p

Riviere MC, Robinson ND, Tough K, Watson PA (2010) 4D Sedismic surveillance over the Azeri-Chirag-Gunashli Fields, South Caspian Sea, Azerbaijan, 72nd EAGE Conference and Exhibition, Barcellona, Spain, EAGE, p 5

Roberts G, Peace D (2007) Hydrocarbon plays and prospectively of the Levantine Basin, offshore Lebanon and Syria from modern seismic data. GeoArabia 12:99–124

Rose PR (2001) Risk analysis and management of petroleum exploration ventures. American Association of Petroleum Geologists, Tulsa, OK, 178 p

Rose PR (2012) Risk analysis and management of petroleum exploration ventures (multimedia CD). American Association of Petroleum Geologists, Tulsa, OK, p 178

Schenk CJ, Kirschbaum MA, Charpentier RR, Klett TR, Brownfield ME, Pitman JK, Cook TA, Tennyson ME (2012) Assessment of undiscovered oil and gas resources of the Levant Basin Province, Eastern Mediterranean. World Petroleum Resources Project. United States Geological Survey, Reston, VI

Schlumberger (2015) Oilfield glossary. Schlumberger Corporation. http://www.glossary.oilfield.slb.com/

Schwochow SD, Nuccio VF (eds) (2002) Coalbed Methand of North America: II. Rocky Mountain Association of Geologists, Denver, CO, 108 p

Steinmetz R (ed) (1992) The business of petroleum exploration: treatise of petroleum geology; handbook of petroleum geology. American Association of Petroleum Geologists, Tulsa, OK, 382 p

Stieglitz T, Spoors R, Peace D, Johnson M (2011) An integrated approach to imaging the Levantine Basin and Eastern Mediterranean: new and emerging plays in the Eastern Mediterranean, p 15–19

Whitson CH (1992) Petroleum reservoir fluid properties. In: Morton-Thompson D, Woods AM (eds) Development geology reference manual. American Association of Petroleum Geologists, Tulsa, OK, pp 504–507

Wikipedia (2014) Schlumberger brothers, Wikipedia. http://en.wikipedia.org/wiki/Schlumberger_brothers

Wikipedia (2015) Thomas Henry Huxley, Wikipedia. http://en.wikiquote.org/wiki/Thomas_Henry_Huxley

Yilmaz O (2008a) Introduction. In Doherty S, Yilmaz O (eds) Seismic data analysis: processing, inversion, and interpretation of seismic data: investigations in geophysics No 10, vol. 1. Society of Exploration Geophysicists, pp 1–24

Yilmaz O (2008a) Seismic data analysis: processing, inversion, and interpretation of seismic data. In: Yilmaz O (ed) Investigations in geophysics, No 10. Society of Exploration Geophysicists, Tulsa, OK, p 2028

Chapter 2
The Basics of Traps, Seals, Reservoirs and Shows

Contents

Abstract Hydrocarbon traps from when reservoirs receive a charge from hydrocarbons migrating from a source rock at a time when effective seals and trap geometries are in place. Exploration that focuses on traps along a migration route is termed conventional exploration. Conventional exploration deals with understanding secondary migration. In the last 20 years, there has been an increasing focus on unconventional exploration, which focuses on the hydrocarbons remaining in the source

J. Dolson, *Understanding Oil and Gas Shows and Seals in the Search for Hydrocarbons*, DOI 10.1007/978-3-319-29710-1_2

rock itself. The generation of oil and gas within a source rock is termed primary migration.

There are a multitude of different trap geometries, all of which rely on the concept of closure. Closure is defined as where structural contours along a migration route terminate into seals. Defining the geometry of the seals and the migration route requires understanding rock properties, burial history and pressure changes. Trap size is controlled by the capacity of the weakest seal as well as the amount of hydrocarbons available to reach the trap. If buoyancy pressure at the top of the trap exceeds the weakest seal capacity, the trap leaks updip.

Porosity in the rock provides the space to hold hydrocarbons, but it is the distribution of the pore throats connecting the porosity system that is a primary control on water saturation and seal capacity and the oil-water contact vs. the free water level. Residual hydrocarbon shows are always below the free water level and must be distinguished from continuous phase shows, which are above it, and in the trap.

2.1 The Petroleum System: Primary, Secondary Migration, and 'Unconventional' Exploration

A petroleum system consists of four major elements: (1) a kerogen rich source rock which has expelled hydrocarbons during burial and heating; (2) an effective migration pathway out of the source rock; (3) seals to trap the oil and gas on a migration pathway; and (4) reservoirs to hold the oil and gas. The process of oil and gas generation in the source rock is termed primary migration. Oil and gas molecules in primary migration move only short distances and stay within the source beds themselves. If these hydrocarbons enter a permeable layer of rock they will migrate updip until reaching a trap or dissipating at the surface. This process of migrating out of the source rocks themselves into permeable carrier beds is termed secondary migration (Fig. 2.1). Exploration efforts now focus on both types of systems, exploiting not only the oil left in the kerogen-rich source rocks, but that which has been trapped in permeable beds along secondary migration pathways.

There are many different kinds of oil and gas traps formed during secondary migration, but they all have the basics in common: a favorable set of seal geometries along a migration pathway. Exploration plays are grossly lumped as targeting (1) conventional oil and gas traps and (2) unconventional traps.

'Unconventionals' are rapidly becoming a type of 'conventional' exploration as an increasing success rate is beginning to redefine the term as the industry practices in the 'unconventionals' become more routine. Throughout this book, however, the term 'unconventional' refers to exploration targeting the primary migration paths in the source rocks. The term 'unconventional' also includes coal gas deposits and some types of tight gas sands, where the trap itself is poorly defined but the reservoir producible.

The source rocks generally require hydraulic fracturing to produce and the plays are confined to mature oil and gas maturation windows where the oil and gas remains trapped in the source rock. One of the most important drivers of

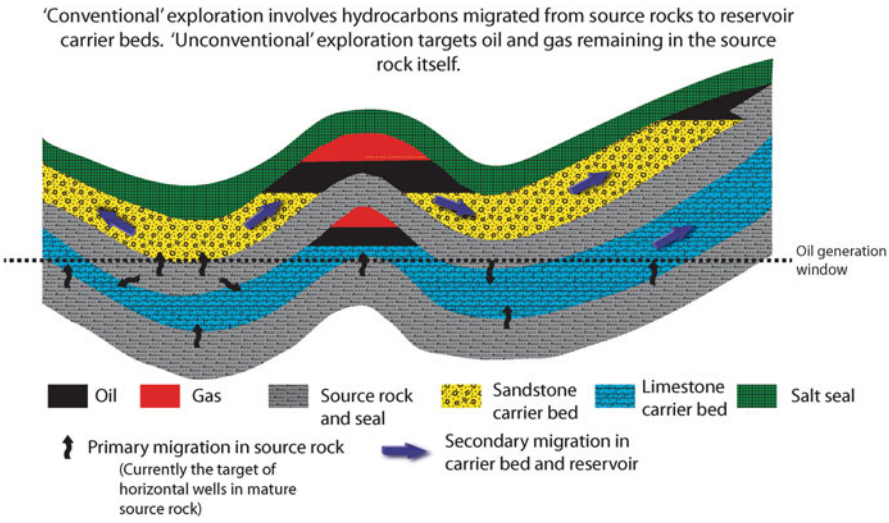

Fig. 2.1 Conventional vs. unconventional traps and migration. Modified from England et al. (1991)

unconventional source rock plays is simply the fact that large amounts of oil remain trapped in the kerogen and never access a secondary migration pathway. Hence, for any given basin, the bulk of the generated hydrocarbons often is remaining in the source rocks themselves. The term 'conventional exploration' refers to identifying secondary migration pathways into reservoirs in structural, stratigraphic or hydrodynamic traps, where migration has occurred from the source rock laterally or vertically into traps. Oil and gas show analysis can help find both primary and secondary migration pathways. When drilling through source rocks, for instance, drill bit friction frequently generates hydrocarbons in the source rock, and oil and gas shows are picked up in tools on the rigs, frequently with mud gas increases. Likewise, migration pathways are frequently recognized from shows in cuttings, particularly underneath regional seals along carrier beds, or in fluid inclusions in the rocks. We'll cover much of this in more detail later.

2.2 Traps, Porosity, Spill Points and Seals

There are a large number of potential trap types. Figure 2.2 illustrates common trap types and the concept of trap closure and spill point. Hydrocarbon traps require a combination of migration, reservoir and seal geometries which form closed containers to hold hydrocarbons. Reservoir rocks are most commonly sandstones or carbonates, but can be fractured granites, volcanics or even shales (unconventionals). In short, reservoirs exist wherever there is a porosity system in the rock with enough room to hold hydrocarbon molecules. Porosity is the percentage void space in a rock.

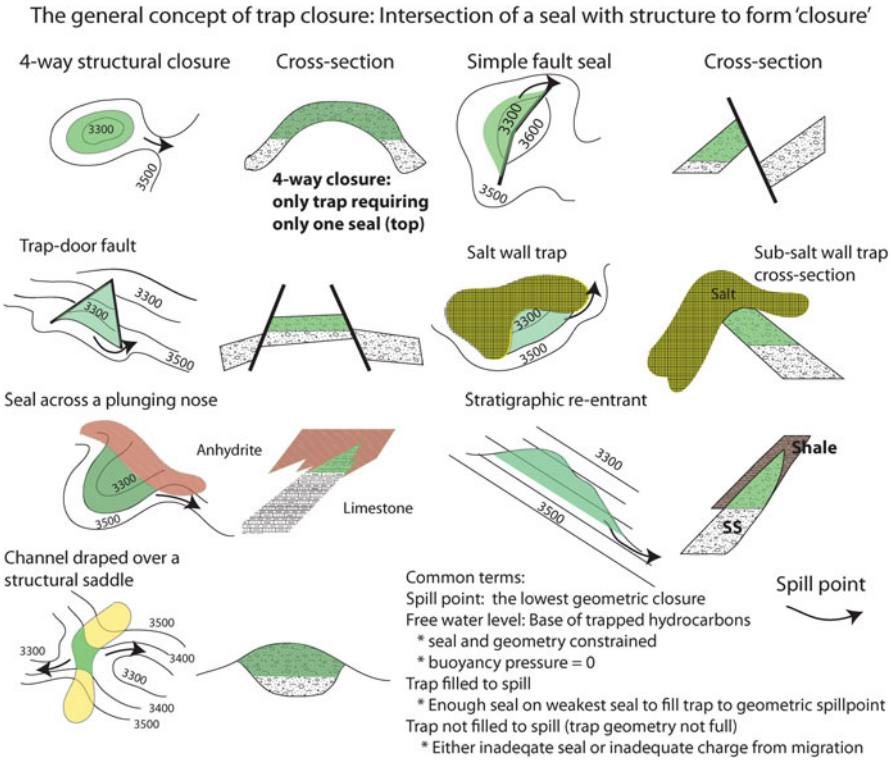

Fig. 2.2 General trap types and closure concepts

If not present, there is no room for oil, gas or water. Porosity is discussed in more detail later in this chapter, but can be thought of as analogous to the inside of a house, where the rooms are pores. Porosity voids are connected to each other by pore-throats, which are analogous to doors between rooms. Porosity and pore throat size plays a large role in determining if a formation can hold hydrocarbons. The larger the pore throats (doors), the better connected are the pores (the rooms) and the easier it is to get oil and gas into the reservoir. The mechanics of how this works has nothing to do with the size of oil and gas molecules relative to the pore throats (which are much, much larger than hydrocarbon molecules), but by the capillary pressure properties of the fluid and rock systems, a topic dealt with in detail in Chap. 5.

Seals, by contrast, are low porosity or micro-porous pore throats that migrating hydrocarbons cannot move through and hence become trapped if geometries are right. Seals come in a wide variety of lithologies, and are most commonly thought of as forming in shales, siltstones, tight carbonates or evaporites and salts. However, seals can form wherever there is a reduction in pore space geometry or energy sufficient to overcome the forces driving migration. In Chaps. 4 and 5, we cover quantification of seal capacity from rock and pressure data and ways to recognize seals from changes in oil and gas shows, drilling information or recoveries from tests.

The term ‘closure’ was developed early on from making structural contours maps of surface anticlines. When the contours ‘closed’ in a circle or oval around a high, the trap was considered ‘closed’. With time, the term closure was broadened to encompass any contour that intersects a seal and is closed on both sides (Fig. 2.2). Most traps require geometric combinations of multiple seals, typically, top, lateral and bottom seals. The point where the contours fail to close is termed the ‘spill point’. Pre-drill, most prospects are evaluated with the assumption there has been adequate oil charge and migration from the basin. This may not always be the case, but if all the seals work and there is an adequate volume of oil reaching the trap, it will be ‘filled to spill’ and the down dip limit of the accumulation will usually conform to a structural level at spill point.

The most commonly sought after and prolific traps are structural four-way closures, where reservoirs are folded into domes or closed anticlines where the accumulation is controlled dominantly by the top seal capacity vs. the structural closure relief. In these kinds of traps, multiple ‘stacked pays’ are possible, with many different oil/water contacts and even fluid types stratified vertically. They are by far the easiest traps to map seismically and lowest risk to drill if on a well-defined migration pathway or within the oil and gas window where interbedded source, reservoir and seal are present inside the trap.

Sub-salt or salt-wall closures are also fairly easy to recognize, but require accurate seismic processing and depth conversion to image properly, a process that can be difficult and expensive. In these cases, simple maps of the structural contours going into the fault are sufficient to quickly see the ‘closure’ and the trap. Traps related to complex salt domes and detached salt nappes also hold very large, ‘stacked pay’ reserves. Salt and other evaporites form outstanding seals and can hold very long columns. Much of the world’s deep-water drilling today focuses on ‘sub-salt’ accumulations where reservoirs are folded or faulted into salt walls, under salt overhangs or under completely detached nappes. These are attractive prospects, but require special acquisition and processing techniques of seismic to image.

The closure itself, however, may not define the size of the accumulation. Column height is defined as the true vertical height that any trap can hold. If the trap is filled completely, it is termed ‘filled to spill’. Column height can be an indirect measure of seal capacity. In a trap with a proven 500 m column, it is a given that the minimum seal capacity on the weakest seal, for that hydrocarbon-water system, is 500 m.

Many structures, however, are not filled to spill, as one or more seals have less capacity to hold a column than the maximum closure geometry. These traps are ‘filled to seal capacity’. However, another reason for not being filled to spill point is simply that an inadequate volume of oil or gas has reached the trap along the migration route. These kinds of accumulations are ‘charge limited’ traps.

But if charge risk is eliminated, one is still faced with risk on seal capacity. Seal failure may well be one of the biggest reasons for drilling dry holes in any basin. Seal capacity is generally thought of in terms of meters or feet of column height.

An example of a structure not filled to its geometric spill point is shown in Fig. 2.3. The geometric spill, if the faults seal, would be at about 2400 m TVDSS (true vertical depth subsea, in this case, in positive numbers, so 2400 is the lowest).

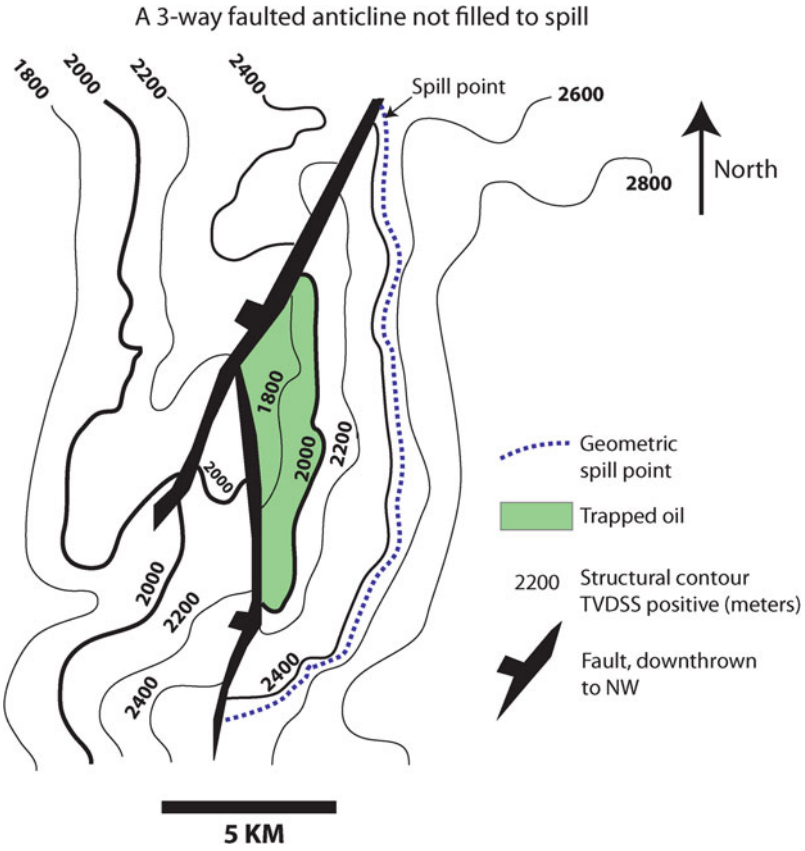

Fig. 2.3 A structure not filled to spill. The cause may be insufficient charge from migrating oil or fault seal capacity, in this case limited to 20 m to oil on one or both of the faults

However, the accumulation is filled only to 200 m. In this case, if there is adequate charge along a migration pathway, the only explanation for the trap not being filled to spill is either top seal or fault seal leakage. With only a 200 m column, the seal capacity on the weakest seal (whatever that is) must be 200 m to the fluid-water system encountered.

Some excellent seals can be in thin layers and the thickness of the seal is not important unless there are faults present which might offset the seal. Hence, thicker seals are desirable in faulted terrain, but thin seals can be highly effective. As an example (Fig. 2.4), shows outstanding seals in Miocene and Cretaceous shales. One industry 'paradigm' I was taught early in my career is that basal sandstones on unconformities are migration pathways, and cannot form seals. Shabandag Field in Azerbaijan is one of thousands of exceptions to that 'rule', with transgressive shoreline facies sealed by sub-cropping Miocene shales and top and lateral seals within the individual shoreline reservoirs layers. Column heights are substantial. In some

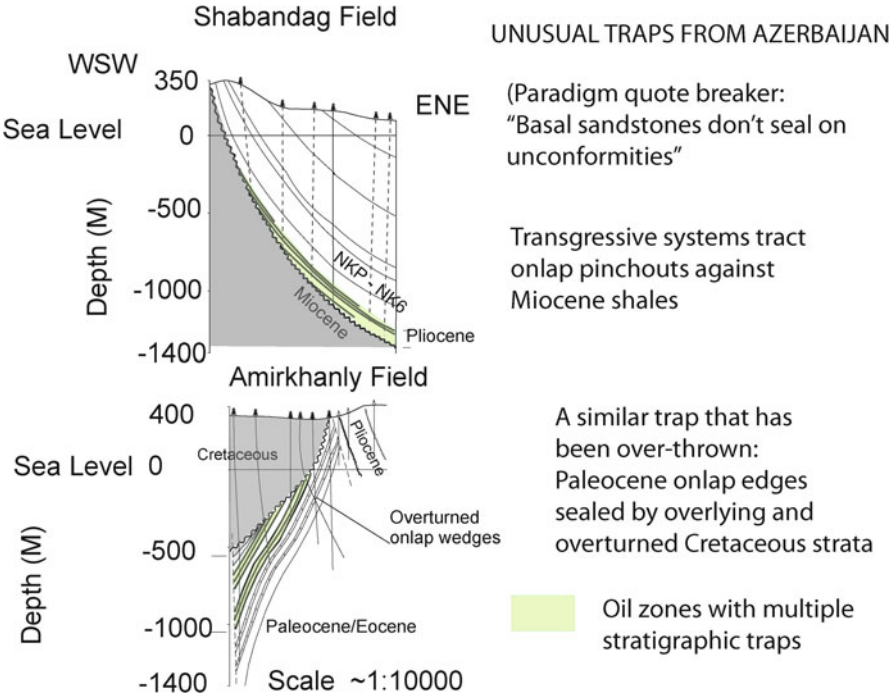

Fig. 2.4 Unusually effective shale seals holding long columns of oil in steep and complex structural settings. Original figures courtesy of Akif Narimanov, SOCAR Company, Baku, Azerbaijan

cases (Amirkhanly Field, Fig. 2.4), the onlap traps have even been overturned and still hold a substantial column.

Even subtle diagenetic changes can set up significant seals. Along subaerial unconformities for example, paleosols can completely occlude porosity systems and set up substantial traps. Several examples in the Lower Cretaceous Muddy Formation of Wyoming have been documented by Martinsen et al. (1994).

Another key point to remember is that for any given rock type, the seal capacity changes with the type of fluid. This is because gas is much lighter than oil and thus more buoyant in the sub-surface. Buoyancy pressure builds up as a trap fills, with the top of the trap having the highest buoyancy pressure. In contrast, at the base of the trap, or (FWL), the buoyancy pressure is zero. The higher the buoyancy pressure, the more likely it is to cause seal failure.

Conceptually, this is like floating in a pool. If you want to sink, you exhale air and reduce your body density until you drop to a point that you can no longer go down. In an oil or gas field, that point of equilibrium is the free water level. If you add weights to become denser, you sink even further. So at the crest of a trap with 500 m of closure, a gas field may actually have so much buoyancy pressure that it breaks the weakest seal at a 300 m column height. That trap, even if it has 500 m of geometric closure, will never accumulate more than 300 m of hydrocarbons. However, in a heavy oil fluid-water sys-

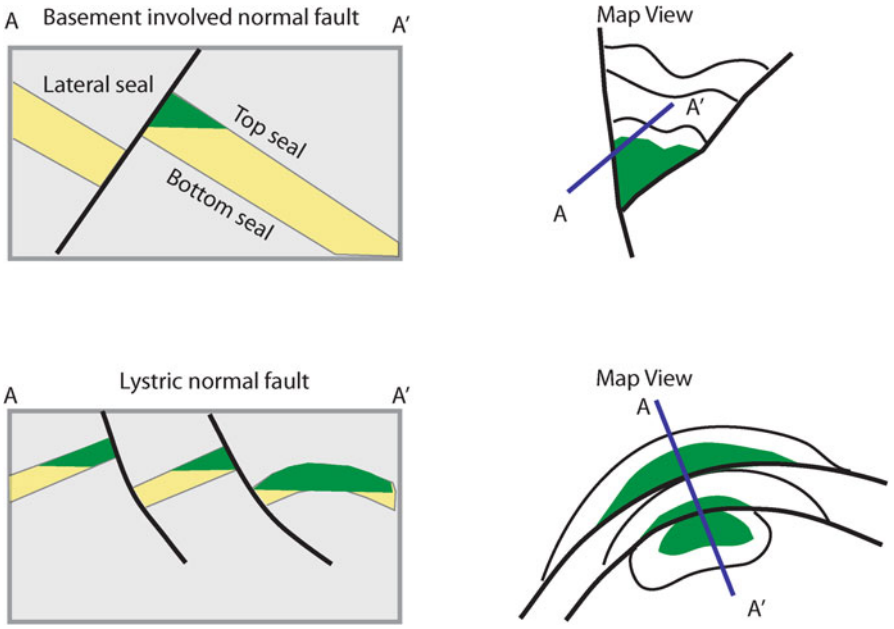

Fig. 2.5 Typical fault traps. As in stratigraphic traps, multiple seals are needed to trap hydrocarbons. Trap A requires a total of 4–6 seals and only one seal failure will mean no trap at all. Modified from Biddle and Weilchowsky (1994). Reprinted by permission of the AAPG, whose further permission is required for further use

tem in the same trap, where buoyancy pressure is less due to density differences of the hydrocarbons and water, the trap could easily be filled to geometric spill point.

Faulted anticlines and fault traps (Fig. 2.5) are another fairly easy trap type to identify, but carry additional risk beyond a four-way closure. Where four-way closures only require an effective top seal, fault and all other traps require multiple seals. Fault traps are attractive as, like four-way closures, many stacked pays can be built up on both sides of the fault, creating large accumulations with multiple hydrocarbon columns and oil or gas-water contacts. Fault seal failure is common, however, either by faults leaking directly through open fractures or from juxtaposition of reservoir against reservoir across the fault, leading to leakage.

Combination traps refer to structures where the stratigraphic overprint is strong, perhaps even dominant, like a facies change occurring over a plunging nose or channel draped over a structural saddle.

Stratigraphic traps occur where reservoir facies pinch out laterally updip into seals. These traps form in a wide variety of depositional settings (Dolson et al. 1999). Figure 2.6 illustrates common primary depositional geometries that can set up regional traps in passive margin continental settings.

As in fault traps, multiple seals are required, but unlike fault traps, there are seldom ‘stacked pays’ or multiple combinations of seal and reservoir yielding large aggregate reserves. Most stratigraphic traps involve a single reservoir layer, and are thus not as attractive as fault and four-way closures. Stratigraphic traps, while sta-

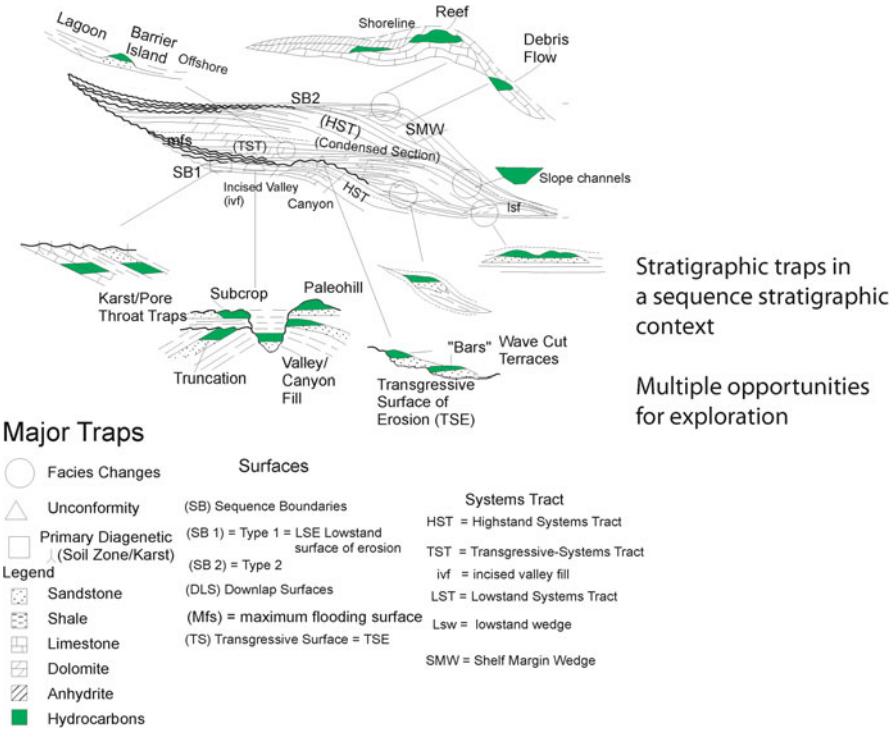

Fig. 2.6 Common depositional systems that form stratigraphic traps. Modified form Dolson et al. (1999). Reprinted by permission of the AAPG, whose further permission is required for further use

tistically containing fewer giant fields, are perhaps the most common trap type globally, and occur in virtually every hydrocarbon province.

Figure 2.7 shows a typical stratigraphic trap caused by erosion beneath a regional unconformity. A paleo-hill is flanked to the northeast and south by erosional lows noted by an isopach thick of the Opeche Shale. These thick trends are part of paleo-river systems, likely desert valleys, which were filled largely with red shales during later transgressions, forming fairly good seals. Ultimately, the Opeche Shale buried the reservoir interval completely, forming both top and lateral seals. The sandstone reservoir interval, once part of a desert dune field, is underlain by a tight dolomite, which forms another seal. Later structural tilting and oil migration trapped oil stratigraphically as the proper seal geometries were set up. As in all stratigraphic traps, all three of these seals need to work together to preserve and trap the oil.

Giant stratigraphic traps (fields defined as > 100 million barrels recoverable) are possible, often in large angular unconformity traps like Prudhoe Bay (Specht et al. 1987) or East Texas Field (Wescott 1994), but giant stratigraphic trap fields have been found in virtually every type of depositional system. In some cases, stratigraphic traps are not even recognized until structures are drilled up and anomalous oil or gas shows and production occurring below closure levels persist, telling the interpreter that 'all is not what it seems to be'.

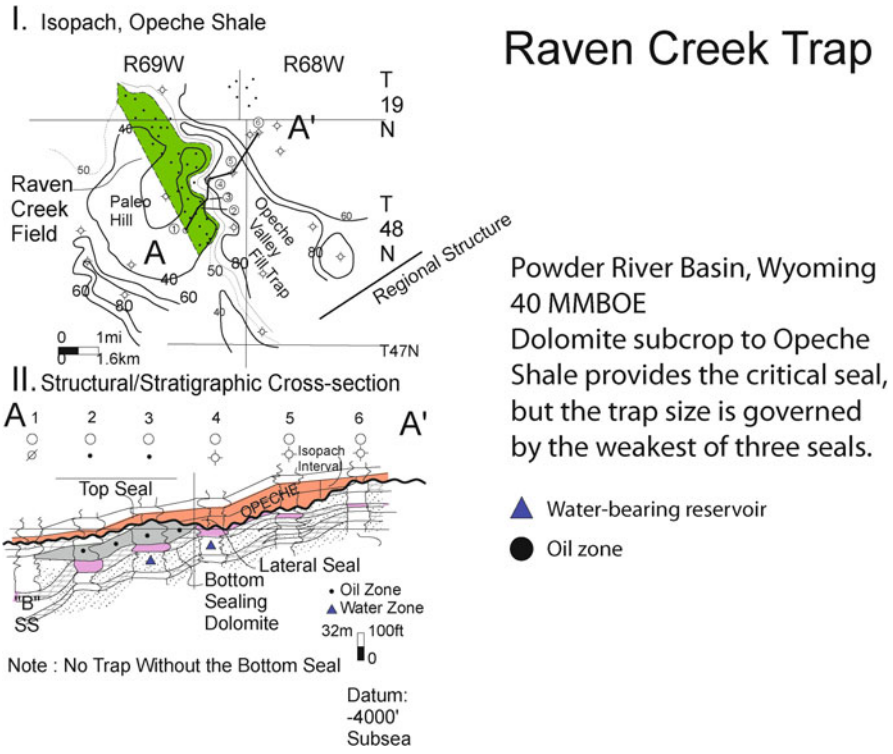

Fig. 2.7 A typical stratigraphic trap. As in faults, top, lateral and bottom seals must be present. The column height is controlled by the trap geometry as well as the sealing capacity of the weakest seal. From Dolson et al. (1999). Reprinted by permission of the AAPG, whose further permission is required for further use

Variations on stratigraphic traps are diagenetically modified traps or fluidic traps (Fig. 2.8).

Diagenetic traps form where cements alter pore networks and set up internal seals which are often difficult to detect without quantifying shows and seals in the system from logs, cores, pressures or other data. These kinds of traps are plentiful and can be prolific, reinforcing the concept that not all seals are in shales, salt or other obvious lithologies. Many seals are simply a change in pore-throat geometry. An example is shown in Fig. 2.9, where anhydrite cements plug an otherwise porous dolomite, forming a lateral seal.

Fluidic and hydrodynamics traps are also common (Vincelette et al. 1999), and frequently go unrecognized. Fluidic traps are caused by changes in fluid density or excess pressure. Many fields have commercial light oil preserved down dip of tar mats at the surface, where the fluid change itself sets up part of the seal to the lighter hydrocarbons. Hydrodynamic traps occur where water flow is present, both in the shallow and deep basins, and the pressure differential, or head, pushes the oil and gas into flank positions on the trap (Fig. 2.10). This topic is covered in detail in Chap. 4.

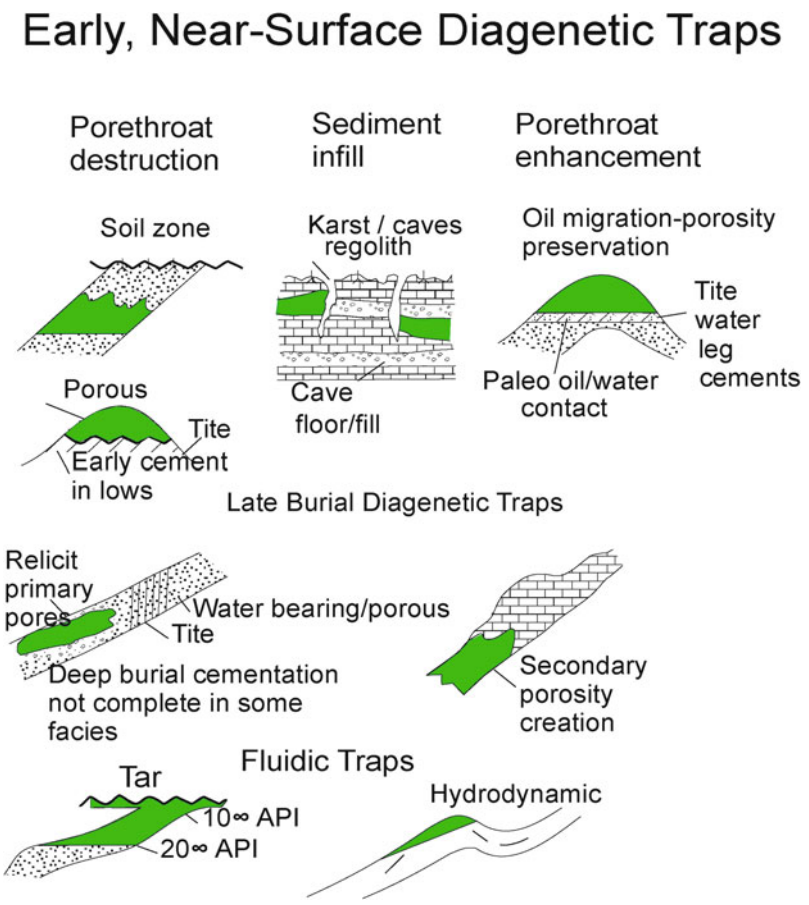

Fig. 2.8 Diagenetic traps. From Dolson et al. (1999). Reprinted by permission of the AAPG, whose further permission is required for further use

These traps are often overlooked, especially in over-pressured basins. Many traps may remain to be found where structures have been tested at the crest to find only short columns when the real 'prize' is off the flank due to hydrodynamic tilting.

2.2.1 You Don't Need to Know Why a Trap Exists If You Can Figure Out Where It Is from the Test and Show Data

Some traps are difficult to define and only found through a careful examination of oil and gas shows. A good example are 'basin centered' gas accumulations, which occur in traps downdip of water bearing zones in areas of no obvious structural or stratigraphic closure. A good example is the giant Wattenberg Field in Colorado (Fig. 2.11).

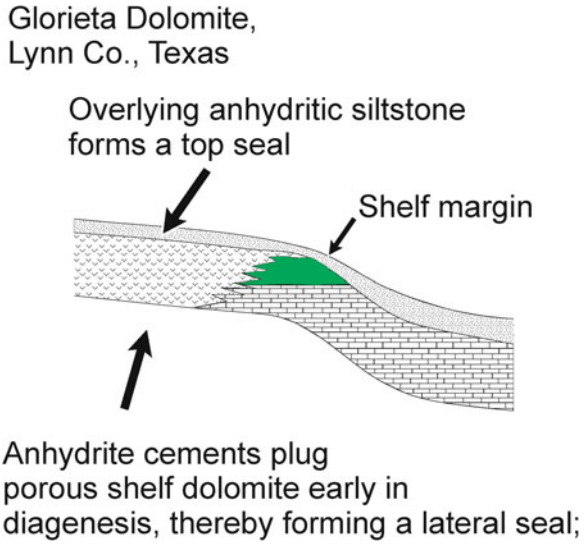

Fig. 2.9 A diagenetically modified dolomite lateral seal caused by anhydritic cements. Carbonate seals, in particular, can be complex, requiring careful analysis of test and show data to identify seals not obvious from well log alone. From Dolson et al. (1999). Reprinted by the permission of AAPG, whose further permission is required for further use

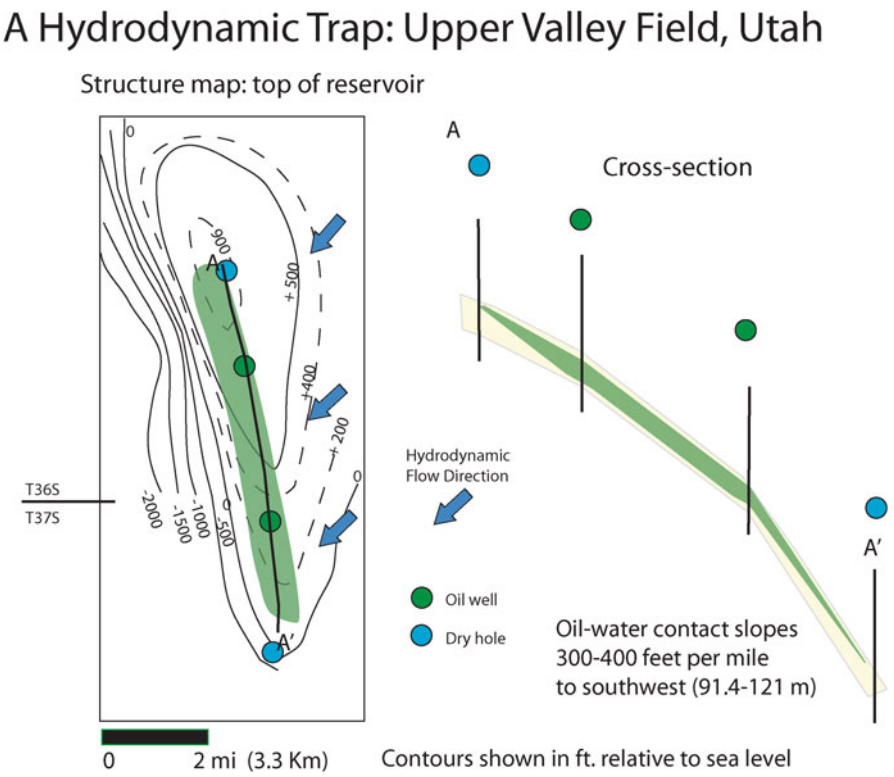

Fig. 2.10 A hydrodynamic trap. Modified from Vincelette et al. (1999)

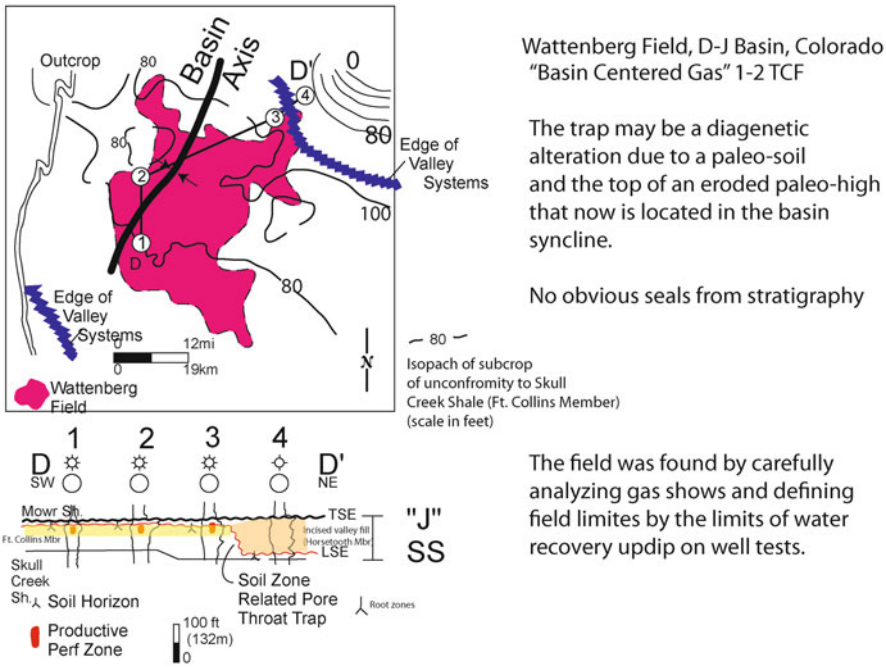

Fig. 2.11 A 'basin centered' gas accumulation found from careful show analysis. No obvious trap could be recognized from stratigraphic or structural data alone. The trap may be related to paleosol development at the top of a 'buried hill' flanked by porous and permeable incised valley networks, but sealed by diagenetic pore-throat plugging along the unconformity surface. TSE refers to a 'transgressive surface of erosion' and LSE to a 'lowstand surface of erosion. Modified from Weimer et al. (1986)

The field was discovered in 1970 by R. A. "Pete" Matuszczak, a geologist with Amoco Production Company who noticed that over a dozen wells in the bottom of the Denver Basin had indications of moveable gas from tests, mud-logs or shows in low porosity Lower Cretaceous sandstones. He made a map of fluid recoveries from wells around the area and noticed that the amount of water recovered on dry holes steadily decreased toward the basin center. Without understanding the cause (which is still under debate), he drew a line on the map where he saw no evidence of moveable water, only tight sandstones with gas saturations. He speculated that perhaps hydraulic fracturing could be used to make these wells economic and proposed to management that a giant gas field lay almost under the Denver office with a market access to one million people along the Front Range of Colorado. Initially, management was more than a little skeptical as he couldn't explain the trap or how fortuitous it might be to have the building sitting on top of a giant field others had drilled through and walked away from. As a result, he was continually denied funds to test his idea. Eventually, he wore management down, got his permission to drill a well and 'the rest is history', with the discovery well proving his concept. The field continues to produce 40 years later. This is a superb example of why understanding oil and gas shows is an important part of looking for oil where others have missed it.

2.3 Assessing Risk: Thinking About Seals, Structure and Reservoir Quality

In all exploratory prospects, quantitative assessment of the seal is essential. In traps where there is no limit to charge from migrating hydrocarbons, the column height will be determined by the weakest seal. There is no exception to this rule. Significantly higher risks are encountered when dealing with multiple seals. Consider the case shown below in Fig. 2.12.

Pre-drill, the four-way structural trap prospect has been given a 70 % probability of the top seal working. Well offset information shows good reservoir and charged structures eliminating risk of any other factors. In this case, the pre-drill four-way prospect has a 70 % chance of success. In a stratigraphic paleo aeolian dune trap, in contrast, the trap needs a top, lateral and bottom seal to work. Even if charge and reservoir are certain, substantially more risk is present. An isopach or structure map of the overlying top seal may show closure of the top of the buried hill, but if the

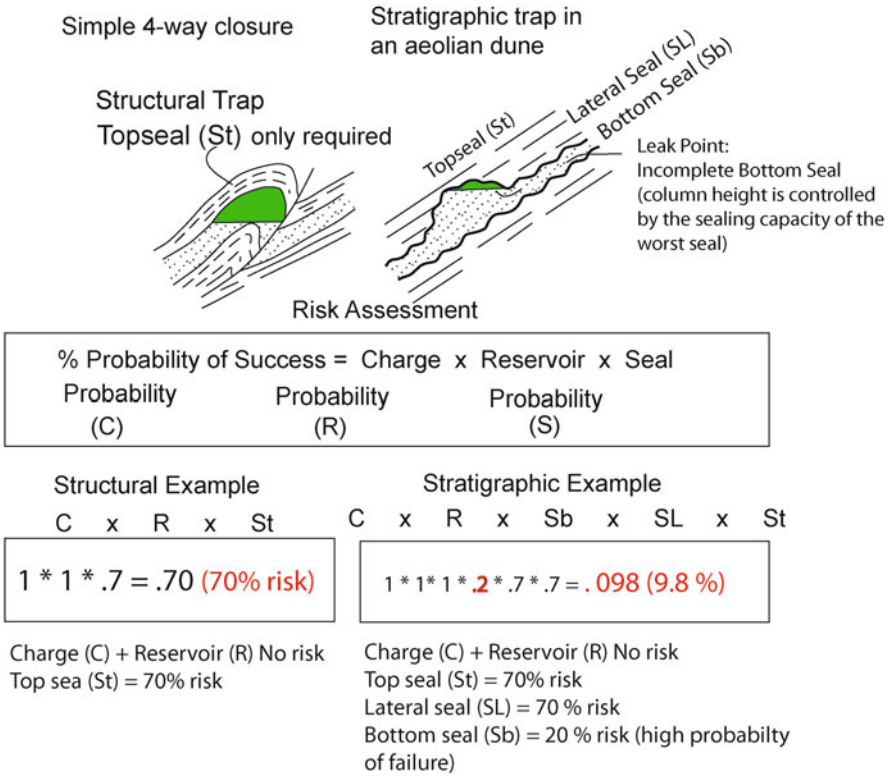

Fig. 2.12 Trap size controlled by weakest seal and effect on pre-drill risk of prospect size using seal evaluation. From Dolson et al. (1999). Reprinted by the permission of the AAPG, whose further permission is required for further use

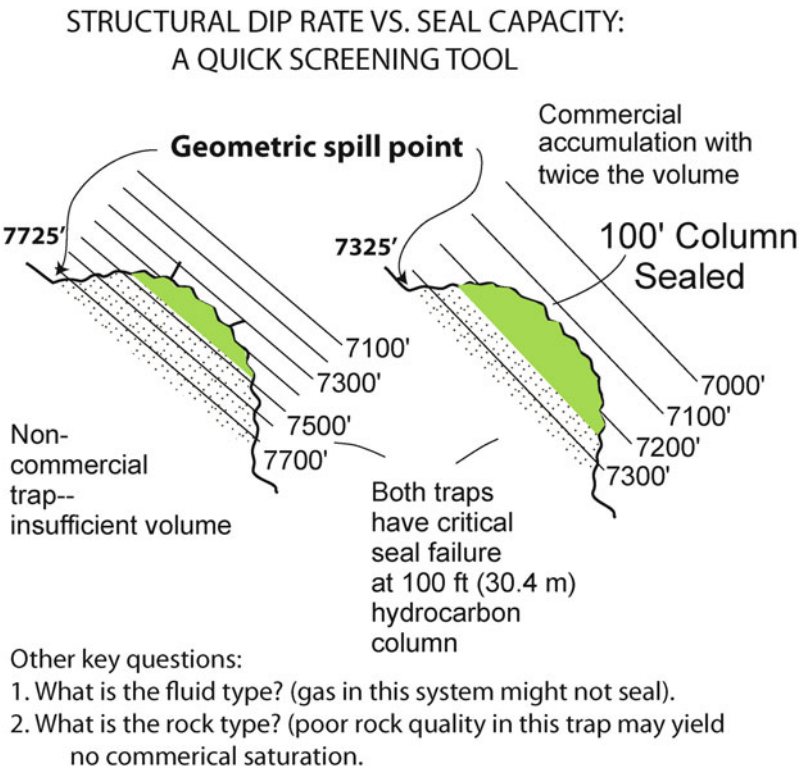

Fig. 2.13 Screening tools and things to think about. Structural dip rate vs. seal capacity of the weakest seal. This trap example is not 'filled to spill' but, rather, 'filled to seal capacity of the weakest seal'. Reprinted by the permission of the AAPG, whose further permission is required for further use

bottom seal has only a 20 % probability of success and top and lateral seals 70 % probability of success, the prospect will have only a 10 % probability of working. So, having a 'closure' at only one seal level is not enough.

Fault seals work the same way. Countless dry structures have been drilled on three-way fault closures where the fault juxtaposition failed to place a seal across the fault or within the fault zone and the subsequent wells were dry. Pre-drill assessment of fault or stratigraphic seal capacity and risks are essential to adequately evaluate a prospect pre-drill.

In addition, the structural relief within closure must be looked at early to assess how good seals must be to hold the accumulation. In Chaps. 4 and 5, this is addressed in more detail, but thinking about structural relief and fluid type is key to pre-drill assessment. A simple screening criteria is simply a qualitative understanding of the column height vs. trap geometry. In the example of Fig. 2.13, a stratigraphic re-entrant trap typical in a meandering fluvial channel is shown against two different regional structural dip rates. Even though the geometry of the trap is the same, the

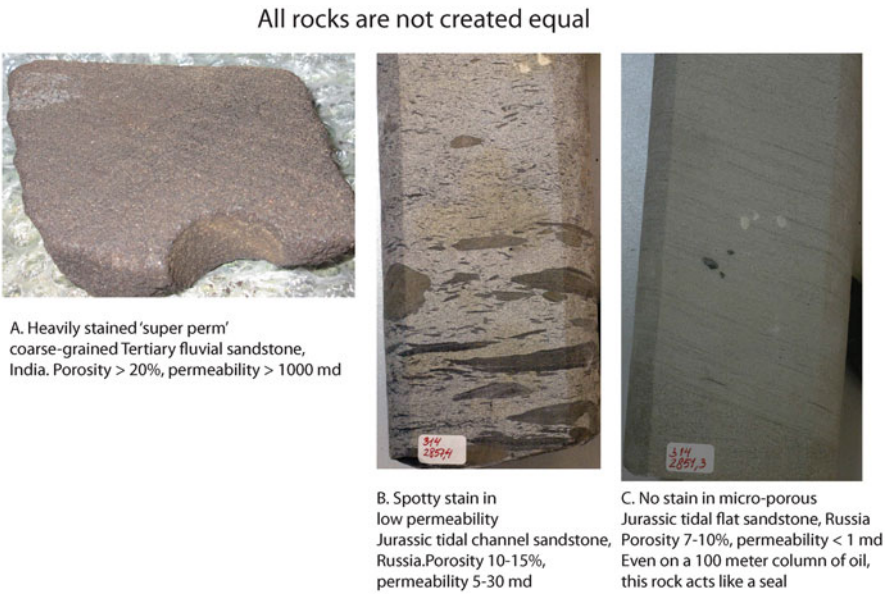

Fig. 2.14 Some rocks require significant column heights and buoyancy pressure to fill with commercial hydrocarbons. The sandstone shown in (**a**) is the highest quality reservoir and heavily stained. Only spotty stain is recorded in much tighter rock (**b**) and virtually no stain in the microporous rock (**c**)

structural spills differ due to the structural dip rate. Neither trap is filled to geometric spill due to seal limitations of 100′ capacity on the weakest seal. However, the lower structural dip rate case will have a lot more oil trapped because if covers a larger area.

Another key question is fluid type. A seal that can hold a 100 ft (32.8 m) gas column might easily be capable of holding a 500 ft (152 m) oil column. The traps shown in Fig. 2.13, if they had a 100′ (32 m) seal capacity for gas, might hold 500′ (152 m) or more of column if oil. In a more dense fluid like heavy oil, they would be filled to spill point. Fluid density differences play a big role in seal capacity and gas, with its lighter density, is harder to seal than oil. The mechanics of this are detailed more in Chap. 5 and in the next section. In gas plays in particular, there are wide ranges of potential densities and seal capacity for each type of hydrocarbon-water system can change accordingly (see Table 2.2 for density variations by fluid phase).

When evaluating traps, the geometric spill point should initially be treated as the maximum possible trap size. Minimum trap size might be determined by your best guess at seal capacity on the weakest seal. When presenting a prospect, you need to show both scenarios so your funders or managers understand what kind of risk they are facing. Your economic analysis will be based on both 'risked and un-risked' volumes, so the 'upside' is clear but so are the risks. In most cases, the economic decisions will be made on a portfolio basis of prospects or the significance of the wells as a potential play opener. Risked volumes pre-drill will play a big role in that decision making.

Complicating this further, a commercial trap may not be possible in a 100 m column trap, if the rock properties aren't right in the reservoir. Reservoir quality can vary substantially by rock type and also vary rapidly laterally and vertically within a trap. An example of variable reservoir quality and saturation are is shown in Fig. 2.14. Oil stain in these rocks are substantially different, reflecting in part how difficult it is to get oil into the pore spaces. Figure 2.14a is a heavily stained channel sandstone with outstanding porosity and permeability. This rock is fully saturated with oil. In contrast, the other two rocks are considerably poorer reservoirs. The fine-grained sandstone in Fig. 2.14c has virtually no oil in it, despite being inside a substantial trap. It simply is too tight to contain hydrocarbons for the amount of closure and oil-water system the trap is in.

Chapter 5 covers quantifying rock properties in detail and ways to assess oil and gas saturation vs. column height. A trap with a 50 m column may be commercial in a good reservoir, but uneconomic or even unable to produce any oil or gas at all if it is a poor reservoir.

In this case, a trap with 50 m of closure may look like a great prospect, but will fail if the reservoir is poor quality. Many small traps have been drilled which fail economically for this reason alone.

Surprisingly, this is where the opportunity lies in dry hole post-appraisal for many explorers. Companies frequently abandon a disappointing well without the proper post-appraisal as to the implications for other prospects. For example, a 50 m trap closure might be targeting a fluvial channel sandstone. When it is drilled, the well tests only the tight, poor quality levee deposits adjacent the channel. Some oil and gas saturations are found, but not enough and the well is abandoned. Years later, another geoscientist thinks about that dry hole differently. The presence of oil means a trap and that means a column of oil. He decides that if he can find a better reservoir within that trap and column, he can find commercial oil. The geoscientist recommends a 3D seismic survey and the seismic imaging reveals the elusive and highly permeable channel sandstone. A subsequent well is drilled next to the old dry hole and flows commercial oil. This is not an uncommon occurrence, but rather, a good result that can come from carefully thinking through oil shows and saturations in old dry holes.

2.3.1 Making the Right Maps

It is one thing to understand rock properties and saturations, but quite another to make the right map. Consider the dilemma of stratigraphic and hydrodynamic traps. Without the right map, they aren't even apparent! These maps are more difficult and time-consuming to make than structure maps. The easiest thing to do with seismic and well logs is to make a simple structure map. While proper fault geometries are difficult to get right until you have 3D seismic, you can do pretty good work with faults on 2D seismic if you are careful to quality control your map with basic contour balancing rules (Tearpock and Bischke 2003). However, if you stop at the structure map, you will be limited in the number of prospects you can find.

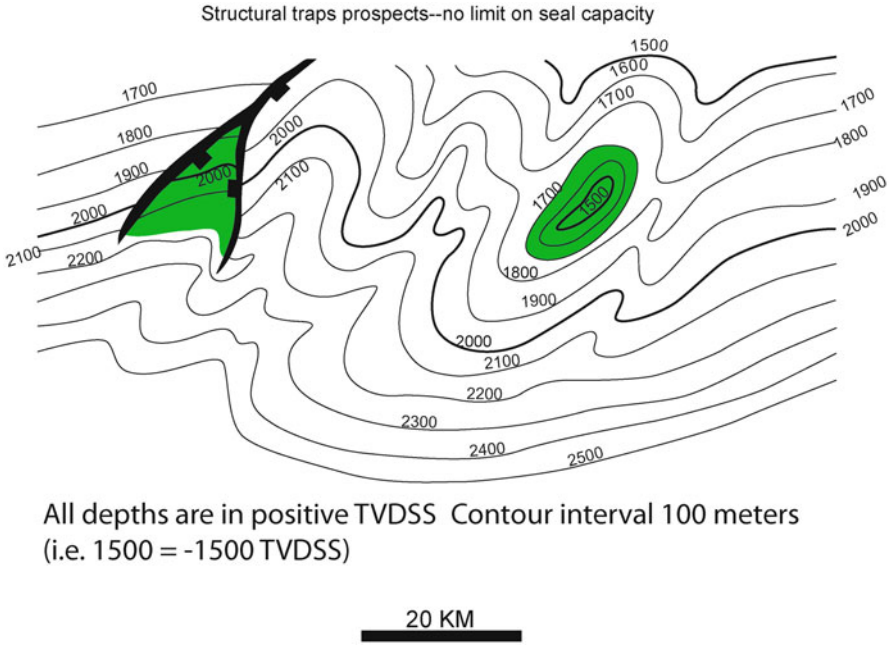

Fig. 2.15 Structure map on a top-seal with prospects filled to spill

For argument's sake, for example, let's assume you have a perfect structure map with faults (Fig. 2.15). Assuming unlimited seal capacity and traps filled to geometric spill point, two basic prospects show up (1) a four-way closure (2) a downthrown fault trap.

These two prospects will be relatively easy to obtain funding for if you only make this map and do not take into consideration where the reservoirs and seals are.

In Fig. 2.16, a facies map constrained by seismic and wells is overlain on the same structural map. The map helps you visualize this depositional system and begin to quantify seals. This map, however, may also have errors, but it is the best you can do with the data you have. So assume it is right. A red shale and anhydrite supratidal shoreline is updip of, and inter-fingers with, a porous limestone facies downdip. Your view of the area now changes. The structural four-way will be a dry hole with no reservoir. If the fault trap is drilled too far updip, it will not find reservoir and will be a dry hole. If the seal capacity is unlimited on the top and lateral seals, a giant stratigraphic trap can occur downdip of the four-way closure, with the trap filled to geometric spill point. The contour at 2200 m marks the free water level and spill point. The column height is from 1800 m at the highest point on the trap to 2200 m at the base, or 400 m.

In this simplified scenario, if there are no complex reservoir changes or faults to disrupt fluid continuity, the trap at one end will have the same production response with time as the trap at the other end. This is actually unusual in nature, but pressure

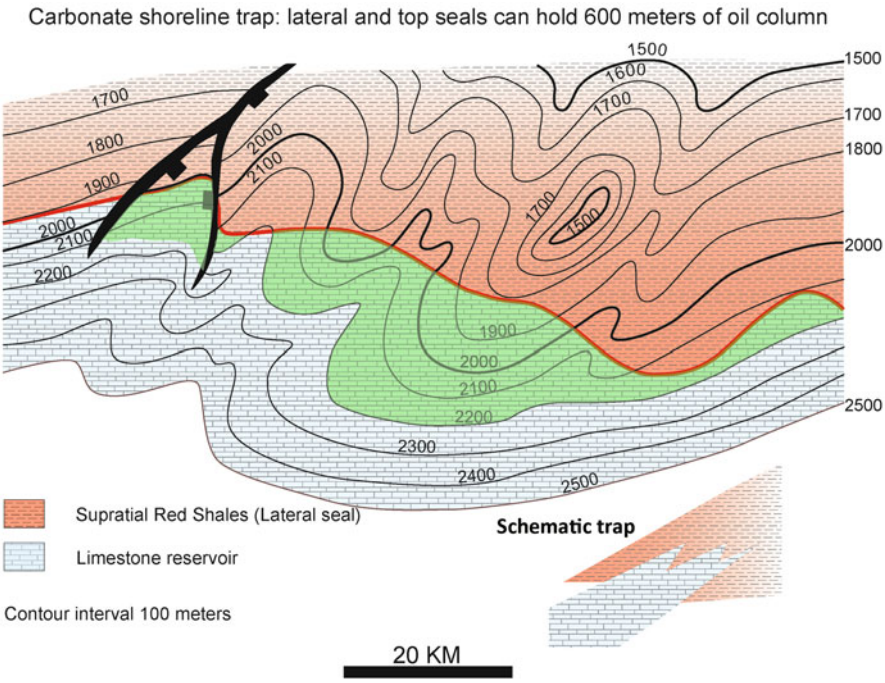

Fig. 2.16 Carbonate shoreline trap map filled to spill

across that broad area would draw down evenly as the field is produced, and the base of the trap, or 'free water level' would be the same across that broad area.

This scenario of large stratigraphic traps downdip of dry structures has been proven over and over globally. To find these fields you often have to understand your dry holes and have outstanding facies maps built from both seismic, core and well logs. Before the advent of high quality 3D seismic, such traps were found by innovative mapping of the updip seal geometries to match to the oil and gas recoveries or shows in dry holes. It is an art, and remains so today, but with better tools to refine that geometry. In some cases, fields like this were found downdip of dry holes which had penetrated tight rocks with oil or gas shows that were near the top of the trap in uneconomic reservoirs called 'waste zones' (Schowalter and Hess 1982). Drilling downdip into the better reservoirs was the key.

Some of the best examples are in Permian carbonates of West Texas (Ward et al. 1986). The Permian Slaughter-Levelland Field, for example, took over 40 years to be recognized for its true size. Wells in poor reservoir in the updip 'waste zone' of the trap had small recoveries of oil and had been off-set updip for years into every increasingly poor reservoir. The real prize lay downdip in porous dolomites that had commercial saturations. Initially, the trap was thought to be made of separate pools of oil, one named the Slaughter Field and the other the Levelland Field. Over time, these and other separate pools were proven to be part of a multi-billion barrel giant

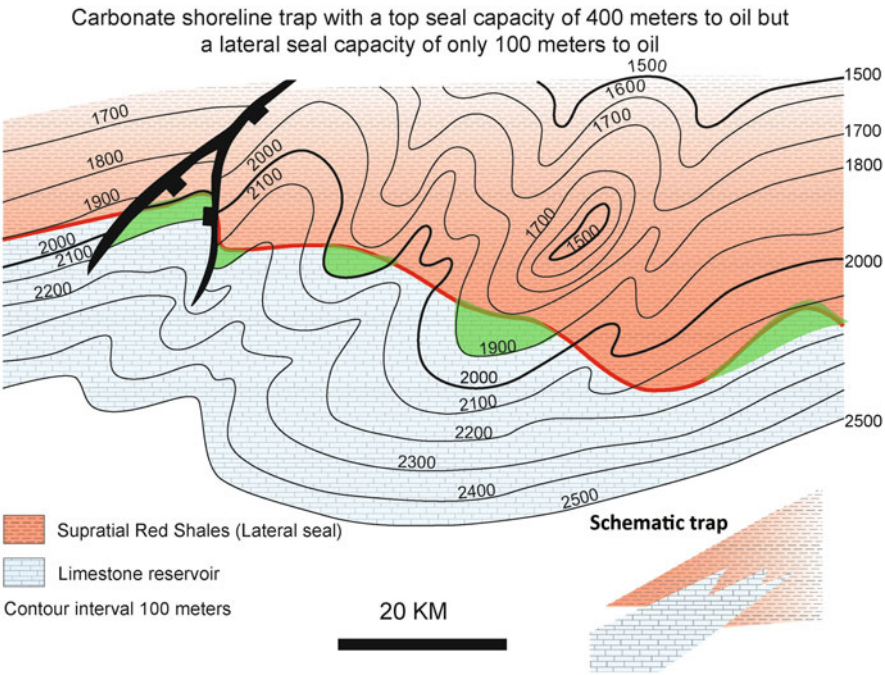

Fig. 2.17 Same trap geometry as Fig. 2.16, but with the weakest seal capable of holding only 100 m of oil. This trap is filled only to seal capacity, not geometric spill points

field complex. Recognizing the trap from simple well log correlations was not enough.

Now, consider the case where the same structural geometry exists but introduce a leaky seal in the shoreline facies and limit the seal capacity to 100 m to oil (Fig. 2.17).

In this case, the trap consists of 4–5 separate pools, each of which would be under a different pressure regime and different 'free water' levels and oil/water contacts. Spill point will be 100 m from the top of any trap geometry set up by the regional seal. All of these pools would be easy to miss! Just as importantly, none of the wells in these pools would be in pressure continuity with one another. They would all act as separate traps, which they are.

2.3.2 Some Thoughts on Stratigraphic Traps

In 1989, I participated in a study at Amoco Production Company in subtle or stratigraphic trap exploration. We had recognized that a number of giant stratigraphic traps had been found by much smaller companies in the Rocky Mountains and Mid-continent. Amoco staff had never recognized the potential, and we were asked to assess our technical strategies and determine why we had missed these and other opportunities.

Looking at over 300 stratigraphic traps world-wide, we found that only about 10 % of the stratigraphic traps were 'giants'—traps which contained over 100 million barrels of oil. Four major reasons for this are (1) single story pay zones (2) high probability of seal failure from the weakest seal (3) seal geometries which made for small closures (4) poor reservoir quality on small traps that made for poor accumulations. I believe the single story pay and seal failures, however, are the dominant reason for the large number of smaller pools vs. good anticlinal, fault and salt-related traps.

In the last decade, a number of giant stratigraphic traps have been found, usually by smaller companies with highly experienced staff, simply by building the proper facies maps, understanding oil and gas shows and deliberately looking for them. Many are in deep water turbidite fan and channel facies. Just two examples are the Jubilee Field in offshore Ghana, West Africa (Jewell 2011) and the Buzzard Field in the North Sea (Editors 2005; Ray et al. 2010).

Another spectacular example of using dry hole information to prove a working petroleum system and then focus on the reservoirs and combination traps was the recent opening of oil discoveries in the Falkland Islands (Richards 2012; Saucier 2014). Interestingly, Shell had drilled a number of dry holes which proved a working petroleum system, but not viable reservoir. After dropping the acreage, the smaller company came in and found the reservoirs and the combination and stratigraphic traps that made the blocks commercial. All of these newer discoveries were found using 3D seismic, which, under the right circumstances, can image the reservoir and seals much more accurately than can be envisioned from 2D seismic or well control alone. As a result, these plays are finally increasingly easy to make.

Another key statistic was that the average time to recognize a giant stratigraphic trap in a mature basin province was up to 11 years! I suspect that number is lower now, with 3D seismic, but perhaps not in some basins where the coverage is still dominantly 2D seismic. But in older wells or mature basins, where 3D was not used in the exploration process, many stratigraphic traps were actually drilled through and plugged without recognizing the significance of the oil and gas shows, perhaps because only tight reservoirs with shows were found.

Good facies and stratigraphic trap maps take time to make but are important, if for no other reason than many stratigraphic traps develop on the flanks of structural closures or plunging anticlinal noses. The crests of these features will almost always be targeted first, and may thus miss the reservoir. This is common because many of these structures, during deposition of the reservoirs facies, are already structurally high and facies belts like incised valleys and non-marine and deep water channel systems deflect around the paleo-highs during deposition, setting up flank traps. Good examples from Russia are documented in West Siberia Jurassic reservoirs (Dolson et al. 2014). Thus, many early wells penetrate the structural crest of a feature only to find sealing facies or waste zone wells (like overbank siltstones and crevasse splays in non-marine channel siltstones). Tight reservoirs with oil shows may well mean a trap has been discovered, sometimes with a substantial column, but the well may be abandoned as dry since the reservoir might not produce any

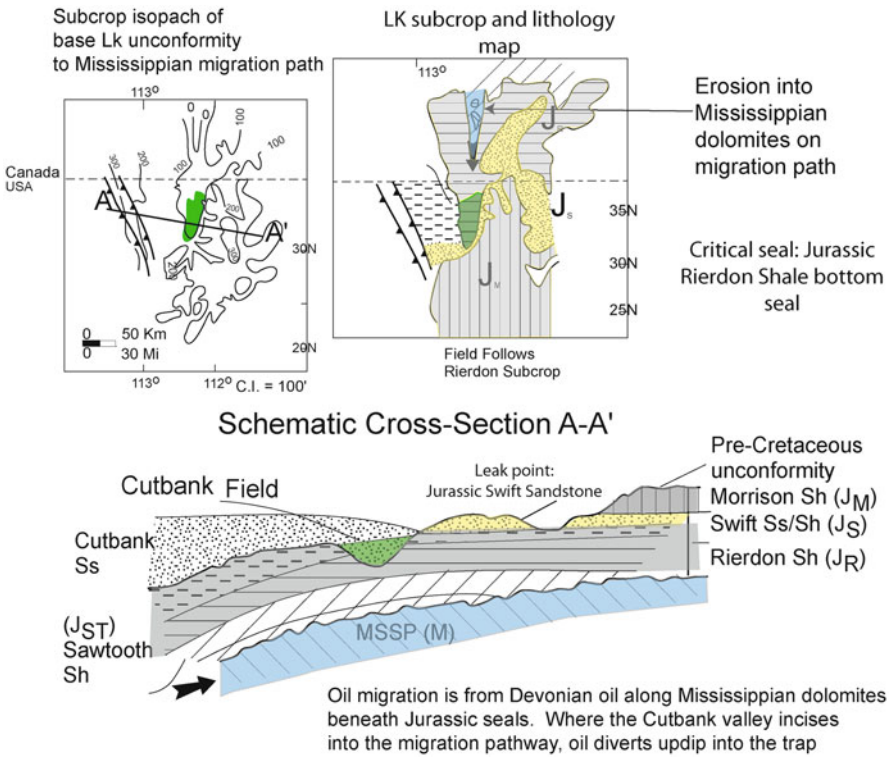

Fig. 2.18 Cutbank Field, Montana. Summarized from Dolson et al. (1993). Migration pathways from Devonian to Mississippian and into the Lower Cretaceous sandstones were unraveled with oil and gas shows mapping and geochemical ties of oils to source rock

commercial oil, or flow an oil at all. Many of these old dry holes are not offset for years, and may actually be one location away from a prolific well with a different reservoir facies within the trap.

Another good example of a stratigraphic trap is the giant Cutbank Field of Montana (Dolson et al. 1993; Dolson and Piombino 1994). This trap is an incised valley fill trap located on the flank of a large structural dome but out of structural closure (Fig. 2.18). Oil and gas show data, plus subsurface geochemical signatures of Lower Cretaceous oil typed to a Devonian source rock, illustrate complex vertical and lateral migration from source to trap. The field, discovered by accident in the 1920s with cable tool rigs drilling down-dip of a structural closure, might have easily been missed today, as a quick look at the area would show good reservoir, but no viable thermally mature or rich source rock anywhere near this location. Pools of this nature were found by 'chasing the oil and gas shows'. The oil is actually from a Devonian source rock which generated mature oil to the west and migrated vertically through thick Mississippian carbonates via fractures, then

traveled under a regional Jurassic unconformity until it reached a spot where the Lower Cretaceous unconformity beveled into that migration pathway. The oil then migrated south from Canada to the US in the porous valley-fill network of the Cutbank Sandstone. Details of how the migration pathways were determined at this field are covered in Chap. 8.

In many cases, the larger stratigraphic traps have been found because someone was paying attention to the production performance or oil shows in a few anomalous wells, where cumulative oil production was more than the structural spill would account for or the oil shows were much deeper than the structural closure. In these cases, the trap geometries themselves have to be rethought. Sometimes, it take years and attention to detail to recognize that the structural trap geometries alone do not explain where the oil is.

The reason for these oversights and a focus on structural traps are simple. Oil companies will always prefer to drill a fault or four-way closure of salt-wall trap before venturing to test the stratigraphic traps unless there are direct hydrocarbon indicators (DHI's) on the seismic which directly show where the fluids are in the trap. The attraction of multi-storied pay zones and multiple seals and reservoirs makes these targets much less risky.

In mature onshore basins, however, most or all of the structural anomalies have been tested and what is left are the more difficult stratigraphic, pore-throat, hydrodynamic and now, unconventional oil and gas shale traps. Getting the reservoir and seal geometries right requires careful and time-consuming work with 3D seismic, cores, cuttings and well logs, some of which is often not available. I have actually heard managers instruct staff not to look for stratigraphic traps as they require too many seals, are difficult to map and 'won't be part of our portfolio'. That is good news for the rest of us, who believe a lot more oil remains to be found in these kinds of traps. In all these cases, oil and gas show analysis is critical to find the overlooked accumulations.

By example, and to illustrate how subtle some of these traps can be, the two largest conventional traps in North America are the angular unconformity traps of East Texas Field and Prudhoe Bay Field (Alaska). On seismic, some of these traps are remarkably subtle. This five billion barrel East Texas Field is a truncation trap miles from mature source rock (Wescott 1994). Seals are set up by the top-seal of the Cretaceous Austin Chalk, and lateral seals where shales beneath the porous Woodbine Formation sandstones sub-crop the Austin Chalk on a very low relief angular unconformity. Figure 2.19 shows an old 2D seismic line once framed and hung on the wall of Amoco Production Company's President (1980–1981) as a reminder of how subtle some big stratigraphic traps can be.

East Texas Field was found by chance, drilled by an oil patch land promoter named Marion "Dad" Joiner. He and his partner, A. D. 'Doc' Lloyd, put together a fictitious prospect in Rusk County, Texas, based on non-existent "faults, folds and salt anticlines" and sold shares for $25 to raise money for wildcats. Professional geologists at Humble (now Exxon) dismissed the acreage as non-prospective due to no obvious structure. One critic even promised to "drink all the oil you find there"—

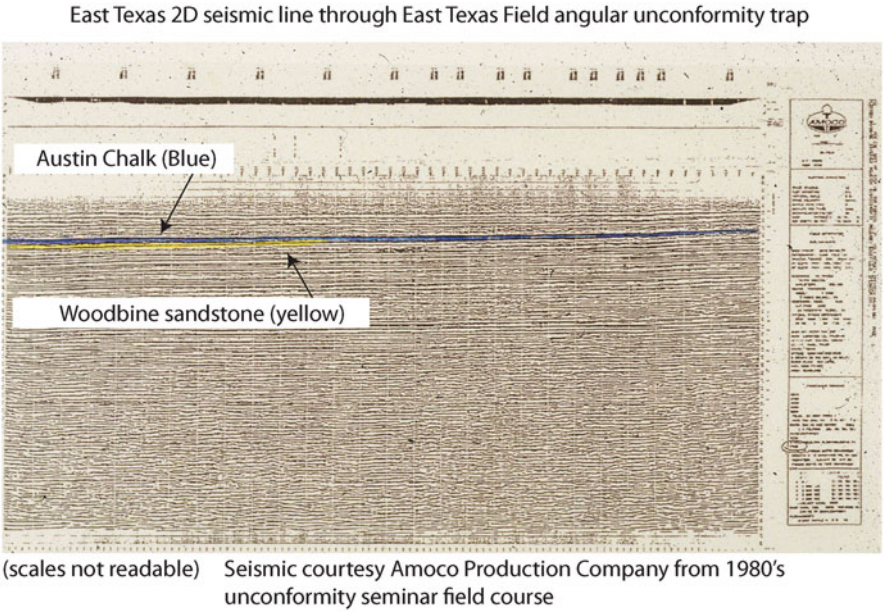

Fig. 2.19 Unpublished East Texas seismic. Date and quality of acquisition unknown. The angular unconformity trap truncation is shown in *yellow*, with the overlying Austin Chalk the top-seal and lateral seals shales sub-cropping the Woodbine Sandstone. Seismic courtesy of Amoco Production Company from unpublished 1987 Unconformity Field Seminar

something that is a very dangerous thing to do in this business, as noted earlier. By sheer luck, his third well, in 1930, found the largest oil deposit in the world for that time period.

Pre-drill, Prudhoe Bay, another angular unconformity trap, was considered high risk with a low probability of success. The trap was mapped as a small fault closure but turned out to be a giant unconformity trap. In both these fields, oil has migrated relatively long distance both vertically and laterally from the 'source kitchen' (Specht et al. 1987).

Lastly, diagenetic overprints can often obscure even the most seemingly obvious trap geometries (example in Fig. 2.20).

Post-accumulation cements may seal in a trap at the paleo-oil water contact and subsequent later structural tilting may make that trap very difficult to find. Many carbonate traps are notorious for diagenetic modifications which can make even the highest part of the trap non-commercial and part of the 'waste zone'. When these traps are drilled, the real prize might actually be down dip or somewhere along trend structurally where the facies improve. Often, even 3D seismic cannot image these subtle changes in rock type properly and the show information for the wells has to be used to understand the trap and prospectivity.

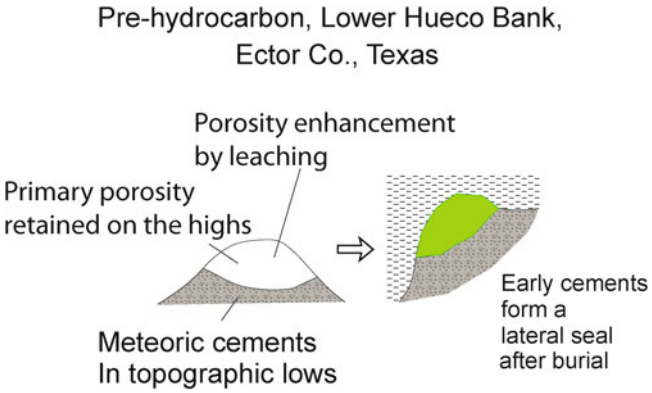

Fig. 2.20 Example of a diagenetically sealed trap where early cements sealed an accumulation which was later tilted structurally. (Figure courtesy of Rick Tobin)

2.4 The Basics of Rock Properties, Free Water Levels, Buoyancy Pressure and Hydrocarbon Shows

Understanding rock properties in relation to oil and gas shows is essential to interpret subsurface data. An excellent overview of reservoir quality and hydrocarbon saturations is covered by (Hartmann and Beaumont 1999) and in Chap. 5, this topic is covered in much more detail. However, it is important to have an early understanding of some basic rock petrophysics terms and ways to classify oil and gas shows, reservoirs and seals.

2.4.1 Porosity

Porosity (PHI) is the total amount of 'void' space between the grains that can hold oil, gas or water. It is expressed in percentage of total rock volume. Porosity systems in rocks are complex. Pores in rocks are connected to each other through narrow passes called 'pore throats'. The pore throat shapes are key to productivity and exert a dominant control on how much oil can enter a reservoir during trap filling.

The pore and pore-throat systems are commonly unevenly distributed. A thorough treatment of porosity types and pore networks is beyond the scope of this introduction and is well covered in other literature, particularly that of (Choquette and Pray 1970). The importance of understanding porosity type and pore geometries has been emphasized for years (Berg 1975; Gunter et al. 1997; Hartmann and Beaumont 1999; Pittman 1992; Schowalter 1979; Schowalter and Hess 1982; Swanson 1977, 1981).

The most common methods for estimating porosity (Fig. 2.21) are from analysis of cores, various well log tools, thin sections and scanning electron microscopy

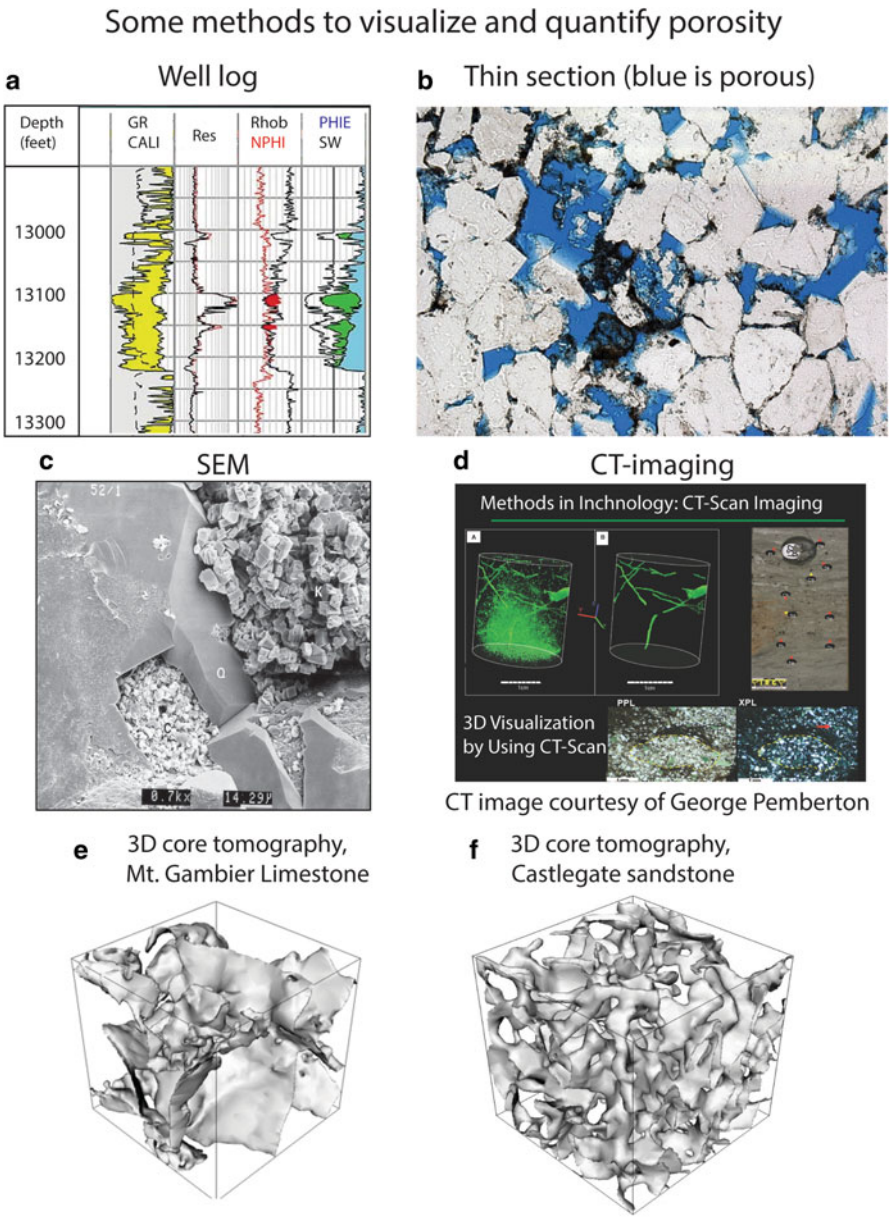

Fig. 2.21 Methods to image and measure porosity. Well logs (**a**) are the most common method, but thin sections (**b**) and scanning electron microscopy (SEM) (**c**) provide critical detail on clays and mineralogy. CT scans (**d**) and 3D core tomography (**e**, **f**) are increasingly used to visualize pore networks. Images (**e**, **f**) from Sheppard (2015), with permission from the Australian National University

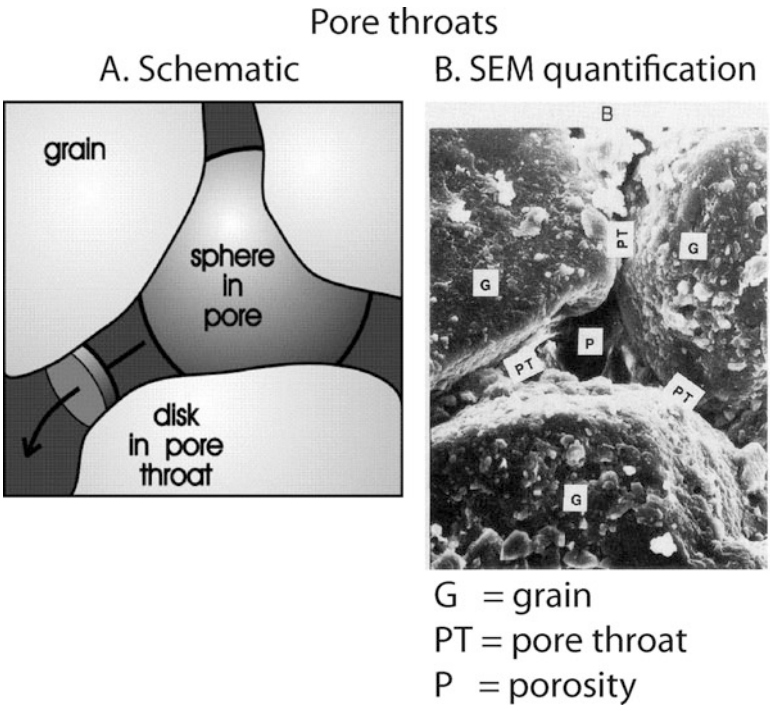

Fig. 2.22 Pore throats exert a strong control on water saturation and volume of oil in a trap at any position. Pore diagram from Coalson et al. (1994), courtesy of the RMAG

Table 2.1 Pore size classifications and implications (modified from Hartmann and Beaumont (1999)

Pore category	Size in microns (mu)	Comments
Nanno	<0.1	Excellent seals
Micro	0.1–0.5	Can be seals or poor reservoirs
Meso	0.5–2	Often transition zone saturations unless high on a trap or in gas reservoirs
Macro	2–10	High quality reservoirs
Mega	>10	High quality reservoirs

(SEM). More recently, tools such as CT scanning (Fig. 2.21d) and 3D core tomography (Fig. 2.21e and f) are providing much better visualization and quantification of how porosity systems differ in three dimensions.

As mentioned, however, the key thing to consider is not just the porosity system, but the geometry and size of the pore throats themselves.

The pore throat concept is critical to understand in order to quantify seal capacity, reservoir performance and hydrocarbon saturation (Fig. 2.22). Pore throat size is measure in microns, and there are basically five classes (Table 2.1).

Understanding the geometry of a pore network is fundamental to understanding oil and gas shows, predict new traps, identify migration pathways and understand potential production. Pore throat size and distribution exerts a strong control on how much oil and gas can enter a pore system during trap filling. The pore throats act like small capillary tubes (covered quantitatively in Chap. 5) initially filled (usually) with water that must be displaced by oil and gas during migration and trap filling.

Mega and macro pores offer almost no resistance to hydrocarbon entry. Micro pores, in contrast, require significant pressure to overcome resistive forces operating at the pore throats in order to displace water with hydrocarbons. This is done through increasing the buoyancy pressure higher and higher on the trap.

2.4.2 Buoyancy Pressure (Pb), Pressure vs. Depth Plots, Free Water Levels and Water Saturation

What is buoyancy pressure (Pb)? Because hydrocarbons are lighter than water, pressure builds up inside a trap due to hydrocarbon/water density differences. This pressure differential is called buoyancy pressure (Pb). Pressures are routinely collected at rigs with down-hole tools or estimated from the mud-weights required to control the well (Chaps. 3 and 4). These data can be analyzed in pressure vs. depth plots and the gradients and buoyancy pressures of the hydrocarbons measured directly as shown in Fig. 2.23. The slope of the lines defines the density of the fluids and the gap between the hydrocarbon densities and water defines the buoyancy pressure. The point where the Pb = 0 is the free water level, and marks the base of the trap and its spill point. Pressure-depth plots are the best way to determine the free water level in any trap, although the use of capillary pressure diagrams (Chap. 5) can give answers if the data is good enough.

On a pressure/depth plot (Fig. 2.23), the slope of the lines is in pounds per square inch (psi) vs. depth (feet). Water densities are normally 0.43–0.5 psi/ft, depending on if it is fresh or salt water (salt water is denser than fresh water). A great example of buoyancy pressure is from swimmers trying to float in a fresh water lake on a hot summer day. Holding in breath creates a less dense body, and floating is possible. Floating, however, is much easier in the salt-saturated Dead Sea, where the density difference between your body and the denser salt water is higher.

The density differences show up on the pressure vs. depth plots. Intersections of different fluids defines contacts. Hence on Fig. 2.23, the water line has a slope of 0.493 psi/ft, a salt water gradient. The oil gradient, in contrast is 0.377 psi/ft and the gas gradient 0.05 psi/ft. The changes in slope and intersections define gas/oil and the free water level.

Some common gradients and densities are shown in Table 2.2.

Oil densities are most commonly presented in grams/cubic centimeter (g/cc) or as API units. The API unit (named for the American Petroleum Institute) is a common unit of measure describing densities.

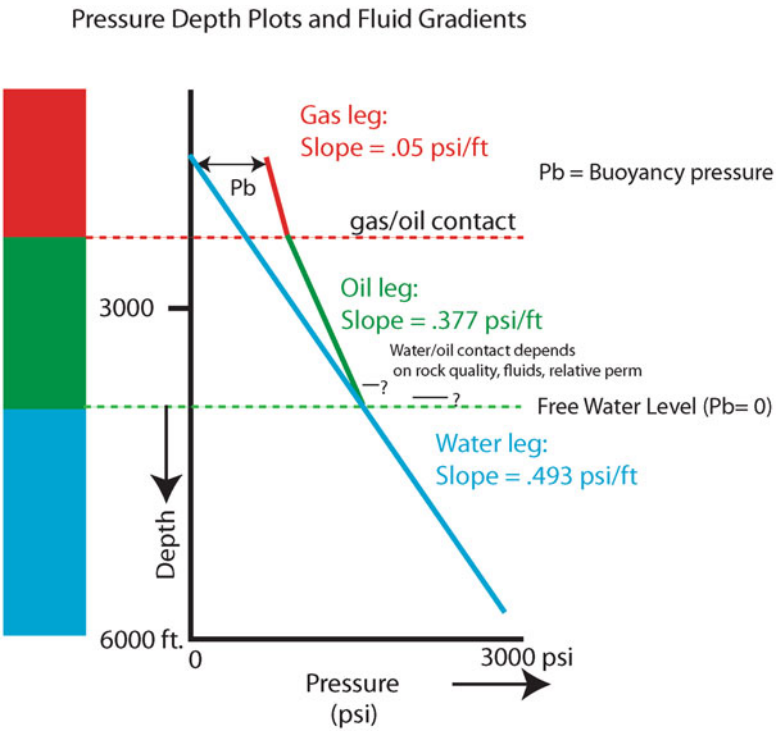

Fig. 2.23 Buoyancy pressure. Modified from Dahlberg (1995) courtesy of Springer-Verlag

Table 2.2 Some common densities. See Appendix A for more formulas and conversions

Fluid	API gravity	Density in g/cc	Density in psi/ft	Comments
Fresh water		1	0.43	1 g/cc = 0.43 psi/ft
Salt water		1.1	0.47	
Extra heavy oil	<10	>1		
Heavy oil	10–22.3	0.92–1.0	0.38–0.43	
Medium oil	22.3–31.1	0.87–0.92	0.37–0.38	
Light oil	31–50	0.87–0.5	0.37–0.216	
Condensate	60	0.73	0.319	
Wet gas		0.5	0.216	
Dry gas		0.2	0.086	

The API gravity formula by Eq. (2.1):

$$\frac{141.5}{SG\,at\,60^{\circ}\mathrm{F}} - 131.5 \tag{2.1}$$

Where SG equals specific gravity, measured in the lab or on the rig at 60 °F.

Table 2.2 compares API gravity and common density measurements. From both Table 2.2 and Fig. 2.23, it is clear that gas accumulations for any given height in a trap, will have higher buoyancy pressure than oil pools, due to greater density differences in the fluids.

Pressure depth plots are the only accurate way to determine the (FWL), or base of the trap, and hence, are extraordinarily useful plots to make if you have the data from your wells. At the base of the trap, there is no oil in the reservoir, and Pb = 0. The structural elevation of the FWL is important to determine, as there will be oil everywhere above it, but not necessarily in commercial saturations. That will depend on other factors like pore throat distribution and fluid phase.

Finding the FWL is key to understanding oil shows and it should not be mistaken as the oil or gas/water contact. A failure to understand the differences between an oil or gas/water contact and the free water level may well be one of the more common problems for geoscientists globally. Understanding the differences quantitatively requires an understanding of capillary properties of the rock (Chap. 5).

To start understanding capillarity, however, learn to interpret and understand height above free water plots.

2.4.3 Water and Hydrocarbon Saturations and Height Above Free Water Plots

When oil enters a trap there are forces called 'capillary pressure' which resist displacement of whatever fluid is already in the pore. In most cases, this is water. For now, consider the pore throat as the primary resistive force that needs to be overcome to get oil to displace water in a trap. The larger the pore throat, the easier it is to overcome the capillary forces that resist migration. Smaller pores, however, require significant buoyancy pressure to bridge ever increasingly small pore throats. This is analogous to capillaries in a human body. It is easy to pump blood into a large artery, but difficult to get blood into ever smaller capillaries. When a human heart becomes weaker with age, smaller capillaries no longer receive the oxygen and blood flow they need and problems result. This is not unlike, conceptually, oil filling a trap using buoyancy pressure.

Because pore geometries are not all created equal (recall Fig. 2.14), the volume of oil that enters a reservoir is strongly controlled by the pore networks. Small pore throats simply take more pressure to displace water than large pore throats.

The percentage of pore space occupied by water is called 'water saturation' (Sw). It is expressed in percentage of pore space filled with water. Hydrocarbon saturations are defined as (1-Sw), and designated as So. A water saturation of 90 %, then, means a hydrocarbon saturation (So) of 10 %. Likewise, an Sw of 20 % is an So of 80 %. Pore geometries vary significantly by rock type, but can be quantitatively visualized on a plot of water saturation vs. height above free water. The pore throat distribution must be known or estimated to do this, as well as the fluid/water phase (gas or oil densities vs. salt or fresh water) and chemical properties of the fluids and finally another property, called 'wettability' which relates to the walls of the pore throat (Chap. 5).

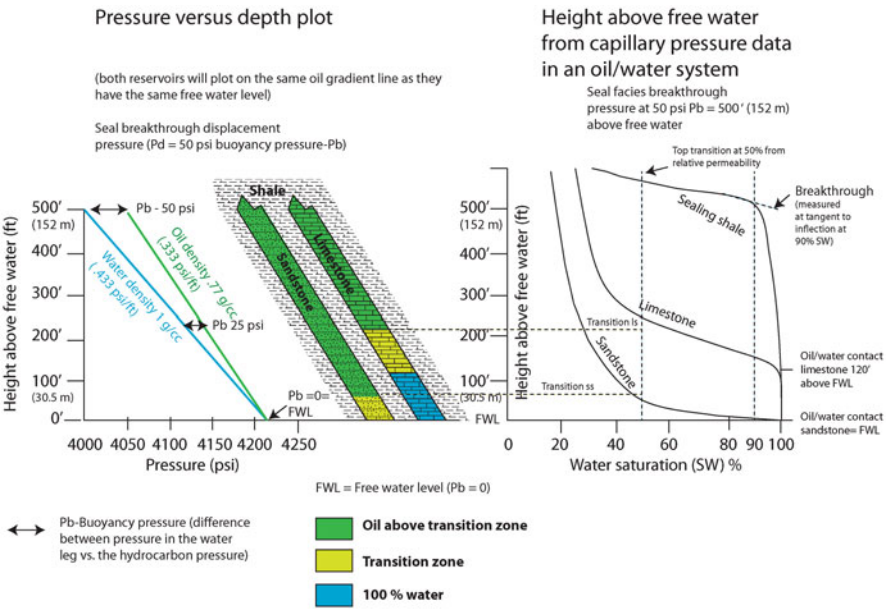

Fig. 2.24 Rock properties from height above free water and the relationship to a pressure vs. depth plot. The three rock types shown have different pore geometries and hence different saturations at any point in a trap. Modified in part from Schowalter (1979); Schowalter and Hess (1982)

Ignoring the math and physics for now, assume you have plots showing a calculated height above free water vs. Sw for three rock types (Fig. 2.24). The changes in the shape of each rock type are due strictly to the changes in pore geometry. The pore geometries change because the rock properties are fundamentally different. A well sorted, highly permeable sandstone will have a completely different height above free water plot than a tight dolomite or shale.

In Fig. 2.24, for example, there are three rock types that are part of the same trap and seal combination. The sandstone and limestone share a common pressure system and a common free water level and thus have the same spill point. In a case like this, both the limestone and the sandstone would be in pressure communication and pressure points would plot precisely on the oil gradient line on the pressure-depth plot. At the base of the trap, Pb = 0 and at the top, Pb = 50 psi. This is true for both lithologies, so they have equal Pb at any given height in the trap. Obviously, the top of the trap has much higher Pb than the base.

2.4.4 *Oil-Water Contacts, Top of Transition Zones vs. FWL and Relative Permeability*

Figure 2.24 also illustrates how the oil-water contacts and top of transition zones can vary within a trap simply by rock type changes. Oil-water contacts should be set at the 100 % Sw line. The top of transition zone, however, is the point at which a

well physically begins to produce water, and that is a function of its rock type and saturation.

Height above free water vs. saturation plots tell a lot about how a well might perform when drilled. In Fig. 2.24, top of transition zones and oil water contacts are substantially different. Examine, for instance, the 50 % SW point for all the rocks. For illustration purposes, the top of the transition zone is set at 50 % SW for both the sandstone and the limestone. Despite being in equal Pb conditions, the sandstone has a larger pore-throat network and reaches 50 % SW at 75 ft (20 m) above free water. In contrast, the limestone doesn't reach 50 % SW until over 200 ft (61 m) into the trap. The shale never reaches 50 % SW because it is the seal and can only hold 500′ (152 m) of oil before it leaks.

Another critical point is where the rock has 100 % Sw. This is the actual oil-water contact. The oil-water contact will also correspond roughly to the seal capacity of the rock. That point can be found by examining the right side of the diagram at the 90 % Sw line. This saturation value is often used as an approximation of seal capacity, but if you have plots like this, a line drawn tangent to the curve at that point and projected back to 100 % Sw is a better approximation of both seal capacity and the oil-water contact (Jennings 1987).

By example, the third rock type is the shale seal. The shale has many tiny micro and nanno pore throats which can only be breached at 50 psi Pb at the top of the trap. The line tangent to the curve at 90 % Sw shows a value of 500′ (152 m) to an oil/water system, or the seal capacity of the shale. The sandstone, in contrast, has no seal capacity and the oil/water contact is the same as the FWL. This means the pore throats in the sandstone are large (like arteries) and it takes only a little Pb to displace water and begin filling the reservoir with oil. The limestone, a third rock type, can seal a 120′ (36 m) column and the oil water-contact will be 120′ (36 m) above the FWL. The pore throat sizes in the limestone are smaller and more difficult to displace water from than the sandstones, but much bigger than those of the shale.

Yet another key part of these plots is where the curve steepens rapidly on the left side of the diagram. When the line goes vertical, or nearly so, this is termed the irreducible water saturation (Swi). Note the sandstone curve still has quite a bit of water remaining until it gets to 40 or 50 % SW, after which it fills rapidly. At Swi, the water in the smaller pore throats can no longer be displaced and will remain in the trap, but not produced when the well flows. In this case the Swi for the sandstone is around 18 % and for the limestone about 30 %.

However, if the operator tries to perforate and produce the sandstone a few feet above the FWL, despite having some oil saturation, it will probably flow only water, regardless of the lithology. At 25′ above the FWL, for example the saturations in the sandstone will be 80–90 % Sw. This may be too high a water saturation to produce anything but water, despite have 10–20 % oil saturation. The reason for this is a phenomenon called 'relative permeability' which is covered more in Chap. 5. From a shows standpoint, a well testing water low on a trap but near the FWL can easily

be mistaken as 'not being in a trap' as the Sw will be very high and there may be no recovery of hydrocarbons.

Another problem arises with the shallower oil-water contact on the limestone. If this is the only well drilled on the trap, the oil-water contact may easily be mistaken from the FWL. That would mean the operator has under-valued the trap by an additional 120′ (32 m) of closure. An offset well might encounter the sandstone at the same level (or lower) as the limestone and find excellent low Sw. The sandstone, at 120 ft (32 m) above FWL, has an SW of about 30 %, and would likely produce oil with no water!

This is the essence of understanding oil shows at the most basic level. Saturations vary as a function of rock type and position in the column. Oil-water contacts can be different across a field and in the same trap, in pressure continuity and with the same FWL, but different contacts due to varying rock type.

If this were changed to a gas-water system, the curves would change again and the seal capacity would be reduced substantially (due to increased Pb in the gas/water cases). Saturations would be lower in all three rock types than they are in the oil/water case.

Here are the points to remember:

1. Sw varies not just by height above free water, but by rock type and pore throat distribution.
2. Gas/water systems have higher Pb (buoyancy pressure) at any given point in a trap than oil/water systems (so seal capacity is reduced for any given rock type). What seals long columns of oil may only seal small columns of gas. There are some caveats to this statement, however:
   (a) Interfacial tension (discussed in Chap. 5) can be high in gas/water systems, and this will increase the seal capacity of any trapping facies.
   (b) There are wide variations in density in gas accumulations and the lighter the gas, the more difficult it can be to seal. So not all 'gas' traps are equal in terms of seals needed to form the traps.
3. The FWL is where Pb = 0. There will ALWAYS be SOME oil saturation above the FWL, but high SW zones can actually test all water and be misinterpreted as below an oil water contact or not in a trap.
4. Pressure/depth plots are the ONLY way to accurately confirm a FWL. Other techniques, like capillary pressure analysis (Chap. 5) offer good approximations.
5. Gas/oil, oil/water and gas/water contacts can be recognized on pressure-depth plots.
6. Oil and gas/water contacts MAY NOT equal the FWL. It is possible to have 100 % SW in a rock with small pore throats high into a trap.
7. Many, many fields are drilled into and undersized or missed because of point 6! Understand your rock quality and look at shows data carefully to see if 100 % SW is below the FWL or simply in really tight rock!

2.4.5 Permeability

Permeability is the rate of flow of a liquid or gas through a porous material. There is commonly a lack of understanding of the difference between pore throat geometry and permeability. Permeability in cores is a measured value (Hartmann and Beaumont 1999) calculated from:

1. Atmospheric pressure
2. Cross-sectional area of a core plug
3. The flow in cm^3/s
4. The length of the plug
5. Pressure at the input end in atmospheres (atm)
6. Pressure at the output end in atm
7. Air viscosity in cp (centipoise)

The standard unit of measure is the millidarcy (md). At a qualitative level, 100 md would be considered a good permeability, 1000 md or higher outstanding, and the rock would probably be called 'tight or low perm' below 1 md. How much a well flows will depend not just on the permeability of the rock, but the pressure drop across the wellbore when it is flowed, the cross-sectional area of the perforated interval, and the fluid viscosity. Because of viscosity variations, a 10 md rock might have high flow rates in gas but low flow rates in heavy oil.

Engineers, in particular, talk in terms of porosity and permeability, as the permeability measures the rate at which oil is produced in a well. A geologist, on the other hand, should learn to think in terms of the distribution of pore throats and their impact on water saturation and water cut when a well is produced. As will be shown in Chap. 5, a high porosity rock can have low permeability and be micro-porous, requiring a long hydrocarbon column and high buoyancy pressure to saturate the reservoir. In contrast, some low porosity rocks have very good permeability and very well connected pore networks, requiring very little Pb to fill to irreducible water saturation. A high porosity zone does not necessarily equate to high permeability and vice versa!

Thus, Swi may be as low as 3 % in some rocks and fluid combinations and as high as 80 % in others, but is typically in the 10–25 % range for rocks with 'normal' ranges of porosity and permeability. In understanding shows, interpreters need to think in terms of pore geometries, not porosity or permeability, and in terms of saturation in the context of rock type, fluid type, buoyancy and position in a trap.

2.4.6 Waste Zones

The term 'waste zone' (Schowalter and Hess 1982), as mentioned earlier, has been used to describe updip, poor reservoir, low saturation facies that are largely uneconomic in a trap. Hence, the monetary value is 'wasted on these rocks'. Waste zones

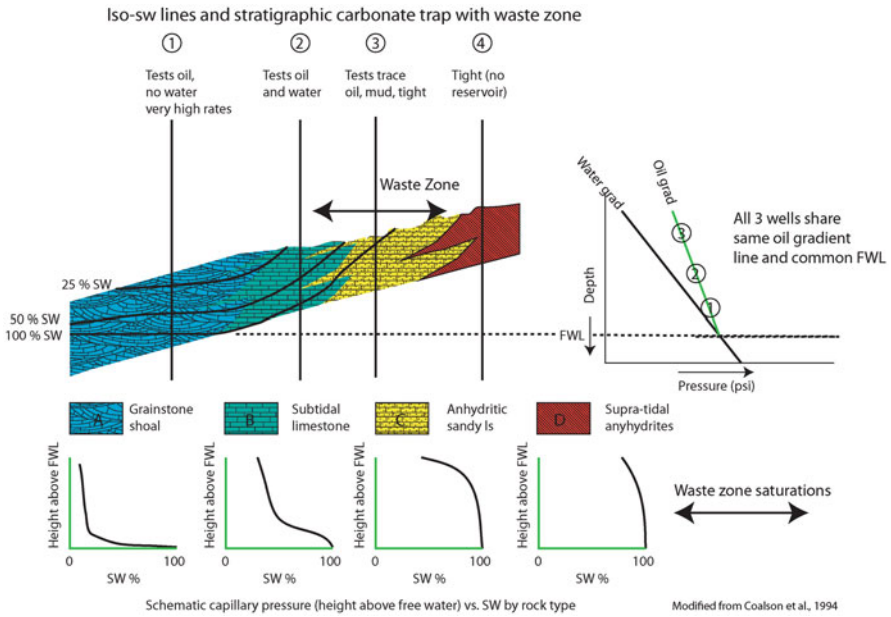

Fig. 2.25 Relationship between SW and pressure in a stratigraphic trap with an updip waste zone and variable rock properties. Modified from Coalson et al. (1994)

are important to recognize in any well or dry hole. Waste zone rocks are generally meso or micro-porous, depending on the fluid system and position in a trap. For instance, in heavy oil, a meso-porous rock may act like a 'waste zone', but in a gas reservoir, with increased Pb, it may be an outstanding reservoir flowing at very high rates.

Evaluations of well shows, tests, recoveries and pressures require a constant ability to think about pore-throat geometries and the density of the hydrocarbon/water system and other things that affect capillary pressure fluid displacement and water saturation.

Consider Fig. 2.25, where a carbonate grainstone shoal with mega pore systems passes gradually updip into meso-porous sub-tidal limestones and then micro-porous anhydritic shoreline limestones and, ultimately, to an evaporite seal. How you initially view this trap may well depend on the order in which you drill the wells! If you drill well 3 first, you will get very high water saturations high on the trap and may well misinterpret this well as 'wet' and 'not in a trap'. You would be wrong. A pressure-depth plot shows that wells 1–3 are in pressure communication on an oil leg, sharing a common FWL. The only reason for the poor result in well 3 is the rock type!

If you drill well 1 first, you and your management will head to lunch to celebrate. You may correctly recognize the high quality rock and feel comfortable making the oil/water contact the FWL. You look at your map and run volumetrics, getting a great number. Then you drill well 2 and the great saturations, almost certainly to

exist updip, go away. No one is buying lunch now. You scratch your head, along with your management. The reserves you estimated have been reduced. Unfortunately, your team also might easily interpret well 2, in the absence of pressure data, as in 'being in a different trap' because the water saturations are so different that it will calculate 100 % SW near the base of the reservoir. Someone in your team, almost certainly, will see the 100 % SW line in well 2 as the FWL and also equate that to the oil-water contact. They will be wrong.

Drill well 2 first and you will have a dilemma. The water saturations are not great. Your management will be urging you to 'drill updip' for more buoyancy pressure and better saturations. You do that and get well 3, a huge disappointment. You go home depressed.

If you have cut core or looked at cuttings, you might recognize that well 2 is mesoporous rock and well 3 micro-porous, but both have saturations. Because you understand shows and height above free water plots, you recognize that this is possible only in the presence of a substantial oil column and large trap. You think this through and decide you need a better reservoir within the trap, maybe even downdip. You carefully build a facies map from all available data. You find a well downdip that is highly porous, in a grainstone shoal, and it doesn't look like wells 2 or 3 on logs. You decide there is a significant facies change downdip and you map it out. If are lucky, you have 3D seismic. If not, you might want to recommend it if you think it will show the facies boundaries.

You take your final facies map back in and recommend to your management to drill downdip of well 2 to find really good saturations in the grainstone shoal. Someone in the management team, almost certainly, will think you are a tad insane, and may even tell you so. They will argue you already found an oil/water contact in well 2, so why go down-dip? If you have pressure points in wells 2 and 3 you can point out that the points fall on the same oil gradient which matches the API gravity of the recovered oil. If not, you have to be persuasive on the basis of rock properties alone. It is not an 'easy sell'.

You talk at length about 'waste zones', buoyancy pressure and rock type until your prospect concept is clear. You argue that both wells 2 and 3 have proven the trap, just not the commercial saturation. Eventually you get some money and drill well 1. While it is drilling, you lose some sleep worrying about the results, as you are taking a gamble, moving downdip of an oil/water contact and high saturations and guaranteeing the result will be good.

The well comes in and everyone goes out to dinner and celebrates. Your manager proclaims he is a genius to have thought of such a novel idea himself. He gets promoted. You get a free lunch and a great reputation with peers. It is clear the old saying 'every dry hole is fatherless, every discovery has multiple parents' is true.

2.4.7 Oil Show Types

With an understanding of rock types and buoyancy, understanding oil shows can begin to make sense. Perhaps the most fundamental papers written on the topic of show classification are those of Schowalter (1979) and Schowalter and Hess (1982),

and expanded upon in summary form significantly by Hartmann and Beaumont (1999) and Vavra et al. (1992).

Even in the last decade there have been many advances in the tools used to identify oil and gas shows but the fundamental issue of how to use them in exploration remains one of an 'art of integration'. Too often, interpreters lack the background in pressures, petrophysics or geochemistry to take full advantage of the huge amount of information available in any basin or field that helps understand oil occurrences. The rest of this book provides more detail on how to interpret key data sets and make exploration and production decisions with oil and gas show information.

To start, Schowalter's papers define four basic show types. Details of how to recognize these shows and where the pitfalls occur in interpretation are subjects for later chapters (Table 2.3).

Continuous phase shows (Fig. 2.26) will always be above the free water level. Immediately above the FWL the first continuous filaments of oil bridge the largest pore throats (hence the name).

Residual oils (Fig. 2.27) occur where oil was once trapped or migrated but has been lost. These shows are always below the FWL, but can have substantial residual saturations and even stain and odor in cuttings. Techniques for assessing residual vs. continuous phase oils are covered by O'Sullivan et al. (2010) and good case history of residual formation by exhuming or rotating older traps into newer structural positions and spilling hydrocarbons updip is presented by several authors (Farrimond et al. 2015; Igoshkin et al. 2008; Littke et al. 1999; Naidu et al. in press; Sorenson 2003). Chapters 5 and 6 deal with this subject in much more detail.

If a well tests measureable amounts of oil and gas, it is clearly in a continuous phase trap. A well testing 1 BOPD and 1000 BWPD (barrels of water per day) is in

Table 2.3 Classification of oil shows (Schowalter and Hess 1982)

Show type	Definition	Comments
Continuous phase shows	Oil above the free water level	Occurs as continuous filaments of oil bridging the largest pores. Difficult to recognize if saturations are low enough to not test oil.
Residual shows	Traces of oil left behind from prior accumulations which have been lost or along migration pathways. Always below the FWL.	Can be difficult to tell from continuous phase shows. Will always test water and be within a water gradient on a pressure-depth plot.
Dissolved gasses	Gas being released from formation water by pressure drops while drilling	Not significant in conventional exploration, but some high permeable sands in the Gulf of Mexico (USA) are being looked into for unconventional gas production (Tim Schowalter, personal communication).
Kerogen-rich source rocks	Oil and gas liberated by drill bit heat and friction in immature source rocks or oil and gas remaining in the source rocks after generation	Significant and large unconventional shale oil and gas resources. Generally requires hydraulic fracturing or natural fractures to produce economically.

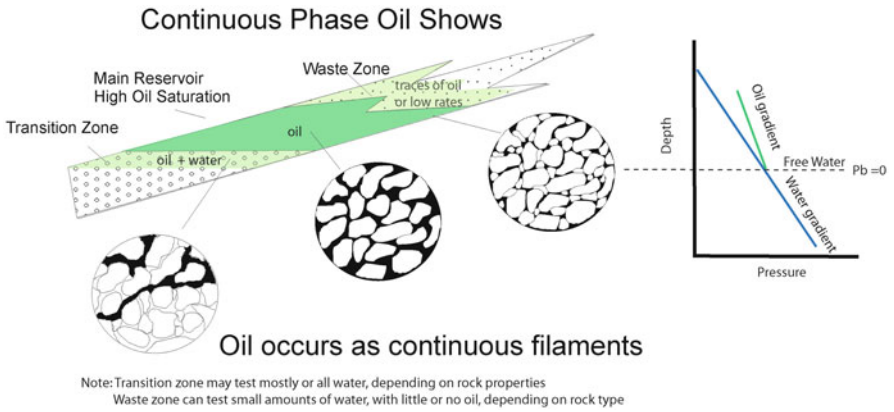

Fig. 2.26 Continuous phase oils. Modified from Meckel (1995) and Hartmann and Beaumont (1999)

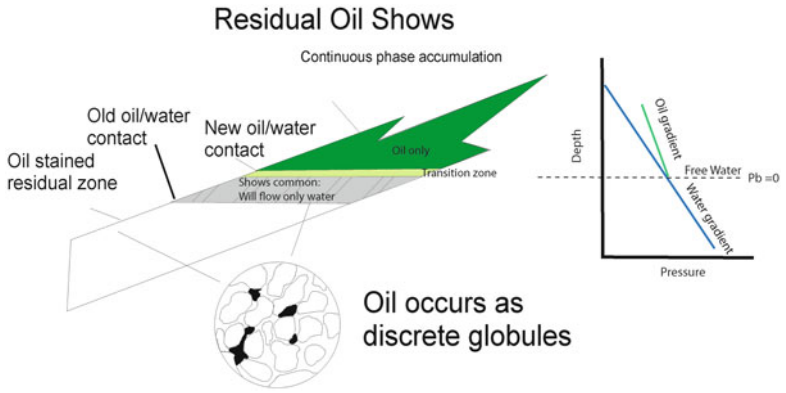

Fig. 2.27 Residual oil shows. Modified from Meckel (1995) and Hartmann and Beaumont (1999)

a trap. Given the high rates, it is probably near the free water level or oil/water contact. A well testing 1 BOPD in very tight rock is also in a trap. Both of these examples are continuous phase shows and must be looked at carefully to see where to drill another well. The tight well is probably in a waste zone.

I lived and worked in Russia for 4 years with TNK-BP. It was common for us to find hundreds of abandoned wells which tested very low rates of oil in very tight tock and were abandoned as 'dry'. More careful work in one area (Dolson et al. 2014) led to recognition of billions of barrels of stratigraphically trapped hydrocarbons in an area peppered with non-commercial 'dry holes'. Careful pressure, core and facies analysis finally revealed the traps.

Residual shows are problematic, as the issue is 'where did the oil go'? More examples are shown in Chap. 5, but it can be very difficult on well logs or cuttings

alone to recognize that some substantial oil shows are residual. Residual oils are very common in older fields undergoing water flood, as the water flooding has displaced the oils and left only residual droplets behind. In many cases, these residual saturations are substantial (60–90 % SW, which equates to 40–10 % oil), but they can't be recovered with conventional means as the droplets are no longer connected.

Often, chemicals (RPSEA 2009) are introduced into these oil fields to change the other capillary properties of the rocks (like wettability and interfacial tension, covered in Chap. 5). These chemical changes allow the droplets to re-connect and be produced. There are enormous volumes of residual oils remaining in old fields globally if we can find ways to produce them.

2.4.8 Kerogen-Rich Source Rocks

Easily one of the most exciting developments in the last century has been the recognition that vast amounts of oil remain trapped in shales and tite limestones in the kerogen-rich source rocks themselves. This is the realm of 'unconventional exploration' and it deals with how to get oil from rocks still trapped in the primary migration phase. The continuous phase and residual shows are associated with secondary migration and require a different set of techniques to evaluate.

This book only briefly touches upon unconventional exploration but suffice it to say that when oil is generated in a source rock, quite a bit remains in the fine pore spaces until the kerogens are completely 'cooked out' during the maturation process. One of the pioneers of unconventional exploration was Fred Meissner (Meissner 1978) who recognized that oil in the Bakken Shales of North Dakota had billions of untapped barrels of oil still remaining in the shales. Early attempts to produce from these shales with vertical well bores and hydraulic fracturing were disappointing, but technically successful. In fact, some of the oldest fields in North America occur in fractured shale and oil formations like the Florence Field of Colorado and the Marcellus shales of Pennsylvania, where early drillers and pioneers could extract the oil and gas from open fractures at very shallow depths, sometimes even lowering buckets into the fractures to lift out the oil.

Horizontal well drilling and a process called multi-stage hydraulic fracturing has finally made access to these resources possible. Unconventional resource assessment is most comprehensively covered by (EIA 2008a, b, 2009a, b, 2010a, b, 2011). Some excellent technical summaries are also provided by (DCNR 2014; Harper and Kostelnik 2013a, b, c; Smith and Leone 2010; Wrightstone 2009, 2010; Zammerilli 2010).

When drill bits encounter shales with kerogens remaining in the pore spaces, bit friction and heat liberate these kerogens as free hydrocarbons. Later chapters deal more comprehensively with new tools to evaluate oil and gas shows in shales, but they are important to distinguish as different from shows in conventional reservoir rocks.

2.4.9 Thinking Like a Molecule

This chapter establishes the foundation for most of the subsequent chapters—which explore techniques of pressures, rock properties, petrophysics, show and geochemical data capture and migration analysis in more detail.

More than one person I know has insisted that successful oil finders are those who 'get back to the basics' and 'think like a molecule of oil', using a solid understanding of rock properties, migration and water saturation analysis to map out where oil goes once it leaves the source rock beds during maturation. Modern software packages allow migration modeling to be simulated, but still need geological insight on carrier beds, seals, source rock characteristics and timing of migration and validation of the models with oil shows databases from dry holes and other data.

Downey (2014) stresses that too little emphasis is often given to the fundamentals of mapping, characterizing and understanding oil and gas shows, regardless of years of experience. Understanding oil shows is often difficult and confusing. But changes in saturation are easier to understand for those who understand the petrophysical basics of this chapter and the rest of this book.

Exploring for oil and gas is not easy. It requires ever increasing sophisticated skills with computers, software, seismic, geochemistry, well logs, engineering, economics and other tools. A favorite quote of mine is that attributed to Parke Dickey from many years ago, but still holds true today.

> We usually find oil in new places with old ideas. Sometimes, also, we find oil in an old place with a new idea, but we seldom find much oil in an old place with an old idea. Several times in the past we have thought that we were running out of oil, whereas actually we were only running out of ideas.

Studying, characterizing and thinking about oil and gas shows in the context of position in a trap, rock type, seals and migration can be a key to unlocking that 'new field in an old area with a new idea' or just as applicably, to opening up a huge new play overlooked by others.

2.5 Summary

Exploration today involves looking at plays in both the source rocks where only primary migration has occurred, and in reservoirs, along secondary migration pathways. There are a multitude of different traps types, seals and reservoir lithologies. Understanding oil and gas shows fundamentally boils down to being able to quantify or conceptually evaluate what oil shows mean. Are the shows residual in leaked traps or along migration pathways, or are they within a trap above the free water level?

The size of the trap is governed by the weakest seal and if traps are not filled to spill, they are either not charged fully or the weakest seal is less than the total trap closure. Being able to differentiate between these two scenarios may lead to recognizing additional potential updip along other migration pathways. Waste zones are

common within traps, and can be recognized as poor quality rock testing only small amounts of oil and gas. Free oil and gas tested in a waste zone indicates that a column is present. Sometimes, that column is significant and all that is needed is a change in facies laterally or updip or downdip to better reservoir to develop an economic field.

Because of varying rock properties, oil-water contacts should not be confused with free water levels. Different facies in the same trap can be in the same pressure system, in continuity with one another, but with different oil-water contacts. Many a field has been underestimated in size when poor quality rock, well above the free water level, calculates 90–100 % Sw and thus the trap is assumed uncommercial or to have failed by some mechanism like seal failure. Astute interpreters learn to recognize additional field potential just by analyzing the geometry of the different reservoir facies and looking for better places to drill high quality reservoirs, often downdip of wells that appear 'wet' on logs but are actually simply in waste zones.

References

Berg R (1975) Capillary pressures in stratigraphic traps. Am Assoc Pet Geol Bull 59:939–956

Biddle K, Wielchowsky CC (1994) Hydrocarbon traps. In: Magoon LB, Dow WG (eds) The Petroleum System—from source to trap: Tulsa. The American Association of Petroleum Geologists, Oklahoma, pp 221–235.

Choquette PW, Pray LC (1970) Geologic nomenclature and classification of porosity in sedimentary carbonates. Am Assoc Pet Geol Bull 54:207–250

Coalson EB, Goolsby SM, Franklin MH (1994) Subtle seals and fluid-flow barriers in carbonate rocks. In: Dolson JC, Hendricks ML, Wescott WA (eds) Unconformity related hydrocarbons in sedimentary sequences, vol 1. Rocky Mountain Association of Geologists, Denver, CO, pp 45–59

Dahlberg EC (1995) Applied hydrodynamics in petroleum exploration, 2nd edn. Springer, New York, 295 p

DCNR (2014) Thermal maturation and petroleum generation. Pennsylvania Department of conservation and Natural Resources (DCNR), p. 1. http://www.dcnr.state.pa.us/topogeo/econresource/oilandgas/marcellus/sourcerock_index/sourcerock_maturation/index.htm

Dolson JC, Bahorich MS, Tobin RC, Beaumont EA, Terlikoski LJ, Hendricks ML (1999) Exploring for stratigraphic traps. In: Beaumont EA, Foster NH (eds) Exploring for oil and gas traps: treatise of petroleum geology, handbook of petroleum geology, vol 1. American Association of Petroleum Geologists, Tulsa, OK, pp 21.2–21.68

Dolson JC, Pemberton SG, Hafizov S, Bratkova V, Volfovich E, Averyanova I (2014) Giant incised vally fill and shoreface ravinement traps, Urna, Ust-Teguss and Tyamkinskoe Field areas, southern West Sibertian Basin, Russia, American Association of Petroleum Geologists Annual Convention, Houston, Texas, Search and Discovery Article #1838534, p. 33

Dolson JC, Piombino J, Franklin M, Harwood R (1993) Devonian oil in Mississippian and Mesozoic reservoirs—unconformity controls on migration and accumulation, vol 30. The Mountain Geologists, Sweetgrass Arch, MT, pp 125–146

Dolson JC, Piombino JT (1994) Giant proximal foreland basin non-marine wedge trap: lower Cretaceous Cutbank Sandstone, Montana. In: Dolson JC, Hendricks ML, Wescott WA (eds) Unconformity-related hydrocarbons in sedimentary sequences. The Rocky Mountain Association of Geologists, Denver, CO, pp 135–148

Downey M (2014) Thinking like oil, the AAPG explorer. American Association of Petroleum Geologists, Tulsa, OK, p 3
Editors (2005) Buzzard- a discovery based on sound geological thinking. GEO ExPro, pp. 34–38.
EIA (2008a) Barnett Shale, Ft. Worth Basin, Texas. Wells by year of first production and orientation. Energy Information Administration Office of Oil and Gas, Washington, DC, p 1
EIA (2008b) Fayetteville Shale, Arkova Basin, Arkansas: key geological features. Energy Information Administration Office of Oil and Gas, Washington, DC, p 1
EIA (2009a) Haynesville-Bossier Shale play, Texas-Louisiana salt basin. Energy Information Administration Office of Oil and Gas, Washington, DC, p 1
EIA (2009b) Marcellus Shale gas play, Appalachian Basin. Energy Information Administration Office of Oil and Gas, Washington, DC, p 1
EIA (2010a) Shale gas plays, lower 48 states. Energy Information Administration Office of Oil and Gas, Washington, DC, p 1
EIA (2010b) Woodford Shale play, Arkoma Basin, Oklahoma: key geological features. Energy Information Administration Office of Oil and Gas, Washington, DC, p 1
EIA (2011) World shale gas resources: an initial assessment of 14 regions outside the United States. Energy Information Administration Office of Oil and Gas, Washington, DC, p 1
England WA, Mann AL, Mann DM (1991) Migration from source to trap. In: Merrill RK (ed) AAPG treatise of petroleum geology, handbook of petroleum geology. The American Association of Petroleum Geologists, Tulsa, OK, pp 23–46
Farrimond P, Naidu BS, Burley SD, Dolson J, Whiteley N, Kothari V (2015) Geochemical characterization of oils and their source rocks in the Barmer Basin, vol 21. Petroleum Geoscience, Rajasthan, India, pp 301–321
Gunter GW, Finneran JM, Hartmann DJ, Miller JD (1997) Early determination of reservoir flow units using an integrated petrophysical method. Society of Petroleum Engineers, v. SPE 38679, pp. 1–8.
Harper JA, Kostelnik J (2013a) The Marcellus Shale Play in Pennsylvania, geological survey. Pennsylvania Department of Conservation and Natural Resources, Middletown, PA, p 21
Harper JA, Kostelnik J (2013b) The Marcellus Shale Play in Pennsylvania part 2: basic geology, geological survey. Pennsylvania Department of Conservation and Natural Resources, Middletown, PA, p 21
Harper JA, Kostelnik J (2013c) The Marcellus Shale Play in Pennsylvania part 4: drilling and completion, geological survey. Pennsylvania Department of Conservation and Natural Resources, Middletown, PA, p 18
Hartmann DJ, Beaumont EA (1999) Predicting reservoir system quality and performance. In: Beaumont EA, Foster NH (eds) Exploring for oil and gas traps: treatise of petroleum geology, handbook of petroleum geology, vol 1. American Association of Petroleum Geologists, Tulsa, OK, pp 3–154
Igoshkin VJ, Dolson JC, Sidorov D, Bakuev O, Herbert R (2008) New interpretations of the evolution of the West Siberian Basin, Russia. Implications for Exploration, American Association of Petroleum Geologists. Annual conference and exhibition, San Antonio, TX, AAPG Search and Discovery Article #1016, pp 1–35
Jennings JB (1987) Capillary pressure techniques: application to exploration and development geology. Am Assoc Pet Geol Bull 71:1196–1209
Jewell G (2011) Exploration of the Tano Basin and discovery of the Jubilee Field, Ghana: a new deepwater game-changing hydrocarbon Play in the transform Margin of West Africa, AAPG Annual Convention and Exhibition, Houston, Texas, AAPG Search and Discovery Article #110156, p. 22
Littke R, Cramer B, Gerling P, Lopatin NV, Poelchau HS, Schaefer RG, Welte DH (1999) Gas generation and accumulation in the West Siberian Basin. Am Assoc Pet Geol Bull 83:1642–1665
Martinsen RS, Jiao ZS, Iverson WP, Surdam RC (1994) Paleosol and subunconformity traps: examples from the Muddy Sandstone, Powder River Basin, Wyoming. In: Dolson JC, Hendricks

ML, Wescott WA (eds) Unconformity-related hydrocarbons in sedimentary sequences. The Rocky Mountain Association of Geologists, Denver, CO, pp 119–286
Meckel L (1995) Seals and shows. Chapter V: Shows (unpublished workshop notes). In: Traugott MO, Gibson R, Dolson J (eds) Seals and shows workshop, September 10–14, 1995. Amoco and Gulf of Suez Petroleum Company, Cairo, Egypt, p 21
Meissner FF (1978) Petroleum Geology of the Bakken Formation, Williston basin, North Dakota and Montana. The economic geology of the Williston basin: Proceedings of the Montana Geological Society, 24th annual conference, pp 207–227
Naidu BS, Burley SD, Dolson J, Farrimond P, Sunder VR, Kothari V, Mohapatra P, Whiteley N (in press) Hydrocarbon generation and migration modelling in the Barmer Basin of western Rajasthan, India: lessons for exploration in rift basins with late stage inversion, uplit and tilting, Petroleum System Case Studies, v. Memoir 112. American Association of Petroleum Geologists, Tulsa, OK
O'Sullivan T, Praveer K, Shanley K, Dolson JC, Woodhouse R (2010) Residual hydrocarbons—a trap for the unwary. SPE, v. 128013, pp 1–14
Pittman E (1992) Relationship of porosity and permeability to various parameters derived from mercury injection-capillary pressure curves for sandstone. Am Assoc Pet Geol Bull 76:191–198
Ray FM, Pinnock SJ, Katamish H, Turnbull JB (2010) The Buzzard Field: anatomy of the reservoir from appraisal to production. Petroleum Geology conference series 2010, pp 369–386
Richards P (2012) Entrepreneurs finished the Falklands' story, AAPG Explorer. American Association of Petroleum Geologists, Tulsa, OK, p 1
RPSEA (2009) First ever ROZ (Residual Oil Zone) symposium, Midland, Texas, Research Partnership to Secure Energy for America (RPSEA), p. 59
Saucier H (2014) Mom and Pop E&P makes unlikely success: Rockhopper hits it big offshore Falklands, AAPG Explorer. American Association of Petroleum Geologists, Tulsa, OK, p 1
Schowalter TT (1979) Mechanics of secondary hydrocarbon migration and entrapment. Am Assoc Pet Geol Bull 63:723–760
Schowalter TT, Hess PD (1982) Interpretation of subsurface hydrocarbon shows. Am Assoc Pet Geol Bull 66:1302–1327
Sheppard A (2015) The network generation comparison forum: a collaborative project for objective comparison of network generation algorithms for 3D tomographic data sets of porous media. In Sheppard A (ed.). Australian National University, Canberra, Australia. http://people.physics.anu.edu.au/~aps110/network_comparison/
Smith LB, Leone J (2010) Integrated characterization of Utica and Marcellus Black Shale gas plays, New York State, AAPG Annual Convention and Exhibition, New Orleans, Louisiana, AAPG Search and Discovery Article #50289, p 36
Sorenson RP (2003) A dynamic model for the Permian Panhandle and Hugoton Fields, Western Anadarko Basin, 2003 AAPG mid-continent section meeting, Tulsa, OK, AAPG Search and Discovery Article #20015, p 11
Specht RN, Brown AE, Selman CH, Carlisle JH (1987) Geophysical case history, Prudhoe Bay Field, Alaskan North Slope geology, volumes I and II, pacific section. SEPM (Society for Sedimentary Geology), Tulsa, OK, pp 19–30
Swanson BF (1977) Visualizing pores and non-wetting phase in porous rocks. Society of Petroleum Engineers, vol. SPE Paper 6857, p 10
Swanson VF (1981) A simple correlation between permeabilities and mercury capillary pressures. J Pet Technol 33(4):2488–2504
Tearpock DJ, Bischke RE (2003) Applied subsurface geological mapping- with structural methods, 2nd edn. Printice Hall PTR, Upper Saddle River, NJ, 822 p
Vavra CL, Kaldi JG, Sneider RM (1992) Geological applications of capillary pressure: a review. Am Assoc Pet Geol Bull 76:840–850
Vincelette RR, Beaumont EA, Foster NH (1999) Classification of exploration traps. In: Beaumont EA, Foster NH (eds) Exploring for oil and gas traps: treatise of petroleum geology, handbook of petroleum geology, vol 1. American Association of Petroleum Geologists, Tulsa, OK, pp 2.1–2.42

Ward RF, Kendall CGSC, Harris PM (1986) Upper Permian (Guadalupian) facies and their association with hydrocarbons—Permian Basin, West Texas and New Mexico. Am Assoc Pet Geol Bull 70:239–262

Weimer RJ, Sonnenberg SA, Young GB (1986) Wattenberg field, Denver basin, Colorado. In: Mast RF, Spencer CW (eds) Geology of tight gas reservoirs, vol 24, AAPG Studies in Geology. American Association of Petroleum Geologists, Tulsa, OK, pp 143–164

Wescott WA (1994) Migration pathways and seismic expression of a North American Giant: East Texas Field. In: Dolson JC, Hendricks ML, Wescott WA (eds) Unconformity-related hydrocarbons in sedimentary sequences. Denver, CO, The Rocky Mountain Association of Geologists, pp 131–134

Wrightstone G (2009) Marcellus Shale-geologic controls on production. AAPG annual convention. Denver, CO, AAPG Search and Discovery Article #10206, p 10

Wrightstone G (2010) A shale tale: Marcellus odds and ends, 2010 winter meeting of the independent oil and gas association of West Virginia, p 32

Zammerilli AM (2010) Projecting the economic impact of Marcellus Shale Gas development in West Virginia: a preliminary analysis using publicly available data. Department of Energy National Energy technology Laboratory, p 37

Chapter 3
Drilling, Mud-Logging, Wireline Logs and Cores

Contents

J. Dolson, *Understanding Oil and Gas Shows and Seals in the Search for Hydrocarbons*, DOI 10.1007/978-3-319-29710-1_3

Abstract Wells are drilled with mud or oil-based systems which allow stabilization of the well bore and prevention of blowouts from reservoir layers that have a higher pressure than the drilling fluids. Well site geologists and engineers monitor pressures and capture cuttings and core data while the well is drilled. If the well is drilled over-balanced, or with a higher equivalent mud weight pressure than the formation pressure, flushing of drill fluids occurs into the formations. This can cause suppression of hydrocarbon shows and can be recognized on wireline logs by separation of the resistivity profiles and the mud cake layers. Even core data is affected by invasion and saturations from conventional core will normally residual unless care is taken in handling the core and analyzing the uninvaded portions.

Casing strings are set to seal off problematic reservoir layers and become progressively smaller as the well deepens. Wireline logs measure a wide range of electrical, magnetic, resistivity or other properties and come in a wide variety of types and contracting companies. Logs come in both scanned (raster) and digital (.las ASCII) formats. Final well reports contain all in the information of the wells during drilling and production testing and are important to review carefully if available. Despite all the efforts to recognize oil and gas in a well bore, it is possible to not recognize key hydrocarbon shows and leave a productive zone untested or a productive well abandoned as a dry hole.

3.1 Historical Context Around Understanding Shows and Drilling Wells

People have been drilling wells for centuries. The oldest mechanical methods are those of cable tool rigs, mostly designed to drill a few hundred feet or meters in largely unconsolidated rock. The oldest mechanical wells were drilled using Chinese 'spring pole' technology documented as early as 450 BC using bent trees or levered bamboo poles which were pulled back and then rebounded, driving a chisel or other cutting device into the ground (AOGHS 2015). In the US, widespread use of spring-pole technology was first used to drill shallow salt brine wells in West Virginia in 1809.

Before long, this technology was adapted to steam driven cable tool rigs (Fig. 3.1) capable of drilling faster and deeper, but essentially the same 'percussion' drilling technology. The first use of a cable tool rig to actually drill an oil well was used in Baku, Azerbaijan in 1946 (Mir-Babayev 2002), and in the US in 1959 with the 69.5 ft. deep (21 m) Drake oil well discovery in Pennsylvania. Soon, cable tool rigs dotted the landscape globally.

Drilling an oil well is a complex, highly technical and expensive effort, operating like a small city with teams of drillers, geologists and engineers monitoring the wells. Costs are significant. Many onshore US wells vary from 1 to 15 million dollars per well. Offshore, costs can skyrocket to hundreds of millions of dollars. Operations in high arctic conditions may approach one billion dollars in total investment for a single exploratory well.

Most exploratory wells are drilled vertically, but many wells are drilled horizontally, or directionally, particularly in unconventional shale plays.

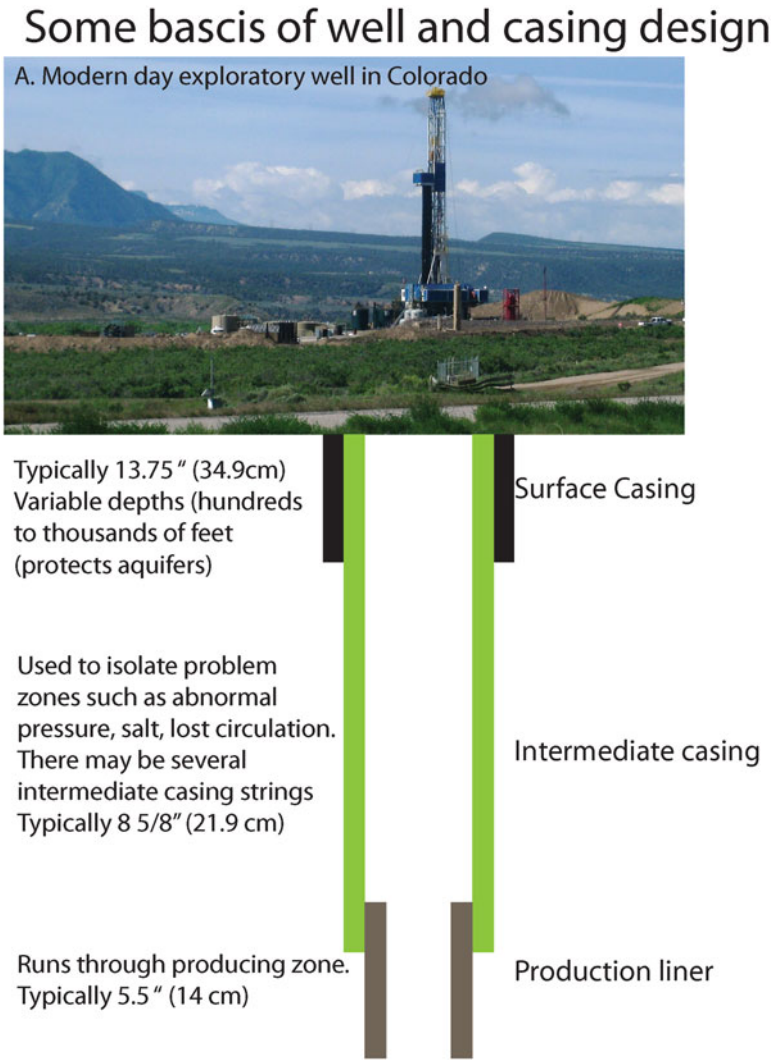

Fig. 3.1 Basics of well design. Steel casing pipe casing is set at various stages of the drilling process, becoming progressively smaller in diameter at depth. The pipe stabilizes the hole and protects aquifers from contamination. Intermediate casing is set over problem zones and more than one casing string might be needed in difficult drilling situations. Photo courtesy of Debbie Dolson

While the details of well design vary greatly, in basic principle, they all share some common characteristics (Fig. 3.1). Modern rigs use rotary drill bits in contrast to the earlier chisel technology. Wells are drilled in all conditions, from deep water offshore to harsh arctic conditions and are kept running 24 h a day if possible. Housing generally exists in trailers (onshore) or in living quarters (offshore). Workers offshore frequently spend a week or two on the rig and then a week or two home, working in rotations, but on call 24 h per day on the rig site.

Steel pipe in successively smaller diameter casing strings are set as the well is deepened. The location of the start of a new casing string is determined by the geology and pressures of the formations being drilled. The casing strings stabilize the hole and allow further well completion operations such as perforations and hydraulic fracturing to take place. Samples must be circulated to the surface, sampled and disposed of and drilling mud must be available as the wells drill. When the well is completed, an assembly called a 'Christmas tree' caps the well and allows the formation fluids to be sent to a pipeline or trucks to haul to market.

Many wells are drilled directionally from one drilling platform. The initial well is vertical, but the drill bit can be deviated as it deepens to horizontal or sub-horizontal positions to reach multiple formations from a single surface site. This helps reduce the 'footprint' of the drilling, allowing one platform to replace dozens of wells that would have to be drilled vertically over a large area to tap the same formations.

3.1.1 Horizontal Wells and Multi-Stage Fracturing

One of the most important innovations in the last 40 years has been horizontal drilling (Fig. 3.2).

Hydraulic fracturing was first done with dynamite in the 1860s, but the first successful applications with modern wells were in 1950. Since then, over 2.5 million

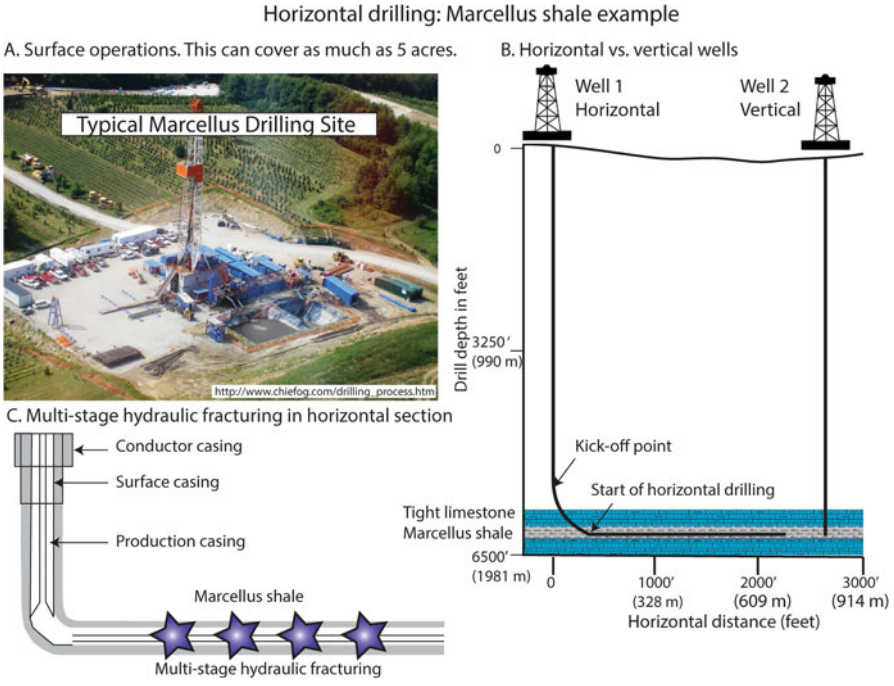

Fig. 3.2 A typical horizontal well set up. Horizontal wells are reaching extended drilling lengths of over 3 km on some wells. Figure modified from (Harper and Kostelnik 2013c)

wells have been hydraulically fractured worldwide. The process involves high pressure injection of liquids, typically a mixture of water and sand and other chemicals into a tight hydrocarbon-bearing formation which would normally not flow commercial rates in a simple completion. The fractures radiate out from the wellbore hundreds of meters, helping to connect pore systems and provide pathways for hydrocarbons to move through to the wellbore.

Explorers love to find high quality rocks that can be completed without hydraulic fracturing, but nature doesn't fully cooperate and many wells encounter tight, low permeability formations that simply won't give up their hydrocarbons without stimulation by fracturing. Horizontal wells offer huge benefits over vertical wells in tight rocks. A vertical well perforation, for instance, in the Marcellus Shale of Pennsylvania (USA), may be attempting to flow from a 15 m thick zone. A horizontal well put into that same zone, however, and run 900 m or more horizontally, accesses an enormous surface area relative to the vertical well. Some recent wells have exceeded 37,000 ft (11,227 m) in horizontal well lengths (PetroWiki 2015).

In a vertical well, one fracture treatment is enough. In a horizontal well, there will be multiple hydraulic fracture 'stages'. A typical Marcellus well may use up to 2.5 million gallons of water for one fracturing job. The frac fluid is pumped out of the well after the frac, allowing the gas and oil to enter the wellbore. Increasingly, hydraulic fracture fluids and water are being recycled for use on other wells, instead of being disposed of after treatment.

Good overviews of operations, geological and hydraulic fracturing factors affecting the Marcellus Shale play are covered by (EIA 2009; Engelder 2014; Hardage et al. 2013; Harper and Kostelnik 2013a, b, c; Wrightstone 2010).

Regardless of well type, samples are collected and analyzed on all wells and wireline logging tools are run into the hole to provide a quantitative assessment of the hydrocarbons present.

3.1.2 East vs. West: Evolution of Different Evaluation Techniques

The wealth from the Caspian Sea oil fields built up the financial empires of the Nobel brothers and the Rothchilds, among others. By 1894, the volume of oil produced annually in Baku equaled that of the US. Baku became the eastern-most cultural and industrial capital of Europe, with most of its oil going north to Russia. With the advent of the Russian revolution in 1917, the Baku oil industry went into a long period of decline until recently being re-vitalized after the collapse of the Former Soviet Union (FSU).

For the ensuing 90+ years under Soviet rule, the Azerbaijan and Russian oil industries developed technology which was largely not transported to, nor influenced by, the west. Driven by a deeply held desire to become energy independent of the west following the devastation in WWII, the Russian oil and gas industry

launched an exploration campaign that managed to find more oil and gas than any other country, often in very hostile arctic conditions and remote areas. Success was measured in footage drilled, and economics played almost no role in the strategy. In contrast, wells in the west would not be drilled unless some assurance was offered that what would be found would pay for the effort.

In evaluating Russian wells, a huge emphasis was placed on extracting core for direct examination of shows, rock type and quality. Traditional well logging techniques, however, relied heavily on resistivity tools (discussed later), in contrast to a much wider suite of tools developed during the same period in the west. Resistivity tools are still a huge part of both western and eastern technology, as they measure the conductivity of the rocks and fluids that currents are passed through. Salt water, for instance, is more conductive (less resistive) than fresh water, and will have a lowered resistivity measurement. Likewise, conductive minerals like pyrite can have very low resistivity. Oil and gas is resistive, however, and changes in resistivity in formations can also, therefore, indicate the presence or absence of hydrocarbons vs. water.

My first exposure to Russian logs and methodologies was in 1993, 4 years after the initial collapse of the FSU and only about 1 year after westerners were allowed to visit technical institutions in Baku and other locations. The result, for me, was a huge new learning curve in techniques to evaluate wells and understand oil and gas shows and ways to explore. The same held true for my Russian colleagues.

In contrast to most companies today, the Russian oil industry, for many years, was highly fragmented. Geophysicists, geologists, biostratigraphers, researchers, engineers and drillers were not only located in different buildings, but in different cities. Exploration was done largely with a drill bit, with seismic providing approximate locations, but with exploration departments that were funded to drill as many wells as possible. Academic institutions, therefore, placed a huge value on understanding how to evaluate a well, and core analysis provided much of that understanding, but with analytical technique that were much cruder than those developed in western companies. Highly integrated interdisciplinary teams which made maps honoring all the data were thus rare or absent, but are a trademark of companies operating today.

In the west, the success of the 1859 Drake oil well in Pennsylvania spawned a huge new industry. The oil boom that followed changed the face of the country, providing an abundance of a new source of energy to light homes, and soon, to power cars and planes. Driven by competition and capitalism, technology advances were rapid, but looking for seeps dominated exploration processes for many years. Ironically, it also saved the world's whale population, collapsing the demand for whale oil and effectively destroying the whaling industry. Oil exploration also exploded globally, notably with the Dutch East India Company (now Shell Exploration) which opened up Indonesia to oil and gas exploration and development at about the same time period.

This chapter covers the basics of western-style drilling, mud-logging and conventional wireline logs. In Chap. 6 we will look at some basic log analysis 'quick look' techniques and more theory behind how hydrocarbons are recognized

with wireline logging tools. The technological pace of change in how to evaluate and drill wells continues at a rapid rate, with new tools and techniques developed annually. At times, it is difficult to keep up with the innovations!

3.1.3 Seeps

In some parts of the world, seeps still play an important role in exploration. A large number of vendors continue to monitor and sell databases of 'offshore slicks and seeps' studies. Offshore, satellite imagery is used to spot oil slicks on the surface or at shallow depths on the sea floor. When possible, these seeps are sampled physically and the oil analyzed to determine its quality as well as other parameters such as possible source rock it originated from and the maturity level of that source rock. We touch in Chap. 8 on some of these geochemical techniques.

Offshore seeps databases seek to differentiate between oil slicks from leaky ships or sunken vessels and natural seeps on the ocean floor. These studies are often essential to purchase to understand potential in untested deep waters or even shallow water previously off-limits to exploration. Onshore, there are still many untested oil and gas seeps, especially in remote basins or countries with difficult access due to political or security issues. These seeps remain 'teasers', with nearby basins and potential traps either untested or poorly tested. Recognizing seeps, then, is still a major part of oil and gas exploration in many frontier areas.

Microseepage studies are another technique which looks for traces of hydrocarbons at shallow depths from subtle chemical alterations in the soil (McCoy et al. 2001; Schumacher 1999, 2012). Seeps and microseepage share a common characteristic of hydrocarbons migrating to the surface, often through tortuous migration pathways and even very long vertical and lateral distances.

Drilling near seeps, however, doesn't always guarantee a discovery. In the overthrust belt of Wyoming, seeps were so abundant that settlers going west to California in the 1800s stopped as they encountered them to lubricate the their wagon wheels with the oil. But over 52 dry holes were drilled in the overthrust belt before Amoco discovered the giant Ryckman Creek Field (Ploeg 1980). The trap, an overturned anticline, was below highly folded and faulted salt structures. The surface seep locations and surface anticlines had no physical relationship to the deeper thrusted anticlines that contained the giant fields. It took years to recognize the structural setting of the productive Jurassic Nugget Sandstones.

All that failure generated yet more bias and paradigms needing to be broken. Yet another Amoco top manager made that fateful comment "I'll drink all the oil and gas that comes out the overthrust belt". After the discovery of the giant Painter Field, he became remarkably silent.

Suffice it to say that seeps indicate working petroleum systems and the terminal point of migration of some sort of hydrocarbon system. Finding where oil and gas remains trapped downdip of the seeps requires a lot of effort, expense and imagination.

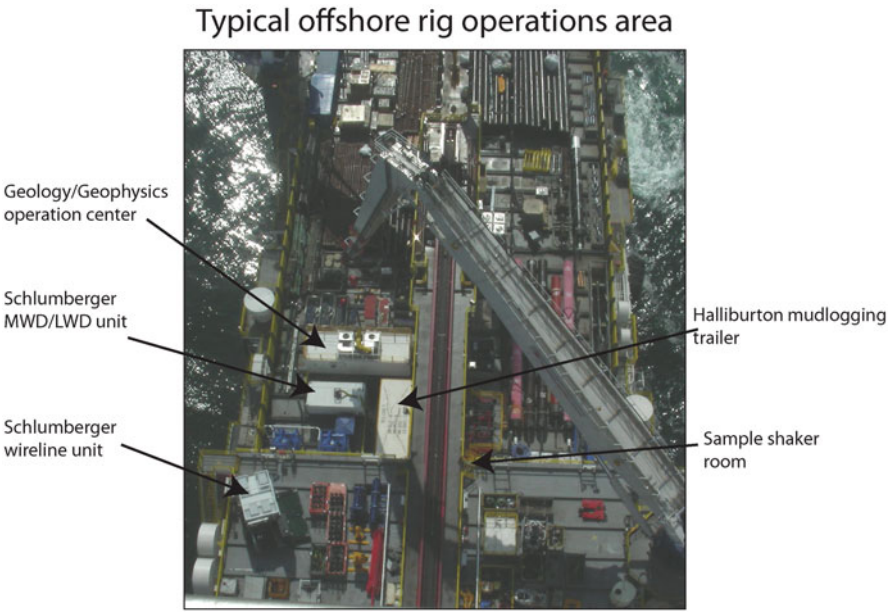

Fig. 3.3 Modern offshore rig operations setup. Modified from BP/Chevron Drilling Consortium course notes. Used with permission

3.1.4 Drilling with Mud

Just as concepts concerning exploration have changed dramatically in the last 100 years, so have the methods we use to drill wells and collect data. Cable tool rigs either operated with no fluids in the hole or water, which was used to wash cuttings up to the surface and help clean out the hole.

Lubricants like mud were not used in these rigs and the holes were generally shallow. Large chunks of rock came back from the drill string which were easy to look at and see both lithology and signs of oil and gas. I've read many old well reports from these kinds of wells, and they usually have very crude descriptions, in contrast to the kinds of descriptions developed later on as rig technology advanced. The main emphasis was on recognition of oil directly in the cuttings from odor or visual inspection, with less attention to the details of rock typing. Today's modern rigs (Figs. 3.1 and 3.3) capture enormous amounts of information, not just on the oil and gas shows, but the rock type, its ages, cements, mineralogy, grain sizes, sorting, and a host of other attributes.

In the earliest years of mechanical drilling, success was noted by oil flowing into the wellbore. In the northeast US corridor in Pennsylvania, Ohio and West Virginia, most wells flowed at modest rates. High pressure wells and blowouts did not occur, and water and air as a drilling medium worked well. However, by the late 1880s word was reaching the US of blowouts in Russia with huge rates per day of oil spewing out over the derrick floor and flinging hundreds of meters of steel pipe into the air.

'Gushers', while making great Hollywood stories, are unwanted results on a rig. Blow outs, in the early days of mechanical drilling, were far too common, and thousands of deaths occurred annually to unlucky drillers happening to be too slow to get off a rig before a blowout. Blowouts are still a serious issue and enormous effort is spent to avoid them. Despite that, as recently as 2010, 11 people were killed when BP's Deep Water Horizon well blew out in the Gulf of Mexico (DHSG 2011).

Perhaps the most innovative technology for drilling wells was the introduction of mud systems to pump into the drill string. The mud not only cools the bit, but chemicals are added to it to increase its density and the stability of the wellbore. The weight of the column of the mud helps hold back oil as the bit goes through an oil-bearing section. Because of both buoyancy pressure and the pressure of the formation itself, it is important to drill at least 'balanced' or 'slightly overbalanced' relative to the formation pressure. This ensures that the well will not suffer a catastrophic blowout.

Mud engineers are assigned to every well and monitor pressures while drilling from sophisticated equipment on the rig. Every geoscientist needs to understand the basic construction of a well, and the tools on rigs to capture information about the subsurface lithologies, pressures and oil and gas shows.

3.1.5 Wellbore Design, Pressures and Rig Safety

The first documented use of mud to stabilize a wellbore was in 1901 at the Lucas well at Spindletop Field in Texas (Clark and Halbouty 2000). Two brothers Al, age 24 and an ex-cattleman, and Curt Hamill, 28, an ex-salesman, stumbled into this breakthrough technology through intuition and innovation. The Hamills were using new steam-driven drilling technology instead of the customary cable tool rigs. Until the Lucas well, drillers had previously only used water to stabilize the wellbore (GeoExpro 2008). The Lucas well prospect was a ground-breaking discovery, opening up the oil industry not only to south Texas, but to the world because of the huge volumes of oil discovered and the new drilling technology used to develop it.

Like many breakthrough discoveries, it was a 'surprise' to the 'experts' of the day, as a local self-taught geologist from Beaumont, Texas, Patillo Higgins, thought an interesting hill near town that had oil and gas seeps bubbling around it might contain oil. Higgins, born into a prominent Texas pioneer family, was a local character. He had one arm, the other lost in a gun-fight, and a reputation as a local rogue obsessed with finding huge oil deposits in south Texas where none had been found before. He had tried drilling on the hill since 1893 but couldn't get deeper than 300 ft. (100 m) and was broke with no money to show for his efforts. No more prominent authority than the Texas State Geologist told Higgins his idea was foolish and he should get back to drilling for water instead. Higgins tried unsuccessfully to get his prospect drilled for over 8 years with no buyers and no luck.

Higgins's technical luck turned around when he met a naturalized American citizen from Austria who was a mining engineer and also a self-taught geologist, Anthony

Lucas, who shared his convictions of big oil in Texas. Lucas secured funding from backers from Pittsburgh, Pennsylvania (then the heart of the oil patch) to get the prospect drilled. Unfortunately for Higgins, the deal didn't include him in the royalties. From the start, the Hamill brothers had trouble drilling the well, as a high pressure water layer kept causing the wellbore to fill up with loose sand and stop the drilling. Frustrated, they looked across a field at a pond being trampled by a herd of cattle. In what might have been a pure act of desperation, they moved the herd to their drill site and had them churn up tons of mud which then they introduced into the wellbore.

Despite the desperate move, the trick worked, the wellbore stabilized and they were able to drill 24 h per day. At 347 m, the well blew out with a 50 m high gusher at rates over 100,000 BOPD, taking 9 days to bring under control. To control the blowout on a well gushing at such unprecedented rates, an event which had never been seen in the United States before, the Hamill's also improvised the first oil field Christmas tree, a device used to cap the well and divert the flow into a pipeline and out into open pits. Christmas trees, much more complex and sturdy than the one improvised on the fly back in 1901, are now standard parts of any drilling well and, along with blowout preventers, critical to control catastrophic blowouts.

As an aside, Higgins sued Lucas for $4,000,000 when the well came in and settled for a lot less. The oil boom launched a change that has reverberated across the last century, not just in the volumes of oil found in the field, but in the ground-breaking drilling technology which allowed a new era in drilling to begin.

3.1.6 Background on Muds, Mud-Weights and Circulation Time

The most important information coming from a drilling well are the cuttings and gasses which come up the drill string as the mud is circulated. These cuttings hold a wealth of information on lithologies, porosity, rock properties and most importantly, the presence or absence of hydrocarbons. Understanding this information is the first critical step in evaluating a formation for presence or absence of oil and gas.

Unfortunately, with the advent of modern day diamond bits, it is more difficult to evaluate the lithologies being drilled because many of the samples have been ground finely by the bit, in contrast to the earlier cable tool rigs and conventional bits which often circulated larger samples to the surface. In addition, there is a lag time involved between penetrating the formation and getting the samples to the surface which must be taken into consideration when deriving a mud log to display the lithologies of the formation. On top of this, the higher mud weights in the wellbore frequently creates a 'flushed zone' around the wellbore which pushes the formation fluids away from the wellbore, including the oil and gas that may be present. In some cases, the flushing is high enough that the shows are suppressed and unrecognized.

On a modern rig, (Fig. 3.3) there is generally a G&G (Geology and Geophysics) operating center, well wireline logging units, MWD/LWD (Measurement While

Drilling/Logging While Drilling) and a mud logging trailer. Staff working in these areas are responsible for full and continuous monitoring of the drilling activity and results. Daily geological reports are generated which summarize the drilling rates, oil and gas shows while drilling, estimated pore pressure from mud-weights and other tools, collection and filing of samples and often, on-site biostratigraphic evaluation of cuttings to determine the age of the formation being penetrated. Well site operation is a science unto itself, with great care taken to monitor the influx of gas into the mud system which might indicated a hydrocarbon bearing zone or indicate the presence of higher pressure gas zones that might be a problem for drilling and potential blow-outs. As such, safety is the first issue of any wellbore operation, but the capture and archival of the rock data is critical. An excellent on-line reference for well site operations geology is that of (Seubert 2004).

Samples arrive on a screened surface which is continuously shaken to loosen the samples from the mud. This area is called the 'shale shaker' and is where an on-sight geologist or technician retrieves and archives rock samples at intervals determined pre-drill by the drilling team and geologists. The samples are stored as both 'wet' and 'dry' samples and analyzed immediately at the rig with information on grain size, lithology, porosity, estimated permeability and oil and gas indicators. All of this information is captured in the reports and as spreadsheets of information which are later converted to digital curves used on workstations and in final displays with other data.

Three common reports are generated: (1) daily drilling report (2) daily geological report (3) end of well report. The drilling report summarizes all unscheduled events encountered (like sharp increases in gas or decisions to increase or decrease mud weight, records of the weight on bit, penetration rate, temperature and other key data. The daily geological report usually contains geological summaries of significant events and lithological descriptions, shows, biostratigraphic results, pore pressure evaluation, drill bit and casing design and a petrophysical summary. The end of well report summarizes the entire history of the well and is often required by state and governmental agencies as a record of the results.

3.2 Mud Logs, Gasses and Cuttings Descriptions

3.2.1 The Mud Log

Perhaps the most important tool for the geoscientist and engineer is the mud log (Fig. 3.4).

An excellent reference on mud logs is that of (Whittaker 1992b) and (Whittaker 1992a; Whittaker and Morton-Thompson 1992). The mud log keeps a record of the mud weights, flowing temperature in and out of the wellbore, mud salinity and resistivities, pit levels and volume, standpipe pressure, weight on bit, rotary torque and revolution, pump stroke rate, pressure, bit revolution and penetration by depth and time. 'Lag time' is the time delay or lag between drilling in a particular formation and arrival at the surface. The lag time varies by hole size, annular volumes

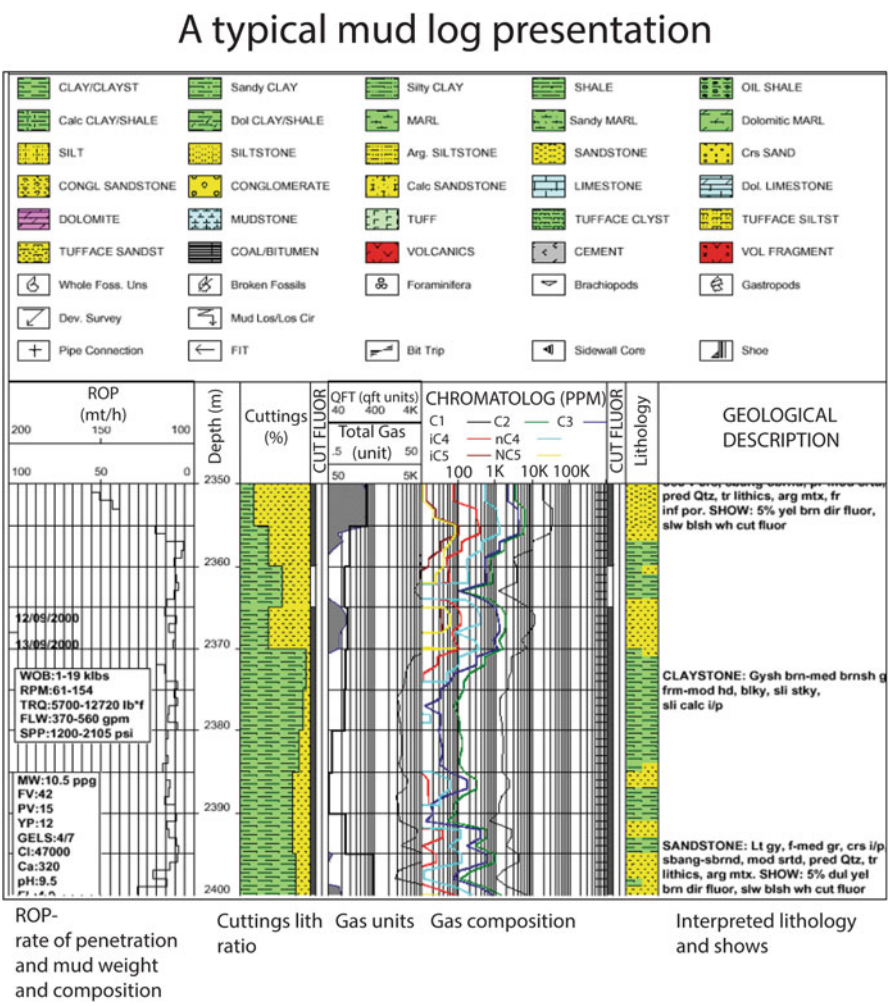

Fig. 3.4 A typical mud log presentation

(volume of mud in the pipe) and circulation rate. It is best described as the volume of the wellbore annulus and the volume of mud discharge by one stroke of the circulating pumps. An example of how to calculate lag time is shown in the Fig. 3.5.

For the final report, the cuttings descriptions are often adjusted to more accurately match information from the wireline logging done when the well is completed.

One of the more important things to note are gas readings commonly displayed in gas units and on a chromatalog in parts per million (ppm). Increases in gasses signify influx of hydrocarbons to the wellbore. Sharp increases may indicate an overpressured zone, perhaps near the top of an oil or gas column or simply a high pressured sand layer. When these 'gas kicks' are encountered, mud weights are

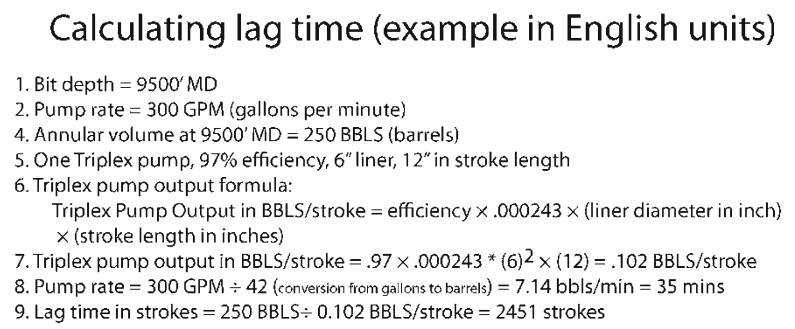

Fig. 3.5 Typical equations used on the rig to understand lag time and ways to mark which depths the shale shaker samples came from. Example for BP/Chevron drilling consortium course notes, by permission

often increased to prevent blow-outs over these intervals. It may also indicate the well is being drilled underbalanced and mud weight need to be increased for additional safety measures.

Mud gasses are commonly recorded from C1 to C5, but other components may also be measured (Table 3.1). Influx of C5 gasses may indicate an oil bearing zone vs. a pure gas bearing zone.

3.2.2 Analyzing Mud Gasses: Wet to Light Gas Ratio Analysis

Figure 3.6 shows the standard method of displaying these chromatogram records and determining fluid type (Haworth et al. 1985). Three types of curves are calculated from the mud log chromatogram data; Wetness, Balanced and CH ratios (see Fig. 3.6 for equations and definitions).

Wetness ratio (Wh) curves are generated by fraction of C_2–C_5 hydrocarbons to total C_1–C_5 hydrocarbons (in ppm) from the chromatogram. High Wh readings mean a lot of wet gas or oil in the system. Balanced ratio (Bh) curves are the fractions of C_1 and C_2 to C_3–C_5. The higher the number the lighter the gasses in the formation. The character ratio (Ch) is calculated as a ratio of C_4–C_5 gasses to C_3. Light gasses have a CH ratio under 0.5 and heavier gasses or oil a ratio greater than 0.5. Various cutoffs and idealized log displays are shown in Fig. 3.6. Of particular utility is the potential to differentiate residual from continuous (trapped) hydrocarbon shows, when the balanced curves are much lower than the wetness curves and the wetness curves >40. Residual shows are common in many basins and attempting to distinguish them from trapped oil and gas is a key part of understanding migration in any petroleum system.

Figure 3.7 provides a practical example from an offshore discovery in India. This discovery tested a new play concept of a deep water debris flow stratigraphic

Table 3.1 Mud gas classifications in mol % and common density measures. The heavier components (C_5 and higher) are often indicators of an oil or wet gas zone. Modified from Whitson (1992)

Component	Description	Dry gas Mol %	Wet gas Mol %	Gas condensate Mol %	Volatile oil Mol%	Black oil Mol%	Comments
CO_2	Carbon dioxide	0.1	1.41	2.37	1.82	0.02	
N_2		2.07	0.25	0.31	0.24	0.34	
C_1	Methane	86.12	92.46	73.19	57.6	34.62	
C_2	Ethane	5.91	3.18	7.8	7.35	4.11	
C_3	Propane	3.58	1.01	3.55	4.21	1.01	
iC_4	Isobutane	1.72	0.8	0.71	0.74	0.76	
nC_4	Normal butane		0.24	1.45	2.07	0.49	
iC_5	Isopentane	0.5	0.13	0.64	0.53	0.43	C_5 and higher are important possible oil show indicators
nC_5	Normal pentane		0.08	0.68	0.95	0.21	
C_{6s}	Hexane		0.14	1.09	1.92	1.16	
C_{7+}	Heptane		0.82	8.21	22.57	56.4	
Density measures							
GOR (SCF/STB)	Gas oil ratio (standard ft^3/ stock tank barrel)		69000	5965	1465	320	
OGR (STB/ MMSCF)	Oil gas ratio (stock tank barrels/million standard ft^3	0	15	165	680	3125	
API gravity	API gravity		65	48.5	36.7	23.6	

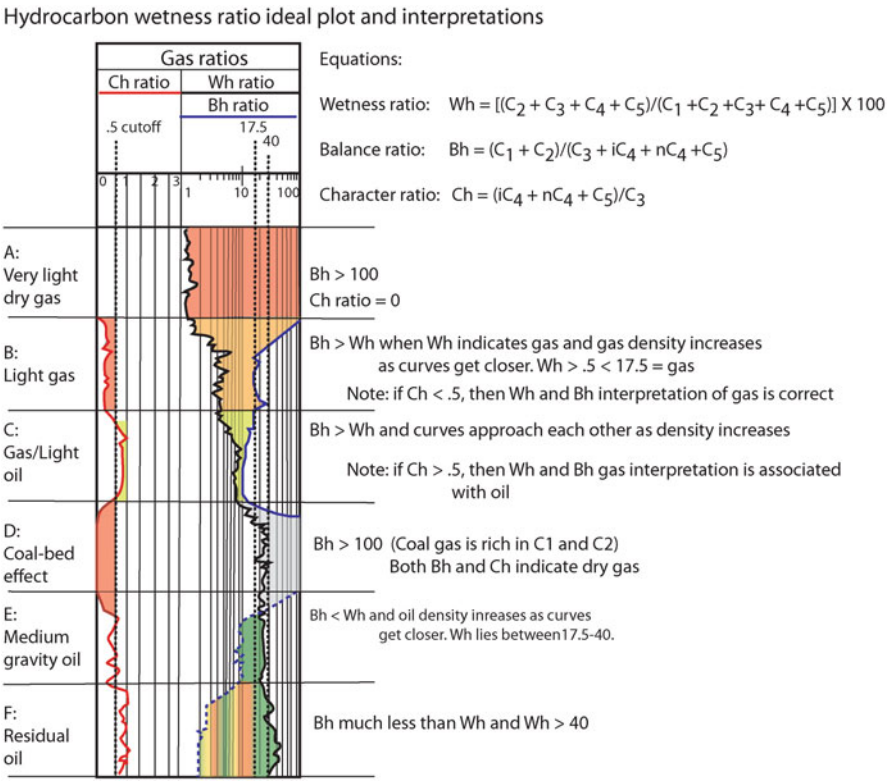

Fig. 3.6 Hydrocarbon wetness plots as a means of identifying fluid type from mud log gasses. Modified from Haworth et al. (1985)

trap. The trap has a long hydrocarbon column, but in low permeability and poorly sorted rocks with meso and micro pore throats. Hence, the best saturations are only seen in the top portion of the trap, where buoyancy pressure is highest. But with hydraulic fracturing, the well flowed substantial rates from a number of zones. The increase in total gas (Tgas) vertically, and the accompanied widening of the gap between the Wh and Bh curves confirms that the gas content is higher at the top of the trap than at the base.

Of additional interest is the long section from 4151 to 4331 m that never goes below 50 % Sw. This is due to high bound-water in tight, shaly sandstones. Water of this type of tight reservoir remains attached to the pores in the reservoir and cannot be produced, but contributes to a percentage of water calculated in the reservoir. Despite the 50–60 % water saturations, the well did not test water. Chapter 5 deals with the concept of relative permeability as a function of rock type and explains how shaly, high water saturation wells can flow oil with no water recovery.

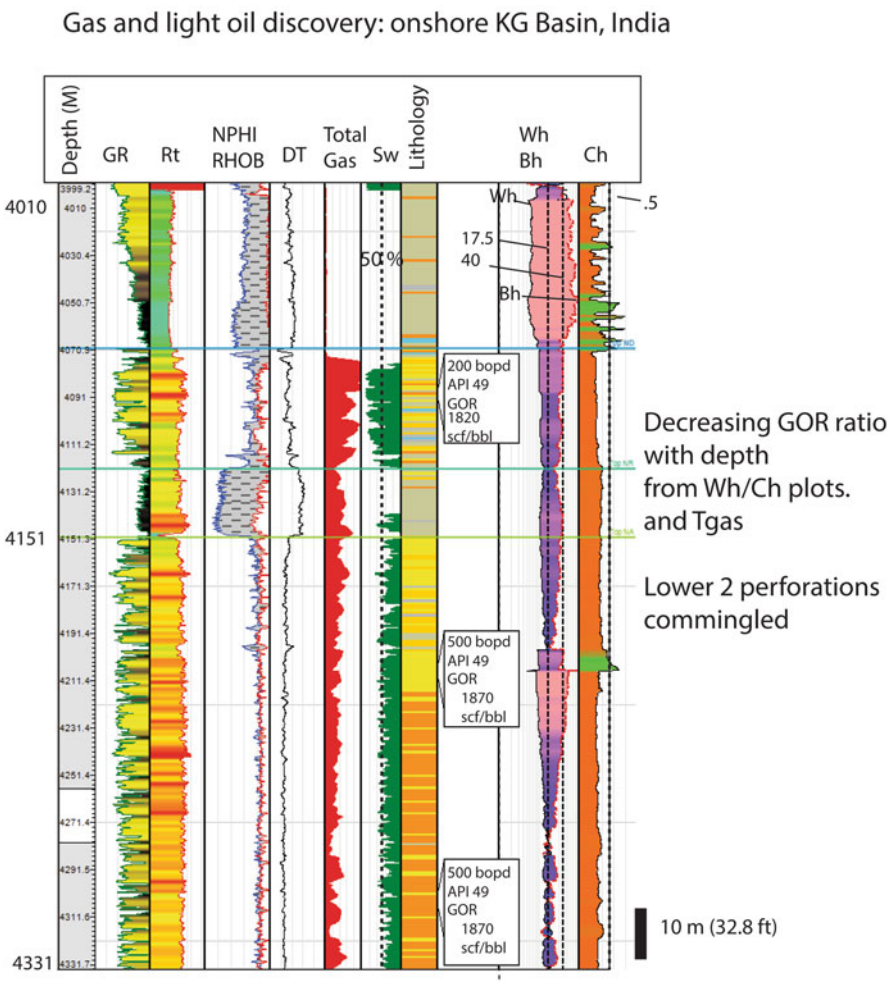

Fig. 3.7 Use of gas chromatography analysis to identify gassy oil zones, offshore India Cretaceous deep water debris flow. Figure courtesy of Cairn Energy India, Pty. and Shubhodip Konar and Bikashkali Jana. GR = gamma ray; Rt = True resistivity; NPHI = neutron porosity; RHOB = density (g/cc); Sw = water saturation. Figure courtesy of Cairn India. Used with permission

3.2.3 Wellbore Flushing and Over and Underbalanced Drilling

Chapter 4 deals with pressure in much more detail, but a brief discussion is needed to understand the concept of wellbore flushing. As described in Chap. 2, pressure-depth plots are used to estimate formation pressure, connectivity between producing zones, seal capacity and other data pertinent not only to an evaluation of the trap and prospect, but for safe drilling of a well. The causes of over or underpressure in wells

Table 3.2 Pressure gradients. Modified from BP-Chevron Drilling Consortium course notes. Used with permission

Mud Weight in LB/GAL (ppg)	Pressure gradient in PSI/FT	SG (specific gravity)	KPa/M (Kilo-Pascal/m)	Term	Comment
1.0	0.051948	0.12	1.18	Unit equivalencies	Conversion units to translate to mud-weight
<8.3	<0.433			Underpressure	Gradients less than fresh water density
8.3	0.433	1.00	9.9	Normal pressure	Fresh water gradient
8.6	0.446	1.03	10.3	Normal pressure	Salt water gradient
9.0	0.467	1.08	10.6	Mild overpressure	Highly saline salt water
12.0	0.624	1.44	14.2	Moderate overpressure	
13.0	0.676	1.56	15.3	Moderate overpressure	
15.0	0.780	1.8	17.7	High overpressure	Difficult wells
19.2	1.0	2.31	22.5	Maximum overburden pressure	Onshore, this is an approximate for the pressure from the overburden rock layers. Offshore, overburden pressure varies.

are varied, but can come from hydrocarbon generation, rapid burial, basin uplift and erosion and other factors discussed in the next chapter. Gradients and definitions of over and underpressure are shown in Table 3.2.

From a drilling perspective, the drillers want to have a mud column weight that is approximately equal at depth to the pressure of the formations being drilled. In any drilling well, fluids from the mud system will flush hydrocarbons away from the wellbore (Fig. 3.8) and the degree of flushing and depth of invasion is dependent not just on the pressure differential between the mud and the formation, but formation permeability. The flushed zones are studied in detail in any well for information needed for log analysis, as tools that measure the hydrocarbon saturations need to have information measured away from the wellbore in the unflushed zones not contaminated by drilling mud.

There are three types of drilling situations:

1. Underbalanced (mud weight below the pressure of the formation)
2. Normally balanced (mud weight approximately equal to the formation pressure)
3. Overbalanced drilling (mud weight more than the formation pressure).

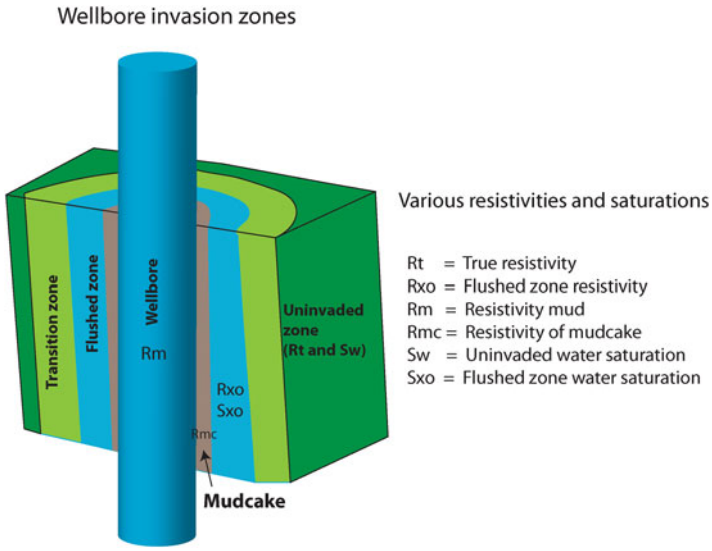

Fig. 3.8 Well bore invasion created by drilling mud. The resistivity measurements (Rm, Rxo, Sxo and Rmc) reflect changes in salinity of fluids away from the wellbore. Rt is the true resistivity (salinity) of the formation, and is in the uninvaded zone

Table 3.2 shows typical gradients and pressures associated with different pressure regimes and mud weights. Gradients lower than that of fresh or salt water are considered underpressured. Normally pressured zones have mud weights equivalent to fresh or salt water. When gradients exceed salt water densities, the formations are overpressured. Hard pressure or high overpressure occurs when gradients exceed 0.78 psi/ft (15 ppg). While the causes of these variations in pore pressure are varied, from a drilling perspective, it is critical for safety and wellbore stability to predict pressure ahead of the bit and have the right mud weight when entering any zone that might flow.

If overpressured conditions are not anticipated, most wells are drilled with balanced mud weights or slightly over or underpressured. Figure 3.8 illustrates formation invasion from drilling fluids when drilling through a formation. If the well is underbalanced, invasion profiles are generally not very deep. The permeability of the formation may also be a factor in depth of invasion.

When pressure is anticipated, over-balanced drilling is usually done for safety reasons. In these cases, invasion profiles may be fairly deep. From a shows standpoint, the more over-balanced a well is, the more the oil and gas shows are suppressed at the wellbore. In some cases, this is enough that a formation with good hydrocarbon saturation is actually drilled with no shows logged. The invading fluids can also damage the formation by clogging up pore systems. A damaged

wellbore may never flow hydrocarbons to the well, despite them being present in the formation.

Underbalanced drilling is an excellent way to avoid formation damage, limit invasion and minimize the flushed zone (Bennion and Thomas 1994; Jacobs 2015). Overbalanced drilling has an additional problem of potentially sticking the drill bit, cores or logging tools against the formation, often resulting in having to junk (abandon) the well and drill a new hole or sidetrack. This is common when drilling in producing fields where production withdrawal from a zone may have lowered the pore pressure more than anticipated. Having 'stuck pipe' myself in at least one situation like this, I can personally attest to how unsettling it is to management and drillers to have to drill a new well and junk the old one from failure to get the pore pressure right.

It is possible to drill through an oil zone and not recognize it because of an overbalanced mud weight where shows were suppressed or not recorded. That is a situation that every geoscientist fears on any well. There is no worse fate for a geologist than to appraise a well as dry only to have someone come in years later and drill right next to it and make a discovery. On the other hand, for the astute explorer, a careful analysis of old dry holes frequently yields new insight and recognition of by-passed pay or near misses that were not properly followed up on by the original operators. Understanding the drilling mud weights and formation pressures is a key part of this kind of post-appraisal.

Interestingly, in unconventional shale plays, thousands of wells have been drilled through what are now productive source rock intervals that had few to no shows in the prior wells. Even when drilling the shale zones underbalanced, low permeability kept the oil and gas shows from the wellbores. As explorers were looking for conventional pays in other zones, these highly productive shale intervals went unrecognized for over a century in many basins.

The zone of flushing of hydrocarbons around a wellbore is important to understand in detail and to quantify. Logging tools can record the resistivity of formation waters at various depths away from the wellbore. If the formation contains salt water, and the well is drilled with fresh water, zones nearest the wellbore will be much less saline than a zone not flushed by the drilling fluid itself. A layer of mud forms at the edge of the formation being penetrated. This "mud cake" thickness can be guide to the permeability of the rocks and depth of invasion. Three major zones exist: (1) the flushed zone, where salinities are close to those of the drilling fluid (2) the transition zone, where more and more formation water is encountered and (3) the uninvaded zone. Well log analysis attempts to resolve the resistivities and salinities of all of these intervals. Invaded zones are given a subscript of xo (like Rxo, Sxo) and the true resistivity of the uninvaded zone is indicated as an Rt. Mud cake resistivity is given as Rmc.

Because hydrocarbons are resistive electrically, if they are present in a formation, the resistivity measured will usually be higher than that of an adjacent water bearing

zone. Exceptions can occur due to mineralogy of the formation itself, but that is subject for a later chapter. The essence of hydrocarbon analysis from logs is based on observations of changes in resistivity in a formation that yields higher resistivity values than expected from layers with 100 % water saturation.

3.2.4 Cuttings and Oil Shows

Oil shows are detected in cuttings by examination under a microscope and recording the ultraviolet fluorescence. Several outstanding references cover the topic of sample and show evaluation (Paul et al. 1992) and (Swanson 1981; Swanson and Fogt 2005).

Solvents such as chlorothene, acetone, alcohol, hot water and acid are used to liberate oil from cuttings (Fig. 3.9). Visual stain indicates hydrocarbons have been in the rock at some time in the past and may be present now. But a lack of visual stain does not mean the formation is barren of oil. Because of the flushing in the near well bore, samples may be retrieved that have had their hydrocarbons repressed while drilling.

Hydrocarbons normally fluoresce in ultra-violet light, but so do many minerals. Dolomite, aragonite, limestones, some shales, anhydrites and other minerals may fluoresce and give a false indicator of oil. An astute mud-logger may identify these as 'mineral fluorescence' in the mud log. In addition, some muds have additives of diesel fuel or oil-based muds which make recognition of real oil shows more difficult.

'Cut fluorescence' is oil liberated from the cuttings by a solvent and will normally be designated as such on the mud log. Color of the sample in plain light, under ultraviolet light, the cut color and liberation rate, intensity and residue are all captured. In highly permeable zones, the cut may be a very rapid 'flash cut' while in low permeable reservoirs, it may be described as 'bleeding', slow streaming or slowly blooming. Table 3.3 summarizes most of these physical tests.

The color of the oil stain can be a guide to its API gravity and fluid type. The lighter the color of the oil staining, the less dense the hydrocarbons (Table 3.4).

In addition, odor is often also recorded, even if other shows are not present. Comments such as 'faint odor' or 'strong odor' can be significant observations in the absence of direct fluorescence, where it is possible to drive off the hydrocarbons during the sample drying process. Odor will only be present in the heavier hydrocarbons, as lighter gases like methane and butane are odorless.

3.2.4.1 Residual Shows

One of the more problematic issues with oil shows are residual oils. (Schowalter and Hess 1982) and O'Sullivan et al. (2010) summarize many ways to recognize residual hydrocarbons in a well. Residual hydrocarbons indicate accumulations or migration pathways that no longer contain connected 'continuous filaments' of oil and gas across the pores. They cannot be produced with conventional completion techniques. Residual shows are common in paleo-oil water contacts, paleo-oil fields

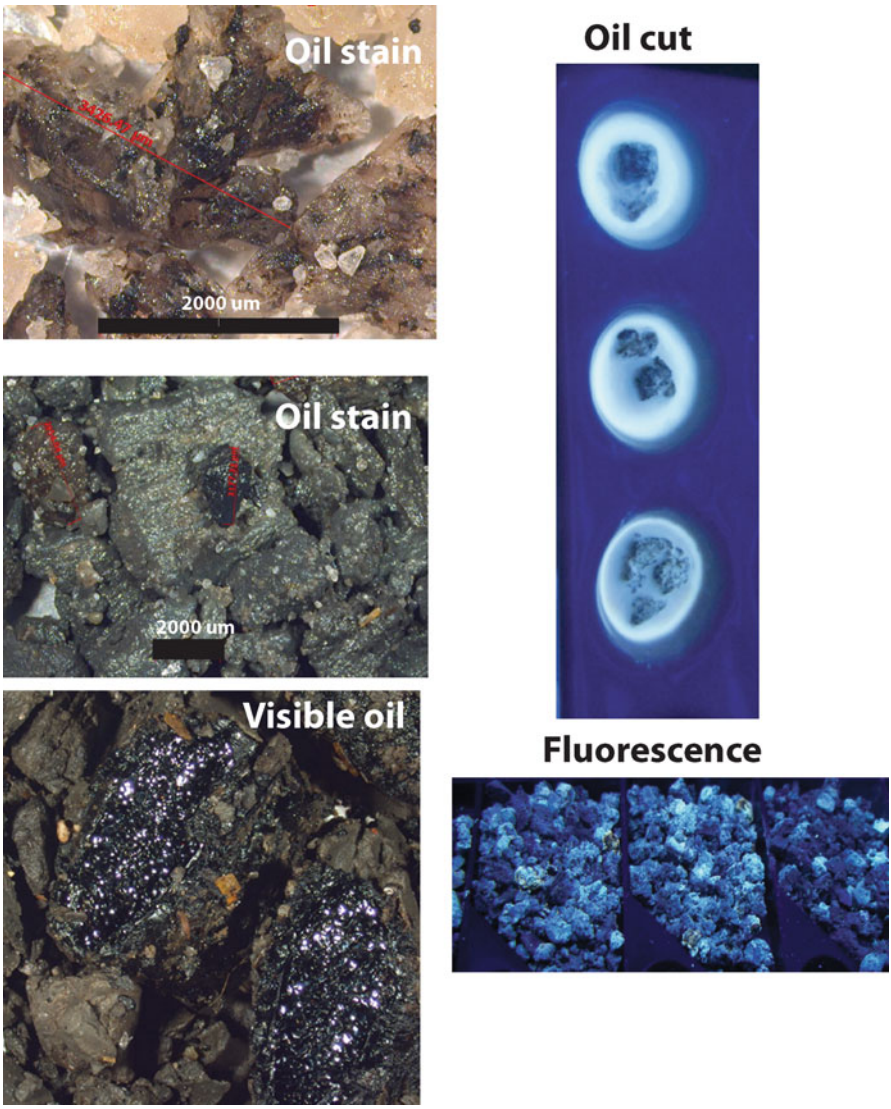

Fig. 3.9 Examples of oil shows in cuttings. Photos courtesy of BP-Chevron Drilling Consortium course notes. Used with permission

and along migration pathways. They can easily be mistaken for continuous phase shows.

Some heavy oils may not fluoresce at all. Frequently, the term 'residual' cut is seen on a mud log. A residual cut occurs when there is a fluorescent ring or residue left after the solvent is evaporated. However, the term 'residual cut' does not necessarily mean the sample is a 'residual show'.

Table 3.3 Cut and fluorescence terms and tests. Modified from Swanson (1981) and Swanson and Fogt (2005)

Term	Definition
Acetone test	Good for heavy hydrocarbons, not recommended for routine detection.
Acetone-water test	Powdered rock placed in a test tube with acetone added and then filtered to another test tube where water is added. A milky white dispersion occurs if there are hydrocarbons.
Bobbing test	Used in limestones. Samples are dropped in a beaker of dilute hydrochloric acid. Carbon dioxide gas from the reaction is released. If hydrocarbons are present, it traps the gas, causing the sample to bob up and down in the beaker as bubbles form.
Chlorothene test	Most common reagent. May become contaminated after a long time period.
Cut	Hydrocarbon extracted with a reagent.
Cut fluorescence	Also called 'wet cut'. The most reliable test. Done on dried samples in pure solvent. Often described as have 'streaming cuts' in porous rocks or slow bleeding cuts (tighter rock).
Dead oil	Thermally dead solid hydrocarbons that will not fluoresce or give cut. A frequently misused term.
Hot-water test	Water at least 170 °F (77 °C) added to unwashed cuttings. An oil film observable under ultra-violet light forms if oil is present.
Iridescence test	Observable in a wet sample tray. Iridescence without stain may be light oil or condensate.
Pyrolysis test	Samples placed in thick-walled test tube and placed over a propane torch. Oily brown residue may be produced. Useful to for identifying unconventional source rocks but will not produce a result in over-mature source rocks.
Residual cut	Cut that doesn't stream, but leaves a fluorescence ring or residue in the dish after the reagent evaporates.
Wettability test	Drops of water on the surface will not soak into the surface if hydrocarbons are present.

Table 3.4 API gravity and fluorescence and oil color. The lighter the color, the lighter the hydrocarbons

API Gravity	Color	Comments
Below 15 api	Brown	Heavy oils, possibly residual tars.
15–25 api	Orange	
25–35 api	Yellow to cream	
35–45 api	White	
Over 45 api	Blue-white	Approaching condensates.

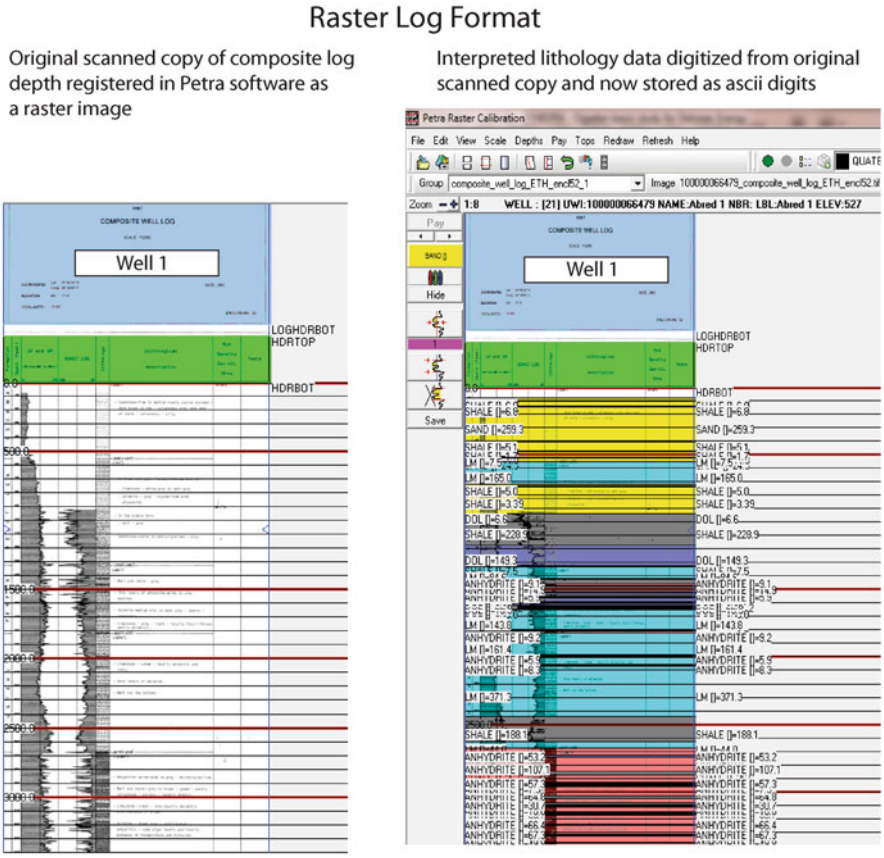

Fig. 3.10 Example of a scanned image of a well log that has been depth registered in a workstation (*left*). On the right are hand-digitized lithologies captured from the logs and text on the original raster. These interpreted lithologies are stored as ASCII curve data, and subsequently be used for calculations or display in cross-sections

3.3 Basics of Well Logs

3.3.1 Well log Formats: Digital vs. Raster

Wireline logs are essential tools to understand. There are hundreds of types of logs and many different service companies. New tools are invented annually, making it challenging to keep up with advances. In this section, we look at the most basic log types used to understand lithology, porosity and to calculate water saturation using resistivity measurements.

Before the widespread use of computers, service companies logged wells and stored the data in tape libraries and delivered multiple hard copy prints of the logging information which was then stored in company well files. To understand these logs, geoscientists had to visit the company library, check out the hard copy logs and work with them in their offices. The work was cumbersome and slow. Stratigraphic and structural cross-sections using the well logs were tedious to make. Log analysis of water saturation and porosity was done manually, reading the curve values directly off the hard copy and calculating with hand-held calculators, often with the aid of numerous charts provided by service companies.

A decision to add a new well to a cross-section required re-doing the existing cross-section and making more hard copies. Millions of these hard copy logs were generated over the last century and the original tapes often lost over the years or degraded to the point they were no longer readable. I am personally thrilled to see the hard copy log period vanish.

With the rapid acceptance of personal computers in the 1980s companies began to collect the old hard copy logs and scan them for use on workstations. Today, these types of log displays are termed 'raster logs'. Any scanned image of a well log can be loaded to a workstation (Fig. 3.10) in multiple formats and then have the depth scale registered so that the image can then be displayed and worked with in digital cross-sections. The scanned images frequently capture not only the curve data, but any annotations written on the logs and lithology and show information.

As computer usage increase, service companies began to provide logs in digital format, often binary files which required specialty software to read, but more often, in .LAS format (Log ASCII Standard). These records are much easier to share and load very quickly to a geological workstation where they can be used quantitatively. Cross-sections can be drawn quickly and scaled to any depths and wells added or dropped as needed.

Figure 3.11 shows some overall views of .las files on a workstation. The digital files can be viewed quickly as curve data (A), or as numerical digits (B). LAS file headers have the same structure and provide basic information on the well, its location and what curves are contained in the file (Fig. 3.11c).

3.3.2 The Well Header and Common Logs

Table 3.5 lists many of the most common well logs run at any well site. This is just a partial listing as there are many log acronyms and many different vendors (Table 3.6).

One of the vexing issues with digital data, however, remains records lost on older wells that are not contained in a .LAS file or found on raster images. One of the most important pieces of information is the log header table (Fig. 3.12). Without a detailed end of well report, the well header information may be the only type of information telling what kind of mud system was used, which logs were run and what the temperatures and resistivities were of the drilling fluids. This information

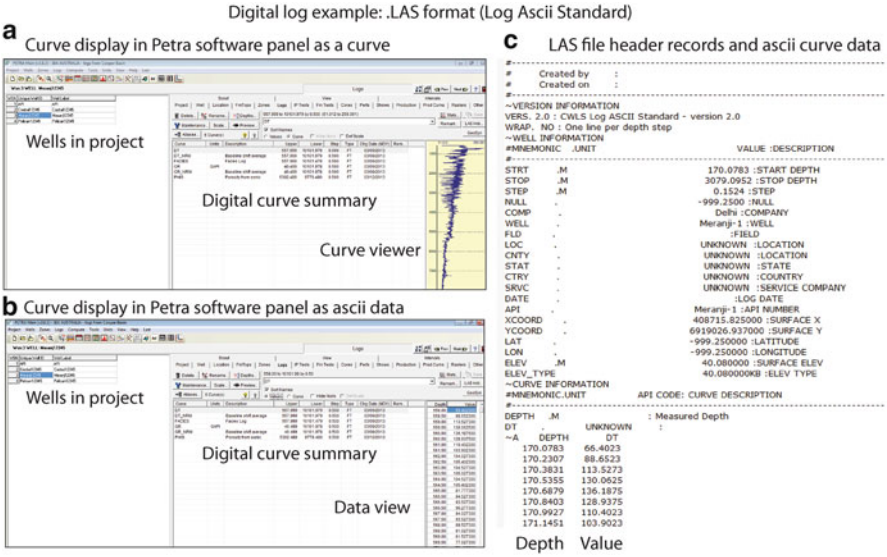

Fig. 3.11 LAS format digital logs. (**a**) Displayed in a summary panel as a curve view (**b**) displayed as digits (**c**) input .las header file with well information

is needed to help determine the salinities and resistivities of the drilling fluids and formation at depth. Temperature corrections have to be made to any measurements of fluid resistivities recorded at the surface. In the absence of this kind of information, many assumptions have to be made about temperatures and salinities critical to well log analysis. The only available information is the well header is not available may be from offset wells only.

3.3.3 Common Log Displays and the Basics of Log Interpretation

Once the data is ready in a workstation, various 'templates' can be set up to display the log data for analysis and visualization in geological cross sections, or even displayed on seismic. Typically, log templates place logs which are indicators of lithology in the left-most track (track 1), a depth track in the center, and resistivity logs in track 2 immediately right of the depth track, and porosity and water saturation and other curves in more tracks to the right. Comments, information on shows, tests, perforations and other data can also be stored in tables and displayed on the same log templates. The result is a quick visualization of the well information in ways meaningful to the individual interpreter.

Figure 3.13 provides a good example. A digital lithology track has been added next to the track 1 which is displaying an SP (spontaneous potential) and GR

Table 3.5 Common log types and their uses. See (Asquith and Krygowski 2004a) for a much more comprehensive review of these logs and log analysis

Log name	Uses	Comments
Caliper (CALI)	Measures hole size and shape	
GR (Gamma ray)	Measures natural radioactivity. Useful for lithology identification and measuring shale content.	Low readings normally indicate a clean reservoir, but some reservoirs can be radioactive (common in sandstones interbedded with volcanics), in which case the GR log can look like a shale, with high readings.
SP (Spontaneous potential)	Records direct current voltage (called potential) between an electrode in the well and one fixed at the surface. Used for lithology and identification of permeable zones.	One of the oldest logging techniques. Can be used to determine the formation water resistivity (Rw). In hydrocarbon zones, it is often suppressed, giving an indicator of oil and gas saturation.
Resistivity (R)	Measures electrical resistivity of a formation. Critical in determining pore fluid type	
Density	Measures the bulk density of the matrix rock in the formation. Used to determine lithology and porosity.	
Neutron	Measures the amount of hydrogen in a formation. Used to calculate porosity and identify gas zones.	
Sonic	Measures travel time in the formation. Used to calculate porosity and lithology.	A key log used by geophysicists to generate synthetics and time-depth relationships for seismic sections. Critical to have to view logs on seismic sections, which are usually displayed only in two-way travel time.

(gamma-ray) log. These are two of the most common logs used to identify potential reservoirs layers. Scales are set so that deflections to the left generally are showing increasingly better quality reservoirs. Deflections to the right are showing higher shale content. It is common to pick a 'shale baseline' from one of these curves and use that baseline to quantify what is pure shale and what is a shale free carbonate or sandstone reservoir.

The resistivity (track 2) displays an ILD log (induction lateral log deep), an MFL (micro-spherically focused log) and an SFL (spherically focused log). The ILD log reads the deepest of all logs into the formation and the MFL log the shallowest. As a result, these three logs are used to measure the resistivity of the fluids in the flushed, transitions and uninvaded zones. The ILD has the best chance in this case of reading the true formation resistivity. Sometimes, corrections need to be made to the ILD log based on depth of invasion to extrapolate to Rt (true formation resistivity).

Table 3.6 Some log types, acronyms and uses

Log name	Name	Comments
LLD	Deep laterolog	Measures Rt in the uninvaded zone.
AND	Azimuthal Density Neutron	Combination porosity, lithology, dipmeter and hole size logs (acoustic caliper).
ARC	Array Resistivity Compensated	Resistivity and GR log combination.
BHC	Borehole compensated sonic	Designed to minimize effect of borehole sizes variations. Usually measured in μs/m or μs/ft (microseconds per meter or foot).
CALI	Caliper	Measures hole size and shape.
CGR	Total Gamma Ray minus Uranium	A log curve from the SGR tool.
CMR	Combined magnetic resonance	A type of NMR log enhancing precision of the tool. Often can be run in combination with MDT pressure recording devices (Chap. 4 covers pressure tools).
CNL	Compensate Neutron Log	
Density logs	Measure bulk density (RHOB) and matrix density	General unit of measure is in g/cm^3. Density porosity estimates require a knowledge of the fluid in the pore system and the matrix density of the formation. Bulk density (RHOB) measures the density of the fluids and the rock. The matrix density is the density of the solid lithology and does not take into account porosity.
DPHI	Density derived porosity	Corrections need to be made for fluid type as well as matrix type to derive this curve.
DRHO	Density correction curve	The curve shows the amount of corrections made to the RHOB curve due to hole size or mud cake thickness. It is usually in g/cm^3 or Kg/m^3.
DT	Sonic log (travel time)	A key log used by geophysicists to generate synthetics and time-depth relationships for seismic sections. Critical to have to view logs on seismic sections, which are usually displayed only in two-way travel time. This is also a common porosity tool and used in lithology identification.
DTCO	DTCO (compressional slowness computer downhole)	Used for pore pressure calculations, seismic velocity, porosity and lithology.
FDC-CNL	Formation Density and Compensate Neutron log combination	The most widely used measurement for porosity and lithology identification.
FMI	Formation Micro Imager	Measures micro-resistivity and produces images and analysis which can reveal thin-bedded lithology, sedimentary structures and formation dip and strike directions.

(continued)

Table 3.6 (continued)

Log name	Name	Comments
GR	Gamma ray	Measures natural radioactivity. Low readings normally indicate a clean reservoir, but some reservoirs can be radioactive (common in sandstones interbedded with volcanics), in which case the GR log can look like a shale, with high readings.
ILD	Deep induction log	Reads the deepest into the formation to measure Rt (true resistivity of the uninvaded zone).
ILM	Medium induction log	Measures resistivity of the invaded zone.
LLS	Shallow laterolog	Measures resistivity in the invaded zone (Ri).
LWD	Logging while drilling	Tools are run right behind the drill bit. Saves rig time, so it saves cost. Borehole conditions are close to the original state so there is less caving and generally less invasion. In some high angle wells, it may be the only tool that can be used.
MRIL	Magnetic resonance imaging log	A type of NMR log used in laminated, shaly reservoirs to enhance resolution and accuracy where other logging suites might underestimate resistivity.
Neutron logs		Measure hydrogen content. Very susceptible to pores filled with gas. When filled with gas the reported porosity is much less than the formation porosity. This decrease in apparent porosity is called gas effect and in combination with density porosity logs, can identify gas zones.
NMR	Nuclear Magnetic Resonance	Uses magnetic responses to estimate porosity and fluid types, mostly in the invaded and mixed zones. Porosity measurements can be less susceptible to lithology changes.
NPHI	Neutron porosity	Porosity calculated from the neutron log
OBMI	Oil-Base Micro Imager	A type of micro resistivity imaging using oil-base mud systems. These images, like an FMI log, allow visualization of thin beds, stratigraphy and structural dip and strike.
PEF	Photo electric curve	Used to determine lithology from density logs.
RHOB	Bulk density	A very common measurement, usually in g/cm^3. It measures the total density of the entire formation (both matrix solids and fluids). Matrix density, in contrast, would be the density of the rock framework in the absence of porosity.
Rxo	Microresistivity	Measures resistivity in the flushed zone (Rxo).
SFLU	Spherically focused log	Measures resistivity in the flushed zone.
SGR	Spectral Gamma Ray	Used to break out different radioactive elements, like uranium, potassium and thorium. Useful for shale identification, recognition of radioactive reservoirs that might look like shales but are not, source rocks, potash, clay types and fracture detection. Measurements are in API units.

(continued)

Table 3.6 (continued)

Log name	Name	Comments
SNL	Sidewall Neutron log	Susceptible to hole size.
SP	Spontaneous potential	One of the oldest logging techniques. Can be used to determine the formation water resistivity (Rw). In hydrocarbon zones, it is often suppressed, giving an indicator of oil and gas saturation. It records the direct current voltage (potential) between an electrode at the surface and another at the well. It can also be a good indicator of permeability.
SPHI	SPHI (sonic porosity)	A porosity estimate made from interval transit time.
WIRELINE	Logging that is done after the well is drilled.	This is done after the hole is drilled. It is less expensive than LWD, wider ranges of measurements and generally more accurate than LWD. 'Hostile environment' tools are available to log difficult sections not possible with LWD.

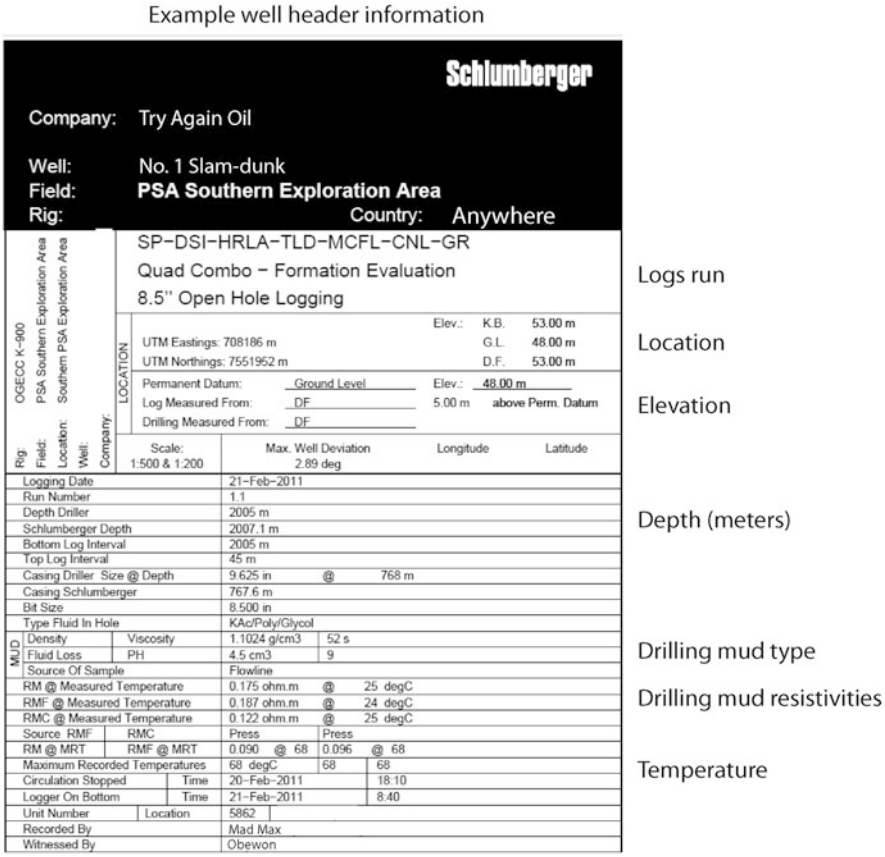

Fig. 3.12 Scanned copy of a log header to a well. Information contained in this part of a hard copy log is essential to understand many details necessary to interpret the logs. Unfortunately, many log headers have been lost over the years. Mud type, temperature and information on logging runs are just some of the data needed to do more quantitative work on a well log

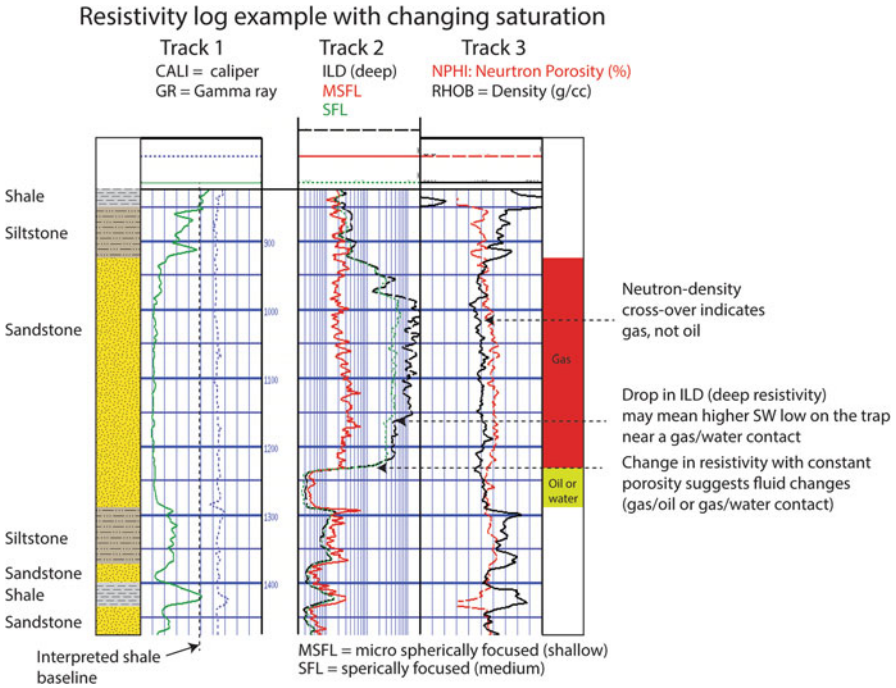

Fig. 3.13 Example of a simple well log template display with logs indicating lithology on the left, and logs showing resistivity and porosity on the right. Modified from Schroeder (2004), AAPG online well log lecture

In track 3 are NPHI (neutron porosity) and RHOB (density) logs. These are commonly run to estimate the porosity of a formation and for identification of gas zones. The NPHI log is displayed in porosity units and the RHOB in g/cc. The density log can also help define the rock type, as rocks like limestones, dolomites, or anhydrites, for instance, are much higher density than sandstones or shales. The neutron log measures the amount of hydrogen in the pore system. At the scales shown on this For example, when the neutron log 'crosses over' the RHOB log and shows less porosity than the density log this is called a 'gas effect'. Neutron-density cross-over is a very good quick look for gas saturated zones.

Figure 3.13 also illustrates an important point on how to recognize resistivity changes that might indicate hydrocarbons vs. water. In track 3, the density log over the thick sandstone remains relatively constant, as does the neutron log. This signals that the lithology is of one type and constant porosity. The GR and SP logs support that interpretation. However, in track 2, the resistivity logs show changes with depth. At 1250 m, the resistivity in all the resistivity logs drops suddenly to a very low value. This indicates, then, a change in fluid content, as the rock type and porosity has been shown to be constant over that interval.

This change is very probably due to the presence of hydrocarbons. The gas effect show on the NPHI/RHOB cross-plot is a zone of high resistivity, consistent with highly resistive gas in the formation and not water. It is not possible without further

work to tell if this drop at 1250 m is due to an oil zone with lower hydrocarbon saturation or a water zone, but it certainly no longer looks like gas. So the basal part of the sandstone might be water, with a gas/water contact at 1250 m, or it could be an oil zone with a gas/oil contact at 1250 m.

This is the essence of log analysis.

3.3.4 Gamma Ray (GR) and Spontaneous Potential (SP) Logs

GR and SP logs are routinely used to identify 'clean' reservoir horizons, usually sandstones or carbonates. The GR log, in particular, is used to quantify the amount of shale in a formation as radioactivity is generally associated with shales. So GR values that exhibit high readings often have high shale content. Exceptions occur when radioactive reservoirs are encountered.

SP logs have great utility as they can be used to quantify formation water resistivity, identify permeable zones and often indicate hydrocarbons directly as the curve may be suppressed over an oil or gas zone. SP logs respond to fluid changes in the formation, whereas the GR does not. The direction the SP curve deflects is afunction of the different salinities of the drilling mud (Rmf-resistivity of mud filtrate) vs. the formation fluids (Rw). The SP curve is generally shown with a negative value on the left and a positive value to the right. When the Rmf = Rw, no current is generated and the curve remains flat. If the Rmf > Rw (fresher water filtrate vs. a more saline formation water), the deflection is to the left. If Rmf < Rw (mud filtrate more saline than the formation water), the deflection is to the right. An example is shown in Fig. 3.14.

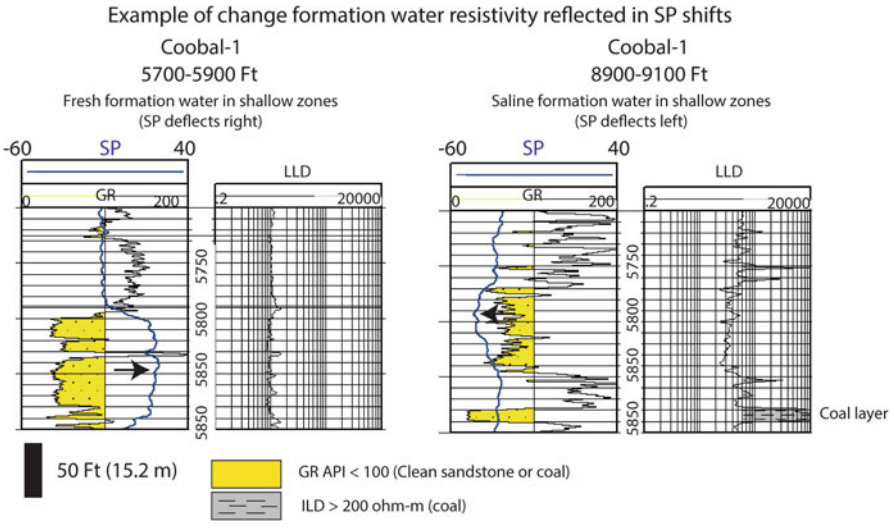

Fig. 3.14 SP deflections in clean sandstones indicating fresh formation waters at shallow depths and saline formation waters at depth, relative to the Rmf (mud filtrate resistivity)

If the resistivity of the mud filtrate is known, then the deflection recorded by the SP curve can be used to calculate the formation Rw. Getting the formation Rw right is critical to calculate hydrocarbon saturation. More of this will be covered in Chap. 6, but good references are provided by Asquith and Krygowski (2004c) and Hartmann and Beaumont (1999).

3.3.5 Porosity Logs, Volume of Shale Calculations and Total vs. Effective Porosity

It is important to remember that porosity tools do not measure porosity directly. Rather, they measure things like travel time (DT), density (RHOB) and liquid filled porosity (NPHI). All three of these families of logs are affected by lithology as well as gas and oil content. Calculation of porosity is a key step in log analysis and will be touched on further in Chap. 6, but more detail is covered in many publications and through charts provided by service companies. Excellent summaries are available in a number of publications (Asquith and Krygowski 2004b; Krygowski 2003; Krygowski and Cluff 2012). Commonly, these tools are used in combination with one another to determine both lithology and porosity.

Porosity calculations also respond to clay minerals in pore systems. The large surface area of clays and micro-porous pore systems can have very high total porosity, but virtually no permeability and micro or nanno pore throats. Without stimulation with hydraulic fracturing or natural fracture networks, these shales, even if saturated with hydrocarbons, will not flow. I like to think of this as analogous to a screen door in the house. The total porosity of the screen is nearly that of the open door, but nothing passes through the screen. Slashing the screen with a knife is analogous to a fracture porosity network, allowing things to pass through and the micro-pores to be connected.

Many pure shales, for example, may have a total porosity (PHIT) >30 %, but virtually no effective porosity (PHIE). Effective porosity is the amount of porosity in a system which can actually contribute to moveable hydrocarbon saturations. This is important, as clay minerals in the pore systems of some reservoirs inhibit permeability and contain a considerable amount of 'bound water'. As stated earlier, bound water is molecularly attached to the clay particle itself, but is not producible in a well. It will, however, show up as a percentage of water in a log calculation. Wells with highly shaly reservoirs can have water saturations as high as 80 % and still flow 100 % oil.

Creation of a volume of shale (Vsh) curve not only allows discriminations of siltstones, shaly limestones or marls or other clean lithologies, but is used to calculate a PHIE curve. Calculating a Vshale curve normally uses SP or GR logs. A shale baseline (Fig. 3.15) is established at the lowest values marking the maximum shale content.

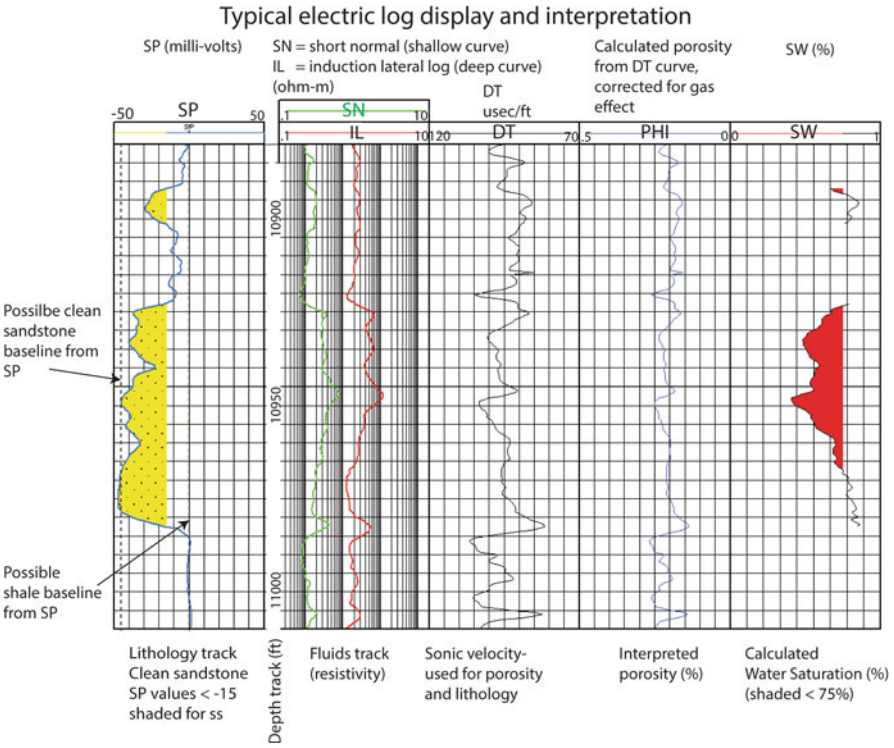

Fig. 3.15 Other curve displays and ways to find a shale baseline for calculating the volume of shale in a formation. Original .las curves from Asquith and Krygowski (2004a)

The Vsh curve itself is calculated from Eq. 3.1. This formula which uses GR logs values, but could also use SP values over short intervals:

$$Vsh = \frac{GRlog - GRmin}{GRmax - GRmin} \tag{3.1}$$

The maximum value (GR_{max}) is determined by visual inspection of the highest value and then that value is set as a 100 % shale baseline. The same is done for the minimum value (GR_{min}), which is assumed to be a clean formation. Various cutoffs can then be set to display clean sandstones, siltstones, shales or ratios of shaliness.

Figure 3.16 shows a Vsh curve overlain on a GR curve, as well as resistivity, porosity and interpreted PHIE curve.

A simple way to use Vsh to convert PHIT to PHIE is given by Eq. 3.2:

$$PHIE = PHIT \times (1 - Vsh) \tag{3.2}$$

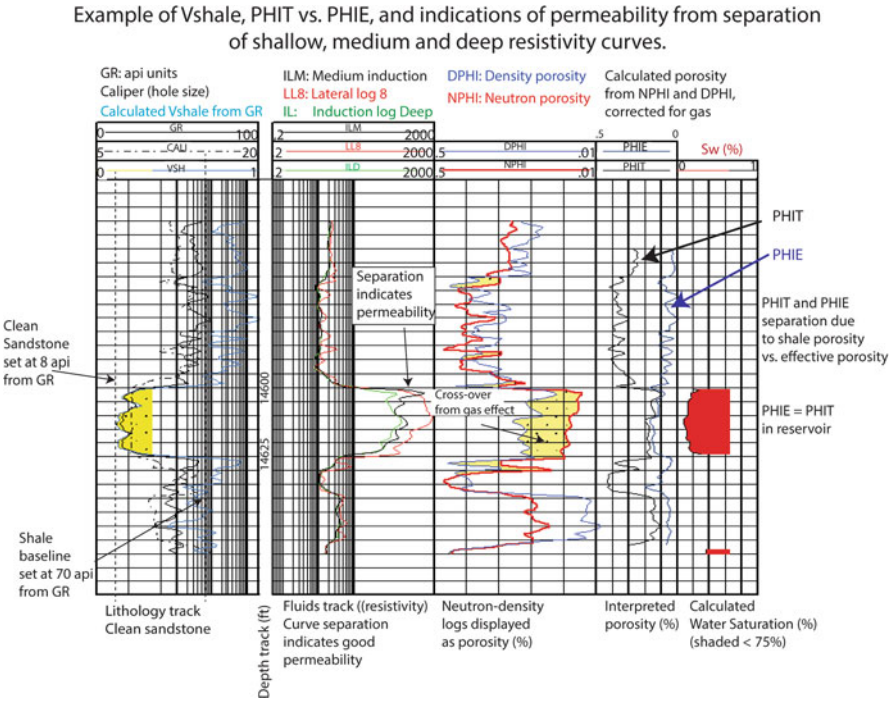

Fig. 3.16 More log curves, gas effect and calculation of a Vshale curve (track 1) to quantify shale percentage in a formation. Original .las curves are from Asquith and Krygowski (2004)

A zone with 50 % Vsh (like a silty sandstone), might have a total porosity (PHIT) of 20 % but the PHIE value will calculate to 10 %, greatly reducing the calculated volume of oil or gas in place in the reservoir. The separation of the PHIT and PHIE curves in Fig. 3.16 indicates the degree of shaliness. When the separation is zero, the formation has little to no clay.

3.3.6 Quick Look for Gas Effect and Permeability from Resistivity Profiles

Figure 3.16 also shows good separation of the resistivity values from the short, medium and deep induction logs. This is a good qualitative guide to permeability, indicating some significant invasion into the formation. When the separation is small, formations are frequently fairly tight with low permeability. This is a good quick look technique to estimate prospective horizons that might flow easily. Also shown on Fig. 3.16 is classic neutron-density cross-over. In the presence of gas, the neutron log will read considerably lower than the density porosity. This is one of the reasons that service companies so routinely run FDC-CNL logs, which are combination tools that measure both density and neutron porosity.

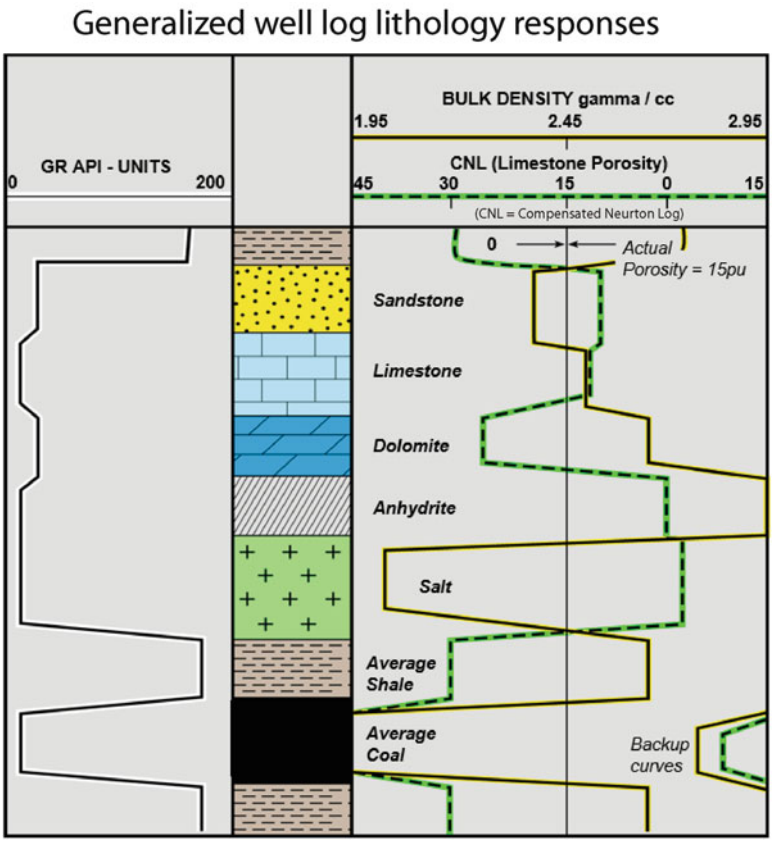

Fig. 3.17 Schematic of responses of various log types to changes in lithology. Digital lithology logs are a critical part of mapping any reservoir bearing intervals. Figure courtesy of BP/Chevron Drilling Consortium course notes. Used with permission

3.3.7 Calculating Lithology

A full discussion of this topic is beyond the purpose of this chapter, but Fig. 3.17 shows some typical log responses to various lithologies. Lithology determination, when done well with logs, should match the sample descriptions and provide good adjustments to porosity calculations which are affected by the matrix of the formation itself. Combinations of a variety of tools provide the best solutions. Surprisingly, it is not uncommon to have a lithology calculated or described incorrectly, leading to errors in analysis or even missing an oil zone completely. Cross-checking the log interpreted values against what has been described in samples is an important quality control on any well.

3.4 Capturing and Interpreting Core Data

3.4.1 Core Data

There is no substitute for cores to understand the details of a formation. Core and sample data remain the only information that is not inferred from other tools like wireline logs and seismic. Core data provides the litmus test to calibrate all log interpretations and gives a direct measurement of porosity, grain size, sorting, cements, lithology and pore-throat distribution and saturation. Slabbed cores also give definitive insight in the sedimentary structures critical to determining depositional environments, as well as higher resolution biostratigraphic sampling for age data.

Core is, however, expensive and time-consuming to acquire, so a lot of thought goes into why and how to capture core data. Core data basically comes in two types (Fig. 3.18), sidewall and conventional cores.

Sidewall cores have the advantage of being made after the well is drilled and logged. Zones of interest can be accurately sampled by the sidewall coring tools.

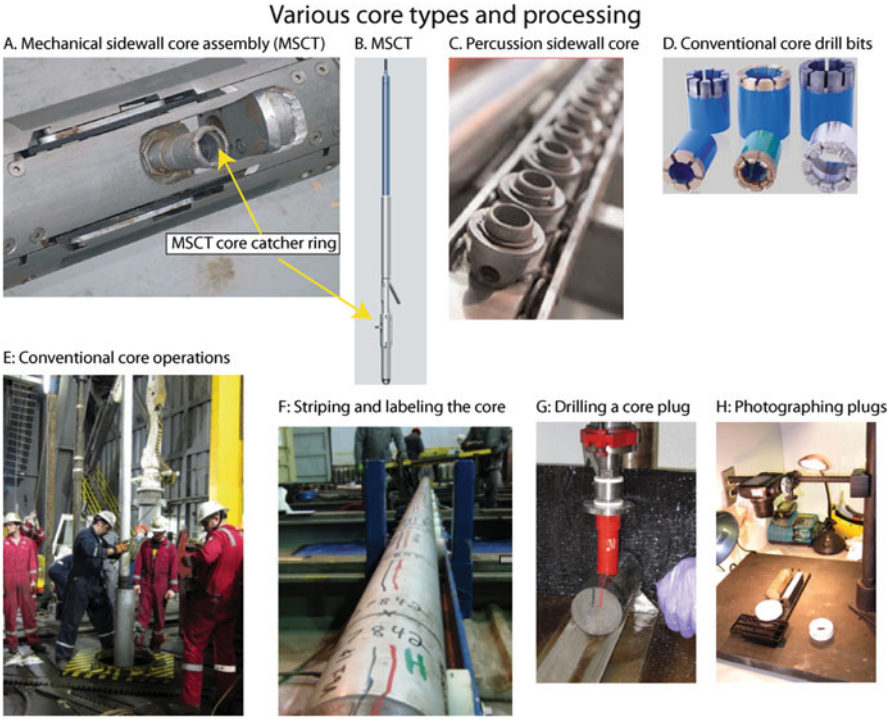

Fig. 3.18 Types of cores and some core handling procedures. Photos courtesy of BP/Chevron Drilling Consortium course notes, used with permission

There are two approaches: (1) mechanical sidewall coring (2) percussion sidewall coring. The sidewall coring assembly is lowered into the wellbore and pressed against the side of the formation at designated intervals. Plugs are taken by small rotary drill bits and retrieved with the core catcher ring. Percussion cores utilize small explosives to extract a plug from the formation, often inducing fractures in the process, an unwanted result, but may be the only way of capturing data in un-cemented reservoirs.

Conventional coring uses a variety of drill bits and coring assemblies to capture an entire section of rock. Where to start the core or 'core point' is determined by geologists on-site from mud log and drill rate data based on a prediction of where the formation in question is located. This is termed 'heads up coring'. Since the section has not yet been drilled, the cores sometimes miss the key horizon or start too late and drill below it. To avoid this, many companies do 'by-pass' coring'. By-pass coring involves drilling a straight hole first and logging it. Later, a drill hole is cut in the side of the first hole above the desired formation to core and a second hole started parallel to the first borehole. The second hole is then cored, since the chance of missing the formation now is greatly minimized.

When conventional cores reach the surface, they are laid out on the derrick floor and striped to record which end is the top and which is the bottom, as well as marked to indicate the depths of the core. If this is done incorrectly, the core might end up being displayed upside down, something that causes a lot of problems for interpreters! During one of my first trips to Baku in 1994, we cut a core at the giant Gunashli Field for a detailed petrophysical study. On the rig site, we were shocked when the core reached the surface and was not striped or labeled. Worse yet, the core was broken into three vertical pieces, each to be sent to a different department for analysis. After a bit of haggling, we convinced our counterparts to keep the entire core, stripe it and label it so we knew which was top and bottom and later, to slab the core in vertical slices so that each department could then have part of a continuous core of the entire interval. Sadly, I cannot tell you how many cores I have examined that have not been labeled correctly, and had the rocks out of order or upside down!

Additional great care is taken in the sealing of the core with many methods beyond the scope of this short overview, some of which is summarizes succinctly in (Bajsarowicz 1992).

3.4.2 Saturation Changes in Coring

One of the prime reasons to cut core is to measure directly the hydrocarbon saturation in the formation. As in a wellbore, however, invasion of drilling mud occurs during the coring process (Fig. 3.19).

This is shown visually in Fig. 3.19a, where core from the giant Mangala Field in India (O'Sullivan et al. 2008) has a rim of invasion from the drilling fluid. In the center of the core however, the rock has not been invaded. Core plugs are often cut

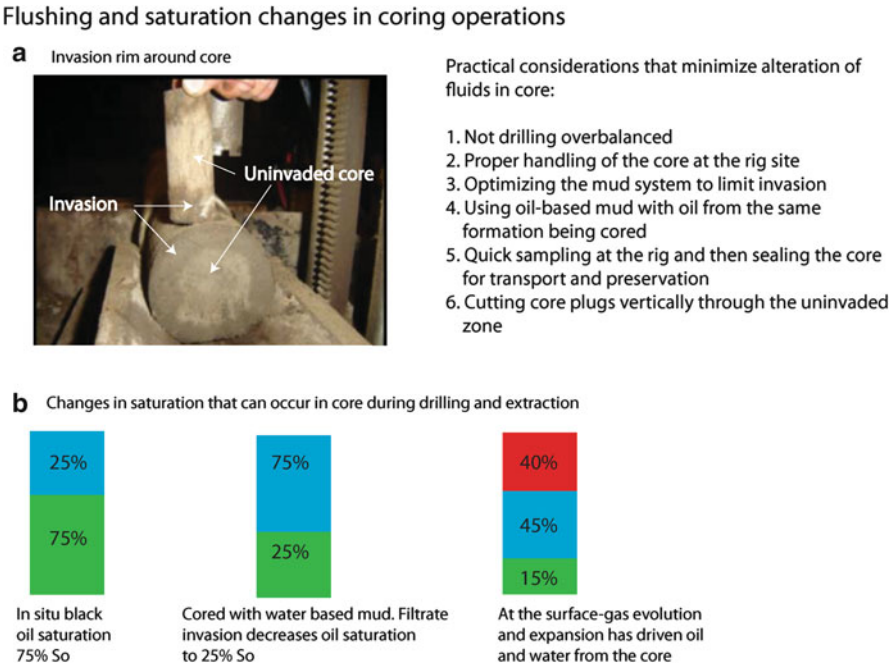

Fig. 3.19 Fluid changes and invasion during coring. (**a**) modified from O'Sullivan et al. (2008). (**b**) adapted from Bajsarowicz (1992)

vertically into a core like this to sample the uninvaded zone. A number of ways to minimize invasion are summarized in Fig. 3.19. Foremost of these is trying to drill the formation at a pressure approximately equal to that of the formation, or to even drill it underbalanced if necessary. Tracer chemicals can be put in the mud system and then analyzed in the core to determine zones that have not been affected by mud filtrate.

In addition, because of pressure and temperature changes from the in-situ hydrocarbons in the formation, saturation changes occur (Fig. 3.19b) which can substantially change the final saturation at the surface. Differences in how much the Sw analyzed in a core vs. what is in the subsurface can be substantial, depending on the type of drilling and methods of core capture.

As a result, relying largely on the saturations measured in a core as the right saturations for a formation can be misleading. If the core has been extensively flushed or miss-handled in preparation or storage, the Sw values can be much higher than in the actual formation, leading to pessimistic interpretations.

In another Russian example from as recent as 2006, I watched a Russian technician hosing down a core with water to clean it off so the geologist would be able to see the sedimentary structures better. Unfortunately, the core was still whole core waiting plugging and analysis for hydrocarbon saturation. I suspect whoever looked at those core results was perhaps a bit surprised at the high water saturations encountered!

3.5 How to Miss Good Hydrocarbon Shows and Case Histories

3.5.1 Ways to Miss Hydrocarbon Shows

There are, surprisingly, many ways to miss hydrocarbon shows and leave an oil pool behind. More examples will be covered in Chapter 8, but Table 3.7 summarizes a few.

3.5.2 Suppressed Resistivity and 'Hot Gamma Ray' Reservoirs

The pitfalls listed in Table 3.7 need to be thought about when evaluating any well or old dry hole. More thorough discussion of pitfalls from log analysis are covered more extensively in Chapter 6, but it is worth mentioning here that some minerals can cause real confusion when recognizing reservoirs or pay zones. Radioactive reservoirs, for instance, will have 'hot' gamma ray signatures that

Table 3.7 Common ways to miss hydrocarbon shows

Activity	Comment
Sloppy mud-logging by poorly trained personnel.	All too common, as many entry level positions are filled on a rig by poorly educated geoscientists or technicians.
Overbalanced mud systems.	Particularly common in unconventional shale reservoirs or low permeability zones where no influx of gasses occurs.
High mud filtrate loss into formation and lost circulation.	
Failure to collect samples at the shale shaker.	
Controlled drilling where drill breaks in porous formations are not recorded.	
Shaly sandstone reservoirs or finely laminated sandstones and shales that look like shale or siltstone on a log but contain permeable layers beyond the vertical resolution of the tool (covered in Chap. 6).	This is very common in turbidite systems and any depositional environment where thin (centime scale) reservoir layers are interbedded with shales or siltstones. The zones end up looking wet or shaly instead of charged and permeable.
Formations with conductive minerals like pyrite that cause 'pay zones' to look 'wet' on wireline logs (covered in Chap. 6).	Very common in some formations and especially common in shaly, laminated reservoirs where conventional resistivity logs fail to accurately measure formation resistivity (next chapter).
Lost circulation material.	
Cavings from previously penetrated beds.	
Radioactive sandstones or other lithologies that are misinterpreted as shales.	

look like shale. These kinds of reservoirs occur in both carbonates and sandstones, most commonly associated with volcanics, but also common along unconformities due to digenetic changes or in any setting where radioactive minerals are precipitated in a reservoir. A good case history is shown in the next section in the Williston Basin.

In other cases, interstitial clays or cements like some varieties of chlorite or pyrite are conductive enough that the resistivity curves are suppressed and look like water on logs. While many wells are adequately tested, missing oil and gas pools because of conductive minerals is not uncommon. An example is recognition of a significant oil leg beneath gas in the Inhassoro Gas Field in Mozambique (Trueblood 2013) where zones that looked wet on wireline logs due to their low resistivity, were actually oil pools. The discovery of oil within this field occurred in 2003, 38 years after the initial gas field discovery. The suppressed resistivity was due to a mineral called glauconite, which was noted in the sample descriptions, but the oil shows were overlooked.

In addition, resistivity tools themselves can have limited resolution and in reservoirs with thinly bedded reservoirs intermixed with clays, the resistivity curves, as well as the GR logs, are subdued, making the formations look wet or like shales. A good case history of this is shown in the Barmer Basin in the next section and this topic is covered in more detail in Chap. 6.

3.5.3 Case History 1: Russian River SE Field: "Hot" Dolomite and by-Passed Pay, Williston Basin, Montana

An excellent example of using basic shows and logs to locate a missed field is that of the discovery of the Russian River SE field (now called Simon Butte Field). The author is indebted to Tim Schowalter, who provided the case history background. In 1978, Amoco drilled the Wolberg No. 1 well (Fig. 3.20). A good mud log show in the Silurian Interlake Formation was not tested, and despite good mud gas readings with levels consistent with other offset producers, no shows were recorded. A shallower test was a misrun and a deeper perforated interval at 12,477–12,488 ft. swabbed 5 barrels of oil and 87 barrels of water over 9 h. After repeated completion attempts, this deeper zone flowed 6 barrels of oil and 145 barrels of water per day. The well was subsequently plugged and abandoned.

The recovery of free oil demonstrated that a trap existed at least at the deep level. In 1988, a geologist named Jim Courdin re-examined this well in more detail, focusing on the mud log shows in the Silurian. While the samples clearly identified the zone as a dolomite, the GR log had a 'hot signature' that, to the novice, might look like a shale. However, both the neutron and density logs indicated this zone was not a shale. In addition, the resistivity logs showed excellent separation from deep to shallow, indicating the zone was permeable.

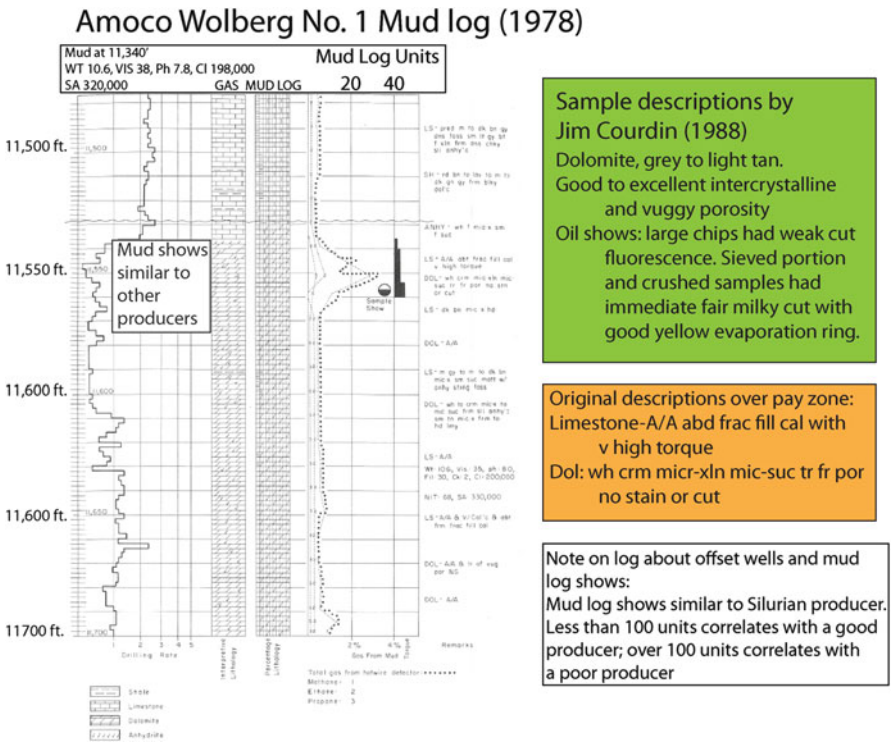

Fig. 3.20 Amoco Wolberg No. 1 mud log and descriptions. Original figure and case history provided by Tim Schowalter

Further examination of the cuttings, even 10 years later, showed good fluorescence and stain. Using Rw values from nearby wells, and porosity from the neutron-density, the Silurian hot dolomite zone calculated 22 % Sw, or pay, probably near irreducible saturations.

Further work on with 2D seismic and showed the well had been drilled on the flanks of a plunging anticlinal closure at the shallower Mississippian Midale level (Fig. 3.21). The potential, then existed for a deeper structural closure at the Interlake Dolomite, the zone with the oil show and calculated by-passed pay (Fig. 3.22).

Stratigraphic cross-section A-A′ (Fig. 3.23) showed that a combination trap might be possible at the Silurian level, as the 'hot dolomite' zone was truncated by an angular unconformity updip and to the southeast. Interestingly, the 'Wolberg Zone' was a normal dolomite downdip in the Russian River Field, where it was also productive. Updip, near the erosional edge, digenetic changes and a mixing of sandstone with dolomite apparently created the radioactive dolomite. In all probability, in screening the well in 1978, this zone was misinterpreted as a shale and never tested.

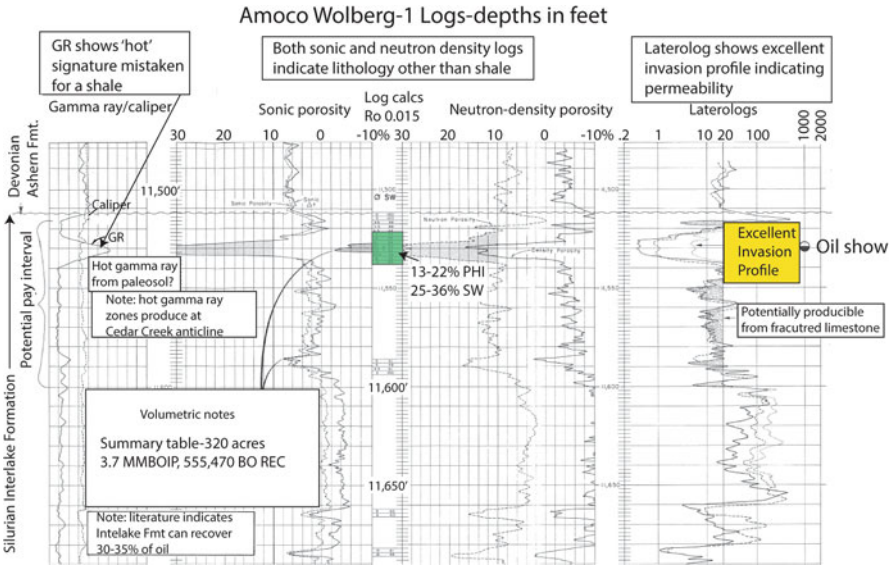

Fig. 3.21 Well logs over the good mud log show, Silurian Interlake Formation, Amoco Wolberg-1. Original figure and case history provided by Tim Schowalter

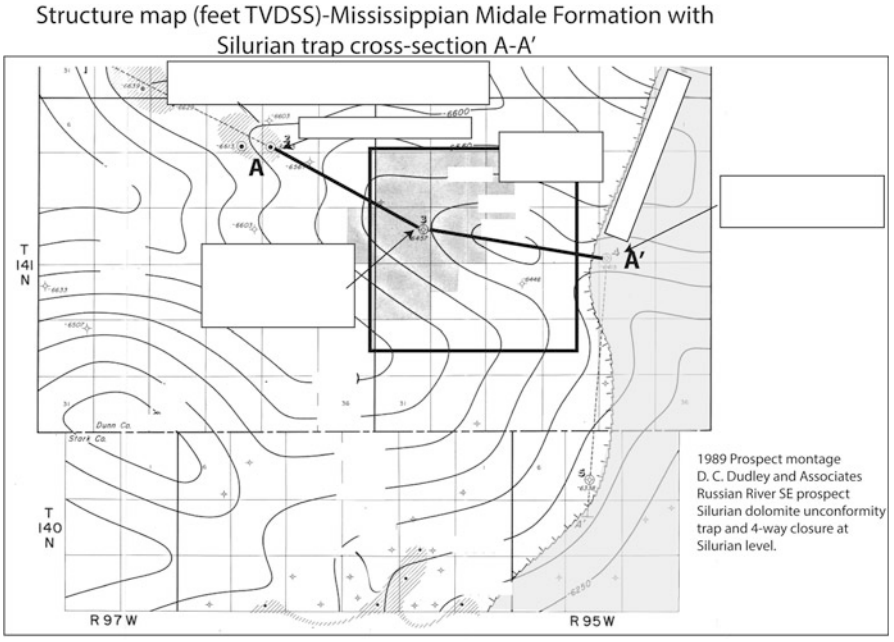

Fig. 3.22 Midale (Mississippian) structure map and cross-section location. The *grey area* is a stratigraphic pinchout edge of the Silurian dolomite with shows. Original figure and case history provided by Tim Schowalter

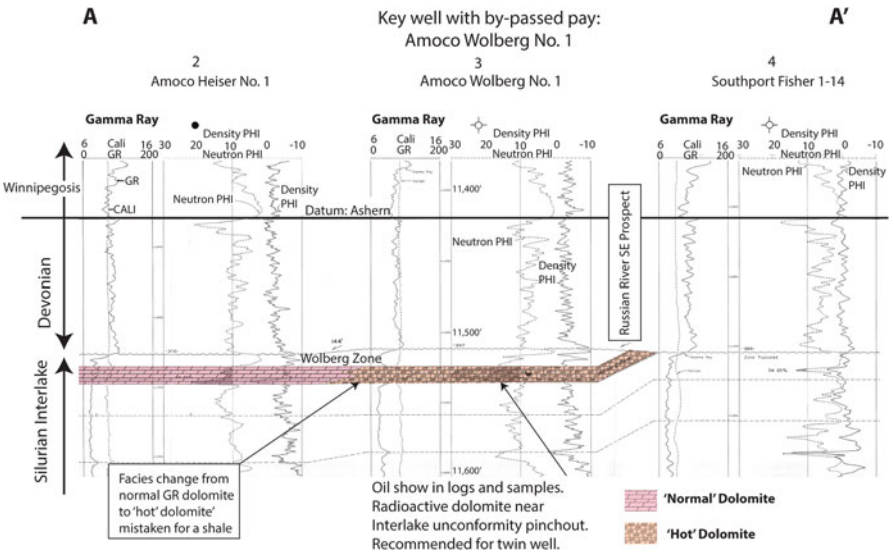

Fig. 3.23 Stratigraphic cross-section showing the change from 'normal' dolomite, to 'hot' dolomite and then an updip truncation of the Wolberg show zone. Original figure and case history provided by Tim Schowalter

The prospect was brought to Dudley and Associates in 1988 and, based on a 2D seismic time map (Fig. 3.24) interpretation of the Silurian level as being on a 4-way closure, acreage was acquired and the well drilled, twinning the Amoco Wolberg-1.

The well flowed at 1000 BOPD water free and has since cumulated over one million barrels of oil. The field has produced 2.856 million barrels of oil from five different stratigraphic levels, and is now undergoing exploitation for the prolific Bakken unconventional shale resource.

This case history is but one example of the reason to pay close attention to oil and gas shows. The recovery of free oil in the deeper horizon indicated a trap was present, possibly low on the closure. The mud log shows were legitimate and it just took a bit more care to look at the logs to recognize the by-passed pay and the potential for a larger field.

3.5.4 Case History 2: Using Gas Wetness mud log Analysis to Discover of a New Turbidite Oil Play Fairway, Eocene Dharvi Dungar Formation, Barmer Basin, India

3.5.4.1 Acknowledgements and Introduction

Special thanks is owed Cairn India Limited for permission to publish this material. Kaushal Pander and Maniesh Singh did most of the work on this prospect and subsequent post-appraisal and have contributed to this case history.

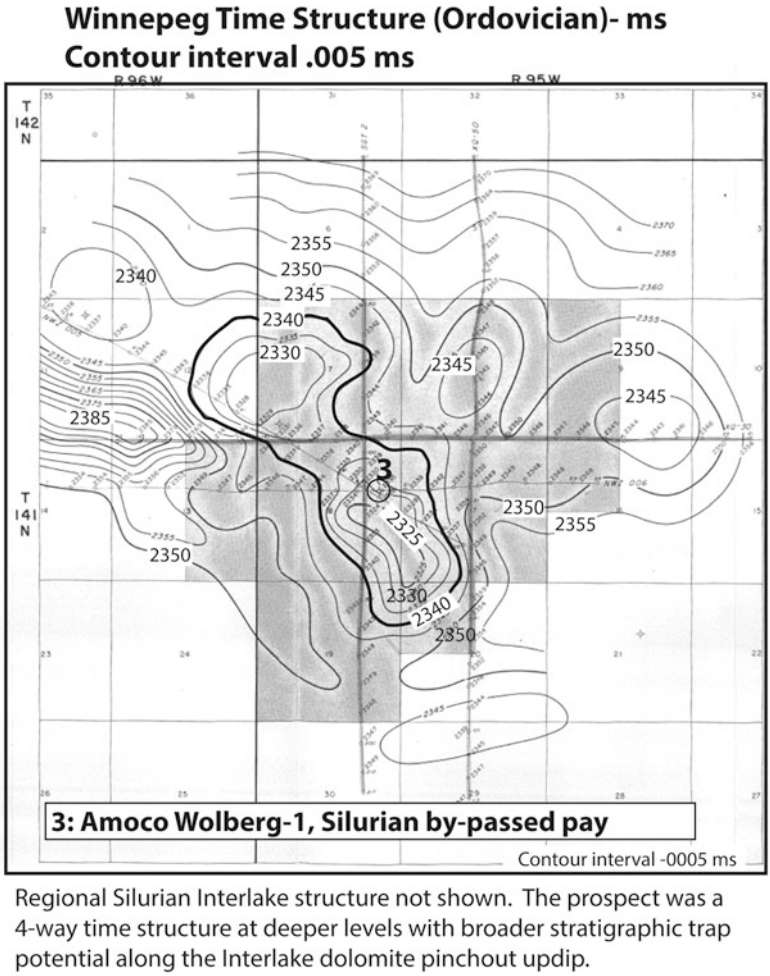

Fig. 3.24 Time structure map, Ordovician Winnepeg level with Amoco Wolberg location. Shaded areas are acreage blocks acquired around the prospect. Original figure and case history provided by Tim Schowalter

The Barmer Basin is a relatively young exploration province, having only had its first significant discovery made in 2004. The history of exploration is detailed, along with the petroleum geology in (Dolson et al. 2015). Geochemical interpretations and migration, while not discussed in this section, are available in (Farrimond et al. 2015; Naidu et al. in press).

The case study is an example of a play that can be developed by looking creatively at seismic signatures, but more importantly, by recognizing from mud log data that deeper oil potential exists in an area where only gas has been found at shallower levels.

3.5.4.2 Regional Setting

The Eocene Dharvi Dungar Formation is a syn-rift deposit in a Tertiary lacustrine rift that has no surface topographic expression or overlying oil seeps. It was found by analysis of gravity and magnetics, followed by 2D seismic and then a drilling campaign from 1999 to 2006. Initial results by Shell and ONGC were discouraging, only finding thin non-commercial oil and gas in the southern portion of the basin. Shell exited the basin, turning over operatorship to Cairn India. On Cairn's 14th well, they discovered the giant Mangala Field in 2004 and as they say 'the rest is history'. As exploration discoveries continued following the Mangala discovery, emphasis was placed primarily on the older sediments of the Fatehgarh and Barmer Hill formations. The Dharvi Dungar Formation, originally part of the uneconomic zones found by Shell to the south in thin fluvial and lacustrine sediments, was largely ignored, despite sporadic production around the basin.

In 2007, a shallow well was drilled in the younger Thumbli Formation at Well 1 (Fig. 3.25).

This well encountered gas pay in Thumbli sandstones (Fig. 3.26). The gas was a bit of a surprise, as to the south, Thumbli pays zones were largely oil. Maturation maps indicate that only the deeper Barmer Hill source rocks are thermally mature at this location, suggesting strong vertical migration into the Thumbli trap.

The most intriguing piece of information in this well, however, was how the wetness increased below the gas zone with depth (Fig. 3.27). The pattern of increased wetness (Wh curve) and decreased balanced curves (Bh) is described in Chap. 3 and (Haworth et al. 1985) of indicative of deeper oil potential.

This increasing wetness trend was immediately recognized and discussed, but deeper levels in the well had only siltstone lenses and no reservoir and the well was TD'd at 1450 m in the Dharvi Dungar Formation. In addition, the siltstones at 950 m appear to be oil saturated, but were not tested. The saturations were good enough to flag as type I continuous phase shows potentially within a trap, and exploration moved on to easier targets elsewhere in the basin.

By 2011, Cairn staff had begun to re-assess the regional geology of the Dharvi Dungar and recognized several pulses of deep water lake deposition that could contain turbidite deposits as reservoirs (Fig. 3.25).

Examination of seismic (Fig. 3.28) showed a seismic facies interpreted as a turbidite fan adjacent to the gas and oil shows in the 950 m level of Well 1.

Detailed mapping of this anomaly resulted in recognition of a bigger trap (Fig. 3.29) with a potentially better reservoir within closure. The structural geometry and facies, based on seismic amplitudes, revealed a combination trap. The detailed mapping showed a robust prospect with Well 1 oil saturated siltstones within closure, but outside of the amplitude map, suggesting these were waste zone shows.

The Well 2 discovery was drilled in 2014 and tested oil on an MDT with a subsequent flow rate 270 BOPD (Fig. 3.30).

Over 50 m of oil bearing section was encountered. Interestingly, the log patterns consist of very thin interbedded sandstone, shale and siltstones and are very shaly on conventional logs. As discussed in Chap. 6, this is common in turbidite facies

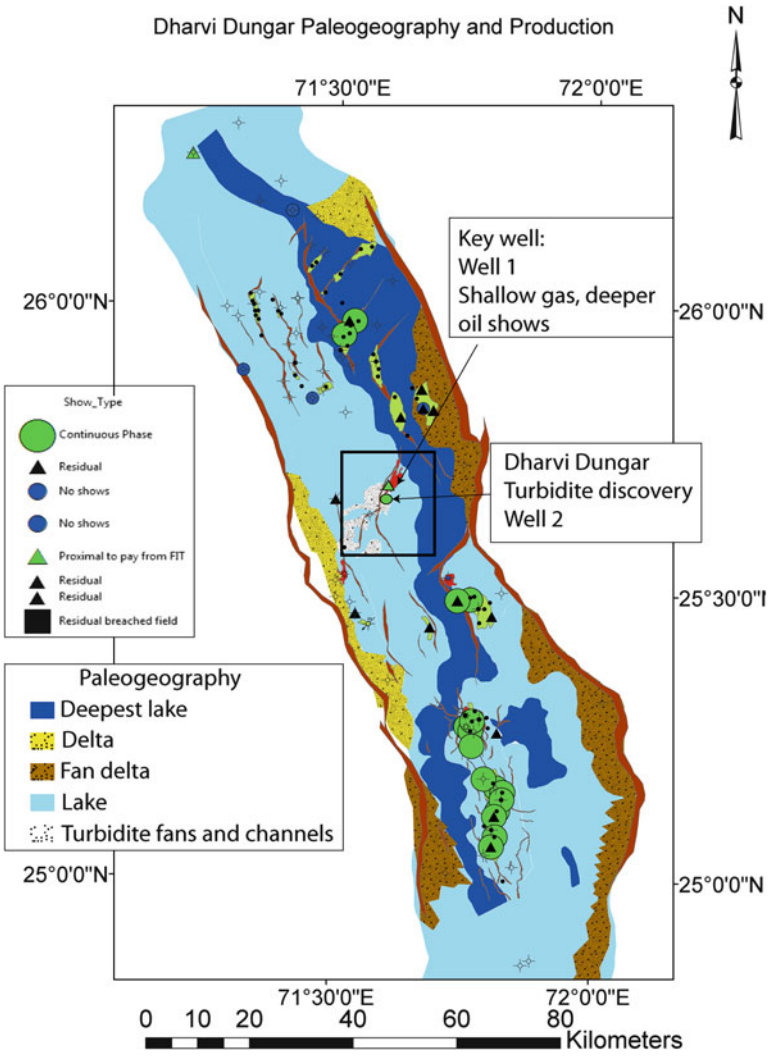

Fig. 3.25 Paleogeography of the Dharvi Dungar Formation and oil and gas shows in the Dharvi Dungar Formation, formed during a lake level highstand. Proximal pay oil and gas shows from Fluid Inclusion Technology (FIT) is discussed in Chapter 7. Brown polygons are faults. Courtesy of Cairn India Limited

and probably represents centimeter scale laminar flows of sandstone, siltstone and shale termed 'Bouma cycles' (original described in Bouma 1962). These thin beds are difficult to resolve with conventional logging suites. Volumetrics are often difficult to assess in these types of reservoirs without extensive testing. Hence, not all of the section has been fully tested and significant additional potential remains on this trap.

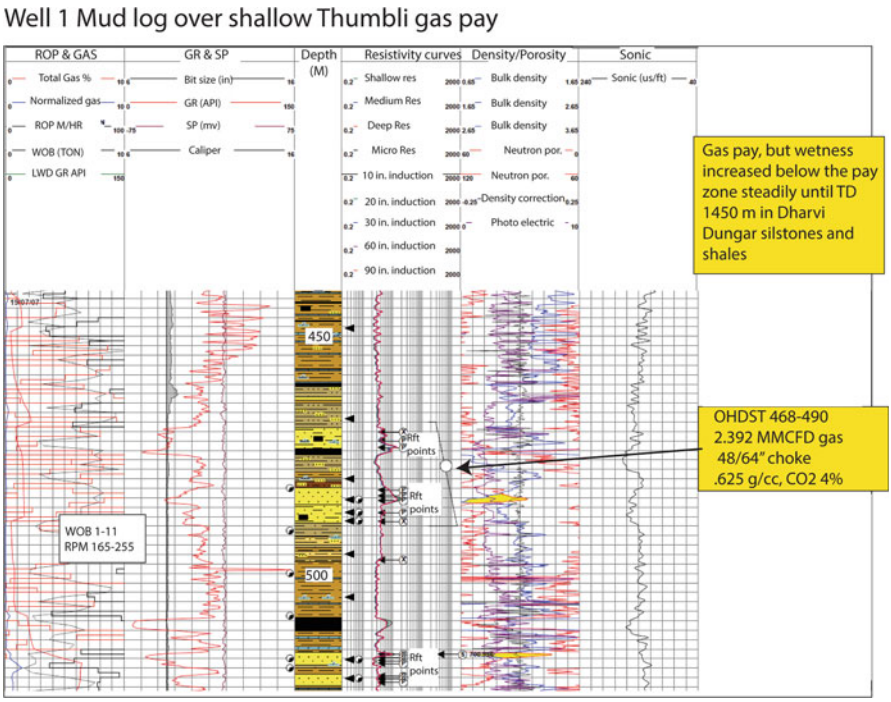

Fig. 3.26 Well 1 composite log. Courtesy of Cairn India Limited. The Younger Thumbli Formation pay zones are dominantly dry gas with good porosity and permeability

3.5.4.3 Summary and Impact

The Dharvi Dungar reservoirs are now considered an additional exploration target. Much of the middle lower portion of the Dharvi Dungar shales are in the oil window, which eliminates charge risk. Stratigraphic traps should thus be abundant elsewhere in the basin, and renewed effort has been placed on finding them.

It is unlikely this play would have been pursued without the key piece of information on increased wetness with depth noted on the deeper part of Well 1. In addition, it took careful and creative analysis of the seismic to recognize that turbidite fans and channels existed in this basin in a horizon that was frequently viewed as just another shale sequence to drill through to get to the main pays.

3.6 Summary

Tremendous advances have been made in the last 50 years with quantification of shows on rigs and from well logs and drilling data. Mud systems and logging is designed to capture as much information on the fluids in a rock, the rock

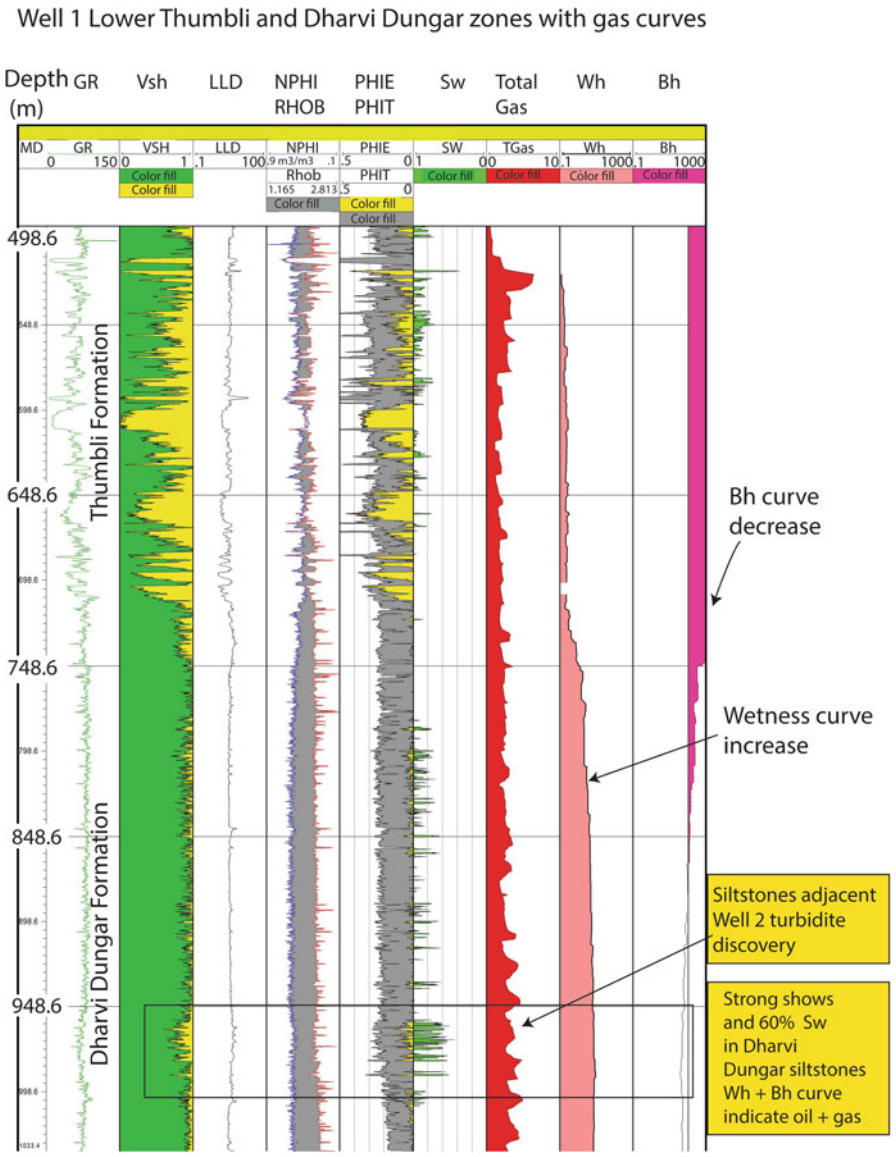

Fig. 3.27 Well 1 gas wetness curves indicating deeper oil. Significant water saturations in siltstone suggested a possible trap had been drilled, but no high quality reservoir found. Courtesy of Courtesy of Cairn India Limited

composition and formation pressures. It is the job of the wellsite geologist to ensure that accurate analysis of the cuttings shows is done, but quality of that work can vary substantially by the interpreter.

Depending on how the well is drilled, hydrocarbons can be flushed away from the wellbore if the mud systems are overbalanced. This can result in a suppression

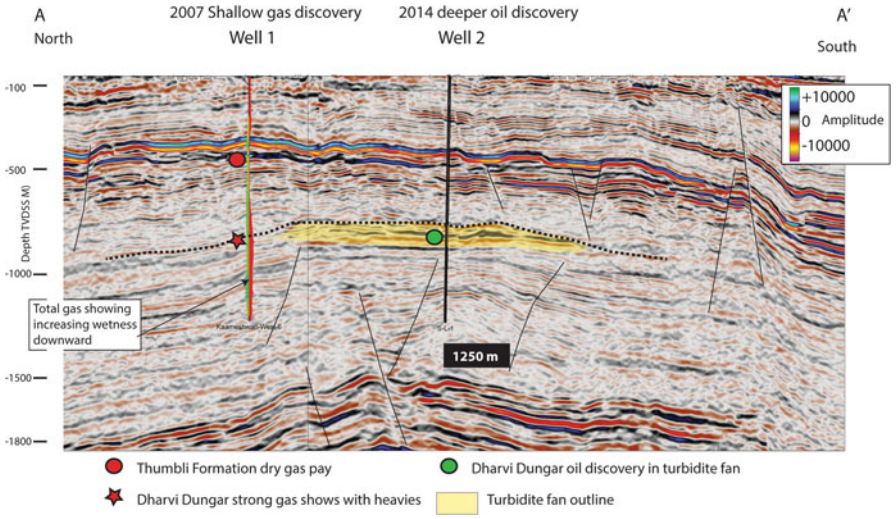

Fig. 3.28 North-south seismic section showing turbidite fan anomaly. Courtesy of Courtesy of Cairn India Limited

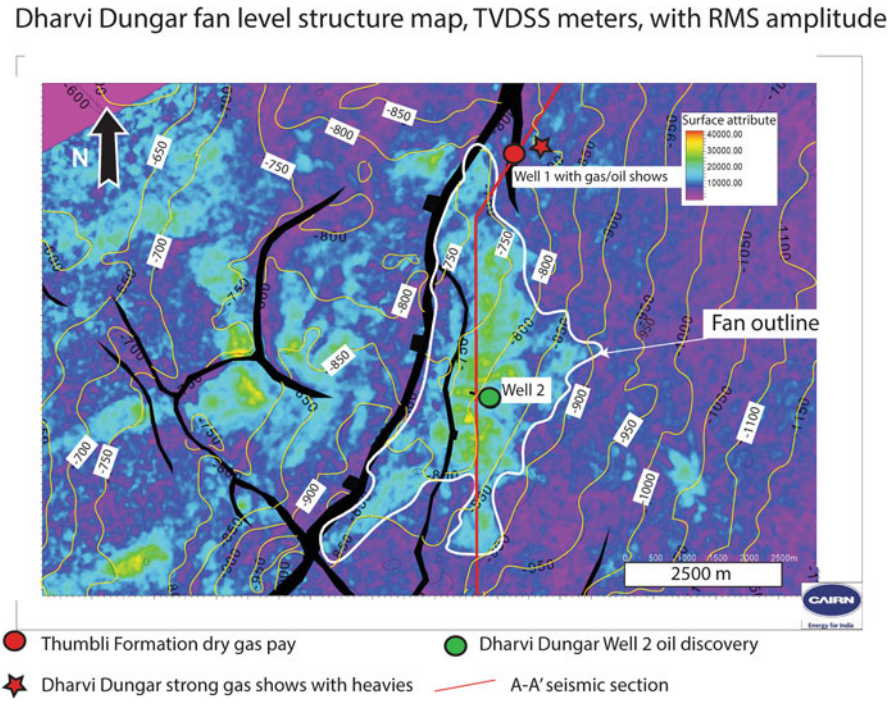

Fig. 3.29 Dharvi Dungar fan trap based on seismic amplitude and facies. Courtesy of Cairn India Limited

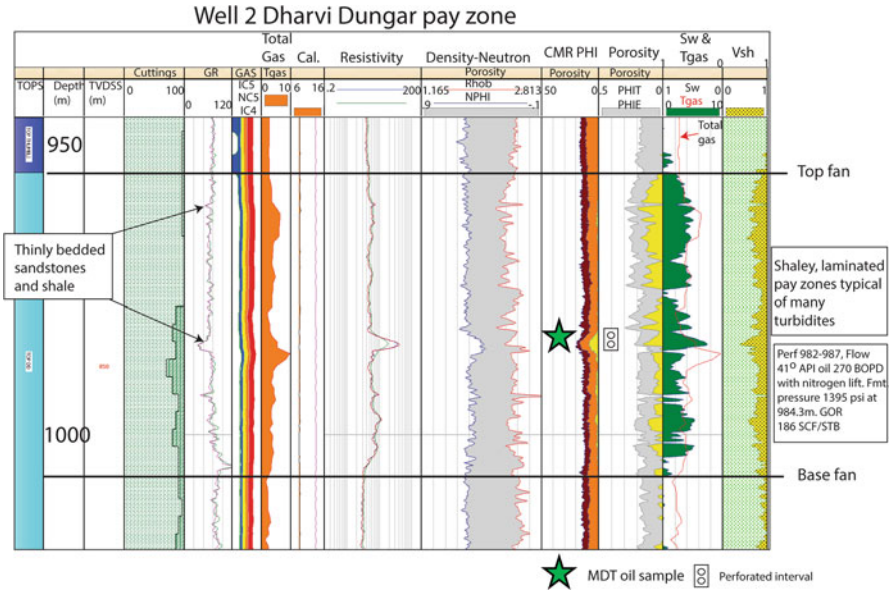

Fig. 3.30 Pay zones in the discovery well. The pay zones a laminated sandstones, siltstones and shales typical of many turbidite deposits. Only 10 m of a 50 m interval was perforated, but oil recoveries of 270 BOPD confirmed the deeper oil pool beneath the overlying dry gas accumulation. Courtesy of Courtesy of Cairn India Limited. Other log suites (FMI, OBI) show the interval is quite sand-rich, but in thin laminations that give a GR signature that looks only like siltstone and shale

of shows in the cuttings as wells as gasses. The resulting invasion profiles are highest in highly permeable rock and can be recognized with resistivity logs by separation of the deep and shallow curves, providing a quick look at potential permeability zones where separation is high.

Gamma ray and SP logs are the most common logs used to identify clean lithologies, but the SP log is affected by formation salinity changes as it relates to the salinity of the mud system. Likewise, naturally radioactive sandstones, dolomites or limestones, although unusual, do occur, potentially causing some reservoirs to be mistaken as shale. FDC-CNL logs are by far the most common log suites run, as these combination tools provide good porosity estimates and lithology information.

Conventional log analysis relies on the assumption that resistivity changes that are different from the resistivity of the formation waters in pore systems reflect hydrocarbons, especially if the porosity and lithology remain constant. Variations from this rule, however, occur where there are conductive minerals or shales or clays with high bound water that might mask hydrocarbons by giving low resistivities across hydrocarbon-bearing zones.

Core data is by far the best way to analyze a reservoir for rock properties, sensitivity to formation damage, petrology and saturations. However, core saturations are almost always residual in nature, as flushing occurs from the mud systems during

coring unless special procedures are taken to prevent this. Hence, using core-derived saturations can many times result in under-estimating hydrocarbon saturation due to flushing.

The Williston Basin case history shown in this chapter illustrates how significant cuttings or mud log shows can be missed, causing a significant discovery to be plugged and abandoned. The Barmer Basin case history also shows has how proper analysis of changing wetness ratios in a mud log lead to an oil discovery beneath a dry gas accumulation.

3.6.1 The Worst Thing I Ever Heard a Mud Logger Say

In the end, despite all the technology employed on a rig and how good the interpretations are boils down to the skill and integrity of the people involved. I sat a well in Kansas in 1982 that managed to find not a trace of oil and gas. It was a relatively cheap well, drilled in about 5 days, and a number of us followed this as part of our well site training.

As we were preparing to leave, I watched the mud logger record a strong oil and gas show at the base of the well. When I asked him what he was doing, he replied, "I always try to give a company hope".

I wish that story weren't true, but it is.

References

AOGHS (2015) Making hole-drilling technology. http://aoghs.org/technology/oil-well-drilling-technology/, American Oil and Gas Historical Society

Asquith G, Krygowski D (eds) (2004a) Basic well log analysis (Second Edition): AAPG methods in exploration series: Tulsa. American Association of Petroleum Geologists, Oklahoma, p 244

Asquith G, Krygowski D (2004b) Porosity logs, basic well Log analysis: AAPG methods in exploration series, v. methods in exploration series No. 16. American Association of Petroleum Geologists, Tulsa, Oklahoma, pp 37–76

Asquith G, Krygowski D (2004c) Spontaneous potential, basic well Log analysis: AAPG methods in exploration series, v. Methods in exploration series No. 16. American Association of Petroleum Geologists, Tulsa, Oklahoma, pp 21–30

Bajsarowicz CJ (1992) Core alteration and preservation. In: Morton-Thompson D, Woods AM (eds) Development geology reference manual. American Association of Petroleum Geologists, Tulsa, Oklahoma, pp 127–130

Bennion DB, Thomas FB (1994) Underbalanced drilling of horizontal wells: does it really eliminate formation damage: society of petroleum engineers. Soc Petrol Eng SPE 27352:153–162

Bouma AH (1962) Sedimentology of some Flysch deposits: a graphic approach to facies interpretation, Elsevier, 168 p

Clark JA, Halbouty MT (2000) Spindletop, v. Special Centennial Edition: Houston, Texas, Gulf Publishing Company, 306 p

DHSG (2011)) Final report on the investigation of the Macondo well blowout, Deepwater Horizon Study Group (DHSG), http://ccrm.berkeley.edu/pdfs_papers/bea_pdfs/dhsgfinalreport-march2011-tag.pdf, Center for catasrophic risk management (CCRM), p. 126

Dolson J, Burley SD, Sunder VR, Kothari V, Naidu B, Whiteley NP, Farrimond P, Taylor A, Direen N, Ananthakrishnan B (2015) The discovery of the Barmer Basin, Rajasthan, India, and its petroleum Geology. Am Assoc Pet Geol Bull 99:433–465

EIA (2009) Marcellus Shale gas play, Appalachian Basin, in O. o. O. a. Gas, ed., Washington, USA, Energy Information Administration, p. 1

Engelder T (2014) Truth and lies about hydraulic fracturing, AAPG Explorer. American Association of Petroleum Geologists, Tulsa, Oklahoma, pp 62–63

Farrimond P, Naidu BS, Burley SD, Dolson J, Whiteley N, Kothari V (2015) Geochemical characterization of oils and their source rocks in the Barmer Basin, Rajasthan, India. Pet Geosci 21:301–321

GeoExpro (2008) The discovery that changed the oil industry for ever, GeoExPro. Geopublishing Ltd., London, England, pp 71–76

Hardage BA, Alkin E, Backus MM, DeAngelo MV, Sava D, Wagner D, Graebner R (2013) Evaluation of fracture systems and stress fields within the Marcellus Shale and Utica Shale and characterization of associated water-disposal reservoirs: Appalachian Basin, Research Partnership to Secure Energy for America. Bureau of Economic Geology, Austin Texas, p 261

Harper JA, Kostelnik J (2013a) The Marcellus shale play in Pennsylvania, geological survey. Pennsylvania Department of Conservation and Natural Resources, Middletown, Pennsylvania

Harper JA, Kostelnik J (2013b) The Marcellus shale play in Pennsylvania part 2: basic geology, geological survey. Pennsylvania Department of Conservation and Natural Resources, Middletown, Pennsylvania, p 21

Harper JA, Kostelnik J (2013c) The Marcellus shale play in Pennsylvania part 4: drilling and completion, geological survey. Pennsylvania Department of Conservation and Natural Resources, Middletown, Pennsylvania, p 18

Hartmann DJ, Beaumont EA (1999) Predicting reservoir system quality and performance. In: Beaumont EA, Foster NH (eds) Exploring for oil and gas traps: treatise of petroleum geology, handbook of petroleum geology, vol 1. American Association of Petroleum Geologists, Tulsa, Oklahoma, pp 9.3–9.154

Haworth JH, Sellens M, Whittaker A (1985) Interpretation of hydrocarbon shows using light (C_1-C_5) hydrocarbon gases from mud-log data. Am Assoc Pet Geol Bull 69:1305–1310

Jacobs T (2015) Going underblanced in unconventional reservoirs. J Petrol Tech 75:50–52

Krygowski DA (2003) Guide to Petrophysical Interpretation. Online report: Wyoming University, Austin, Texas, Daniel A. Krygowski, p. 147

Krygowski DA, Cluff RM (2012) Pattern recognition in a digital age: a gameboard approach to determining petrophysical parameters. AAPG Annual Convention and Exhibition, Long Beach, California, USA, AAPG Search and Discovery Article #40929, p. 6

McCoy R, Blake JG, Andrews KL (2001) Detecting hydrocarbon microseepage using hydrocarbon absorption bands of reflectance spectra of surface oils. Oil Gas J, 3

Mir-Babayev MY (2002) Azerbaijan's oil history: a chronology leading up to the Soviet Era, Azerbaijan. Baku-City that Oil Built, Baku, Azerbaijan, Azerbaijan International, p. 34–40

Naidu BS, Burley SD, Dolson J, Farrimond P, Sunder VR, Kothari V, Mohapatra P (in press) Hydrocarbon generation and migration modelling in the Barmer Basin of western Rajasthan, India: lessons for exploration in rift basins with late stage inversion, uplift and tilting, Petroleum System Case Studies, v. Memoir 112. Tulsa, Oklahoma: American Association of Petroleum Geologists

O'Sullivan T, Zittel RJ, Beliveveau D, Wheaton S, Warner HR, Woodhouse R, Ananthkirshnan B (2008) Very low water saturations within the sandstones of the Northern Barmer Basin, India. SPE 113162:1–14

O'Sullivan T, Praveer K, Shanley K, Dolson JC, Woodhouse R (2010) Residual hydrocarbons—a trap for the unwary. SPE 128013:1–14

Paul A, Daniels J, Finnell DB, Anderson WJ (1992) Show evaluation. In: Morton-Thompson D, Woods AM (eds) Development geology reference manual. American Association of Petroleum Geologists, Tulsa, Oklahoma, pp 109–114

PetroWiki (2015) Extended reach wells, http://petrowiki.org/Extended_reach_wells, Society of Petroleum Engineers, p. 1

Ploeg AJV (1980) The overthrust belt: an overview of an important new oil and gas province, Laramie, Wyoming. The Geological Survey of Wyoming, p. 22

Schroeder FW (2004) Lecture 4: well log data. American Association of Petroleum Geologists, Tulsa, Oklahoma, p 25

Schumacher D (1999) Surface geochemical exploration for petroleum. In: Beaumont EA, Foster NH (eds) Exploring for oil and gas traps: treatise of petroleum geology, handbook of petroleum geology, vol 1. American Association of Petroleum Geologists, Tulsa, Oklahoma, pp 18.4–18.27

Schumacher D (2012) Hydrocarbon microseepage-a significant but underutilized geologic principle with broad applications for oil/gas exploration and production. AAPG Annual Convention and Exhibition. Long Beach, California, American Association of Petroleum Geologists, p. 27

Schowalter TT, Hess PD (1982) Interpretation of subsurface hydrocarbon shows. Am Assoc Pet Geol Bull 66:1302–1327

Seubert BW (2004) The wellsite guide, PetroPEP Nusantara, http://www.petropep.com/download_1_html_files/The%20Wellsite%20Guide_new.pdf, p. 137

Swanson R (1981) MTH01-sample examination manual: methods in exploration. American Association of Petroleum Geologists, Tulsa, Oklahoma, p 117

Swanson R, Fogt D (2005) Sample examination AAPG Video Series on DVD. American Association of Petroleum Geologists

Trueblood S (2013) Finding big oil fields in East Africa: Inhassoro: the southernmost oil field in the East African rift system? SASOL Petroleum International, http://64be6584f535e2968ea8-7b17ad3adbc87099ad3f7b89f2b60a7a.r38.cf2.rackcdn.com/EA%20Oil%20Forum%20-%20Sasol%20Presentation.pdf

Whitson CH (1992) Petroleum reservoir fluid properties. In: Morton-Thompson D, Woods AM (eds) Development geology reference manual. American Association of Petroleum Geologists, Tulsa, Oklahoma, pp 504–507

Whittaker A (1992a) Mudlogging: gas extraction and monitoring. In: Morton-Thompson D, Woods AM (eds) Development geology reference manual. American Association of Petroleum Geologists, Tulsa, Oklahoma, pp 106–108

Whittaker A (1992b) Mudlogging: the Mudlog. In: Morton-Thompson D, Woods AM (eds) Development geology reference manual. American Association of Petroleum Geologists, Tulsa, Oklahoma, pp 101–103

Whittaker A, Morton-Thompson D (1992) Mudlogging: drill cuttings analysis. In: Morton-Thompson D, Woods AM (eds) Development geology reference manual. American Association of Petroleum Geologists, Tulsa, Oklahoma, pp 104–105

Wrightstone G (2010), A shale tale: Marcellus odds and ends, 2010 winter meeting of the independent oil and gas association of West Virginia p. 32.

Chapter 4
Understanding Seals, Pressures and Hydrodynamics

Contents

J. Dolson, *Understanding Oil and Gas Shows and Seals in the Search for Hydrocarbons*, DOI 10.1007/978-3-319-29710-1_4

Abstract Seals occur in virtually every type of lithology, but are most usually recognize from lithologies such as shale, evaporites and salt. All seals leak over time and most seal edges are diffuse. The best way to recognize seals remains analysis of pressure data from well tests, either from simple pressure vs. depth plots or anomalous production indicating barriers between wells. Fault seals are the most problematic, as their character can change rapidly along strike and vertically in the fault system, in response to lithology juxtapositions, shale gouge and/or stress direction.

Analyzing pressure vs. depth plots has great utility in both production and exploration, as this is the best way to define free water levels accurately, tilted oil and gas water contacts and pressure compartments. Reservoirs within the same trap and seal system will plot on the same hydrocarbon gradient on a slope representing the density of the fluid system.

Abnormal pressure is any pressure higher or lower than a fresh or salt water gradient. Causes of abnormal pressure are variable, but include depositional rate, hydrocarbon generation and uplift and erosion. Effective stress is not only important to understand from a drilling standpoint, but exerts a strong control on porosity development. Where effective stress is low, difficult drilling conditions exist and there may be little or no room for a hydrocarbon column before buoyancy pressure exceeds the fracture pressure. Pressure regressions, in high pressure basins, created pressure enhanced seals as well as conduits for migration.

Hydrodynamic flow in a basin may be the norm, not the exception, as excess pressure in overpressured basins creates hydrodynamic flow, as does the movement of meteoric water from uplifts towards the basin center. Tilted hydrocarbon-water contacts can occur in both deep and shallow basin settings and is often difficult to tell from perched water.

This chapter covers methods of using pressure vs. depth plots and hydrodynamic analysis to assess trap size, recognize free water levels, fluid compartmentalization and tilted oil and gas/water contacts. It is divided into five sections.

4.1 Basic Pressure Terms, Uses and Pressure Data Collection

4.1.1 Why Look at Seals from the Standpoint of Pressures and Hydrodynamics?

There are few better ways to find new traps with old data than to carefully evaluate pressures in wells. Pressure data is the only way a free water level can be found accurately, as well as the best way to identify a seal. Recall from Chap. 2 that the free water level is where buoyancy pressure (Pb) equals zero. If there is adequate charge and migration to a trap, the position of the free water level is a function of the seal capacity of the weakest seal and the trap geometry. Hence, quantifying seal capacity early is a key part of prospect evaluation.

Since the free water level marks the absolute base of a trap, any well even a meter above that point is actually within the trap. As already illustrated in Chap. 2, wells are sometimes abandoned simply because their relative position in a trap is unknown or misinterpreted. Tight wells, in particular, are problematic, as they may have 100 % SW well above the FWL. An offset well, in the same trap, with good quality reservoir, may, in contrast, be at irreducible water saturation.

Perhaps the most difficult part of post-appraising dry holes is keeping an open mind to rock type, subtle shows and the potential that a well interpreted as barren of hydrocarbons is actually already in an unrecognized trap. An equally important, and often unrecognized complication are tilted hydrocarbon contacts caused by excess pressure and hydrodynamic flow. Large fields have gone unrecognized for years because of crestal wells that found water with traces of oil or gas that were actually at the top of an accumulation with gas or oil-water contacts tilted off the flank due to hydrodynamics and excess pressure. This occurs in both shallow and deep basin settings. Water flow and tilting in the overpressured deep basin setting is still undervalued as of this writing.

4.1.2 Some Good References

A real breakthrough in understanding hydrodynamics and migration was that of (Hubbert 1953). The principles outlined in this paper form the foundation for most or all petroleum systems migration modeling software. Perhaps the best treatment of pressures and hydrodynamics, however, is that of (Dahlberg 1982, 1995). This short textbook contains virtually all the basic concepts covered in this chapter, and comes complete with exercises that help a beginner learn to deal with pressure data quantitatively. Dahlberg's book stresses methods of hand-generated contour maps utilizing Hubbert's U-V-Z method to model migration and entrapment in hydrodynamic conditions.

This chapter expands on the U-V-Z method by illustrating how to work with grids and software packages to do the calculations. Grid manipulation provides much faster solutions and allows quick testing of alternative models, but utilizes the principles outlined by Hubbert and Dahlberg.

Additional key papers dealing with pressures and hydrodynamics are those of (Beaumont and Fiedler 1999; Berg 1976; Biddle and Wielchowsky 1994; Dennis et al. 2005; England 1994; England et al. 1991; Ferrero et al. 2012; Hartmann and Beaumont 1999; He and Berkman 1999; Muggeridge and Mahmode 2012; Riley 2009; Robertson et al. 2013; Swarbrick and O'Connor 2010).

Chapter 5 deals with seal quantification using capillary pressure, but seals can be recognized easily with pressure vs. depth plots, techniques that are the subject of this chapter. Seal evaluation is covered extensively in the literature, with perhaps the most classic papers those of (Downey 1984; Sales 1997; Skerlec 1999; Vavra et al. 1992; Yielding et al. 1997).

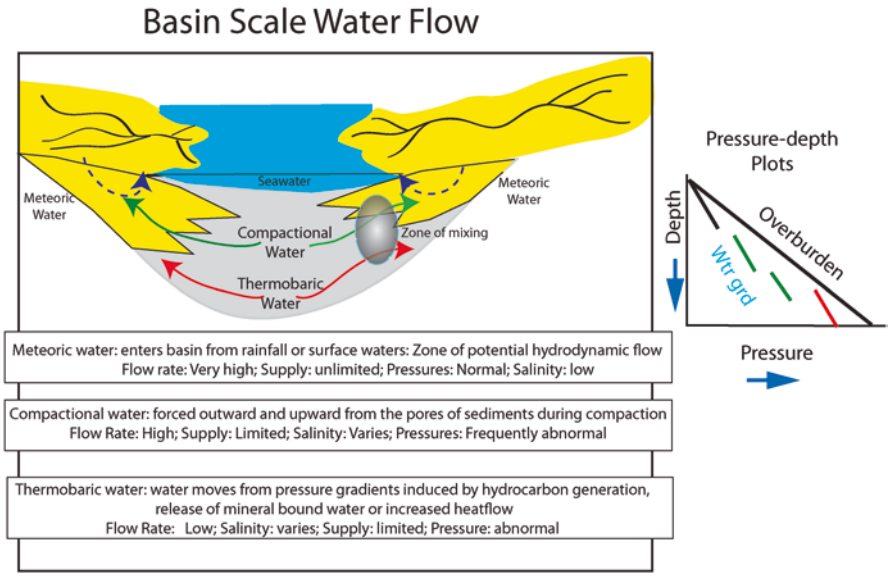

Fig. 4.1 Basin scale water flow. Modified from Hartmann and Beaumont (1999)

Fault seals are especially important to try to quantify, and often, the most difficult. Good treatments of faults seals are covered in an AAPG thematic volume publication (Davies and Handschy 2003) and in a numerous additional publication, some of the more significant of which are (Bjorlykke et al. 2005; Cartwright et al. 2007; Doughty 2003; Faerseth et al. 2007; Gibson 1994; Gibson and Bentham 2003; James et al. 2004; Jones and Hillis 2003).

The origin and recognition of seals and pressure environments is also extensively covered but good basic references are those of (Beaumont and Fiedler 1999; Bradley and Powley 1994; Lee and Deming 2002; Lupa et al. 2002; Shaker 2002, 2005; Swarbrick and O'Connor 2010; Traugott 1997).

Hydrocarbon migration from source to trap inevitably obeys fundamental laws of hydrodynamics and fluid flow. Any force resisting migration along the pathways can set up hydrocarbon traps if the geometric conditions are right. These may be simple seals created by changes in lithology or faulting, or can be modified by excess pressure, either from deep, overpressured basin water flow or from shallow meteoric water flows into the basin.

Figure 4.1 shows three basic hydrodynamic regimes and some characteristics of each: (1) meteoric (2) compactional and (3) thermobaric water. Also shown is a simple pressure-depth plot and an overburden line. Overburden is defined as the total weight of the sediment plus the weight of water (if offshore). Onshore, the gradient is usually about 1 psi/ft. When aquifers have a geometry and burial history where pressure is trapped within the aquifer, it can become overpressured. In these cases, the pressure-depth plot will show sudden shifts of the water pressure gradients. These shifts are caused by the presence of pressure seals which compartmentalize the individual aquifers. If the aquifer pressure becomes so high as to approach

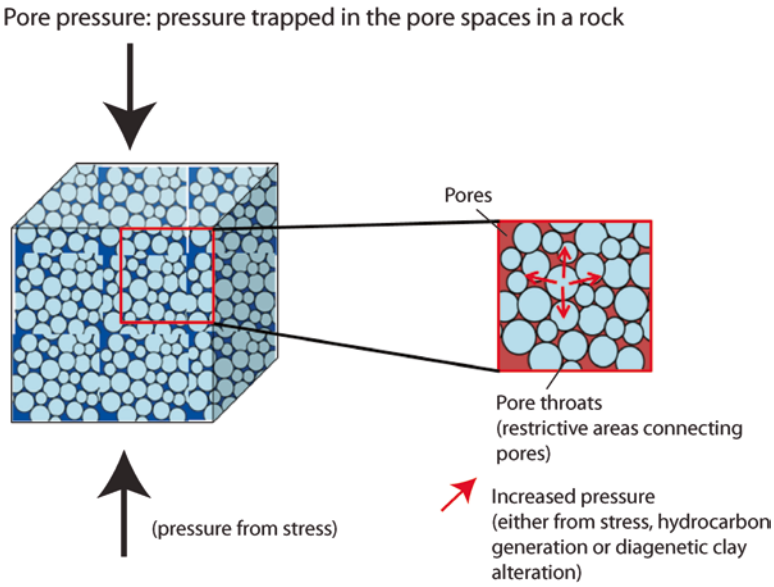

Fig. 4.2 Pore pressure. There are multiple causes of pore pressure above or below hydrostatic gradients. See text for discussion. Modified from BP-Chevron Drilling Consortium course notes, used with permission

the overburden pressure, then there is total seal failure and it is impossible to hold a hydrocarbon accumulation.

Sometimes, it is difficult to tell the cause of the overpressure, but recognizing where they are on pressure-depth plots and other data is important. The seals that set up these compartments are important horizons to map as they will be primary top seals within reservoirs at each aquifer level. If water is moving within these systems, the system is called hydrodynamic. If not, it is hydrostatic. Many explorers, unfortunately, recognize too late that they are in a hydrodynamic basin and fail to build the appropriate fluid flow maps to understand entrapment fully. As will be shown later, the result are frequently missed fields or the wrong volumetric assessment of a trap due to the presence on tilted hydrocarbon-water contacts.

4.1.3 Pore Pressure

Any internal or external force can create excessive pressure within a pore system (Fig. 4.2). Pore pressure predictions plays an important role in hydrocarbon exploration:

1. Safety. Predicting high pressure is critical to prevent blowouts
2. Recognition and quantification of seals
3. Determining free water levels

Table 4.1 Geological factors affecting pressure

Geological factor	Example	Comments
Total stress	Gravity, overburden or tectonics	Tectonically induced pressures occur in places like overthrust belts where strong horizontal stresses may create abnormal pressure.
Rate of Sedimentary loading (compaction disequilibrium)	Depositional environment Stratigraphic age Seal level changes with time	Compaction disequilibrium is a major source of overpressure in rapidly subsiding Tertiary basins. Fluids are not expelled from the rocks fast enough as the sediment is loaded. Often, older rocks have had sufficient time to equilibrate pressure as to remain normally pressured.
Diagenetic changes	Transformation of clay minerals from smectite to illite or other changes.	As clays change molecular shape, water is expelled and higher pore pressure is produced.
Hydrocarbon generation	Volume expansion due to hydrocarbon generation or expansion due to conversion of oil to gas.	Tops of traps with long oil and gas columns can also become overpressured due to added buoyancy. In some basins, the top of overpressure coincides with the top of the oil or gas window. This is common in many basins in the Rocky Mountains.
Diapirism and compressional folding	Compressional folding shale or salt diapirs	Shale and salt diapirs are commonly highly overpressured. In some cases mud volcanoes actually erupt at the surface as pressure builds up.
Uplift and erosion	Can cause both high pressure and subnormal pressure	If a normally pressured reservoir is uplifted as a basin changes shape, but adequate seals are in place, the original pressure is preserved and brought to a shallower depth, creating overpressure. In contrast, if a basin cools during uplift, subnormal pressures can result.
Reservoir depletion	Creates subnormal pressures	Very common in older fields where pressure drawdown has occurred as a field is produced.

4. Determining if reservoirs are hydraulically connected to one another (degree of compartmentalization) at a reservoir level
5. Quantitative mapping of water, oil and gas fluid flow-directions, magnitude and hydrocarbon entrapment
6. Porosity prediction. Normally, rocks compact along fairly predictable lines as they are buried, losing porosity in the process. But if overpressured conditions are reached, excess pore pressure can slow the compaction forces, preserving considerable amounts of porosity.

Abnormal pressures are any pressures that deviate from a salt or fresh water gradient. Table 4.1 summarizes some of the major cause of abnormal pressure.

There are a number of terms critical to remember when dealing with pressure-depth plots and analyzing pressure systems (Fig. 4.3).

Overburden pressure is the total weight of the rock plus any column of water. Onshore, the gradient approximates 1 psi/ft but offshore, there can be a number of other gradient equations. Fracture gradient is the point at which a rock will fracture

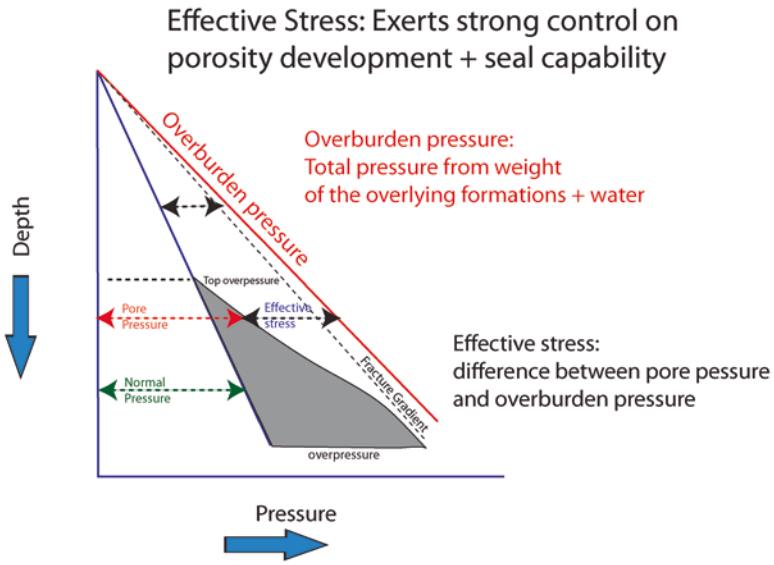

Fig. 4.3 Pore pressure terms. Fracture gradients are determined from well tests or theoretical algorithms, but are the points at which a rock will fracture under high pressure, regardless of lithology of the seals

when the horizontal stress created by the overburden pressure is exceeded by the pore pressure.

Fracture gradients can be estimated from equations but are routinely measured in a well with a test called a 'leak off test'. During leak off tests, pump pressures are increased in a well until fluid leakoff into the formation is detected. A series of these points, plotted on a pressure vs. depth graph (Fig. 4.4) will show a better approximation of the fracture gradient. It is important to note that exceeding fracture gradient while drilling can result in blowouts. In addition, if pore pressure in the rock approaches that of the fracture gradient, there is no hope for a hydrocarbon column accumulation, as even a short column will have enough additional buoyancy from the added buoyancy pressure to cause seal failure and loss of trap.

In a normally pressured environment, the pressure increase follows that of the density of the water system, which is 0.433 psi/ft (1 g/cc) for fresh water and 0.48–0.5 psi/ft for salt water. When these gradients are exceeded, the formation is overpressured. Pore pressure itself if the direct measure of the pore pressure at the point of measurement.

Effective stress is the difference in pore pressure between the overburden and the reservoir. It is an important concept, as effective stress can also be a significant factor is preserving or creating porosity at depth. The higher the effective stress, the more the rocks are compacted and the less porous they become. In cases where overpressure is common, the effective stress is decreased and porosity destruction slowed or halted.

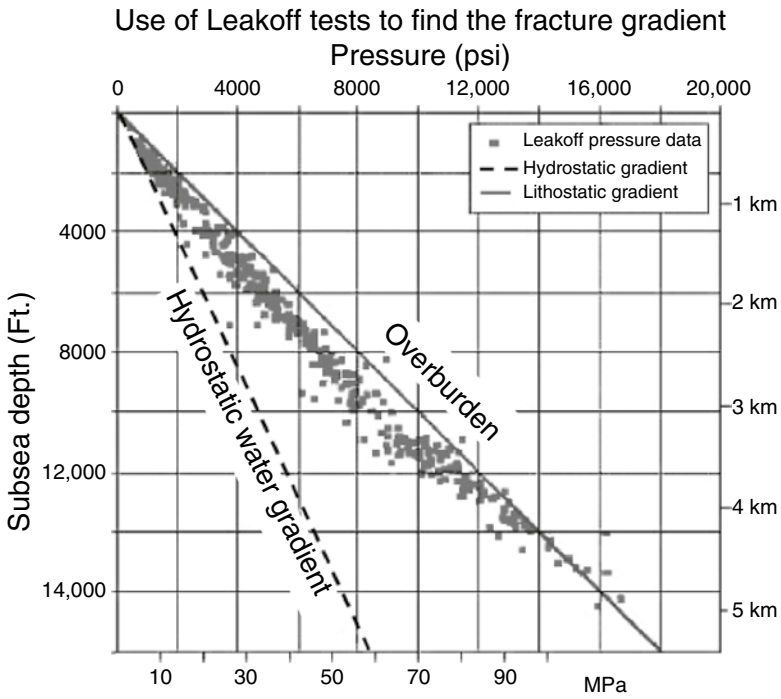

Fig. 4.4 Using leak-off tests to measure the fracture gradient directly. From Bjorlykke et al. 2005. Reprinted with permission of the AAPG, whose further permissions is required for further use

Another fundamental concept in analyzing these plots relates to density of the fluids (Fig. 4.5). Slopes of the pressure points represent changes in density of the fluids, as discussed earlier in Chap. 2. Gas columns have much lower density than oil columns and this is reflected in an increase in the slope of the graph. Supernormal pressures occur when gradients exceed an equivalent 15 lb/gal mud weight, and underpressured zones, if water bearing, have densities less than that of salt water.

Table 4.2 shows some of the common equivalencies used in making pressure vs. depth plots. In the USA, as well as many parts of the world, psi/ft is a standard unit of measure, but units in g/cc or kPa/M are also common. When making plots it is useful to keep the horizontal and vertical scales the same so as to be able to visualize gradients (densities) better.

When working with pressure, it is important to know the densities of the various fluids involved. Table 4.3 provides a summary with some common units used. Direct measurements of pressure, if there are enough points on a pressure-depth plot the graph has added utility in that the slopes measured reflect the actual density in the subsurface temperature and pressure conditions. When densities of fluids are recorded on a rig, in contrast, they are at surface temperatures and pressures and must be converted to equivalent gravities at depth. Adjustments for reservoir conditions, particularly with gas, can be significant, as densities change rapidly as a func-

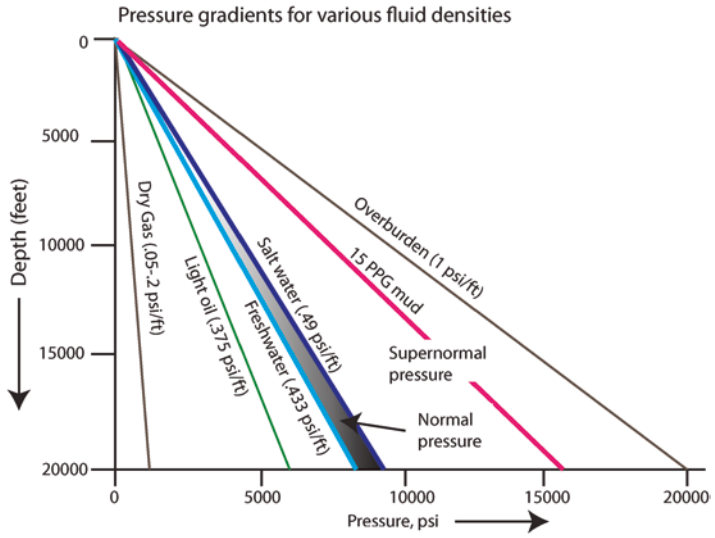

Fig. 4.5 Pressure gradients for various fluids and zone of supernormal pressure. Modified from BP-Chevron drilling consortium notes, used with permission

Table 4.2 Common units of pressure measurement. Additional equations and equivalencies are given in Appendix A

Pressure units	Definition
1 g/cc = 0.4335 psi/ft	pounds per square inch and g/cc
g/cc = 8.345 ppg	pounds per gallon
g/cc = 9.806 kPa/m = 0.009806 MPa/m	kilo pascals and mega pascals per meter
1 psi/ft = 19.25 ppg	
1 psi/ft = 2.307 g/cc	
1 psi/ft = 22.62 kPa/m = 0.02262 MPa/m	
1 ppg = 0.1198 g/cc	
1 ppg = 0.051948 psi/ft	
1 ppg = 1.176 kPa/m = 0.001176 Mpa/m	
1 kPa/m = 0.102 g/cc	
1 kPa/m = 0.0442 psi/ft	
1 kPa/m = 0.9504 ppg	
1 psi = 6.895 kPa = 0.006895 MPa	
1 MPa = 145 psi	
1 kg/cm^2 = 14.19 psi	kilogram/cm^2 and pounds per square inch
Psig	Pressure read from the gauge
1 atm = 14.7 psi	Atmospheric pressure = approximately 14.7 pounds per square inch at sea level (varies slightly with elevation)
Psia = Psig + 1 atm = Psig + 14.7	Absolute pressure. This is the number usually used in pressure-depth plots
Length	
1 m = 0.3048 ft	Meters to feet
1 ft = 3.280804 m (meters)	Feet to meters

tion of molecular composition, compressibility, temperature and pressure. The data in Table 4.3 is thus a rough guideline. When you need very accurate numbers, it is best to consult PVT (pressure, volume, temperature) charts directly or consult an engineer or log analyst in your company.

Sources of additional tables include online calculators and (Gearhart-Owens-Industries 1972).

4.1.4 *Recognizing Seals on Pressure-Depth Plots and Understanding mud Weights*

Figure 4.6 shows a simple pressure-depth plots with a few mud weight equivalent lines superimposed, along with fresh water gradients (blue lines). The points A-F equal pressure values recorded at various depths below sea level for different

Table 4.3 Common density measurements

Fluid	API	Specific Gravity at 60 F	kg/m^3	g/cc	psi/ft	Solids (ppm)	Comments
Highly saline water						**330,000**	**Dead Sea example**
Salt water			**1030**	**1.03**	0.4460	> 100,000	
Fresh water			**1000**	**1**	0.4330	< 100,000	Very fresh formation water <10,000 ppm
Bitumen	**8**	**1.014**	**1012**	**1.012**	0.4382		
Bitumen	**9**	**1.007**	**1005**	**1.005**	0.4352		
Bitumen	**10**	**1.000**	**998**	**0.998**	0.4321		
Heavy oil	**15**	**0.966**	**964**	**0.964**	0.4174		
Heavy oil	**20**	**0.934**	**932**	**0.932**	0.4036		
Normal oil	**25**	**0.904**	**902**	**0.902**	0.3906		
Normal oil	**30**	**0.876**	**874**	**0.874**	0.3784		
Normal oil	**35**	**0.850**	**848**	**0.848**	0.3672		
Normal oil	**40**	**0.825**	**823**	**0.823**	0.3564		
Light oil	**45**	**0.802**	**800**	**0.8**	0.3464		
Light oil	**50**	**0.780**	**778**	**0.778**	0.3369		
Condensate/ gas	**55**	**0.759**	**757**	**0.757**	0.3278		
Condensate/ gas	**58**	**0.747**	**745**	**0.745**	0.3226		
Wet gas			**400**	**0.4**	0.1732		Gas gradients vary substantially with pressure and temperature
Wet gas			**200**	**0.2**	0.0866		
Dry Gas			**100**	0.1	0.0433		
Dry Gas			**7**	**0.007**	0.0030		

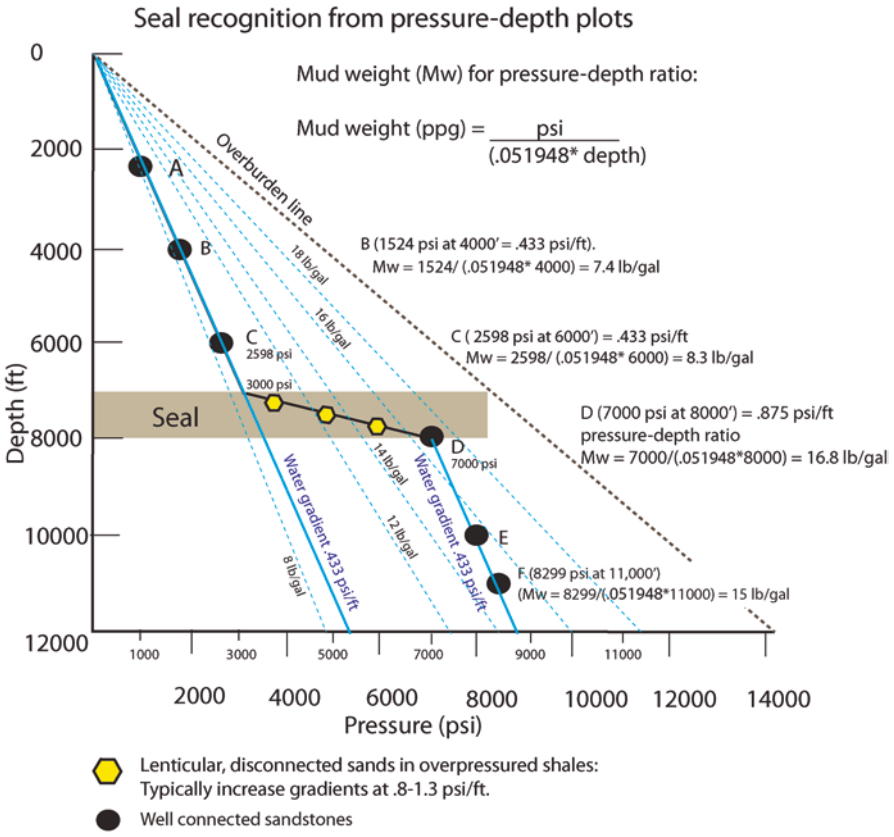

Fig. 4.6 Recognition of seals. Sharp shifts water lines on a pressure depth plot indicate seals capable of holding significant geopressure. The seal above was entered at 3000 psi on a fresh water gradient, with 8.3 lb/gal mud weights. When drilling out of the seal at D, the mud weight would have to be increased to 16.8 lb/gal to contain the pressure, where the pressure-depth ratio increased from 0.433 psi/ft (normal pressure) to 0.875 psi/ft overpressure. The pressure increase across the seal was 4000 psi. Any thin, lenticular sandstones within the sealing shales may take on the pressure ramp shown in the shales and catastrophic blowouts can occur. See text for more discussion

wells. Wells A-C are normally pressured, and fall on the fresh water gradient line, with a surface extrapolation to seal level. At 7000 ft. (2133 m), a thick regional shale seal is encountered. At well D, the pressure ramps from 3000 psi above the seal to 7000 psi below it. The conversion to mud weight equivalent from pore pressure is given by the Eq. 4.1:

$$Mud\,weight\left(Mw\right)in\,ppg = \frac{Pressure\left(psi/ft\right)}{.051948*\left(depth\right)} or, alternatively, Mw = \left(Pressure, psi/ft\right)*19.25 \quad (4.1)$$

Wells A–C could be drilled with an equivalent mud weight of 8.3 lb/gal. Upon entering the shale seal, however, the pressure would increase dramatically, and upon exiting the seal at the equivalent position of well D, a mud weight of 16.8 lb/gal would be need to contain the pore pressure. In practice, because shales are such low permeability, this shale might be drillable at lower mud weights. If, however, then lenticular sandstones are encased in the shale, they can take on the pressure of the shales and thus become dangerous high pressure water sandstones, where mud weights of 8.3 lb/gal cannot control the well. Getting accurate pressure readings in shales is very difficult, and some operators believe the best gauge of a shale pressure (which can vary significantly from pressures in reservoirs) is to find thin zones to test for pressure directly within the shales. In Chap. 5, we look at capillary pressure more quantitatively, and will explain why shales and other formations is micro-porosity systems can have such high capillary pressure and seal capacity. Ramps like this in pressure are often termed pressure seals, but usually can be attributed to a geological features like a widespread shale deposit with good sealing capacity.

It is important to recognize the fundamental difference between the pressure-depth ratio and the pressure-depth gradient. The gradient or slope of the pressure plots reflects fluid density. The absolute pressure-depth ratio reflects over, normal or underpressure. For example, the slope from A-C and the slope from D to F are identical at 0.433 psi/ft (fresh water). But the pressure-depth ratio is different at each point. At D, it is 0.875 psi/ft (equivalent to 16.8 lb/gas), or highly overpressured. At F is 0.75 psi/ft (equivalent to 15 lb/gal).

Pre-drill, plots like this are routinely made from offset wells or from estimates of pore pressure changes from seismic, in order to plan a new well and anticipate pressure ramps.

There is a wealth of additional information that comes from pressure vs. depth plots. However, before a full treatment of this topic, it is important to understand the tools needed to capture pressure information, as well as a more qualitative understanding of how to evaluate both fault and lithology seals in a basin.

An example of seal recognition and different pressure regimes is shown in Fig. 4.7 from the Nile Delta in Egypt. The Nile Delta is a young Tertiary basin with a high deposition rate in the central part of the delta offshore. Rapid burial has caused overpressure at a number of levels. The gray bars show the location of regional pressure seals. Water gradients are shown in blue and gas columns in red. There is an area of subnormal pressure on the graph which has resulted from taking readings in fields where there has been pressure drawdown from production. These trends show up as underpressured and the values do not represent original reservoir pressure.

Also highlighted are changes in effective stress. Not that at very shallow depths, the effective stress (Efs) is very low. In these settings, there is little or no room to build up a gas column as the buoyancy pressure at the top of the trap will exceed the fracture gradient. This is the reason that a lot of time and money is spent by oil companies to identified shallow gas sands or high pressure shallow water zones that could cause blow-outs. Entire teams are placed on looking for shallow hazards and then designing the wellbore to avoid them as it drills to the deeper targets. Just as importantly, there is a steady increase in effective stress with depth for all wells falling on the normally pressured fresh water gradient line.

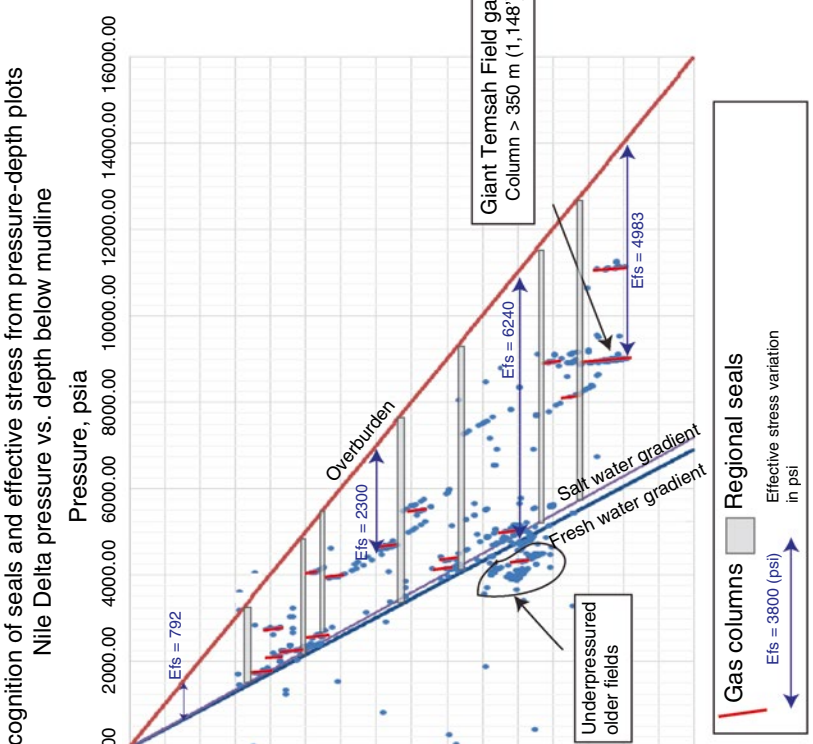

Fig. 4.7 Example of seal recognition and changes in effective stress, Nile Delta, Egypt. The porosity in the Miocene of the Temsah Field is far better than formations at equivalent depths in the normally pressured environment, due to decreased effective stress in the overpressured setting. A number of regional seals are apparent on the plot

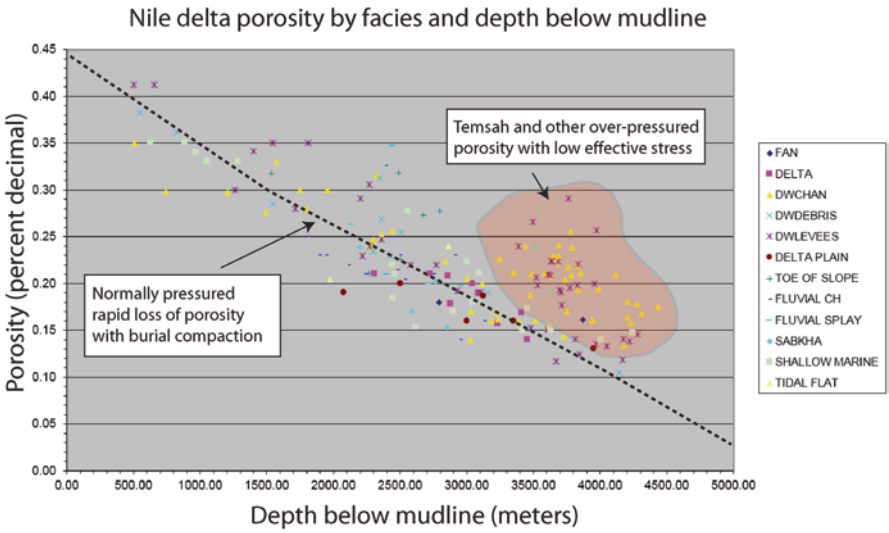

Fig. 4.8 Porosity preservation, Nile Delta, due to overpressure halting normal compaction process. See Fig. 4.6 for pressure depth plots that show the effective stress in the Temsah Field area

Figure 4.8 is a plot of reservoir porosity vs. depth. The plot has been broken out by depositional facies from studies of logs and cores, in an effort to see if there was a primary depositional control on porosity. The plot showed conclusively that normal compaction porosity loss (black dotted line) indicated that many of the reservoirs had uneconomic porosities at depths approaching 3500 m below mud line (sea floor). However, there were quite a few dramatic exceptions (red outline) where porosities as high as 28 % occurred >3500 m below mud line. Closer examination revealed virtually all of these points were overpressured. The giant Temsah Field is a case in point. It has porosities in excess of 20 % and is overpressured at >0.7 psi/ft. In contrast, reservoirs with normal pressure at the same depth had porosities below 10 %.

This plot was successfully used to recommend deeper drilling in the overpressured basin. BP has now drilled a number of very deep gas discoveries in the Nile Delta, all of which have encountered excellent porosity at depths exceeding 6 km below mud line.

4.1.5 Tools and Data Capture for Pressure Analysis

There is a wealth of critical information that can be gleaned from pressure analysis, but before covering that in detail, it is important to understand the tools used for data capture, as well as a more qualitative understanding of how to evaluate fault and lithology seals. Figure 4.9 summarizes four of the most common tools designed to measure formation pressure directly. While indirect measurements can be made

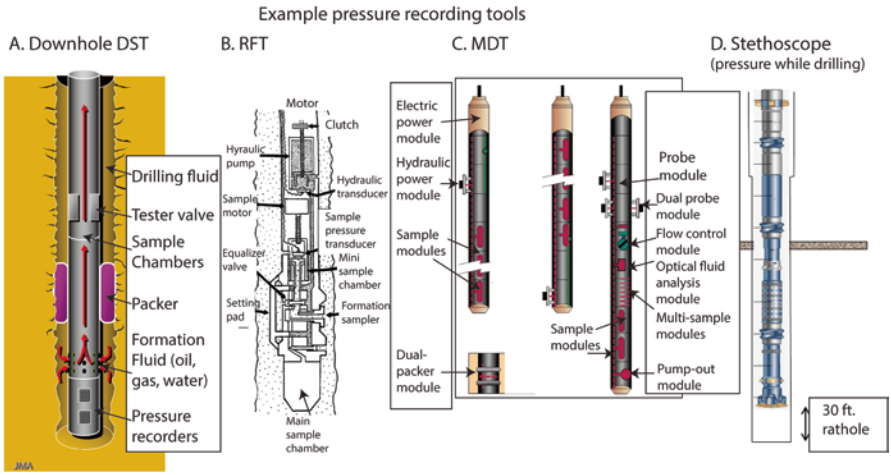

Fig. 4.9 Various pressure recording devices. DST = Drill Stem Test. MDT = Modular Formation Dynamics Tester. C = Repeat Formation Tester. Stethoscopes are special tools that measure pressure directly behind the drill bit, so they can save time tripping out of the hole to put on another pressure tool. Figure A courtesy of John Armentrout. Figure B from Dahlberg 1995. Figure C modified from Ayan et al. (1996), courtesy of Schlumberger. Figure D courtesy of BP-chevron drilling consortium

from plotting mud weight vs. depth, there is no substitute for accurate pressure readings from a downhole tool.

A good summary of pressure recording tools is provided by Beaumont and Fiedler (1999) and Dahlberg (1995) and on company websites, where operation and design of the tools are covered in detail.

Drill stem tests (DST) are one of the most reliable ways to capture formation pressure and fluid information. An excellent source of quick understanding of the DST methodology is that of (Borah 1992). The tool is lowered into the hole and inflatable packers are expanded to seal off the formation completely, with the pressure recorders and sample chambers located adjacent the interval of interest. The tests are expensive and can take considerable time, but basically work like an open hole completion of the zone. When the test works, it provides reliable samples of the fluids, the temperature of the formation and its pressure. A wealth of information results.

Other methods involve MDT and RFT tools. Both these tools can be run into a wellbore and work somewhat like a sidewall coring tool, in that intervals are selected to measure and the tool is raised or lowered until opposite a formation and probes pressed against the reservoir and then opened for both sample and pressure measurement. They offer the ability to sample many more points, but are not as accurate as the DST tool. However, their utility in collecting a lot of data quickly saves time and money. There are other tools with specialized design and names, but functionally, these four types of tools represent the basic ways pressure is taken in a well. The advantages and disadvantages of various tools are summarize in Table 4.4.

Table 4.4 Advantages and disadvantage of each tool type (in part from Beaumont and Fiedler 1999)

Consideration	DST	RFT	MDT	Stethoscope
Advantage	Best recoveries, pressures, evaluation	Quick and samples many points at a high resolution scale	Best tool for accurate formation fluids and quick stabilized pressures	Saves rig time and can capture fluid data in the event that an MDT or RFT later fails.
Time to take measurement	Longest	Less than 5 min if permeable	Similar to RFT	Similar to RFT.
Drilling delay	Two trips	About one logging run	Similar to RFT	No delays except time to take pressure
Sampling interval	Covers several feet or more	<1 in. (<2 cm.)	Similar to RFT	Requires zones > 10 ft (3.28 m) thick
No. of samples	Few	Many	Many	Many, but less than RFT.
Expense	Large	Small	Small	Moderate
Fractured reservoir	Good if fractures intersect the wellbore	Not reliable	Not reliable	Good
Problems	Getting a good packer seat and depth determination	Difficult to get seated at times Screen plugging with drilling mud		Must be performed in unreamed smaller hole section. Unreliable in shaly zones.
Laminated reservoirs	Can be good if many levels tested	Not representative		Difficult
Skin damage	Can be measured or corrected	Can be a major error		

Tripping in and out of a wellbore to assemble a probe and then lower back in the well takes hours to days of rig time. Hence, some companies offer a tool referred to as a stethoscope (D). The stethoscope is run behind the drill bit and can be run as soon as a reservoir layer is penetrated. This saves rig time, but has its own set of problems, not the least of which is potentially complicating the drilling process.

4.1.5.1 Data Reporting Formats

Once the data is collected, the data is recorded and preserved both digitally and in hard copy reports. In an ideal world, all of the pressure information and fluid information is available to look at. In older wells, however, there may be only scant mention of the pressure tests, with the reports long lost or held privately with an operator. However, a little information, if accurate, can go a long way and should be looked for carefully.

Figure 4.10 shows a pressure build-up chart from a DST. It is a plot of pressure vs. time and a number of key inflection points mark changes in the types and

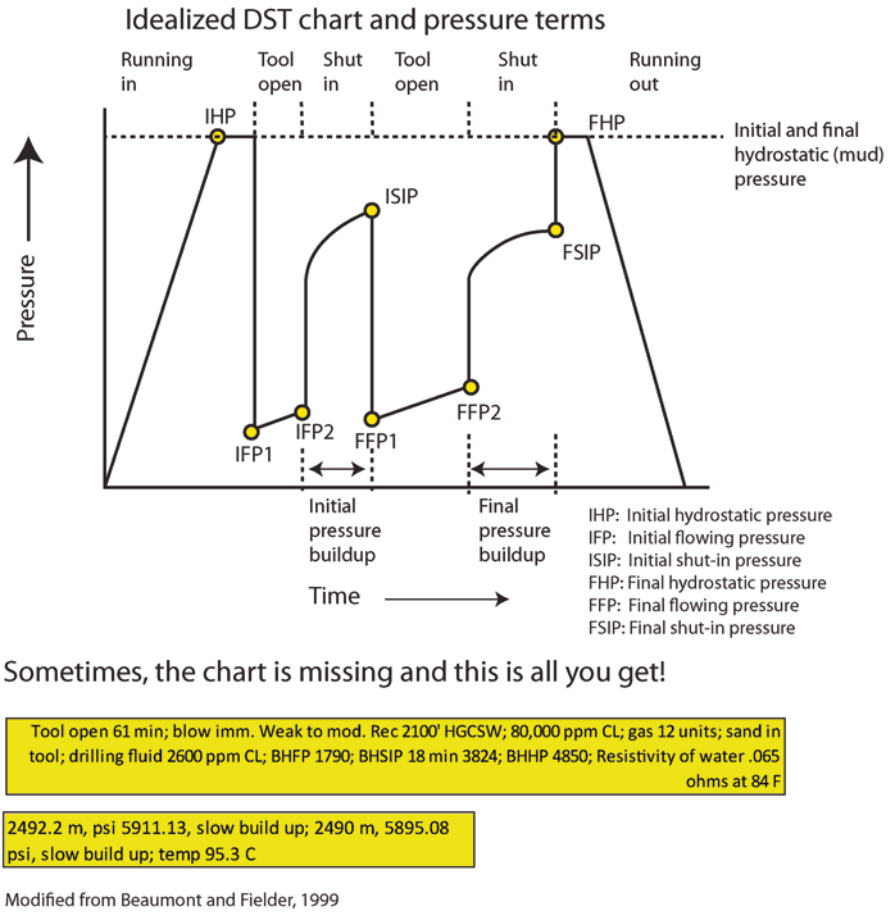

Fig. 4.10 A DST chart. Often, you don't have the chart, only comments on the pressure changes with time and recoveries. Modified from Beaumont and Fielder 1999. Reprinted with permission of the AAPG, whose further permissions is required for further use

amounts of pressure recorded. As the tool is run into the hole the pressure from the mud column rapidly builds up to a maximum called the IHP. At that point, the tool is opened and allowed to flow the pressure at the start of the flow (IFP1) is recorded as is the pressure when the test is stopped (IFP2). The slope of these lines can be a good measurement of permeability. Rapid buildup can indicate a good reservoir, whereas flat to no buildup a very tight reservoir.

After the first flow period, the well is shut in and the pressure allowed to build up, reaching a stabilized formation pressure called the ISIP (initial shut in pressure). It is important that this pressure represent a stabilized maximum pressure and if not, that it is corrected to what it would reach given more time. Correcting DST's pressure to the maximum formation pressure is done through analysis of pressure changes in the test over time, and is done by constructing 'Horner plots). How to do

this is covered in (Horner 1951), Beaumont and Fielder (1999) and Dahlberg (1995). Where possible, Horner corrected values should be used.

The tool is opened and flowed for a second time (FFP1 N FFP2) and more samples taken. The FSIP (final shut in pressure) is then recorded. Hopefully, the FSIP and ISIP are close to one another and are recording the true formation pressure. The FHP is recorded last, measuring the weight of the mud column. The IHP and FHP should be within 5 psi of one another if the tool is accurate.

Frequently, packers fail and the chart shows the test was not successful, with plots that look dramatically different from this one. Examples of various successful and failed test data are shown in (Borah 1992).

Generally the FSIP is taken as the formation pressure for a pressure depth plot, but the higher of the ISIP or FSIP may also be used.

A wealth of additional information is captured on a DST. An example of an older report with data from scanned hard copy reports is shown for a well drilled on a small 4-way structural closure in the Cooper Basin of Australia (Fig. 4.11).

Shown on the diagram (A) is a modern log analysis from the digital log curves, with pay flagged green in the figure. Coals are shaded with gray stipples. This is a

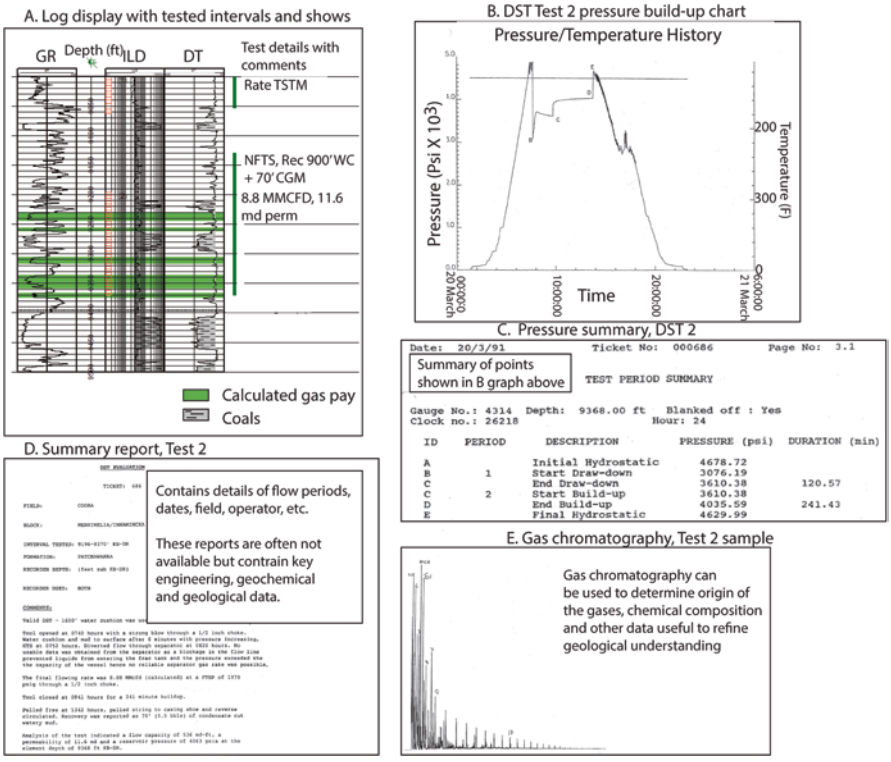

Fig. 4.11 Types of analysis that come with modern log analysis mixed with information from older reports

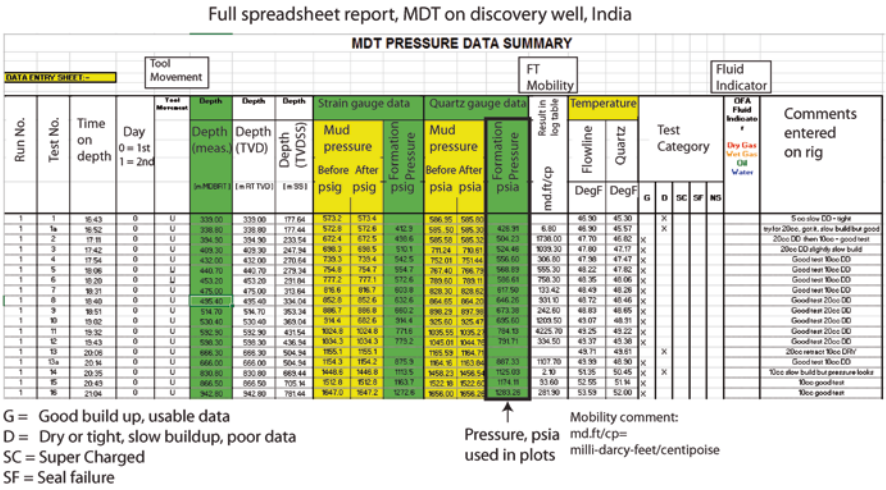

Fig. 4.12 MDT reporting format in a spreadsheet. The green columns show the depths and formation pressure that would be used in a pressure-depth plot. Super charged points are tight zones and the results are unusable, as are zones labeled dry or seal failure

gas discovery in lenticular, fluvial sandstones and the DST intervals and summarized results have been put into data tables in the software and are posted on 11 A. A copy of the DST record is shown on 11B, with a summary of pressure buildups in 11C. A detailed report was available on the test rates, volumes of oil and gas recovered, formation temperature and density and type of fluid (11 D). All of this information can be used in further analysis of the shows in this well to determine if the reservoirs are connected hydraulically and what the permeability and fluid properties are. The Gas chromatogram shown in 11E can be useful not just to an engineer evaluating the discovery, but to geochemists, who may use it to show what likely source rock the fluid was derived from and how thermally mature the sample may be. All of that information can be input into petroleum systems migration modeling software to determine where to look next in the basin for other fluids and traps. Chapter 8 deals with geochemical analysis in more detail.

With RFT and MDT data, reports are commonly preserved in spreadsheets.

A fairly complete spreadsheet on an MDT tool is shown in Fig. 4.12. Buildup times and mobility, but perhaps most importantly, quality of the test if recorded. Only points labeled good or excellent should be used in a pressure-depth plot. The Quartz gauge records (black outline, green box) are the most accurate points to plot.

Many RFT reports have very brief summaries that are the only record you'll get on the test, with details buried well within company files or someone's desk. An example is shown in Fig. 4.13. Again, only use the good points, usually determined by the service company providing the dat. The mobility records are very useful, as they can be converted to approximate permeability.

Example of spreadsheet format reporting: RFT test, India

	Quality	PSIA	MD	TVDSS	mobility	
1	good	3666.54	2248.50	2089.10	7.40	(Ctrl), Stable As A Rock - Good Pressure
2	sc		2359.00	2199.13		Still Building Slowly At 4156 ... Heading for ca. 4200
2	sc	4163.34	2359.00	2199.13	0.20	Still Building Slowly At 4164 ... Heading for ca. 4175-4200
3	dry		2395.00	2234.93		Zero Pressure - Tight/Dry
3	missing		2441.50	2281.12		Missing
3	sc	4432.57	2441.50	2281.13	0.10	Still Building Slowly At 4433 ... Heading for ca. 4500
1	good	3676.57	2468.00	2307.46	0.70	Moderate Quick Build, Stable As A Rock - Good Pressure
1	good	3867.52	2480.00	2319.36	0.30	Moderate Quick Build, Stable As A Rock - Good Pressure
1	good	3784.23	2490.50	2329.78	3.10	Moderate Quick Build, Stable As A Rock - Good Pressure
3	dry		2507.00	2346.14		Zero Pressure - Tight/Dry
2	sc	3877.63	2541.00	2379.86		Still Building Quickish At 4156 ... Heading for ca. 4200-4600
3	seal		2558.50	2397.21		Lost Seal - No Data
3	seal		2565.90	2404.55		Lost Seal - No Data
3	seal		2565.90	2404.55		Lost Seal - No Data
2	sc	4589.66	2599.00	2437.36	0.50	Almost Built Up At 4589.7 ... Heading for ca. 4590-4592
3	seal	5246.22	2656.00	2493.87	0.30	Heading For Hydrostatic - Probably Leaky Seal
3	seal	5290.09	2716.50	2554.07		Two Tests Here But Both Heading For Hydrostatic - Probably Leaky Seal
3	seal		2740.50	2577.98		Lost Seal - No Data
2	sc	5062.13	2755.20	2592.63	0.10	Still Building Slowly At 5062 ... Heading for ca. 5100
3	seal		2764.00	2601.40		Lost Seal - No Data
3	seal		2777.50	2614.85		Lost Seal - No Data
2	sc	5497.17	2822.00	2659.23	0.20	Moderate Quick Build, Moderately Stable - Good Pressure
comp test		3640.00	2466.00	2306.00		

Good Good mobility, good pressure buildup, usable data

Seal = lost seal, data unusable

SC = Supercharged, data unreliable

Dry = tight, no recovery or usable pressure

Mobility- can be converted to permeability

Fig. 4.13 RFT spreadsheet. Only points determined to be good values should be used

4.2 Understanding Facies and Fault Seals Qualitatively

4.2.1 Seals Overview: Facies and Fault Seals

Pressure plots allow quantification and recognition of seals in basins. Other ways to estimate seal capacity come from direct observation of column heights in known fields, as well as quantifying seal capacity from capillary pressure test data (Chap. 5). Fault and facies seals, where traps are filled to spill and column heights known, will at least give minimum seal capacities for the hydrocarbon-water systems encountered. Entire books have been written on facies and fault seals. Some of the best references are those of (Boult and Kaldi 2005; Downey 1984; Vavra et al. 1992).

The best sealing lithologies are salts, anhydrites and shales. Shale seal capacity, however can vary greatly and seals can exit in any other lithology where the pore-throats are small enough to trap hydrocarbons. There are a number of key points to remember regarding seals:

1. Seals leak when the driving force (buoyancy) exceeds the resistance force (capillary pressure). With ever changing geological conditions, all seals leak over

time. The older the age of hydrocarbon generation and entrapment, the better the seals have to be.
2. The size of the trap is limited by the weakest seal.
3. The thickness of a seal is not what controls seal capacity. Seal capacity is controlled by capillary properties, fluid-water density differences and pore throat size. However, thicker seals are desirable in areas where there is extensive faulting, as top seals will be breached if the throw on the fault is greater than the thickness of the top seal.
4. Seals are strongly fluid dependent. What is a good seal for heavy oil might not seal at all for a gas accumulation. Other factors like capillary changes, wettability and interfacial tension (Chap. 5) can significantly alter seal capacity. Oil-wet rocks (where the pore throat walls are lined with oil), for instance, have much lower seal capacity than water-wet rocks (where the pore throat walls are lined with water).
5. Seal edges, particularly in stratigraphic traps, are commonly diffuse. The edges can be difficult to map.
6. Faults can be problematic. Fault seal quantification requires careful geometric analysis, as well as regional stress patterns, likely location of open fractures, or tectonic stresses that might close faults.
7. Shale and gouged material drug down a fault plane can create a seal even with reservoir juxtaposition directly across the fault on both sides.
8. Many laterally continuous source rock beds act as good seals, but are still good exploration targets for oil remaining trapped in the primary migration pathway.
9. Seal effectiveness is often best approximated from known accumulations and pressure information.
10. Open fractures within a sealing lithology can cause the seal to fail.
11. Differential pressure heads across a fault can cause the fault to leak.

In Chapter 5, we cover the quantification of seal capacity from mercury injection capillary tests. This is an excellent way to quantify seal capacity, but may not be fully representative of the seal except at the single point sampled. Lateral and vertical variations in seal capacity are common simply due to facies geometries and changes along faults. Accurate prediction of capacity can be difficult as a result and it is best, when using seals in migration simulation, to test multiple working models and calibrate the final result using oil show analysis.

4.2.1.1 Seal Quality, Pressures and Time

There are two end-member shale seals: (1) hard shales (brittle) (2) soft shales (ductile). Soft shales generally form better seals, as they are less prone to fracturing. Hard shales are more common in older lithologies and in carbonate rich marls. Young Tertiary basins commonly have very plastic, soft shales that make better seals.

Table 4.5 Seal attributes by facies, Talang Akar Formation, Indonesia. Modified from Vavra et al. 1992

Facies	Calculated seal capacity (ft)	Thickness (ft)	Extent	Seal Potential	Comment
Shelf carbonates	2500–10,000	<10	1–10s mi^2	Moderate	
Delta front shales	1000–1400	1100–1500	1–10s mi^2	Good	
Pro-delta shales	270–1800	300–2000	1–10s mi^2	Moderate	
Channel abandonment siltstones	90–320	100–300	<10	Poor	From personal experience, these often provide effective baffles to production in fields, creating compartmentalized reservoirs systems.
Delta plain shales	80–90	90–100	1–10s mi^2	Poor	
Channel sandstone	6.5	–	10–100	Reservoir	

Seals are calculated based on oil-water systems. Seal capacity for a gas-water system would be less. Reprinted with permission of the AAPG, whose further permissions is required for further use

A common screening criteria is the sonic log. Hard shales generally have travel times less than 90 μs/ft., with soft shales velocities >90 μs/ft. In addition, hard shale often have high resistivity, in contrast to lower resistivities in the soft shales.

Seal capacity can also change with depositional systems. A good summary is shown in Table 4.5.

Building good facies maps is a pre-requisite to understand lateral changes in seal capacity. These maps should be as accurate as possible from cores, logs and seismic information, but may still have uncertainty, especially at facies boundaries. Sharp lateral changes in facies are unusual unless unconformities are involved. As such, facies belts are notoriously diffuse at their edges. What works in one location may be enough different in the next location as to cause seal failure.

An example of diffuse seal edges is shown in Fig. 4.14 for the Jurassic Khatatba Formation in the Western Desert of Egypt. (Dolson et al. 2014). The facies belts cover thousands of square kilometers and are composed of multiple tectonic as well as sea level induced transgressions and regressions. The result is a complex interlaying of reservoir and seals. The seals become progressively worse southwestward into the coastal plain and continental sandstones, where traps are often more difficult to find due to a lack of good seals. Along the coastline, especially in the lagoon and carbonate reef belts, the opposite is true, and reservoir facies are the key challenge. A relative seal risk map is shown on the top right. Note that most of the proven fields (shown as pie charts with relative oil, gas and condensate recoverable) are within the low risk seal area to the north.

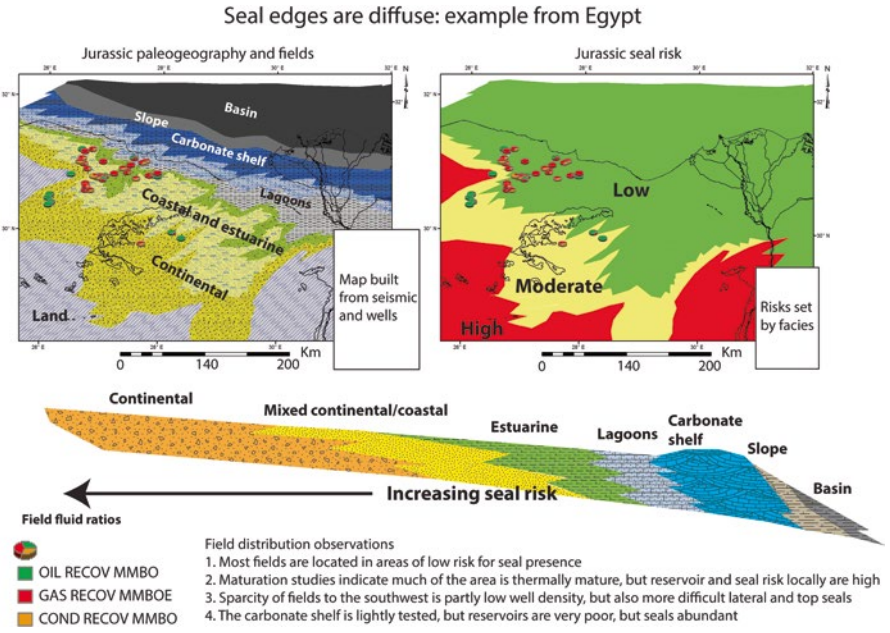

Fig. 4.14 Example of diffuse seal edges

The Jurassic section in the Western Desert offers another look at the importance of mapping top seals. Figure 4.15 (top) shows the location of fields producing the Upper Cretaceous Bahariya and Abu Roash Formations. North of the Rosetta fault, there are a number of fields which appear to be source from Jurassic Khatatba source rocks, based on prior geochemical work and regional basin analysis. In this area, Cretaceous age source rocks are thermally immature and cannot explain the accumulations at the Upper Cretaceous levels.

Overlain on this map are the locations of Jurassic faults as well as the isopach of the top seal to the Khatatba, the Masajid Formation (top map). Areas colored red or orange are where the Masajid Formation is thin to absent, eroded by an overlying unconformity. These areas correspond to a large number of Upper Cretaceous accumulations, indicating substantial vertical migration along faults or upward into pervasive and regionally thick sandstones of the Lower Cretaceous AEB Formation. Oil shows from a commercial database are posted on a geological cross-section (Bottom figure) built with Trinity software which shows probable migration pathways from the thermally mature Jurassic source beds upwards into the AEB and shallower. The most regional top-seals are within the Abu Roash and Khoman Formations, which is where most of the accumulations in this area stop. There are a multitude number of four-way closures and excellent 3-way fault taps at the Upper Cretaceous level in the areas of thick Masajid, but with no hydrocarbons, suggesting a total failure of vertical migration.

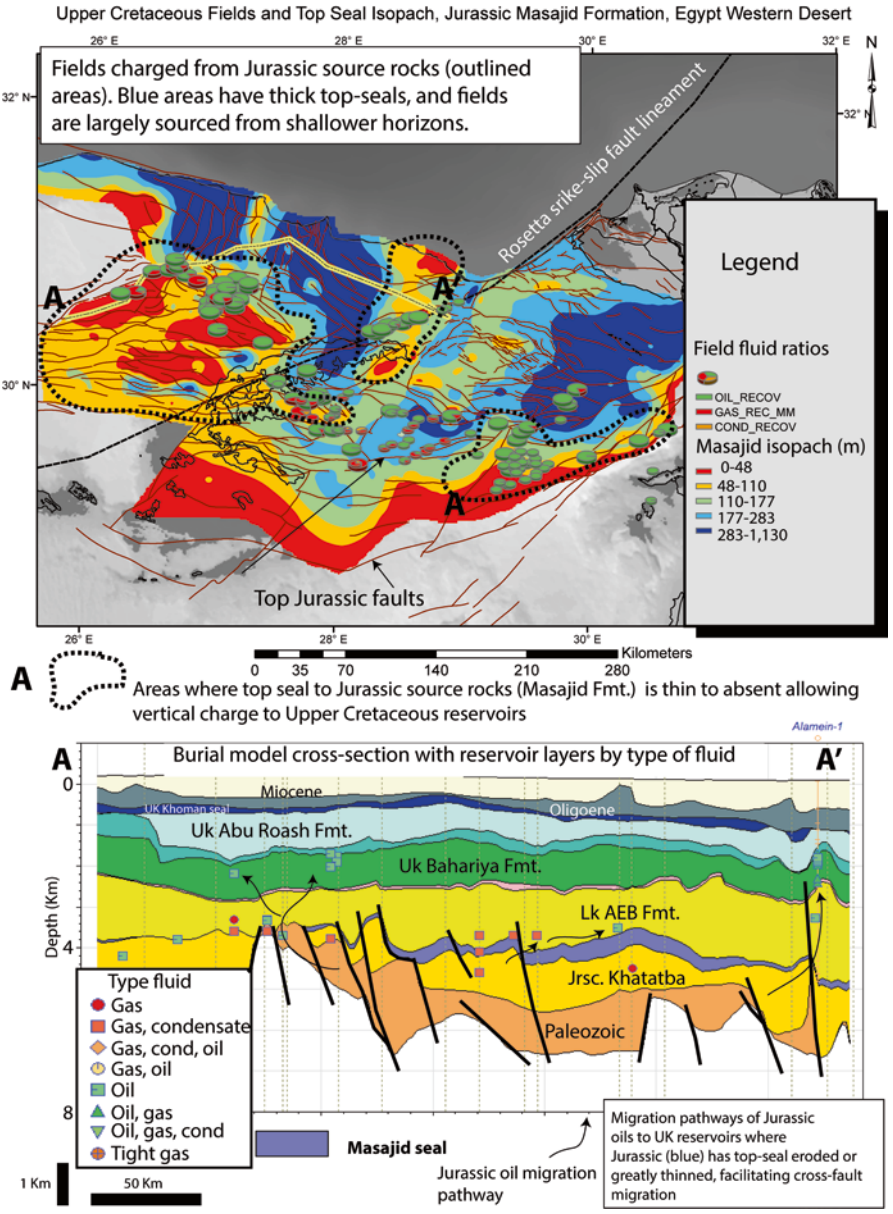

Fig. 4.15 Top seal failure on the Jurassic Masajid Formation failure and vertical leakage to overlying Cretaceous reservoirs

Another insight provided by Downey (1984) is quantification of how much oil and gas might be lost due to a small fracture at the top of an accumulation (Fig. 4.16). Although the numbers of loss are impressive, in nature, things are more complex, and forgiving. Many fractures don't extend far enough into the seal to do more than

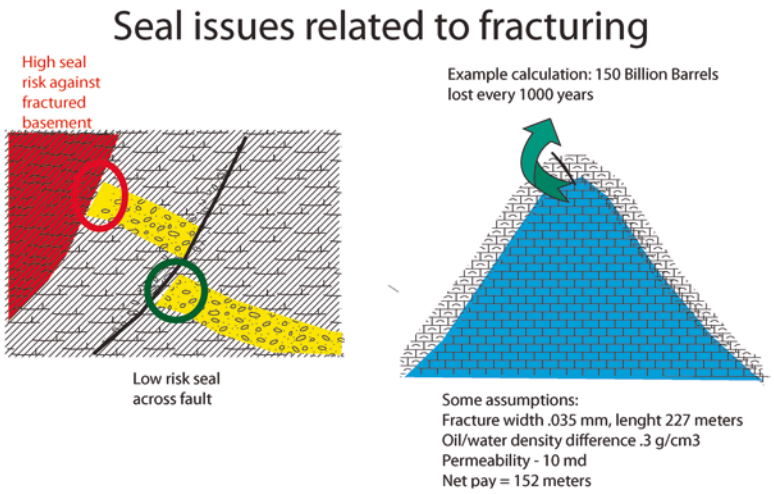

Fig. 4.16 Fractures causing fault sealing. Modified from Downey 1984. Reprinted with permission of the AAPG, whose further permissions is required for further use

create a complex waste zone. A common bias in exploration is that basement seals, due to their brittle lithology (Fig. 4.16, left) are high risk oil and gas candidates.

While this is certainly worth considering, there are large numbers of field globally producing not just from fractured basement itself, but from fault seals along basement. Some of the best recent examples are down-thrown traps in Lake Albert of Uganda (Cloke 2009; Smith and Rose 2002). Field work and careful work with pressures and shows can sometimes derisk these types of geological scenarios.

Another key point is understanding pressure regimes and impacts on seals. Downey (1984) correctly points out that pressure differential across a fault can lead to hydrocarbon leakage. In Fig. 4.16 another example from Egypt of seal failure across a fault due to differential and excess pressure. Seismic velocities are routinely used to estimate pore pressure. A full discussion of this is beyond the capability of this book, but will be covered briefly later. In Fig. 4.17, seismic pore pressure analysis shows areas of overpressure shown by dark blue, green and beige colors. A prominent growth fault west of the EEM-1 well is overpressured on to the southwest and normally pressured to the northeast (Heppard et al. 2000). A shallow well, Ringa-1 was drilled to test a robust fault closure on the upthrown side of the fault. When drilled, it found only a fraction of the hydrocarbon expected. Pressure-depth plots revealed a residual gas column 58 m long (Fig. 4.17c) beneath a small continuous phase producible gas zone. The well was drilled on seismic DHI's (direct hydrocarbon indictors) which showed an excellent correlation with a paleo gas-water contact at the base of the residual gas shows. The best explanation for the failure was that the original trap was much larger, but due to excess pressure, bled off across the fault, leaving only a much smaller commercial column behind. Unfortunately, seismic DHI's are sensitive to enough 10 % gas saturations, where they look like robust traps, but are nothing but residual accumulations.

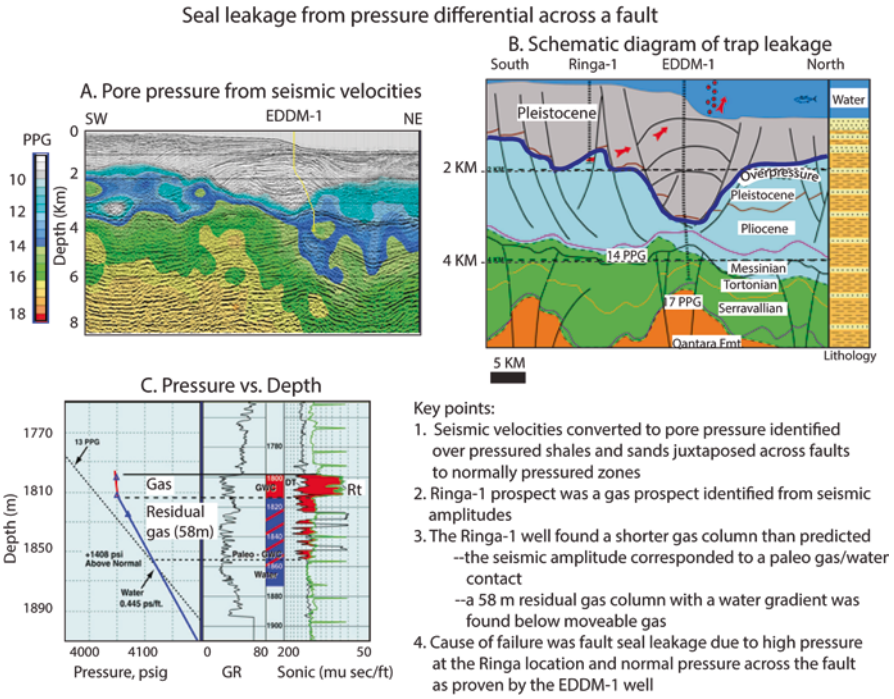

Fig. 4.17 Leakage across a fault due to higher excess pressure. A significant residual gas column beneath continuous phase gas in the Ringa-1 well is from a paleo-column leaked across a fault due to pressure differentials. From Heppard et al. 2000

We drilled more than one paleo-accumulation in the Nile Delta during my tenure in that basin from 1999 to 2002. Unfortunately, you have to drill a well to find out if it is still there. You win some. You lose some.

4.2.2 Fault Seals

4.2.2.1 Fault Traps, Gouge and Juxtaposition Analysis

Fault traps are second only to 4-way closure in providing reasonably easy prospects to identify. They offer the additional potential for a number of stacked pay horizons if the fault seals at multiple levels. In some basins, particularly in rifts, fault plays are the dominant trap type. The Gulf of Suez in Egypt (Fig. 4.18) is a case in point, with fault traps comprising virtually all of the exploration activity over the last half century. Even in this basin, however, fault seal failures are common at some levels and surprises are made at others.

I spent 5 years exploring in the Gulf of Suez as part of a large team at GUPCO. Enormous effort was put into mapping faults and building 3D computer models with fault planes and facies changes to try to look for both new fields and

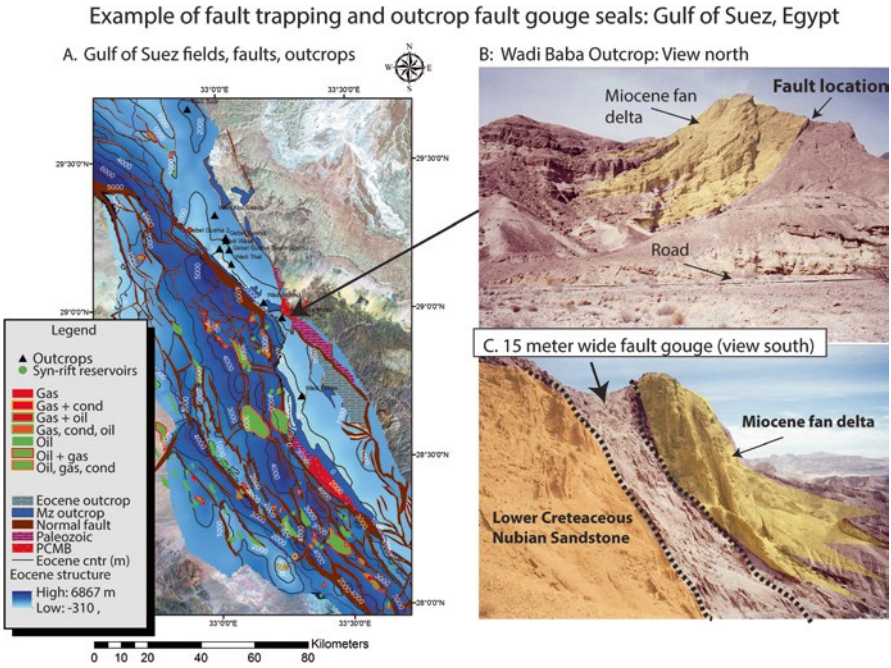

Fig. 4.18 A rifted basin with fault traps as the dominant play: the Gulf of Suez, Egypt. Fault traps remain the dominant play in this basin after more than 50 years of exploration offshore

better infill well locations. Quantitative dip analysis of the beds (Bengtson 1981) was done routinely with computer software designed to analyze digital dipmeter data (logs that record the dip and strike of a formation) in order to accurately detect fault locations, throw, direction and type. Integrated into this analysis was close look at hydrocarbon shows and pressures that would indicate fault seals between wells, some of which were below seismic resolution.

Today, a large number of service companies offer software and training to evaluate fault geometries and seals. A number of these vendors and tools are listed in Table 4.6. As this topic is huge and many books devoted to fault seals alone, this section summarizes many of the basic issues and techniques used to evaluate fault seals. Practical applications in petroleum systems modeling software to test fault seal models quickly and calibrate to subsurface shows is also illustrated.

As such, understanding ways to evaluate fault seal risk predrill is an important part of any prospect assessment.

Figure 4.18 also shows the stratigraphic and structural changes occurring during active faulting, and subsequent fault gouge created in a major fault zone. Figure 4.18b shows a very thick (see road bed for scale) Miocene fan delta developed on the downside of a large basin-bounding normal fault. Details of the geology of this area, beautifully visible in three dimensions on the Sinai margin outcrops, is covered well by (Gawthorpe et al. 2002; Sharp et al. 2000; Young et al. 2002). On the upthrown

Table 4.6 A partial list of software packages and vendors for fault seal analysis

Vendor	Software package	Links
Badley Geoscience Limited	T Seven (Trap Tester)	http://www.badleys.co.uk/traptester-overview.php
FaultSeal Pty Ltd	FaultRisk	https://www.faultseal.com/
Paradigm	SKUA Fault seal	http://www.pdgm.com/getdoc/c3e50ad1-debe-48 cd-bacf-32dd9a335167/skua-fault-seal/
Emerson Process Management	RMSfaulseal (ROXAR)	http://www2.emersonprocess.com/en-us/brands/roxar/reservoirmanagement/reservoirsimulation/pages/rmsfaultseal.aspx
Schlumberger	VISAGE, ECLIPSE, Petrel	http://www.slb.com/services/technical_challenges/geomechanics/reservoir_management/fault_seal_analysis.aspx

side of the fault is the massive Lower Cretaceous Nubian sandstone. The Nubian Sandstone contains almost no effective seals, and certainly none on a regional basis or at this location. However, there is a 15+meter wide gouge zone separating the Cretaceous and Miocene reservoirs. This gouge is created as the rocks are crushed in the fault plane and can provide at least some seal capacity to hydrocarbons, especially if the fluid is a heavier oil. In the subsurface, many examples exist of columns located on the down thrown side of faults in Miocene strata that often juxtapose Lower Cretaceous reservoirs.

One of the oldest and well established methods of dealing with fault seal analysis remains that of fault plane mapping, where lithologies on the hanging wall and footwall are visualized in cross-section along a fault plane. These maps are termed Allan fault plane maps (Allan 1989) and illustrated in Fig. 4.19 (Yielding et al. 1997).

Construction of these cross sections, if done by hand, takes a great deal of time and requires an detailed understanding of the facies relationships at each structural level, as well as a clear idea of the vertical stacking of seals and reservoirs. In the real world, facies changes within the depositional systems may further complicate map construction. In fluvial systems, for example, seals may change rapidly along the fault plane, as the reservoirs are highly lenticular. This type of analysis is done much quicker with computers, which can build a 3D model of reservoir-seal pairs and then model cross sections in any view. Given the level of detail required to build the maps, this technique has its best application within fields, in areas of densely spaced wells or where 3D seismic is available to help with the facies geometries.

At an exploration scale, there are even more difficult to work with, as layer cake seals and reservoirs are uncommon in many provinces, especially in syn-tectonic settings where active growth faulting may deposit thick reservoirs on one side of a fault and have the other side barren. Rifts are also notorious to deal with in this manner, due to extremely rapid facies changes and complex reservoir geometries. Nonetheless, where stratigraphy provides a more layered geometry of reservoir and seal, these kinds of analysis are essential to understand trapping potential and risk early.

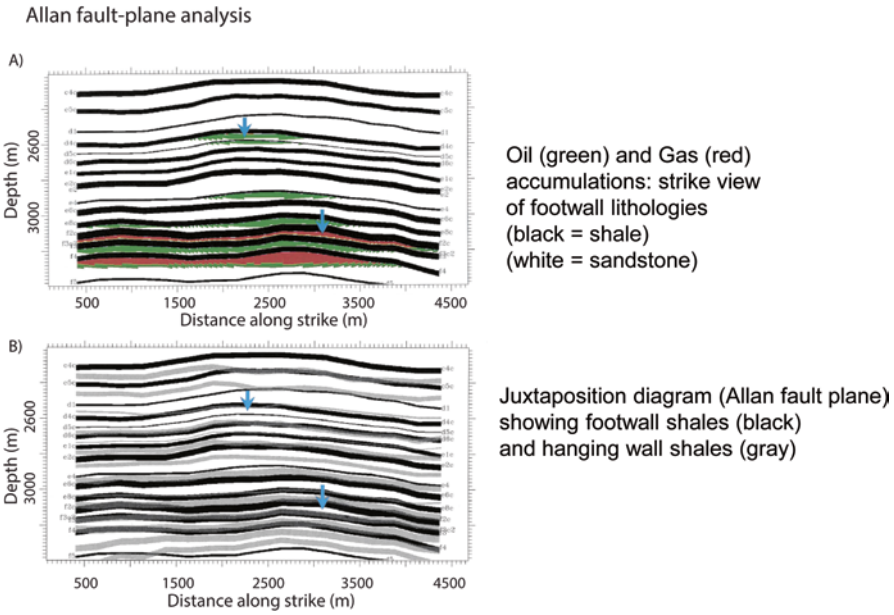

Fig. 4.19 Allan fault plane analysis. From Yielding et al. 1997. Reprinted with permission of the AAPG, whose further permissions is required for further use

Another common evaluation technique is calculation of the Shale Gouge Ratio (SGR), a value that can help determine if a fault will seal just from the lithology mix in the fault plane itself, regardless of reservoir juxtaposition on each side. This is illustrated in Fig. 4.20. Some people prefer to run the reciprocal of this equation, calculating the clay smear or shale smear factor (Fig. 4.21).

In either case, a quantitative assessment of the ratio of sand and shale at each level across the fault is necessary to derive the numbers. The numbers themselves are fairly useless unless calibrated with pressure or shows data to determine what an effective SGR seal would be, and for what kind of fluid.

An example of a simple calibration is illustrated by Gibson (1994), for stacked pay zones in a growth-fault province in Trinidad (Fig. 4.22).

In the Trinidad case, SGR ratios of 30 % or more had 100 % of the faults sealing. Predrill, then, SGR estimates became a valuable tool to determine low risk locations for additional untapped or undrained oil pools.

Other factors that need to be kept in mind include:

1. Pressures
2. Burial history
3. Timing of migration vs. faulting

As in the case of lithology seals, what works in heavy oil might not work in gas, due to increased buoyancy pressure.

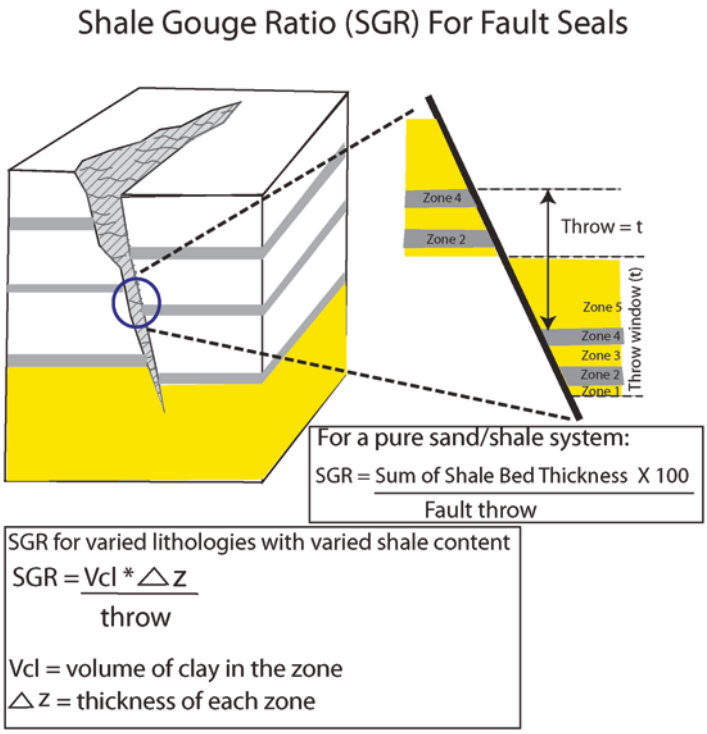

Fig. 4.20 Calculating volume of shale in a fault plane that can act as seals. Modified from Yielding (2002). Used with permission from the Norwegian Petroleum Society

(Bretan et al. 2003) provides an excellent summary diagram of some of these factors and the impact on fault sealing using SGR analysis (Fig. 4.23).

As Fig. 4.23 shows, the buoyancy pressure in an oil water system is much lower than that of a gas-water system. Leak points can be determined from capillary pressure analysis (Chap. 5) and also calibrated to known column heights in existing fields. Figure 4.23a (right side of diagram) shows impacts on seal capacity as a function of burial depth in an oil-water system. As a general rule, the deeper the burial, the more brittle the rocks become and the sealing capacity decreases. Figure 4.23b (lower right) gives a column height estimate vs. the fluid phase present. Note that a SGR of 30 for a heavy oil system can trap up to 1100 m of oil but in a gas system, only 100 m.

Fault type is also important. Strike-slip faults can have an enormous amount of crushed rock along the fault plane, acting as a seal, but with values that are not simple to quantify. A case in point is the giant Jonah Field, a tight gas accumulation in Wyoming (Fig. 4.24), documented well by (Hanson et al. 2004; Montgomery and Robinson 1997; Shanley 2004; Surdam et al. 2001). The field is a classic showcase for why to pay attention to shows and pressure.

I had worked the Johan area as a young geoscientist in 1983 with Amoco and was asked to look at this part of the Green River basin where there were intriguing gas

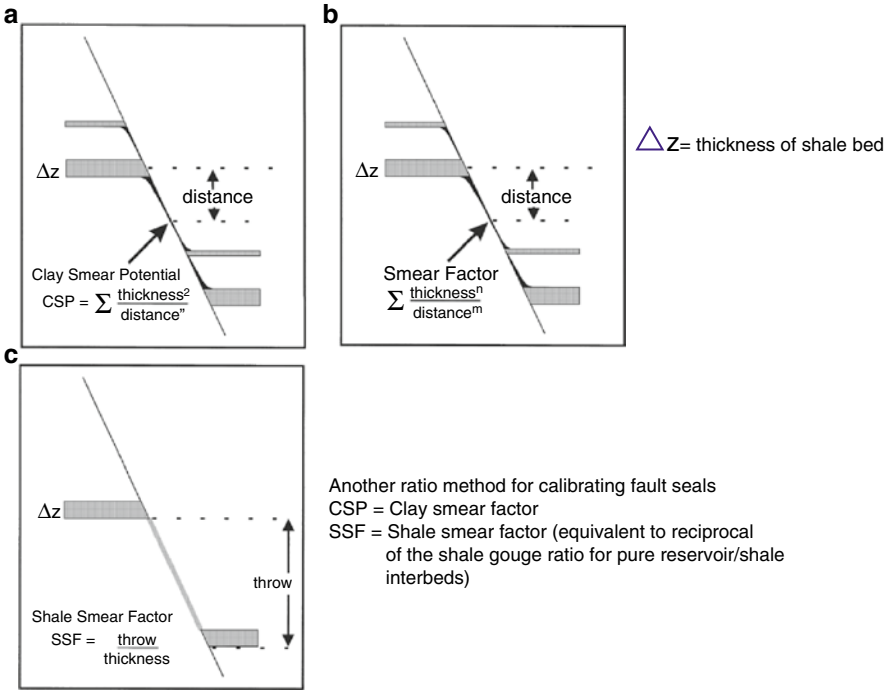

Fig. 4.21 Clay smear ratio. Modified from Yielding et al. 1997. Reprinted with permission of the AAPG, whose further permissions is required for further use

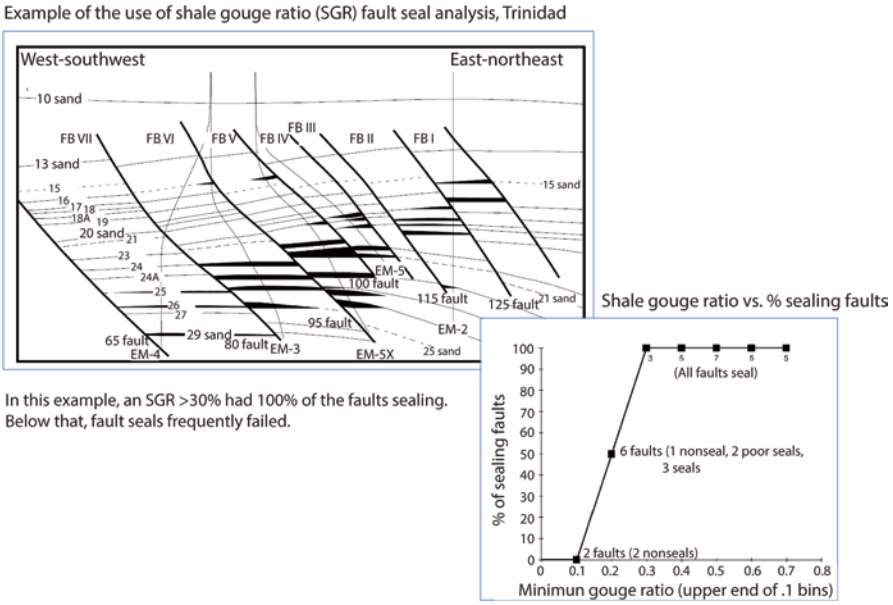

Fig. 4.22 Example of calibration of SGR ratio with sealing faults based on pressures and hydrocarbon columns in a complexly faulted field in Trinidad. Modified from Gibson and Bentham 2003. Reprinted with permission of the AAPG, whose further permissions is required for further use

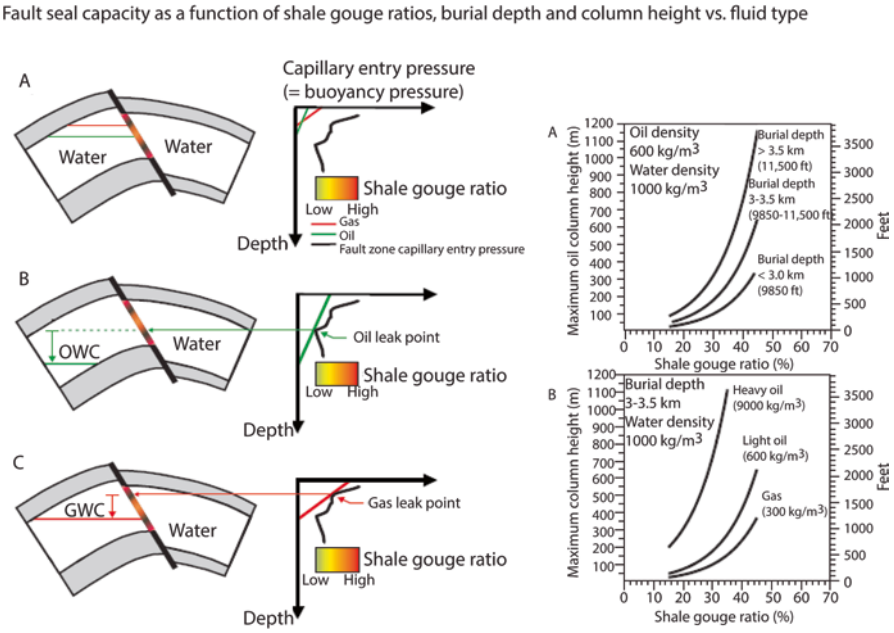

Fig. 4.23 Column height and seal capacity in SGR calculations as a function of fluid density and burial depth. From Bretan et al. (2003). Reprinted with permission of the AAPG, whose further permissions is required for further use

shows, but many dry holes. Structurally, the area was largely ramp dip with few faults and limited seismic. What seismic was available was 2D and older vintages. I pointed out that low rates of gas had actually been tested in some wells, all of which were plugged and abandoned as dry holes. I could not explain the trap.

Years later a few of my colleagues (with other, smaller companies) took a more practical approach. In the Jonah area, one dry hole existed that had quite an apparent column of very tight, but gas saturated reservoirs in the Tertiary and Cretaceous reservoirs. The well was overpressured. Updip, the Corona 7–24 well was wet and normally pressured. This information proved that a seal existed between the wells, although what caused the seal was unknown. A dry hole with apparent pay behind pipe in the overpressured area proved the presence of a gas field. The accumulation might be small, or it might be large. The issue was size and location, but not presence.

Log correlations between the dry holes showed extensive sandstone development, but no obvious trap. But with the pressure and pay observations in mind, they proceeded to purchase as much acreage as possible around the well with the gas and overpressure. As they say, the ‘rest is history’. After applying hydraulic fracturing and some more novel completion techniques to avoid formation damage, they unlocked an 8 + TCF gas field. After 3D seismic was shot, the trapping faults became visible (Fig. 4.24).

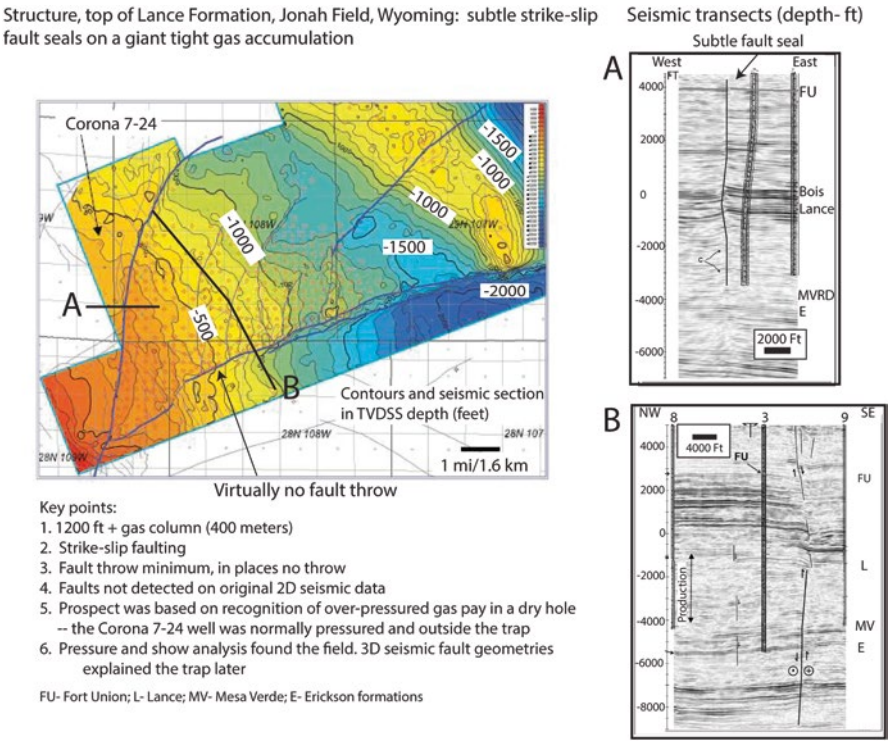

Fig. 4.24 Strike slip fault sealing with minimal to no throw along the sealing faults. Map from Shanley 2004. Seismic depth sections are from Hanson et al. 2004. Reprinted with permission of the AAPG, whose further permissions is required for further use

Both of these faults are near vertical and have strike-slip components. What is important to note is that along the faults, there are numerous places where the throw goes to zero. Despite that, the faults are sealing a 1200′ (400 m) gas column.

From a personal perspective, when I have to deal with strike slip faults, I think of them as potentially low risk seals and then seek to find other data that might support or debunk that idea.

4.2.2.2 Stress Direction: Borehole Breakout

No discussion of fault seal risk is complete without an understanding of regional and local stress fields. Faults that are undergoing tension can be likely to leak and those under compression more likely to seal. Many unconventional shale plays use analysis of regional stress directions to determine optimum potential natural fracture orientations in shales that might enhance permeability during a hydraulic fracture, or, in some cases, allow a vertical well to produce. A good

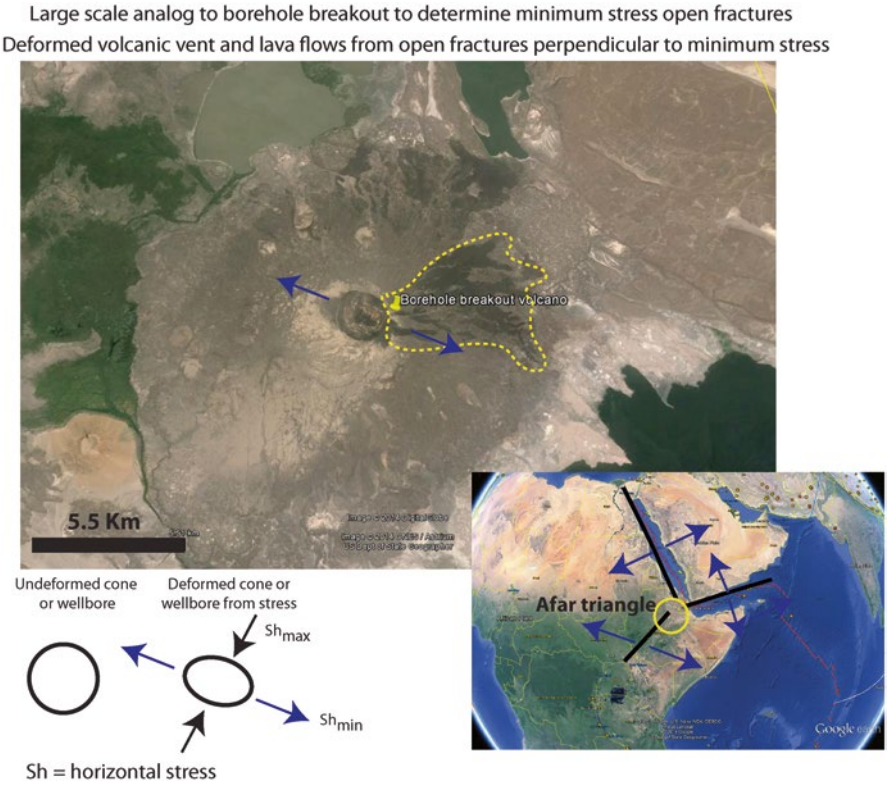

Fig. 4.25 Borehole breakout analogy, volcano in the Afar triangle

summary of techniques used from outcrop and wells is that of (Engelder et al. 2009).

One of the most common methods of determining stress in wellbores is that of wellbore breakout. The concept is fairly simple, in that a borehole would be perfectly cylindrical, in theory, if stress directions are equal. If the borehole shape is elliptical, however, that means differential stress is acting on the wellbore, deforming it. Caliper logs can readily measure wellbore diameter and stress diagrams determined as a result.

A good way to visualize this is at a much larger scale, with volcanos in active tectonic regimes (Fig. 4.25). The Afar triangle is part of an active triple junction where Tertiary rifting is occurring with extensional stress oriented NW-SE. Fractures will preferentially occur perpendicular to the minimum horizontal stress. A prominent volcano show clear elongation in that direction and associated lava flows emanating largely from fracture systems running NE-SW, or perpendicular to the minimum horizontal stress.

When modeling fault seal capacity, this is an additional step that can be taken to evaluate seal capacity. A fairly good treatment of this topic, as well as stress evolution through time is that of (Bjorlykke et al. 2005).

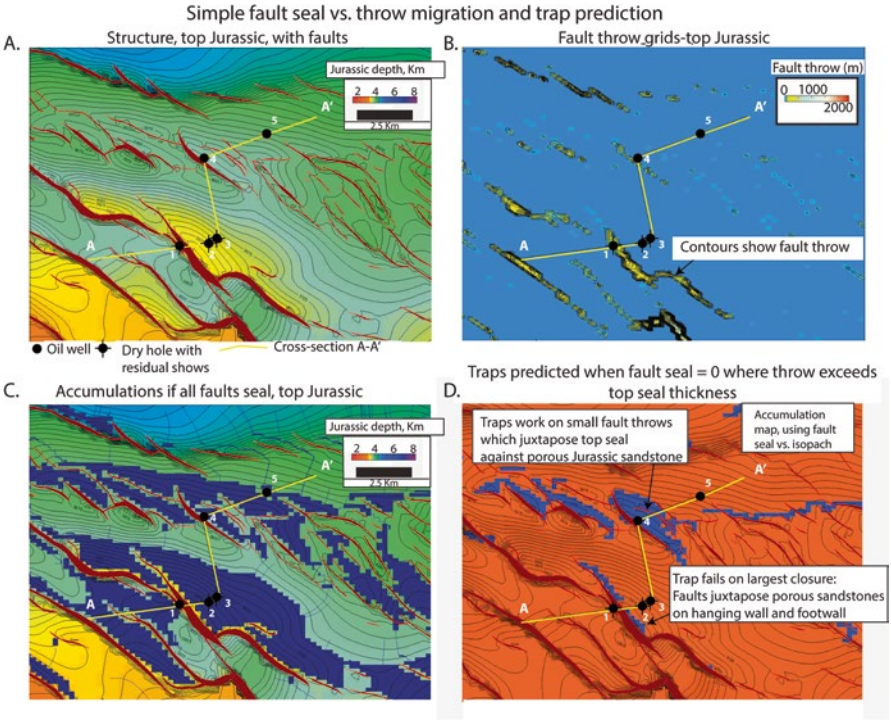

Fig. 4.26 Fault throw mapping and seal analysis, Egypt

In the end, faults seal needs to be approached from a variety of models and techniques and there are seldom definitive answers given to every fault in a study area. However, getting models built which can reduce risk is highly desirable. One of the keys remains, however, continue calibration of the models to pressure, hydrocarbon phases on both sides of the faults, shows, and other data, to validate the models. An example follows.

4.2.2.3 Testing Fault Models with Shows

Only your ability to calibrate your ideas to observed data that will let you effectively evaluate seals and traps. Figure 4.26 shows a Trinity migration model using a couple of scenarios of fault sealing and then calibration against the results of the wells. Figure 4.26a is a structure map on the target horizon (top Jurassic). A large 3-way structural closure at well locations 2 and 3. This area has the structural geometry and faulting well constrained by 3D seismic, which greatly aides in assessment. Figure 4.26b is a fault throw map made by calculating the difference in elevation on both sides of the fault. This map provides a grid of values at each fault polygon that can then be used to create seal grids from a variety of parameters. For example,

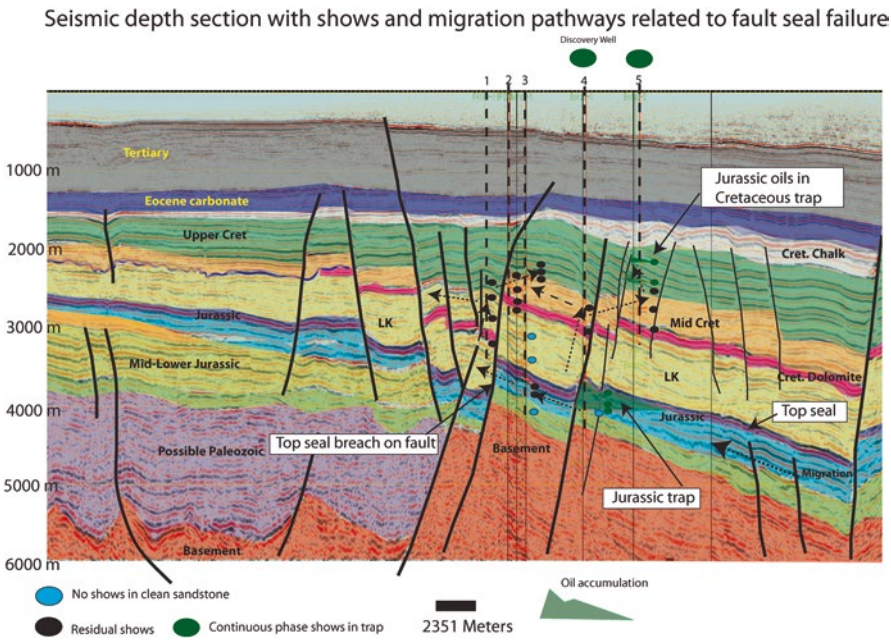

Fig. 4.27 Seismic depth section A-A′ showing residual vs. continuous phase oil shows. See Fig. 4.24 for location

since the fault throw is known, if the relative ratios of shale and reservoir over the faulted area are known, a shale gouge ratio map could be constructed using the fault throw map. Likewise, all faults can be set to seal (Fig. 4.26c) or set to seal based on their throw relative to top seal thickness (Fig. 4.26d).

A migration model, run using all faults as sealing, shows the predicted accumulations at the target level (Fig. 4.26c). Unfortunately, there are three dry holes (1,2,3) drilled around or within the largest 3-way structure. As in any basin, knowledge of top seal thickness and lithology is essential. By setting all faults as sealing, that component of seal risk was missed and undervalued. For the model run in Fig. 4.24d, the fault throw map was subtracted from the regional isopach of the top seal. Where the throw exceeded top seal thickness, the faults are set to leak.

The results in Fig. 4.36d show that the large trap failed because the throw was so big it juxtaposed porous Lower Cretaceous reservoirs against porous Jurassic reservoirs across the main fault. The Trinity fault seal model also successfully predicted (pre-drill) that accumulations would be possible where the throw did not breach the top seal. On a more regional scale, virtually all of the dry holes at this level were easily explained by using seal capacity from throw vs. top seal isopach.

A good image of the seismic and facies from Fig. 4.26 is with a 3D seismic cross-section through wells 1–5 (Fig. 4.27). Well 4 is a discovery at the Jurassic level, as well as higher levels in the section. Trinity 3D models helped de-risk this area pre-drill. Information from fluid inclusions in well 1 (topic covered in Chap. 7) showed

that residual shows were clearly present at the Jurassic level (blue horizon) on both sides of the mail fault in wells 1–3. However, a significant prospect (well 4), where fault throw did not exceed top seal thickness, came in as predicted. Interestingly, there is considerably vertical migration in this area up to terminal regional seals in Cretaceous chalks. A significant oil discovery that geochemical data suggests came from a Jurassic source rock, was made at the Upper Cretaceous Abu Roash level in well 5. That accumulation was also predicted pre-drill in a Trinity migration model.

4.3 Building and Interpreting Pressure Vs. Depth Plots and Hydrodynamic Flow

4.3.1 The Basics of Pressure-Depth Plots and Recognition of Hydrodynamic Flow

Pressure vs. depth plots, in the simplest cases, where there is a hydrocarbon-water contact in a thick reservoir, will give an exact depth to the free water level and a direct reading of the hydrocarbon and water density (Fig. 4.28). Any points lining up on the same gradient indicate they are in the same fluid and hydraulic compartment. Recall

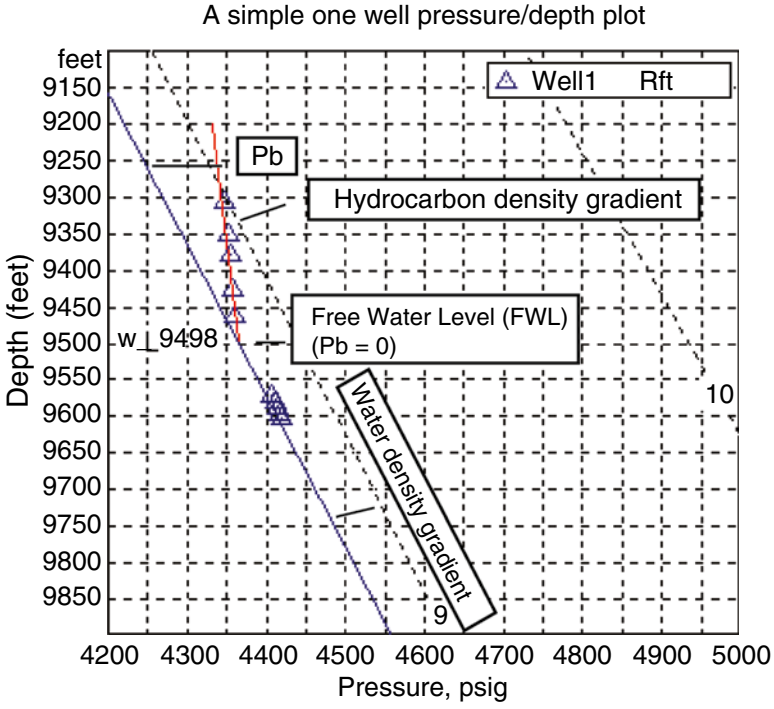

Fig. 4.28 A simple pressure depth plot and location of the free water level (FWL)

also that the psi difference at any point between the hydrocarbon and water phase is a direct measure of the buoyancy pressure (Pb). At 9250 ft. in this trap, the buoyancy pressure is 100 psi. It is zero at the FWL. It is crucial to remember that the FWL is not necessarily at the oil or gas/water contact. That contact is determined by the capillary properties of the reservoir and its pore throat size. Oil water contacts can be significantly higher than the FWL if the rock is of poor quality. It is, again, possible to drill a dry hole with near 100 % Sw on a viable trap and assume the trap failed. Pressure data, if available, can help understand and recognize those situations.

However, add more wells and more horizons and the plots can become significantly more difficult to read. Understanding pressure vs. depth plots boils down to understanding the 'plumbing' in your reservoir system and how you interpreted the causes of pressure differences. The differences may be due to faulting, facies seals, hydrodynamics or other factors.

Figure 4.29 provides a good illustration of the problems associated with interpreting pressure-depth plots.

In basins where there is no movement of water, the setting is termed hydrostatic (Fig. 4.29a). In this tank experiment, pressure is put downward equally on the rock-fluid system and water rises to equal levels A and B in the tubes inserted into the tank. These tube simulate wells. The level to which the water rises in the wells is referred to as the potentiometric surface. The difference in elevation of water levels in wells is a reflection of what is termed hydraulic head. In a hydrostatic situation, there is no hydraulic head (Hw) and flow is zero.

In some cases, basins behave in a very simple hydrostatic situation, such as in parts of the Devonian carbonate trend in Alberta (Fig. 4.30). In this area, reef development in Devonian carbonates creates numerous stratigraphic traps that frequently overly the same aquifer system. This is an ideal situation, because an oil discovery, once the pressure is taken, can determine the FWL directly. By plotting a line showing the density of the oil, the point it intersects the aquifer will be the FWL and base of the trap. In practice, however, I have seldom seen this. Life is usually much more complex.

In flowing situations (Fig. 4.29b), however, the situation is different. Water will always flow from high hydraulic head to low. In the case of tilted potentiometric surfaces, there is subsurface flow of water due to the potential energy differences created by the different fluid levels. A common misconception I find with many geoscientists and engineers is that 'water flows from high pressure to low pressure'. That is actually physically impossible. If it were true, you could not drink a cup of coffee, as the pressure at the bottom of a cup is higher than at the top. Water flow is gravity driven. Water falls exist because of gravity, not because of pressure.

One of my first professional jobs as a geologist was working as a hydrogeology field assistant for the United States Geological Survey in Denver, Colorado. My job entailed driving to farms in eastern Colorado, and, once I had fended off the inevitable farm-house dogs, made friends with the owners and then thrown rocks in down wells to look for rattlesnakes, I had to sample the well. At each well, I lowered a steel tape into the well and retrieved it, marking the depth to the water table. That was followed by actually sampling the water for its salinity and other mineral

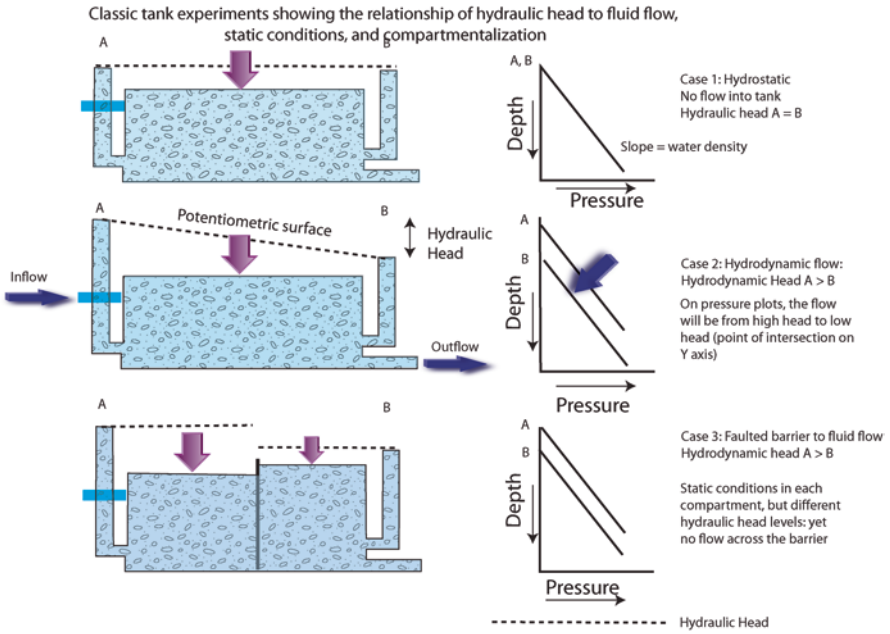

Fig. 4.29 Principles of hydrostatic, hydrodynamic and sealed compartments from pressure-depth plots. From Dahlberg 1995. Reprinted with permission from Springer-Verlag

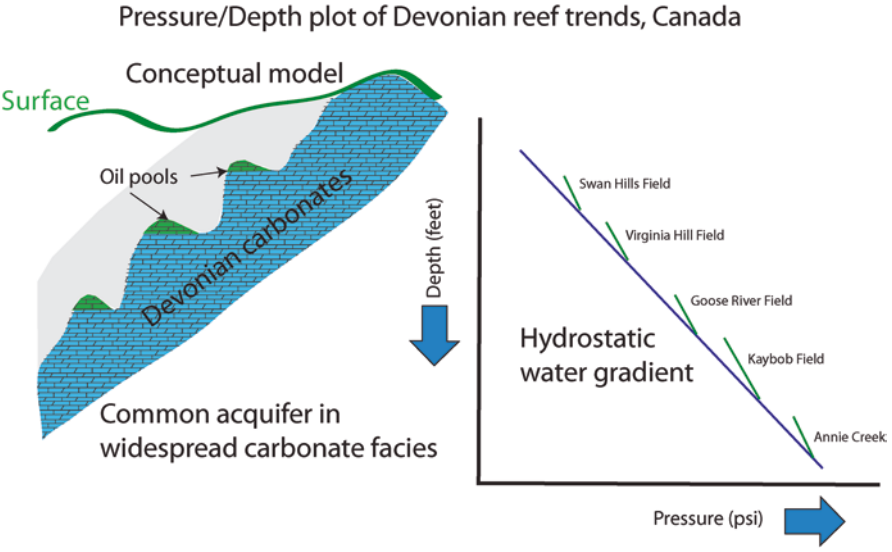

Fig. 4.30 A simple hydrostatic case with a regional aquifer that is shared between multipole traps. Modified from Dahlberg 1995

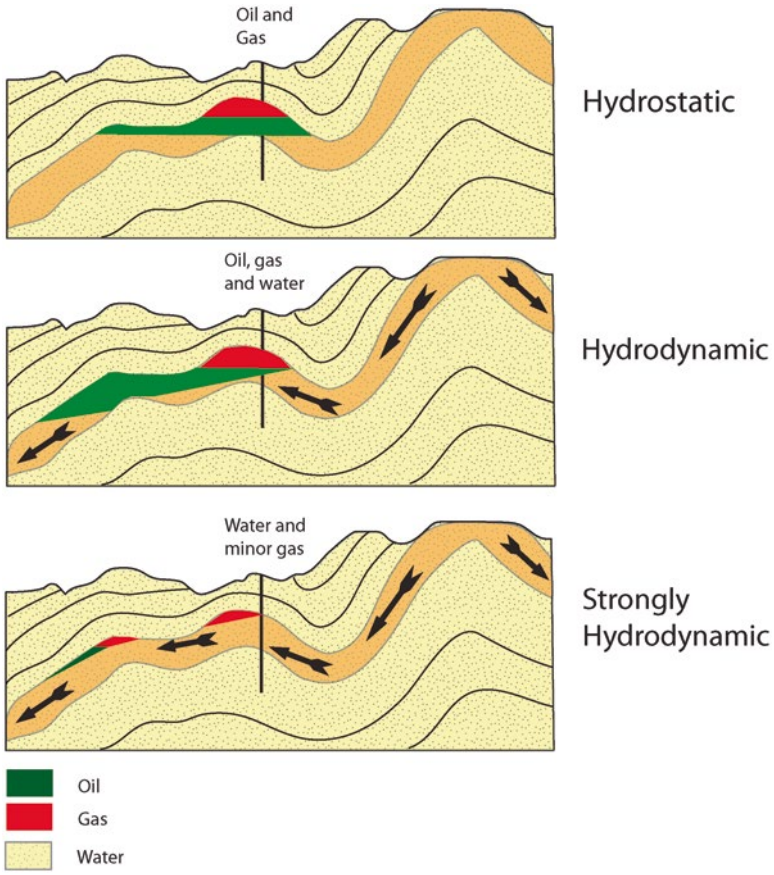

Fig. 4.31 Impact of hydrodynamic flow on an oil or gas accumulation. The degree of tilt is a function of the hydrocarbon-water density differences and the intensity of the water flow. If the gradient is high enough, structures can have their accumulations swept from the trap. From Dahlberg 1995

content. Back in the office, the location of each point went into a computer and then was contoured, building a potentiometric surface map. The map not only quantified the depth to drill to any aquifer but also the rate of flow and direction.

In the oil and gas industry, far too few companies bother to make these maps, operating instead under the assumption that there is no water flow in their basin or even if there is, it isn't that important. As will be shown throughout this section, that omission can lead to missing oil and gas fields, as flowing water has the potential to tilt hydrocarbon contacts and to completely flush potential traps in some locations (Fig. 4.31).

On a pressure-depth plot, hydrodynamic flow is indicated by parallel lines between the wells that intersect the Y axis at different levels. As the slope of the lines is the water density, the point where the trend intersections the Y axis is the

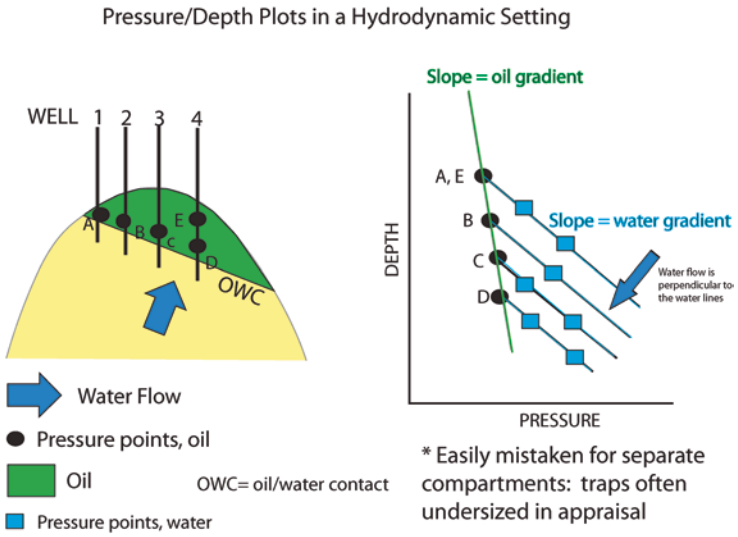

Fig. 4.32 Pattern recognition of potential hydrodynamic flow from pressure depth plots. The hydrocarbon phase will plot on one gradient and the water phase at multiple levels to the right. The direction of water flow and tilt is perpendicular to the water lines. From England et al.(1991). Reprinted with permission of the AAPG, whose further permissions is required for further use

actual depth of the potentiometric surface. In the case of Fig. 4.29b, flow is from well A to well B and well A plots higher on the pressure-depth plot than well B. Flow is perpendicular to the lines on the plot. Figure 4.32 shows a pressure vs. depth plot in a hydrodynamic setting with a titled oil-water contact.

Unfortunately, the exact same pattern can occur if there is a barrier in the wells and the differential forces on each compartment are a bit different. In this case, simulating a fault. The barrier between wells A and B in Fig. 4.29 (bottom example) could just as easily be a facies change. The pattern would be the same. This is shown schematically in Fig. 4.33, where two different aquifer systems are present, but the basin is hydrostatic. This kind of plot has great utility in exploration and development as it allows identification of which reservoirs share the same FWL and pressure system and which reservoirs are in separate traps. The ability to visualize connectivity directly from pressure data is one of the prime reasons it is so important to collect his kind of information.

Compartmentalization is important to recognize, especially for engineers, as wells that are not in pressure continuity will produce at different rates. Compartmentalization studies are used to modify where wells are drilled to top undrained reservoirs and to place water flood wells to be more effective in pressure support. Sometimes, the pressure changes are fairly subtle and require careful analysis.

An example is shown on Fig. 4.34. The well is a gas field discovery made on a 4-way closure in Australia. The depositional environment consists of highly

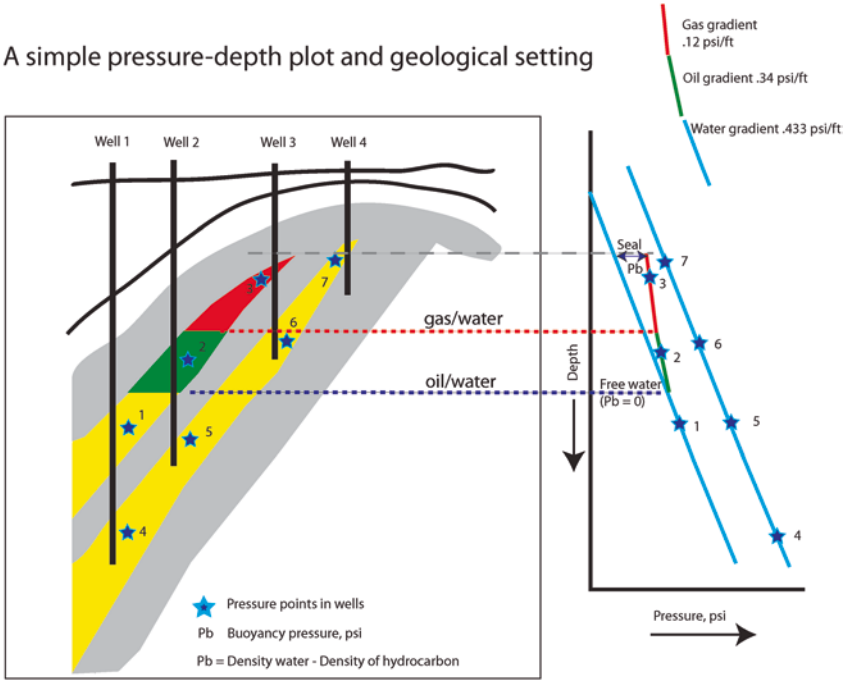

Fig. 4.33 Pressure vs. depth plot showing disconnected reservoirs in a hydrostatic environment. Modified from Dahlberg 1995

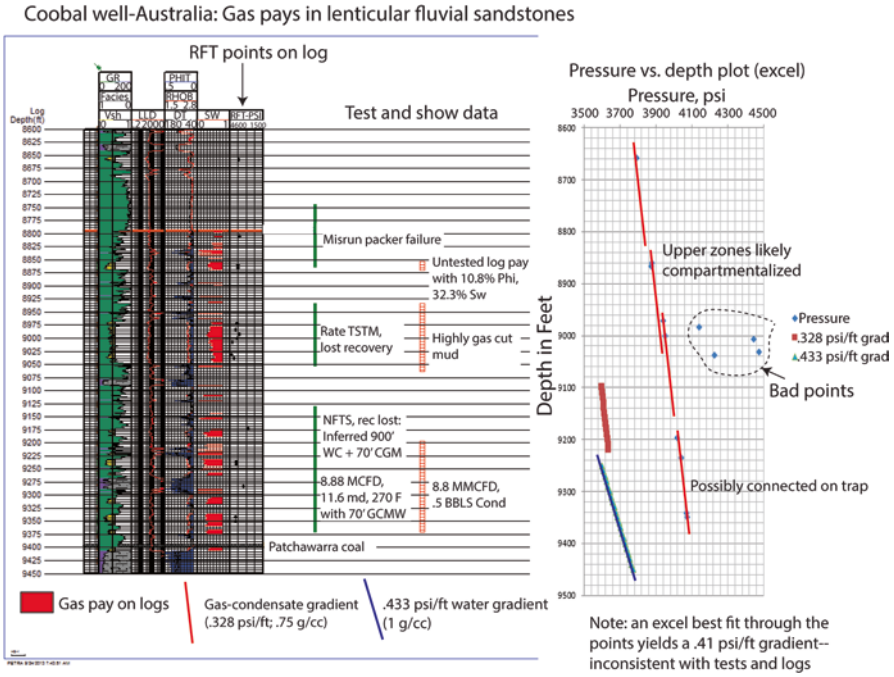

Fig. 4.34 Pressure analysis of a gas discovery, Cooper Basin, Australia. Note: An excel best fir through the points yields a 0.41 psi/ft gradient—inconsistent with tests and logs

lenticular, thin, fluvial sandstones. In these cases, compartments are almost to be expected, as the reservoirs can be so narrow. In fact, in many of these settings, the well spacing, often at 160–640 acres per well, misses a lot of pay zones, as multiple separate channels can fit between the wells.

When looking at compartmentalization, it is important to use all the data and display the pressure-depth plot at the same scale relative to the logs and petrophysical analysis. The DST and RFT data showed the gas gradient is that of a wet gas at 0.328 psi/ft (shown as red lines on the plot). The aquifers are fresh water (blue line). A number of pressure points are unreliable and have to be ignored (or better yet, not plotted). Attempts to connect all the points into one line would yield something that has a steep gradient, but that line (tried by some students of mine), yields a 0.41 psi/ft., which is inconsistent with the measured densities of the gas. A better interpretation is one of slight pressure compartments as shown. It is possible the thicker zones toward the bottom are actually sharing the same FWL, but I am reasonably confident the zones above will have separate seals and free water levels.

4.3.2 *Making Potentiometric Surface Maps and Modeling Hydrodynamic Entrapment*

Potentiometric surface maps measure the potential energy in a water-hydrocarbon system. Building these maps is necessary to add as a component to petroleum systems migration analysis if water flow occurs in your basin. Potentiometric surface maps are easy to make, involving rather simple calculations. The issue is always finding enough good pressure points to build one.

A simple diagram (Fig. 4.35) shows a couple of ways to approach this. The classic formula is Eq. 4.2 (Hubbert 1953):

$$Hw\left(hydraulic\,head\right) = Z + \left(\frac{P}{Pgrad}\right) \tag{4.2}$$

Where Z=TVDSS depth, P=Formation pressure at point of measurement, Pgrad=density of water (0.433 psi/ft if fresh water). The full Hubbert equations use a gravitational constant g multiplied by Z to express potential. However, since that is gravity is a constant, for practical purposes, it can be dropped and the resulting equation then is expressed in feet or meters. Hw maps can then be used to map the potential energy across a basin in any fluid system. The concept of fluid potential and flow is also covered by (England et al. 1987).

Note in the Fig. 4.35 that wells A and B have the exact same pore pressure (6250 psi), but flow is from well A to well B. Note also that the vertical intersection of the pressure-depth plot is Hw, and extends far above the overburden line. This is because the math is quantifying fluid potential. In highly overpressured basins, the fluid potential is high and a potentiometric surface map may have very high numbers. A good website for understanding migration and hydrodynamic map construction is available on the Trinity site (www.zetaware.com).

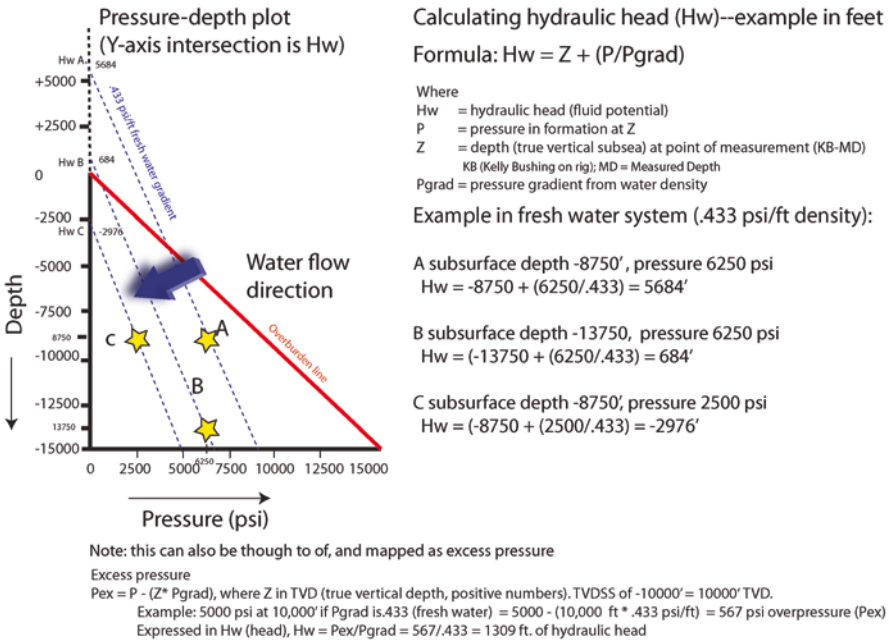

Fig. 4.35 Equations for calculating hydraulic head. The stars are pressure points from various wells. Water gradient lines passing through each pressure point extrapolate to the Y axis as hydraulic head values, giving a graphical solution that can be mathematically calculated as shown on the figure. Note: This can also be through to of, and mapped as excess pressure. Excess pressure: Pex = P-(Z* Pgard), where Z in TVD (true vertical depth, positive numbers). TVDSS of -10,000′ = 10,000′ TVD. Example: 5000 psi at 10,000′ of Pgrad is 0.433 (fresh water) = 5000-(10,000 ft * .0433 psi/ft) = 567 psi overpressure (Pex). Expressed in Hw (head), Hw = Pex/Pgrad = 567/0.433 = 1309 ft of hydraulic head

Additionally, as shown in Fig. 4.35, hydraulic head can be thought of, or mapped, in terms of excess pressure. For those geoscientists who still insist on telling me that water flows from high pressure to low pressure, I remind them it might be better to talk in terms of 'higher excess pressure to lower excess pressure. Calculating excess pressure (Pex) is given by (from www.zetaware.com) as Eq. 4.3.

$$Pex = P - \left(Z * Pgrad\right) \tag{4.3}$$

Where P = pressure in the formation, Z the TVD (positive) at point of measurement, and Pgrad the gradient of the water system. Keeping units in feet, the Pgrad is in psi/ft and P in psi. As shown, if a formation is 5000′ at 10,000′, in a fresh water system (Pgrad = 0.433 psi/ft), The Pex = 567 psi. Calculating head by this approach takes one more step (Eq. 4.4):

$$Hw = Pex \,/\, Pgrad \tag{4.4}$$

In this case Hw = 567/.433 = 1309′.

4.3.3 Modeling Hydrodynamic Tilt and Migration Using Potentiometric Surface Maps

In petroleum systems modeling software, fluid potential, which can be expressed as a potentiometric surface map, is used to model migration of hydrocarbons. As buoyancy is a driver, the density of the hydrocarbon phase must also be taken into consideration and the potentiometric surface map scaled for buoyancy pressure for a given hydrocarbon-water density difference.

A mathematical solution to entrapment and flow (England et al. 1987; England et al. 1991) is given by Eq. 4.5:

$$\Phi_p = \Phi_w + \left(\rho_w - \rho_p\right) gZ + Pc \tag{4.5}$$

where Φ_p = Fluid potential of the petroleum and Φ_w = Fluid potential of the water (Hydraulic head Hw), (ρ_w–ρ_p) is the density difference between the water and hydrocarbon, g acceleration of gravity, Z a subsurface depth and Pc capillary Pressure. Capillary pressure is used to quantify the effect of seals along the migration pathway. That component of the fluid potential map is covered in detail in the next chapter.

The (ρ_w–ρ_p)g is another way of expressing buoyancy pressure, and can be expressed in terms of the density difference between the hydrocarbon and water. The equation can be further modified by dividing by (ρ_w–ρ_p)g to Eq. 4.6.

$$\Phi_w / \left(\rho_w - \rho_p\right) g + Z + Pc / \left(\rho_w - \rho_p\right) g \tag{4.6}$$

If the capillary pressure component is ignored for now, then fluid potential from hydrodynamic flow adjusted for buoyancy is shown as Eq. 4.7.

$$\Phi_p = \Phi_w / \left(\rho_w - \rho_p\right) g + Z \tag{4.7}$$

The g component (gravity) is effectively constant, and can be dropped for practical mapping purposes, further reducing the solution to Eq. 4.8.

$$\Phi_p = \Phi_w / \left(\rho_w - \rho_p\right) + Z, with\, \Phi_w \tag{4.8}$$

with Φ_w being approximated with the hydraulic head (Hw) map. In this approach, Z is a subsurface depth in positive meters or feet, depending on the units being used for the potentiometric (Hw) map.

The effect of fluid flow on migrating hydrocarbons can be seen graphically in Fig. 4.36. Upward flow magnitude is determined by the pressure gradient vs. the density of the fluid. Oil and gas, being less dense than water, have a stronger vertical flow component. In a hydrostatic environment, where Fw (flow component of water) = 0, the migration is vertical. But when water flow is present, the vector solutions show that oil and gas will migrate, due to buoyancy, oblique to water flow as shown graphically. The vector component of gas is steeper than that of oil.

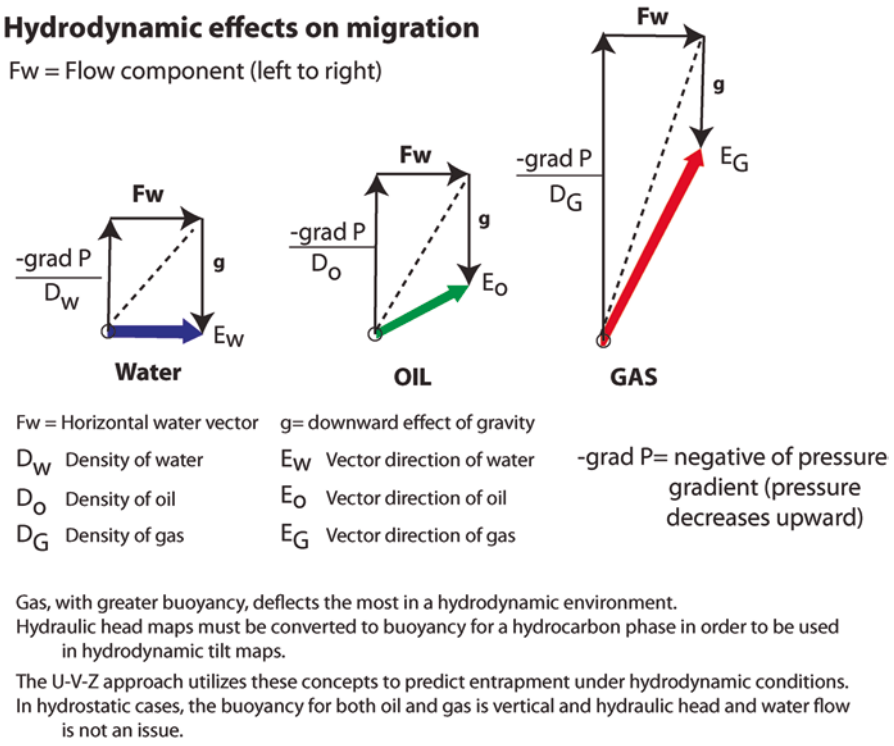

Fig. 4.36 Graphic representation of the effect of hydrodynamic flow on migrating hydrocarbons. Upward forces (vertical lines) are driven by the pressure gradient and the fluid density, with gravity exerting a downward force. Vertical hydrocarbon buoyancy is greater than water so the vector resolution produces a different flow path. Because of density differences, gas in more buoyant than oil and the result vector direction of gas (E_G) will be steeper than that of oil (E_o). Modified from Dahlberg (1995)

So, making this simple, by scaling the potentiometric map to the difference between the hydrocarbon-water density, it can be used, when added to the structure map (Eq. 4.7), to show fluid potential for the hydrocarbons.

This also assumes the density of hydrocarbon remains the same over the migrating distance, which is a source of potential error where longer distance migration is occurring and density changes may occur due to reduced pressure and temperature and other factors. However, those changes are difficult to model and simple approximations are better than no approximations at all. Maps of equal fluid potential lines will define the direction and rate of fluid flow. Where the fluid potential contours close on a map, traps exist. It is important to remember that it is not the water that is tilting the hydrocarbon columns, but the excess fluid potential created by buoyancy. The potentiometric surface map directly measures the water fluid potential and when adjusted for buoyancy, approximates the fluid potential of migrating hydrocarbons of any given density. Thus, building a good potentiometric surface map is the first step in being able to model hydrodynamic tilt and flow.

4.3.4 *A Practical Example of Hydrodynamic Tilting Using Trinity Software*

An excellent tutorial using Trinity software to modeling hydrodynamic tilting is given on the Trinity website, but downloadable files and data. Documentation of the Qatar Arch hydrodynamic maps in the following section can be found in (He and Berkman 1999).

Figure 4.37 shows the structural and hydrodynamic setting of the Qatar arch. Figure 4.37a is a structural map with field located (green). A simple migration map without hydrodynamic flow and subsequent accumulations is shown in Fig. 4.34b. These accumulations do not exist as predicted in a hydrostatic migration model, where only buoyancy is the driver. If they did, a very large structural trap would be filled at the top of the map, as shown on the cross-section, where flat oil-water contacts would be developed. Instead, the contacts are known to be tilted in this area.

Figure 4.37c shows the potentiometric surface for the formation directly above the Shuaiba Formation reservoir, which has been modeled in migration. There is a fairly strong hydrodynamic flow to the NE as shown by the slope of the potentiometric surface map. By selecting the potentiometric map to predict tilting and different potential energy available for migration, the correct position of the accumulations show up in Fig. 4.37d. Within the software, the density of both the fluid and water phases also have to be defined.

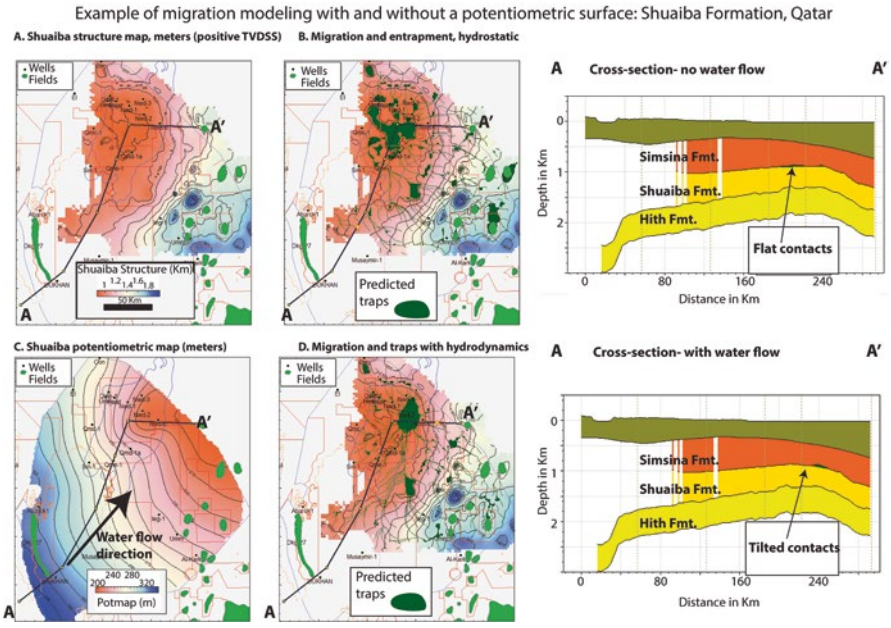

Fig. 4.37 Trinity Qatar arch tilted oil-water contacts and migration. Images created from Qatar migration model exercise, www.zetaware.com, by permission. Also, see He and Berkman 1999

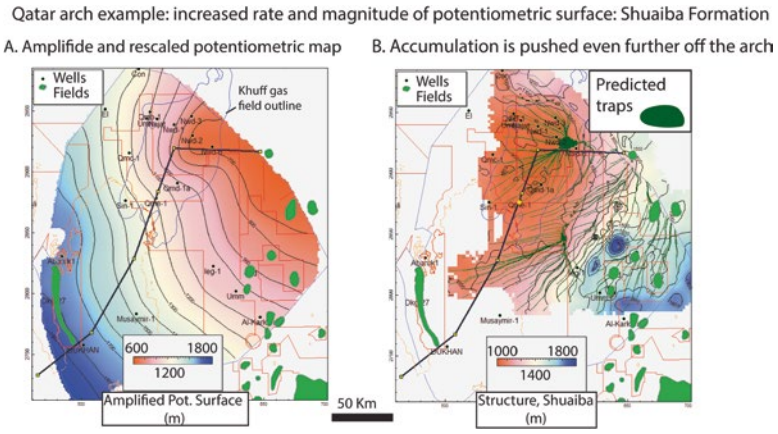

Fig. 4.38 Effect of increasing the potential energy in the water system on migration, Qatar arch example. The accumulation would be pushed even further off the crest of the structure. In a strongly hydrodynamic environment, there might be no accumulation left at all

As a way of further illustrating the impact of water flow on tilting columns, I amplified and scaled the potentiometric surface map to reflect higher water flow and potential. The results (Fig. 4.38), push the accumulation even further off the side of the structure.

4.3.5 Example of Tilted Contacts in an Overpressured Environment

Until recently, most of the examples of tilted oil and gas water contacts due to hydrodynamic flow has been from relatively shallow accumulations involving meteoric water flow. Within the last decade a number of significant papers, however, have showed that overpressured basins can have very active deep aquifers that also caused tilted on and gas contacts. Some of these references are (Dennis et al. 2005; O'Connor and Swarbrick 2008; Riley 2009; Swarbrick and O'Connor 2010). I am personally convinced this is an under evaluated situation and that many dry holes with free gas but overpressured water legs may actually be part of the top of a larger trap.

Conceptually, it makes a great deal of sense that overpressured basins should have active aquifer systems, since the extreme overpressure provides the addition potential energy and head to create a very high potentiometric surface. A dramatic example is documented in Riley (2009) in the Caspian Basin (Fig. 4.39).

My first exposure to this basin was a trip to Baku in 1993, shortly after the first westerners were allowed into the county to bid on oil and gas properties for the first time in almost 90 years. Amoco was involved heavily in the acquisition of the Azeri, Gunashli, and Chiraq fields (termed AGC and shown on Fig. 4.38. At the time, the Azeri field only a few exploratory wells in it and, while it was recognized as a

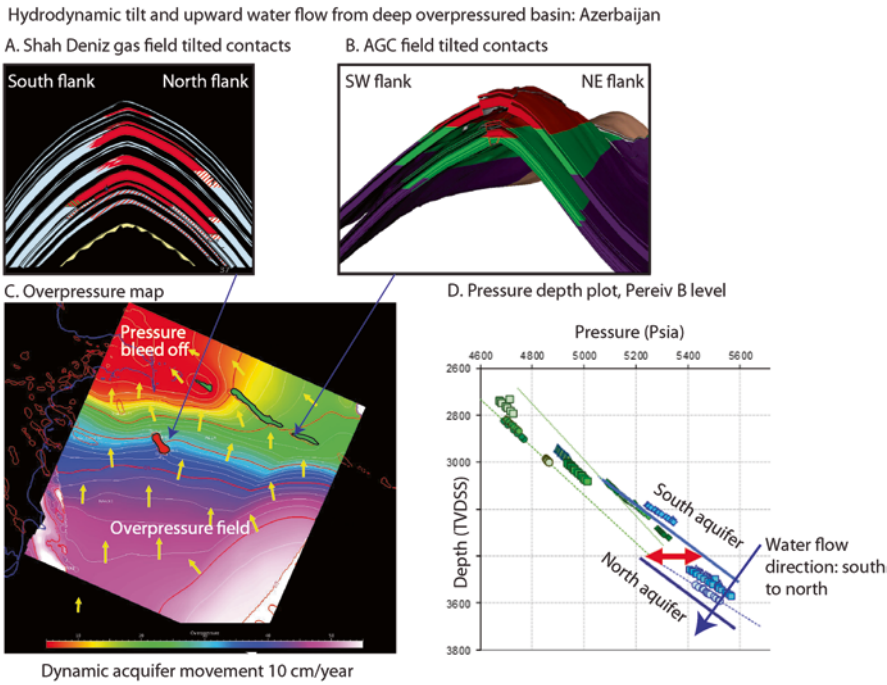

Fig. 4.39 Tilted contacts due to upward water flow from highly overpressured basin, Caspian Sea, Azerbaijan. From Riley 2009. Used with permission

world-class giant field, it was assumed that the oil-water contacts were flat. Reserve estimates were thus initially made on that assumption.

In addition, a very large offshore closure downdip of these fields, was a tantalizing prospect. Amoco bid heavily on this acreage, winning a substantial percentage. The deep prospect (now Shah Deniz) Field, a supergiant gas accumulation, was a primary exploration target. Extreme overpressure in the basin was well documented, with numerous active mud volcanos onshore, the result of seal failure along mud diapirs associated with dewatering and hydrocarbon generation. Despite this, thinking of the fields as having tilted contacts seemed unlikely at the time. Reserve estimates on fields were calculated with flat oil and gas-water contacts.

Interestingly, Amoco acquired quite a bit of data on surrounding oil and gas shows and fields and maps of fluid recoveries showed progressively higher GOR's downdip toward the Shah Deniz prospect. These data, plus petroleum systems modeling of the major source rock (Oligocene Mykop Formation) suggested the prospect would be a gas field. Other companies bet heavily on oil, due to the proximity to the giant onshore or shallow water oil fields.

When Shah Deniz was finally drilled, it came in as a rich gas-condensate field. Again, initial studies suggested flat gas-water contacts. In all the fields bid upon, however, as drilling continued, it became apparent that the contacts were tilted substantially to the northeast (Fig. 4.38a, b).

Some truly outstanding pore pressure work from wells and seismic, plus state of the art petroleum systems modeling now shows quantitatively that the South Caspian Basin is subsiding so rapidly that water is being expelled from the shales and reservoirs at a rate of up to 10 cm/year, which is a very high rate (Fig. 4.38c). A pressure-depth plot (Fig. 4.38d) shows the hydraulic head differential between the southern and northern aquifers.

4.3.6 *Building Your Own Hydrodynamic Maps: A Bit More Theory Behind Migration and Hydrodynamics: The U-V-Z Method*

It is useful to understand the workflow in a bit more detail on how to construct these kinds of maps. A frequent complaint I run into is that of a lack of software to generate hydrodynamically tilted maps easily. However, there are many simple gridding packages available on the market and most geoscientists today have at least some software tools that deal with grid manipulation. So understanding a bit more theory, but in a practical workflow example, is useful (Fig. 4.40).

Hubbert (1953) established what has become known as the U-V-Z method of quantifying subsurface migration and entrapment. The equations developed by

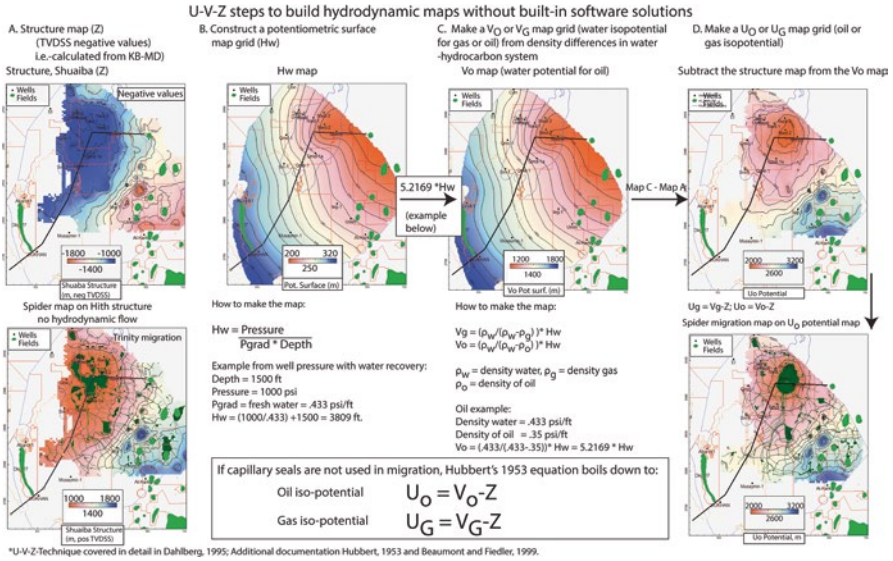

Fig. 4.40 Steps to make a hydrocarbon potential map using the U-V-Z methodology. This is a grid-based approach following the U-V-Z methodology. Any program that can deal with simple grid math can follow these steps to create hydrodynamic entrapment analysis. These maps were made without using the built-in capabilities of Trinity. They simply illustrate the process for deriving the same result with any simple gridding package. Dahlberg (1995) covers this topic in much more detail

Hubbert (1953) are the underpinning of all petroleum system migration software packages. The method is carefully and repeatedly illustrated, along with exercises, in Dahlberg (1995), using hand drawn structure maps and overlays. A simpler approach is simply to use basic math grid manipulation to derive the same results.

The methodology relies on:

1. A good structure map (Z) (in these equations, the structure map is TVDSS relative to sea level, or KB rig elevation – Measured depth).
2. A good potentiometric surface map (Hw).
3. Constructing a water isopotential map (V) with respect to oil (Vo) or gas (Vg)
4. Subtracting the structure map from the Vo or Vg map to create U (Oil or Gas potential maps-Uo or Ug).

Vg or Vo maps rely on the same equations, but with different densities (Eqs. 4.9 and 4.10)

Gas

$$Vg = \frac{Dw}{\left(Dw - Dg\right)} \times Hw \tag{4.9}$$

where Dw = density of water, Dg = density of gas, Hw = hydraulic head

Oil

$$Vo = \frac{Dw}{Dw - Do} \times Hw, \tag{4.10}$$

where Dw = density of water, Dg = density of gas, Hw = hydraulic head

The ultimate map desired is U (or oil or gas potential, Eqs. 4.11 and 4.12):

$$Ug = Vg - Z\left(Where\ Z\ is\ expressed\ in\ negative\ TVDSS, from\ KB - Depth\right) \tag{4.11}$$

$$Uo = Vo - Z\left(Where\ Z\ is\ expressed\ in\ negative\ TVDSS, from\ KB - Depth\right) \tag{4.12}$$

These final maps can be treated like structure maps where closures show where hydrocarbon entrapment might be. The reader is encouraged to delve much more into the theory than is presented in this short summary, with the best treatment that of (Dahlberg 1995).

4.3.6.1 A Note on the Value of Z in Many Petroleum Systems Software Packages

Most mapping packages, when dealing with structural maps, are generated by subtracting measured depth (MD) in a well from the surface elevation, usually set at the KB (Kelly bushing) on the rig floor. In some cases, you may only have the ground level to work with, and that number is usually close enough if the KB isn't recorded. The numbers, then, will always be negative, and calculating the hydraulic head and Ug or Uo equations works as shown above in Eqs. 4.8–4.11.

However, many petroleum systems software packages work on positive TVDSS values, actually multiplying the TVDSS grids by -1 to 'flip' them. In these cases, the equations work the same but Ug = Vg + Z and Uo = Vo + Z. In this book, examples of how to work with grids without petroleum systems software will use the negative TVDSS values (KB-MD).

4.3.6.2 Hubbert's Full Equation with Seal Capacity Added

Lastly, Hubbert's full fluid potential equation also involves entrapment due to capillarity and facies or fault seals (Chap. 5).

Hubbert's full equation (similar to what is shown in Eq. 4.5) is Eq. 4.13.

$$\Phi p\left(\textit{fluid potential}\right) = gZ + \frac{P}{\rho} + \frac{Pc}{\rho}, \tag{4.13}$$

where Z = structural elevation (TVDSS), P = pressure at that elevation, ρ = density of the fluid (water, oil or gas), Pc = capillary pressure.

As g is a constant, for practical mapping purposes it is dropped and Uo or Ug maps used.

When the g is dropped, the density units (ρ) are now in units of pressure gradient (Eq. 4.14).

$$\Phi p\left(\textit{fluid potential}\right) = Z + \frac{P}{Pgrad} + \frac{Pc}{Pgrad} \tag{4.14}$$

Where Pgrad is oil or gas density in psi/ft (for example, 0.35 psi/ft for oil). Equation 4.13, then, results in values in feet or meters, depending on the units used for Z (subsurface structure). These values are then contoured, producing an equipotential map that reflects both fluid phase, seals on the migration pathway and hydrodynamic flow.

A full U-V-Z approach approximates the total fluid potential from:

1. Hydrodynamic flow maps (expressed in meters or feet (this chapter examples)
2. Seal capacity maps (expressed in meters or feet—next chapter)
3. Amplified seal and flow maps (total fluid potential) based on potential from hydrodynamic flow + seals along the migration route

The hydrodynamic U-V-Z approach shown in this chapter deals only with equipotential surfaces of hydrocarbon migration in an active hydrodynamic environment. Further modification of trap geometries occur where seals are present along migration pathways.

Chapter 5 covers how to make the $\frac{Pc}{Pgrad}$ part of the equations directly from capillary pressure, or estimates from knowledge of the area, of pseudo-capillary pressure, in feet or meters of seal capacity. A full hydrocarbon entrapment model

requires having quantitative seal maps build from fault and facies analysis, as well as potentiometric surface maps to model the fluid flow (if the system is hydrodynamic).

4.3.7 *Perched Water—Another Problem That Can Look Hydrodynamic*

The term 'perched water' is classically applied to shallow water aquifer systems, where geometries are such that some water gets trapped above a regional water table. Within oil and gas fields in is frequently encountered (or interpreted) in situations where lenticular sands, structural sags or the base of channels (especially in thick turbidite slope channels) trap water that is not expelled during trap filling. I reasonably well documented occurrence in the Gulf of Mexico is that of (Kendrick 1998).

As in the case of a hydrodynamically tilted contact, failure to recognize perched water contacts inevitably results in a gross underestimation of reserves, as a flat hydrocarbon-water contact in the discovery well will discount oil or gas downdip. Perched water can be very difficult to tell from a hydrodynamically tilted contact, as the pressure-depth plots are essentially similar, with wells in the hydrocarbon phase lining up on the same density gradient, but with higher pressure water points out to the side (Fig. 4.41).

One of the observations about the water gradients is that they appear to be over-pressured or have density gradients from pressure plots that are greater than fresh water. An explanation has been that, since these are water legs trapped inside gas or oil columns, the buoyancy pressure of the hydrocarbon phase is pressing on the relatively small volume of trapped water, causing overpressure. This has been a

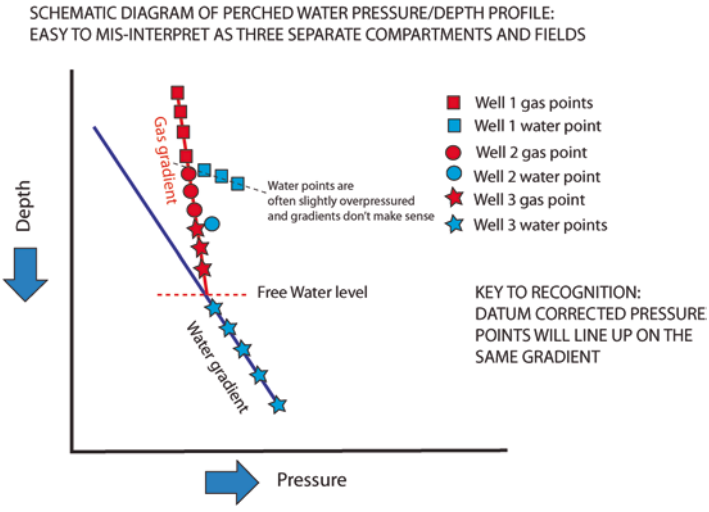

Fig. 4.41 Perched water pressure-depth plot

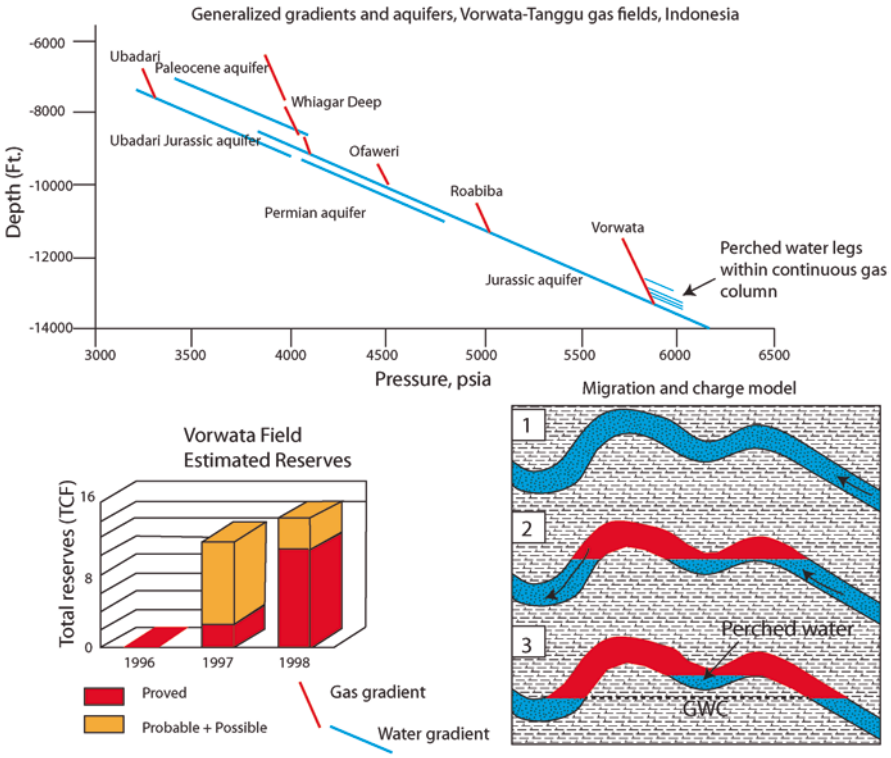

Fig. 4.42 Perched water reserve growth, Indonesia. Modified from Marcou et al. (2004). Used with permission of the Indonesian Petroleum Association

criteria of an anomalously pressured water gradient has been used to identify perching in many wells. The impact on reserve growth can be huge as shown in Fig. 4.42 (Marcou et al. 2004). A number of separate aquifer legs are shown in the Tanguu area, with numerous separate gas field. The Vorwata Field, in particular, showed evidence of either hydraulic flow or perched water, with a continuous gas column through multiple wells, but pockets of water disconnected from the gas found in numerous others. Initially, the field was seen as highly compartmentalized, with multiple small gas caps and multiple gas-water contacts and free water levels. However, production and pressure data indicated the hydrocarbon phase was connected and there were limited numbers of problems with production. Wells did better than predicted volumetrically. By 1997, proved reserves were estimated at about 2 TCF of gas, with an additional probable 10 TCF. As the model became refined, by 1998 the proved reserves had jumped to 10 CF with an additional 4 TCF possible. Diagrammatically, the perched legs are show in depositional and synclinal lows over the top of a gas field interpreted as having flat gas contacts.

Another example proposing a perched water model is that shown on Fig. 4.43 (Cross et al. 2009). One of my first exposures to perched water was during the

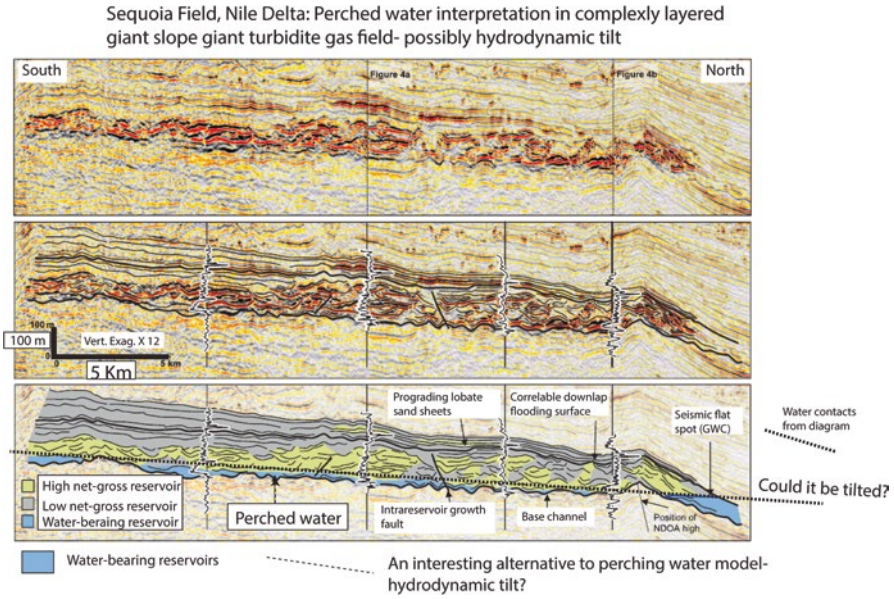

Fig. 4.43 Sequoia Field perched water model. The contacts in this area have long been recognized as lower on the north side of the trap than the south. A possible hydrodynamic model may also explain the water bearing zones. The proposed tilted gas-water contact is pure speculation on my part, but would fit with other, later discoveries in this and deeper horizons in the Nile Delta. Modified from Cross et al. (2009). Reprinted with permission of the AAPG, whose further permission is required for further use

discovery in the late 1990s of a multi-TCF slope channel complex by British Gas (Samuel et al. 2003) over a large anticline with acreage dropped by Amoco in 1995. The structure underlying these Pliocene fields had been drilled in the early 1980s by Exxon, hoping to find oil but finding gas in thin and poorly developed sands and siltstones. What was missed by Amoco was the potential away from that abandoned well, which proved the trap, but not the reservoir. BG began testing Pliocene seismic DHI anomalies over the block and discovered over 10 TCF of reserves.

Aside from the embarrassment of leaving such a large accumulation untouched, the discovery and development wells began to surprise all operators as the gas columns looked continuous from pressure, but numerous water legs were found at the base of many of the slope turbidite channel sandstones. These water zones were subsequently interpreted as perched, as shown in the diagram below. Volumetrically, they are relatively insignificant water legs.

Interestingly, it was also noted, not just from wells, but seismic, that gas contacts on the south side of the structure were higher than on the north. Again, the difference was attributed to perching. An alternative, albeit pure speculation without hard data, is shown on Fig. 4.43 (bottom). Many of these basal sandstones could, alternatively, be below a tilted gas-water contact.

While this tilt model can't be proved without additional work, a number of colleagues working the basin in recent years believe that hydrodynamic tilting is actually much more common in this basin than previously recognized. More documentation follows later with a discussion of the Temsah Gas Field.

4.3.7.1 Ormen-Lange Field, Norway—Perched or Tilted?

An example where a perched water contact model has been changed to a hydrodynamic model is shown in a case history of the Ormen-Lange gas field in Norway (Cade et al. 1999; Ferrero et al. 2012). The discovery well was downdip, and in a different trap than an updip, and encountered substantial gas and then an 'apparent' water leg and transition zone. The pressure plot (Fig. 4.44, Cade et al. 1999) had points in the tighter interbedded sandstones and mudstones at the base with pressure points that were progressively higher deeper, but did not fit a calculated water density. This difference in slope was attributed to a perched water table, or, alternatively, thin lenticular reservoirs within a low permeability seal that were taking on the pressures of a sealing siltstone (as mentioned previously in Fig. 4.6.

The well log (Fig. 4.45) clearly shows the loss of porosity and reservoir deeper in the well at the point the anomalous pressure points were taken. The zone interpreted as 'water sands', through petrographic work, was shown to be due to high bound water in chlorite clays in the pore spaces. This bound water shows up on the logs as high Sw and low porosity. Note also that the gas gradients extend to 2790 m through very tight rock with high SW interbedded with streaks of favorable satura-

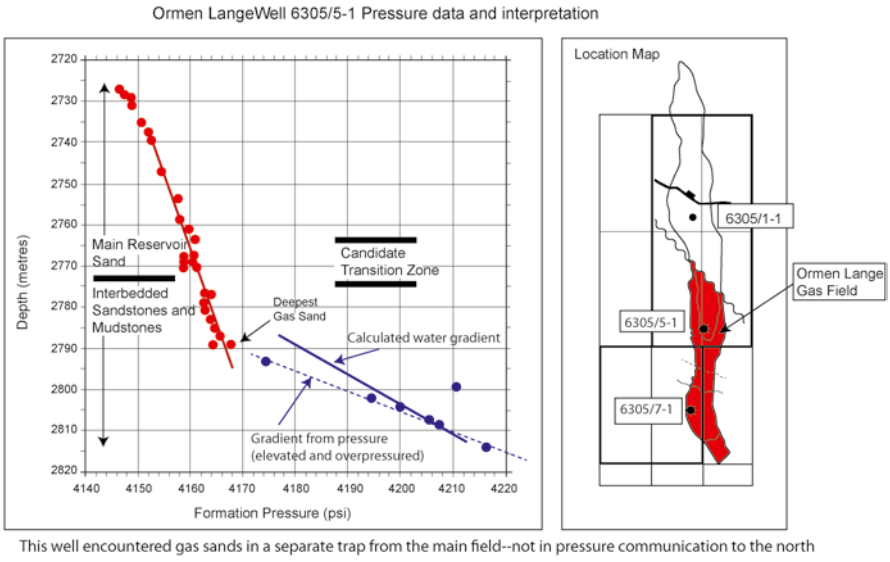

Fig. 4.44 Discovery well, Ormen Lange Field, Norway. Modified from Cade et al. (1999). Used by permission of the EAGE

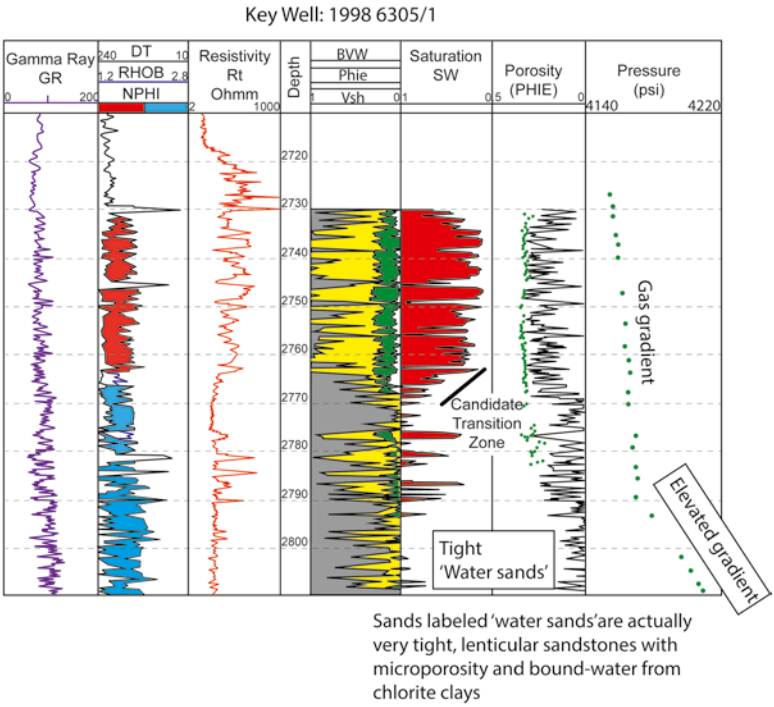

Fig. 4.45 Discovery well log and pressures, Ormen Lange Field, Norway. Modified from Cade et al. (1999). Used by permission of the EAGE

tion. This is a classic case of high bound water in tight rock within a transition zone type of saturation. Base on the perched water interpretation, and conclusions that a free water level had not been reached, a second well was drilled downdip. The second well found more gas, all of which was in pressure communication with the updip discovery.

As more wells were drilled and data collected, the perched water model was re-evaluated and in 2012, a hydrodynamic tilt model was proposed (Ferrero et al. 2012). The model differences are summarized in Fig. 4.46. The hydrodynamic model appears robust and more simply explains the trap and water discovered. The model also predicts flushing of gas with time as the tilt amplified, leaving residual gas zones at the top of the trap. Differential aquifer drawdown with time is also noted.

As will be shown in the Temsah Field case study later, you don't have to have the model right when the first well is drilled if you have a concept from the shows and pressure data that successfully predicts a downdip location and larger reserves with tilted or deeper contacts.

The analysis done by Cade and other in the late 1990s on the discovery well showed convincingly that there was no gas-water contact in the well, and that the high water saturations were part of a tighter transition zone. That was enough information to drill a second well and find a large trap. Without it, the trap may have been overlooked as uneconomic.

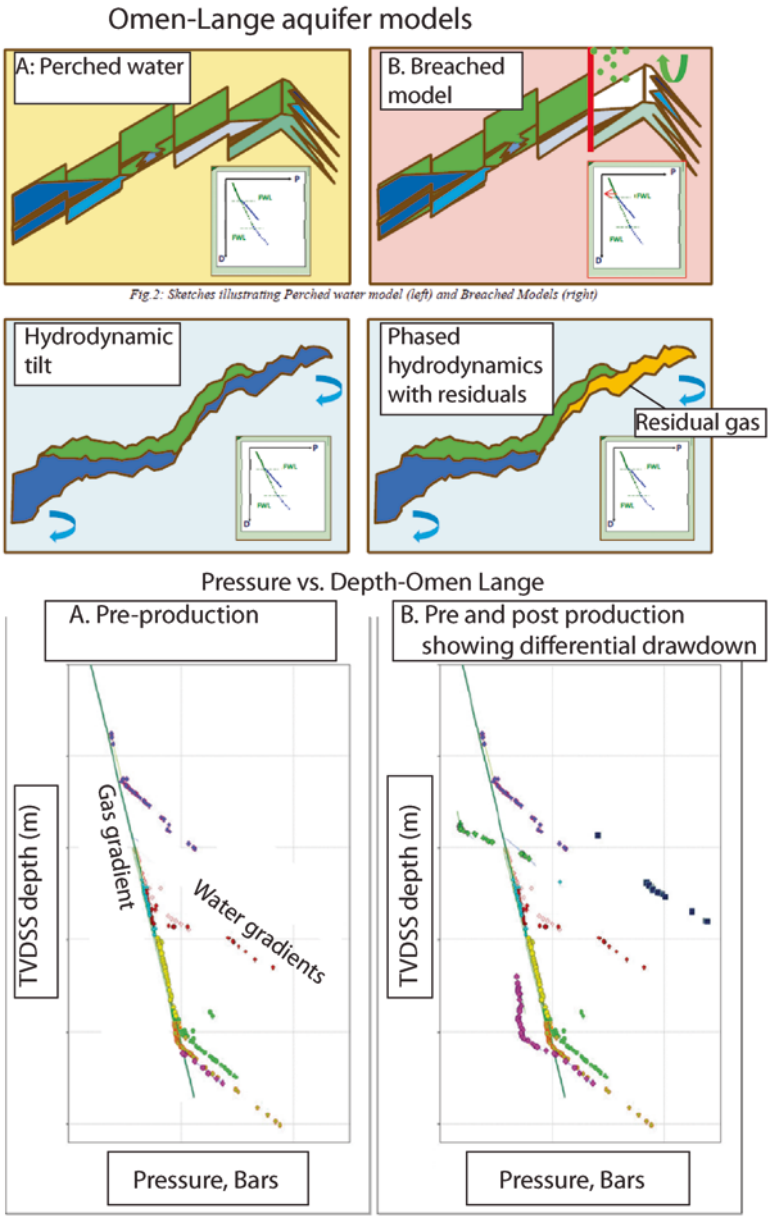

Fig. 4.46 Hydrodynamic tilt model for Ormen Lange Field. (Ferrero et al. 2012). Reprinted by permission of SPE

4.4 High Pressure Systems, Pressure Regressions and Fracture Seal Breaching

Overpressured basins are common worldwide. While causes are varied, recognition of overpressure is critical to safe well design, but also to understand fluid flow and migration. Hence, many companies have entire teams devoted to mapping and predicting overpressure before drilling a well, monitoring a wells pressure real time with seismic and logs and then post-appraisal of results.

Perhaps no better visualization of overpressure is that of active mud volcanoes (Fig. 4.47).

Some excellent references on shale diapirs and mud volcanoes are those of (Battani et al. 2010; Bonini 2008; Davies and Stewart 2005; Duerto and McClay 2002; Henry et al. 2010; Jackson et al. 2002; Sautkin et al. 2003; Stewart and Davies 2006; Yusifov 2004). These features, while creating significant drilling and shallow hazards problems, are also proven vertical migration pathways for oil and gas.

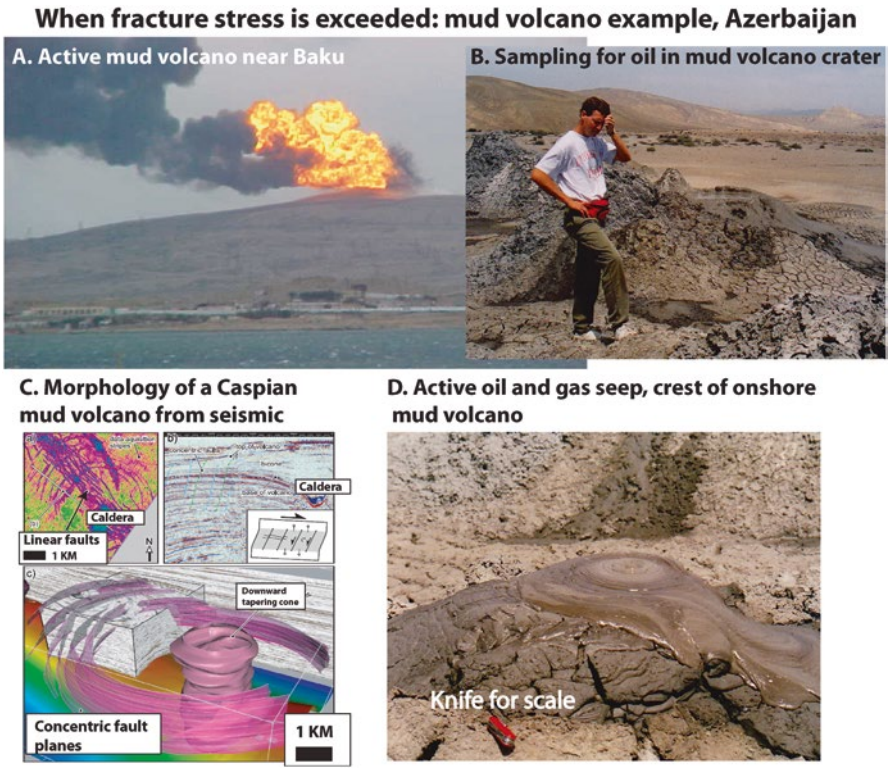

Fig. 4.47 Active mud volcano, Azerbaijan. Caspian Basin mud volcanoes tap mature source rocks as deep as 20,000' (6500 m) and frequently build up enough pressure to exceed fracture gradient, Oil and gas seeps are ubiquitous at the surface, as well as occasional spectacular eruptions. Figure 4.47a courtesy of Greg Riley, BP. Figure 4.47c from Stewart and Davie (2006) and reprinted by the permission of AAPG, whose further permission is required for further use)

4.4.1 Maps of Over Pressure

Largely because of safety issues with drilling in overpessured basins, maps of geopressure are routinely made by geoscientists in oil companies. An example is shown in Fig. 4.48 from (Burke et al. 2012). These maps are not only used by drillers to determine the wellbore design, but can be converted to potentiometric surface maps for use in migration and entrapment maps using principles outline earlier.

One of the easiest sources of data to approximate pressure with depth are mud weights, as most well reports contain mud weight information as part of routine reporting and display. Figure 4.49 shows an example from the Gulf of Mexico. These maps can readily be converted to pressure in psi/ft or other units by simple conversions. When converting to pressure offshore, the subsea depths used should be relative to the mudline (sea floor), as the water column does not increase effective stress. Another way to say this is the psi/ft gradient offshore is psi minus sea water pressure divided by the depth below mudline.

An example is shown in Fig. 4.49 (Heppard et al. 2000). This regional mud weight map is based on well data at the Miocene level. It can be converted to psi/ft by a simple multiplication of the mud weight map by Eq. 4.15:

$$Pressure\left(in\frac{psi}{ft}\right) = Mud\ weight\ in\ lb/gal * .051948 \tag{4.15}$$

The resultant map (Fig. 4.50b) is an approximation of pressure in psi/ft. If the structural level is known for the formation relative to mudline, this can be further

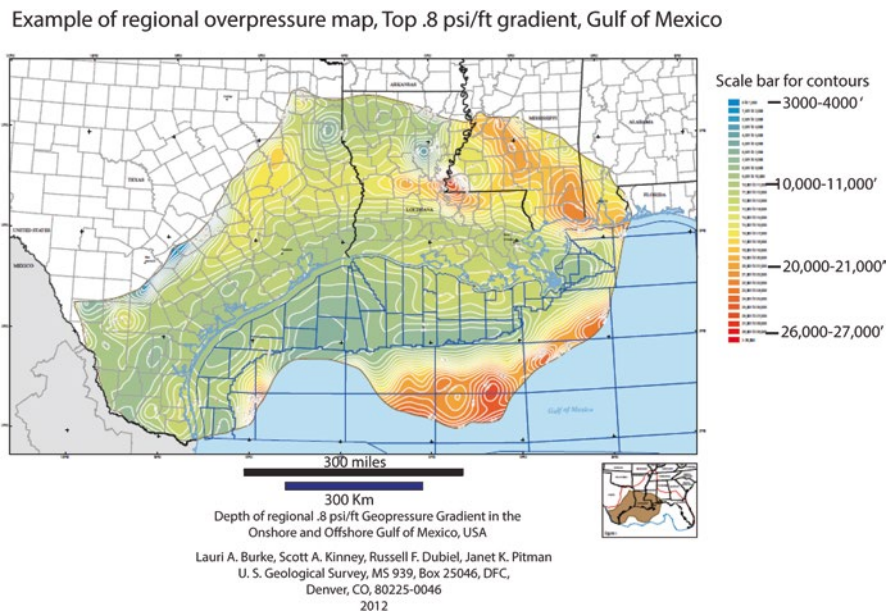

Fig. 4.48 Public access database of top of overpressure. (Burke et al. 2012). The entire database is also available from AAPG online

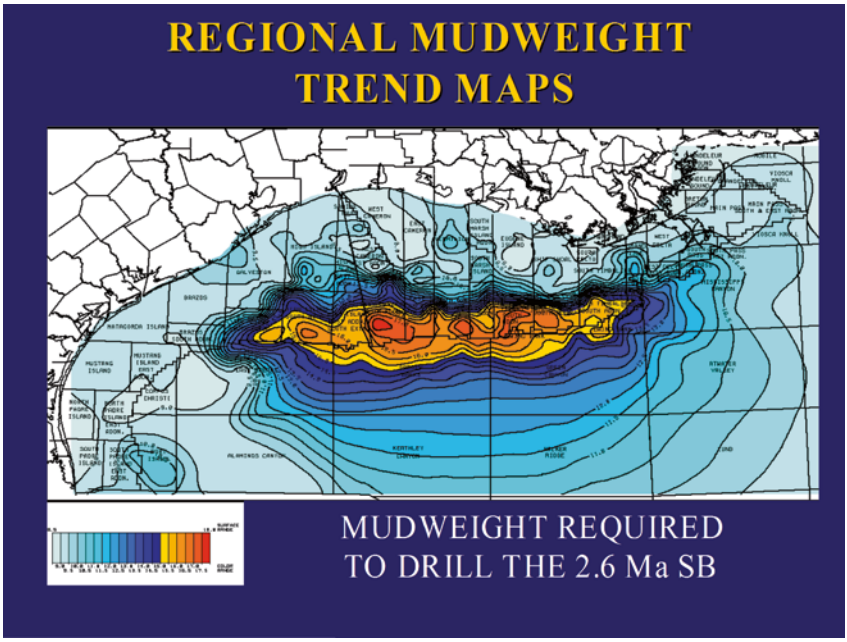

Fig. 4.49 Pressures to drill the 2.6 MA sequence boundary, Gulf of Mexico. Figure courtesy of BP-Chevron drilling consortium course notes, used with permission

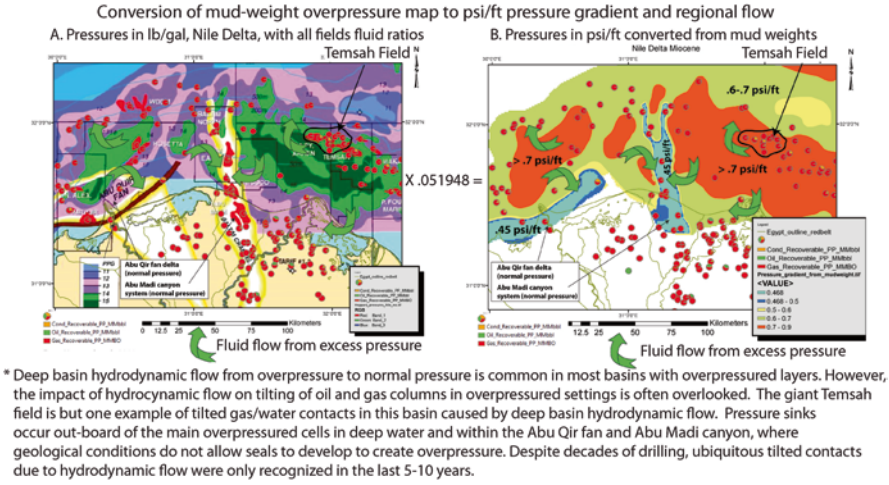

Fig. 4.50 Mud weight map of the Nile Delta converted to psi/ft pressure gradient map

converted to formation pressure and further converted to a hydraulic heat (potentiometric surface) map from excess pressure relative to hydrostatic.

Another way to view this map is from an exploration standpoint. Because the map is showing excess pressure, water flow will be away from the overpressured parts of the basin toward lower excess pressure. This is a key part of building hydro-

dynamic tilt maps. An example will be covered in more detail using a case history of the giant Temsah Field later in this chapter.

4.4.2 *Deep Overpressure and Log and Seismic Methods of Prediction*

By far the most common way to develop overpressure is rapid burial and expulsion of water as shales compact. This process of pressure disequilibrium is common any many basins where deltaic deposition has created high overpressure in the. Another schematic diagram from Heppard et al. 2000 is shown in Fig. 4.50.

The primary cause of overpressure in the Nile Delta is compaction disequilibrium, caused by rapid Plio-Pleistocene burial in the core of the delta. Note in Fig. 4.51 that the overpressured areas cross-cut stratigraphy, as the pressure is driven by burial, not necessarily the stratigraphy or structural setting of the individual formations. The highest pressures (orange) are located under the main depocenter of the Nile delta. Excess pressure in this area will tend to force hydrocarbons to lower excess pressure areas, shown schematically with black arrows. This creates strong vertical and lateral migration and water movement. Hydrocarbon pools at multiple levels result from complex migration assisted by cross-fault juxtaposi-

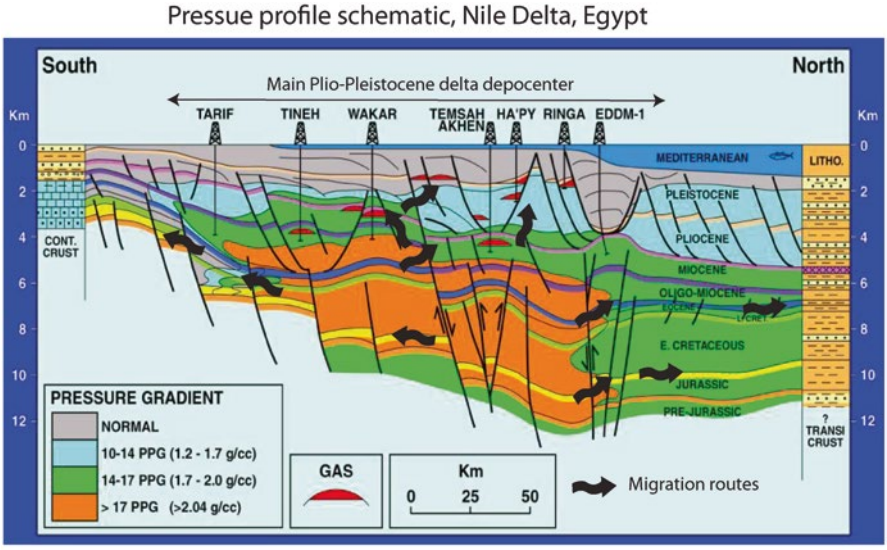

Key points:
1. Highest pressure is condined to thickest are of Plio-Pleistocene deltaic deposition (rapid burial drives compaction disequilibrium overpressure at depth)
2. Pressure crosses stratigraphic boundaries
3. Hydrocarbon migration routes are set up by excess pressure and flow across fault juxtapositions and regionally extensive reservoir trends

Fig. 4.51 Pressure and migration schematic, Nile Delta

tion of reservoirs, with migration occurring over many kilometers of vertical distance into multiple stacked traps. This phenomenon is typical of most overpressured basins, as illustrated earlier with an example from the Caspian Basin.

Mud weights, however, and direct measurements from RFT, DST or MDT tools are not the only ways to map pressure regimes. Wirelines logs and seismic can also be used. One of the landmark papers dealing with pressure prediction from well logs is that of (Eaton 1975). A concise summary of these and other techniques is also shown by (Bowers 2001).

The most commonly used well logs for pore pressure prediction are resistivity and sonic logs (Fig. 4.52).

Sonic and resistivity logs are ideal for calibrating to pressures. This is because, as shales compact with burial, the effective stress decreases and the changes show up as trends of normal compaction lines. When the normal compaction in deviates from the regional trend, it is most often due to changes in the pressure regime. As shown in Fig. 4.52, resistivity profiles decrease at the top of overpressure and sonic travel time increases. Both phenomenon are caused by a general decrease in porosity and effective stress with depth in the normally pressured section, as shown earlier on Figs. 4.7 and 4.8. In the overpessured window, effective stress is decreased, and porosity increased, causing the changes detected by the well logs. Software pack-

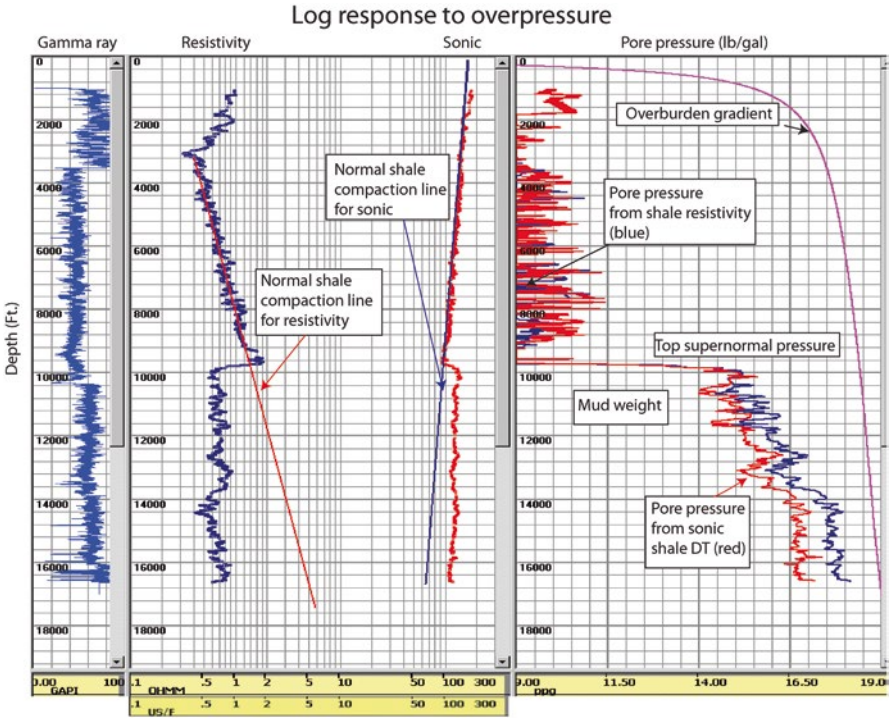

Fig. 4.52 Log profiles in an overpressured setting. Figure modified from BP-Chevron Drilling Consortium course notes, by permission

ages allow interactive picking of shales from GR or other logs and smoothing and filtering of the regional trends to predict pore pressure. Calibration to MDT, mud weight or other pressure data is critical to validate the models, but the ability to use well logs gives a much better regional picture.

Another example of sonic response to pore pressure is shown in Fig. 4.53 (Henry et al. 2010). In this example, a well in Trinidad was drilled to test a structural close that turned out to be related to shale diapirism and a mud volcano. The Haberno-1 well encountered very high pressure at shallow depths, mudflows into the wellbore and very difficult drilling. Logs from offset wells away from the mud diaper showed the degree the sonic and porosity logs in the Haberno-1 well deviated from regional porosity trends and travel time.

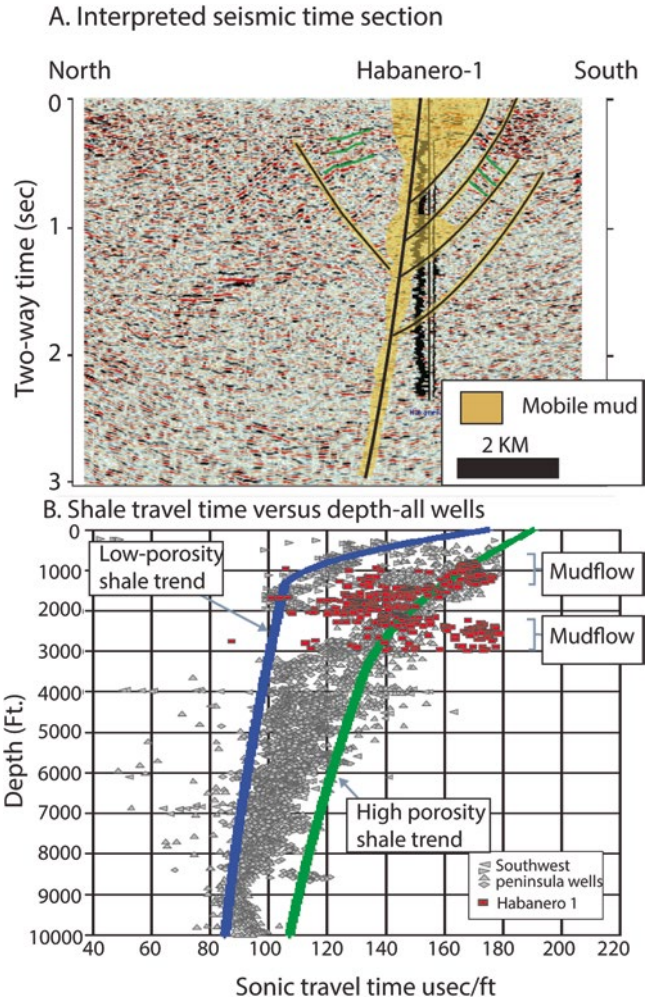

Fig. 4.53 High pressures associated with a mud volcano, and sonic log response. Modified Henry et al. (2010). Reprinted by permission of the AAPG, whose further permission is needed for further use

An equally important tool involves pressure prediction from seismic. A full discussion of how this is done is beyond the scope of this summary, but suffice it to say that as seismic measures travel time, it can serve as a proxy for sonic logs to derive pore pressure. Most deep, overpressured wells today have seismic pore pressure prediction as a key part of the well planning, much of it done on 3D seismic. An example is shown on Fig. 4.54, where high pressure is encountered above and below a salt structure in the Gulf of Mexico.

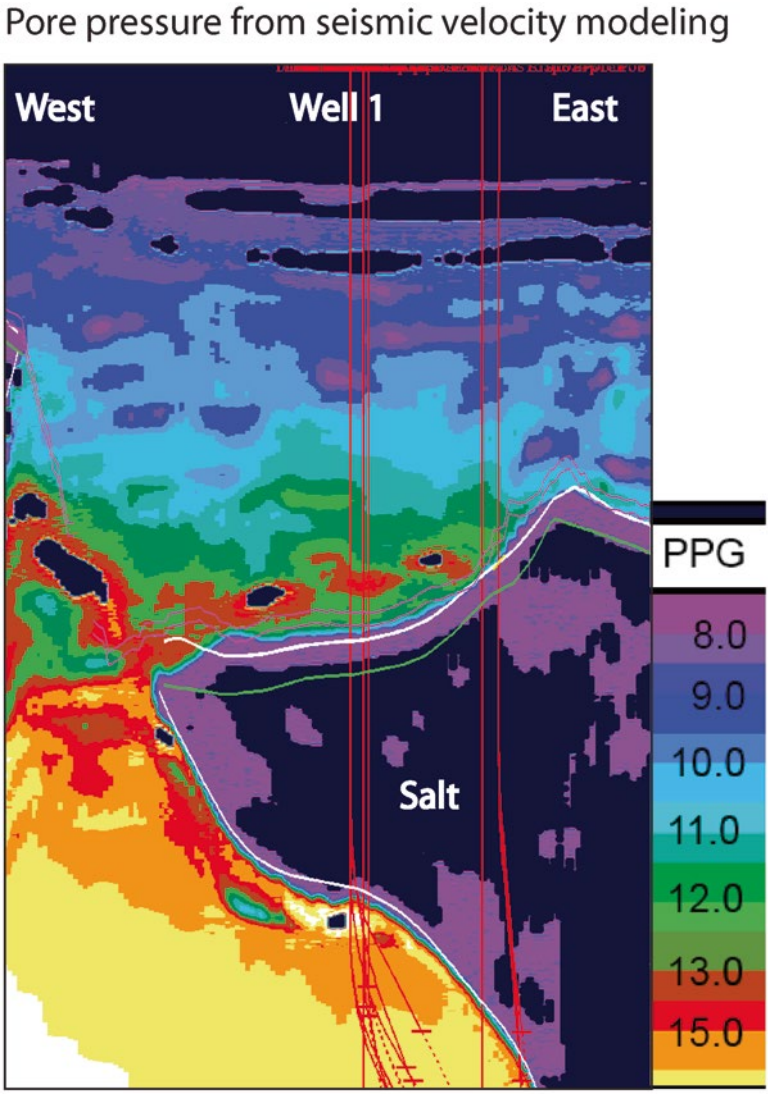

Fig. 4.54 Seismic pore pressure prediction, Gulf of Mexico. Modified from BP/Chevron Drilling Consortium course notes, used with permission

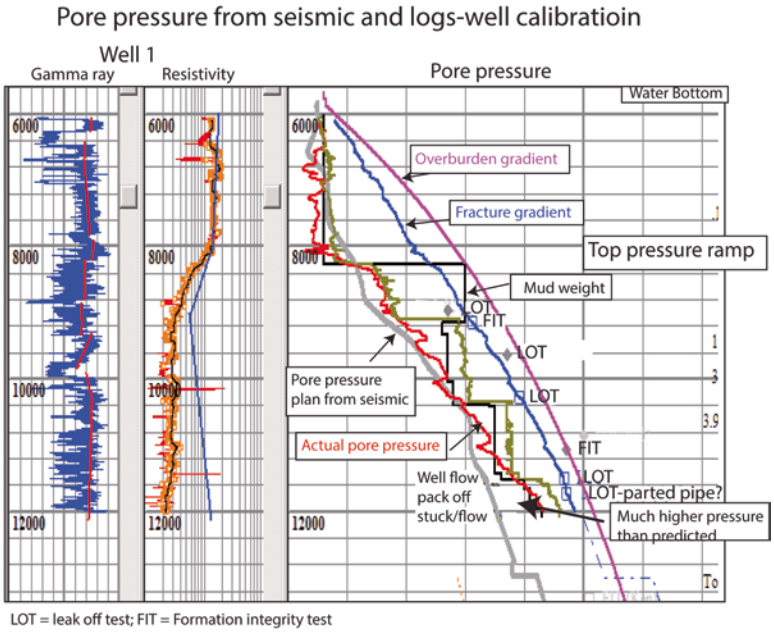

Fig. 4.55 Calibration of logs and seismic to measurement in a well. Modified from BP/Chevron Drilling Consortium course notes, used with permission

Seismic pore pressure prediction has its limits, however, as resolution is much less than that of well logs or direct measurement. But in many cases, particularly frontier exploration wells, it may be the only reliable way to predict pressure. An example of the calibration to the BN-2 well shown in Fig. 4.54 is shown in Fig. 4.55.

A sharp reduction in resistivity occurs at 8000 ft. in the well, a point that is clearly the top of a major pressure ramp. Leak off and formation integrity tests from the well confirm the predicted fracture gradient. Note that the actual pressure recorded at the base of the well is considerably higher than predicted from the seismic velocities alone, but the general trend of overpressure has been detected.

4.4.3 Pressure Regressions and Fracture Gradients- Casing Design, Room for Accumulations and Enhanced Seal Capacity

One of the most important concepts in exploration in overpressured settings is that of pressure regressions. Pressure regressions (Fig. 4.56) occur where geometries of the reservoirs set up favorable conditions for the reservoir pressure to be substantially less than the surrounding shales. Thick, laterally continuous reservoir belts

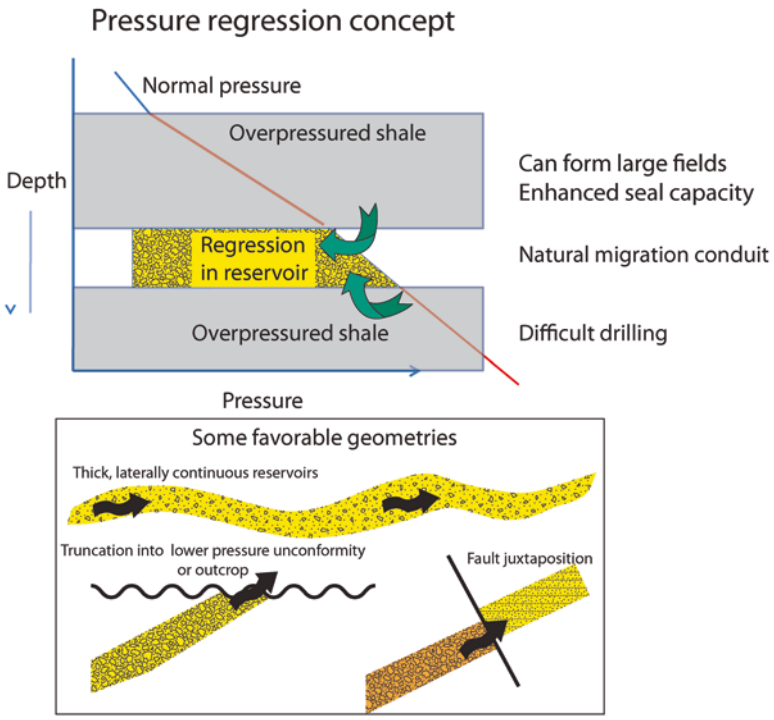

Fig. 4.56 Pressure regressions. Laterally continuous reservoirs or geological conditions such as pressure changes across faults or unconformities can cause reduced pressures in the reservoirs relative to the bounding shales. These settings create both enhance pressure seals and natural conduits of migration for oil and gas

and juxtaposition of overpressured reservoirs by faults or unconformities to lower pressure strata are some of the causes.

Because of the excess pressure in the shales relative to sands in pressure regression, ideal conduits for migration are created due to hydrodynamic flow. In addition, the encasing seals provide pressure enhanced seal capacity.

The importance of pressure regressions from both a well design and exploration standpoint are shown in Fig. 4.56. When fracture gradients are exceeded, there is not only no hope for a column to accumulate, but catastrophic blowouts can occur. Note that there is virtually no room for a column in both the shallow gas example and deep overpressured accumulations shown in Fig. 4.57, where short columns of gas or oil can readily reach the fracture gradient. However, there is substantial room for a long hydrocarbon column in the deep reservoir undergoing a pressure regression, as well as for any traps that fall on a regional hydrostatic gradient.

Geometry and scale of reservoirs makes all the difference. If the reservoirs being drilled are thin and highly lenticular, however, they often cannot bleed pressure off

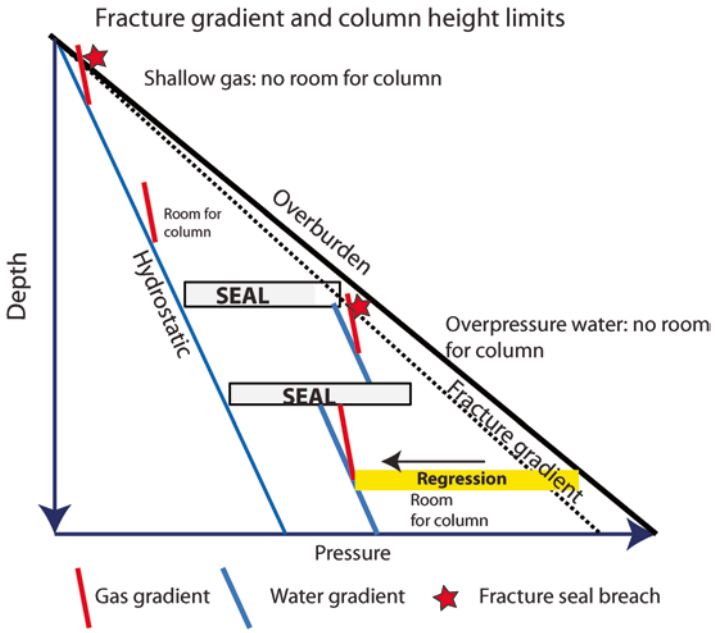

Fig. 4.57 Decreased room for columns in a highly pressured settings. Water overpressured water gradients are very high, any gas column can build up additional pressure from buoyancy that reaches the fracture gradient. When this happens, seals are broken and the trap leaks. In the shallowest areas of the basin, fracture gradients and overburden are also close the normally pressured water gradients. As in the deep case, there is little room to build up a gas column before reaching fracture gradient. This is why shallow gas hazards need to be avoided in order to prevent catastrophic blowouts

and take on the pressure of the surrounding shales, creating serious drilling hazards. An example from Azerbaijan is shown in Fig. 4.58.

Extreme overpressure (>0.8 psi/ft or 15 lb/gal mud weight) is encountered at very shallow depths in the Caspian basin (Riley 2009) and very difficult drilling conditions exist, as highly lenticular, isolated reservoirs in the shallow section take on the pressure of the encasing shales (Fig. 4.58, top). However, at depth, some very well developed, laterally extensive reservoirs are connected to the outcrop and have pressure regressions back to normal pressure gradients, as shown from a pressure plot from the giant Shah Deniz Field (Fig. 4.58, bottom).

Shah Deniz Field also has shallow gas accumulations so close to the fracture gradient that it is effectively impossible to drill the crest of the structure. As a result, there is a 'no drill window' (Fig. 4.59) which wells must be deviated around to avoid the shallow gas hazards. In addition casing design is complex, as the wells cannot drill with 16 lb/gal mud into the normally pressured deep formations without large mud losses or sticking pipe in the lower pressured reservoirs.

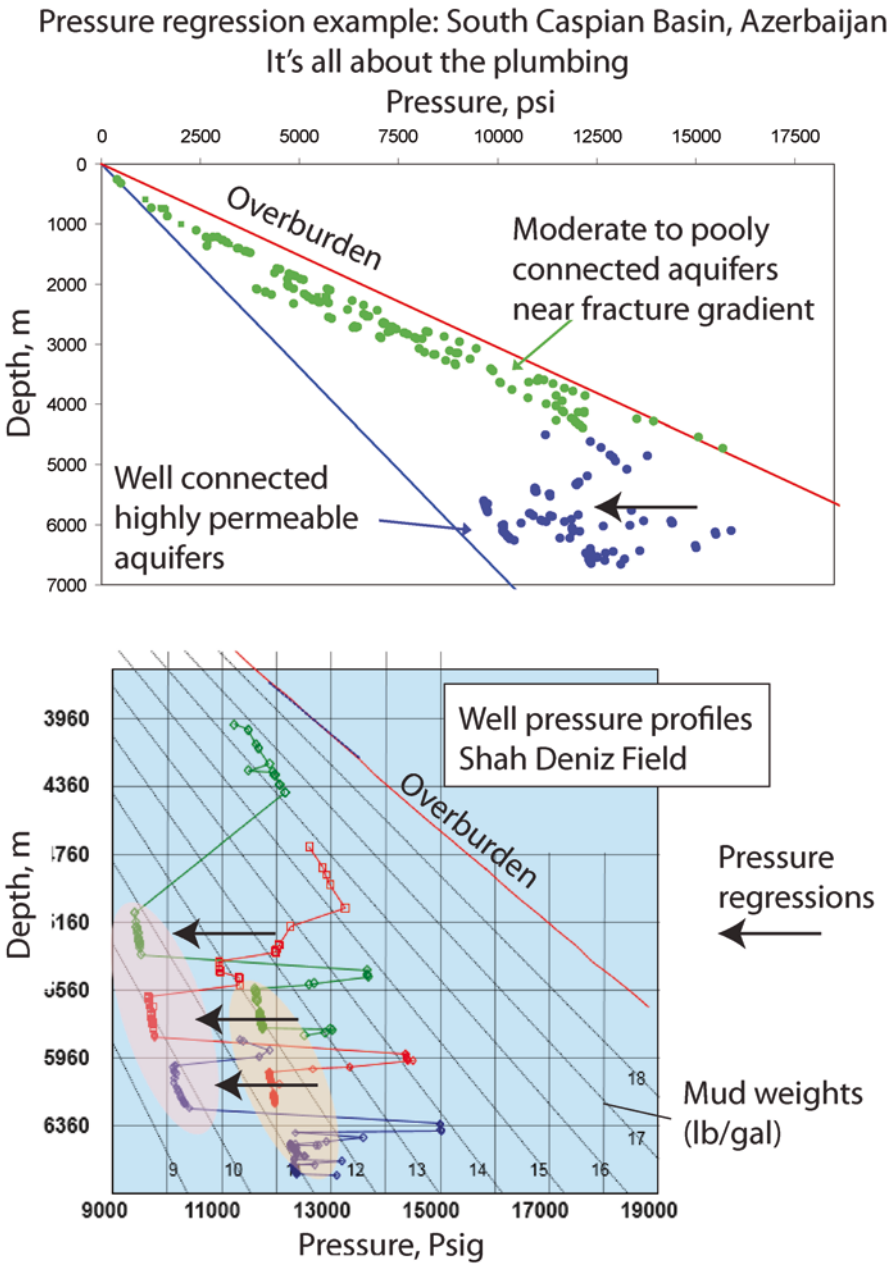

Fig. 4.58 Lenticular vs. regionally connected reservoirs in an overpressured basin (*Top*). 'Ricochet' drilling profile (*bottom*) caused by high pressure shales separated by thick sandstone in pressure regression. This creates very difficult drilling conditions. Modified from Riley (2009). Figures used with permission

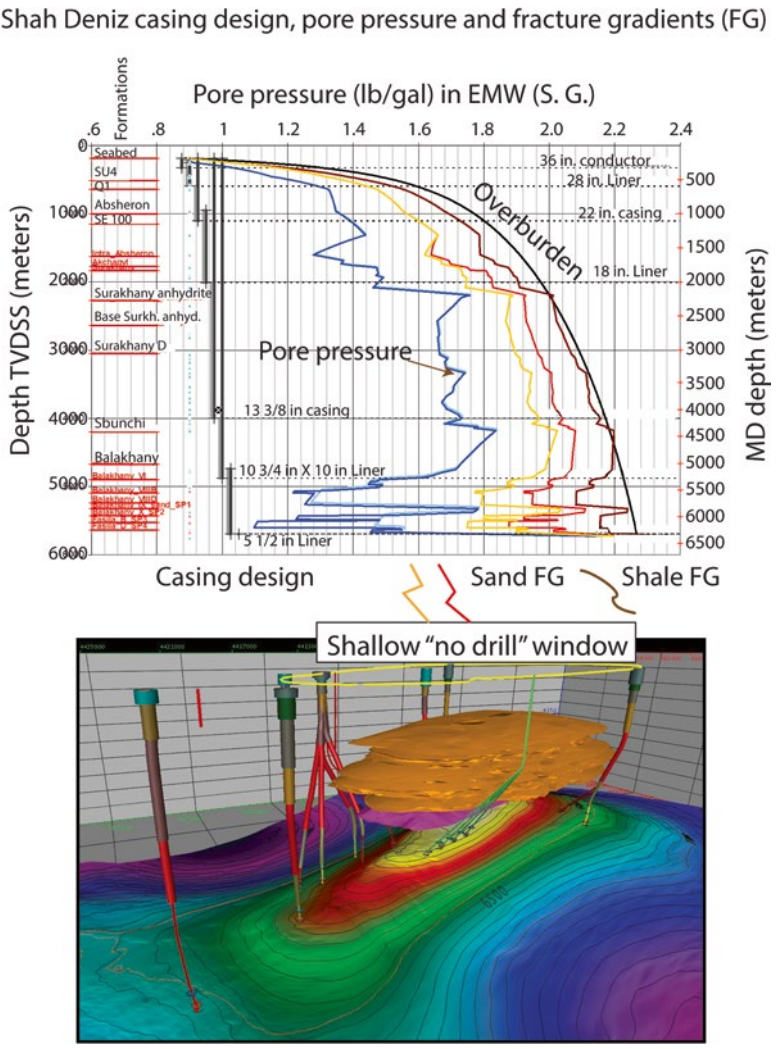

Fig. 4.59 Casing design, Shah Deniz Field. Pore pressure in the shallow gas column is near the fracture gradient, so wells are drilled around the shallow gas caps to tap the deeper pools. Figure from Afgan Huseynov (2012) and Greg Riley, BP, used with permission

Casing designs in overpressure settings are driven by the geometry of the reservoirs and shales, and can be quite varied (Fig. 4.60).

In the end, it is up to the interpretive team, using all the tools available, to understand and predict the pore pressure, not just from a drilling standpoint, but from a prospect evaluation standpoint.

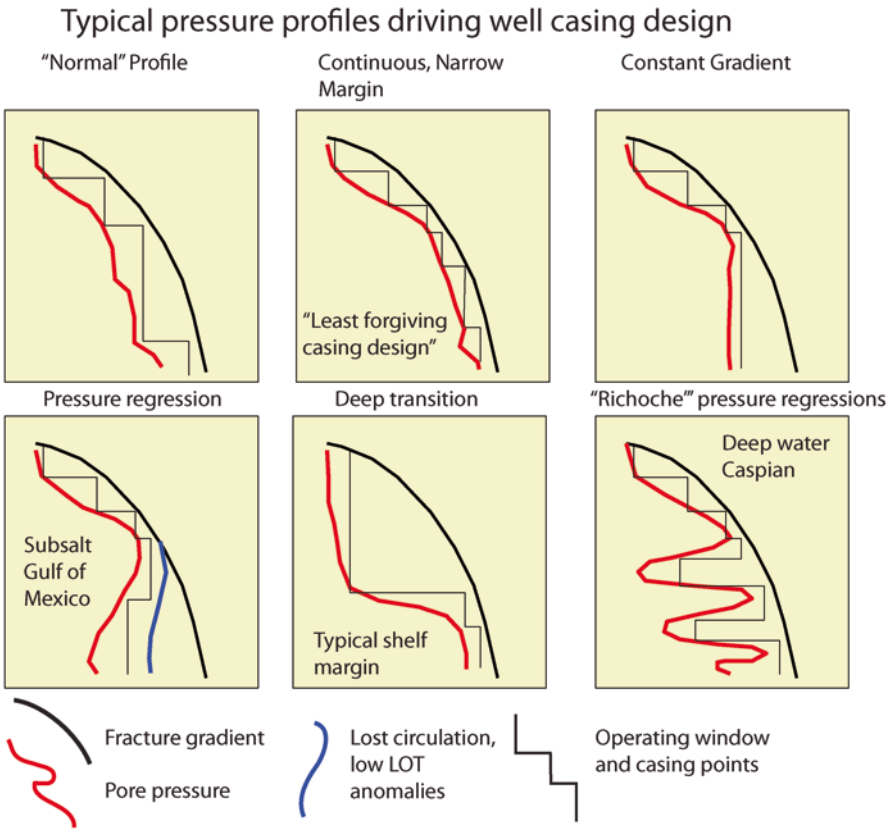

Fig. 4.60 Variations in casing design as a function of pore pressure changes. Modified form BP/Chevron Drilling Consortium course notes. Used with permission

4.4.4 Bigger Isn't Always Better-the Role of Pressures and Centroids in Fracture Seal Breach and Exploration Failure

When post appraising dry holes in overpressured basins, as well as when predicting new accumulations, it is important to target reservoirs that have the best likelihood of having pressure regressions allowing hydrocarbon columns to be developed without reaching fracture gradients. Many a dry hole has been drilled where high shale pore pressure and a lack of a pressure regression has prevented a viable trap from forming.

The Bougaz-1 well in the Nile Delta is a case in point (Fig. 4.61). This well was drilled in 1982 to test a very large structural closure at the Oligocene and Cretaceous levels.

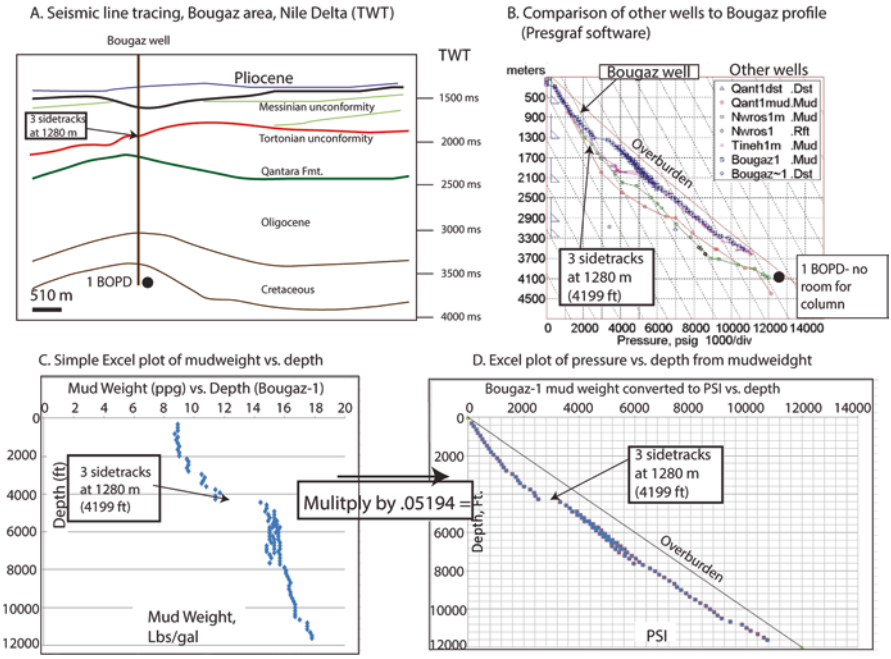

Fig. 4.61 Bougaz dry hole—no room for an accumulation

An extreme pressure ramp was encountered at 1280 m after crossing a major pressure sealing unconformity. From that point to TD, the well was drilled within a few psi of the fracture gradient, and three sidetracks had to be made before the wellbore design allowed further drilling. Simple mud weight vs. depth plots, converted to pressure (Fig. 4.61c, d) show the onerous drilling conditions encountered. This well was significantly anomalous in pore pressure relative to other wells in the area at similar depths (Fig. 4.61b). Without a pressure regression in the deep reservoirs, there is no hope for an accumulation as any column at all would reach fracture gradient and cause seal failure.

The well tested 1 BOPD in the Cretaceous from a highly pressured sandstones which was not in pressure regression. The presence of oil and a reservoir confirmed a working deep petroleum system, a key observation that later would help unlock the deep, overpressured Oligocene play (next section discussion on the Habbar-1 dry hole).

In contrast, the deep Miocene play in the Nile Delta is possible because a number of regionally extensive submarine slope channel systems are in pressure regressions relative to the surrounding shales. An example of pore pressure analysis in the Akhen-1 well (Fig. 4.62) shows a significant pressure regression that sets up column heights in this area of up to 400 m to gas. Figure 4.62 also shows calibration to seismic pore pressure vs. actual measured data from the well. The slight deflections from the seismic profile were used for later well planning to try to estimate where additional

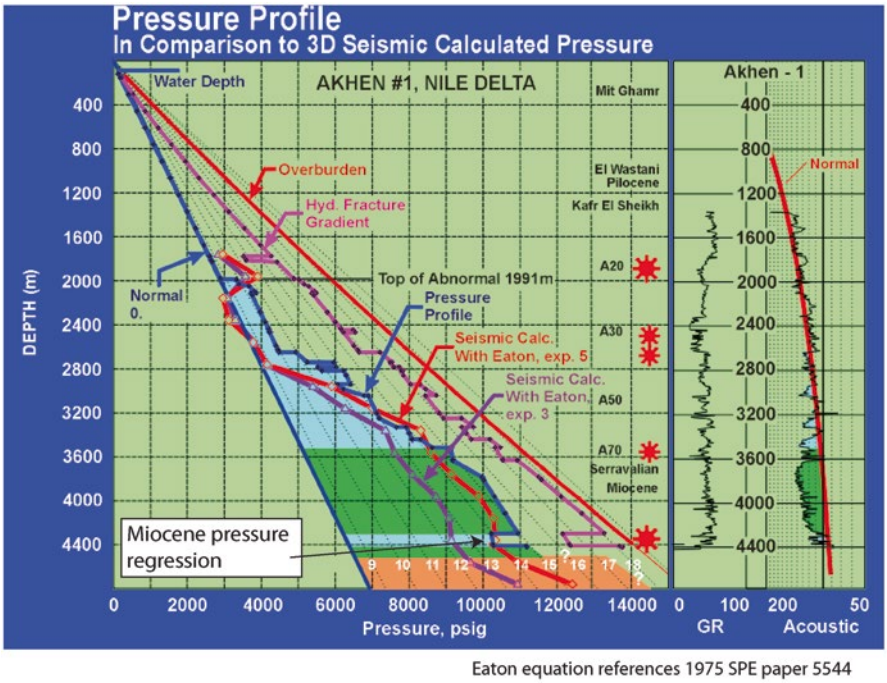

Fig. 4.62 Pressure regression in Miocene reservoirs-Akhen Field, Nile Delta. From Heppard et al. (2000)

thick reservoirs might be present. Some of that work late led to the Raven discovery in 2003 (Dolson et al. 2002a, b; Dolson et al. 2005; Saxon 2011; Whaley 2008).

No discussion of highly pressured systems is complete without mentioning the centroid concept (Figs. 4.62 and 4.63).

The centroid concept was introduced in 1997 (Traugott 1997) and a nice short summary is provided by Shaker (2005). It is sometimes referred to as 'lateral pressure transfer'. In extreme overpressured settings, shale pore pressures can take on a very high pressure gradient. Structural or stratigraphic traps in reservoirs caught up in these shales may have geometries which cause the centroid effect to take place. Essentially, pore pressure in the structural low has fluid pressure transferred from the shales into the reservoirs and transmitted towards the crest of the trap. The term 'centroid' derives from the point at which the pressure in the reservoir is equal to the pressure in the shales themselves. Below this point, the shale pressures are transmitting pressure into the reservoir and above it, the reservoir pressures exceed those of the surrounding shales. If the traps are big enough that the top of the trap reaches fracture gradient, there will be a breached seal.

Schematically, this can be shown in Fig. 4.64.

In this example, 3 different reservoirs geometries are shown (A, B, C). Almost without exception, any exploration company seeing a structural closure as big as the

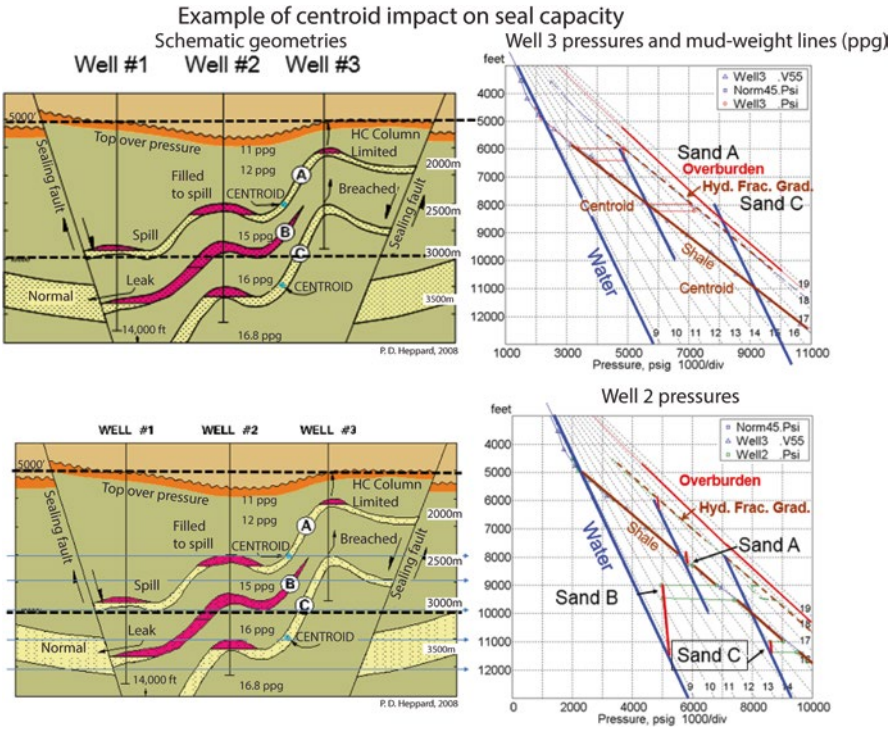

Fig. 4.63 The centroid concept. Modified from a Fig. provided by Phil Heppard

one targeted by well 3 would have this prospect at the top of their lists of things to drill. A look at well 3 pressures, however (top right) shows that the target reservoirs have centroid-translated pressures which put the top of the trap at or near fracture gradient, due to lateral pressure transfer from the deep syncline. Well 3, as a result, has only a limited column at reservoir level A (room for a small accumulation only), but nothing at all in reservoir C, where the fracture gradient and topseal has been breached.

In contrast, well 2 has a number of viable traps. Reservoir A has room for a column and is filled to spill. Reservoir B, which is in pressure communication across a fault downdip, and 'plumbed' into a normal pressure system, has a pressure-enhanced seal and a very long column

In the end, 'bigger is not always better'.

4.4.5 Summary of Part IV

Pressure analysis is a fundamental part of show and seal evaluation. Excess pressures, can set up enhanced seals, control migration pathways and determine if commercial columns can accumulate without reaching topseal fracture gradients. While

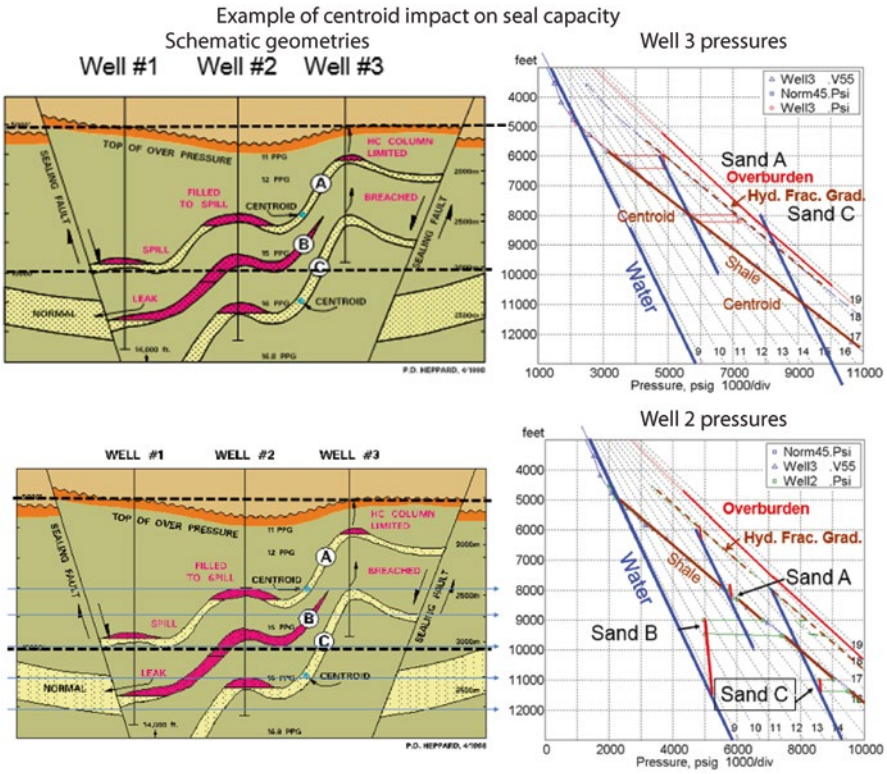

Fig. 4.64 Geometric examples of how centroids might play a role in seal breaching in highly pressured settings. Steeply sloping red lines are gas gradients. Blue lines water gradients. Figures courtesy of Phil Heppard

pressure analysis is often treated largely as a tool for wellbore design, it is a critical part of any exploration program or well post-appraisal.

Well logs, seismic and regional geological thinking need to be integrated into a coherent story. In practice, this is often done with teams of specialists, but the objectives are the same, the drilling of a safe and cost effective well and proper assessment of migration and seals pre-drill.

4.5 Case Histories

Two case histories from the Nile Delta offer a glimpse into how difficult it is sometimes to think creatively about pressure and shows information in exploration. The first case history is that of the Temsah Field complex, which has taken 25 years to recognize its full size and a hydrodynamically tilted contact . The second case

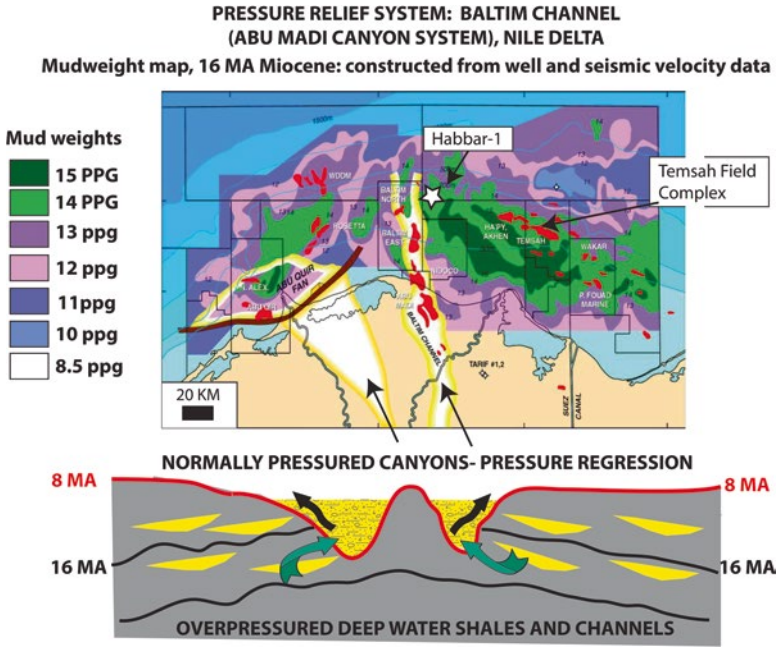

Fig. 4.65 Nile delta regional pressure regression. MA = millions of years ago. A major canyon incision (Abu Madi valley) formed during a regional seal level drop and tectonic uplift between 8 and 5MA ago. The Messinian Abu Madi canyons are normally pressured, but incise into overpressured Miocene shales in the 16 MA Serravallian age strata. This provides a 'pressure relief' and natural conduits for migration of fluids from the overpressured Serravallian reservoirs in the Abu Madi canyon. Mudweight map from Heppard et al. 2000

history details the opening of the deep overpressured Oligocene play from dry hole analysis of the Habbar-1 dry hole (see Fig. 4.65 for locations). In both cases, pressure regressions have played an essential role in exploration success, particularly in the Habbar-1 example.

One of the unique settings in the Nile Delta is the presence of a 550 m deep canyon system called the Abu Madi canyon. It formed during a regional sea level drop which began about 8 MA and ended with burial of the canyon system by Pliocene transgressions approximately 3.3 MA ((Dalla et al. 1997; Dolson et al. 2002c, 2014; McClelland et al. 1996; Nashaat et al. 1996; Palmieri et al. 1996). This system is deeply incised into overpressured Miocene shale in many locations, providing a critical pressure relief that sets up some of the deep pressure regressions favorable to migration and entrapment. Much of the background data on the Nile Delta comes from (Moussa and Matbouly 1994).

4.5.1 *Temsah Field: 25 Years to Recognition of a Tilted Gas-Water Contact*

The Temsah field was fist drilled by Mobil in 1977. The objective was a huge structural closure at the Miocene level and the hope was that oil would be found. The only available seismic at the time was a 2D grid and data quality very poor, and only a generic shape was truly mapped out.

Unfortunately, the discovery well was a major disappointment. Not only was it gas with some condensate, but it had much shorter column than anticipated, and tested water in the lower part of the reservoir. Flow rates were encouraging, with 310 BOPD, 4.9 MMCFD but 2100 BWPD on DST 2 and 6.4 MMCFD with 62.4 BOPD and 2730 BWPD on DST 1. The water leg was significantly overpressured.

I have often wondered who recommended the well and what it felt like to get that result. The target was, after all, a huge closure and I am certain the initial post-well interpretation revolved around the structure being potentially charge or seal limited, as water was found high on the crest.

Temsah-2 was drilled in 1982, however, and found more gas, structurally flat to the initial well, but with a longer gas column. Mobil, which did not have gas rights at the time, dropped the acreage in 1982 and the acreage remained open until 1992 which it was acquired by IEOC and Amoco. A seismic 3D survey was acquired in the late 1990s and revealed that the reservoir was considerably more complex than thought, consisting of highly variable slope channels draped over the structural closure (Fig. 4.66).

Appraisal wells found more and more gas down-flank on the northern part of the structure, but also many puzzling overpressured gas-water contacts. Pressure-depth plots, however, showed most of the gas zones were in pressure continuity on one simple trap (Fig. 4.67). The presence of multiple gas-water contacts resulted in the interpretation of the water legs as perched water, with complex interlayers of isolated channels trapped within a large gas column. This model, however, could not readily explain the progressive deepening of the gas contacts to the north.

Some of the high pressure water points are shown on Fig. 4.67. The field was thought at that time to be highly compartmentalized and difficult to develop (a belief still held by many). Small scale sub-seismic faults and stratigraphic seals not mappable with seismic or clearly seen on logs were called upon to explain the compartmentalization. Initial reserves were thus pessimistic, with 50 BCF growing to 100, then 500 and then as production was established to well over 1 TCF of gas. Despite this, the continuity in the gas phase was recognized, and the larger field reserves speculated upon booked.

Around 2007, the perched concept was challenged by looking at the possibility of hydrodynamic tilt. Having been a proponent of the perched model, when I heard about the new BP model of hydrodynamic tilt, the answer seemed simple and elegant. One way to test the model is simply run a migration model with hydrodynamic flow (Fig. 4.68).

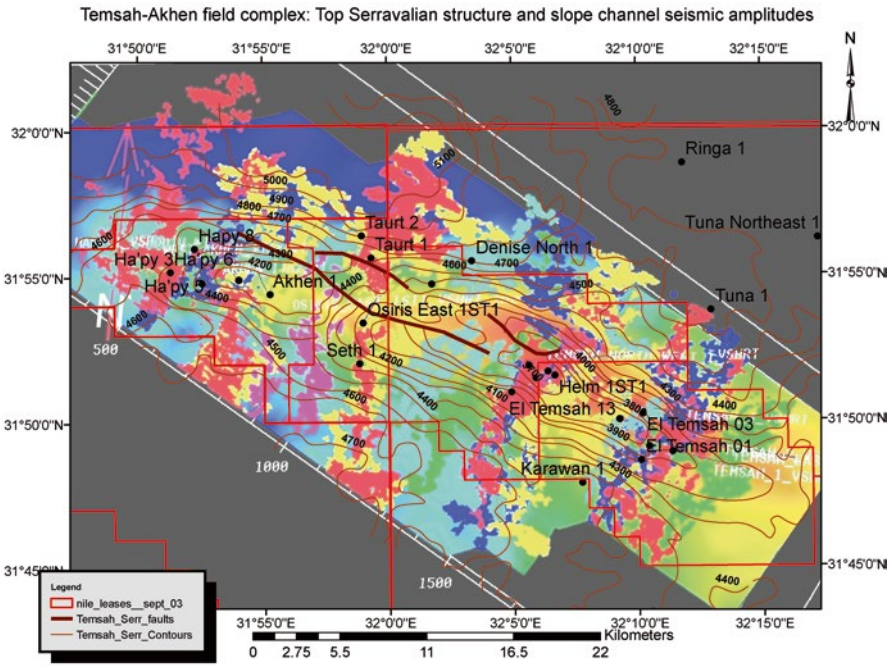

Fig. 4.66 Slope channel interpretation and gas field outline, Temsah-Akhen complex. A number of interpretations of complexity ranging from perching to seal capacity and tilt have been proposed for the gas distribution

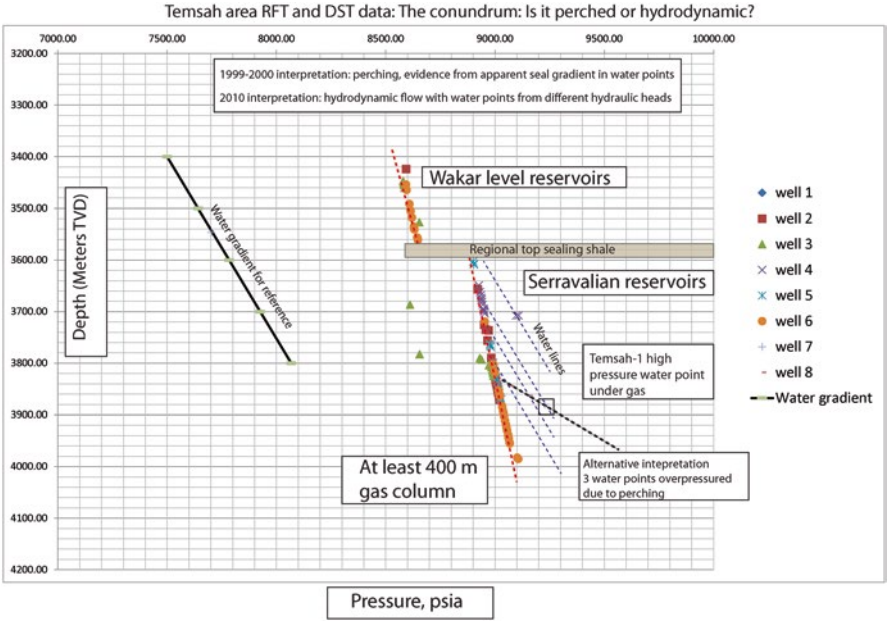

Fig. 4.67 Pressure vs. depth plot, Temsah Field area. See text for discussion

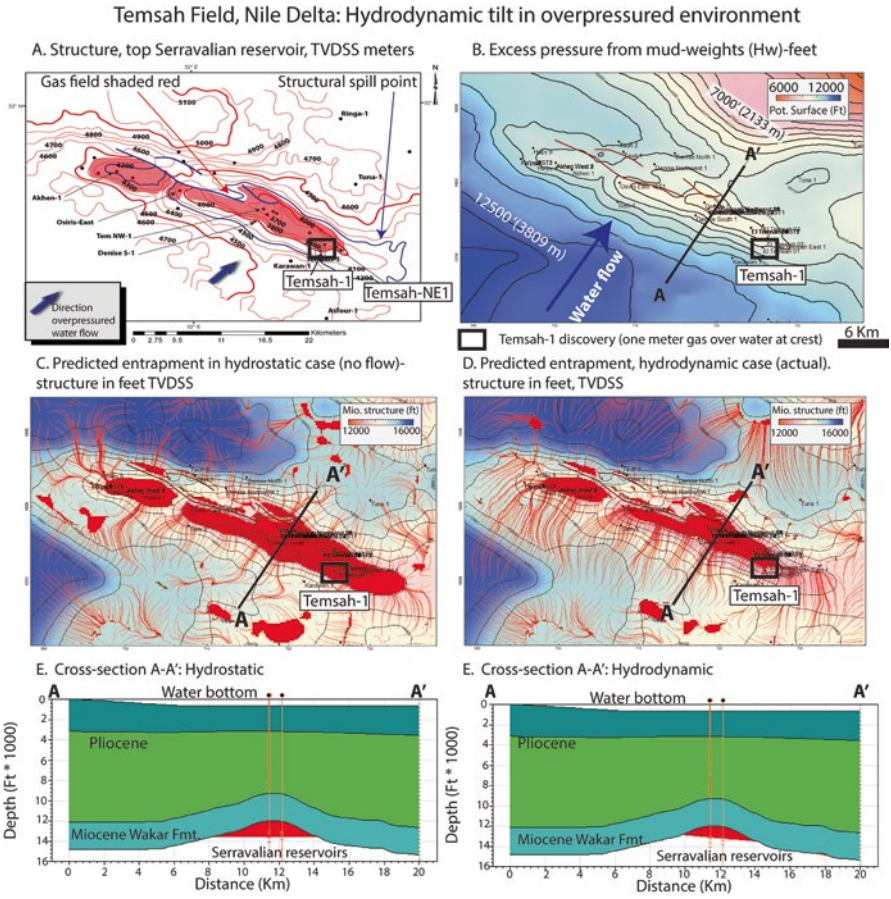

Fig. 4.68 Hydrodynamic tilt model for Temsah made by converting regional mud weight map to a potentiometric surface. The Temsah-1 well is shown with a *black box*

Converting the original regional mud-weight map (Fig. 4.65) to a pressure gradient map and then to pressure from the structure map shown in Fig. 4.68 provides a probable answer. Because of the high overpressure south of the field, and lower pressure to the north, water flow from the deep basin flows from SW to NE toward the deeper water portion of the Nile Delta where burial rates are less and excess pressure lower. If the structure were filled to spill and top seals adequate to hold 400–500 m of gas, but the basin was hydrostatic, the accumulation should have looked like Fig. 4.68c. In that case, there should have been no water found in Temsah-1 or any of the other wells at the crest of the structure.

However, using the potentiometric surface maps from the regional pressure maps, migration and entrapment with hydrodynamic flow predicts a tilted contact as shown in Fig. 4.68d. That distribution of predicted gas is very close to what has been found in the wells. Temsah-1, with the initial high water cut, is actually at the top of the trap.

So, it took from 1977 to 2007 to get the tilt right. It took from 1977 to around 2002 to get the reserves right and recognize the continuous column of gas on the pressure plots. This late recognition of hydrodynamic flow in the basin is not unique, but has been demonstrated in other basins as well. Reserves noted in one commercial database are a conservative 1.5 TCF, making it a true giant discovery. Along with other accumulations on the structure, the complex itself may well hold many more TCF of gas.

4.5.2 Deep Nile Delta Play Opener: Pressures and Shows Identified the Play

Easily the most significant deep exploratory play development in the Nile Delta and Mediterranean Levant Basin (to the east off Israel and Syria), has been the Oligocene play. The relatively recent extension of the play into the Levant Basin has been a huge success globally in the last decade (Belopolsky et al. 2012; Gardosh et al. 2007, 2009a, b; Lie et al. 2011; Peace 2011; Roberts and Peace 2007; Schenk et al. 2012; Stieglitz et al. 2011).

The Oligocene play was speculated upon (Dolson and Boucher 2002; Dolson et al. 2002a, b, 2004), but met with much resistance. The primary concern was that it relied on a deeper source rock in the Oligocene than had ever been proven anywhere in Egypt, despite thousands of onshore wells having fully penetrated the Oligocene stratigraphy. Figure 4.69 shows the overall stratigraphic setting of the Oligocene in Egypt and the key wells used to speculate a deeper play was possible.

Prevailing wisdom also was that overpressures would be so high there would be no chance for accumulations, the reservoirs would have low porosity and permeability due to great depth and the play would be undrillable.

The team I was working with in the Nile Delta looked at the data a little differently, as there were a number of key dry holes that suggested the deep play would actually work. These same dry holes had been used by many others to condemn the play as 'proof' it would not work. The most obvious 'NULF' (nasty, ugly little fact) was the undeveloped and uneconomic Tineh Field in the offshore, drilled in 1981. The Tineh-1 well flowed 1600 BOPD, 29.3° API and water, from high quality Oligocene sands. Two offsets were dry at the same level. The zone was overpressured. The pay zones were also well below the 'proven' source rock in the Miocene Qantara Formation.

A second 'NULF' was the Bougaz-1 well, discussed earlier. Post-appraisal of it showed a working petroleum system as deep as the Cretaceous, with extreme overpressure exceeding the fracture gradient. Thirdly, a dry Oligocene penetration at Temsah Field, which encountered very high pressure, had no reservoir, and thus could be discounted as not proving the play concept.

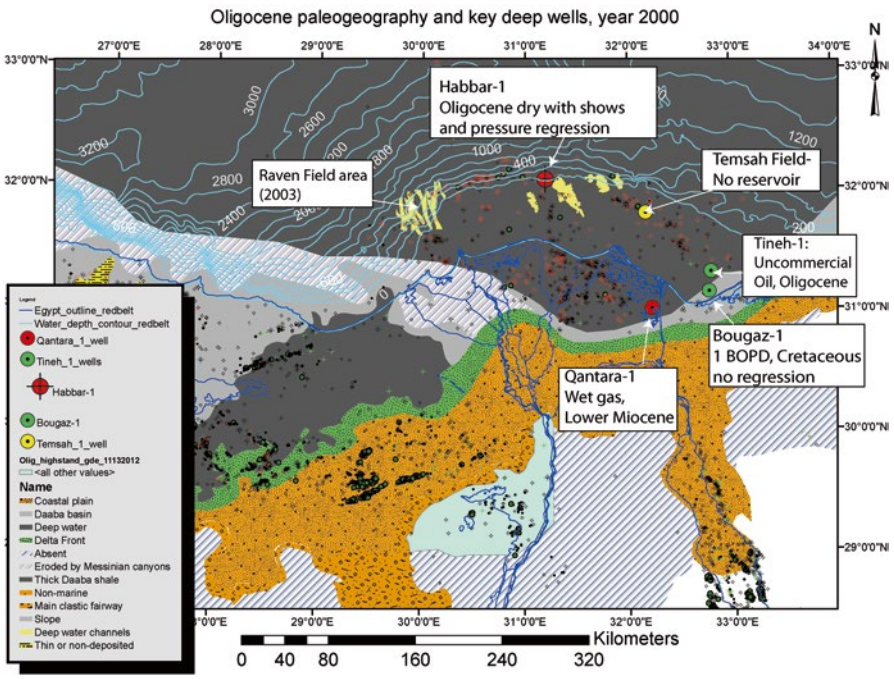

Fig. 4.69 Oligocene paleogeography at late sea level highstand and key wells available pre-Raven discovery in year 2000 deep potential evaluation. Modified from Dolson et al. (2014)

Fourth, a deep overpressured zone in the lower Miocene Qantara Formation had also tested gas and condensate (Qantara-1). That reservoir was also below what was thought to be the main source rock interval. Lastly, in 1999, IEOC and Amoco drilled the Habbar-1, testing a huge fault trap at the Oligocene level. It came in dry, again, reinforcing the idea that the Oligocene play was hopeless.

However, post-appraisal of the pressure data in the Habbar-1 well indicated that a major pressure regression was present. The well drilled a normally pressured Messinian section, crossed the major unconformity shown schematically on Fig. 4.69, and ramped up to 17 ppg mud weights. However, in two thick Oligocene reservoirs, the pressure broke back to 12 ppg, indicating seal breach at the Messinian unconformity (Fig. 4.70).

Additional work on the cuttings and logs provided other encouragement. The log analysis indicated the presence of residual gas throughout the Oligocene reservoirs, proving that hydrocarbons had migrated through the reservoir in the past. Samples were sent out for fluid inclusions (Chap. 7) and came back with 29–43 API oil in the inclusions, proving the migrating fluids had oil and condensate as well as gas. The reservoir quality was also high, negating concerns about lack of porosity at depth. This higher quality reservoir is due in large part, to low effective stress in the over-pressured environment.

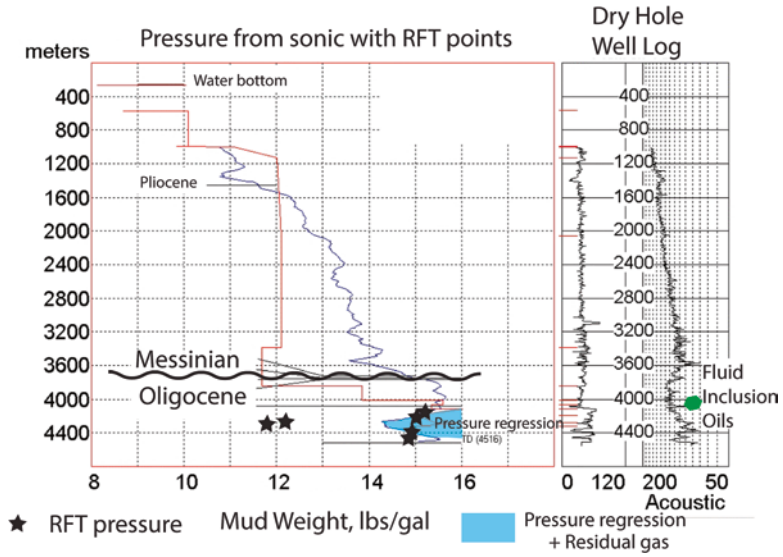

Fig. 4.70 Habbar-1 pressure data

A schematic diagram (Fig. 4.71) shows how this information allowed a new look at the play. First, there was direct evidence of migration, despite any evidence of a viable source rock. Secondly, the pressure regression into the Messinian Abu Madi valley concept was already well known. What was obvious on the seismic, however, was that many deep 4-way and fault trap closures existed downdip of the Habbar-1 well and were not breached at the unconformity. These undrilled structures, however, were tapped into the lower pressure system encountered in the Habbar-1 well, making them ideal targets for pressure regressions and enhanced pressure seals.

With this interpretation in hand, BP proceeded to negotiate in 2002 for acreage over all of the untested deeper structures that were 'plumbed' into the Habbar-1 top-seal breach. In 2008, BP drilled the deep giant gas-condensate Satis Field discovery, complete with a pressure regression and good condensate yields. Since then, a number of other traps have been found and the play is still being pursued as of this writing, with multi-TCF discoveries.

Interestingly, another paradigm was broken with discovery of the Satis-1 well. Oligocene source rocks, in part of the section never penetrated and analyzed by prior wells, were found to be the source for the oil and gas in Satis and many of the shallower accumulations in the eastern and central Nile Delta (Dolson et al. 2014). Once again, the old saying "the absence of evidence is not evidence of absence" held true.

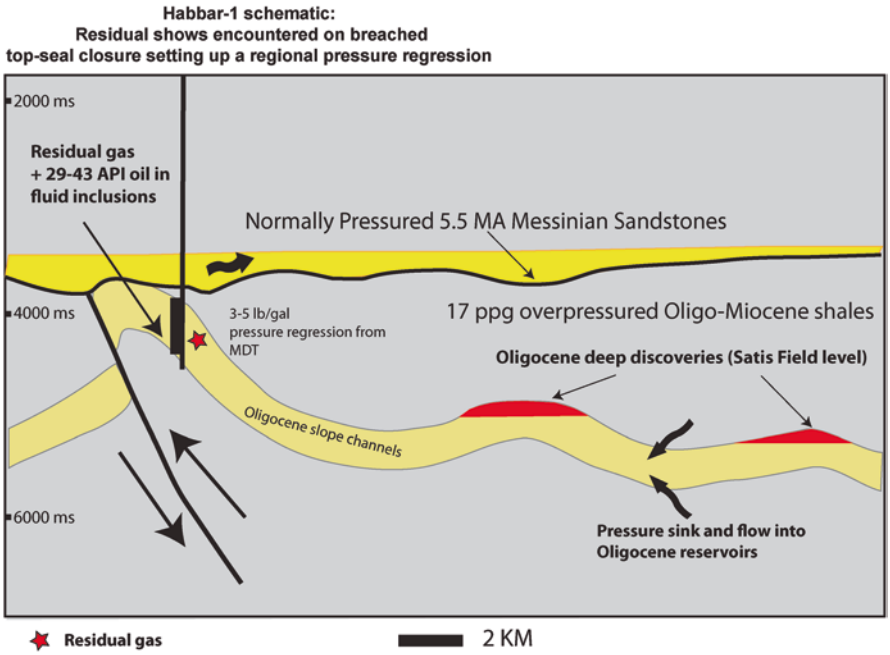

Fig. 4.71 Habbar-1 trap schematic and play concept, deep Oligocene structures. From Dolson et al. (2014). Reprinted with permission of the AAPG, whose further permission is required for further use

4.6 Summary

Pressure analysis is critical to any exploration and development program. Compartments, seals, tilted contacts, free water levels and quantification of buoyancy pressure is a critical part of interpreting shows data. Wells cannot be drilled safely without good pre-drill pressure analysis and post-drill analysis of the pressure is essential to understand what has been found and what might remain to be found.

High porosity is often created and preserved as effective stress drops where overpressure occurs, allowing ever deeper exploratory wells to be successful finding viable reservoirs. Pressure regressions in high overpressure settings are a key to developing effective seals and enhance migration pathways. Deep basin water flow in overpressured settings is real and common, as are titled and compartmentalized fluid contacts.

The case histories shown in this chapter are just two of many examples of how pressure and shows data, put in the proper context, can help break paradigms and find new reserves. As explorers, we often become so ingrained in our beliefs in how basins and plays work that we stop thinking about alternatives or worse, don't deliberately get the information required from existing wells to challenge old ideas. Source rocks that are proven are not always the only source rocks in the basin. Sometimes, the shows information tells you there are still things out there you don't know but ought to think about.

References

Allan US (1989) Model for hydrocarbon migration and entrapment within faulted structures. Am Assoc Pet Geol Bull 72:803–811

Ayan C, Douglas A, Kuchuk F (1996) A revolution in reservoir characterization. Middle East Well Eval Re 16:24–55

Battani A, Prinzhofer A, Deville E, Ballentine CJ (2010) Trinidad mud volcanoes: the origin of the gas. In: Wood L (ed) Shale tectonics. Tulsa, Oklahoma, American Association of Petroleum Geologist, pp 225–238

Berg R (1976) Trapping mechanisms for oil in Lower Cretaceous Muddy Sandstone at Recluse Field, Wyoming, Guidebook, 29th Annual Field Conference: Wyoming Geological Society, p. 261–272

Beaumont EA, Fiedler F (1999) Formation fluid pressure and its application. In: Beaumont EA, Foster NH (eds) Exploring for oil and gas traps: treatise of petroleum geology, handbook of petroleum geology, vol 1. American Association of Petroleum Geologists, Tulsa, Oklahoma, p 64

Belopolsky A, Tari G, Craig J, Illife J (eds) (2012) New and emerging plays in the eastern Mediterranean: an introduction, vol 18. Petroleum Geoscience, The Geological Society of London, London, p 372

Bengtson CA (1981) Statistical curvature analysis techniques for structural interpretation of dip-meter data. Am Assoc Pet Geol Bull 65:312–332

Biddle K, Wielchowsky CC (1994) Hydrocarbon traps. In: Dow WG, Magoon LB (eds) The petroleum system—from source to trap. The American Association of Petroleum Geologists, Tulsa, Oklahoma, pp 221–235

Bjorlykke K, Hoeg K, Faleide JI, Jahren J (2005) When do faults in sedimentary basins leak? Stress and deformation in sedimentary basins: examples from the North Sea and Haltenbaqnken, offshore Norway. Am Assoc Pet Geol Bull 89:1019–1031

Bonini M (2008) Elliptical mud volcano caldera as stress indicator in an active compressional setting (Nirano, Pede-Apennine margin, northern Italy). Geology 36:131–134

Borah I (1992) Drill stem te4sting. In: Morton-Thompson D, Woods AM (eds) Development geology reference manual. Tulsa, Oklahoma, American Association of Petroleum Geologists, pp 131–139

Boult P, Kaldi J (eds) (2005) Evaluating fault and Cap rock seals: AAPG Hedberg series, No. 2. American Association of Petroleum Geologists, Tulsa, Oklahoma, p 268

Bowers GL (2001) Determinnig an appropriate pore-pressure estimation. Offshore Technology Conference, Offshore Technology Conference

Bradley JS, Powley DE (1994) Pressure compartments in sedimentary basins: a review. In: Ortoleva PJ (ed) M61: basin compartments and seals. American Association of Petroleum Geologists, Tulsa, Oklahoma, pp 3–26

Bretan PG, Yielding G, Jones H (2003) Using calibrated shale gouge ratio to estimate hydrocarbon column heights. Am Assoc Pet Geol Bull 87:397–413

Burke LA, Kinney SA, Dubiel RF, Pitman JK (2012) Distribution of regional pressure in the onshore and offshore Gulf of Mexico Basin, USA, Spatial Library GIS Open File http://www.datapages.com/Partners/AAPGGISPublicationsCommittee/GISOpenFiles/DepthofRegionalGeopressureGradientsintheOnshoreandOffshoreGulfofMexicoBasinUSA.aspx, Denver, Colorado, United States Geological Survey, p. 24

Cade CA, Grant SM, Witt CJ (1999) Integrated petrographic and petrophysical analysis for risk reduction, Ormen Lange area, Norway: European Association of Geologists and Engineers 61st Conference and Technical Exhibition, p. 4

Cartwright J, Huuse M, Aplin A (2007) Seal bypass systems. Am Assoc Pet Geol Bull 91:1141–1166

Cloke I (2009) The Albert Rift, Uganda: A history of successful exploration, IRC-Egyptian Petroleum Exploration Society (EPEX), Cairo, Egypt, AAPG Search and Discovery Article #10192

Cross NE, Cuningham A, Cook RJ, Taha A, Esmaie E, Swidan NE (2009) Three-dimensional seismic geomorphology of a deep-water slope-channel system. The Sequoia field, offshore west Nile Delta, Egypt. Am Assoc Pet Geol Bull 93:1063–1086

Dahlberg EC (1982) Applied hydrodynamics in petroleum exploration. Springer Verlag, New York, p 161

Dahlberg EC (1995) Applied hydrodynamics in petroleum exploration, 2nd edn. Springer Verlag, New York, p 295

Dalla S, Harby H, Serazzi M (1997) Hydrocarbon exploration in a complex incised valley fill: an example from the late Messinian Abu Madi Formation (Nile Delta basin, Egypt). Lead Edge 16:1819–1824

Davies RJ, Stewart SA (2005) Emplacement of giant mud volcanoes in the South Caspian Basin: 3D seismic reflection imaging of their root zones. J Geol Soc 162:1–4

Davies RK, Handschy JW (2003) Introduction to AAPG Bulletin thematic issue on fault seals. Am Assoc Pet Geol Bull 87:377–380

Dennis H, Bergmo P, Holt T (2005) Tilted oil-water contacts: modelling the effects of aquifer heterogeneity: Petroleum Geology conference series 2005, p. 145–158

Dolson JC, Atta M, Blanchard D, Sehim A, Villinski J, Loutit T, Romine K (2014) Egypt's future petroleum resources: A revised look in the 21st Century. In: Marlow L, Kendall C, Yose L (eds) Petroleum Systems of the Tethyan Region, v. Memoir 106: Tulsa, Oklahoma, American Association of Petroleum Geologists, p. 143–178

Dolson JC, Boucher PJ (2002) The petroleum potential of the emerging Mediterranean offshore gas plays. Egypt: Annual Meeting, AAPG

Dolson JC, Boucher PJ, Dodd T, Ismail J (2002a) The petroleum potential of the emerging Mediterranean offshore gas plays, Egypt. Oil Gas J 32–37

Dolson JC, Boucher PJ, Ismail J, Dodd T (2002b) Pre-Pliocene potential in the Nile Delta/ Mediterranean, offshore Egypt: an emerging giant gas and condensate play? (abs.): International Petroleum Conference and Exhibition, p. A25

Dolson JC, Boucher PJ, Siok J, Heppard PD (2004) Key challenges to realizing full potential in an emerging giant gas province: Nile Delta/Mediterranean offshore, deep water, Egypt: Petroleum Geology: North-West Europe and Global Perspectives—Proceedings of the 6th Petroleum Geology Conference, p. 607–624

Dolson JC, Boucher PJ, Siok J, Heppard PD (2005) Key challenges to realizing full potential in an emerging giant gas province: Nile Delta/Mediterranean offshore, deep water, Egypt: 6th Petroleum Geology Conference, p. 607–624

Dolson JC, Martinsen RS, Sisi ZE (2002c) Messinian incised-valley systems in the Mediterranean along the Egyptian coastline: paleogeography and internal fill: evidence from cores and seismic (abs.): AAPG International Petroleum Conference and Exhibition, p. A25

Doughty PT (2003) Clay smear seals and fault sealing potential of an exhumed growth fault, Rio Grande rift, New Mexico. Am Assoc Pet Geol Bull 87:427–444

Downey MW (1984) Evaluating seals for hydrocarbon accumulations. Am Assoc Pet Geol Bull 68:1752–1753

Duerto L, McClay K (2002) 3D geometry and evolution of shale diapirs in the Eastern Venezuelan Basin (3 posters), AAPG Annual Convention, Houston, Texas, Search and Discovery Article #10026 (2002), p. 3 posters

Eaton BA (1975) The equation for Geopessure prediction from well logs. SPE 50th Annual Fall Meeting, Society of Petroleum Engineers

Engelder T, Lash GG, Uzcategui RS (2009) Joint sets that enhance production from Middle and Upper Devonian gas shale of the Appalachian Basin. Am Assoc Pet Geol Bull 93:857–889

England WA (1994) Secondary migration and accumulation of hydrocarbons. In: Dow WG, Magoon LB (eds) The petroleum system—from source to trap. The American Association of Petroleum Geologists, Tulsa, Oklahoma, pp 211–217

England WA, Mackenzie AW, Mann DM, Quigley TM (1987) The movement and entrapment of petroleum fluids in the subsurface. J Geol Soc Lond 144:327–347

England WA, Mann AL, Mann DM (1991) Migration from source to trap. In: Merrill RK (ed) AAPG treatise of petroleum geology, handbook of petroleum geology. Tulsa, Oklahoma, The American Association of Petroleum Geologists, pp 23–46

Faerseth RB, Johnsen E, Sperrevik S (2007) Methodology for risking fault seal capacity: Implications of fault zone architecture. Am Assoc Pet Geol Bull 91:1231–1246

Ferrero MB, Price S, Hognestad J (2012) Predicting water in the crest of a giant gas field: Ormen Lange hydrodynamic aquifer model: Society of Petroleum Engineers. v. SPE 153507, p. 1–13

Gardosh M, Druckman Y, Buchbinder B, Calvo R (2007) The Oligo-Mocene deepwater system of the Levant Basin. Geophysical Institute of Israel. p 73

Gardosh M, Druckman Y, Buchbiner B (2009a) The Late Tertiary deep-water siliciclastic system of the Levant margin—An emerging play offshore Israel, AAPG Search and Discovery Article #10211

Gardosh MA, Druckman H, Buchbinder B (2009b) The late Tertiary deep-water siliclastic system of the Levant Margin: an emerging play in Israel, American Association of Petroleum Geologists Annual Convention, Denver, Colorado, AAPG Search and Discovery Article #10211, p. 1–19

Gawthorpe RL, Moustafa AR Pivnik D, Sharp I (2002) Syntectonic sedimentation in rifts: Examples from the Sinai margin and subsurface of the Gulf of Suez, Egypt: A field guidebook, AAPG International Conference and Exhibition, Cairo, Egypt, American Association of Petroleum Geologists, p. 116

Gearhart-Owens-Industries (1972) GO Log InterpretationReference Data Handbook, Gearhart-Owens Industries, Inc., 226 p

Gibson RG (1994) Fault-zone seals in siliciclastic strata of the Columbus Basin, offshore Trinidad. Am Assoc Pet Geol Bull 78:1372–1385

Gibson RG, Bentham PA (2003) Use of fault-seal analysis in understanding petroleum migration in a complexly faulted anticlinal trap, Am Assoc Pet Geol Bull 87:465–478

Hanson WB, Vega V, Cox D (eds) (2004) Structural geology, seismic imaging, and genesis of the giant Jonah Gas field, Wyoming, U.S.A.: Jonah field: case study of a giant tight-gas fluvial reservoir: AAPG studies in geology 52 and rocky mountain association of geologists 2004 guidebook. American Association of Petroleum Geologists, Tulsa, Oklahoma, pp 61–92

Hartmann DJ, Beaumont EA (1999) Predicting reservoir system quality and performance. In: Beaumont EA, Foster NH (eds) Exploring for oil and gas traps: treatise of petroleum geology, handbook of petroleum geology, v. 1: Tulsa, Oklahoma, American Association of Petroleum Geologists, p. 9.3–9.154.

He Z, Berkman T (1999) Interactive charge modeling of the Qatar arch petroleum systems, AAPG Hedberg conference on multi-dimensional basin modeling, Colorado springs. American Association of Petroleum Geologists, Colorado

Henry M, Pentilla M, Hoyer D (2010) Observations from exploration drilling in an active mud volcano in the southern basin of Trinidad, West Indies. In: Wood L (ed) Shale tectonics. Tulsa, Oklahoma, American Association of Petroleum Geologist, pp 63–78

Heppard PD, Dolson JC, Allegar NC, Scholtz SM (2000) Overpressure evaluation and hydrocarbon systems of offshore Nile Delta, Egypt: Mediterranean Offshore Conference, p. CD

Horner DR (1951) Pressuer build-up in wells. Proceedings of the Thrid World Petroleum Congress, The Hague, Netherlands, p. 503–521

Hubbert MK (1953) Entrapment of petroleum under hydrodynamic conditions. Am Assoc Pet Geol Bull 37:1954–2026

Huseynov A (2012) Pore pressure principles course-training materials (in-house course), Baku, Azerbaijan, BP

Jackson J, Priestley K, Allen M, Berberian M (2002) Active tectonics of the south Caspian basin. Geophys J Int 148:214–245

James WR, Fairchild LH, Nakayama GP, Hippler SJ, Vrolijk PJ (2004) Fault-seal analysis using a stochastic multifault approach. Am Assoc Pet Geol Bull 88:885–904

Jones RM, Hillis RR (2003) An integrated, quantitative approach to assessing fault-seal risk. Am Assoc Pet Geol Bull 87:507–524

Kendrick JW (1998) Turbidite reservoir architecture in the Gulf of Mexico—insights from field development, EAGE/AAPG 3rd Research Symposium—Developing and Managing Turbidite Reservoirs p. 287–289

Lee Y, Deming D (2002) Overpressures in the Anadarko Basin, southwestern Oklahoma: static or dynamic? Am Assoc Pet Geol Bull 86:145–160

Lie O, Skiple C, Lowrey C (2011) New insights into the Levantine Basin, GeoExPro. Geopublishing Ltd., London, pp 24–27

Lupa J, Flemings P, Tennant S (2002) Pressure and trap integrity in the deepwater Gulf of Mexico. Lead Edge 21:142–183

Marcou JA, Samsu D, Kasim A, Meizarwin, Davis N (2004) Tangguh LNG's gas resource: discovery, appraisal and certification, IPA-AAPG Deepwater and Frontier Exploration in Asia and Australiasia Symposium, Indonesian Petroleum Association

McClelland E, Finegan B, Butler RWHA (1996) A magnetostratigraphic study of the onset of the Mediterranean Messinian salinity crisis: Calanisetta Basin, Sicily. In: Morris A, Tarling DH (eds) Paleomagnetism and Tectonics of the Mediterranean Region, v. Publication No. 105: London, The Geological Society, p. 205–218

Montgomery SL, Robinson JW (1997) Jonah field, Sublette county, Wyoming: Gas production from overpressured upper cretaceous lance sandstones of the green river basin. Am Assoc Pet Geol Bull 81:1049–1062

Moussa DS, Matbouly DS (eds) (1994) Nile delta and north Sinai: fields, discoveries and hydrocarbon potentials (a comprehensive overview). The Egyptian General Petroleum Corporation, Cairo, Egypt, 387 p

Muggeridge A, Mahmode H (2012) Hydrodynamic acquifer or reservoir compartmentalization? Am Assoc Pet Geol Bull 96:315–336

Nashaat M, Carlin S, BagnoliG, Moussa A (1996) The pre-Messinian overpressure study in the Nile Delta area: a supporting methodology for understanding hydrocarbon accumulation. In: Youssef M (ed) 13th Petroleum Conference, v. 1: Cairo, Egypt, The Egyptian General Petroleum Corporation, p. 193–202

O'Connor SA, Swarbrick RE (2008) Pressusre regression, fluid drainage and hydrodynamically controlled fluid contact in the north Sea, lower cretaceous, Britannia sandstone formation. Pet Geosci 14:115–126

Palmieri G, Harby H, Marini JA,Hashem F, Dalla S, Shash M (1996) Baltim fields complex: an outstanding example of hydrocarbon accumulations in a fluvial Messinian incised valley. In: Youssef M (ed) Proceedings of the 13th Petroleum Conference, v. 1: Cairo, Egypt, The Egyptian General Petroleum Corporation, p. 256–269

Peace D (2011) Eastern Mediterranean: the Hot New exploration region, GeoExPro. Geopublishing Ltd., London, pp 36–41

Riley G (2009) Supergiant fields in an overpressured lacustrine petroleum system: the south Caspian basin, AAPG 2009 distinguished lecture series. American Association of Petroleum Geologists, Tulsa, Oklahoma, p 32

Roberts G, Peace D (2007) Hydrocarbon plays and prospectively of the Levantine Basin, offshore Lebanon and Syria from modern seismic data. Geo Arabia 12:99–124

Robertson J, Goulty NR, Swarbrick RE (2013) Overpressure distributions in Palaeogene reservoirs of the UK Central North Sea and implications for lateral and vertical fluid flow. Pet Geosci 19:223–236

Sales JK (1997) Seal strength vs. trap closure-A fundamental control on the distribution of oil and gas. In Surdam RC (ed) Seals, traps and the petroleum system, v. Memoir 67: Tulsa, Oklahoma, American Association of Petroleum Geologists p. 57–83

Samuel A, Kneller B, Raslan S, Sharp A, Parsons C (2003) Prolific deep-marine slope channels of the Nile Delta, Egypt. Am Assoc Pet Geol Bull 87:541–560

Sautkin A, Talukder AR, Comas MC, Soto JI, Alekseev A (2003) Mud volcanoes in the Alboran Sea: evidence from micropaleontological and geophysical data. Mar Geol 195:237–261

Saxon J (2011) 'Water Way' to gas identification in Raven, New and Emerging Plays in the Eastern Mediterranean. The Geological Society of London, London, p 59

Schenk CJ, Kirschbaum MA, Charpentier RR, Klett TR, Brownfield ME, Pitman JK, Cook TA, Tennyson ME (2012) Assessment of undiscovered oil and gas resources of the Levant Basin Province, Eastern Mediterranean, Reston, Virginia, World Petroleum Resources Project United States Geological Survey

Shaker SS (2002) Geopressure progression-regression: an effective risk assessment tool in Gulf of Mexico Deep Water. Gulf Coast Assoc Geol Soc Trans 52:893–898

Shaker SS (2005) Geopressure centroid: perception and pitfalls, 2005 SEG Annual Meeting. Houston, Texas, Society of Exploration Geophysicists, p 4

Shanley KW (2004) Fluvial reservoir description for a giant low-permeability gas field: Jonah Field, Green River Basin, Wyoming, USA. In: Robinson JW, Shanley KW (eds) Jonah Field: Case Study of a Tight-gas Fluvial Reservoir, v. 52, American Association of Petroleum Geologists Studies in Geology, p. 159–182

Sharp I, Gawthorpe RL, Underhill J, Gupta S (2000) Fault-propagation folding in extensional settings: Examples of structural style and synrift sedimentary response from the Suez rift, Sinai, Egypt. Geol Soc Am Bull 112:1877–1899

Skerlec GM (1999) Evaluating top and fault seal. In: Beaumont ANHFEA (ed) Exploring for Oil and Gas Traps: Treatise of Petroleum Geology, Handbook of Petroleum Geology, v. 1: Tulsa, Oklahoma, American Association of Petroleum Geologists, p. 10-3–10-94

Smith B, Rose J (2002) Uganda's Albert graben due first serious exploration test. Oil Gas J

Stewart SA, Davies RJ (2006) Structure and emplacement of mud volcano systems in the South Caspian Basin. Am Assoc Pet Geol Bull 90:771–786

Stieglitz T, Spoors R, Peace D, Johnson M (2011) An integrated approach to imaging the Levantine Basin and Eastern Mediterranean: New and emerging plays in the Eastern Mediterranean, p 15–19

Surdam RC, Robinson J, Jiao ZS, Nicholas KB II (2001) Delineation of Jonah Field using seismic and sonic velocity interpretations. In Anderson D (ed) Gas in the Rockies, Rocky Mountain Association of Geologists, p. 189–209

Swarbrick R, O'Connor S (2010) Low pressure to high pressures--how regional overpressure mapping helps find trapped hydrocarbons, Finding Petroleum, Immarsat Conference Center, London, United Kingdom, Finding Petroleum

Traugott M (1997) Pore pressure and fracture pressure determinations in deepwater: World Oil, v. Deepwater Technology supplement to World Oil p. 68–70

Vavra CL, Kaldi JG, Sneider RM (1992) Geological applications of capillary pressure: a review. Am Assoc Pet Geol Bull 76:840–850

Whaley J (2008) The Raven field: planning for success, GEOEXPRO. United Kingdom, GEOEXPRO, p. 36–40

Yielding G (2002) Shale gouge ratio-calibration by geohistory. Norwegian Petroleum Soc Special Publications 11:1–15

Yielding GB, Freeman B, Needham DT (1997) Quantitative fault seal prediction. Am Assoc Pet Geol Bull 81:897–917

Young MJ, Gawthorpe RL, Sharp IR (2002) Architecture and evolution of the syn-rift clastic depositional systems towards the tip of a major fault segment, Suez Rift, Egypt. Basin Res 14:1–23

Yusifov M (2004) Seismic interpretation and classification of mud volcanoes on the South Caspian Basin, offshore Azerbaijan. Texas A&M University, College Station, Texas, p 104

Chapter 5
Quantifying Seals and Saturations: Capillary Pressure, Pseudo-capillary Pressure and Quantitative Show Assessment

Contents

Abstract Capillary pressure exerts a fundamental control on seal capacity and reservoir behavior. Pore throat radius is a key factor in seal capacity, with the smallest pore throats requiring the most buoyancy pressure to displace water in the pore systems with hydrocarbons. Interfacial tension and wettability play additional roles. When converted to height above free water plots, capillary pressure data can give a good approximation of the free water level if the water saturation is known.

J. Dolson, *Understanding Oil and Gas Shows and Seals in the Search for Hydrocarbons*, DOI 10.1007/978-3-319-29710-1_5

Capillary pressure data can be expensive and time consuming to require. However, by studying flow units in rocks using Winland analysis, porosity and permeability can be used to estimate a pore throat radius. Once this is done, pseudo-capillary pressure plots can be make which give a good approximation of the height above fee water from the permeability and porosity data alone. These data can then be used to estimate seal capacities and reservoir performance.

Seals and traps along migration routes can be modeled using software packages or with simple grid manipulation. Quantitative show analysis can help identify seals, force modification of paleogeographic maps to fit hydrocarbon shows, or help determine seal capacities on faults. Once this is done, migration can be modeled using seals along the migration pathways, providing a much more robust prospect inventory than can be achieved by looking for four-way closures alone.

In addition, Appendix B shows how to build an Excel spreadsheet to visualize potential pore throats sizes. Appendix C illustrates how to build Excel spreadsheets to analyze mercury-injection capillary pressure data and Appendix D similar solutions for pseudo-capillary pressure using porosity and permeability as inputs. Appendix E provides some tips on how to create a seal grid for trap analysis using ARCGIS shapefiles and feature classes.

The major intent of this chapter is to get the reader to the point where a simple knowledge of porosity and permeability, from any source, can lead to a quantitative estimate of seal capacity or reservoir performance. To get to this point, you will learn how to construct pseudo-capillary pressure curves from calculations using regression equations which estimate pore throat size from porosity and permeability data.

Being able to assess seal capacity or position in a trap from Sw in terms of height above free water is key to understanding traps and hydrocarbon shows.

5.1 The Fundamentals of Capillary Pressure

5.1.1 The Importance of Understanding Capillary Pressure

Before going further, it is probably important to understand relative pore throats sizes, as capillary pressure models fluid displacement in the pore throat networks. In a sense, pore throats in rocks act like arteries and capillaries in a human body, with a complex arrangement of networks from big to very small. A micron is 10^{-3} mm. A 70 μm rock has a pore network the size of a human hair, is mega-porous and would be capable of huge flow rates. Meso-porous rocks, which are between 0.5 and 2 μm, have pore networks about the size of some bacteria. Shale pore networks are less than soap film in size. Fortunately, oil and gas molecules are smaller still and can comfortably fit into these small spaces.

Capillary pressure forces provide seals that trap hydrocarbons. The saturation reached in a trap will be limited by the weakest of those capillary seals and the amount of buoyancy pressure required to overcome the capillary seals as the trap fills. Chapter 2 provided an introduction to the concepts of free water levels and saturation vs. height for various rock types, as well as basic trap geometries related to seals.

Understanding how capillary pressure is calculated and is an additional key, then, to actually quantifying where an oil or gas show is within a trap. Determining if an Sw, for instance, of 65 % is at the top of a trap is in a waste zone, or low on a hydrocarbon column in the transition zone, requires a knowledge of how to look at the reservoirs from a capillary pressure standpoint. If rock properties are well understood from capillary pressure, then how a well tests under production is usually easier to understand and quantify.

In addition, Chap. 4 covered the basics of pressure analysis and fluid flow in hydrodynamic conditions, but did not cover the additional trapping component created by seals. In this chapter, we cover ways to estimate seal capacity from capillary pressure data, direct observation of shows data and/or the use of pseudo-capillary spreadsheets using porosity and permeability data.

5.1.2 *Fluid Potential (Entrapment) Maps Using Capillary Pressure Seals*

Understanding how to generate maps that utilize both hydrodynamic conditions and seals requires understanding Hubbert's full equation for entrapment (Chap. 4 and Hubbert 1953). Equation 5.1 provides the full equation for fluid entrapment (potential).

$$\Phi p\left(\textit{fluid potential}\right) = gZ + \frac{P}{\rho} + \frac{Pc}{\rho}; \tag{5.1}$$

where Z = structural elevation (TVDSS), P = pressure at that elevation, ρ = density of the fluid (water, oil or gas), Pc = capillary pressure, g = gravitational component.

As gravity is a constant, for practical mapping purposes (Dahlberg 1995), it can be dropped and the equation reduces to:

$$\Phi p\left(\textit{fluid potential}\right) = Z + \frac{P}{\rho} + \frac{Pc}{\rho} \tag{5.2}$$

This can be re-written in terms of pressure gradients as:

$$\varnothing\left(\textit{fluid potential}\right) = Z + \frac{P}{Pgrad} + \frac{Pc}{Pgrad} \tag{5.3}$$

Where Pgrad is oil or gas density in psi/ft (for example, .35 psi/ft for oil).

It is useful to remember when dealing with densities, that 1 g/cc = 0.433 psi/ft and hence converting density in g/cc to psi/ft is by Eq. 5.4.

$$\text{Pgrad}\left(\text{psi / ft}\right) = \text{Density}\left(\text{g / cc}\right) * .433 \tag{5.4}$$

The math used in generating hydrodynamic tilt maps using the U-V-Z method discussed in Chap. 4, however, does not use the full Hubbert equation, but only the $Z + \frac{P}{\rho}$

component. The additional component $\left(\frac{Pc}{\rho}\right)$ is the seal capacity of a rock due to its capillary pressure properties. Modeling traps quantitatively requires, then, a knowledge not just of the water flow, but the capillary pressure seal capacity of facies or faults along a migration route. The impact can be substantial, as fault and facies changes can add hundreds of meters of seal capacity to a trap undergoing hydrodynamic tilting and flushing. Clearly, the most complicated traps involve both water movement and capillary seals, and these should be modeled to understand trap geometries.

If a basin has no lateral gradient in the water head, the equation for fluid potential reduces to:

$$\Phi p\left(\textit{fluid potential}\right) = Z + \frac{Pc}{\rho} \tag{5.5}$$

because the hydrodynamic head is constant over the area.

In this chapter, we cover how to calculate the seal component $\left(\frac{Pc}{\rho}\right)$, as values of feet or meter of column height of seal capacity for any fluid-water combination. With that number in hand, migration maps can be run using the U-V-Z method that add additional trapping due to fault or facies seals.

If a basin has hydrodynamic flow, then the Vo or Vg maps from hydraulic head must be added to the seal capacity maps and then the U-V-Z approach tried. When this is done, the resultant maps have a much better chance of predicting new fields and explaining existing accumulations.

5.1.3 Capillary Pressure

Capillary pressure is the force that causes water to rise in a series of tubes are immersed in a tube half filled with water and half filled with oil, as shown on Fig. 5.1 (modified from Dahlberg (1995)). The smaller the tube, the higher the rise of the water phase, which is said to be 'wetting' the walls of the tube. The height that the water or 'wetting phase' rises in the tube is controlled by capillary pressure, which is in turn a function of the radius of the tube and the properties of the wetting and nonwetting phase. In this case, the nonwetting phase is oil. To displace the water in the tube with oil, extra pressure is required to force the water from the tube. In hydrocarbon traps, that displacing force is provided by buoyancy pressure, which is a function of the density differences between the oil and water and the trap geometry, which controls the column height. High on the trap, more fluid from smaller tubes can be displaced, but not until the capillary pressure in the tubes are overcome.

Excellent short reviews of capillary pressure are covered by (Abdallah et al. 2007; Hartmann and Beaumont 1999; Jennings 1987; Vavra et al. 1992). Additional classic references are those of (Berg 1975; Schowalter 1979; Swanson 1981; Thomeer 1960).

Capillary pressure is defined as the difference in pressure across the meniscus of the capillary tube, but is probably easier thought of as the amount of extra pressure

required to force the nonwetting phase (in this case oil) to displace the wetting phase (in this case water). Capillary pressure arises from forces acting on the interface between cohesive forces at the water and oil interface and the adhesive forces between the liquid and the wall of the capillary. These forces are highest in the smallest capillaries. The forces acting on the fluid interfaces are termed 'interfacial tension' and those along the wall of the capillary as the 'wettability'.

In Fig. 5.1, three generic rock types gradually change facies across an anticline. Capillary forces are highest in the smallest pore throats, and lowest in the largest. Hence, water rise is high in the shale and very low in the sandstone. Reservoirs can be thought of as a nearly infinite distribution of capillary tubes and thus, in a case like this, if the capillary radius gradually decreases updip, then an oil-water contact will actually have a slope or tilt. As mentioned in Chap. 2, saturation can be viewed as a saturation-height function (right side of Fig. 5.1). The point that hydrocarbons breakthrough or displace the water in the capillarity not only defines the oil-water contact for that rock type, but also the seal capacity.

Also shown on Fig. 5.1 is the similarity between hydraulic head and the height to which the water rises in the tube. Thought of in terms of fluid flow, there is a high degree of potential energy in the shales relative to the other reservoirs.

The basic equation to express capillarity quantitatively (Vavra et al. 1992) is by Eqs. 5.6 and 5.7 and graphically as shown in Fig. 5.2.

$$\mathrm{Pc} = gh^{*}\left(\rho_{w-}\rho_{nw}\right) \tag{5.6}$$

where

ρ_w = density of wetting phase
ρ_{nw} = density of nonwetting phase
g = gravitational constant
h = height above the free water level

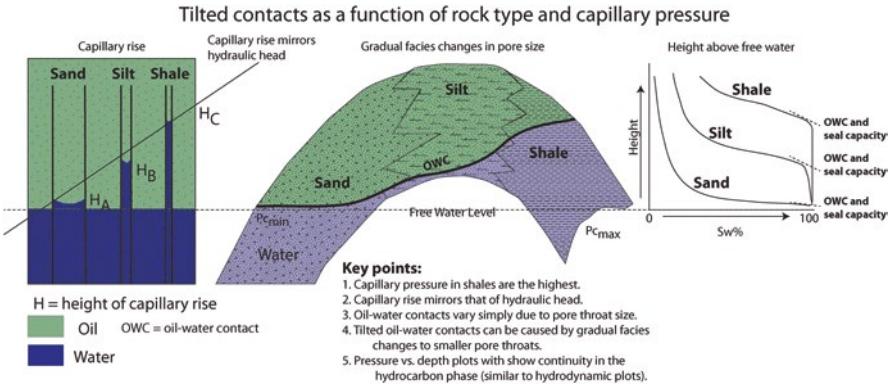

Fig. 5.1 Conceptual diagram of capillary pressure vs. rock type and height above free water. Shales or any seals have high capillary pressure relative to porous reservoirs. For this reason, pore throat changes to smaller sizes updip in a trap can create a tilted oil-water contact simply because of capillarity. Modified from Dahlberg 1995

This can be re-written as Eq. 5.7:

$$Pc = \frac{2\gamma cos\theta}{R} \tag{5.7}$$

where γ = interfacial tension in dynes / cm
θ = wettability angle
R = Radius of pore throat in centimeters (10,000 μm = 1 cm)
The answer is in dynes/cm^2 units (69035 dyn/cm^2 = 1 psi)
Conversion to psi is by Eq. 5.8 or 5.9:

$$Pc\left(in\ psi\ units\right) = \frac{2\gamma cos\theta}{R} * 145 \times 10^{-5} \tag{5.8}$$

If R is entered in microns, then conversion to psi is:

$$\mathrm{Pc} = \frac{2\gamma cos\theta}{R} * .145 \tag{5.9}$$

Density differences in the oil and water phases drive buoyancy. Therefore, capillary pressure is easily understood in the context of pressure vs. depth plots In Fig. 5.2, the capillary pressure, like buoyancy pressure, is the difference between the wetting and non-wetting phases (in most cases, between the water density and hydrocarbon density). The free water level is where Pc = 0.

So, what are the additional numbers of interfacial tension and wettability? Overcoming capillary pressure also means overcoming resistive forces of interfacial tension (IFT) and wettability. Wettability and interfacial tension work together. The forces at the liquid to liquid interface (IFT) are termed cohesive, and are caused by molecular changes at the interface of the liquids. Wettability is an adhesive force operating between the wetting phase and the capillary walls. Conceptually, when water does not run down a windshield, it is because gravitational forces are less than the adhesive forces (wettability).

Normally, rocks are assumed to have water as the wetting phase and are thus termed water wet. If oil is the wetting phase, it is oil wet. An example of a water wetting phase is shown in Fig. 5.3a, where the contact angle is less than 90°. Conversely, if the surface is oil wet, the water beads up as shown in Fig. 5.3b. Interfacial tension can be viewed as the forces acting at the fluid interface, as shown visually by the water spider on Fig. 5.3c.

Oil wet rocks are relatively rare, and can reach very low water saturations (O'Sullivan et al. 2008). More commonly, pores may be slightly oil wet, as shown in 5.3d. An example of interfacial tension and wettability working together is shown in 5.3e. There can be intimate linkage between wettability and interfacial tension. If IFT is reduced, for instance, a formerly non-wetting liquid can become wetting.

This may be exactly what happens in some oil-wet reservoirs. Initial conditions may have been water wet, but chemical reactions with certain types of asphaltine-rich oils or iron-rich cements may alter wettability with time. In any event, changing the IFT or contact angle in a capillary pressure analysis can have significant impacts on saturation-height functions. A practical application involving changing wettability and IFT values is from deliberate chemical injection into drained

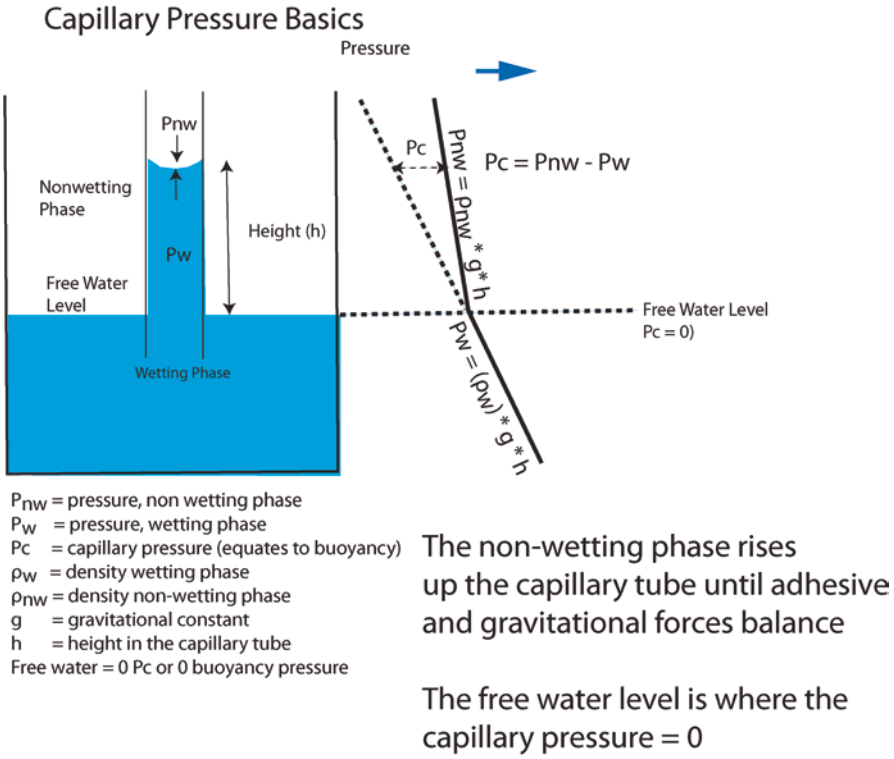

Fig. 5.2 Basic capillary pressure definition. The equations for Pc can best be thought of in terms of a pressure vs. depth plot, with Pb (buoyancy) pressure equivalent to Pc. The free water level is where Pc = 0. After Vavra et al. (1992). Reprinted by permission of the AAPG, whose further permission is required for further use

oil pools to change both values and allow residual oil to once again be produced (RPSEA 2009) as the capillary properties of the drained reservoir are changed.

5.1.3.1 Mercury Injection Capillary Pressure Analysis

Capillary pressure is quantified in a number of ways, one of the most common of which is mercury capillary injection pressure (MCIP). Centrifuge and porous plate methodology is also used, but for the rest of this book, we are going to be dealing with mercury injection data. The process involves cutting core plugs, heating and drying the plug to remove all liquids, both water and hydrocarbons, so that nothing but pore space is left. Next, the evacuated plug is put in an apparatus where mercury is injected at increasingly higher pressures until the pore system is filled up to a finite state. MCIP injection pressures are typically at 2000 psi, but can reached 60,000 psi or higher for tests in really tight strata or shale.

With this test, air in the pores is the wetting phase and the mercury is the non-wetting phase. The displacement by mercury simulates migration of oil and gas filling a trap. When mercury is being injected, the curve that results of percentage

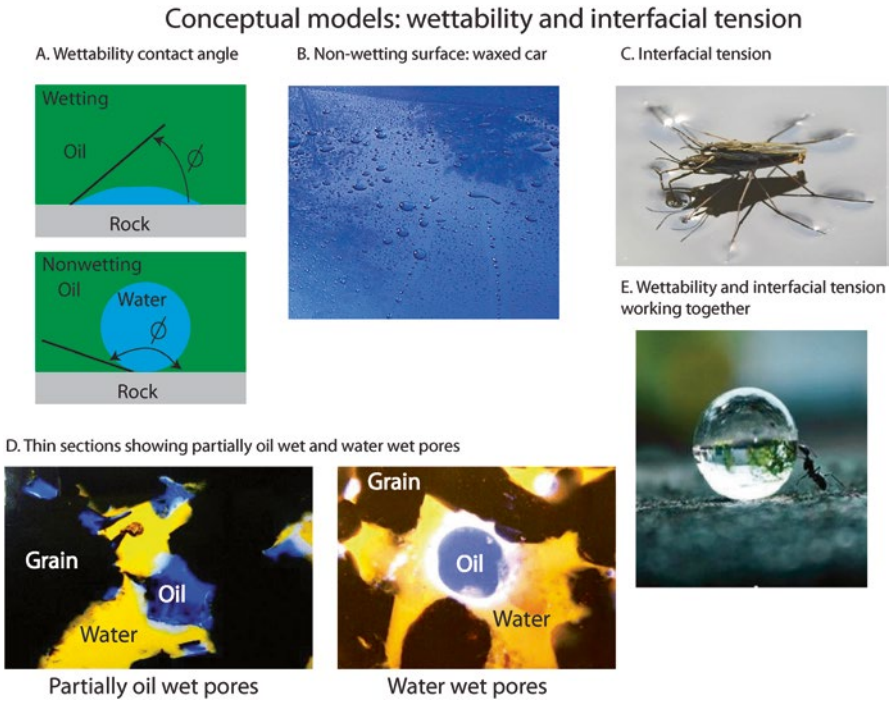

Fig. 5.3 Conceptual models of wettability and interfacial tension

mercury vs. pressure is called the 'drainage' curve direction (Fig. 5.4). On these plots, a number of important pieces of information can be obtained:

1. The curves can be converted to height above free water if the densities of the hydrocarbon-water system are known, as well as the IFT and wettability of the hydrocarbon phase.
2. Pore throat size distributions can be calculated directly from the curve as the IFT of air-mercury and wettability of mercury are known. The equation for pore throat size thus becomes Eq. 5.10:

$$R = \frac{2\gamma cos\theta}{Pc}, \tag{5.10}$$

and as the IFT of mercury-air = 485 dyn/cm, and $\theta = 140^{o}$

Note: While θ for mercury-air is given as 140^{o} in this and other examples, the value of 40^{o} should be used in order to return a positive value for cos θ as the original equation for mercury-air pore throat size (Washburn 1921) takes the absolute value of cos (140^{o}).

3. This equation can further be rewritten as Eq. 5.10 (Pittman 1992):

$$\mathrm{R}\left(\mathrm{microns}\right) = \frac{107}{Pc\left(psia\right)} \tag{5.11}$$

Pseudo-capillary pressure analysis involves calculation of the pore throat radius from simple porosity and permeability algorithms. If the pore throat radius, IFT and wettability can be estimated, then a seal capacity or saturation at other pore throat radii can be obtained. This is covered in the next section.

Capillary pressure plots that come back from service companies often have the pore throat distribution calculated and displayed for each sample. In reality, because of the very complex distribution of pores, the calculated value actually represents the effective size of the throats, but not the actual dimensions (Vavra et al. 1992). However, the shape of the curves gives a good idea of the type of pore throat system and rock type.

Key points to remember are:

1. The inflection point at the 10 % mercury saturation line is called the displacement pressure. A line drawn tangent to the curve (Fig. 5.4, left), not only gives the seal capacity of the rock, but a theoretical oil-water contact, once conversions to a hydrocarbon-water system are made.
2. The pore throat size statistically represented at the 35th percentile mercury (65 % Sw) has been shown to be have a strong correlation with reservoir performance (Pittman 1992; Winland 1972, 1976).

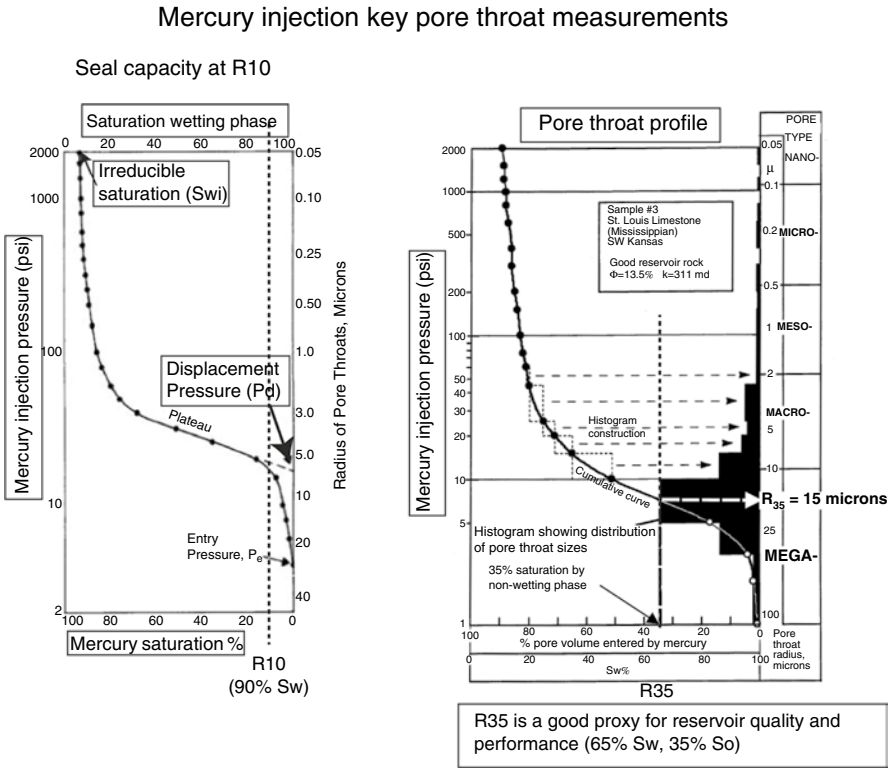

Fig. 5.4 Mercury injection pore throat distributions. From Jennings (1987) and Hartmann and Beaumont (1999). Reprinted by permission of AAPG whose permission is required for further use

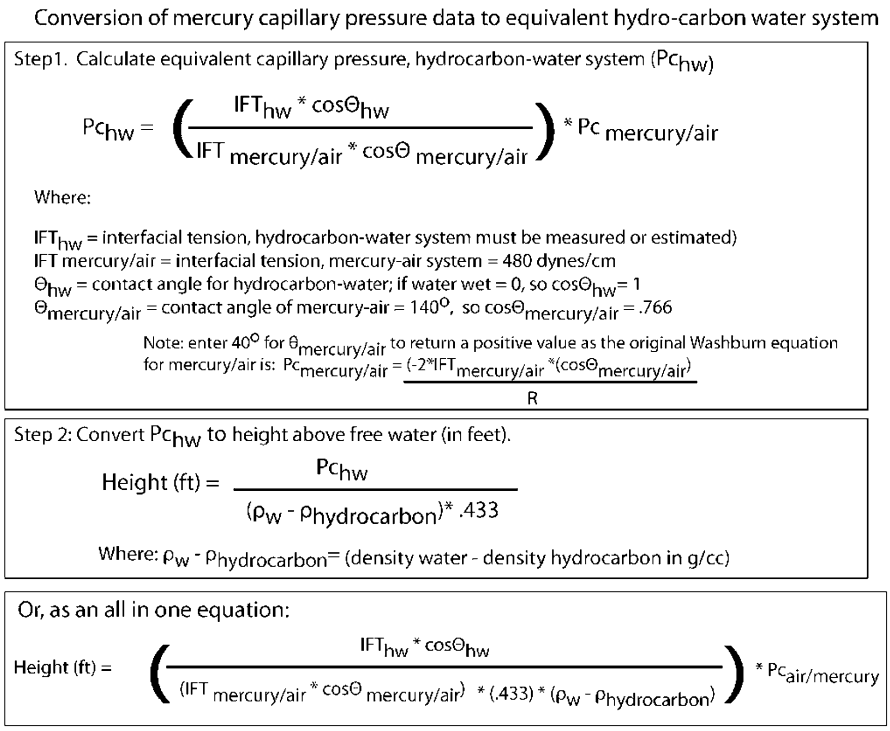

Fig. 5.5 Conversion equations. IFT and wettability numbers must be estimated or known from special core and fluid analysis. Table 5.1 summarizes some of the common numbers used for various fluids

3. The point where the curves go vertical and no further saturation is possible despite increased pressure marks the irreducible water saturation (Swi). When converted to height above free water in a hydrocarbon-water system, this is the lowest Sw that can be obtained. Some bound water remains in the pores, forever attached to the smaller pore throat walls, but is not displaceable.

Making these measurements useful to you and management requires converting the values to a height above free water plot. Figure 5.5 summarizes the steps. Step 1 is to calculate the capillary pressure (Pc_{hw}). Step 2 is to convert Pc_{hw} to height above free water. The equations are shown on Fig. 5.5.

Clearly, it is best to build spreadsheets to do these kinds of calculations quickly and test sensitivities to different inputs. Appendix C shows a simple spreadsheet construction to produce height above free water plots. One of the more difficult things to get right, however, are the contact angles and IFT values, as they are seldom available unless an engineer or log analyst has had the samples run to obtain the numbers. Also, the density values must be correct to subsurface conditions, something that is best done by working with an engineer with PVT reports from your area, or trying to adjust with a knowledge of subsurface temperatures and pressure. This is particularly sensitive in gas zones, where pressure and temperature can have a big impact on density.

Tab. 5.1 Typical ranges used in height above free water calculations. Modified from Vavra et al. (1992)

System	Contact angle (Θ)	Interfacial tension (IFT)	Comments
Air/mercury	140 (enter 40 in equations to keep numbers positive)	480	These are standard numbers and fixed for use in equations
Oil-water < 30 api	0	30	Partially oil wet reservoirs contact angles = 30
Oil/water (30–40 api)	0	21	Partially oil wet reservoirs contact angles = 30
Oil/water > 40 api	0	15	Partially oil wet reservoirs contact angles = 30
Methane/water	0	50–72	These numbers are susceptible to high temperature and pressure changes. An IFT of 30 has been suggested for higher pressure gasses (Zhiyong He, personal communication).
Oil-wet reservoirs	50–80		

Table 5.1 provides some ranges commonly used for 'quick looks' where detailed information is not available. The spreadsheets off the added benefit of testing sensitivities by visually comparing how much changes occur with each variable or combination used.

Some caution also needs to be used in setting IFT values for high temperature and pressure wells. Much of the literature showing the relationship between IFT and temperature for instance (as in Schowalter 1979) has been shown to be erroneous in higher temperature and pressure setting (O'Connor 2000; Pepper 2007). Unfortunately, few publications deal with this topic in a way that is useful to provide meaningful prediction beyond having the samples actually measured. Hence, it is best to deal with ranges of uncertainty from using variable inputs to assess the impact of the changes. Where possible, several modern techniques measure IFT at reservoir conditions, providing the best possible answer.

Figure 5.6, for example, shows the impact of varying the wettability on capillary pressure data obtained for a well in Russia. Although oil-wet reservoirs are unusual, changing the contact angle has a profound effect. If Fig. 5.6 (left) the reservoir is treated as partially oil-wet, while on the right, strongly oil-wet. In actual practice, these sample are water-wet reservoirs. Changes to the saturation-height functions if changed to oil-wet are profound. Note the samples indicated with seal capacity on the sides of both diagrams. In the partially oil-wet case, some micro-porous tidal flat reservoirs actually have seal capacities of 80–150 m. As we don't normally think of sandstone as sealing, in this setting, these facies can form significant seals. Also note that the best reservoir reaches an irreducible saturation around 300 m into the trap, and only 20 % Sw at that.

In contrast, the oil wet samples reach irreducible Sw as low as 7 % and the seal capacity of the tidal flat facies is reduced to 25–50 m, making them potential productive reservoirs if on a column greater than 50 m.

Generally, however, the greatest impact on these curves are the density contrasts between the fluids (Fig. 5.7).

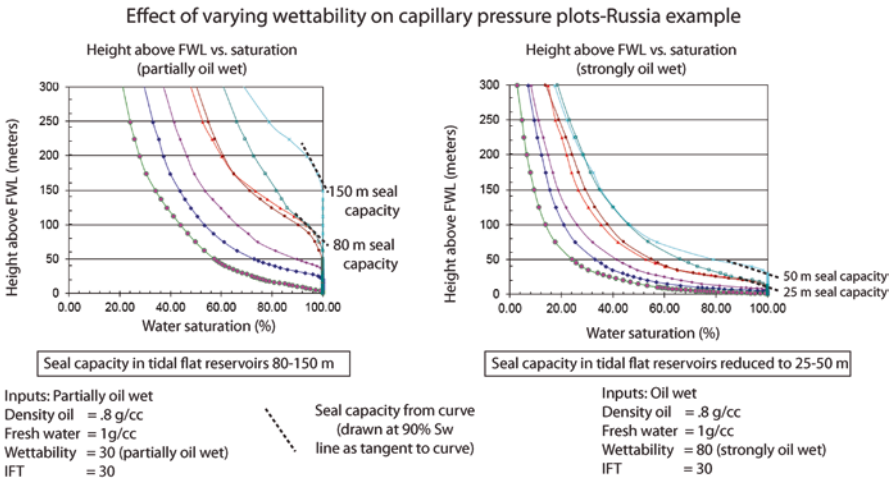

Fig. 5.6 Impact of varying wettability. Frequently, seals are assumed to be water wet, with a contact angle of 0

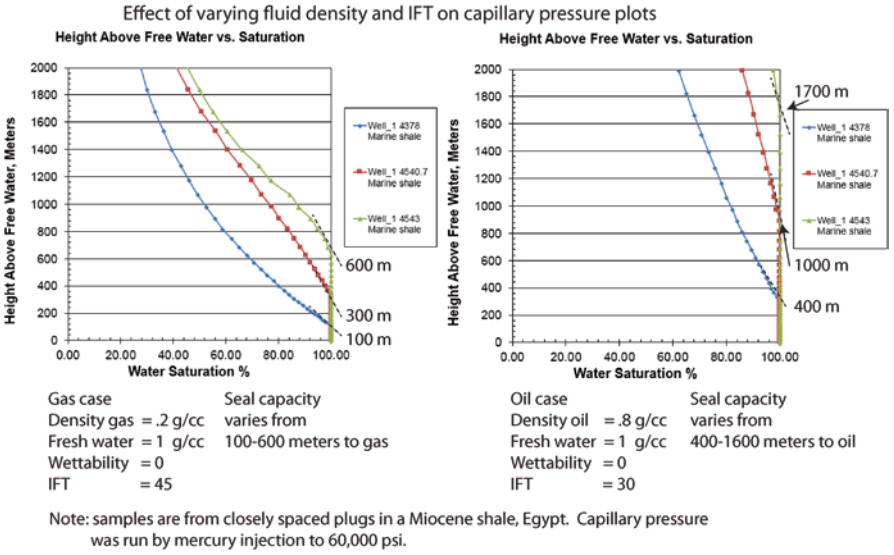

Fig. 5.7 Changing density and IFT on shale seal samples, Egypt

The samples in Fig. 5.7 are from a Miocene shale in Egypt that provides the topseal to the Temsah Field, discussed earlier in Chap. 4. The mercury injection pressure was run to 60,000 psi. In the gas case (left), seal capacity varies from 100 to 600 m. In the oil case (right), the seal capacity jumps to 400–1700 m, driven primarily by the density differences. Note also that the samples were very close to one another in the core (within inches), but have a widely variant seal capacity for each plug. I am always struck by how some workers will run a plot like this on a shale and proclaim that is the

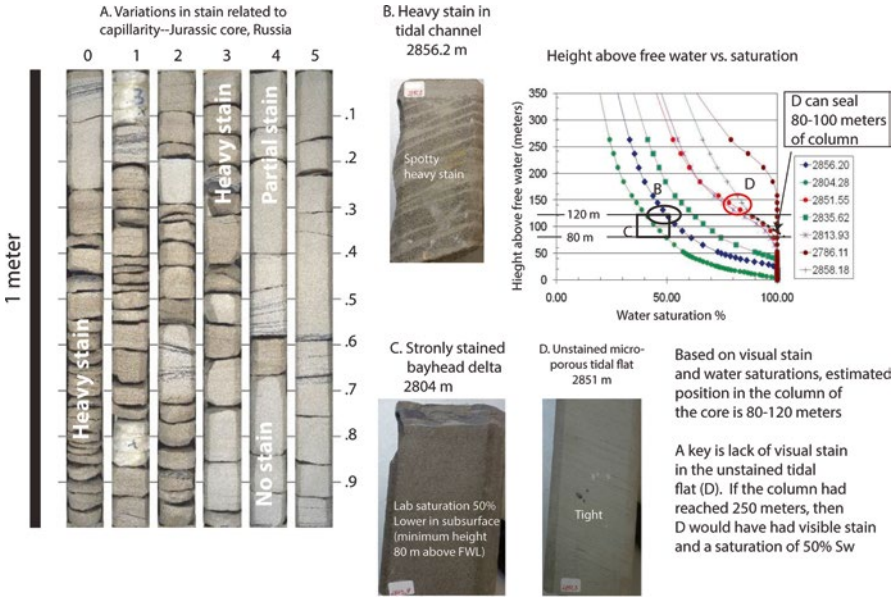

Fig. 5.8 Example of estimating height above free water for a core in Russia

regional seal capacity. IFT values can be much higher in gas than oil, causing some shale seals to be underestimated (Tim Schowalter, personal communication).

In reality, because pore geometries vary rapidly both laterally vertically, it is best to build up a database with ranges of values and use those to input into trap and migration maps. In addition, the best way to calibrate capacity is to actually look at the column heights proven on four-way closures that are filled to spill. That at least provides a set of minimum numbers.

5.1.4 Estimating Height Above Free Water from Capillary Pressure Data

One of the great utilities capillary pressure data is the ability back out the approximate position any sample is within a trap relative to the free water level.

Figure 5.8 shows a core from Russia in Jurassic estuarine facies in an area with regionally low structural dip and oil shows and tests which did not conform to structure (Dolson et al. 2014), indicating significant stratigraphic trap potential. This well tested five BOPD and no water, with pressure data showing the overall interval was low porosity and permeability. The structure map indicated the well was drilled on the edge of a 15 m closure, near spill point. Such subtle structures are problematic in that even slight seismic velocity changes can cause the closures to disappear in depth. Aside from that, however, the capillary pressure data showed that there would be no oil saturation in this well at 15 m above free water, except, perhaps slight stain in the most porous rock (green on the saturation-height plot).

Further examination of the core showed rapid variation in stain, with many facies completely un-stained, indicating micro-pore-throats. Plugs for capillary pressure were taken in a variety of facies and saturation levels, from the best saturation to the worst (unstained rock). The core was not captured to preserve original water saturations (such as using a native-state core process) core, so the reported saturations in the core from measurement would be residual at best and not as low as they would be in the subsurface. Sample B, for example, had an Sw from core of 50 %, which, using the plot above, would yield a hydrocarbon column at that point of 80 m. If the saturations were as low as 40 % in the subsurface, the column height would increase to 120 m. Thus, the position in the trap can reasonably be assumed to vary from 80 to 120 m.

With the right kind of core and analysis, with accurate, uninvaded SW measurement on the sample, the solution becomes more accurate. In this case, however, comparison of visual stain and saturations alone indicated that the unstained samples (D) cannot be more than 120 m above free water, as they might start to show some saturation. The best analysis from all data confirmed a likely minimum column at the well of 80 m, with potential upside to 120 m. That information proved the well was not in a structural trap, but part of a much larger stratigraphic trap, one exceed a physical area of over 800 km^2. Paleogeographic maps readjusted to explain regional seals that would match the downdip limit of the deepest oil shows and provide the 80–120 m of column in this well, along with 3D seismic of reservoir facies, showed the potential for a giant accumulation (Dolson et al. 2014).

5.1.5 Relative Permeability, Water Cut and Oil-Water Contacts

When interpreting well test information, it is important to be able to understand the relationships between rock type, saturation, position in a column and water cut. This requires additional information (Fig. 5.9).

Take for instance, the examples shown in Vavra et al. 1992 for various rock types and the saturation-height profiles. As discussed earlier, seal capacity and the position of oil-water contacts is highly variable with facies and pore throat distribution. Rocks, A and C, for instance, are very forgiving reservoirs, with the oil-water contact located at or near the free water level. However, D and E will act as seals in this example, and may even be tight limestones or sandstones not normally thought of as conventional seals. But what will they test? Will the 50 % water saturations shown in B and D flow oil or water, or both?

Unravelling this takes an understanding of relative permeability.

Figure 5.10 is a typical relative permeability curve for a fairly good quality reservoir (Schowalter and Hess 1982). In a two phase water-hydrocarbon pore network, permeability is not constant, but changes with the saturation, and thus, by rock type and position in the trap. Shown on the diagram are critical Sw cutoffs. At 20 % Sw, this rock will flow 100 % oil and at 80 % Sw it will flow 100 % water. From 20–80 % Sw, it will test oil and water, with increasing water cut occurring in the higher saturations. Trap evaluation becomes particularly difficult if a well happens to drill into this trap, with this kind of relative permeability and end up with 80 % Sw. The interpreter is likely to call this an oil-water contact and when the zone is

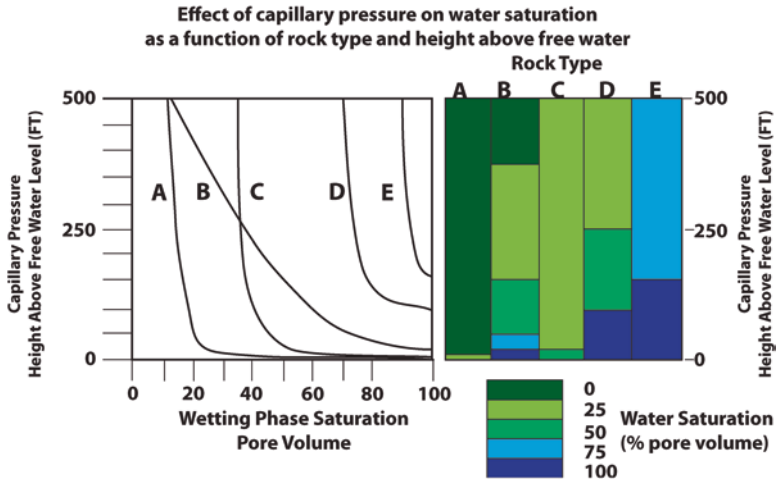

Fig. 5.9 Saturation changes with rock type. Modified from Vavra et al. (1992). Note that oil-water contacts, within the same trap, can vary considerably due to capillarity alone. Reprinted by permission of the AAPG, whose further permission is required for further use

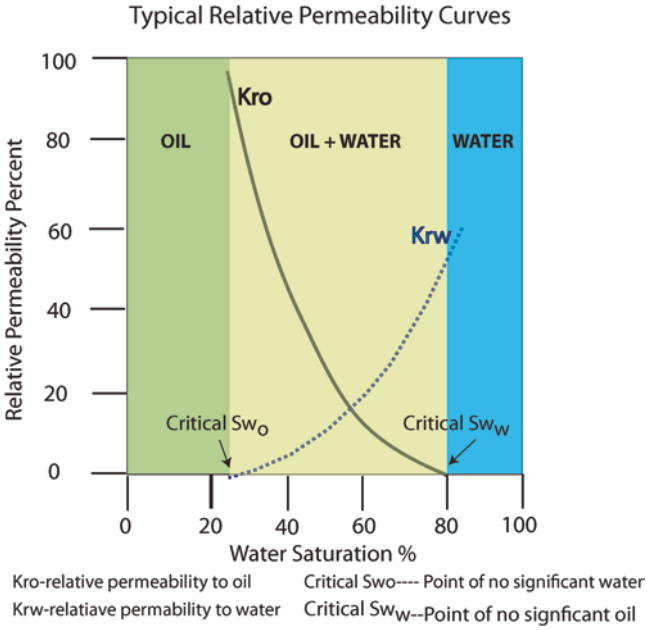

Fig. 5.10 Relative permeability curve. A critical Sw_o of 25 % indicates the saturation below which water will be tested along with oil. At 80 % Sw, a critical Sw_w is reached, at which point the well will test only water. Note that at 80 % Sw, there is still 20 % of the formation saturated with oil, but none will be tested. This is one of the things that makes determination of a residual vs. continuous phase accumulation difficult low on a transition zone. Complicating matters, different rock types in the same trap have different relative permeability curves. Modified from Schowalter and Hess (1982)

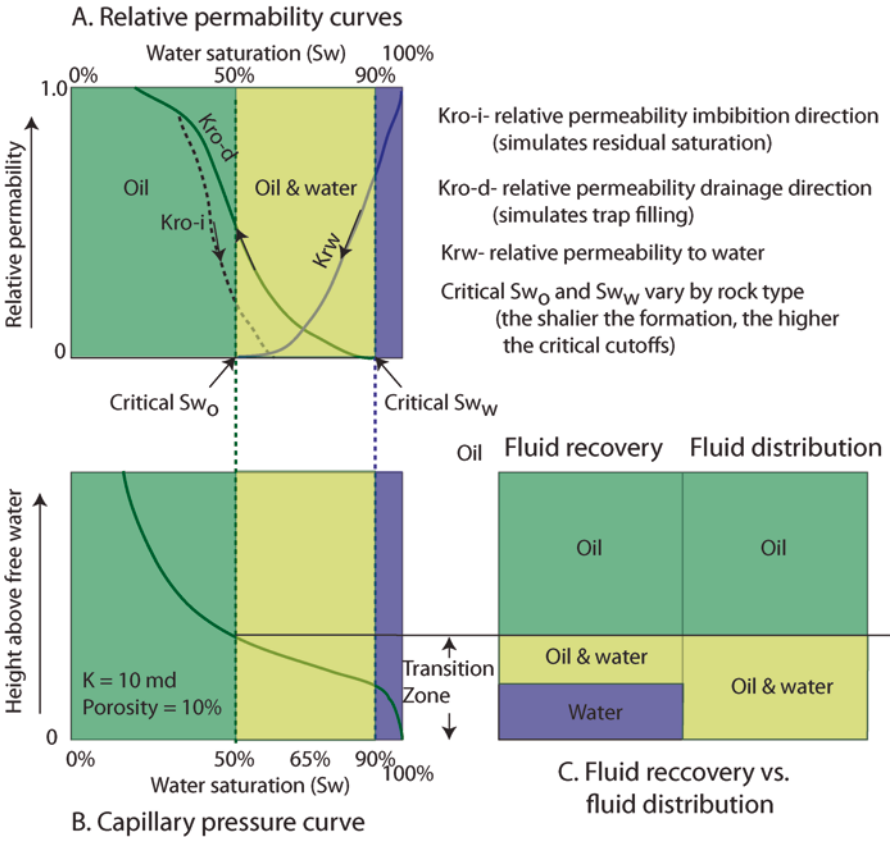

Fig. 5.11 Relative permeability and oil production vs oil presence. Modified from Hartmann and Beaumont (1999). Reprinted by permission of the AAPG, whose further permission is required for further use

tested, it may flow very high rates of oil with no water thus 'proving' in the mind of some, that the trap has failed. In fact, an 80 % Sw means that 20 % oil is in the trap, and an offset should potentially be drilled somewhere else.

As covered in Chaps. 2 and 3, the point where a well begins to test significant water is called the top of the transition zone. The transition zone extends all the way down to the free water level, but may actually test all water near the base of the trap. Transition zone saturations also vary by rock type, with more clay-rich reservoirs having higher Sw cutoffs than highly permeable rocks.

The impact of relative permeability of test results vs. saturation is best shown graphically as in Fig. 5.11 (from Hartmann and Beaumont 1999). Two types of relative permeability curves are shown: (1) drainage direction (2) imbibition direction. This is covered in the next section, but suffice it to say that in this example, the critical Sw_o is at 50 % and the critical Sw_w at 90 %. These critical saturations mark the point where water begins to flow with oil (Sw_o) and where the formation can no longer flow any oil at all (Sw_w).

Table 5.2 Critical Sw_o volumes for different pore types. Modified from Hartmann and Beaumont (1999)

Pore type	Micro	Meso	Macro
Critical Sw_o	60–80 %	20–60 %	<20 %
Length of transition zone	>30 m	2–30 m	0–2 m

In many cases, the 90 % Sw line or any point with high water cut and no oil may be mistaken for the free-water level or picked as an oil-water contact, which it is not. High rates of water production with minor oil flows often mean a well is located far down the trap in the lower part of the transition zone. Conversely, low rates of oil with little water, if in very tight reservoirs, may indicate the presence of a substantial column with the well potentially in a waste zone.

Critical cutoffs vary by rock type as explained in much more depth in Hartmann and Beaumont (1999), but are summarized as potential 'rules of thumb' when working with variable rock types (Table 5.2). Unfortunately, as in the case of IFT and wettability data, relative permeability for various facies may not be known and thus the critical saturations only estimated or observed from offset wells.

For example, in the Barmer Basin of India (Dolson et al. 2015), reservoir facies are quite variable, from porcellanitic shales, silty non-marine channels, low permeability debris flows and super-perm fluvial sandstones. Critical Sw in these facies for water-free oil are as low as 20 % for the fluvial reservoirs and as high as 70 % for the silty channels.

5.1.6 Imbibition Curves and Residual Saturations

When mercury is injected in a core plug and fills, the curve it follows is termed the drainage direction (Fig. 5.12). After the sample reaches irreducible saturations, the pressure is released and the mercury drains out. This direction is called the imbibition direction. The same kind of analysis is also done on relative permeability curves.

Having a knowledge of the imbibition curve can be very useful in exploration, as the final saturation is the residual saturation. Saturations higher than the residual saturation are not producible as the oil filaments in the pores are no longer connected to one another. This is critical to know in a field development as saturation changes with production, mimicking the imbibition curve.

At an exploration level, or in post-appraising dry holes, residuals are often overlooked or misinterpreted (O'Sullivan et al. 2010). In Fig. 5.12, for example, the residual saturations are as low as 40 %. One of the common causes of residual saturations in nature occurs when older hydrocarbon traps have their geometry changed with later structural movement, a regional change in stress type or uplift and erosion. In many cases, wells are drilled that have residual saturations of 40–50 % and then test all water, puzzling the interpreter, who initially might be inclined to evaluate those saturations as a discovery.

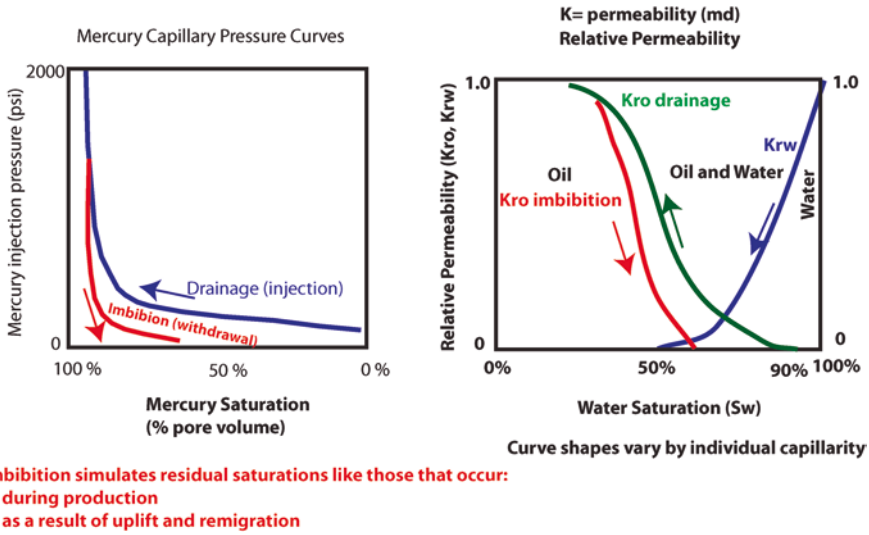

Fig. 5.12 Imbibition and drainage curves, relative permeability and simulating trap filling and later spilling. Modified from Hartmann and Beaumont (1999) and Vavra et al. (1992). Drainage directions simulate trap filling during migration. Imbibition curves simulate loss of hydrocarbons by re-migration by seal loss, uplift and tilting, or production with time. If residual saturations are low Sw, then they can be very difficult to distinguish from continuous phase saturations

Figure 5.13 illustrates the problem from (Shanley 2007 and Byrnes et al. 2009). A tight gas sand has had high pressure mercury injection done on a number of samples, yielding a typical pattern as shown, with residual Sw as low as 38 %. This example is from the Green River Basin in Rocky Mountains, an area which has undergone kilometers of uplift and erosion post-accumulation. Shanley and Cluff (2015) give a thorough treatment of burial history, expulsion and remigration resulting in pervasive residual saturations in this basin. Many tight gas sand wells in this and other basins have low water saturations, but flow water with no sign of hydrocarbons. These kinds of capillary pressure measurements strongly argue that residual saturations in tight rocks may be very difficult to distinguish from trapped, continuous phase gas accumulations.

5.1.7 Summary

Capillary pressure data provides a wealth of information on pore geometries, potential performance of wells as a function of rock type and position in a trap and can be used to estimate height above free water in the absence of pressure data. An understanding of relative permeability is essential to understand why a zone tests hydrocarbons or water, or a mix of both. High water saturations low on a trap that appear ‘wet’ may actually be above the free water level. So test rates alone should not be the sole criteria for identifying a free water level or trap size.

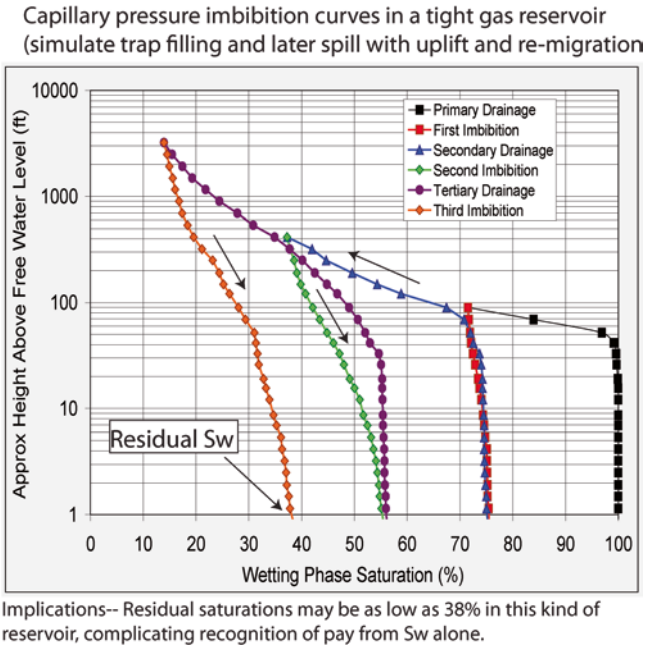

Fig. 5.13 Residual saturations in a tight gas sand. Modified from Byrnes et al. (2009). Note that residual saturations can be quite low, making interpretation of moveable hydrocarbons and pay very difficult

5.2 Flow Units, Winland Plots, Pseudo-capillary Pressure Curves and Mapping Seals

The reality of exploration is that you never have all the data you need. Many explorers don't bother to think of capillary pressure data as they may be cost constrained or not have access to cores or cuttings. However, there are a number of ways to estimate free water levels and rock quality in the absence of cores or cuttings, simply from porosity and permeability. A caveat on the techniques that follow in this chapter are that they apply well to rocks with intergranular and intercrystalline porosity systems that are more or less 'normal' pore throat distributions. Complicated dual porosity systems like disconnected vugular porosity in carbonates, will have very different pore throat distributions and must be treated separately. Also, the techniques discussed in this chapter become increasingly unreliable the lower the porosity and permeability become.

In this book we cover three methods of estimating free water levels (Fig. 5.14).

The only really reliable method is the use of high quality pressure plots, which give a direct measurement. Capillary pressure data, if the IFT, wettability and subsurface densities and Sw are known from the best core data, can give another good

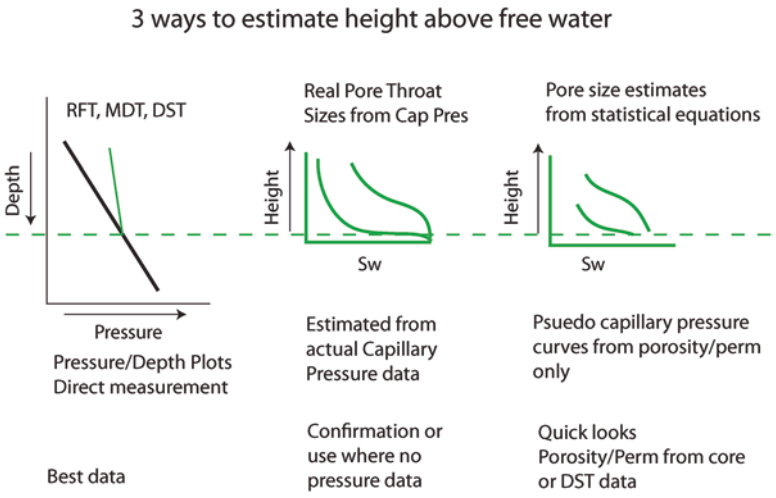

Fig. 5.14 Ways to estimate free water levels discussed in this book. Pressure vs. depth plots are by far the best methods, but capillary pressure and pseudo-capillary pressure data can also be used

answer. As shown, using capillary pressure data where the input variables are uncertain introduces error, but can provide a good approximation. A third technique is called pseudo-capillary pressure, and it uses mathematical estimates of pore throat radius from routine porosity and permeability data to derive a capillary pressure curve.

I have found pseudo-capillary pressure curves to be invaluable in exploration and development, as it can drive significant discussion on the meaning of saturation and oil shows. Often, for instance, DST or MDT pressure data can be used to derive a permeability number, with logs giving the porosity. If the MDT data does not define the free water level (a frequent occurrence as tests are taken high in a column or there is no water in the zone of interest), then the log porosity and test permeability can derive a pseudo-capillary pressure curve.

Before dealing with pseudo-capillary pressure, however, it is useful to understand flow units and facies controls on reservoir performance.

5.2.1 Flow Units and Winland Plots

The concept of flow units is illustrated in Fig. 5.15. Flow unit concepts are covered in more detail in Ebanks et al. (1992) and Gunter et al. (1997). They are important to understand when dealing with reservoir performance and seal prediction.

Facies exert perhaps the most fundamental control on pore throat distribution. However, diagenetic changes related to burial can significantly alter porosity and permeability. These changes introduce heterogeneity to the reservoir system. This

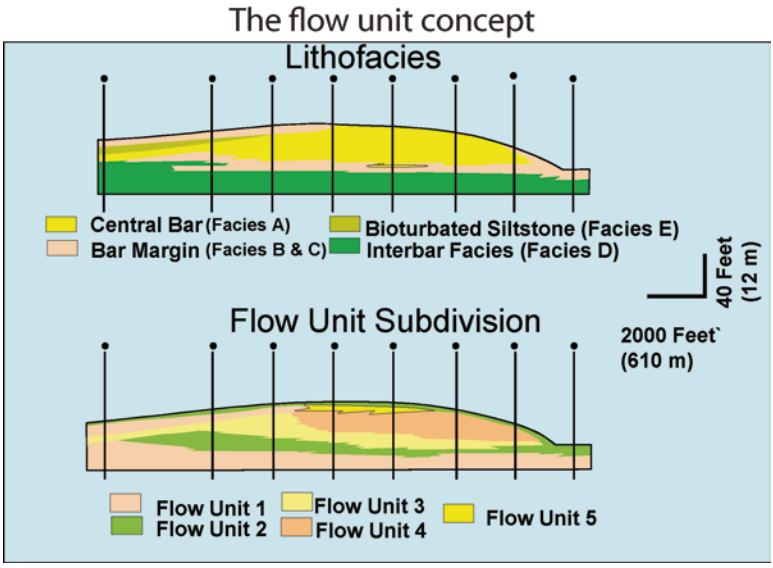

Fig. 5.15 Flow units vs. facies. Modified from Ebanks et al. (1992). While flow units generally follow facies lines, they may cross boundaries depending on variations in rock type and capillarity. Reprinted by permission of the AAPG, whose further permission is required for further use

heterogeneity in turn exerts a strong control on performance. Flow units are defined as mappable units of similar pore type. They can, however, cross-cut primary facies as shown in Fig. 5.15. Note in Fig. 5.16 there are four primary facies, but five defined flow units. Some characteristics of flow units are summaries by Ebanks et al. (1992):

1. Flow units are specific, mappable volumes of a reservoir, in either reservoir quality or non-reservoir quality rocks
2. Flow units are correlative and mappable between wells.
3. Flow units can be recognized on wireline logs.
4. Flow units may be in communication with other flow units.

While there are a number of ways to define flow units, one of the best screening tools is by use of cross-plots of porosity and permeability and comparing to theoretical pore throat aperture from equations developed by Winland (1972) and Pittman (1992) (Fig. 5.16). Winland's (1972) research showed that well performance had a good empirical relationship with the 35th percentile pore-throat radius (R_{35}). Appendices B and D shows the equations in Excel format.

In these equations, the pore throat radii measured are from those calculated with standard mercury injection capillary pressure curves. Hence, they are the reciprocal of Sw when converted to a height above free water plot. R10, for example, is at the 90 % Sw line, and represents an approximation of displacement pressure or seal capacity. R35, in contrast, is at the 65 % Sw and has been shown to empirically

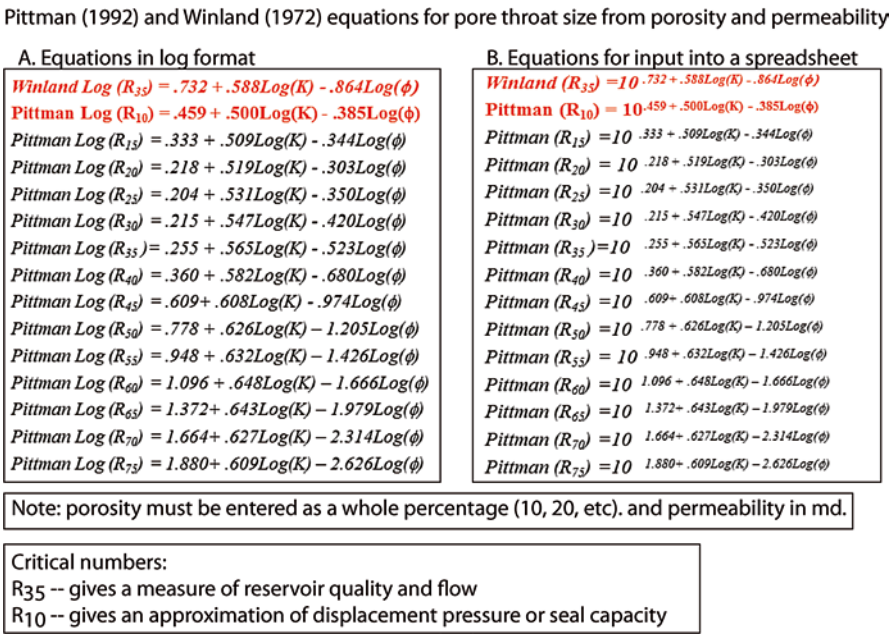

Fig. 5.16 Winland a Pittman pore throat size equations

correspond to reservoir performance, and thus flow units. An example of the utility of these plots in defining flow units is show on Fig. 5.17. The following discussion are from unpublished work I completed with Amoco Production company in 1993, a project that involved thousands of feet of core and hundreds of wireline logs and regional seismic.

Overlain on Fig. 5.17 are curves of equal R35 pore throat size calculated using Winland's equation (top of Fig. 5.16). Values falling below 0.5 μm are micro-porous, those between 0.5 and 2 μm meso-porous and anything above 2 μm mega-porous. Three major cluster of facies show up on the plot:

1. Algal boundstones which formed as reefal buildups
2. Lime mudstones in a supratidal settings
3. Dolomitic limestones also formed in a supratidal setting.

The plot has a number of important observations reinforcing the difference between pore throats and porosity and permeability.

1. The highest porosity rock is in the lime mudstone, reaching 27 % porosity, but seldom exceeds 10 md in permeability. It is only a meso-porous reservoir.
2. The dolomites, at 15 % porosity, are largely micro-porous, and act as seals.
3. The algal boundstones (the key reservoir), at 15 % porosity can have permeabilities up to 800 md. These reservoirs are also effective reservoirs at 6 % porosity, and are macro-porous.

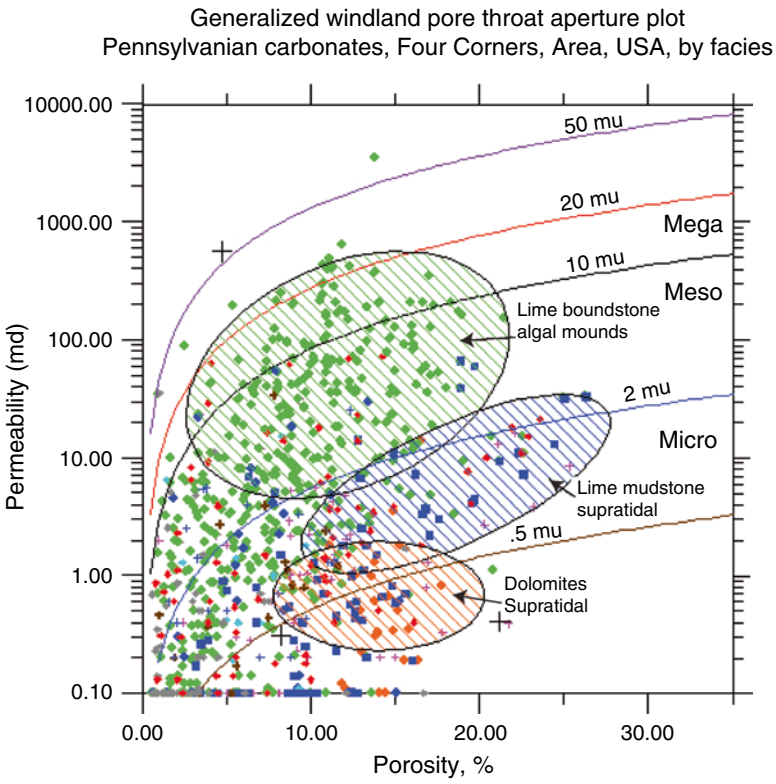

Fig. 5.17 Winland plot, Pennsylvanian carbonate, 4-corners area

A problem is now apparent. On logs, without a knowledge of the pore throat distributions, an explorer might view the 25 % lime mudstones as the best target. Worse yet, a cutoff of 10 % porosity for effective porosity might be applied, which will eliminate a substantial number of algal boundstones as effective targets for exploration or development. In addition, 15 % porosity dolomites might be targeted as attractive when, in fact, they are seals.

Log profiles with the porosity, permeability and R35 pore throat radius posted are a first step in recognizing and correlating flow units (Fig. 5.18).

Figure 5.18 shows clearly that the micro-porous zones, while high porosity, have no deliverability and act as seals and baffles.

Another way to view the Winland plot from the standpoint of flow units is shown in Fig. 5.19.

Essentially, the algal boundstones can be broken into two major flow units by port size as one population has mega pores and the other macro pores. The lime mudstones generally follow one meso-porous profile. Likewise, for the most part, the dolomites are behaving as microporous seals. This is a typical way to view a

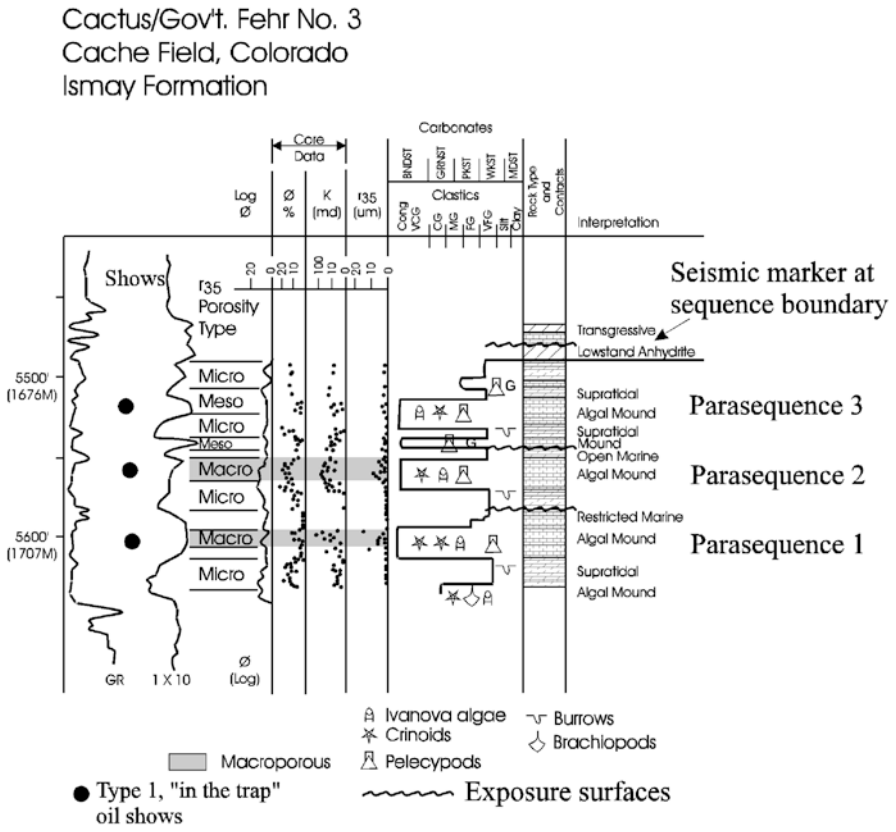

Fig. 5.18 Flow units marked on a log. Porosity is not a good indicator of permeability and pore throat type in these carbonates. Some of the best porosity is in micro-porous dolomites, which have no effective permeability and act as seals. From Dolson et al. (1999). Reprinted by permission of the AAPG, whose further permission is required for further use

Winland plot and to look at flow unit distribution. In this case, three major facies, and four flow units.

Maps of DST or test recoveries can readily point out variations in pore type. The map in Fig. 5.20 is from a 1991 database of test recoveries in the Desert Creek Formation. Colors inside the symbols give relative percentages of oil, gas and mud recoveries. The tightest wells recover only mud and have very small symbols. The largest recoveries are almost completely coming from algal boundstone mega-pore throat reservoirs. Smaller recoveries are from the meso-porous limestones and the smallest recoveries are from supratidal dolomites and other tight facies. As will be shown later in an exploration example, this information can be used with facies maps to prospect for oil and gas. Good facies and flow unit maps will have a good correlation with oil and gas recoveries in wells.

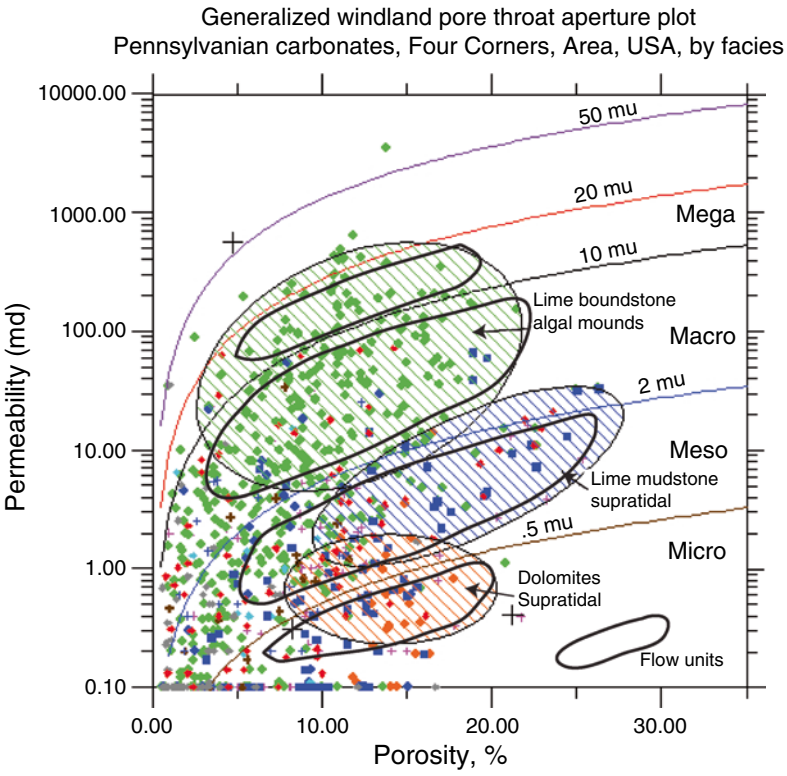

Fig. 5.19 Flow units on a Winland plot

5.2.2 Pseudo-capillary Pressure Curves

An even more effective way of analyzing these data from a show evaluation standpoint, however, is to have an idea of the saturation vs. height functions for each facies. Recall that the fundamental equation for capillary pressure (Eq. 5.2) requires a knowledge of the pore throat size (R) and the IFT and wettability. As discussed earlier, IFT and wettability can be estimated, and with the equations published by Pittman (1992), capillarity can also be estimated by calculating equivalent pore throat size from porosity and permeability. As in analyzing capillary pressure curves, this is best done with spreadsheets. Appendix D shows an example of how to build a pseudo cap pressure spreadsheet using Pittman's equations.

An example of this is shown in Fig. 5.21 using representative porosity and permeability values from Figs. 5.17 and 5.19.

Curious how accurate Pittman's equations were, I compared them with mercury injection data from the same core shown earlier in Fig. 5.8. The comparison were very similar, with discrepancies more in the tighter rock. Using Pittman's equations

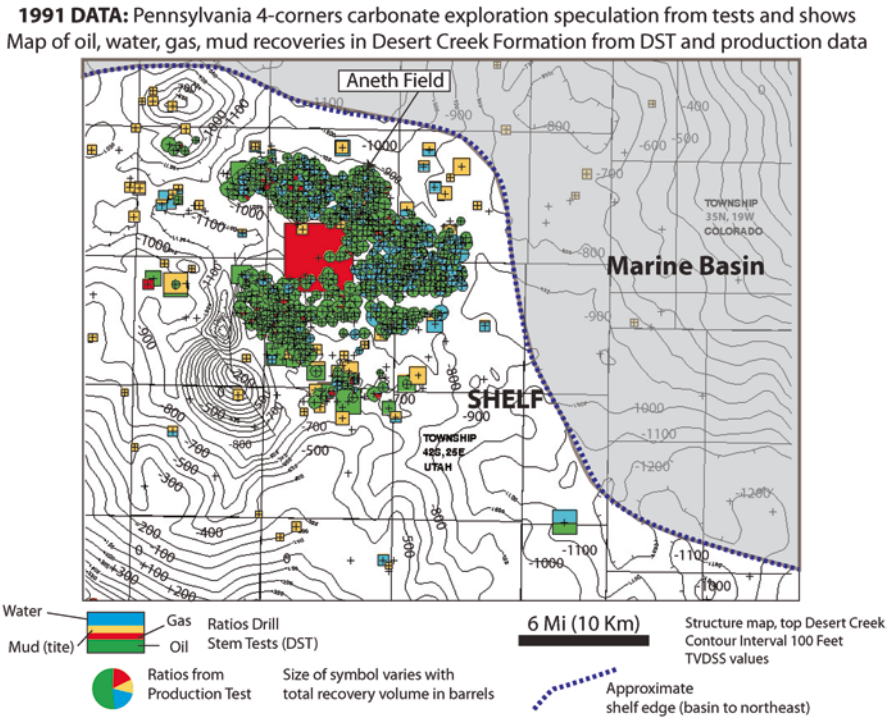

Fig. 5.20 Pore throat radius variations show up in test data. Symbol size varies by total flow on the test. Fluid ratio percentages are shown as oil, water and mud recoveries. Large symbols are macro-porous, smaller ones mesoporous. The smallest symbols, which all show tests of mud only, are microporosity seals. Initial prospecting screening can be done from these data alone without a great deal of knowledge of facies. Detailed work with cores, logs, seismic and facies can refine the prospects to a drillable location

alone, the apex of the height above free water curve is not calculated, and the R10 value is taken as displacement pressure of seal capacity. On a capillary pressure diagram, as discussed, a tangent to the line are breakthrough is taken to the y axis, yielding an accurate seal capacity (Jennings 1987). Still, the results are useful. Pittman's seal capacity on the tightest rock is 125 m and on the actual capillary pressure 150 m. Especially at an exploration scale, that is enough to begin to build maps and test migration and seal models.

A different set of equations, but which yield nearly identical results, were published by (Hawkins et al. 1993) and incorporated into a different pseudo-capillary spreadsheet (courtesy of Keith Shanley). The Hawkins method has the advantage of giving irreducible saturations and the apex curve (Fig. 5.22).

The analysis is for an oil water system, with IFT set at 30 and wettability 0. What is significant is the remarkable difference in capillarity than can now be looked at for reservoir performance and seals. This plot allows discussion of the prospectivity of small closures. A 100 m (328′) closure (big for much of this

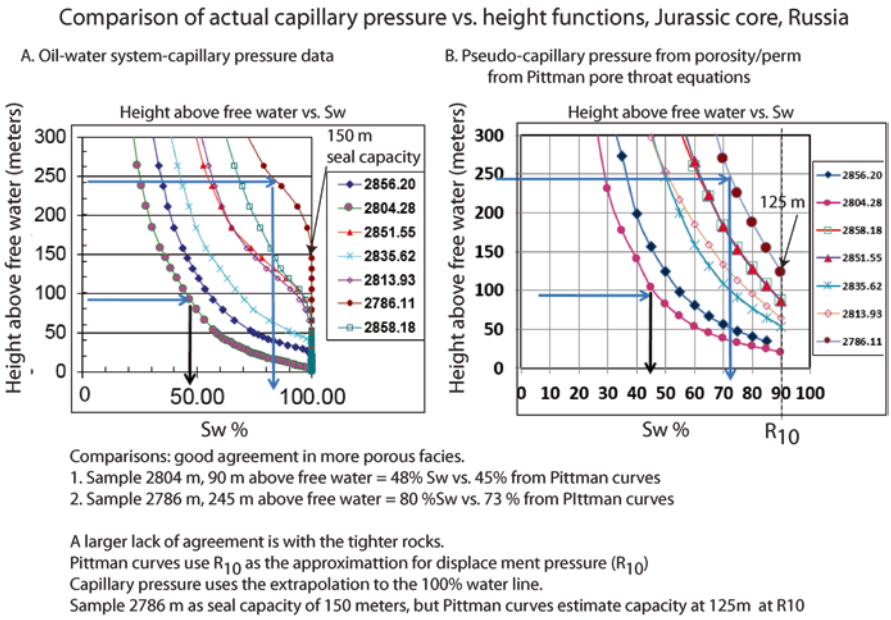

Fig. 5.21 Cap pressure comparisons using PIttman's equations. The values calculated for seal potential and height above free water from actual capillary pressure data (**a**) compare favorably with those calculated by using pore throat radii predicted from the Pittman (1992) equations

area), will be productive in an algal mound, but only reach 45 % SW at the crest of the trap in the supratidal limestones. The R35 port size identifies the supratidal limestones as a transition zone type of meso-porous reservoir, where water cut is likely to be very high and flow rates low. The supratidal dolomite facies will act as a substantial seal, up to 533 ft. (140 m). So the porous dolomites, if mapped and correlated to the test data shown earlier, can now be viewed as a sealing facies, something other interpreters may have completely missed. Small closures are difficult targets if in the wrong facies. Many traps in this area have closure under 25 m (95′) in size. In these cases, the meso-porous limestones act as seals and traps and will have no saturation at all.

As part of my 4-year tenure as Chief Geologist for TNK-BP in Russia, I had a chance to review some prospects in carbonates in the Orenburg area of the Pri-Caspian basin in southern Russia. The prospects being shown were very low relief with structural closures with as little as 10 m (30′). I asked the teams showing these prospects if they had a map of the reservoir facies distributions and flow units. The answer was 'no', followed by a comment that "if it has porosity and is on a trap, it produces. There is no risk". I challenged that assumption and one of my colleagues pulled production data from all the fields with small closures and found they had a 90 % or higher water cut and made very little oil. Without exception, the pore sizes were meso or microporous and thus the small closures mostly failed economically.

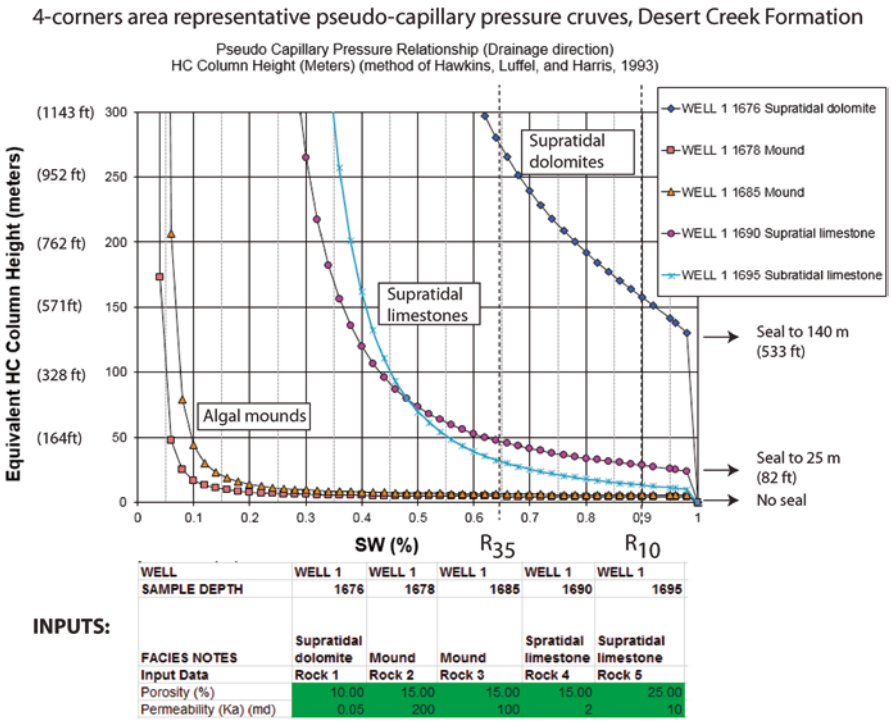

Fig. 5.22 Representative pseudo-capillary pressure curves from the general porosity-permeability relationships shown on Figs. 5.17 and 5.19

5.2.3 *Making a Seal Capacity Estimate When You Do Not Have a Pseudo-capillary Pressure Spreadsheet*

The key to seal capacity from porosity and permeability remains some way to estimate breakthrough displacement pressure. The Winland or Pittman equations can provide an approximation using the R10 values.

Step 1 is to calculate R_{10}, for example using Pittman's 1992 equations (enter porosity as whole percent, i.e., 15, not 0.15) using Eq. 5.12.

$$R_{10} = 10\text{^}\left(\left(0.459 + 0.5 * \mathrm{LOG}(K)\ \ 0.385 * \mathrm{LOG}(\mathrm{Porosity})\right)\right) \tag{5.12}$$

By example, a dolomite with a porosity of 15 % and permeability of 0.1 md will have an R_{10} of 0.32078 μm

Step 2 is to convert to height above free water for the seal capacity. Hartmann and Beaumont (1999) offer a simple equation, with final units in feet using Eq. 5.13:

$$H(\mathrm{ft}) = \left(0.670 * \mathrm{IFT}(\mathrm{Cos}\theta)\right) / \left(R * \left(\rho_w - \rho_h\right)\right) \tag{5.13}$$

Where IFT = Interfacial tension of hydrocarbon-water in dynes/cm
θ = Wettability
ρ_w = Density of water in g/cc
ρ_h = Density of hydrocarbon in g/cc
R = Pore throat radius at R_{10} from above

So if an oil has a wettability of 0 (water wet), and an IFT of 27 and Dw = 1.01 (brackish water) and Dh = 0.85 (oil), and R10 = 0.32078 mu, then H = 352′ ft

This same equation, by substituting other R values from Pittman (1992), yields a pseudo-capillary pressure curve (see Appendix D for spreadsheet construction and other equations).

5.2.3.1 Weyburn Field Example

Another example of micro-porosity seals is that of Weyburn Field (Canada), which is one of the fields first examined by Dale Winland in 1972 (Fig. 5.23).

The Weyburn Field is a giant carbonate stratigraphic trap. Initial exploration targeted the updip pinchout of porous Mississippian Midale Formation carbonate beneath an angular unconformity overlain by Mesozoic seals. An anhydrite caps the Midale Formation, forming a topseal and tight limestones underlie the dolomitic porosity layer, forming a bottom seal. Wells drilled in the position of wells 9, 10 and 11 were tight, and part of the waste zone. The real prize lay downdip of these tight wells. Recognition of the wells as tight was difficult, as they generally had 20–25 % porosity, similar to the downdip productive wells. Wells in the waste zone tested small amounts of oil and water, but at very low rates. Eventually, the downdip macro and mesoporous main field was discovered. Using a simple range of porosities and permeabilities shown in Fig. 5.23, a pseudo capillary pressure shows the sealing capacity of the microporous facies (Fig. 5.24).

Hartmann and Beaumont (1999) detail the petrophysics of this field and derive a column height seal capacity of 283 ft (86 m) meters, using an R_{10} pore diameter. The quick look with pseudo-capillarity reaches a similar range of values (75–100 m). The advantage of using a pseudo-capillary spreadsheet remains speed of interpretation and the ability to test different scenarios. At times, all you have available is published literature or very spotty core or test data. Although the values used in this analysis are different from the details provided by Hartmann and Beaumont (1999), they provide a similar answer. Dahlberg (1995) also suggests downdip hydrodynamic flow is responsible for part of the trap. But the column heights speculated from this analysis are in good agreement with columns shown as in Fig. 5.23 at 250–300 ft.

5.2.4 Migration with Seals: Examples from Aneth Field Area, Utah-Colorado

The quickest way to evaluate a trend and generate a lot of prospects is to generate seal maps and then test migration models using seals to predict traps. Mississippian age carbonates of the four-corners area of Colorado and Utah offer an excellent test

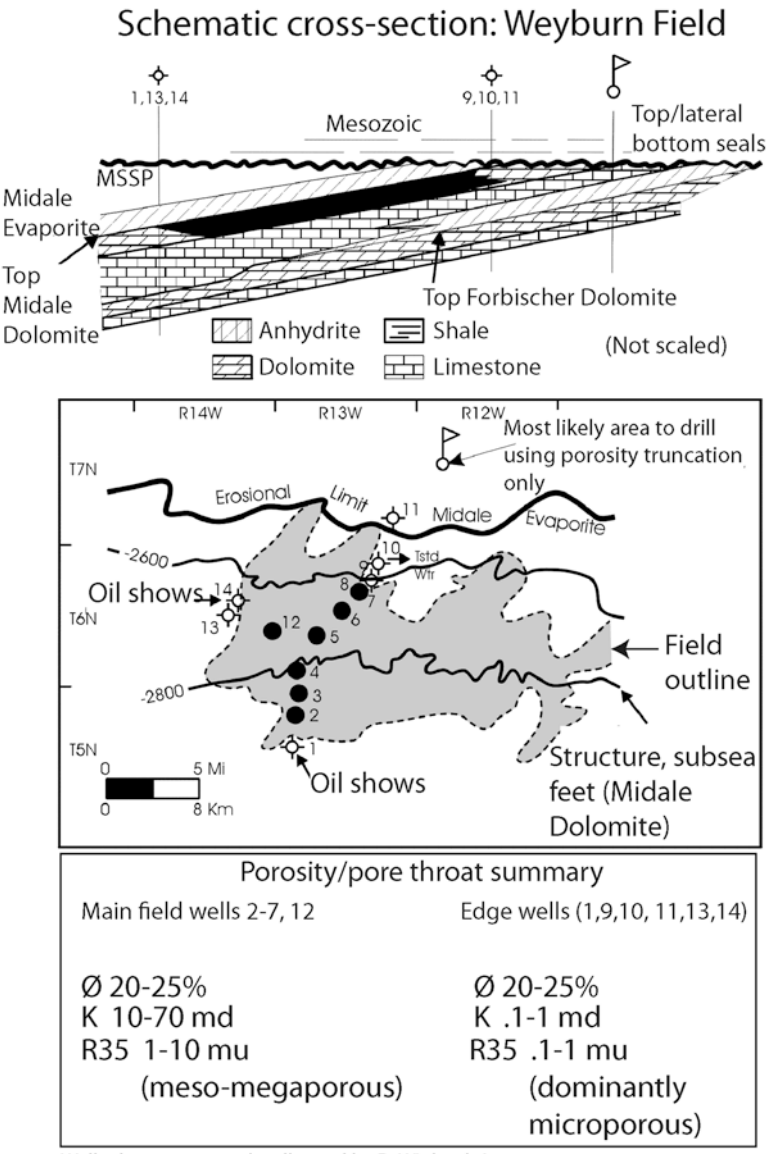

Fig. 5.23 Weyburn Field pore throat trap. Depth is in feet TVDSS. From Dolson et al. (1999), but original figures from Dolson (1999-RMAG core workshop) and unpublished work by Dale Winland, Amoco (1972). Reprinted by the permission of AAPG whose further permission is required for further use

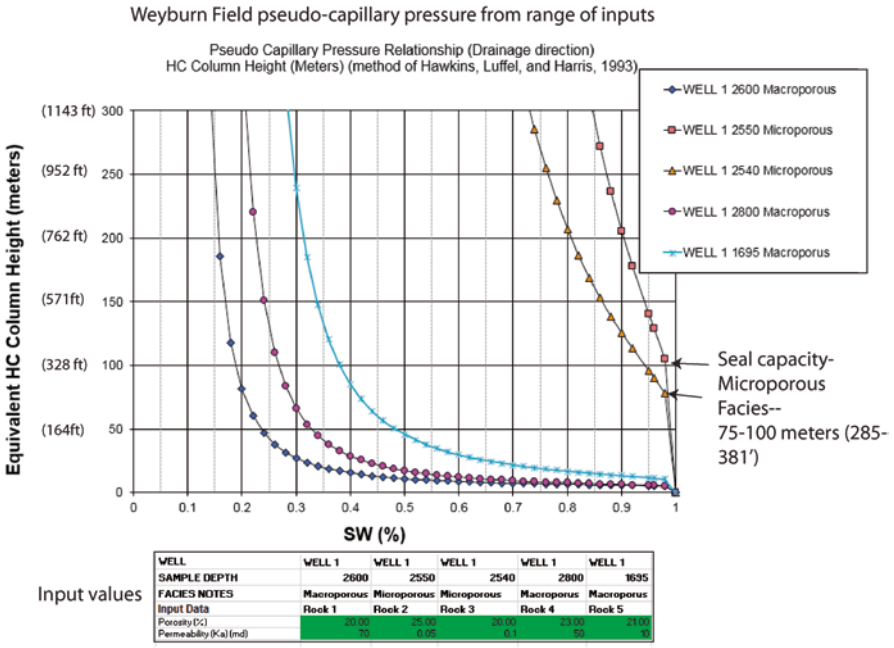

Fig. 5.24 Seal capacity on the microporous facies from pseudo-capillary pressure, Weyburn field, using average values shown in Fig. 5.23

case. My personal experience in this area is dated, going back to 1991–1992, in a comprehensive exploration study for Amoco we completed with about 10,000 ft of core and cuttings sampling, and facies maps (long disappeared within the company) at multiple levels. Of all that data, the only pieces that remain in my repository are an old map of the DST and test data for the main formation (Desert Creek Formation) and the Winland plot discussed earlier.

That is enough, however, to evaluate this trend. Much more detail on the facies, high resolution sequence stratigraphy and regional trends is available in several publications (Coalson and DuChene 2009; Eby et al. 2003; Grammer et al. 1996; McClure et al. 2003; Peterson 1992; Chidsey and Eby 2009; Trudgill and Arbuckle 2009; Wold 1978), and much of that has been used to derive things like the shelf edge line shown on Fig. 5.25. Much earlier in my career, I would have hesitated to take that one map of DST data and sit down and immediately prospect from it. I would have searched out all the cores, logs, seismic and pulled a comprehensive report together, something that would have consumed a minimum of 3 months and perhaps up to a year.

Prospect generation using these concepts can be surprisingly simple, however. The task is to generate a lot of ideas early and then try to disprove them with more data. One of the expressions I like best about exploration is to 'explore like a crooked politician who implores voters to vote often and early'. This often means using whatever show and test data is available, and then diving into more detail later to try

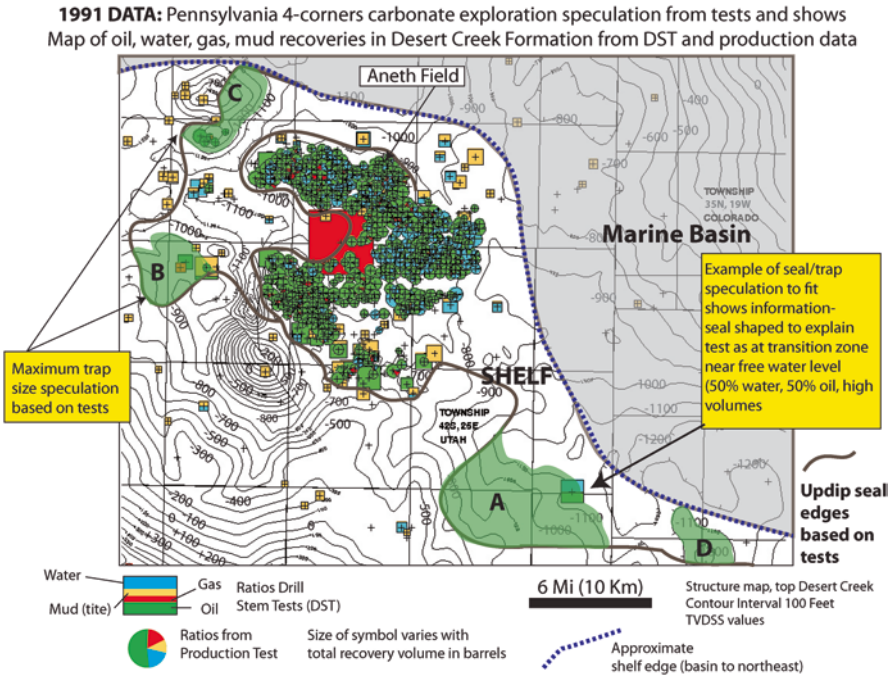

Fig. 5.25 Seals based on test data, Cache Field area, Utah-Colorado. The traps are speculation based on test results. Seal geometries have been drawn to simulate the maximum possible trap size. Further work would be need to refine prospects

to confirm or deny the prospectivity. Recognizing a philosophy advocated in Chap. 1, that 'the map is wrong, it is always wrong, the question is how wrong is it?', the challenge is to go ahead and make a map that may very well be wrong in detail, but sets up leads to test later with more data.

Take Fig. 5.25, for example. Without knowing anything about facies except that the carbonate buildups in the Desert Creek are generally SW of the shelf edge line (blue dashes), there are enough wells testing oil to show approximately where seals must be to set up the trap. The map shows recoveries from drill stem tests of mud, water, oil and gas. Symbol size varies by recovery volume, so large symbols had high flow rates. Small brown squares are really low recoveries of mud, indicating good seals. Smaller volumes of mixed oil, water or mud are from more meso-porous rocks and the big symbols from macro-porous rocks.

There are at least two trends of seals present based on the test data. The speculative seal edges have been placed on the structure map in a way that shows potential leads and spill points or seals that could explain the oil shows from the tests. Note that structural spill points at the base of the prospect areas are drawn to fit the test data where possible and a speculation on the potential largest trap possible. Maps like this can be generated quickly, without have to speculate on all the details necessary to confirm the prospects.

For example, Lead A in Fig. 5.25 capitalizes on a well test that had very high recoveries of water with oil. The high recoveries suggest permeable macro-porous rock low on a column near the oil-water contact or free water level. The seal edge could have been drawn differently, but the spill point of the trap, as speculated upon, passes through the well with the high water and oil cut. How big that trap might be depends on accurate mapping (something to do later) of the seal and reservoir geometries, using core, logs, seismic and pressures. But for now, it is sufficient to high-grade an area of significant prospectivity. At least one seal has to be present updip of the giant Aneth Field and the DST data shows that wells updip of this field are likely meso-porous, and from the pseudo-capillary pressure data shown in Fig. 5.22 could seal 85–100 ft. of column, but also require substantial closure to be productive. A second seal has to exist west of leads B and C, where production has been established down the flank of some structural closures. The test data west of this seal line tests mud with only very small recoveries of any volume at all. It is likely a microporous seal. Prospect D is a simple undrilled four-way (if the map is right) on trend with potential macro-porous rocks.

The play concepts here can readily be tested using migration and seal maps in software like Trinity, although recognizing and drawing the trap geometry requires nothing but some creativity. Note that there is a large faulted anticline SE of lead B, but it has drilled a micro-porous facies and not found to be productive. That does not mean it is not a trap! What that structure is missing, in all probability, is simply a good reservoir.

The first step is to scan and georeference any old maps and then digitize and grid a structure map (Fig. 5.26). The map is in TVDSS values (feet), and the gridding was done in ARCGIS (a geographic information software mapping package). Many petroleum systems software packages work with TVDSS positive values (flipping the grid by −1), and that effectively changes the equations used in Hubbert's U-V-Z technique by simply adding a seal capacity map to the TVDSS positive structure to get the Uo or Ug map required to look for traps. If working with negative subsea grids (a more standard approach in many workstations), then the U-V-Z migration models require the seal map to subtract the TVDSS map (more later in a summary). Note that the structural dip rate is generally very low, something that facilitates stratigraphic entrapment, as subtle seals can set up traps over large areas.

The second step is to use the porosity and permeability as a guide to displacement pressure and thus seal capacity, as shown earlier in Fig. 5.24. For this step, I decided to use the same values as those shown in Fig. 5.24, both for oil-water systems with the same IFT and wettability, but using the Pittman R10 approximation as seal capacity. The results (Fig. 5.27) is nearly identical to that shown in Fig. 5.24. Seal capacity in meters or feet can now be put into a map view and tested with migration.

The third step is to create a seal map. This can take months of work to get right in detail, using seismic facies, core, logs, pressures, etc., but it doesn't hurt to speculate early and often.

Using the ideas and seal values from Figs. 5.25 and 5.27, an estimate of seal capacity is made from each pore type shown on the map. A huge advantage of using

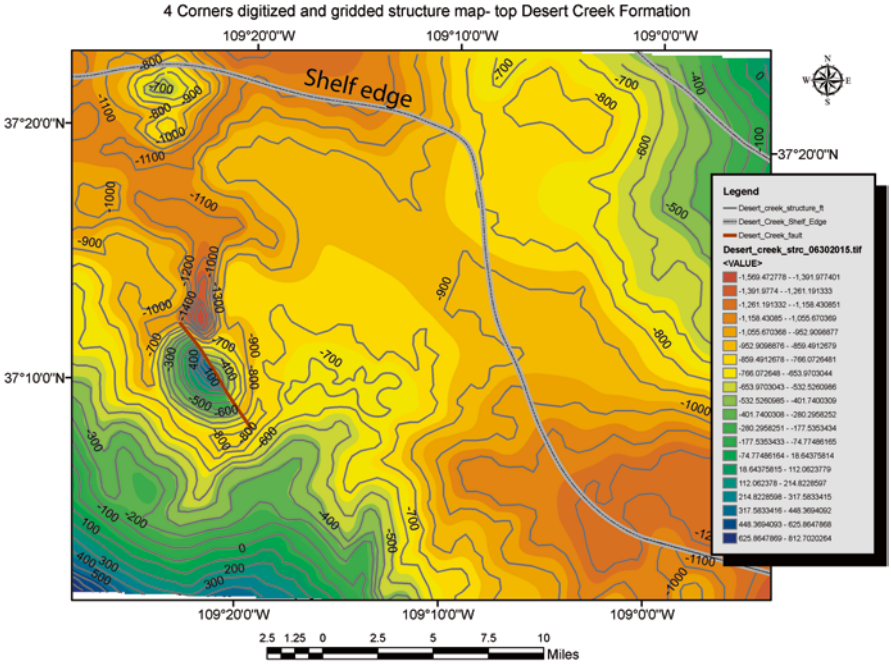

Fig. 5.26 Structure contour grid created by digitizing in ARCGIS (a Geographic Information Systems software package), the structural contours on the georeferenced image from Fig. 5.25

petroleum systems software like Trinity, are built-in tools for changing and modifying grids quickly, so as to test alternative models against real data. In this example, a seal map consisting of polygons was created in ARCGIS software and values entered in a shapefile (the polygon) table of possible ranges of seal capacity from pseudo-capillary pressure runs (see Appendix E for tips on using ARCGIS to do this). The values posted from the analysis are shown in Fig. 5.28. In the basinal facies east of the shelf edge, the Trinity migration models have been set up to have a low seal capacity, allowing the software to readily migrate oil from the basinal source rocks into the carrier beds to the west of the shelf edge.

Modeling migration with the seal map can be done with pure grid manipulation independent of any built-in software algorithms that come with tools petroleum software tools like Trinity, Petromod, and BasinMod of other packages. The workflow on how to do that is summarized in Fig. 5.29. Migration with seal maps are the only way to predict fault or stratigraphic entrapment on a migration route. Otherwise, the software packages simply show flow lies that will show structural shape and closures only. This can also simply be done by looking at seal geometries on your map with a structural overlay and finding closures by hand. It is quick and probably

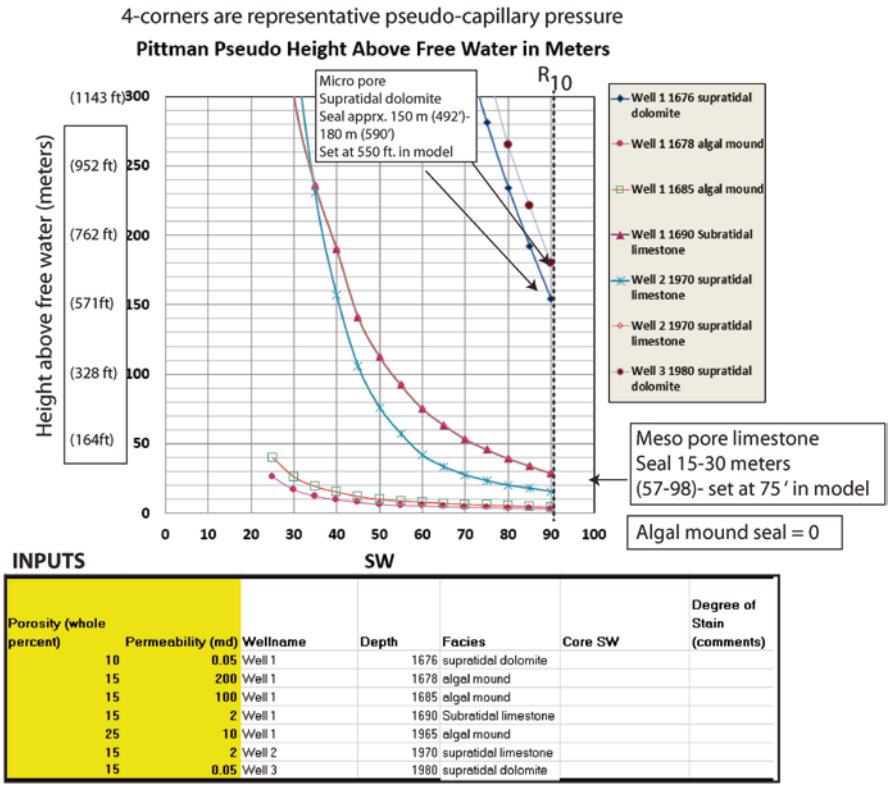

INPUTS SW

Porosity (whole percent)	Permeability (md)	Wellname	Depth	Facies	Core SW	Degree of Stain (comments)
10	0.05	Well 1	1676	supratidal dolomite		
15	200	Well 1	1678	algal mound		
15	100	Well 1	1685	algal mound		
15	2	Well 1	1690	Subratidal limestone		
25	10	Well 1	1965	algal mound		
15	2	Well 2	1970	supratidal limestone		
15	0.05	Well 3	1980	supratidal dolomite		

Fig. 5.27 Seal capacity estimate by facies using a pseudo-capillary pressure spreadsheet for an oil-water system using Pittman equations for pore throat radius from porosity and permeability. The results are nearly identical to those obtained by using the method and equations shown in Fig. 5.24

the most common way people map out fault and facies seal prospects. The digital approach, however, is much quicker and often finds more leads.

The step shown in Fig. 5.29 simulates the U-V-Z approach by subtracting the TVDSS map from the seal map and then running migration on that pseudo-structure map, which now incorporates the seal capacity. Resulting closures (Fig. 5.28d) are potential traps. Note that the input structural grid with this example is in TVDSS, and thus has negative values for this area. As in the cases shown for hydrodynamic entrapment in Chap. 5, most of the petroleum systems software packages invert the TVDSS maps to positive values. In these cases, the seal map is added to the structure map. The results are the same, but be aware of the input elevation type.

When running these kinds of maps in Trinity and other petroleum systems modeling packages, however, there is an added advantage (beyond speed and simplicity) in that top seals can also be set on the carrier beds. The U-V-Z approach does not simulate top seals, so some of the controls on entrapment are lost or underestimated.

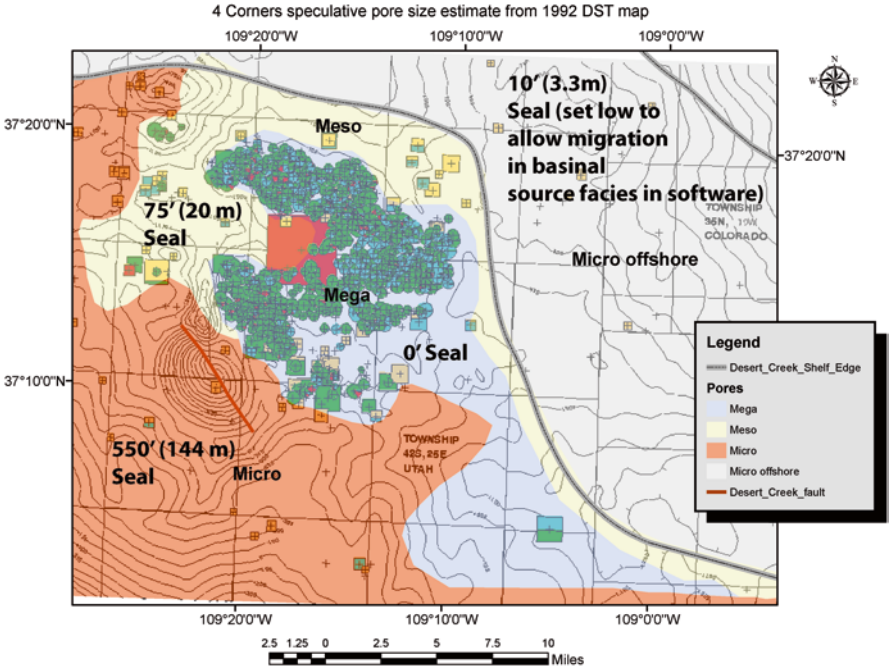

Fig. 5.28 Seal map from relative sizes of the test recoveries and pseudo-capillary pressure analysis from Fig. 5.27 and seal geometry speculated upon in Fig. 5.25

So what do the maps look like and does all the drilling done since 1991 confirm or reject the models shown? Figure 5.30 gives an answer using Trinity migration, with top seals set at 700 ft. (213 m) in an oil-water system. The results are very similar and most of the future oil was found with this simple approach.

The entrapment map, using only these kinds of quick looks, has found well over 80 % of the proven oil fields. Unfortunately, there is no information readily available from the Utah Geological survey as to which zones these wells are productive from (Ismay, Desert Creek or other), but in general, the trends west of the shelf edge on published maps are dominantly a Desert Creek fairway (Eby et al. 2003; McClure et al. 2003; Chidsey and Eby 2009). In detail, things are more complex, as large numbers of dry holes also exist within some of the predicted traps, indicating compartmentalization and multiple seals. Prospect A, for instance, is not as large as speculated, but there is a small field at the key dry hole used to build the seal map, as well as other oil pools to the west. In the end, buying the acreage on this map, long before the other wells were drilled, would have resulted in someone earning a substantial amount of money. The Trinity model, again, uses a top seal limitation of 700 ft. to oil, so the large anticline west of Aneth Field is not filled to spill.

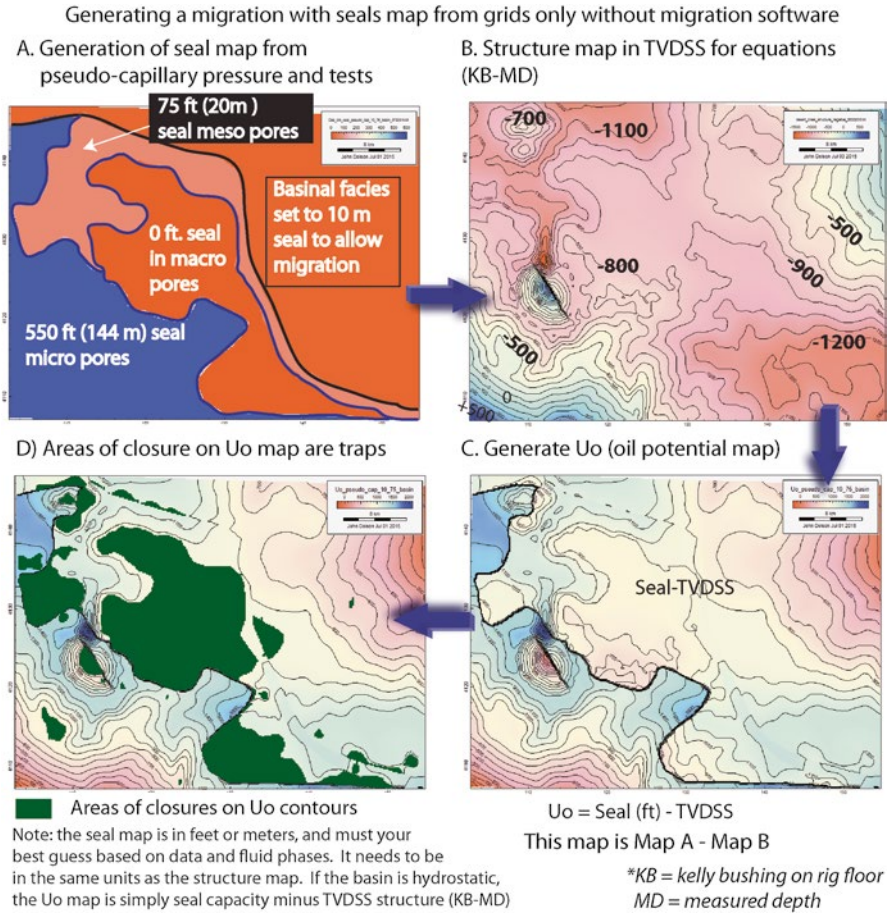

Fig. 5.29 Workflow for migration modeling if only using standard grid manipulation software. This method requires making a seal map in feet or meters based on geometries required to explain oil and gas shows and inputs from pseudo-capillary pressure analysis of seal capacity. This can be done with any software that can deal with grid manipulation. Results will be very similar to those obtained with more expensive petroleum systems tools. Petroleum systems software, however, will allow quicker iterations of various models and better simulation of migration pathways and volumetrics generated, trapped and lost during the evolution of the basin

How good were the results from making the U-V-Z map construction using just grid manipulation without the Trinity software? The results are nearly identical (Fig. 5.31), with the only real difference the large structure southwest of Aneth Field, which has a higher column shown than was established in the Trinity model. This difference is caused by the way Trinity not only handles top seals, but how it models the free water level. Trinity places a free water level from the top of the carrier bed and the U-V-Z method, which uses a deeper structure map due to the

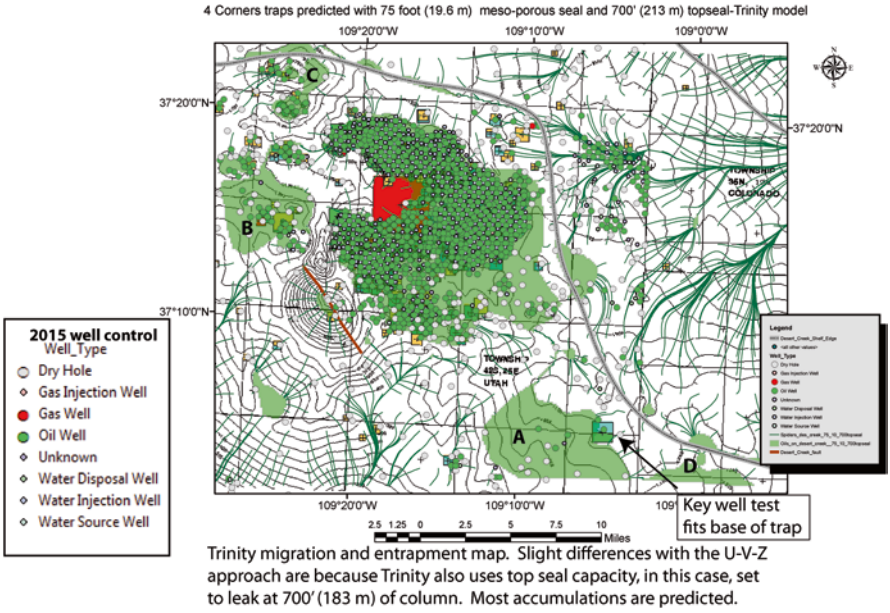

Fig. 5.30 2015 well control overlain on predicted traps map, Desert Creek Formation

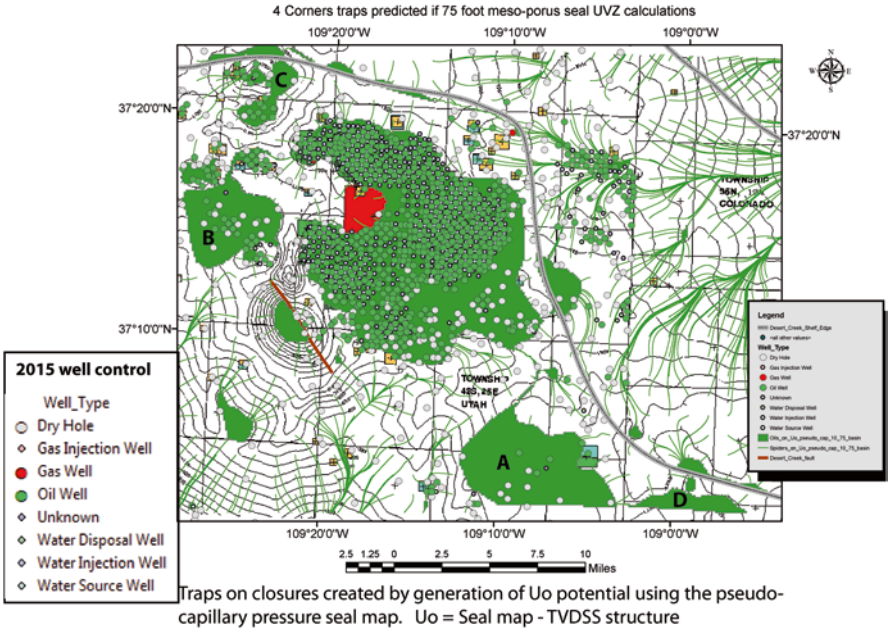

Fig. 5.31 Map produced by U-V-Z technique only

physical addition of the seal capacity grid, will have the contact slightly lower, depending on the structural differences due to seal thickness. The differences are minor, as shown.

For readers that don't have access to migration mapping packages, there are number of tools in GIS software packages like ARCGIS can treat the Uo or Ug potential maps like hydrologic stream flow and thus mirror the migration patterns coming from other software packages.

So, is the map wrong in detail? Of course. Will the map ever be right in detail? Unlikely. Can additional work with cores, facies and seismic make the interpretation much better? Of course. Can I find oil and gas leads and ideas with limited data and sound geological thinking? Absolutely!

This example was actually done as a 'blind test' of the concepts and it works. I've used these techniques globally for many years, and yes, they generate a lot of leads and ideas, but you have to think a bit like a molecule of oil or gas and follow where it goes from start to finish.

5.2.5 Migration with Both Fault Seals and Hydrodynamics-Temsah Field, Egypt

Within a hydrodynamic environment, incorporating fault or facies seals with the hydrodynamic flow is the best way to fully develop a lead inventory. Figure 5.32 provides an example from the Temsah Field (discussed earlier in Chap. 4).

There are two sizable faults on the Temsah structure, and in the earlier hydrodynamic flow discussed in Chap. 4, they were not used in the migration and entrapment scenario. In Fig. 5.32a, fault seal capacity has been arbitrarily set at 600′ (182 m) to wet gas and a trap map run without hydrodynamic flow. The trap is too large, has a flat gas-water contact and does not fit the known accumulations.

Figure 5.32b uses the potentiometric map and is a better fit to known accumulations. It also has a tilted gas/water contact that fits the well data. The best map is probably Fig. 5.32c, however, which uses both fault and hydrodynamic seals. Although the differences are subtle, they are significant in detail. Trinity software, like other petroleum systems software, allows using both fault and potentiometric maps in migration runs. It also has the added feature of setting top seal capacity, something that cannot be done with a simple U-V-Z approach. As inputs can be changed quickly and new runs made, it is possible to develop a much better idea of risk and reward.

Running combined maps like these without a petroleum systems software package is possible by added the Vg or Vo hydrodynamic map to the fault or facies seal map (both of which will be in feet or meters) and then subtracting the TVDSS structure map, also in feet or meters. Remember, these TVDSS maps have negative numbers calculated in the examples shown, as the surfaces are created are from

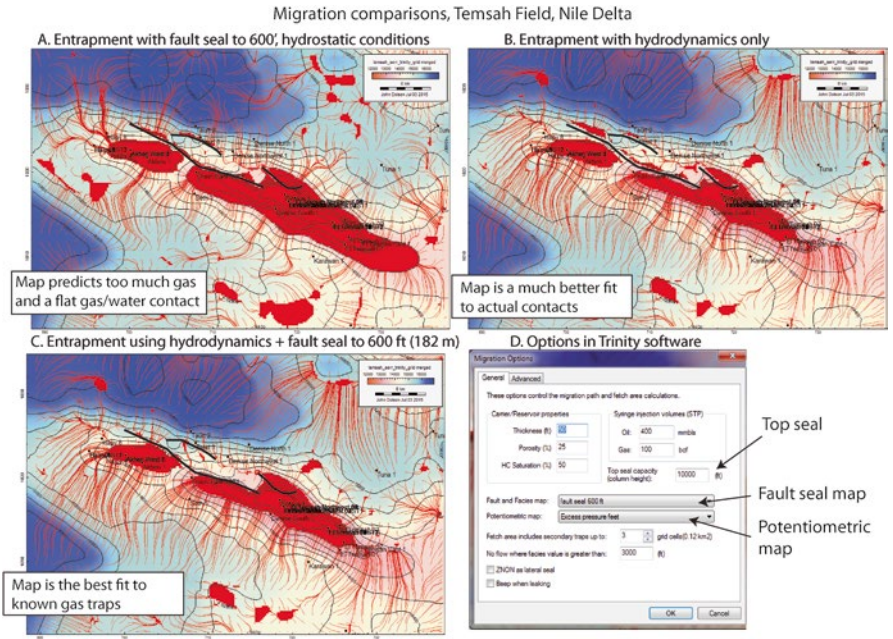

Fig. 5.32 Trap comparisons, using various combinations of fault and hydrodynamic seals, Temsah Field, Egypt

subtraction of the measured depth from the Kelly bushing or ground level elevation. If you are using positive TVDSS numbers, you simply add the Vo (or Vg) + seal + structure and then look for closures.

The physics and detailed understanding of how the U-V-Z approach is derived is complex, as is the math behind capillary pressure analysis. But once you get used to the approaches described in this book from practical examples, and with good spreadsheets on hand to make calculations quickly, your ideas of where oil and gas might remain to be found will increase substantially.

5.2.6 Summary

Porosity and permeability data are usually available either from pressure analyses like RFT, MDT or DST data or reports from core. Capillary pressure data takes time and money to acquire and may not be possible to use in an early evaluation of the prospectivity of an area. However, pseudo-capillary pressure analysis can utilize the porosity and permeability to calculated a like pore-throat radius. This information, in turn, can be used with the Pittman (1992) equations, to create height above free water plots that not only can describe well performance, but estimate sealing capacity.

Seal maps are a critical part of an exploration screening process. They can be built with a good knowledge of facies and faults, oil and gas shows in the area and calibration to capacity predicted from the pseudo-capillary pressure plots. Once seal capacity map is built, with the units in either feet or meters (depending on your structure maps), a fluid potential map can be made to simulate trapping along a migration route. If the primary structure map is in positive TVD numbers, the seal map is added to the structure map and the resultant map contoured. Closures define the trap. If the structure map is in TVDSS numbers (KB – measured depth), then the structure map is subtracted from the seal map.

In either case, a more comprehensive look at entrapment is possible that might be missed by simply generated leads individually based on the shows data. Full entrapment potential is best done with a combination of potentiometric surface and seal maps. Software which offers quick and easy manipulation of the grids, to test alternative models, can go a long way towards improving a prospect inventory in any area.

In the end, whatever maps are made, the shows data should confirm or reject the models, giving a good assessment of the risk for new prospects.

5.3 Show Types and Quantitative Assessment

Oil and gas shows databases, as previously shown, come from a wide variety of sources. Test reports, Calculated Sw from logs, mud logs information, well completion reports, fluid inclusions (Chap. 7) or geochemical data. Seismic data, if the frequencies are right, can also be used, but in this book we concentrate on shows in wells. In some cases, particularly in international exploration, there may only be an old map or listing of shows in wells, often with very little detail. Regardless, it is important to capture that information and try to make sense of it using the principles already described from height above free water, relative permeability and fluid flow and entrapment.

Recall from Chap. 2 that shows are classified into four major categories (Table 5.3), (Schowalter and Hess 1982).

The task of a geoscientist is to go beyond the descriptive show information and make a stab at interpreting the show type and its significance. Does the show indicate a migration pathway or trapped oil? If the Sw is 80 % and tests water, with no shows recorded or recovered is the interval low on the trap in a transition zone or high in a trap in a waste zone? Ways to recognize shows types are summarized on Figs. 5.33, 5.34, and 5.35 (modified from Meckel (1995)) (Table 5.4).

Pickett plots are covered in more detail in Chap. 6, but an excellent reference is in Hartmann and Beaumont (1999) where step by step instructions are given for construction. Wettability bead tests are simply examining how much a drop of water beads up on the surface of a core, for instance. In many residual saturations, the water does not bead up, but flattens out. A strong bead of water indicates oil is coating the surface. The water saturation cutoffs listed in Fig. 5.33 should be taken with

Table 5.3 Show classification adapted from Showalter and Hess (1982)

Show type	Characteristics	Comments
Continuous phase shows	A continuous filament of oil has bridged the large pore networks	Any hydrocarbon above the free water level.
		Can possibly be used to determine position in a trap
		If a well tests measureable rates of hydrocarbons, it is in the trap and a continuous phase show.
		It is difficult to recognize if the Sw is high enough (either low on the trap or in a waste zone) and relative permeability causes the well to test water only.
Residual shows	Occur as isolated droplets within the pore system	Common in depleted reservoirs.
		Common on migration pathways
		Commonly occurs where there is post-accumulation uplift and re-migration.
		Common in hydrodynamically tilted traps in the flushed zones.
		Will always test water and have a water gradient on pressure plots.
Source rock shows	In-situ hydrocarbons adsorbed onto the surface of organic matter	Commonly released by bit friction while drilling—may show up on mud logs as increased gas or oil show in shales or marly limestones.
		Can be used to help identify potential source rocks.
		The rules for evaluation of these shows and production involve different rules—these are primary migration shows, not secondary migration shows.
		Natural fractures or hydraulic fracturing may be needed to produce them (if at all possible).
		These shows and source rocks may hold the bulk of future new reserve growth in many countries, if not globally.
Dissolved hydrocarbons	Molecular scale background gasses and hydrocarbons	No real exploration significance.
		Common in most formations as background gas on mud logs.

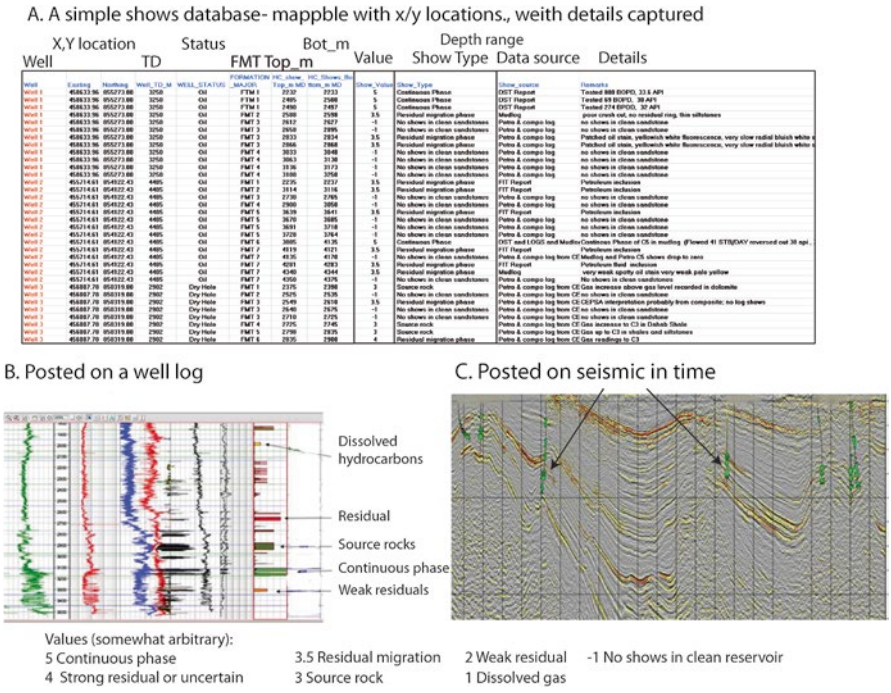

Fig. 5.33 Example of a shows database compilation and displays, Barmer Basin, India

some caution, as some tighter rocks, as shown earlier, can have residual saturations as low as 35 %.

Residual shows are common, and could be recognize a number of criteria (Table 5.5). An excellent summary of how to recognize residual oils is that of (O'Sullivan et al. 2010).

The most significant proof of a residual show are water gradients from DST or RFT data, as the residual shows are always below the FWL. In thick permeable reservoirs, a lack of a clear oil or gas-water contact is also distinctive. Chapter 3 covered another interesting technique dealing with mud gas plots using wetness ratio curves, where the Balance ratio gas curves are much less than the wetness ratio curves over residual zones.

Many times, however, largely due to relative permeability issues and zones of high water saturations in tighter rock, it is difficult to distinguish between residual and continuous phase shows. These cases are summarized in Table 5.6.

These situations take a much more careful look and may, in fact, not be resolvable. Part of any risk assessment is recognition that the answer is unclear. In these cases, it just takes your judgment as to what the implications are for locating a well based on the shows data.

A. Table of shows data from a vendor, Argentina

Well	X, Y location		Depth (m)	Show strength	Flourescence	Porosity
Well	X	Y	Depth	Show_strength	Flourescence	Porosity
AEA.Nq.Gu-1154	2477749.60	5698719.63	1002.00	0	3	0
AEA.Nq.Gu-1154	2477749.60	5698719.63	1010.00	0	1	0
AEA.Nq.Gu-1154	2477749.60	5698719.63	1012.00	0	2	0
AEA.Nq.Gu-1154	2477749.60	5698719.63	1014.00	0	2	0
AEA.Nq.Gu-1154	2477749.60	5698719.63	1016.00	0	2	0
AEA.Nq.Gu-1154	2477749.60	5698719.63	1018.00	0	2	0
AEA.Nq.Gu-1154	2477749.60	5698719.63	1020.00	0	2	0
AEA.Nq.Gu-1154	2477749.60	5698719.63	1022.00	0	1	0
AEA.Nq.Gu-1154	2477749.60	5698719.63	1024.00	0	1	0
AEA.Nq.Gu-1154	2477749.60	5698719.63	1026.00	0	1	0
AEA.Nq.Gu-1154	2477749.60	5698719.63	1028.00	0	1	0
AEA.Nq.Gu-1154	2477749.60	5698719.63	1011.00	0	1	0
AEA.Nq.Gu-1154	2477749.60	5698719.63	1013.00	0	2	0
AEA.Nq.Gu-1154	2477749.60	5698719.63	1015.00	0	2	0
AEA.Nq.Gu-1154	2477749.60	5698719.63	1017.00	0	2	0
AEA.Nq.Gu-1154	2477749.60	5698719.63	1019.00	0	2	0
AEA.Nq.Gu-1154	2477749.60	5698719.63	1021.00	0	2	0
AEA.Nq.Gu-1154	2477749.60	5698719.63	1023.00	0	1	0
AEA.Nq.Gu-1154	2477749.60	5698719.63	1025.00	0	1	0
AEA.Nq.Gu-1154	2477749.60	5698719.63	1027.00	0	1	0
AEA.Nq.Gu-1154	2477749.60	5698719.63	1029.00	0	1	0
AEA.Nq.Gu-1154	2477749.60	5698719.63	1310.00	1	2	2
AEA.Nq.Gu-1154	2477749.60	5698719.63	1311.00	1	2	2
AEA.Nq.Gu-1154	2477749.60	5698719.63	1312.00	1	2	2
AEA.Nq.Gu-1154	2477749.60	5698719.63	1313.00	1	2	2
AEA.Nq.Gu-1154	2477749.60	5698719.63	1316.00	1	2	2
AEA.Nq.Gu-1154	2477749.60	5698719.63	1317.00	1	2	2
AEA.Nq.Gu-1154	2477749.60	5698719.63	1318.00	1	2	2
AEA.Nq.Gu-1154	2477749.60	5698719.63	1319.00	1	2	2
AEA.Nq.Gu-1154	2477749.60	5698719.63	1320.00	1	2	2
AEA.Nq.Gu-1154	2477749.60	5698719.63	1321.00	1	2	2

Numbers vary by interpreted intensity of the show

B. Mud log shows database displayed in Trinity in 3D with multiple wells

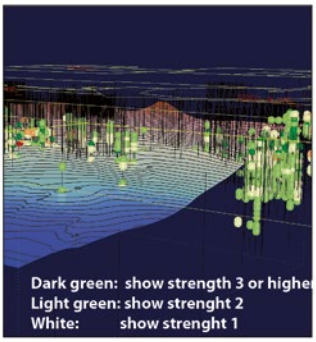

C. Trinity 2D cross-section with vendor shows posted

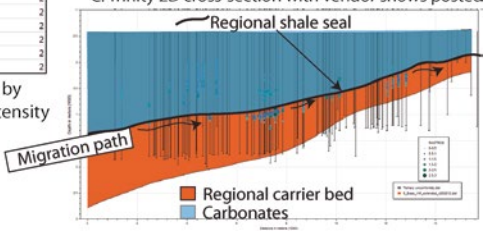

Fig. 5.34 Digital shows formation database from a mud log vendor and visualization in Trinity. The shows clearly define a regional migration pathway beneath thick source rocks and a carbonates

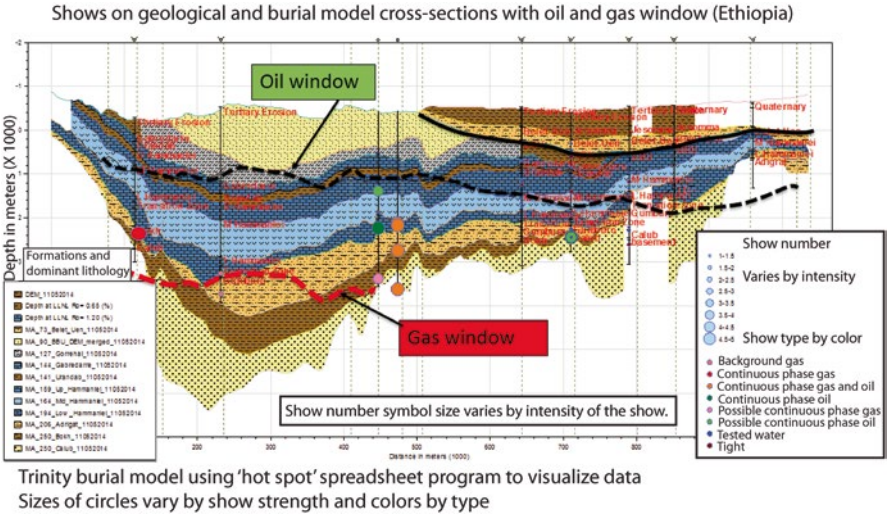

Fig. 5.35 Shows on a petroleum systems oil and gas window model, Ethiopia

Table 5.4 Some possible indicators of continuous phase shows. Modified from Meckel (1995)

Continuous phase shows: data type	Indicators
From formation tests or drilling	
	Free oil or gas.
	Water cut oil, mud cut oil, gas cut oil.
	Oil cut mud, oil on pits.
	Oil cut water cushion, oil cut formation water.
	Gas cut mud, no formation water.
	Gas cut filtrate, no formation water.
	Gas to surface, no formation water.
	Gas to surface in measureable quantities.
	Gas in sample chamber in absence of water.
	RFT pressures indicate hydrocarbon gradient.
From log evaluation	
	Pickett plots indicate continuous phase hydrocarbons.
	Sw 65 % or less in sandstone.
	Sw 45 % or less in limestone or dolomite.
	Calculated moveable hydrocarbon >0.
	Water saturation no constant.
	In highly porous rocks, resistivity and Sw show sharp changes from 100 % Sw to 65 % Sw or less.
From rock samples	
	Visible oil in samples, Sw estimated at 60 % or less.
	Strong streaming cut with gas bubbles.
	Wettability bead tests in conjunction with Sw evaluations indicating low Sw.

Table 5.5 Possible indicators of residual hydrocarbons. Modified from Meckel (2005)

Residual phase shows data type	Possible indicators
Samples	Natural asphalt, such as Gilsonite, in pore spaces.
	Immobile tar in pore space, with no gas shows in cuttings.
Pressure tests	RFT or DST of the horizon has no recovery of hydrocarbons.
	Pressure data yields a water gradient.
Log analysis	A 'lazy Sw profile' over a thick permeable reservoir, with no sign of a clear oil or gas/water contact.
	Sw >65 % for sandstones, >45 % for limestones or dolomites
Mud log or mud isotubes	Mud log plot where the balance ratio (Bh curve) is much less than the wetness ratio (Wh curve).
Show locations regionally	Shows are at the same stratigraphic level beneath seals in multiple wells, indicating a migration pathway

Table 5.6 Cases when it is difficult to determine the type of show. Modified from Meckel (2005)

When it is difficult to determine the type of show data type	Indicators
From formation tests	
	Gas cut mud with water (could be gas in solution).
	Gas cut filtrate with water (could be gas in solution)
	Gas to surface too small to measure (TSTM)-could be as in solution.
	Formation water with only a trace of oil.
	Gas in the sample chamber with water (could be gas in solution).
	Traces of hydrocarbon in formation water (may be migrated from another zone).
From log analysis	
	No calculated moveable hydrocarbons.
	Sw 60–75 % in sandstones, 45–60 % in limestones
While drilling	
	Water flow, trace oil.
	Water flow, gas cut (could be solution gas).
	Gas cut mud (can be from a source rock or residual).
	Mud log shows (could be from a source rock or residual).
From samples	
	Bleeding oil-occurs in low permeability strata (could be remnant shows in tight reservoirs).
	Bleeding gas-occurs in low permeability strata (can be gas coming out of solution).
	Hydrocarbon odor.
	Sample fluorescence.
	Cut with solvent.
	If in a source rock, could be oil/gas released from bit friction during drilling.

5.3.1 Building and Visualizing a Shows Database

I have consulted now globally with many, many companies for over three decades. I am still amazed, however, at how many companies do not maintain or have, a comprehensive shows database. One of the first things any geologist should do when entering a basin is establish a shows database that can be continually updated and improved. It should also be mappable and capable of moving the data to a workstation so as to visualize the data on logs and seismic sections.

Some vendors, particularly large companies like IHS Energy (www.ihs.com) or smaller companies like Nehring and Associates (www.nehringdatabase.com) readily sell databases of oil and gas recoveries or tests by formation or field. All of these data can provide a very quick start on visualizing and thinking about oil and gas shows.

It really doesn't matter what a classification scheme is as long as you have one and can think about what it means and then explore with it. One of the most comprehensive and complete shows databases I have ever worked with has been assembled by Cairn India for the Barmer Basin and some of that results of that work have recently been published (Dolson et al. 2015; Farrimond et al. 2015; Naidu et al. 2016). Figure 5.33 shows an example of the format used. The database covers all of the exploratory wells and a number of significant development wells. It has been used repeatedly to open up a number of new plays and prospects.

The classification used in Fig. 5.33 is fairly rigorous, in that every show has to be classified and given a number for loading to workstations as a curve. The data is visualized on both logs and seismic as a fairly routine part of the interpretive workflow. As much detail as possible is captured in the comments section and the well files are fairly well organized so it is not difficult to track down the original source of data if it needs to be re-examined and changes made.

Figure 5.34, in contrast, provides an example of a much simpler classification from a vendor delivery of shows data from a mud log.

The database is very simple, with a numeric flag by a depth with numbers from 0 to 3 or more with a grade for the show (no show, weak, strong, etc.). It is not interpretive as to type, but can be put on a curve and displayed on logs or seismic or brought into a petroleum systems software package and visualized. Trinity software has the capability to quickly visualize a shows database like this in three dimensional views (Fig. 5.34b) or in cross-sections (Fig. 5.34c). In this example, a regional aeolian sandstone (Tordillo Formation, in orange, Fig. 5.34c) is overlain by a maximum flooding event source rock shale (Vaca Muerta Formation). The shale is in turn overlain by a carbonate shelf reservoir (Quintuco Formation, shown in blue). The digital shows database readily shows a regional migration pathway beneath the shale, as indicated by ubiquitous shows along the upper part of the aeolian sandstone.

Shows data is the only way to calibrate any trap model, but is also useful for understanding petroleum maturation and fluid phase along migration routes. In addition, different source rocks generate different types of hydrocarbons, and that may be recognizable from geochemical signatures or the phase of the show (oil, gas or mixed), thus helping understand the petroleum system better.

In Fig. 5.35, for example, oil and gas shows are displayed on a regional structural cross-section in Ethiopia that is derived from a multi-layer Trinity petroleum systems model.

Different software packages have different ways to visualize shows data, but Trinity has one tool that I have found particularly useful—a spreadsheet visualization tool called 'hot spot'. Hot spot reads excel spreadsheet or other ASCII files that contain x/y location data and depth and allows a lot of quick interactive posting of data in both 3D and 2D views. In the diagram above, the colors indicate the type of fluid (oil, gas, condensate, water) and the size of the symbol the relative strength of the show. The largest circles are any definitive proven continuous phase fluids as confirmed by well tests or logs. The diagram clearly shows some gas (red) above the gas window (dashed red line), which indicates substantial vertical and

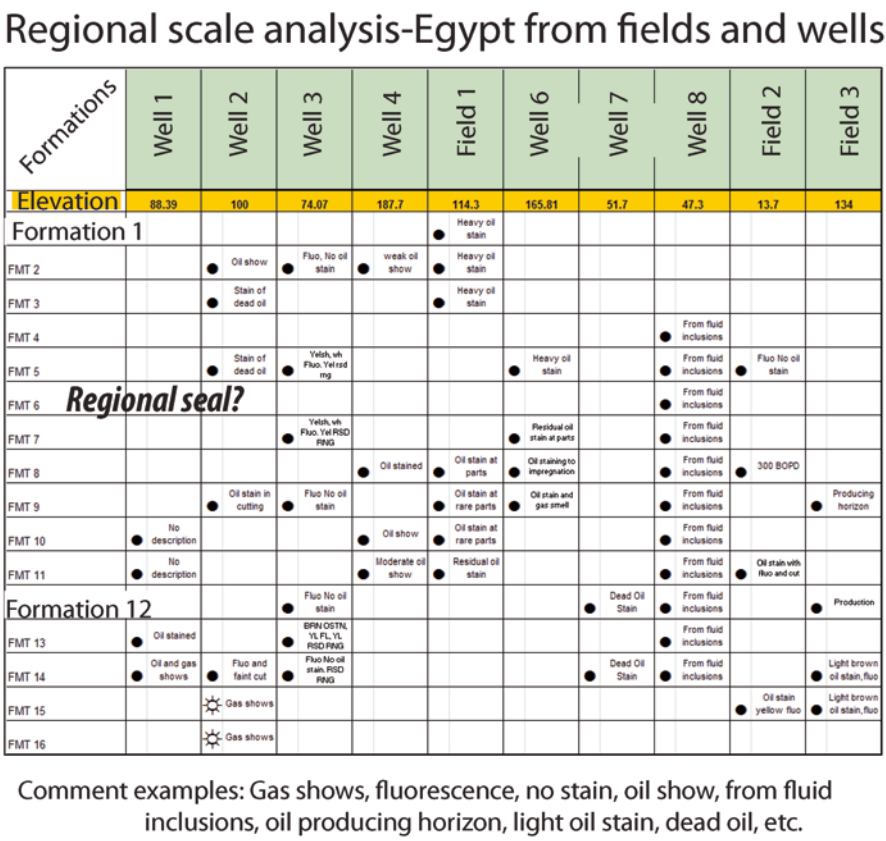

Fig. 5.36 Regional scale assessment of shows. Vertical breaks can indicate regional seals at different formations

lateral migration. Understanding those migration pathways and being able to predict them with the kinds of tools discussed in this book bring a new level of risk reduction to any prospect or play generation.

You don't need software to do this, however. You just need to find a way to post the shows on a cross-section. Doing it by hand is just as good, and sometimes, causes you to think pretty hard in the process. As most work today is done on some kind of workstation, however, it is best to load your shows databases software packages and work with them visually on cross-sections.

Lastly, at the start of entering any new basin, it is good to simply take key wells and summarize the shows from the wells or existing fields so as to understand the basin and plays better.

The data in Fig. 5.36, for example, was done by a company in Egypt and identified Formation 6 as a potential regional seal, where virtually no shows were recorded in it over a wide area. The table contains not just well information, but generalized data from fields from published literature that were near their block.

It really doesn't matter how you capture shows information, as long as you think about it in the context of entrapment and position in a trap or along a migration pathway or within a source rock.

5.3.2 Summary

The most important shows types from an exploration standpoint are continuous phase, residual and source rock shows. Continuous phase shows are clear when there is any measureable amount of oil and gas tested in a well. Even small amounts of oil at low rates indicate a trap is present. Continuous phase shows need to be examined carefully to look for offset potential, either in better rock or higher up on the trap. At times, evaluation of the saturations and height above free water analysis may show that a trap though to be in a structural closure actually may be in a larger stratigraphic trap.

Residual shows indicate either migration pathways or paleo hydrocarbon columns. In either event, looking updip for the terminal trap is the right thing to do. Source rock shows may indicate substantial potential in unconventional plays and this is discussed in more detail in Chap. 8.

Building up a quantitative shows database takes time, but is worth the effort. Analysis should start at a regional scale using information from fields and available well data and then be progressively refined with time. The more information that can be captured in a central database or spreadsheet, the better the end result. Failure to look at shows systematically as an early part of the exploration process generally means a lot of future mistakes will be made and potential overlooked.

5.4 Case Histories

The following case histories reinforce some of the concepts covered so far. They represent both successes and failures. Other case histories are included in subsequent chapters. The first four case histories are from the giant October Field in Egypt. The last three are from the North Sea, Hugoton Field (USA) and the West Siberian Basin (Russia).

5.4.1 Cases 1–4: October Field, Egypt

One of the primary reasons I moved to Egypt in 1994 as the Senior Technical Advisor for GUPCO was simply because it was an opportunity to drill a lot of wells. The giant October Field (about 2 BBOIP) was discovered in 1977 by Amoco and is a complex of large rift-related tilted fault blocks (Fig. 5.40). The main field has four

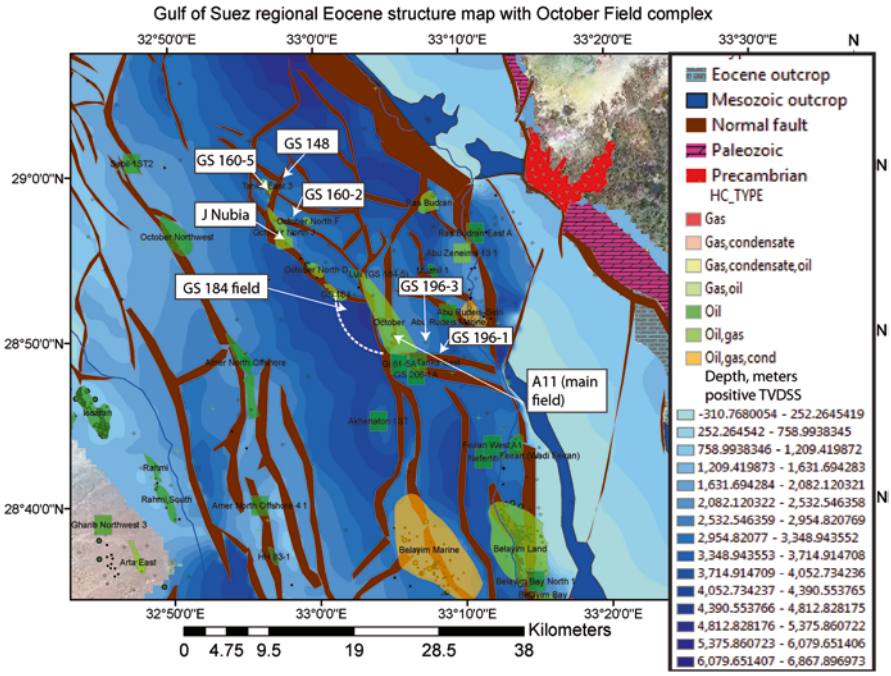

Fig. 5.37 Index map to October Field complex and key wells in case studies

major platforms, with deviated wells drilled to multiple development locations. In 1994, the field was in a fairly mature stage of development, but over the next 5 years we still managed to find over 200 MMBO of new oil, much of that through detailed analysis all dry holes and with teams of very experienced geoscientists.

The bulk of the reserves are from the 2 BBO accumulation are in the Lower Cretaceous Nubian Sandstone (1.5 BBOIP), a multi-darcy, widespread fluvial and aeolian reservoir. The Nubian Sandstones are overlain by the Nezzazat Group, a complexly layered formation of low porosity meso and micro porous tight limestones and sandstones (500 MMBOIP) (Fig. 5.37).

There are a number of smaller fault blocks as well as some down-thrown three-way fault traps in Miocene reservoirs. The Miocene play, involving deeper water turbidites and some deltaic facies, is present only on the down-thrown side of the faults, as the fault blocks were active during deposition and the reservoirs were completely missing over the high structural corners.

Seismic data in the Gulf of Suez is notoriously poor due to multiple attenuation beneath many salt layers in the shallower section. Hence, unlike many other basins, the details of fault orientations are often difficult to image. Consequently, wells frequently encounter unpredicted faults and resolution of reservoir geometries from seismic is difficult or impossible. As a result, subsurface interpretation requires perhaps an even greater reliance on any data from existing wells to understand traps.

5.4.1.1 Case 1: Underestimating a Field Size—Failure to Get the Free Water Level Right, GS 184 Field, October Field Complex, Egypt

Case 1 deals with a down-thrown Miocene trap in the prolific Asl Formation as the GS 184-1 field. Despite extensive exploration which had found the structural high Nubia traps in the late 1970s and early 1980s, drilling success had declined until a down-thrown trap play was identified in 1989. While drilling the crest of a Nubia oil pool on the October D platform, a well accidentally crossed a fault and stumbled into a thick Miocene age calcarenite on the downthrown side, a facies which had never been seen in this part of the basin. The reservoir porosity was low and mud loggers had described the interval as a low permeability limestone, when, in fact, it was a mixed facies of calcite cemented sandstone, with low porosity but good permeability (macro-porous). After nearly deciding to abandon the well as a dry hole, someone convinced management to perforate and test the interval. The well flowed 20,000 BOPD, opening up some serious attempts to find another similar trap.

Subsequent exploration in the north near the "J" Nubia pool (discovered in 1989), found a down-thrown three-way trap in the Asl Formation in the October J-5 well in 1991, again with significant reserves. The GS 184-1 well was then drilled in 1994 to test another, even larger, down-thrown three-way closure in a structural transfer zone between the C and D platforms. A great deal of excitement justifiably existed around this discovery, as the well, drilled vertically from an exploration rig, flowed 10,000 BOPD from a high quality Miocene reservoir. The potential trap covered a reasonably large area, and initial estimates put the OOIP at about 125 MMBO, with recoverable reserves greater than 50 MMBO.

Figure 5.38 shows the generalized structural setting.

We held an exploration discovery party in August, 1994, a custom always held on the top of the Amoco Building in Maadi, Egypt, and expectations at the party were high, as a delineation well, the GS 184-3 was being drilled to confirm the size of the trap. A few weeks later the euphoria was tampered down. The GS 184-3, a very long-reach well drilled from the main field C platform, had reached TD at 13,500′ MD in a very tight limestone with only marginal saturations. The reservoir that produced in the discovery well was not present. It was unclear if the main reservoir had been faulted out or undergone a dramatic thinning and facies change. A facies change was suspected, but one that could explain the geometry shown on Fig. 5.38 had not been seen before in the basin. Rapid facies changes are common in rift settings, however, due to active fault movement during deposition, and this was the expected culprit in the well failure. Because it was essential to try to penetrate the reservoir again, as well as find the oil-water contact, a sidetrack to the GS 184-3 was drilled to 14,962′ MD and unfortunately encountered the same poor facies, again, with minor shows and high Sw (GS 184-3St-1).

What had been euphoria at the exploration party in July of 1994 turned to dismay by November 1994. This discovery had looked like the start of an exploration turnaround, as over the prior 3 years, 32 dry holes had been drilled with no success and the pressure was on to 'get it right' and control costs. We were subsequently given 2 weeks to determine how much oil or gas was in that trap and if it was enough to

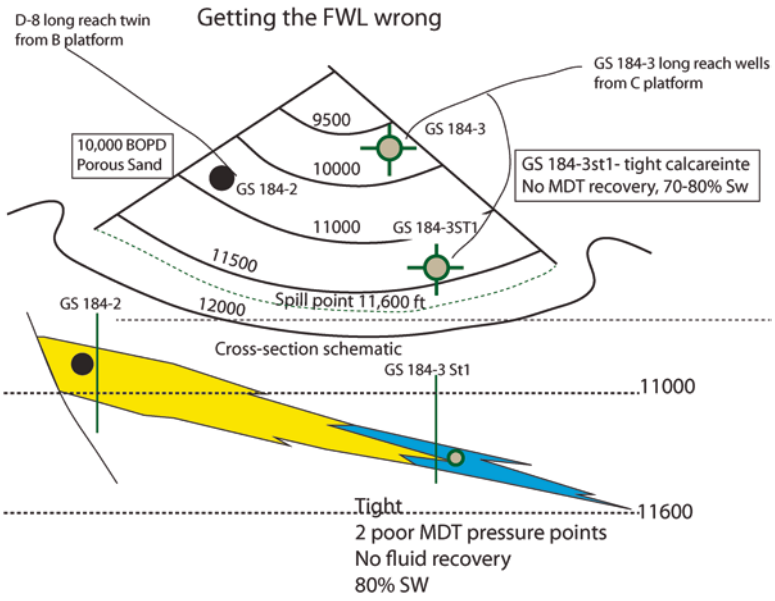

Fig. 5.38 Generalized structural setting and key wells. The trap is a 3-way downthrown trap in a transfer zone to the main field

justify a new platform. An alternative to a new platform would be to simply develop the field with a few more long-reach wells from existing platforms. The long reach wells, however, were difficult to drill and much more expensive than wells from a platform. Hence, the decision to set a platform would come down to field size and economics.

Pressure data had been collected on the GS-184-2 well, and indicated a light oil gradient (Fig. 5.42). TVD corrected depths were compared with two poor pressure points from the GS 184-3ST1 well, which had a Sw of 70–80 % with weak shows. The gradients did not line up on a common gradient, so there was no direct proof of a long, continuous column. The GS 184-3St1, with its high water saturations, was treated as 'wet' despite the shows and 70–80 % Sw. Setting a water gradient at the pressure points gave a FWL of about −11,040′ feet, substantially higher than the spill point at −11,600′ (Fig. 5.39).

The impact on reserves was profound. With a much shallow oil-water contact, plus the loss of reservoir facies to the east, the reserves dropped substantially.

This evaluation gave the field about 50 MMOIP, with much less recoverable. A hotly contested decision to not set the platform was made to keep costs down after the two expensive delineation wells had failed. Perhaps the greatest error made at this point was taking this minimum trap case (Fig. 5.40) at certainty. At the time in GUPCO, risk assessment of alternative sizes of pools was not done. Maps were generated as 'the answer' and wells drilled based upon those maps. A more proper treatment of this discovery should have involved making a 'maximum' map and

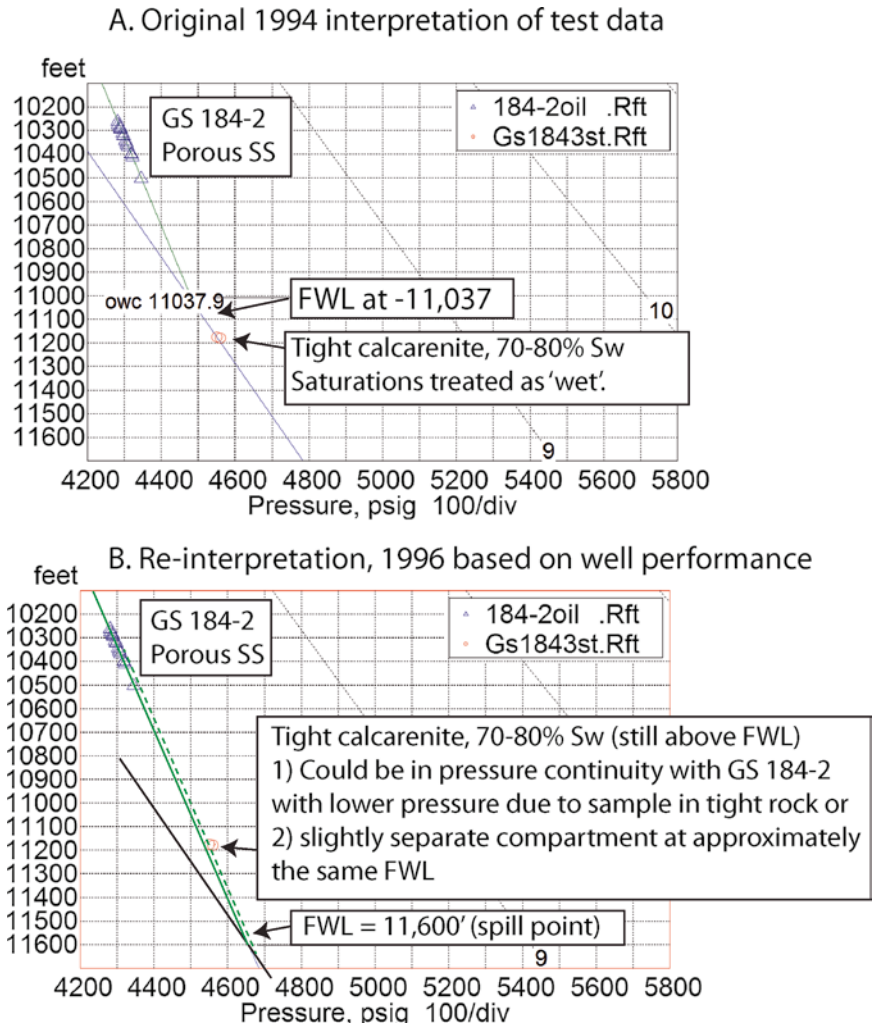

Fig. 5.39 Pressure depth plots used to speculate on free water levels. The original interpretation was incorrect, as it treated a zone with saturation as 'wet' and at or near the free water level. The test in the downdip well did not line up perfectly with the oil column in the GS184-2 well, and should have been interpreted, at least as one possibility, as either compartmentalized above the free water level, or not having reached full pressure on the test in the tight carbonate. A few psi additional extrapolated pressure would have put the downdip well in communication with the updip oil leg, suggesting a larger trap above the FWL

treating this map as the most likely minimum reserve case. That was not done, however, and a long reach well, the D-8, was drilled from the D platform and twinned the GS 184-2 well in 1995.

The D-8 was another surprise, as it came in with even more pay than the GS 184-2 and had developed a second oil-saturated calcarenite sand body below the

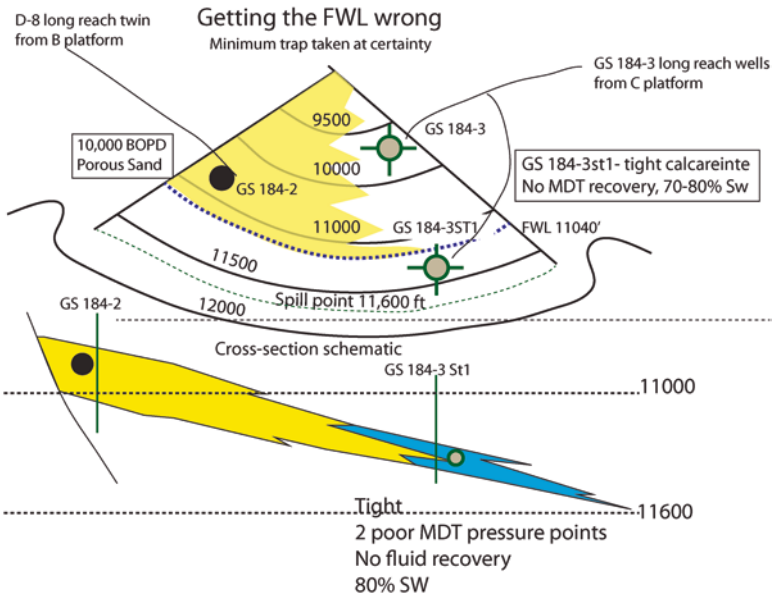

Fig. 5.40 Minimum trap size by treating the 80 % Sw in the GS 184-3ST1 well as wet. This pessimistic evaluation resulted in a decision to not set a platform, a decision that in a year, after production, would prove to be the wrong thing to do

deepest stratigraphic level in the original well. The D-8 flowed at 15,000 BOPD and continued to flow with no pressure drop for over a year. It was the highest flow rate of any well in the Amoco GOS portfolio.

In early 1996, it was clear that the field was much bigger than the one estimated in the minimum case. The D-8 well recovery volumes were large enough, with no pressure drop, to show that the minimum case was clearly wrong. By now, there was enough production and pressure information to determine how much oil was actually in the trap, and the number went back up to near the original estimate of 125 MMBOIP. I was involved in the reassessment, and had to take a hard look at what went wrong earlier in 1994. It is always a difficult task to stare solid data in the face and admit your earlier analysis wrong. Over the prior year, we had developed better facies models for how reservoirs would respond in active structural settings from outcrop field work and analog rift basins. It was now clear that the facies change was real, but we just didn't know exactly where it occurred east of the discovery. It was also clear that the 70–80 % Sw in the tight calcarenite was significant, and that the GS 184-3ST1 should not have been treated as wet, but as a poor saturation well above free water and within a long transition zone for that type of rock.

Why the pressure gradients didn't fall on the same line between remained problematic. One possibility was that the tight MDT data had not reached its ultimate pressure, and was thus too low (Fig. 5.39b). Only a few more PSI would have put the tight limestone in pressure continuity with the main sandstone. An alternative to

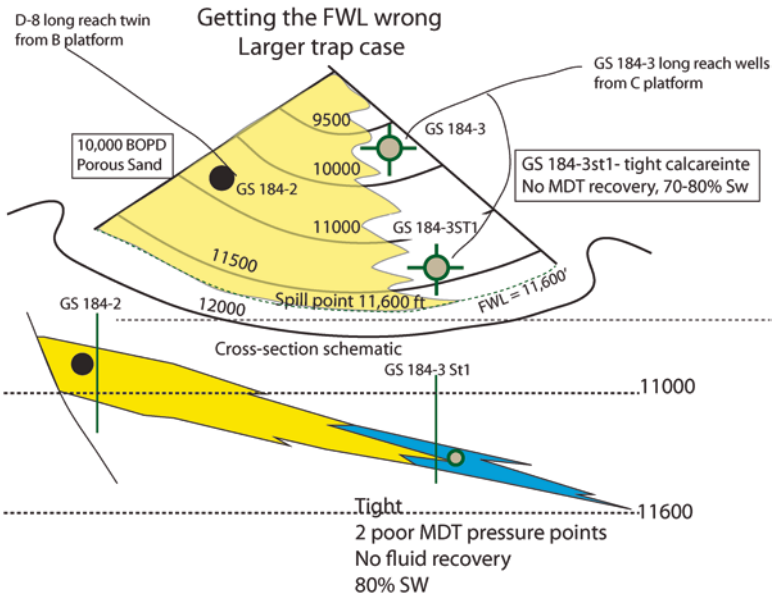

Fig. 5.41 Maximum map which mapped pressure data and production, 1996. The lesson learned in this example is to (1) be reluctant to treat any saturation not 100 % Sw as at the FWL and (2) risk weight probable answers to get a most likely volumetrics. If risking had been done between the volumes from the maximum and minimum cases, a platform would have been set to develop the field. Considerable future expense would have been saved

that was the real possibility that a pressure compartment existed and the tests in the GS 184-3ST1 had a slightly different, but deeper FWL than the main sandstone body.

Either way, the only way we could end up explaining the volumes being recovered in the well was material balance of the volumes vs. pressure decline was to draw a maximum map (Fig. 5.41).

The maximum trap map required a FWL and spill point of −11600 ft., the geometric spill mapped from seismic. It also required the facies edge to extend farther eastward toward the two dry holes. By now, enough money had been spent to make a platform recommendation uneconomic, so another delineation well (the D-9) was drilled form the "D" platform.

The problems weren't over yet, as in 1997, the D9 well (not shown, but northeast of the GS 184-2 well), hit a major fault causing two sidetracks to be made before landing successfully in the main reservoir. Mud loggers, however, as in the case of the GS 183-1, misidentified the calcarenite as limestone and boldly announced we had 'missed the pay'. The announcement further rattled management, and was made before the well logs had been run. More dismay ran through the company, as it looked like 2 years of analysis and expense had been for nothing. However, a number of us confronted the drilling department and told them to 'wait until the logs are in' before passing judgement, pointing out that the reservoir samples described

were identical to the GS 183-1 and that the pressure data almost certainly required the reservoir to be present up on the block.

When the logs arrived, the zone was the same as in the D-8 well downdip and fully saturated, flowing at over 15,000 BOPD from the same low porosity, highly permeable macro porous calcarenite. There was great relief, but also extreme frustration that developing that field had become so much more difficult and expensive with the long-reach wells. The mud logger was reassigned to other duties by the exploration manager who had prematurely announced the D-9 as a dry hole.

By now, the decision not to build the platform was clearly seen as a mistake. In post appraising the process, the problem was in not using maximum and minimum risk maps to give a risk-weighted probabilistic volumetric. Had we re-thought the 70–80 % Sw on the dry downdip well as possibly either too low a pressure reading or a compartment on a longer column in a transition zone, we could have drawn the maximum map. Our final risk-weighted volumes would not have been closer to 125 MMBOIP, but they would have been greater than the 50 MMBOIP used to condemn a platform location. Development wells could have been drilled faster and cheaper from a platform, which could have also been used later for water injection wells.

In 1995, we instituted company-wide peer reviews and quantitative statistical risk assessment in both production and exploration. The result was a substantial increase in predictability to within 10 % of predictions and a success rate in exploration that climbed to 76 % (Dolson et al. 1997).

5.4.1.2 Case 2: Cap Pressure Analysis Leads to Deeper Oil-Water Contact, October Field, Egypt

One of the major changes made to how teams evaluated wells in GUPCO was to centrally locate engineers, geophysicists and geologists into the same physical work areas, so they would have daily exchange of ideas based on diverse disciplines. While this may seem like a standard practice in many companies today, in 1996, within exploration, it was a radical change. At the time, reservoir performance field studies of the October Field were done remotely from Houston, by small teams with a few Egyptian staff re-located to Houston. However, production in the main field was on decline at a much higher rate than many fields being operated by co-located teams within GUPCO's own field development groups. A decision was made to form an 'asset team' for the October Field, shut down the Houston field studies team and co-locate everyone in one building. A lot of good things happened from that move, not the least of which was a complete halt to the field decline over the next 5 years through innovative engineering and geological reassessment of the structural geology.

One of these reassessments involved looking at the Nezzazat Group in the main field. For nearly two decades multiple teams of engineers and geoscientists had worked hard to understand optimum ways to produce the giant October Field. With over 1 BBOE of resources, it was one of the largest and most important economic assets within Amoco. Co-locating team members soon had a major impact on many

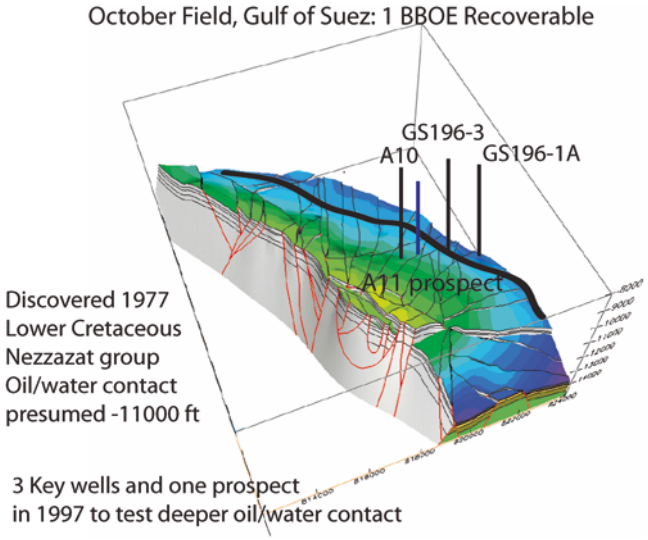

Fig. 5.42 Nezzazat structure, main field

basic assumptions that had gone largely unchallenged since discovery in 1979. One the paradigms, for instance, was that the faults in the Cretaceous level ran north-south, parallel to the main rift bounding faults. Dipmeter analysis (Sercombe et al. 2012) of a number of key wells, however, showed that many of the faults actually ran east-west (Fig. 5.42). The new structural interpretations required an enormous amount of work by the engineers to re-incorporate into new reservoir performance models and the result was the first real matches of well performance history to production.

As part of this effort, a long-held belief that the Nezzazat oil-water contact in the main field was at −11,000′ (3353 m) TVDSS was challenged based on production data (Dolson et al. 1998).

The issue of the depth to the oil-water contact in the Nezzazat Group came under review when anomalously high oil recoveries were noted from a macro-porous reservoir locally called the Wata Channel. The Wata Channel is an incised valley fill tidal channel deposit that is generally not over 50′ (15 m) thick, making it far beyond seismic resolution. The furthest downdip producer (the A10), was making more oil from the Wata Channel than predicted in all the models. Consequently, we set about trying different reservoir geometries and thicknesses, working with an engineer to try to come up with scenarios that might explain the additional oil being recovered. However, we could not do that with the downdip limit of the pay set to −11,000′.

Having already greatly disturbed our engineering management with a re-interpretation of major structural changes to the field, we now set about challenging the 20 year-old accepted wisdom of that oil-water contact in the Nezzazat Group (Fig. 5.43).

Fortunately, the A10 well had a long core through the Wata Channel and we sampled this core for mercury injection capillary pressure data (Fig. 5.46). The well

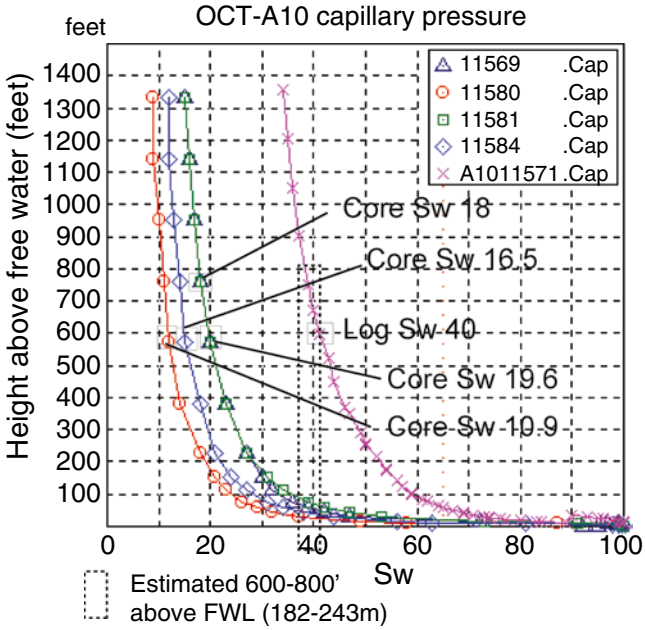

Fig. 5.43 Capillary pressure data from the A10 cores, Wata Channel

was at irreducible water saturations but one sample (A1011571.cap) was in tighter rock with log and estimated subsurface saturations of 40 % Sw or lower. These data suggested the FWL could be much deeper than the −11000′ level accepted as fact. Additional information also supported a deeper contact. We estimated the new level at −11,250 to 11,300′ (3428–3444 m).

The GS 196-3 and another downdip well (GS 196-1) had been drilled in 1991 and 1978, respectively. These two wells were the ones used to set the oil-water contact at −11,000′. These wells had to be re-evaluated, in light of the suspected deeper FWL. This was done with both log analysis and cuttings re-examination (Fig. 5.44).

The downdip GS 196-3 well, despite marginal oil saturations throughout the Nezzazat group, was treated as the downdip 'wet' well, and thus used to set the shallower oil-water contact. The rock types in most of the Nezzazat Group, however, particularly the Matulla-2 and 3 formations, are dramatically different from the Wata Channel. The Matulla 2 and 3 formations are low porosity, low perm mesoporous sandstones and carbonates. Saturations in the GS 196-3 well were also not 100 % water, but hovered between 60 and 80 % Sw. Significantly, a thin, porous sandstone penetrated the Wata Channel in the GS196-3 and was 100 % Sw, giving a lower limit to the FWL.

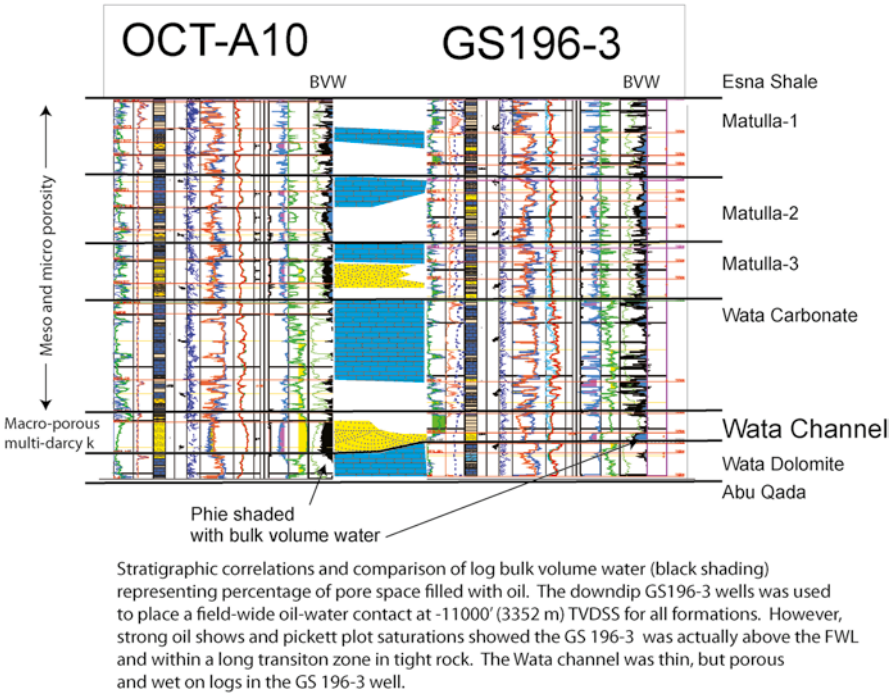

Fig. 5.44 Correlation with A10 with the downdip GS 196-3 well

For the GS 196-3 well, a Pickett plot, a technique discussed in more detail in Chap. 6 and covered well by Hartmann and Beaumont (1999) and Asquith and Krygowski (2004) was used (Fig. 5.45).

Pickett plots are simply a plot of the deep resistivity (RD) against porosity (PHIE). Diagonal lines of water saturation are drawn on the plot based on inputs from water resistivity, cement factors and other components of the 'Archie' equation for Sw (Chap. 6). When zones plot above the 50 % line on a Pickett plot, it is a strong indication of continuous phase shows above the FWL.

The Pickett plot confirmed that the GS 196-3 well was not 'wet' but in a long transition zone in poor rock quality well above a free water level. Sample examination of the GS 196-1 well, which had a much higher water saturation and was physically lower structurally, found strong oil shows in cuttings in high Sw reservoirs down to −11,250′. The Wata Channel was not present in the GS 196-1 well, so the cuttings were done on meso-porous Matulla Formation reservoirs and oil was still visible in cuttings to the deeper depth.

The results are summarized on Fig. 5.46.

The key point in Fig. 5.46 is that the Matulla 2 and 3 transition zone saturations found on the GS 196-3 Pickett plot were below the old field-wide oil-water contact of −11,000′. The −11,000′ contact, while making a good depth cutoff for zones that might flow dominantly oil with low water cut, was certainly not a 100 % Sw cutoff.

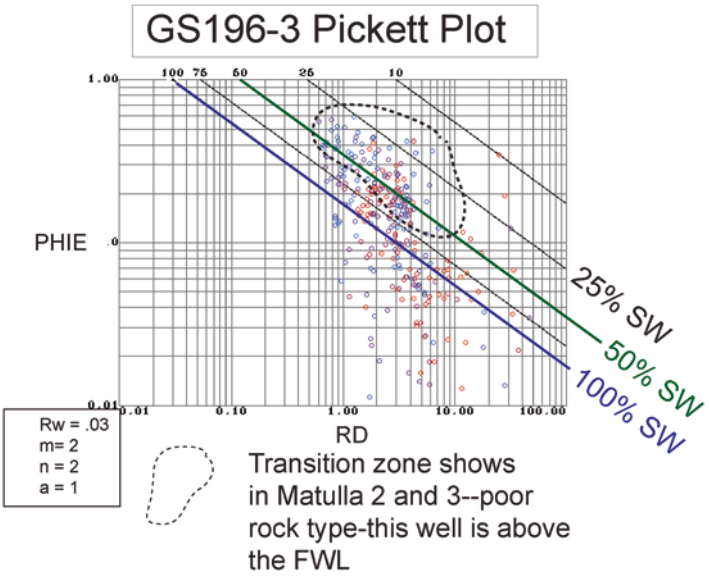

Fig. 5.45 Pickett plot, GS 196-3. The saturations indicated the well was above the FWL, with much of the saturation in a long transition zone in poor quality rock. Therefore, this well could not be used to establish a field wide oil-water contact above it

The difference in saturations between the Matulla and Wata Channel was due to capillarity, with the meso-porous Matulla Formation substantially tighter than the world-class multi-darcy Wata Channel. Base on capillary pressure and shows data, a FWL and OWC for the Wata Channel of at least −11,250′ was proposed, and possibly as deep as −11,300′.

This was not an 'easy sell'. While invalidating paradigms is part of our job, it is never received well by people who have bought into the old paradigm. In 1997, we recommended a new well (A-11) downdip of the A10 to test the concept. The A-11 was going to be the furthest downdip development well ever drilled in the Nezzazat Group. Skepticism that more oil would be found downdip was high.

After an initial well failed due to stuck pipe, a sidetrack (A-11st1) finally drilled to within 47′ the old oil-water contact level (Fig. 5.47). The well encountered irreducible water saturation in the Wata Channel and log saturations to TD with no water, below −11000′. The Wata Channel itself had irreducible saturation to −10.953′, or 47′ (14.3 m) above the postulated oil-water contact of −11,000′. Saturation in tight rock was noted below this to TD of the well, confirming a deeper free water level.

After sweating out the results pre-drill, the well results silenced most of the critics and also found a new, untapped reservoir in the Matulla-1. This reservoir (Figs. 5.46 and 5.57) was in virgin pressure as it had never been deposited updip and was absent in the downdip wells. In all probability, it is a lenticular marine sandstone and unlike other Matulla horizons, had excellent porosity and permeability. The total hydrocarbon pore volume (HPV) of the Oct All-St1 well was the highest

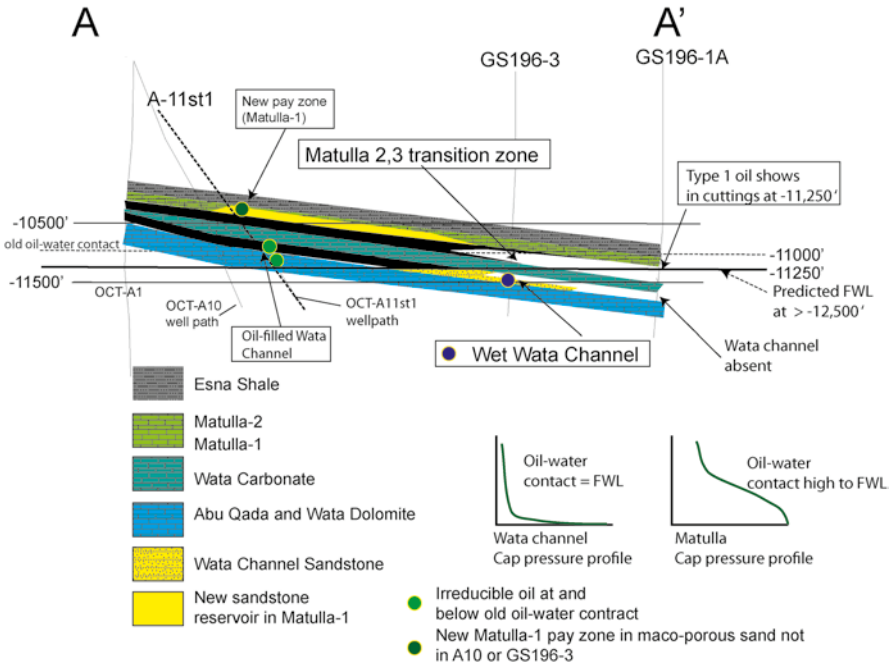

Fig. 5.46 Structural-stratigraphic cross section from A10 to GS 196-1A

of any well in the main field, as well as being the structurally lowest. The Oct A11-St1 well flowed 2600 BOPD, water free.

This work was not done in isolation. I don't believe the well could ever have been recommended without the input of petrologists, log analysis, engineers and certainly drillers ready to test a novel concept. The value of team integration was substantiated.

5.4.1.3 Case 3: Capillary Pressure and Sample Shows in Dry Hole with by-Passed Pay Lead to Updip oil Discovery, October Field, Egypt

The third case history deals with the GS 148-1 and GS 160-5 wells. The GS 148-1 well was drilled in 1981 as part of an aggressive exploration effort by GUPCO to find more satellite fields to the giant October Field complex. It was drilled to target the prolific reservoirs of the Nubia Group. The well found low permeability Nezzazat Group lithologies and shows to a TD of 12,877′, which at the time, was the deepest penetration in the northern Gulf of Suez. The main target, the Nubia Sandstone, was 100 % Sw and the well was plugged and abandoned without testing (Fig. 5.48).

One of the things I enjoyed most about working in GUPCO was the tremendous number of talented geoscientists who came and went through that organization over

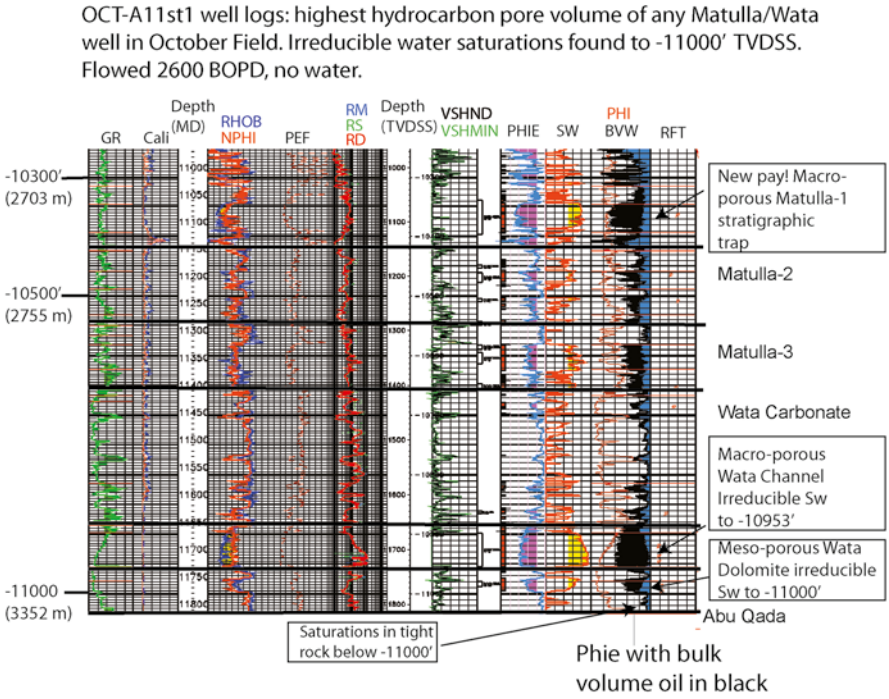

Fig. 5.47 Oct A11-St1 well logs

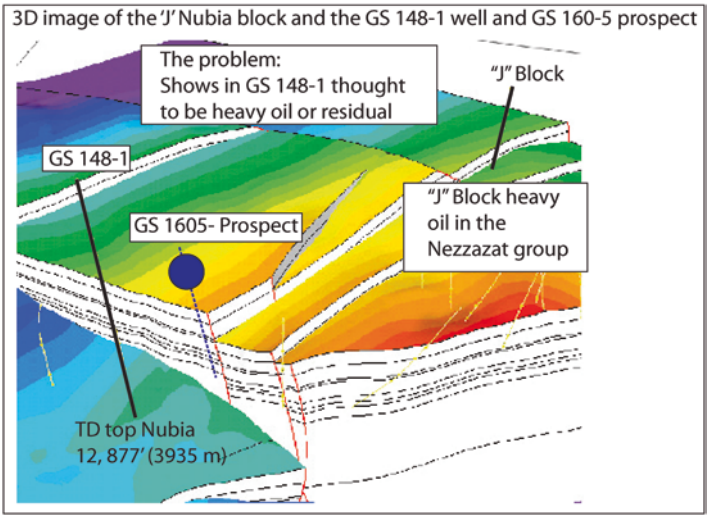

Fig. 5.48 GS 148-1 problem

the years. More than one geoscientist had noted that it looked like there was pay on the logs in the GS 148-1 well and perhaps it had actually drilled into a trap. After 18 years of agonizing over this observation, and by keeping a prospect alive in our inventory for over a decade, we decided to get more aggressive evaluating that block.

One of the prime concerns in this area was that the updip "J" Field Nezzazat Group was a 20° API heavy oil deposit, and unattractively economically. It made no sense to many in management to drill downdip from heavy oil and expect something lighter and better. The debate had raged for years. Curious about it, we decided to do something novel-to look at the rocks themselves! The petrology department pulled the cuttings from both the heavy oil field updip and the GS 148-1 well. They were strikingly different.

In the GS 148-1, the samples had light oil stain, yellow streaming cut and fluorescence and even gas bubbles in the cut, even after 18 years in storage. Along with the log saturations, these shows were a strong indicator of a continuous phase, bypassed accumulation. In contrast, the heavy Nezzazat in the updip block was black with tarry oil.

One would think that would have ended the discussion, but it didn't. Further proof was asked for so we sent the cuttings off for fluid inclusion analysis (Chap. 7). Fluid inclusions (Hall 2008) can trap petroleum in bubbles in reservoir cements and be analyzed for API gravity, temperature of emplacement, oil type and a host of other things discussed in Chap. 7 in more detail. The results confirmed a light oil interpretation (Fig. 5.49), with API gravities as high as 32 API.

In addition, we ran cuttings for mercury injection capillary pressure, to get a feel for the FWL and how high the well was in the trap (Fig. 5.50).

Interestingly the core labs in Cairo did not think it possible to run capillary pressure on cuttings alone, until we pointed out that much of the original work on capillary pressured decades before was done on cuttings, not just core. In any event, as shown in Fig. 5.50, the 50–60 % saturations seen in the core pointed to a FWL as deep as 12,850′. Looking at the cuttings carefully, there were only modest shows and high Sw at −12846′. A range of possible values was placed on the FWL based on uncertainty (Fig. 5.51). The capillary pressure plot, moreover, confirmed the meso porous natures of the reservoir and the need to get high to the old well structurally in order to get better saturations.

Interestingly, with the characteristic horrid seismic common to the Gulf of Suez, we could never determine the seal on this trap to the west, but had an idea where an updip fault might be from the seismic. The initial updip test (GS 160-5) crossed the fault and had to be sidetracked downdip. The well penetrated the Nezzazat 400′ (121 m) high to the GS 148-1 well. We drilled the well without fully understanding the trap, but relying on the now fairly firm observation that an oil field already had been drilled by the old well, and that it had found light oil downdip of heavy oil.

The GS 160-5 ST-1 well (Fig. 5.52) flowed 8500 BOPD water free, with 32 API oil, confirming the pre-drill interpretation. Due to the meso-porous nature of the rock, decline rate was initially high as the largest pores were produced, but the well subsequently stabilized at around 700 BOPD as the finer grained pore systems began to contribute. The well was the first new field structural trap found in the 'back block' east of the field in 20 years.

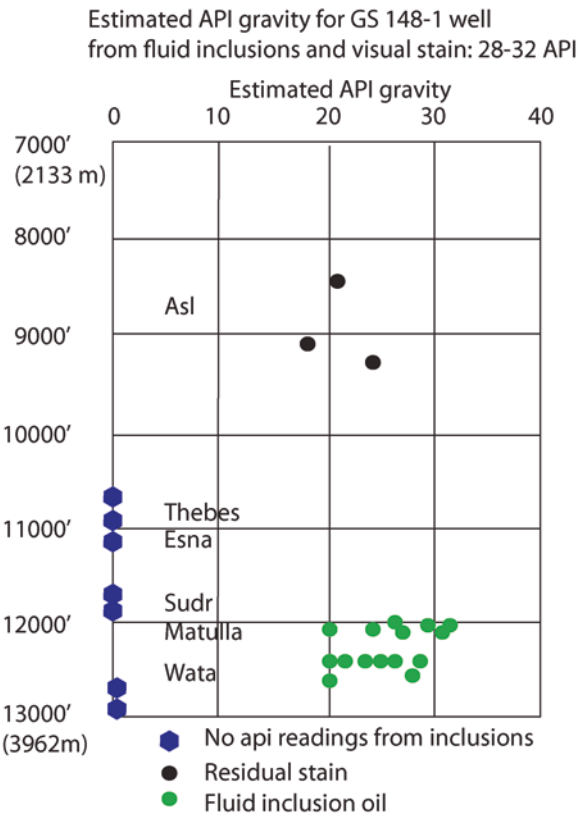

Fig. 5.49 Fluid inclusion results. Light oil gravities of 20–32 API supported visual observations of light oil in the cuttings, indicating a better quality oil downdip of the heavy oil accumulation in the "J" block

5.4.1.4 Case 4: "J" Platform Oil Discovery-Drilling Updip of Residual Oil, October Field, Egypt

The last case history from October Field involves looking updip of residual oil along a migration pathway to a continuous phase accumulation. One of the earliest northern exploratory tests were those of the GS 160-1 an GS 160-2 wells, drilled 1978 and 1979, respectively. Shows were encountered in both wells, but the shows in the GS 160-2 were nothing short of spectacular. Unfortunately, they were all residual oils (Fig. 5.53).

Hundreds of feet of sample and core stain were noted throughout the Nubia Formation, indicating an oil field had at one time existed in this area. The residual nature of the shows was clear from the log analysis, which showed 'lazy' Sw profiles in macro-porous multi-darcy reservoirs over a long interval with virtually no shale breaks or tight layers. If these shows had been in a continuous phase trap, there would have been an extremely sharp oil-water contact corresponding with the free water level, with little to no transition zone.

The interpretation at the time (Fig. 5.56, top right), especially given the poor seismic, was that the fault seals had failed with and vertical leakage or oil from the

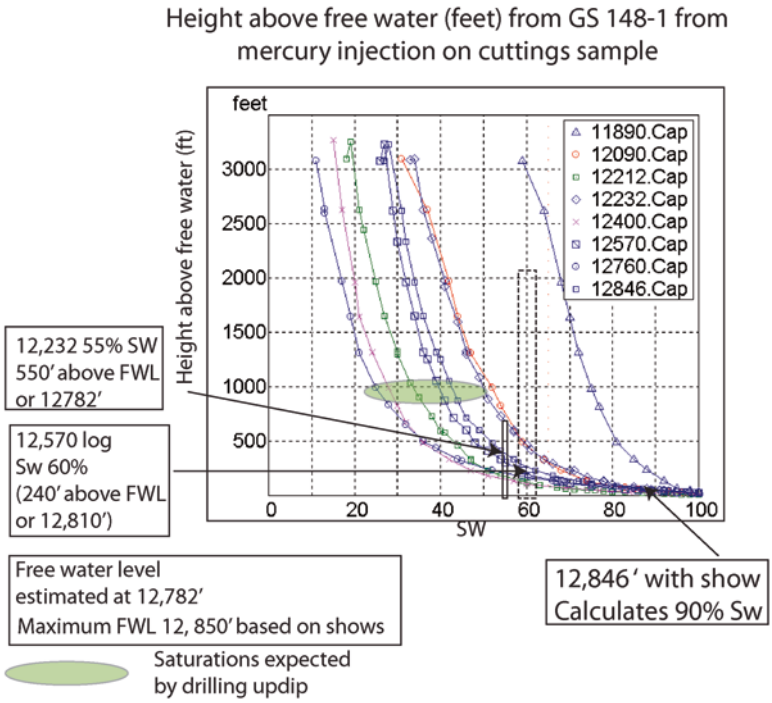

Fig. 5.50 Cap pressure and FWL analysis

older trap. For the next decade, the area was largely ignored as not having an effective seal. The prevailing wisdom at the time was that salt was needed to seal the Nubia. The salt seal concept persisted for many years with many people in the Gulf of Suez, despite the fact that the giant October Field was sealed by Miocene shales and in some areas, down-thrown Nezzazat Group.

In 1988, some additional geological work with dipmeters suggested that perhaps the big fault lay west of the GS 160-2 and there might still be oil located there. The J-1 well was spud in 1988, finding the 62 MMBO recoverable Nubia trap updip of the residual shows. At some point in geological history, the paleo-trap must have been huge, and while there was clear fault seal leakage, enough oil remained updip to make a commercial discovery.

In 1991, the downthrown side of the trap was tested and another 100 MMBOIP Miocene Asl Formation discovery was made. It is unlikely this additional resource would have been found in 1991 without the encouragement of the oil discovery in the adjacent fault block in the Nubia. In addition, the Miocene accumulations could be reached from the J platform, maximizing economic return.

These four case histories offer a glimpse of what can be done with sound geological thinking with cores, logs, cuttings and by working in integrated teams. It also demonstrates that alternative models are always the goal of an explorer and seeking out new data to test a concept is a vital part of the evaluation process. Lastly,

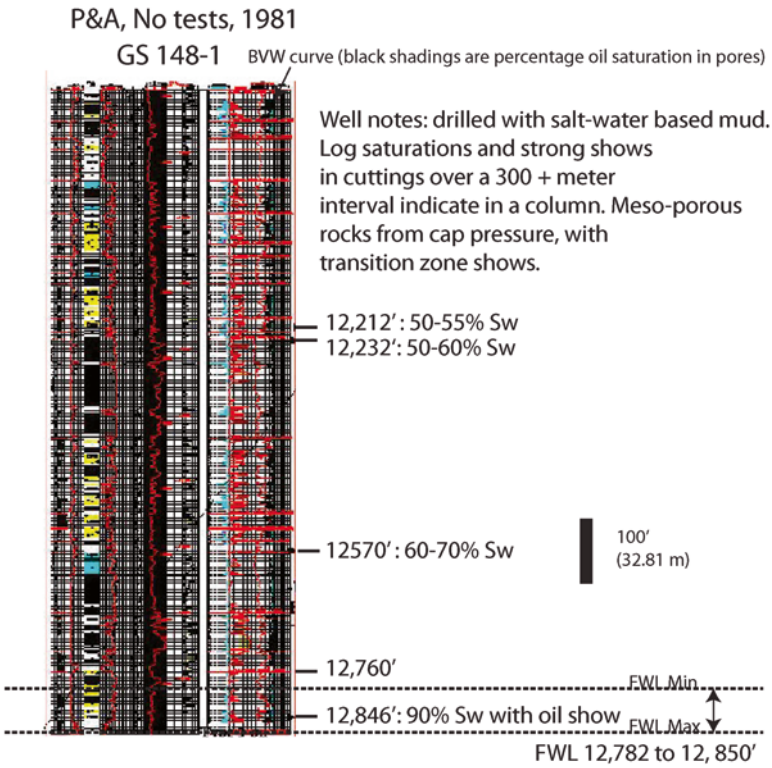

Fig. 5.51 GS 148-1 well log and free water level maximum and minimums

ideas are seldom good enough to insist that only one scenario is right. Quantitative risk assessment, using your best guess of minimum, most likely and maximum results is critical to become an effective explorer.

5.4.1.5 Case History 5: Buzzard Field, United Kingdom. Missing a Key Oil Show

One of the largest discoveries globally made in the last 15 years was that of the Buzzard Field in the North Sea (Carstens 2005; Ray et al. 2010; Robbins and Dore 2005). The prospective acreage block was acquired by Amoco in the late 1995, in partnership with British Gas. A commitment was made to drill one well and shoot 3D seismic (Fig. 5.54).

In 1999, Amoco was acquired by BP and in the subsequent reorganization, in which both companies lost over 70 % of their exploration staff, and much knowledge that went with it, the acreage was dropped as not prospective. Pan Canadian took operatorship of the block after swapping some acreage with BP-Amoco else-

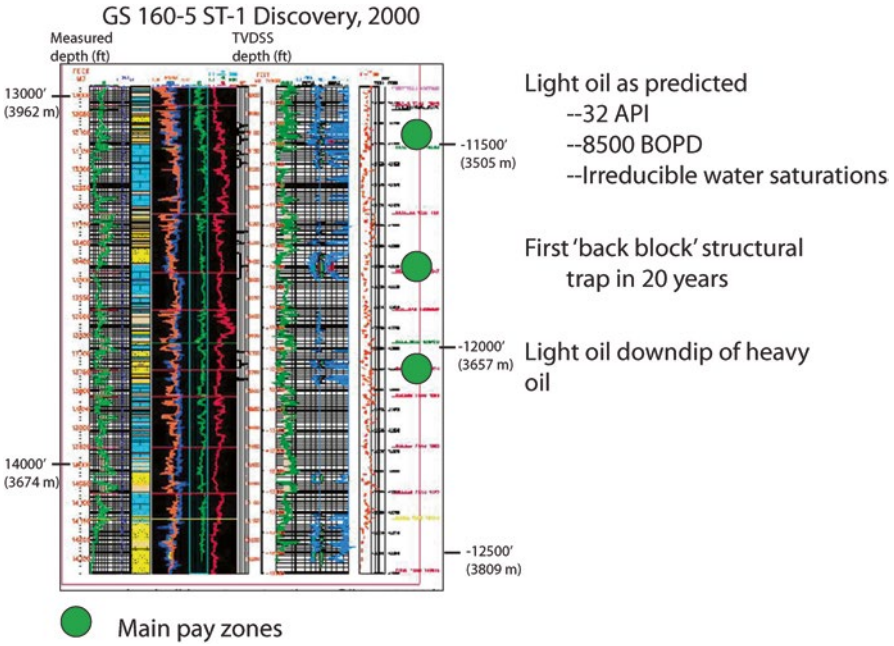

Fig. 5.52 GS 160-5 discovery

where in the world as part of the deal. The reason given at the time for dropping the acreage was that it was too far from the mature source rock and there was no evidence of a trap.

However, for the staff that acquired the acreage, attention to detail paid off. While there was very little structural closure anywhere in the area, a very small structural trap had been drilled in 1986 which found 3.5 m of pay at the top of highly porous and permeable Jurassic turbidite (Fig. 5.55, 20/6-2 Well). The presence of oil in the dry hole effectively dispelled the idea there could be no hydrocarbons on the block due to a lack of migration.

In 2001, the 20/6-3 discovery well was drilled to test a very large updip stratigraphic trap, encountering 300 ft. (121 m) of oil and testing 32° API oil at 6547 BOPD. STOIIP estimate is 1.4BBO, making it a world-class giant field discovery (Ray et al. 2010). The trap is a combination of fault closures on the north and south and stratigraphic closure to the west.

I was located in London with BP at the time the discovery was announced. Needless to say, there was quite a bit of discussion around 'what went wrong' with the decision to drop the acreage. On an aside, petroleum systems modeling is a crucial part of an exploration program, but the chances for lateral migration out of the kitchen should always be considered. There was nothing wrong with the models run by BP, which had accurately outlined the mature source rock kitchen. The oversite came from not looking carefully at the dry holes.

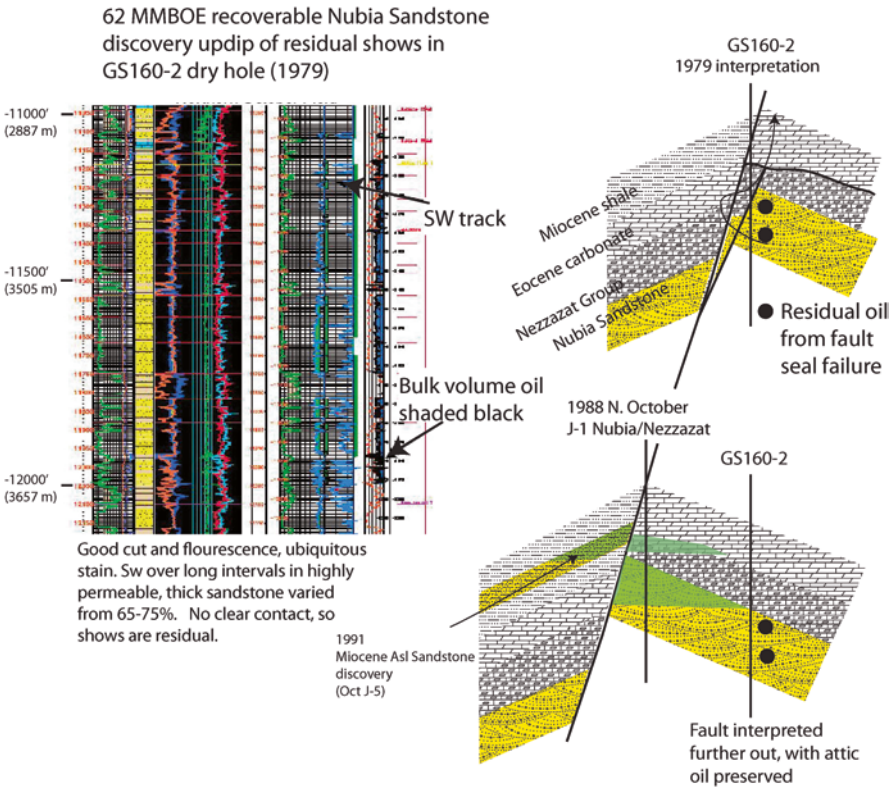

Fig. 5.53 Residual oil and re-interpretation

The only way to calibrate any migration model effectively beyond using algorithms in built into the software, is to look at shows in dry holes. In this case, geologists who had worked the dry holes carefully found that lateral migration had actually occurred on the block, proven by a thin oil pay on a very small trap. Others less familiar with the area did a cursory look a structure maps with no closure, wells labeled as dry holes and dismissed the acreage as not prospective.

In Chap. 9, the topic of how to model migration in both 2D and 3D is covered, with some more examples, but the emphasis on proof of the model will continue to be doing some hard work with the dry hole analysis.

5.4.1.6 Case History 6: Hugoton Field: Giant re-Migration Along Residual Migration Pathway

The following two cases look at re-migration and gas cap expansion and flushing as basins are uplifted and hydrodynamically re-organized. The first deals with the giant Hugoton-Panhandle Field, one of the largest contiguous gas accumulations in the

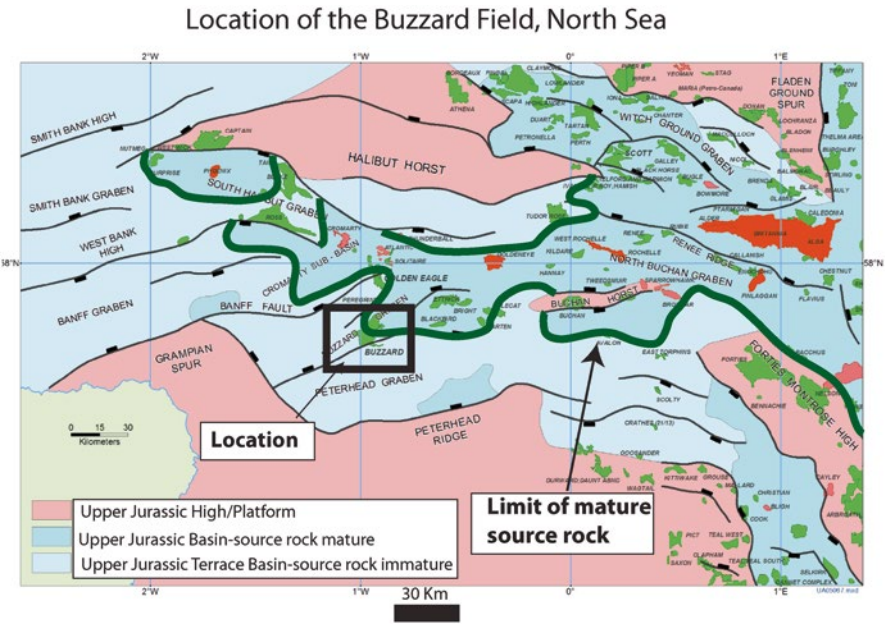

Fig. 5.54 Buzzard field location and edge of mature source rock kitchen. The discovery involved long range migration of 15–20 km from the mature source rocks to work. Figure copyright Nexen Petroleum UK Ltd

United States and the largest source of Helium in the US. The history and geology of the Hugoton Field has been summarized well by many (Frye and Leonard 1952; Pippin 1970; Rascoe 1988; Skelton 2014; Sorenson 2003, 2005). Sorenson's analysis of the uplift and charge history is particularly compelling and is summarized here.

This case history offers a good glimpse a re-migration and residual show development. Residual shows can be significant, as they can mark major migration pathways for re-migrated oil or gas from other traps. Exploration updip along the migration route may then offer new exploration opportunities. In addition, anomalous gas caps are often seen on oil fields that are far from gas generation kitchens. In many cases, these gas caps are from solution gas coming out of the oil column as the region is uplifted and overburden pressure reduced. Most Tertiary basins globally onshore have had extensive uplift and exhumation, and thus residual shows and gas cap expansion is not only common, but to be expected.

Besides the incredible trap size, which spans parts of Texas, Oklahoma and Kansas, the formation pressure is extremely low (435 psi, Fig. 5.56). This is due to Tertiary uplift and erosion, with communication to the outcrop 175 miles (280 km) to the east. It took years to recognize the size of this field after the first well was drilled in 1918 with a well in Texas, 21 mile north of Amarillo, on surface anticlinal closure. The Kansas extension was not discovered until 1922, and the initial well was not deemed that important. In 1939, however, a well hit southwest of the sleepy hamlet of Hugoton in Kansas, and started a drilling boom which lasted decades.

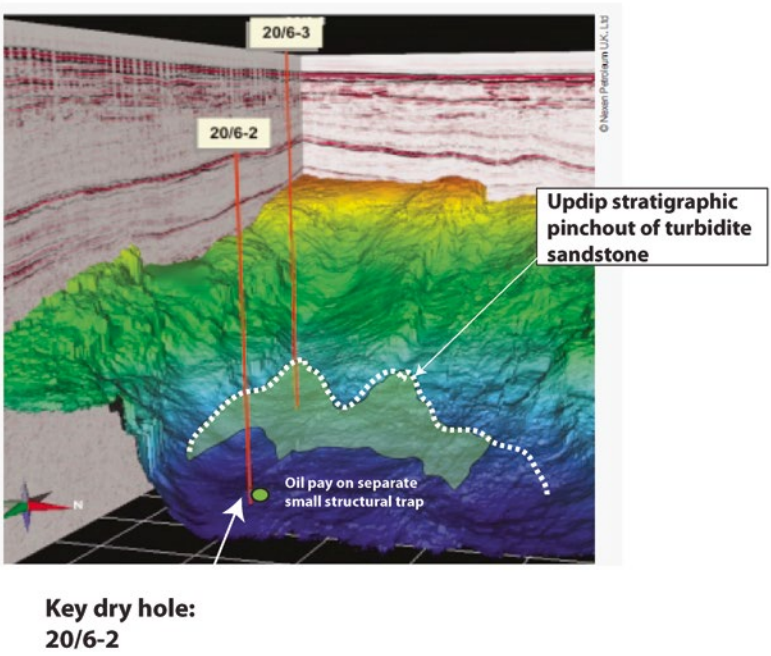

Fig. 5.55 3D view of the Buzzard stratigraphic trap. The trap is a combination of fault trapping on the south end and updip an updip pinchout of the turbidite fan. Modified from Carstens (2005). Figure copyright Nexen Petroleum UK Ltd

Some of the later CEO's and Presidents of Amoco Production Company were involved as younger geoscientists in trying to further delineate the field limits in the 1950s. As the trap wasn't well defined, it was delineated by drilling the center of every square mile (sections) in the Hugoton embayment and simply looking where gas shows stopped and water cut increased. This simple technique was used to lock up a huge tract of land which has been producing for decades.

The trap itself has been debated, as there are well known tilted oil and gas water contacts dipping to the east (Pippin 1970) which support a hydrodynamic component. However, equally important is a facies change from regionally porous carbonates to tight red-bed shales and sandstones of continental facies to the east. The change from macro and meso porous carbonates to tight shales and sands can also produce a tilted contact, due to capillarity. In any event, the field location is well established.

Initial charging was in the late Permian from mature source kitchens to the north of the Panhandle Field, a very large structural closure that first filled migrated oil and gas (Fig. 5.56). This structure would have been filled to spill point and normally pressured at the time of migration (Fig. 5.57).

By Cretaceous time, however, regional stress fields had shifted and the basins reorganized so that tilt toward the west and a Cretaceous sag basin began to reorganize older hydrocarbon accumulations. This tilt direction was reversed in the early

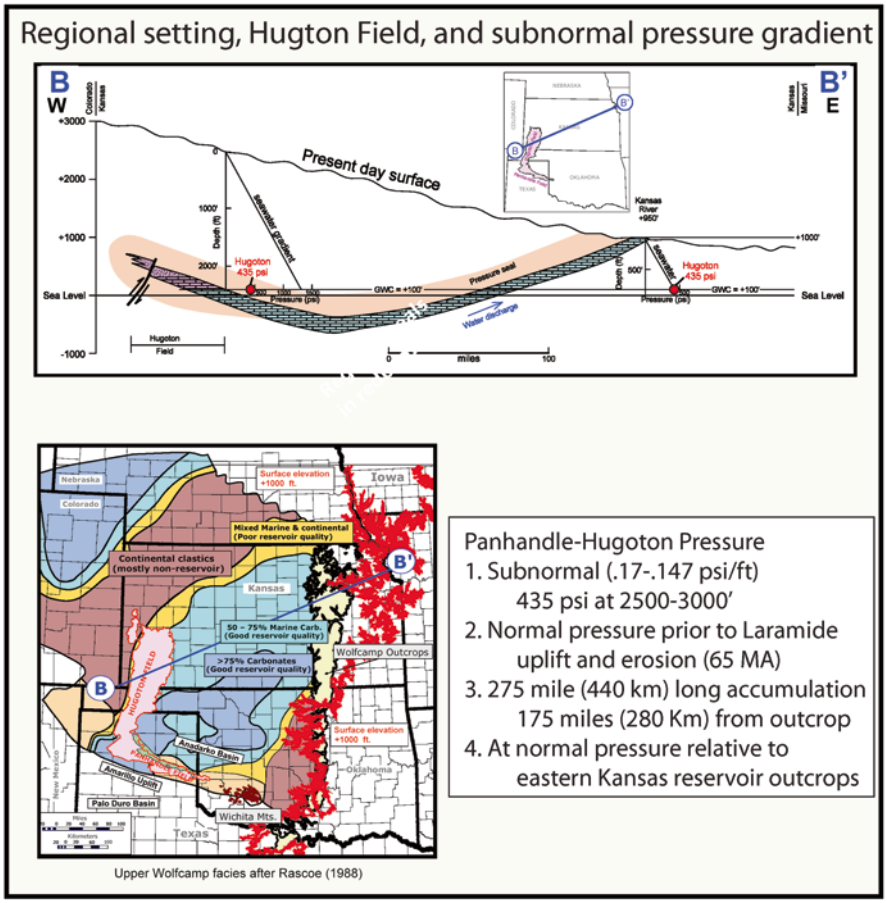

Fig. 5.56 Hugoton field pressure setting, location and facies. The field is underpressured relative to depth the aquifer is normally pressured relative to the outcrop to the east. Figure modified from Sorenson (2003), with permission

Tertiary with the onset of the Laramide orogeny, which gave rise to the Rocky Mountains. As the Western Interior Seaway was uplifted and drained 65 Ma during the Laramide orogeny, major losses of hydrocarbons from the Panhandle Field occurred. A northwestward tilt and spill from the Panhandle Field set up the first major re-migration of hydrocarbons toward a regional stratigraphic trap edge in western Kansas. As tilt and migration accelerated, pressure was dropped as hydrocarbons escaped and extensive residual oil shows were left around the flank and within the Panhandle Field, which was now beginning to develop a substantial gas cap from fluid expansion.

By late Tertiary, enormous quantities of gas and oil had remigrated into a giant stratigraphic trap to the west and north along the edge of the regional seals in the continental red beds. Coincident with continued uplift was erosion of the major

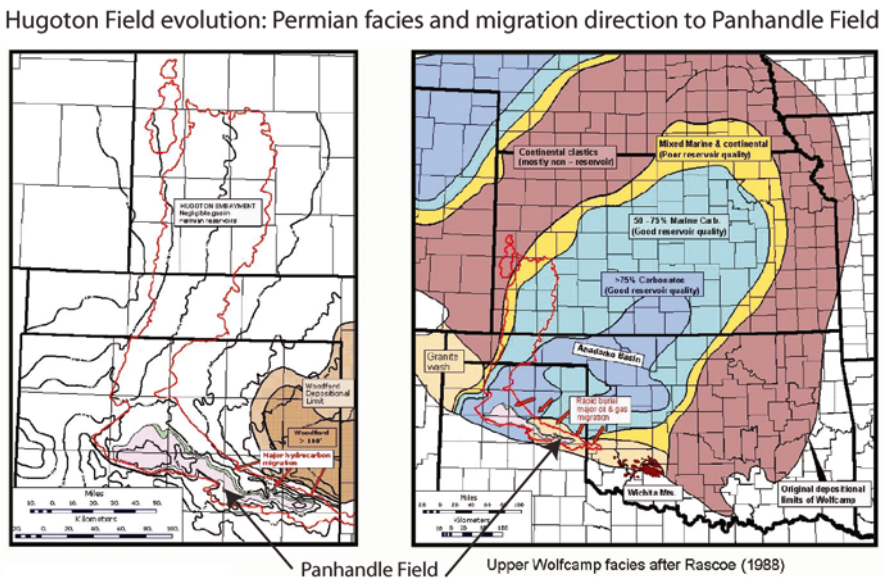

Fig. 5.57 Permian migration into giant structural traps in Panhandle Field. Figure modified from Sorenson (2003), with permission

reservoir facies east of the field in eastern Kansas. Communicating the Hugoton aquifer to the surface eastward resulted in further regional pressure reduction and further gas expansion, displacing even more liquids as gas came out of solution.

If Sorenson's model is correct, the process of final gas cap expansion was complete during the last Pleistocene ice age (Fig. 5.58), when glaciers further exhumed the major reservoir facies in northeastern Kansas. With aquifers cropping out to the east, a regional hydrodynamic flow from west to east was also developed, potentially the cause of the tilted oil and gas water contacts, which, not coincidentally, deepen to the east as would be predicted under hydrodynamic conditions.

While there may be little exploration significance at this time to understanding this process, it provides a good example of uplift and re-migration. There are many, many onshore basins where uplift and remigration has occurred, leaving abundant residual shows which can significantly complicate exploration, but also provide opportunities for those astute enough to figure out where all those older trapped hydrocarbons ended up.

5.4.1.7 Case History 7: West Siberian Basin, Russia: Perhaps the World's Largest Residual Migration Pathway

I had the opportunity with TNK-BP to explore in the West Siberian Basin for 4 years from 2004 to 2008. I can truly say that I have not worked a more petroliferous basin either in volume of source rocks, oil and gas generated or physical size

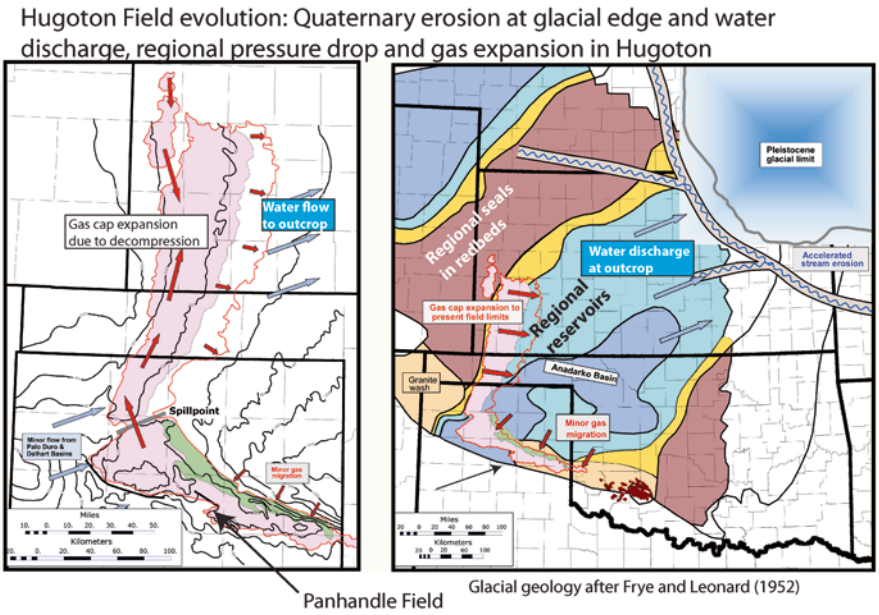

Fig. 5.58 Pleistocene glaciation and pressure release. Figure modified from Sorenson (2003), with permission

anywhere in the world. Much of this discussion is documented in Igoshkin et al. (2008), with a more quantitative look at the gasses and re-migration model presented by Littke et al. (1999).

The basin contains some of the largest hydrocarbon accumulations in the world, dominated by Cretaceous deltaic reservoirs that prograde over and tap into, and underlying rich source rock, the Jurassic Bazhenov Formation, one of the thickest and richest source rocks in the world. The basin is big enough to swallow all of the central United States from the Canadian border to Gulf of Mexico and in width from Ohio to Denver, Colorado (Fig. 5.59).

The Bazhenov Formation is not the only source rocks, as there are others above and below it (Dolson et al. 2014; Hafizov et al. 2014) and it is thermally mature over most of the basin (Fig. 5.60).

There is a good fit to Bazhenov maturation levels and fluid type in the major fields, with the large gas and gas-condensate fields located to the north near the gas kitchens. The fit is not perfect, however, as there are a number of gas fields, as well as fields with thin oil legs and thick gas caps, located in areas that are dominantly oil prone at the Bazhenov level.

The location of the large gas fields, and in particular, fields with reported oil rims and residual shows are shown north of the dashed line. The giant Urengoy Field is a huge structural trap lies in the heart of the gas kitchen but also has significant oil rims on the flanks. It has up to 369 TCF of gas, dwarfing all other fields globally with the exception of North Dome in the Middle East. Particularly anomalous in the

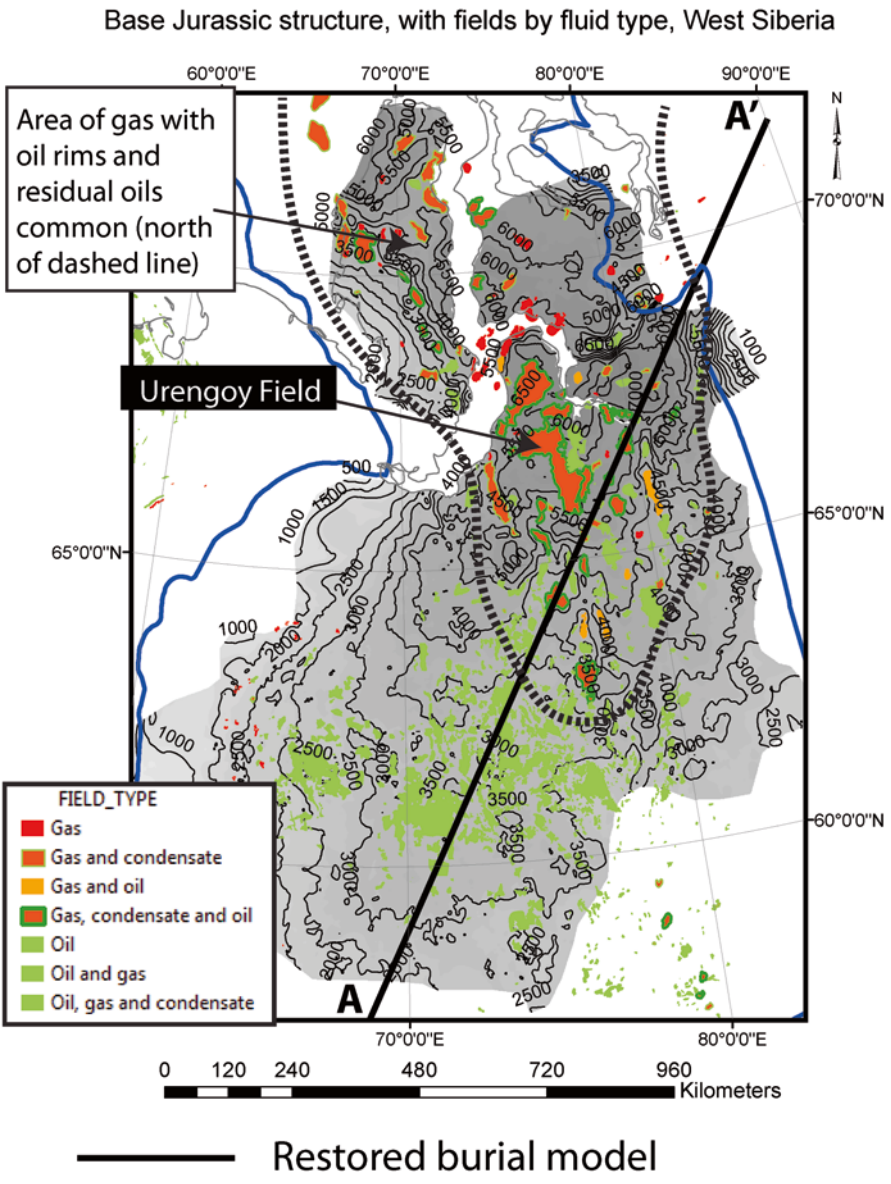

Fig. 5.59 West Siberian Basin structure map, base of Jurassic, with field outlines

Urengoy area is are huge accumulations of dry gas. Five other mega-giant gas traps exist with greater than 90 TCF per trap, collectively forming the largest concentration of giant conventional gas traps in the world.

While some of the changes in gas character might be attributed by some to variability in the source rock type and kinetics of the Bazhenov source rock, Littke et al.

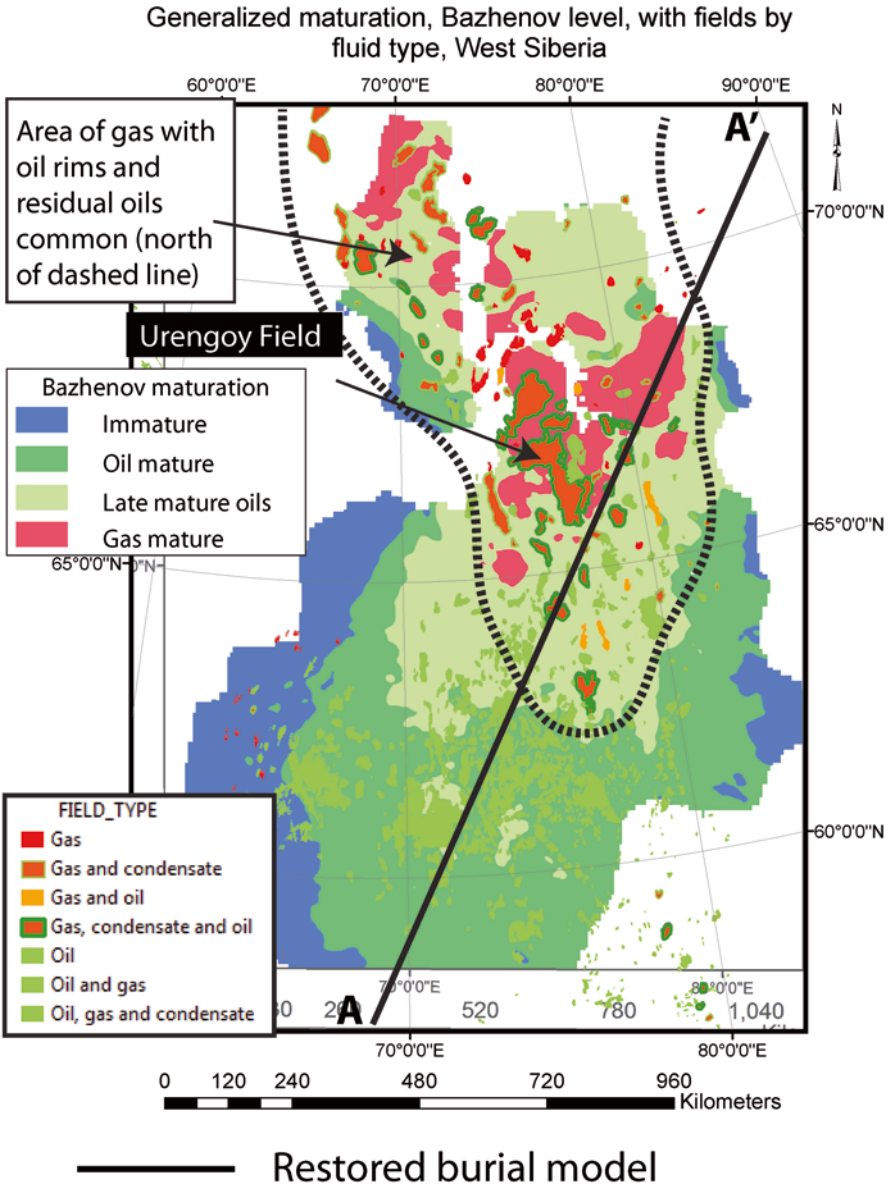

Fig. 5.60 Maturation, Bazhenov Formation. Maturation windows ae somewhat are generalized

(1999) makes a compelling case that much of the dry gas is from gas expansion and flushing of oil as the northern part of the basin was uplifted and eroded in early Eocene time. Work we completed at TNK-BP also supports the Littke model.

A Trinity based erosion restoration and uplift cross section (Fig. 5.61) was built from maps generated by the Geoseis Company in Tyumen, Russia (Igoshkin et al.

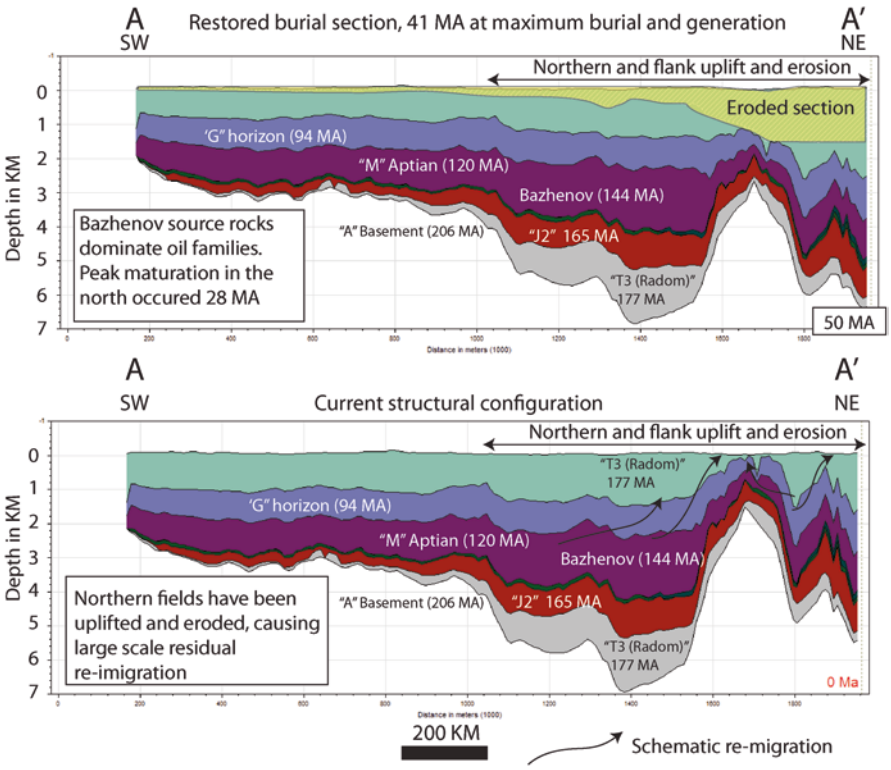

Fig. 5.61 Regional erosion section showing maximum burial at 50 Ma (**a**) and current structural configuration (**b**). See Figs. 5.59 and 5.60 for location

2008). These maps were built using seismic and sonic velocity from wells to try to estimate the magnitude of Tertiary uplift (Fig. 5.62).

Most of the large gas caps occur north of the 200 m erosion line and parts of the basin on the flank have had over 1500 m of uplift. As shown in cross-section A-A′ (Fig. 5.63), any oil trapped prior to the Eocene and Oligocene uplift would be spilled northward and toward the basin edges. Interestingly, the southern basins have not undergone significant erosion, and there are few gas fields or gas caps.

What is the impact? If the models proposed by Littke et al. (1999) are correct, much of the volume of gas found in the northern part of the basin cannot be explained by simple maturation models and gas generated from source rocks. However, they can be explained better as part of the process of dissolution and re-migration as gas caps expanded and flushed heavier hydrocarbons to the flanks of the fields.

Hugoton Field was an example of a giant re-migration. In West Siberia, the volumes and aerial extent of this migration even are an order of magnitude more. The question for exploration might well be "what happened to all that oil?"

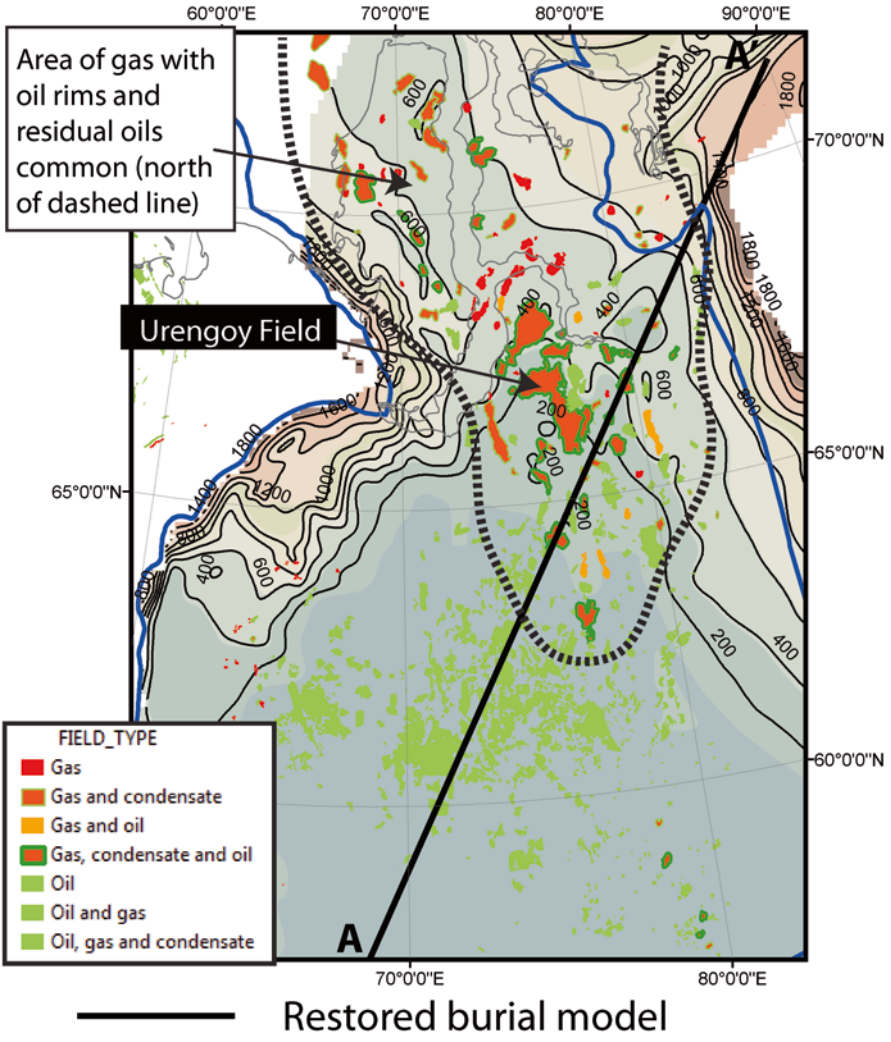

Fig. 5.62 Tertiary erosion map

5.5 Summary

Understanding capillarity is an essential part of any geoscientist's tool kit. Screening plots of rock type using Winland analysis is a quick way to assess pore type and potential facies control on flow. Pseudo-capillary pressure is an especially powerful and quick way to assess seals and reservoirs. Spreadsheets (Appendices B–D) allow rapid testing of seal capacity and reservoir performance. The more detailed your

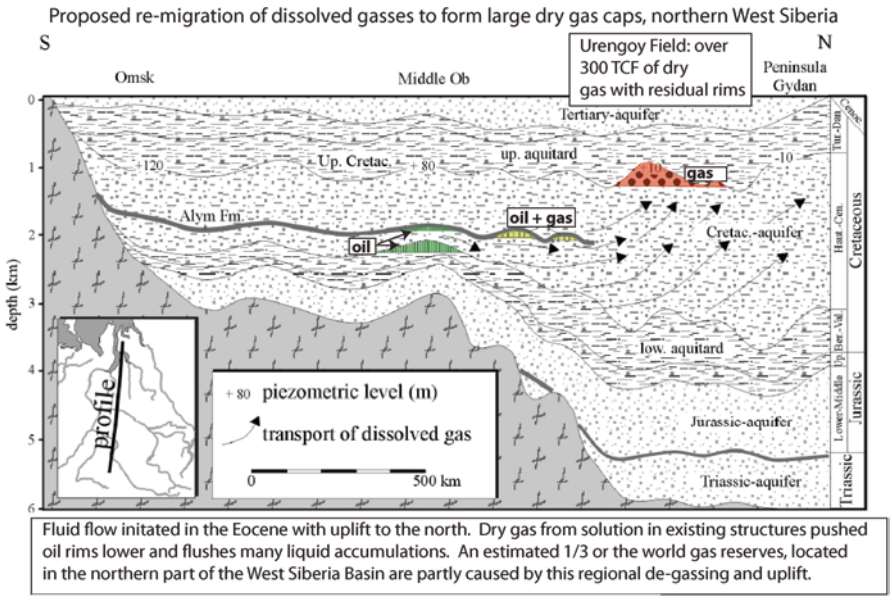

Fig. 5.63 Impact of Tertiary re-migration and gas expansion. Modified from Littke et al. (1999). Reprinted by permission of the AAPG, whose further permission is required for further use

maps become, with geologically and seismically constrained facies and faults, the better your chance of finding new fields.

Any software package capable of dealing with grid math can be used to make both hydrodynamic and seal trap maps. However, making a seal trap map by hand can just as easily be done by examining shows and tests overlain on a good structural map, with seal edges shaped to explain the tests and shows. It doesn't really matter which tools you choose to use.

Recognizing hydrodynamic flow has to come from looking a pressure data or recognition of tilted contacts that can't be explained easily with capillarity. Building fault or facies maps takes good judgement and calibration to cores, known columns, pressures, or test and show data. Failure to build these kinds of maps inevitably means a higher risk of getting the trap wrong or failing to recognize the full potential in an area.

The tools demonstrated in this and other chapters allow you to do that. It is also my personal belief that every explorer should get as familiar with migration modeling as possible, taking the time and expense to acquire the proper tools to test ideas quickly. A huge advantage of petroleum systems tools is the ability to vary the top seals, and visualize and model migration in 3D space (Chap. 9). Additionally, it is possible to incorporate timing of oil and gas generation, migration volume loss, volumes generated, uplifted, eroded and re-migrated with seal and pressure changes through time. These kinds of additional tools can greatly help reduce exploration risk.

The case histories in this chapter illustrate a variety of ways that quantitative show and seal assessment can be made to understand prospectivity as well as reser-

voir scale development. Understanding where you are in a trap, on a migration pathway or within a mature organically rich source rock is essential to successfully explore for and develop hydrocarbons.

References

Abdallah W, Buckley JS, Carnegie A, Edwards J, Fordham E, Graue A, Habashy T, Seleznev N, Signer C, Hussain H, Montaron B, Ziauddin M (2007) Fundamentals of wettability. Oilfield Review, Schlumberger, pp 44–61

Asquith G, Krygowski D (eds) (2004) Basic well log analysis, 2nd edn, AAPG methods in exploration series. American Association of Petroleum Geologists, Tulsa, OK, 244 p

Berg R (1975) Capillary pressures in stratigraphic traps. Am Assoc Pet Geol Bull 59:939–956

Byrnes AP, Cluff RM, Webb JC (2009) Analysis of critical permeability, capillary and electrical properties for mesaverde tight gas sandstones from western U.S. Basins. U.S. Department of Energy final technical report for project #DE-FC26-05NT42660, U. S. Department of Energy, p 355. doi:10.2172/971248

Carstens H (2005) Buzzard- a discovery based on sound geological thinking. GEO ExPro, p 34–38

Chidsey CT Jr, Eby DE (2009) Regional lithofacies trends in the Upper Ismay and Lower Desert Creek zones in the Blanding sub-basin of the Paradox Basin, Utah, the Paradox Basin revisited-new developments in petroleum systems and basin analysis, v. RMAG 2009 Special Publication. Rocky Mountain Association of Geologists, Denver, CO, pp 436–470

Coalson EB, DuChene HR (2009) Deposition of Upper Ismay carbonate mounds, Blanding Subbasin of the Paradox Basin, Utah. The Paradox Basin revisited-new developments in petroleum systems and basin analysis, RMAG Special Publication. Rocky Mountain Association of Geologists, Denver, CO, pp 471–495

Dahlberg EC (1995) Applied hydrodynamics in petroleum exploration, 2nd edn. Springer Verlag, New York, 295 p

Dolson JC, Steer B, Garing J, Osborne G, Gad A, Amr H (1997) 3D seismic and workstation technology brings technical revolution to the Gulf of Suez Petroleum Company. Lead Edge 16:1809–1817

Dolson JC, Sisi ZE, Ader J, Leggett B, Sercombe B, Smith D (1998) Use of cuttings, capillary pressure, oil shows and production data to successfully predict a deeper oil water contact, Wata and Matulla Formations, October Field, Gulf of Suez. In: Eloui M (ed) Proceedings of the 14th petroleum conference, vol 1. The Egyptian General Petroleum Corporation, Cairo, Egypt, pp 298–307

Dolson JC, Bahorich MS, Tobin RC, Beaumont EA, Terlikoski LJ, Hendricks ML (1999) Exploring for stratigraphic traps. In Beaumont EA, Foster NH (eds) Exploring for oil and gas traps: treatise of petroleum geology. Handbook of petroleum geology. American Association of Petroleum Geologists, Tulsa, Oklahoma pp 21.2–21.68.

Dolson JC, Pemberton SG, Hafizov S, Bratkova V, Volfovich E, Averyanova I (2014) Giant incised vally fill and shoreface ravinement traps, Urna, Ust-Teguss and Tyamkinskoe Field areas, southern West Sibertian Basin, Russia, American Association of Petroleum Geologists Annual Convention, Houston, Texas, Search and Discovery Article #1838534, p 33

Dolson J, Burley SD, Sunder VR, Kothari V, Naidu B, Whiteley NP, Farrimond P, Taylor A, Direen N, Ananthakrishnan B (2015) The discovery of the Barmer Basin, Rajasthan, India, and its petroleum geology. Am Assoc Pet Geol Bull 99:433–465

Ebanks J, Scheihing NH, Atkinson CD (1992) Flow units for reservoir characterization. In: Morton-Thompson D, Woods AM (eds) Development geology reference manual, vol 10, AAPG methods in exploration series. American Association of Petroleum Geologists, Tulsa, OK, pp 282–285

Eby DE, Thomas J, Chidsey C, McClure K, Morgan CD (2003) Heterogeneous shallow-shelf carbonate buildups in the Paradox Basin, Utah and Colorado: targets for increased oil production and reserves using horizontal drilling techniques. Utah Geological Survey, Salt Lake City, UT, p 23

Farrimond P, Naidu BS, Burley SD, Dolson J, Whiteley N, Kothari V (2015) Geochemical characterization of oils and their source rocks in the Barmer Basin, Rajasthan, India. Pet Geosci 21:301–321

Frye JC, Leonard AB (1952) Pleistocene geology of Kansas (Bulletin 99). State Geological Survey of Kansas, Lawrence, Kansas, 230 p

Grammer GM, Eberli GP, Buchem FSPV, Stevenson GM, Homewood P (1996) Application of high-resolution sequence stratigraphy to evaluate lateral variability in outcrop and subsurface--Desert Creek and Ismay intervals, Paradox Basin. In: Longman MW, Sonnenfeld MD (eds) Paleozoic systems of the Rocky Mountain Regiona. Rocky Mountain Section, SEPM (Society for Sedimentary Geology), Denver, CO, pp 235–266

Gunter GW, Finneran JM, Hartmann DJ, Miller JD (1997) Early determination of reservoir flow units using an integrated petrophysical method. Society of Petroleum Engineers, v. SPE 38679, pp 1–8

Hafizov S, Dolson JC, Pemberton G, Didenko I, Burova L, Nizyaeva I, Medvedev A (2014) Seismic and core based reservoir characterization of the Giant Priobskoye Field, West Siberia, Russia, American Association of Petroleum Geologists, annual convention, Houston, TX, Search and Discovery Article #1838540, p 31

Hall D (2008) Fluid inclusions in petroleum systems. In: Hall D (ed) AAPG getting started Series No. 15. American Association of Petroleum Geologists, Tulsa, OK

Hartmann DJ, Beaumont EA (1999) Predicting reservoir system quality and performance. In: Beaumont EA, Foster NH (eds) Exploring for oil and gas traps: treatise of petroleum geology, handbook of petroleum geology, vol 1. American Association of Petroleum Geologists, Tulsa, OK, pp 3–154

Hawkins JM, Luffel DL, Harris TG (1993) Capillary pressure model predicts distance to gas/water, oil/water contact. Oil Gas J: 39–43

Hubbert MK (1953) Entrapment of petroleum under hydrodynamic conditions. Am Assoc Pet Geol Bull 37:1954–2026.

Igoshkin VJ, Dolson JC, Sidorov D, Bakuev O, Herbert R (2008) New Interpretations of the Evolution of the West Siberian Basin, Russia. Implications for exploration, American Association of Petroleum Geologists. Annual conference and exhibition, San Antonio, TX, AAPG Search and Discovery Article #1016, p 1–35

Jennings JB (1987) Capillary pressure techniques: application to exploration and development geology. Am Assoc Pet Geol Bull 71:1196–1209

Littke R, Cramer B, Gerling P, Lopatin NV, Poelchau HS, Schaefer RG, Welte DH (1999) Gas generation and accumulation in the West Siberian Basin. Am Assoc Pet Geol Bull 83:1642–1665

McClure K, Thomas J, Chidsey C, Mitchum RM, Morgan CD, Eby DE (2003) Heterogeneous shallow-shelf carbonate buildups in the Paradox Basin, Utah and Colorado: targets for increased oil production and reserves using horizontal drilling techniques: deliverable 1.1.1. Utah Geological Survey, Salt Lake City, UT, p 44

Meckel LD (1995) Chapter 5: Shows. In: Dolson J, Gibson R, Traugott MO (eds) Shows and seals workshop notes (unpublished). Gulf of Suez Petroleum Company (GUPCO)-a subsidiary of Amoco Production Company, Cairo, Egypt

Naidu BS, Burley SD, Dolson J, Farrimond P, Sunder VR, Kothari V, Mohapatra P, Whiteley N (2016) Hydrocarbon generation and migration modelling in the Barmer Basin of western Rajasthan, India: lessons for exploration in rift basins with late stage inversion, uplit and tilting. Petroleum system case studies, v. Memoir 112. American Association of Petroleum Geologists, Tulsa, OK

O'Sullivan T, Zittel RJ, Beliveveau D, Wheaton S, Warner HR, Woodhouse R, Ananthkirshnan B (2008) Very low water saturations within the sandstones of the Northern Barmer Basin, India, SPE, v. 113162, pp 1–14

O'Sullivan T, Praveer K, Shanley K, Dolson JC, Woodhouse R (2010) Residual hydrocarbons--a trap for the unwary, SPE v. 128013, pp 1–14

O'Connor SJ (2000) Hydrocarbon-water interfacial tension values at reservoir conditions. Inconsistencies in the technical literature and the impact on maximum oil and gas column height calculations. Am Assoc Pet Geol Bull 84:1537–1541

Pepper A (2007) Fluid properties: density and interfacial tension (IFT)--quantitative impact on petroleum column capacity evaluation in exploration and production (abs.), AAPG Hedberg Conference: basin modeling perspectives: innovative developments and novel applications. American Association of Petroleum Geologists, The Hague, The Netherlands

Peterson JA (1992) Aneth Field--USA. Paradox Basin, Utah. In: Foster NH, Beaumont EA (eds) Stratigraphic traps III. American Association of Petroleum Geologists, Tulsa, OK, pp 41–82

Pippin L (1970) Panhandle-Hugoton Field, Texas-Oklahoma-Kansas-The first fifty years. In: Halbouty MT (ed) Geology of giant petroleum fields, Memoir 14. American Association of Petroleum Geologists, Tulsa, OK, pp 204–222

Pittman E (1992) Relationship of porosity and permeability to various parameters derived from mercury injection-capillary pressure curves for sandstone. Am Assoc Pet Geol Bull 76:191–198

Rascoe B (1988) Permian system in western Midcontinent. In Morgan WA, Babcock JA (eds) Permian rocks of the midcontinent: Special Publication 1, Midcontinent SEPM, pp 3–12

Ray FM, Pinnock SJ, Katamish H, Turnbull JB (2010) The Buzzard field: anatomy of the reservoir from appraisal to production: petroleum geology conference series 2010, pp 369–386

Robbins J, Dore G (2005) The Buzzard Field, Outer Moray Firth, Central North Sea, AAPG annual conference and exhibition, Calgary, AB, American Association of Petroleum Geologists, Search and Discovery #110016, p 19

RPSEA (2009) First ever ROZ (Residual Oil Zone) symposium, Midland, TX, Research Partnership to Secure Energy for America (RPSEA), p 59

Schowalter TT (1979) Mechanics of secondary hydrocarbon migration and entrapment. Am Assoc Pet Geol Bull 63:723–760

Schowalter TT, Hess PD (1982) Interpretation of subsurface hydrocarbon shows. Am Assoc Pet Geol Bull 66:1302–1327

Sercombe WJ, Thurmon L, Morse J (2012) Advance reservoir modeling in poor seismic: October Field, northern Gulf of Suez, Egypt. AAPG international conference and exhibition, Milan, Italy, American Association of Petroleum Geologists Search and Discovery Article #40872

Shanley KW (2007) Pore-scale to basin-scale impact on gas production from low-permeability sandstones. TNK-BP, Moscow, Turris, p 52

Shanley KW, Cluff RM (2015) The evolution of pore-scale fluid-saturation in low-permeability sandstone reservoirs. Am Assoc Pet Geol Bull 99:1957–1990

Skelton LH (2014) Hugoton's rich history, AAPG explorer. American Association of Petroleum Geologists, Tulsa, OK, pp 40–44

Sorenson RP (2003) A dynamic model for the Permian Panhandle and Hugoton Fields, Western Anadarko Basin. 2003 AAPG mid-continent section meeting, Tulsa, OK, AAPG Search and Discovery Article #20015, p 11

Sorenson RP (2005) A dynamic model for the Permian Panhandle and Hugoton fields, western Anadarko Basin. Am Assoc Pet Geol Bull 89:921–938

Swanson VF (1981) A simple correlation between permeabilities and mercury capillary pressures. J Pet Technol 33:2488–2504

Thomeer JHM (1960) Introduction of a pore geometrical factor defined by capillary pressure curve. J Pet Technol 12:73–77

Trudgill BD, Arbuckle WC (2009) Reservoir characterization of clastic cycle sequences in the Paradox Formation of the Hermosa Group, Paradox Basin, Utah. In: U. G. Survey. Utah Geological Survey, Salt Lake City, UT

Vavra CL, Kaldi JG, Sneider RM (1992) Geological applications of capillary pressure: a review. Am Assoc Pet Geol Bull 76:840–850

Washburn EW (1921) Note on a method of determining the distribution of pore sizes in a porous material. Proc Natl Acad Sci 7:115–116

Winland HD (1972) Oil accumulation in response to pore size changes, Wyburn Field, Saskatchewan. Amoco Production Company report F72-G-25 (unpublished), Tulsa, OK, p 20

Winland HD (1976) Evaluation of gas slippage and pore aperture size in carbonate and sandstone reservoirs. Amoco Production Company report F76-G-5 (unpublished), Tulsa, OK, p 25

Wold JT (1978) Cache field I-II. Four Corners Geological Society, Durango, CO, pp 108–110

Chapter 6
Basic Log Analysis, Quick-Look Techniques, Pitfalls and Volumetrics

Contents

Abstract An understanding of basic log analysis is essential for any geoscientist. The process, however, can be very difficult in some types of rocks and fluid combinations. Conductive minerals can suppress resistivity, making zones look wet that are actually pay zones. Fresh water, likewise, can be difficult to distinguish from hydrocarbons. Thinly laminated pay zones can also be problematic, as both GR and resistivity logs may failure to accurately account for the thin reservoir layers. High clay content with high bound water can also cause low resistivity readings and high water saturations in zones that actually flow hydrocarbons.

J. Dolson, *Understanding Oil and Gas Shows and Seals in the Search for Hydrocarbons*, DOI 10.1007/978-3-319-29710-1_6

Logs do not measure porosities directly, but rather rock properties like travel time or density that must then use further calculations to estimate porosity. Once porosities and lithologies are determined, the Rw of the formation waters must be calculated and used in the water saturation equations. All of these steps introduce some potential error in the final analysis which, which is only as good as the input parameters.

Residual saturations, in tight rock, can be as low as 35 % Sw, and be very difficult to distinguish from moveable hydrocarbons. Lastly, some clays and well completion techniques can cause formation damage which can lead to good pay zones being dismissed as non-prospective.

6.1 Overview

Being able to perform basic log analysis and calculation of porosity and water saturation is a fundamental skill required of every geologist. This is especially true for taking 'quick looks' at potential pay zones and for estimating prospect reserves. A full treatment of this subject is beyond the scope of this book, and basic terms and concepts were outlined previously in Chap. 3. As such, this section highlights basic procedures only, with some examples of useful plots to make to look for continuous phase shows and if the shows are in transition zone or waste zone positions. Log analysis is not just about generating numbers to get an Sw for volumetric and reserve assessment. The results always need to be put back into the context of 'where am I in the trap'? The prior chapters have dealt with that topic in detail, but there are additional techniques with logs covered in this chapter that are very useful.

For serious learners, the best textbook is that of (Asquith and Krygowski 2004), which also comes with .las files of actual wells that can be worked with on any workstation. In addition, it comes with Excel spreadsheets which can provide solutions if the reader does not have access to geological interpretive software. Other good references are (Asquith 1985, 2006; Doveton 1994; Hartmann and Beaumont 1999; Krygowski 2003; Krygowski and Cluff 2012; Lovell and Parkinson 2002; Passey et al. 2006c).

In addition, there are pitfalls to log analysis, in the form of bed resolution, conductive minerals, complex pore networks and even formation damage. I have had more than one well calculate pay and then fail when tested, only to find out later that the formation had been damaged beyond repair by completion fluids, overly clay swelling or migration in pores, acid treatments that react badly with matrix cements, or other causes. Fortunately, these events are not that common, but they do occur. When evaluating your own results or post-appraising dry holes, keeping formation damage in mind or completion techniques sometimes explains why a well didn't test well, but calculated pay.

An additional pitfall are residual oils and gasses, which can have low Sw, particularly in tight rocks, where they might even look like productive pay zones but then flow nothing but water.

These topics are covered in this section, in addition to the basics of how to calculate porosity and Sw. This chapter is intended as only a broad overview of these topics, especially for younger geoscientists with little to no prior background in log analysis.

6.2 The Archie Equation and Finding Rw

Most basic log analysis ultimately comes back to fundamentals identified by Gus Archie (Archie 1942), using resistivity logs (Fig. 6.1). The basic principal guiding this analysis is the assumption that if the resistivity of the formation waters is known, then when more resistive formations are encountered, there may be hydrocarbons present, as they are less conductive than water.

The equation is:

There are limits to the Archie equation, however, in that it works best with the intercrystalline and intergranular porosity. This is also true for the pseudo-capillary pressure analysis discussed in Chap. 5. If rocks have complex pore throat networks (like vugular, disconnected porosity in some oolitic limestones, neither the pseudo-capillary pressure nor Archie equations will work well).

6.2.1 Archie Equation Limits Due to Shaliness

As the degree of shaliness increases, further complications arise. Entire books are devoted to handling that topic alone (Passey et al. 2006b, c, d; Sneider 2003; Sneider and Kulha 1995). The degree of shaliness is important to understand, as relatively clay free reservoirs, in many environments, are the exception. Figure 6.2 (Chai et al. 2008) provide an example from shallow marine tidal flats and burrowed shoreface sandstones in Malaysia. In cases like these, the logs themselves may be limited in resolution and the productive laminated sandstones not even recognized on the logs (more on this in a later section).

Archie Equation

$$Sw = \left(\frac{a * Rw}{(\emptyset^{m} * Rt)} \right)^{\frac{1}{n}}$$

Sw = water saturation, decimal %
a = tortuosity factor (usually assumed as 1)
n = saturation exponent (normally 2 but varies from 1.8-4.0)
Rw = formation water resistivity at formation temperature (ohm-m)
Ø = porosity (decimal %)
m = cementation exponent, normally 2 but varies from 1.7-3
Rt = true resistivity of the formation (ohm-m)
*often the deepest resistivity curve (like an ILD), but corrections may be needed for invasion, borehole irregularities and other factors

Example:
a = 1; n = 2, m = 1.9
Rt = 252 ohm-m
Rw = .14
Ø = .097
Sw = .2147 (21.5%)

$$Sw = \left(\frac{.14}{(.097^{1.9} * 252)} \right)^{\frac{1}{2}}$$

Fig. 6.1 The basic Archie equation for Sw

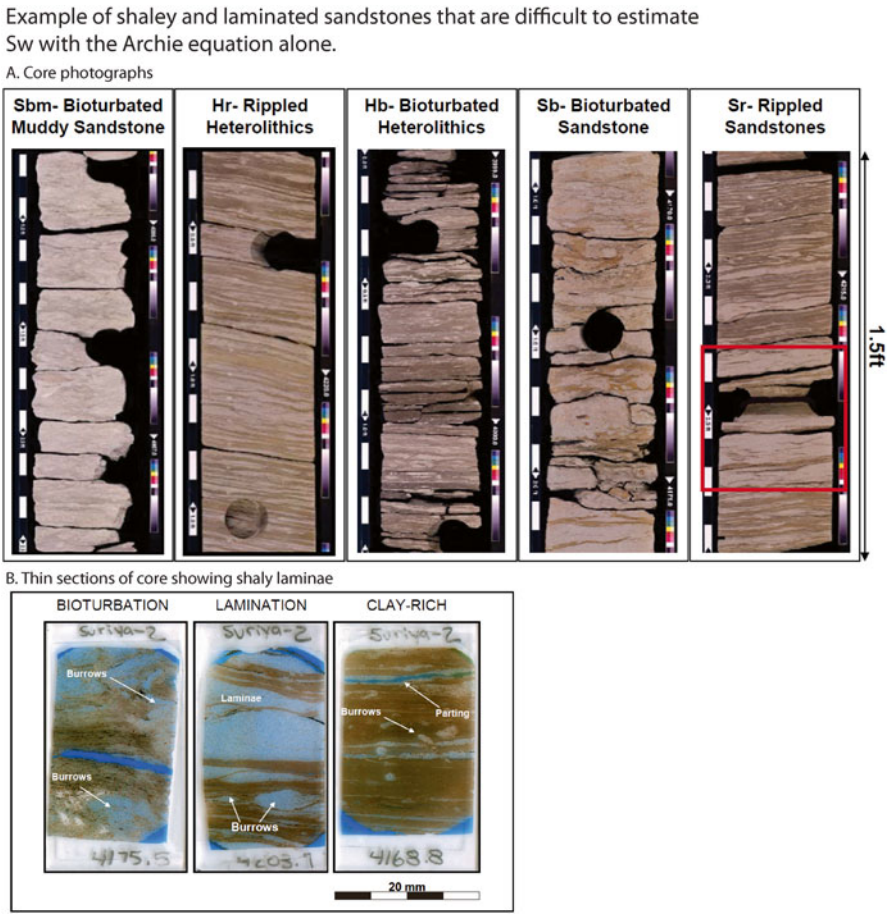

Fig. 6.2 Shaly reservoirs where the Archie approach alone may not work. From Chai et al. (2008). Used with the permission of the Indonesian Petroleum Society

The log expression of this well (Fig. 6.3) is particularly useful in showing the problem with laminated, shaly pay zones. Up to 40 % of the gas pays in this field are in rocks that look like shales on logs. Traditional log analysis in lithologies like these is difficult and core calibration is essential to quantify the pay zones. Frequently, these zones are drilled through and unrecognized as pay, leaving substantial resources behind pipe.

6.2.2 Archie Equation Steps

When lithologies are less complex however, the Archie equation is sufficient. Hartmann and Beaumont (1999) offer useful suggestions for steps to take in log analysis and values to use when dealing with rocks where the Archie equation could work well (Table 6.1).

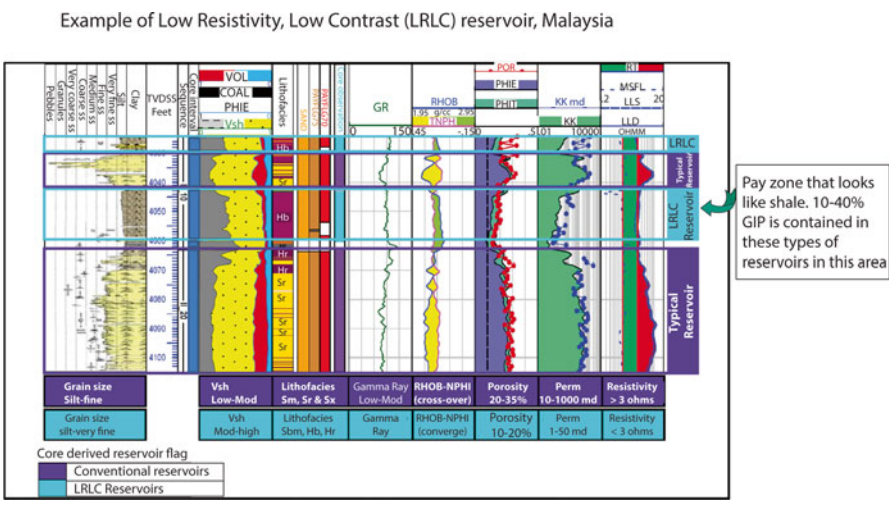

Fig. 6.3 Log expression of the rocks shown in Fig. 6.2, showing a zone that looks like shale from the GR log, but is actually a laminated gas reservoir. Modified from Chai et al. (2008) with the permission of the Indonesian Petroleum Society

6.2.3 Finding Rw

A good estimation of Rw is required to run the Archie equation, as the resistivity of the formation waters in a wet zone need to be compared to those in a hydrocarbon zone. Good porosity measurements are also key. Many companies maintain catalogues of Rw from various formations and depths in an area. But all the measurements of actual fluid resistivities are derived from sample recoveries which, like API gravity and other measurements, are done at surface conditions in a lab or on the rig. Hence, these resistivity values need to be corrected for temperature of the formation itself.

One of the oldest methods involves use of the SP log, which is very sensitive to differences between the drilling mud resistivity and that of the formation (Chap. 3). Those differences are reflected in the degree of SP response. If the resistivities of the drilling mud and formation waters are the same, there is no SP response at all in a clean formation. How much the SP response is depends on how different the drilling mud and formation resistivities are. Unfortunately, many wells, especially in recent years, are not logged with an SP curve. The technique on how to calculate Sw is well illustrated in (Hartmann and Beaumont 1999) and (Asquith and Krygowski 2004) and won't be dealt with in this chapter. There are other techniques like apparent resistivity in a water bearing zone, but not covered here.

A good alternative method calculate Rw is by using Arp's equation (Asquith and Krygowski 2004). Figure 6.4 shows the steps and an example. In any situation, the temperature of the formation must be calculated, as shown in steps 1 and 2. Units should be kept constant (either metric or imperial) in using the Arp's equation. There are also published charts from service companies that allow correcting for measurements in the lab to subsurface temperatures, but Arp's equation provides a close approximation of those charts.

Table 6.1 Suggested steps and parameters from use in calculating Sw (modified from Hartmann and Beaumont (1999) and Asquith and Krygowski (2004)). Reprinted by permission of the AAPG, whose further permission is required for further use

Step	Find	Use…	If…	Then…
1	n	• 2.0 for Archie porosity • 1.8 or less if clayey matrix or fractures • 4.0 for strongly oil-wet rocks	Not sure of rock type	Use 2
2	a	• 1.0 for Clean granular formations and carbonates • 1.65 for shaly sandstones • 0.62 for unconsolidated sandstones	Not sure of rock type	Use 1
3	Rw	• Calculate from an SP log • Calculate from Arp's equation • Estimate from well reports of offset wells or local catalogs • Estimated from a water sample from a test, correcting for subsurface temperature and salinities • Estimate from a Pickett plot		
4	Porosity	From cores, density, density-neutron, sonic or NMR logs	If density-neutron log matrix does not match formation matrix	Density-neutron cross-plot
5	m	• 2.0 for Archie porosity • 1.7–2.0 for shaly sandstones • 2.5–3.0 for vugular porosity with connected vugs • 2.5–3.0 for non-connected moldic porosity • 1.0 for fractured rocks	If unsure	Use 2
6	Rt	Deep resistivity logs (ILD, LLD, RD, RILD or others). If necessary, make corrections from charts.	Extensive invasion, thin beds or borehole washouts	Use chart book corrections

6.3 Porosity Logs and Calculations

There are multiple ways to derive porosity from logs. Where possible, calculated values should be compared to measured core porosities. What is important to remember is that no approach actually measures porosity directly. Rather, values are derived from other properties measured directly by the logs. Generally, the log suites you'll have to work with will be sonic, neutron or density logs. In some wells, nuclear magnetic resonance logs (CMR, MRIL) are run and are the preferred method for obtaining porosity. The reader is referred the Chap. 6 in Asquith and Krygowski (2004) for more detail. In exploration focused analysis, which most of this book addresses, it is unusual to run across these more expensive and new tool MRI tools with logs available from prior drilling.

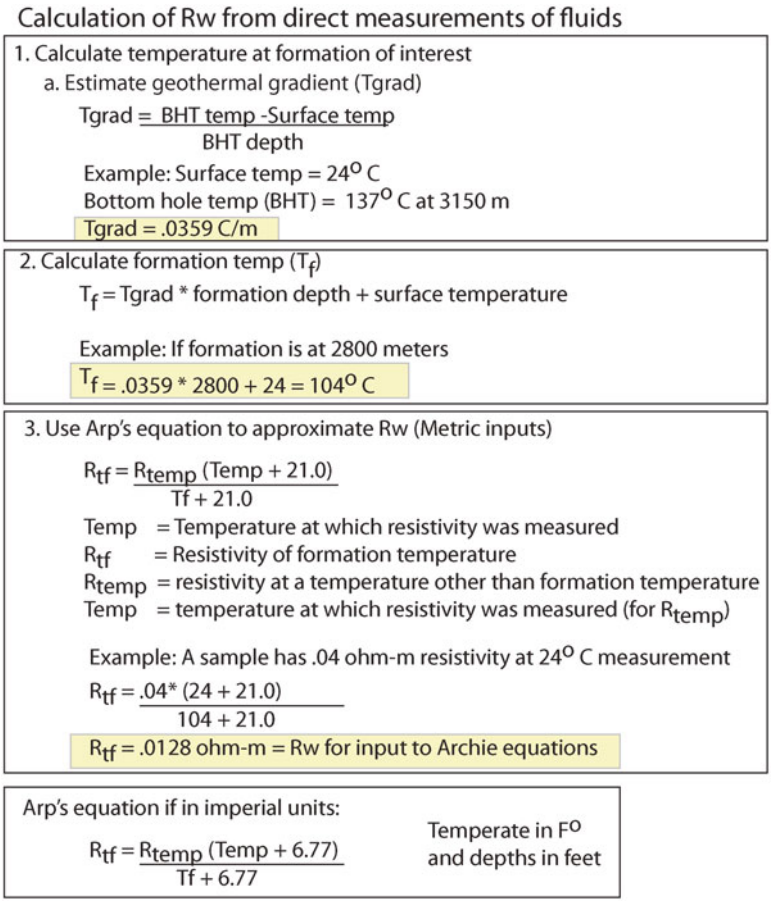

Fig. 6.4 Obtaining Rw using Arp's equation

This section is also designed to be only a general overview of porosity techniques. Porosity evaluation can get quite involved was porosity estimates with logs can be affected by:

1. Lithology
2. Presence of gas or oil (vs. water).
3. Fluid used in the drilling mud and present in the near wellbore flushed zone
4. The formulas used to derive porosity from the company running the logs
5. Condition of the borehole
6. The matrix of the formation the porosity was estimated from

i.e.—density porosity estimated on a limestone when the calibration was done on sandstone matrix density needs correcting

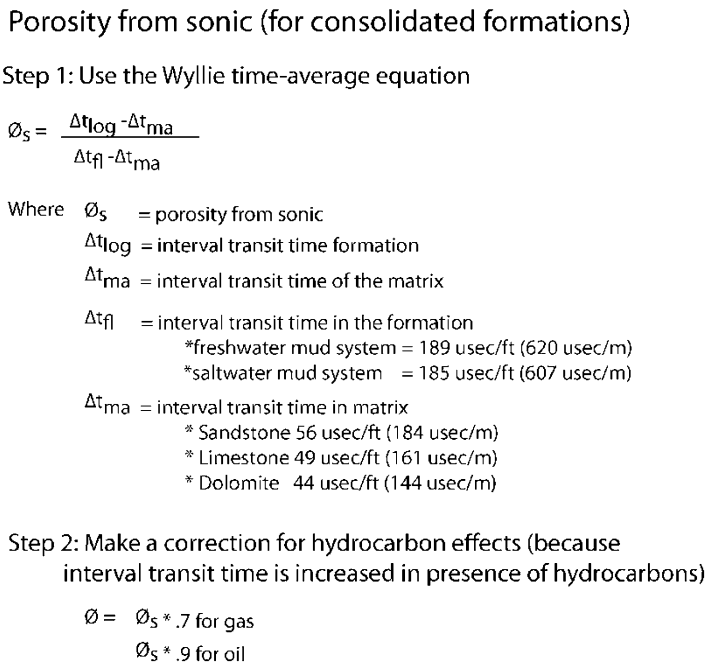

Fig. 6.5 Sonic porosity calculations. Modified from Asquith and Krygowski (2004)

6.3.1 Sonic Log Porosity

One of the oldest methods of obtaining porosity is from the sonic log. Most modern sonic logs are called borehole-compensated (BHC) logs and are designed to minimize effects of washouts and borehole size variations. Measurements are in microseconds per foot (μs/ft) or microseconds per meter (μs/m).

Inputs to the equations are given in Fig. 6.5. Note that the inputs are both lithology sensitive and fluid sensitive. The fluid input, as the log reads close to the wellbore in the flushed zone, is set for either fresh water or salt water based drilling muds. The kind of drilling mud used will be recorded on a lot header, and if not, assumptions need to be made based on offset wells, or sensitivities run on solutions. Oil-based drilling muds would require a different input, but many older exploratory wells were drilled with water-based muds. An additional adjustment needs to be made if there is gas or oil in the formation. Occasionally, this presents a dilemma if you are not sure. The correction for gas is substantial (a reduction by 30%), as shown, and less so for oil. If not corrected, the sonic porosity will be too high.

6.3.2 Density Log Porosity

Density is measured in g/cc and the log itself has a relatively shallow response into the formation. Figure 6.6 summarizes inputs and some values to enter into the equations. In water bearing formations, the inputs for fluid density are those of the fluid

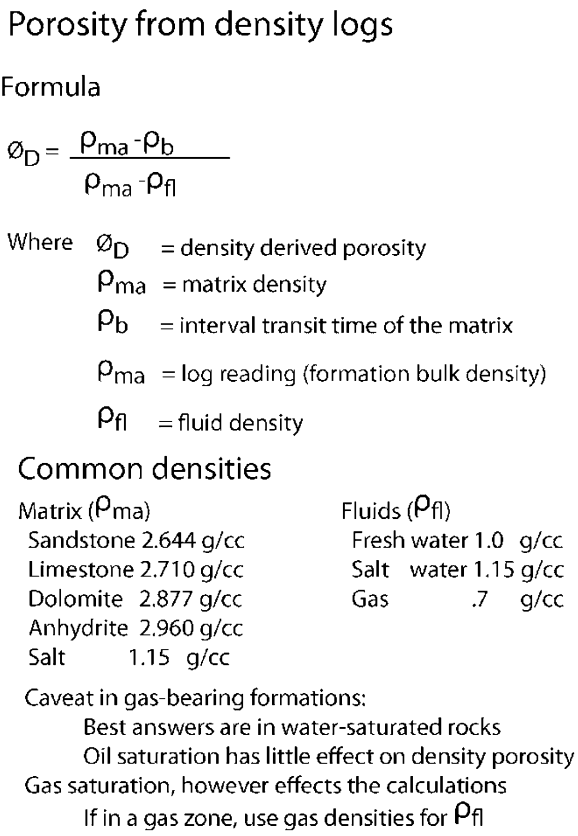

Fig. 6.6 Density porosity calculations. Figure modified from Asquith and Krygowski (2004)

densities in the drilling mud being used (fresh or salt water). If gas is present, corrections, as in the case of the sonic log, must be made.

The bulk density of the formation $\rho_{b \text{ is called RHOB.}}$ It can be used to:

1. Identify evaporite minerals
2. Detect gas-bearing formations
3. Detect hydrocarbon density
4. Evaluate shaly-sand reservoirs and complex lithologies

It is often run with a correction curve (DRHO), used to determine corrections needed and added to the values based on mud cake thickness. The density derived curve is most commonly name DPHI. Inputs to the porosity calculation. An additional density-derived curved called a photoelectric-effect curve (P_e) is often also displayed. This curve is very useful for identifying lithology (Asquith and Krygowski 2004).

There are a number of sources of potential error in using density porosity (DPHI) as shown on a well log:

- Wrong formation density: the matrix density used to calculate the porosity was set for limestone, but the lithology is sandstone. In this case, the porosity will be higher than what is actually in the formation

- Wrong fluid density: the formation is actually salt water, but a fresh water fluid density was used. In this case, the calculated porosity will be too low.

6.3.3 Porosity from Combination Neutron-Density Logs

Neutron logs measure the hydrogen content in a formation. In clean, water bearing formations, it measures liquid-filled porosity. The units can be read directly from the tool without conversions and are usually identified as PHIN or NPHI curves. They vary depending on:

- Differences in detector types
- Spacing between source and receiver
- Lithology

There are various types of neutron logs, but the most common type is the compensated neutron log (CNL). Older logs are the sidewall neutron log (SNL). Different tools and processing, plus lithology differences need to be kept in mind and charts provided by service companies are available to make corrections.

One of the key uses of the neutron log is detection of gas as well as the degree of shaliness in the formation. Clays in a formation, as they contain hydrogen, cause neutron porosities to read higher than density porosities over shaly intervals. When neutron and density porosities converge in water-filled sediments, the formations are largely clay free. In addition, the presence of gas causes the neutron log to read lower porosity than the density log. In these cases, the effect is termed 'cross-over' and is an excellent indicator of the presence of gas.

FDC-CNL logs are logs that are run to measure both neutron and density porosity simultaneously. These logs are the most popular logs to run because of the relative ease of calculating porosity and recognizing gas and shale effects. Input equations are shown on Fig. 6.7.

If the logs have been run on the same density as the formation, the equation in Fig. 6.7 will provide a good solution. If not, then density porosity must be recalculated from the density of the lithologies in the formation being analyzed, as per Fig. 6.6. Many charts exist to use the FDC-CNL combination logs to also calculate porosity (an example of log responses to lithology was shown in Chap. 3). Again, the reader is referred to (Asquith and Krygowski 2004) and (Hartmann and Beaumont 1999) for details.

6.4 Some Quick Look Techniques: Pickett and Buckles Plots

There are two quick and powerful ways to identify Sw in transition zones vs. irreducible water saturation and 100 % water. As any hydrocarbons in a transition zone are above the free water level, they are in the trap and continuous phase shows. But Sw, as illustrated in Chap. 5, can be quite high, especially low on the trap in poor quality rock.

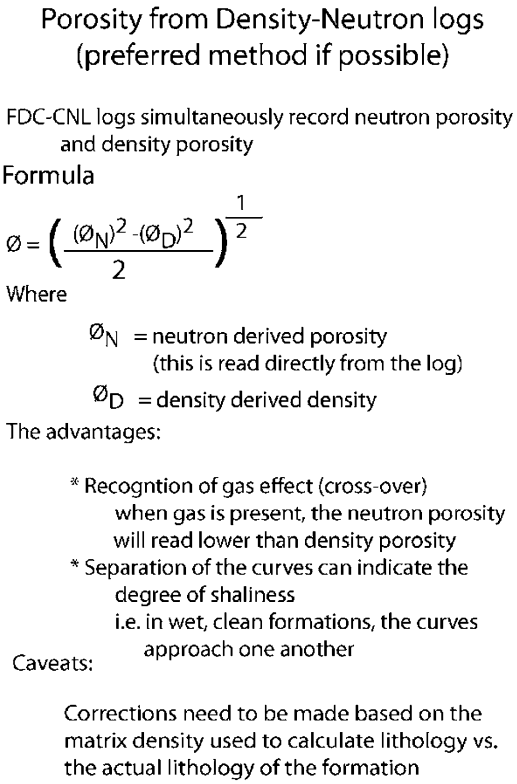

Fig. 6.7 Porosity from density-neutron logs. These are the easiest porosity tools to work with for standard log suites. Modified from Hartmann and Beaumont (1999)

6.4.1 Pickett Plots

One of the simplest ways to view SW, as well as be able to estimate m and Rw from simple porosity vs. resistivity plots is the Pickett plot (Fig. 6.8). Many software packages come with the built-in ability to generate a Pickett plot once the porosity is calculated. Simple instructions on how to generate Pickett plots are shown in Hartmann and Beaumont (1999). A simplified plot and major concepts are shown in Fig. 6.8.

The popularity of the Pickett plots derives from the fact that, if water bearing zones are present, the slope through those zones intersects the y axis with a slope that will equal 'm' on the Archie equation, and intercept that will equal Rw. Points above the water saturation lines shown can easily be looked at as transition zone, waste zone of irreducible or very low water saturations. An example of using a Pickett plot to identify transition zone saturations in the Matulla Group in Egypt, previously identified as below the oil-water contact, was shown in Chap. 5.

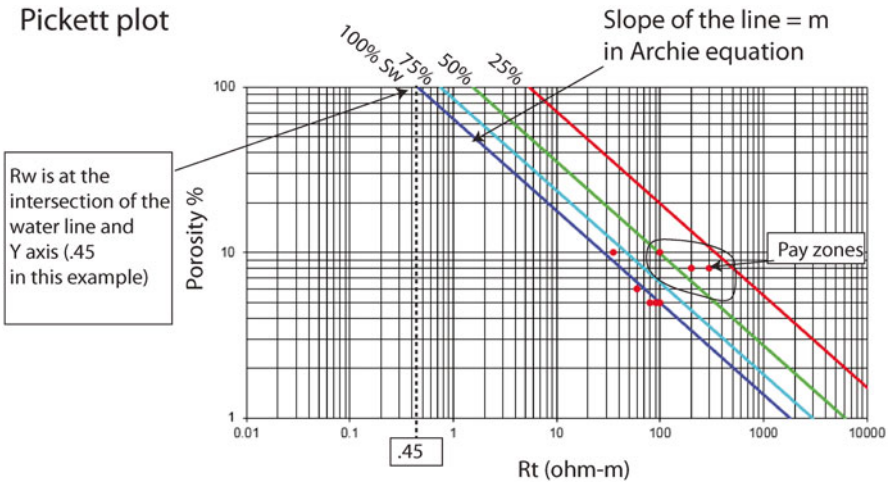

Fig. 6.8 Pickett plot construction: a graphic representation of the Archie equation. Rt values from the deep resistivity logs are plotted against porosity. The intersection of the 100 % SW line and the 100 % porosity line is at the value of Rw in the subsurface. The lines on the graph have slopes equal to the 'm' value in the Archie equations. Wet values fall on or near the 100 % Sw line. And pay zones at increasingly lower SW lines. This can also be used to estimate Rw and m from porosity and resistivity when little is known of the area

6.4.2 Buckles Plots and Bulk Volume Water (BVW)

Bulk Volume Water (BVW) has additional utility in identifying transition zone vs. water zones and zones that will produce water free. This is because BVW, when the pore systems and geometries are the same varies as a function of the height above free water. This is because, for any given rock type, when the porosity and pore throat distributions are the same, SW is a function of that rock type and the height above free water.

The equation is:

$$\mathrm{BVW} = \mathrm{PHI}\left(\mathrm{porosity}\right) * \mathrm{Sw}$$

Shading the BVW curve vs. porosity on a log plot can give a feel for the degree to which hydrocarbons are filling the pore system.

A Buckles plot overlays hyperbolic lines of constant BVW curves on a porosity vs. water saturation plot. If the formations are at irreducible Sw, the porosity and saturation will track the buckles lines. If not, points will fall off the line. If there is no pattern at all, despite having some porosity and water saturation, the formation is not close to irreducible and will produce high volumes of water.

In the example in Fig. 6.9, where the points are tracking the BVW 0.04 line, the points are at or near irreducible water saturation. In cases B and C, some of the

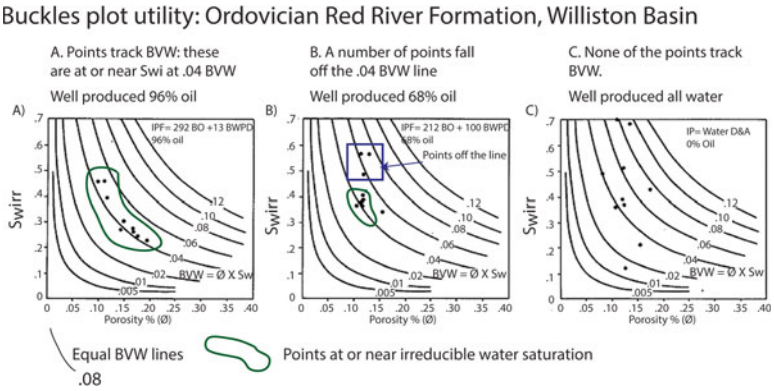

Fig. 6.9 A Buckles plot example. Modified rom Asquith and Krygowski (2004). Reprinted by permission of the AAPG, whose further permission is required for further use

points do not track the BVW 0.04 line and are thus not at irreducible Sw. In case C, despite having some saturation, produced no oil.

6.5 Pattern Recognition of Pay

It is useful to simply learn to visualize some log displays to spot gas effect and shaliness and changes in water saturation. In addition to Sw calculations a useful screening criteria is to use Bulk Volume Water curves (BVW). Here are some tips for fairly conventional reservoirs:

1. If log porosity and lithology and are constant, but resistivity changes, it is probably due to hydrocarbons.
2. Macro-porous rocks will have sharp hydrocarbon-water contacts, as there is little transition zone.
3. Micro and meso-porous rocks will have long transition zones, and can be mistaken for water bearing zones, despite being above the free water level. So look for saturation changes that are tracking changes in porosity. The reason may be pore throat changes well into a trap, not necessarily going lower on the trap.
4. Be careful with low porosity horizons with saturation. They indicate a column, or at least a paleo-column. Residual hydrocarbons in tight rocks can have saturations in the 35–50 % range and will always produce water. Pressure data across these zones will indicate a water gradient, proving the residual nature of the saturation.

6.5.1 *Example 1: Eocene Wilcox Sandstone*

This example (Fig. 6.10) comes from .las files and case studies in Asquith and Krygowski (2004), loaded to a Petra software package and interpreted. A quick look at the SP curve shows good response and deflection, indicating a fairly clean reservoir and a good difference in resistivity between the mud filtrate and the reservoir. The SN and IL curves show good separation, indicating invasion and good permeability. The sonic log was used to derive porosity and in this example, uncorrected PHI for gas is shown (blue) next to corrected PHI for gas effect (red). Porosity was calculated without any shale cutoffs, to it is total porosity, including porosity in the shales. Sw was next calculated given known Rw values in the area and Archie parameters from experience. The Sw curve was subsequently clipped to a null value where there was shale calculated from a Vshale curve (not shown). Lastly, a BVW curve was calculated and displayed with black shading against the porosity curve, indicating there is some saturation all the way to the base of the reservoir.

At the bottom of the sand however, the resistivity and porosity curves both drop rapidly, indicating a decrease in porosity as well as a potential for a decrease in pore throat size and increase the amount of bound water. Water saturations at the base climb to 70–80 % Sw (Fig. 6.11).

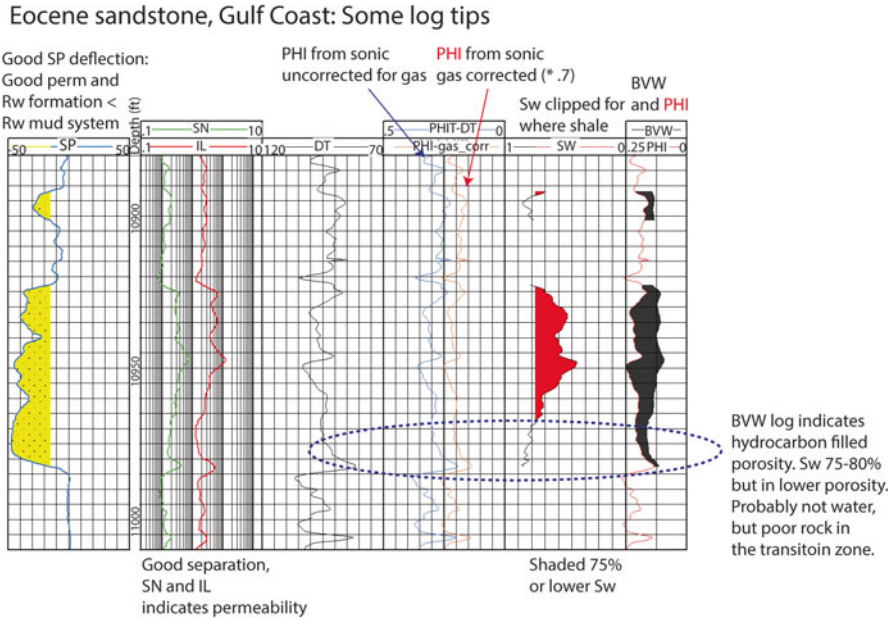

Fig. 6.10 Example of quick look techniques on a Tertiary sandstone. Original .las file from Asquith and Krygowski (2004)

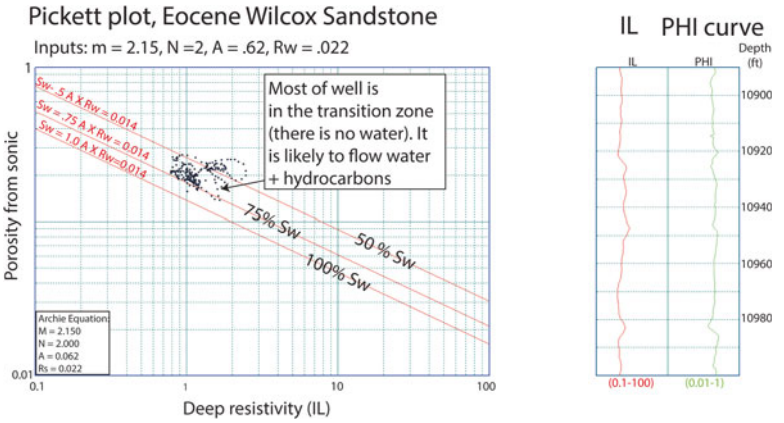

Fig. 6.11 Pickett plot of a pay zone in Oklahoma. Original .las file and case history from Asquith and Krygowski (2004)

Using a well-established Rw for this area, the Pickett plot shows that no points are truly at the 100 % Sw line. However, the saturations are hovering between 75 and 50 % Sw so most of this zone is within the transition zone, potentially low on the trap. Some zones are clearly above the 50 % line and likely to produce oil and gas. This is a productive gas well, but with a high volume of water recovered with the gas.

6.6 Residual Shows on Logs

Residual shows can be very problematic and difficult to distinguish from transition zone or waste zone shows where water saturations are high but the zones still above the free water level. One of the more clear-cut log techniques, however, is when very porous strata are encountered but no clear changes in resistivity are seen. A good example is shown on Fig. 6.12 and also documented in the context of migration and seal loss in Naidu et al. (2016) and Dolson et al. (2015). The well shown in the Barmer Basin of India was drilled to test a fault trap in a portion of the basin which has seen significant uplift and erosion which post-dates timing of hydrocarbon emplacement. Residual oil shows are common. The resistivity in this well is very low and does not change vertically, despite the core data showing permeabilities in excess of two Darcies. The core is heavily stained with a strong hydrocarbon odor. Hence, these oil shows cannot be transition zone low on the trap or there would have been a very sharp oil-water contact on the logs. Two wells produce updip of this location on the same structure. The residual shows were once above a deeper oil-water contact which has been adjusted above this elevation during uplift and remigration.

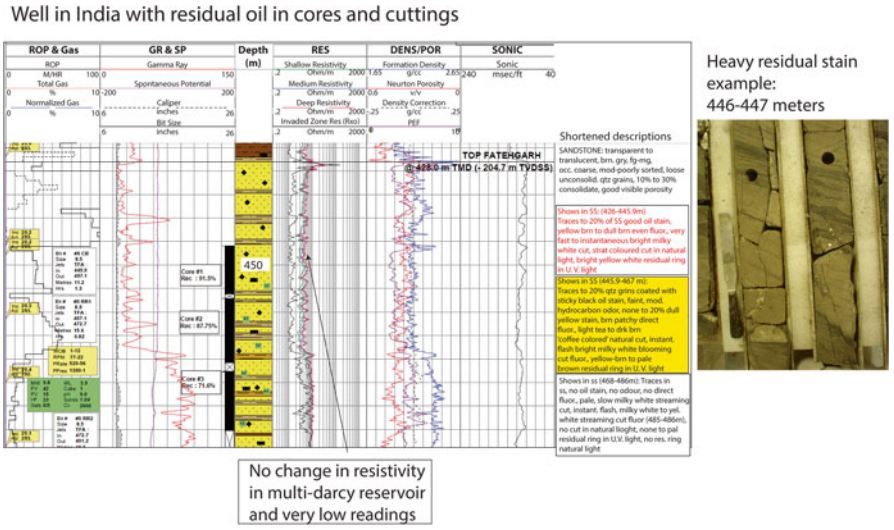

Fig. 6.12 Residual oil stain in core and lack of resistivity response on multi-darcy rock, India. Data courtesy of Cairn India Limited, with permission

Pressure data remains the best way to recognize residual oil and gas, as the gradients through the saturated zones will show a water gradient. Figure 6.13 provides an example in a carbonate in Ethiopia, why hydrodynamic flushing of a low relief structural trap has left residual oil only in the target closure. Log saturations between 45 and 80 % Sw occur throughout this interval but tested only water. Horner corrected pressure data showed a common water gradient through all the points. Further work with hydrodynamic maps showed that the low relief structure is incapable of holding hydrocarbons under hydrodynamic conditions. The shows, then, are clearly residual and not related to effects of relative permeability.

As covered in Chap. 5, residual shows in tighter rock are much more troublesome, as residual saturations can be as low as 35–45 % Sw. In these cases, pressure data indicating water gradients across the interval may be the only definitive way to show these saturations are residual. It is important to remember that even if a zone tests 100 % water, the water flow may be due to relative permeability problems and not a residual zone. At times, it is simply difficult to distinguish the cause of the water flow without more data.

6.7 Pitfalls: Clays, Shales, Laminated Pays

There are a variety of ways to miss hydrocarbons. Clays, shales and laminated thin-bedded reservoirs can be primary causes of misinterpreting wells logs as due to silty or shaly reservoirs with no permeability or in wet sands that contain

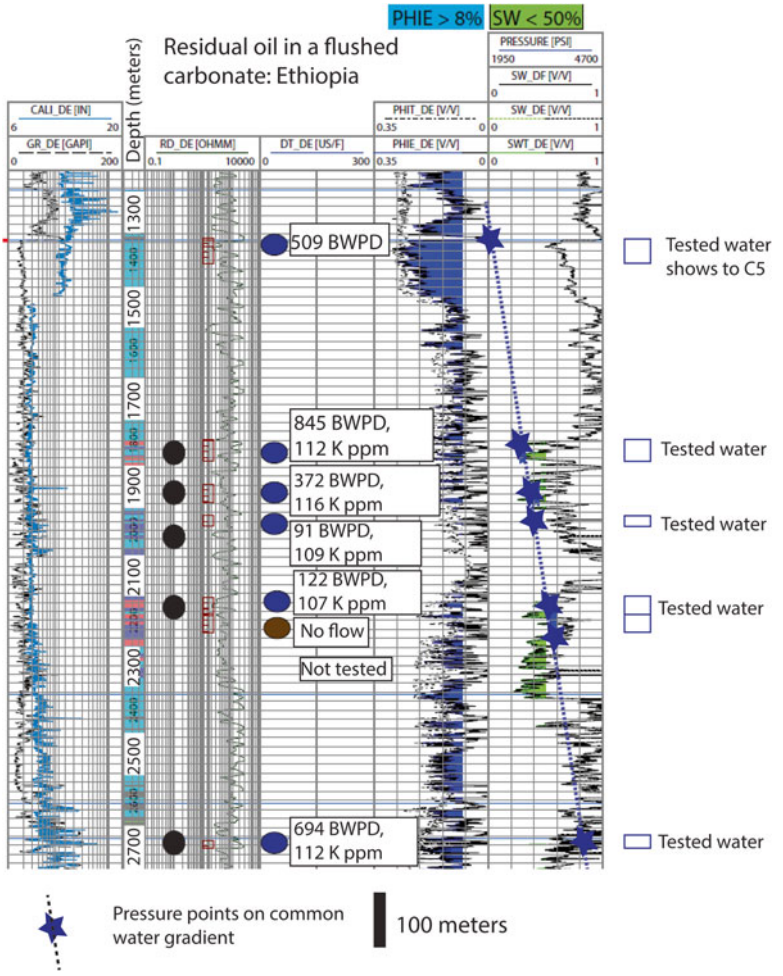

Fig. 6.13 Residual saturations on logs which tested water with no shows and had a common salt water pressure gradient

conductive minerals and high bound water. Compounding these problems, wells with good pay zones can suffer formation damage during drilling and completion. This section provides a brief overview of some of the pitfalls of log analysis, as well as some of the more recently developed logging tools that help in difficult evaluations.

6.7.1 Low Resistivity-Low Contrast Pays (LCLR)

Low resistivity pay reservoirs are commonly considered wet, misidentified as a shale or completely overlooked due to logging instrument limitations. The term low resistivity pay is usually used to describe a pay zone that either had relatively low resistivity or calculated "wet" using conventional well log calculations. Low-resistivity pay is commonly believed to be at the 1.0–5.0 Ω-m (deep) resistivity range, yet productive reservoirs can be found around the 0.5 Ω-m resistivity level. Hence pays are often easy to condemn since they appear "wet" if one tries to conventionally interpret the resistivity measurement as a saturation curve.

In recent years the term "low contrast, low resistivity (LCLR) pay" has replaced "low resistivity pay." The term "low contrast" is added to accentuate that the pay zone resistivity may differ little from adjacent "wet" or "shaly" intervals. This definition also allows classification of subtle pay zones that do not have extremely low resistivities, but have little resistivity contrast with adjacent beds. Low-contrast pay indicates a lack of resistivity contrast between pay sands and adjacent non-reservoirs like shales or wet zones. Low-contrast pay occurs mainly when formation waters are fresh or of low salinity. As a result, resistivity values are not necessarily low, but there is little resistivity contrast between oil and water zones.

Pay zones that produce low resistivity or low contrast log responses are often a consequence of unusual rock or fluid properties and are influenced by a variety of factors associated with mineralogy, particularly clay content, water salinity, and microporosity, as well as bed thickness, dip, and anisotropy. Because of its inherent conductivity, clay minerals, and hence shale, is the primary cause of low-resistivity pay. Causes of LRLC pay include: thinly laminated clean sands high capillary and clay bound water sections such as silts or clays; clay-coated sands or sands with interstitial dispersed clay with high clay bound water volumes; sands with conductive minerals (such as pyrite, glauconite, hematite, or graphite or rock fragments forming continuous electrical pathways); very fine-grained sands (silts) with high irreducible water saturation; microporosity; sands with very high saline formation water, while low salinity water can cause low contrast pays. Often it is also a combination of the above factors.

Of all of the factors listed above, probably the most common cause of low resistivity pay is the combination of thin beds containing highly conductive clays (and their associated bound water), along with thin pay sands, which are below the vertical resolution of the logging instrument. Here the resistivity is dramatically reduced, the apparent clay volume is increased, and the hydrocarbon volume and the permeability calculated from conventional log analysis are underestimated. This topic is covered extensively in the literature with several key papers and books providing essential background (Boyd et al. 1995; Claverie et al. 2010; Passey et al. 2006a, b, c, d; Shepherd 2009; Sneider 2003; Sneider and Kulha 1995; Worthington 2000).

In many cases, zones that look like shales will show subtle increases in resistivity that are responding to hydrocarbons while the GR and other logs still register a shale signature. In some cases, the change may be from 1 Ω-m in a normal shale to 2 or 3 Ω-m in a laminated shale and sandstone complex. Simply spotting those changes on old logs can be a guide to recognizing where by-passed pay might be in a well.

An example is shown as shown in Fig. 6.14 showing a core through a laminated interval.

"Cookbook" style petrophysical calculations of well log data will fail to identify these pays. While conventional analysis can provide reliable water saturation, it does not distinguish clay- and capillary bound water from free water. Also, shaly and silty reservoirs often present a complex mineralogy, which makes estimates of clay volume and grain density uncertain. Standard shaly sand models are not suited

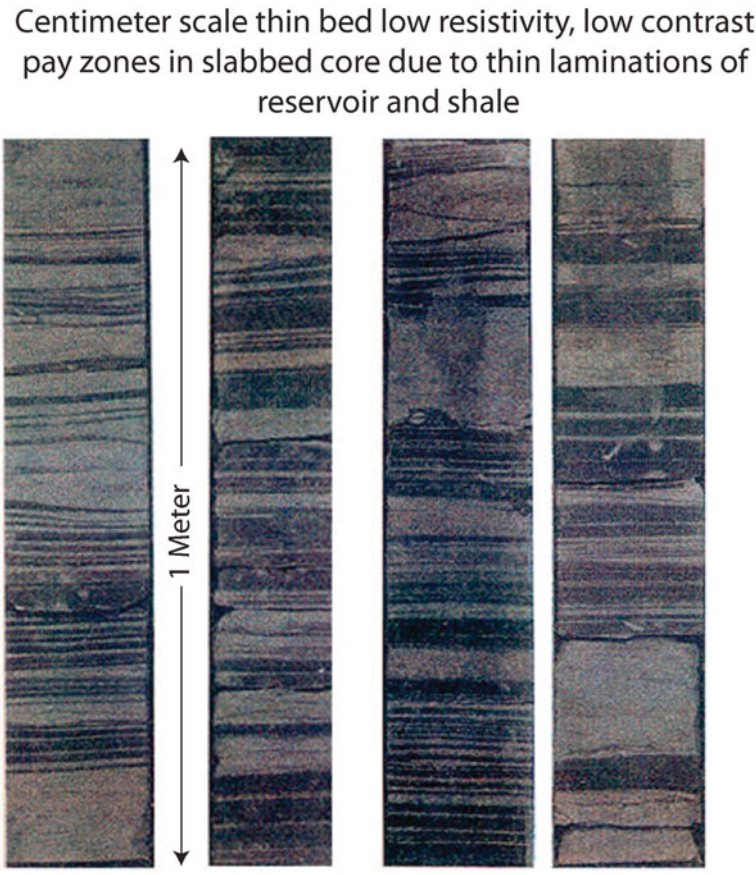

Fig. 6.14 Laminated sandstones interbedded with shales in this core are difficult for conventional logs to evaluate, as resolution of the resistivity tools are not high enough. This interval may well appear to be a shale or siltstone on a GR or resistivity log. Photo courtesy of Bernd Herold

for LRLC evaluation and specialized fit-for-purpose interpretation workflows are necessary in order to reduce uncertainty in saturations and improving producibility prediction.

Low resistivity pays and low contrast pays depositional systems include deep water fans, with levee-channel complexes, delta front and toe deposits, shingle turbidites and alluvial and deltaic channel fills. LRLC pays have been found in clastic basins ranging from the Gulf of Mexico to Alaska, Offshore Brazil to the North Sea, West Africa, and Malaysia. Although LRLC reservoirs have been under production for many years, their identification and the calculation of their reserves and flow properties remains a difficult challenge. They are volumetrically significant hence there is an incentive to understand them fully.

6.7.2 Using Micro-resistivity and NMR Logs in Shaly and Difficult Pay Zones

Over the last 20 years, however, recognition and quantification of laminated pay zones has become increasingly sophisticated. Micro-resistivity logs are particularly useful in identifying thin-bedded pay zones and getting a better look at the potential depositional environment. An example is shown in Fig. 6.15. A zone testing oil in a highly laminated turbidite flowed from very thin beds. In this example, over 50 m of additional thin-bedded pay away perforations, as only a 10 m interval was opened in a zone giving a slightly better GR response. The flow rates indicated good permeability and sand content, despite looking dominantly like a siltstone on the logs.

OMRI logs (Halliburton 2015), like other micro-resistivity tools, are designed to provide very high resolution measurements of resistivity to a vertical resolution of 1 in. (2.54 cm). In many depositional systems, these tools are essential to quantify pay zones. The reader is also referred to Hurley (2004) for more information on borehole image logs.

6.7.2.1 NMR Logs

Nuclear Magnetic Resonance logs are perhaps best summarized by Henderson (2004) and PetroWiki (2015), and have become fairly routine in difficult log analysis settings. NMR technology has been studies for over 50 years (Fukushima and Roeder 1981; Kenyon et al. 1986; Timur 1968, 1969), but only in relatively recently been more widely adapted to difficult reservoirs. A full treatment of this topic is that of (Coates et al. 1999; Cowan 1997) and beyond the scope of this chapter.

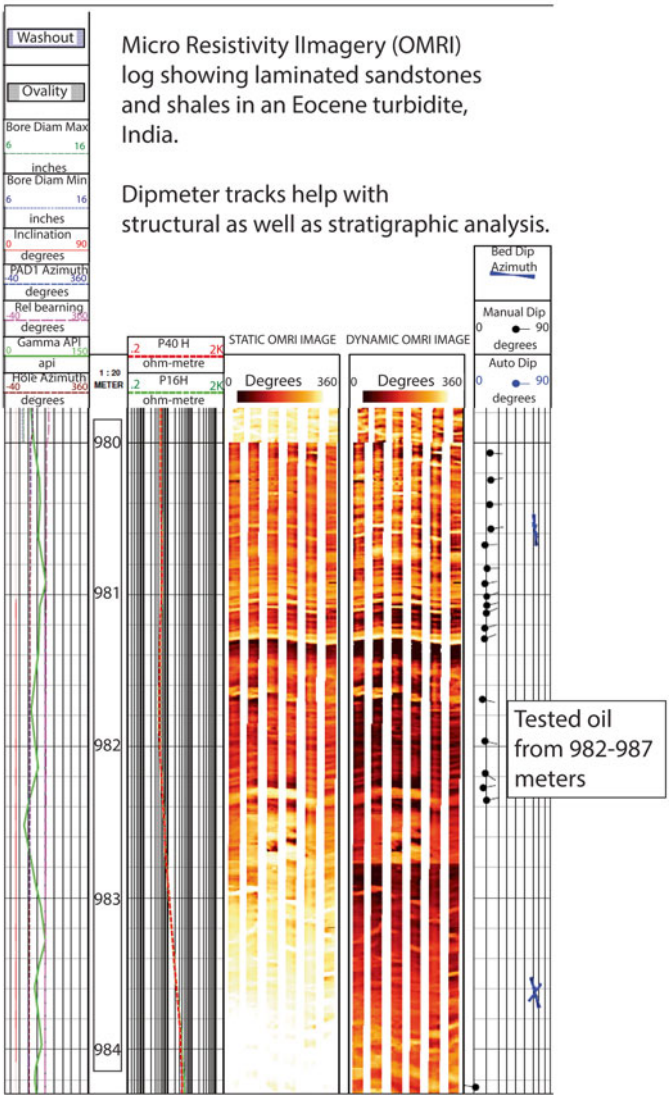

Fig. 6.15 OMRI log over a laminated oil zone, India

NRM logs measure response of hydrogen nuclei to an induced magnetic moment. The NMR tool uses a permanent magnetic field and an oscillating field to polarize the spin axes of protons away from their equilibrium direction. When the oscillating field is removed, the protons starts to tip back, or relax towards their original magnetic field. The rate of this decay is called relaxation time and is

measured to determine properties of the fluid as wells as the geometry of the pore system. A variety of different relaxations times are recorded and the reader is referred to other papers for more detail (Kleinberg and Vinegar 1996; Mardon et al. 1996a; Prammer et al. 1995; Zhang et al. 1998) The time it takes for the protons to get back to their un-polarized states is recorded (the T2 track). Processing is done to then convert these data into meaningful porosity and saturation numbers.

Relaxation time can be affected:

1. Type of fluid (oil, gas or water) in the pores.
2. The strength of the surface relaxation.
3. Rock wettability.
4. Fluid densities.
5. Pore size.

As the tool responds to hydrogen protons it is primarily measuring liquid filled porosity zones. It contrasts with conventional logging suites, which are affected by lithology and clay content as well as porosity and hydrocarbons. The tool is thus used define both clay bound and effective porosity. It can also provide some estimates on permeability, pore size distribution and hydrocarbon type. As in other tools, calibration of the tool to other data, particularly core, significantly enhances the interpretations. NMR porosity is generally the most accurate porosity measurement available amongst all log tools provided when used a number of conditions are met (Murphy 1995), including, among other criteria, good borehole conditions (in gauge, without rugosity and formation damage), and no magnetic minerals in the formation or borehole fluid. NMR porosity can be further refined to free fluid porosity (FFI), thus attempting to differentiate between moveable fluids and bound fluids in the smallest pore throats (Coates et al. 1997; Timur 1969). A number of examples of utility in complex reservoirs follows.

The example in Fig. 6.16 is from a shaly Eocene fan-delta and turbidite complex which gives a log response of largely siltstone and shale. However, it tested gas over the interval shown with a good NMR log show matching shale-adjusted Sw from conventional log analysis. This is a laminated reservoir and the pay was better defined with the NMR log.

Another example involves a porcellanitic reservoir in the Barmer Basin of India. Porcellanitic reservoirs are high porosity, low perm siliceous reservoirs difficult to quantify SW and permeability of logs. Figure 6.16 shows a good agreement on permeability derived from NMR measurements using the Timur-Coates equations (Ahmed et al. 1991; Allen 1988; Coates et al. 1999) (Fig. 6.17).

NMR tools can also help distinguish fluid type (Akkurt et al. 1996a, b; Kleinberg and Vinegar 1996; Mardon et al. 1996b; Moore and Akkurt 1996; Prammer et al. 1995). An example of this is shown in a complex volcanic reservoir where porosity and water saturation are difficult to determine. An example is shown in Fig. 6.18 where conventional logs could not define effective porosity or gas zones.

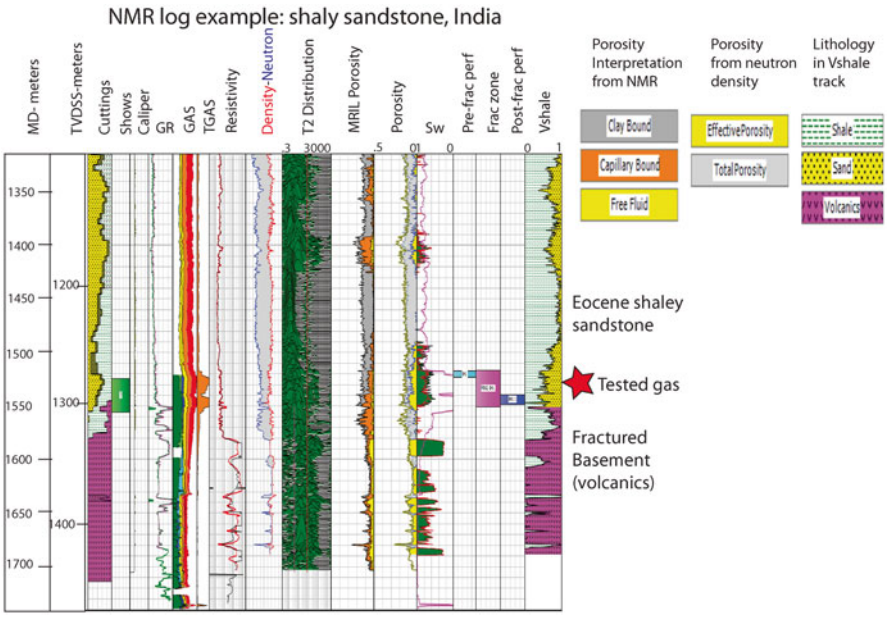

Fig. 6.16 T2 distribution curve and response to a gas zone, with analysis compared to conventional logs over the same interval

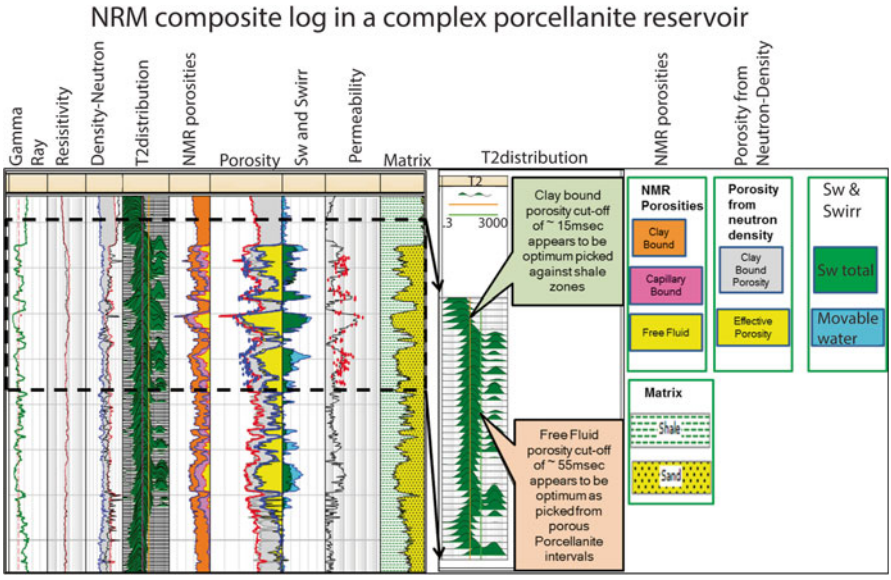

Fig. 6.17 Calibration of NMR derived porosity and conventional log porosity tied to conventional core analysis. NMR computed permeability using the Timur-Coates equations agrees well with core points (*red*). In addition, the Sw and Swirr shows the difference between moveable and bound water in the pore system (*blue* and *green* colors). Porosity type is also identified, showing variations in clay bound porosity (*gray*) effective porosity (*yellow*) in the porosity track and clay bound NMR, capillary bound and free fluid porosity in the NMR porosity track

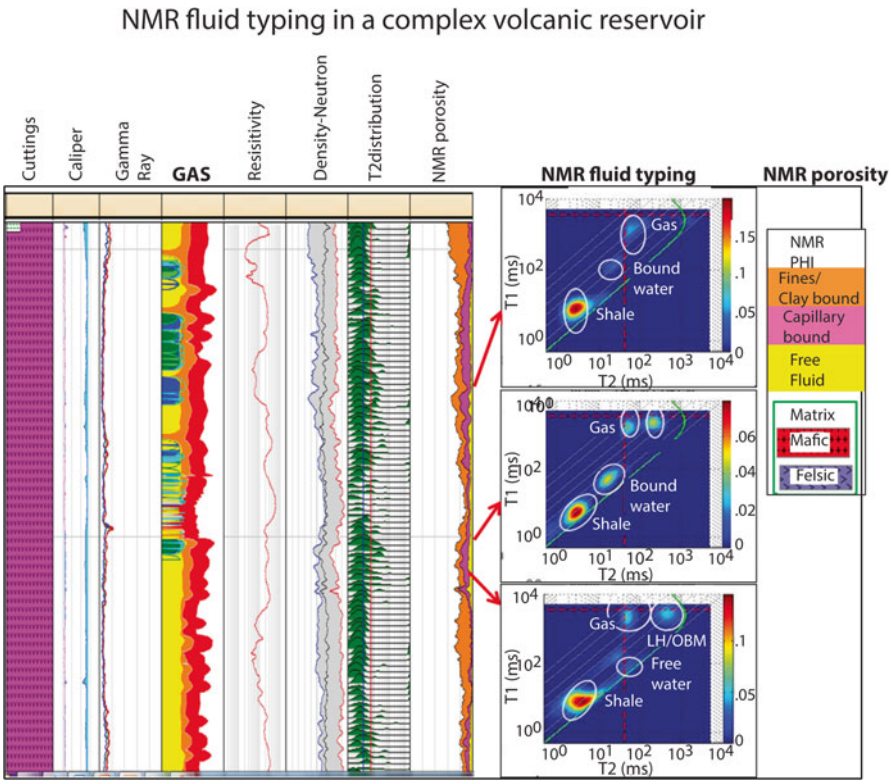

Fig. 6.18 Differentiation of gas bearing zones from NRM logs in a complex volcanic. The well was originally logged with oil based mud using an LWD (logging while drilling) combination, but the conventional logs were unable to identify the gas zones in this well. See text for references on how fluid differentiation is done using NMR logs

6.7.3 More Pitfalls: Clays, Conductive Minerals and Formation Damage

Clays are ubiquitous in most reservoirs, both from original detrital deposition and later diagenetic changes. In addition, some secondary minerals or cements, like glauconite, pyrite, and iron carbonates like siderite can pose significant problems in recognition of pay (through suppressed resistivity) or even formation damage upon completion. When encountering a good show in a well, and then subsequently testing water or having no recovery at all, formation damage must be ruled out. Ubiquitous shows over intervals of very low resistivity need to be looked at from the standpoint of possible conductive minerals that might suppress resistivity and mask hydrocarbons.

The most common clay groups are shown on Fig. 6.19.

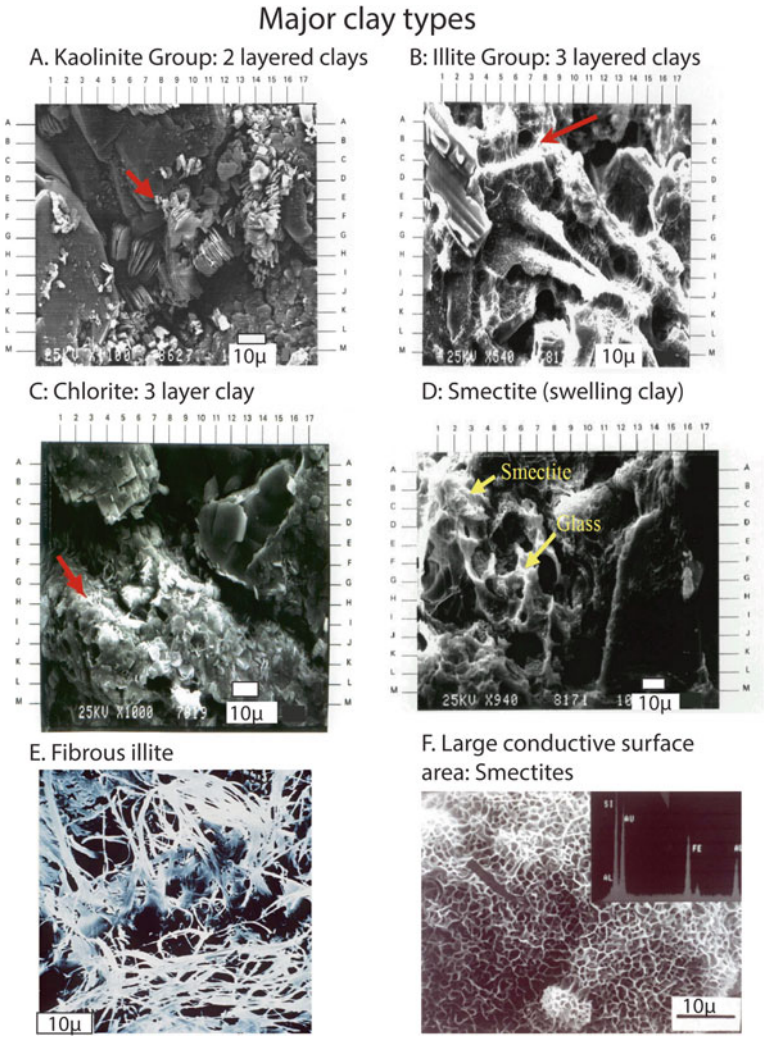

Fig. 6.19 Common clays. Fibrous illite can act like a spider web, trapping other clays (like kaolinite) dislodged during well completion and flow. Other clays are sensitive to water (like smectites) and can swell and plug pore-throats. Other problems result from highly conductive clays or minerals which mask hydrocarbons on resistivity logs and chemical reactions with stimulates than can cause formation damage. Figures (**a**–**d**) courtesy of Jack Thomas. Figures (**e**) and (**f**) courtesy of George King

Formation damage is possible in a number of cases with these clays. One of the best sources on formation damage is that of (King 2009) and some of the summaries used in this text are from Thomas (2001). Some other good references include (Bennion and Thomas 1994; Bennion et al. 1996; Joshi 1991; Kasino and Davies 1979; Minh et al. 2011; Pittman and King 1986).

A common problem with fibrous illite (Fig. 6.19e) is that is acts like a spider-web and during completion, layered clays like Kaolinite can mobilize and flow with oil, gas and water when the well is produced, but then get trapped by the fibrous illite. The result can be a loss of production or significant drop in rate.

Smectite, like other clays in the montmorillonite group, can swell when in contact with water, so formation damage can result is a well is drilled through formations rich in this clay by water-based mud systems. Acid treatments can also react with reservoir cements and clays. Smectitic clays also have very large surface areas that can hold significant bound water, raising Sw levels on logs. Chamosite, an iron-rich variety of chlorite, is conductive enough that it can suppress resistivity over a pay zone, making the interval look wet. This is also common when more than 7 % pyrite is present in reservoirs.

A good example of suppressed resistivity is shown in Fig. 6.20 (Dolly and Mullarkey 1996). In this case, resistivities don't exceed 2–3 Ω-m and the zone looks completely wet on logs. The culprit is a complete family of conductive cements and shaly clays which suppress the resistivity.

An interesting case history of by-passed pay from glauconite-rich sandstones is that of Trimble Field (Cook et al. 1990) in Mississippi, where 100 BCF of gas was found in a zone that looked so wet on logs that the Environmental Protection Agency (EPA) had actually approved the zone that eventually flowed two MMCFD gas as a water disposal well. The structural trap had been drilled twice and abandoned since initial tests in 1963 and 1984, despite good mud log shows. The pay, evaluated with conventional logs, had reminded behind pipe and overlooked for decades. It was only noticed while try to complete the water disposal well in 1987, which flowed gas instead.

More recently, an oil leg was found beneath a large gas field in Mozambique (Trueblood 2013) when wells low on the structure though to be wet flowed oil instead. As in the case of Trimble Field, the Inhassoro Field was discovered in 1965, but the oil leg was not identified until 2003. The logs simply looked wet and the zones remained untested.

Some good examples of suppression of resistivity due to pyrite are given by (Kennedy 2004; Tabarovsky and Georgi 2000) and (Turner 1997).

A summary of problems with cements, logs and completions is shown in Table 6.2.

One of the more difficult tasks when confronted with a well that looks like it should flow hydrocarbons but doesn't is actually that of sitting with engineers and other staff members to sort out the reasons why. There are many ways to damage a well beyond what is discussed here. Eliminating geological causes through good log analysis, pressure data and core information goes a long way to be able to test an idea that a formation has actually been damaged or a zone by-passed due to mineralogy or logging limitations.

There is often a great deal of resistance to acknowledging that a zone may have been damaged. It is often not easy to come to agreement on this topic. The senior

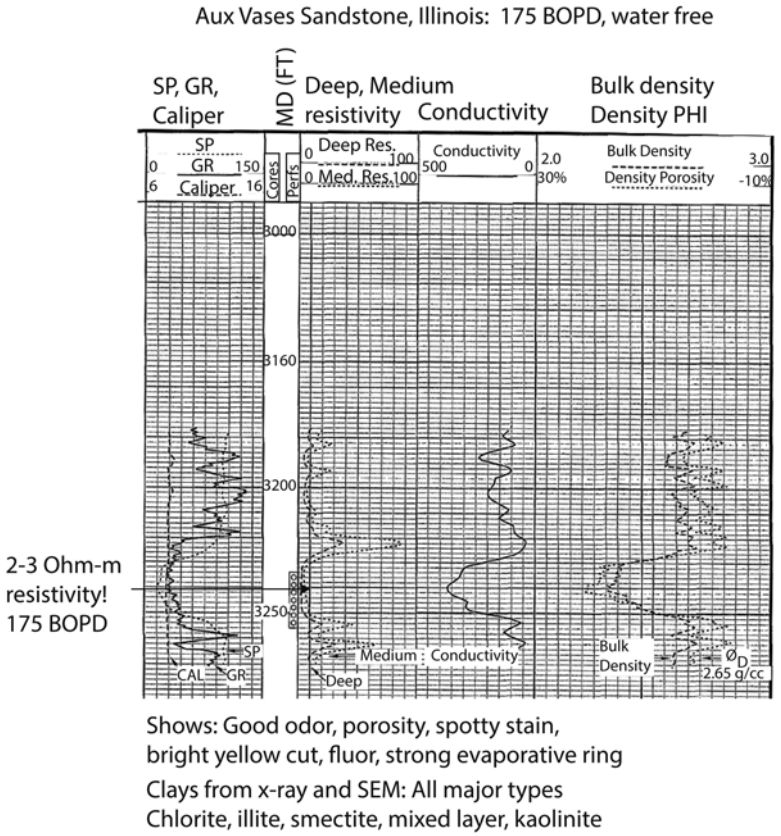

Fig. 6.20 Suppressed resistivity over a pay zone, Illinois. Modified from Dolly and Mullarkey (1996). Used by permission of the RMAG

Table 6.2 Clay minerals, cements and issues with logs and completions

Mineral or cement	Effect on logs or completion
Kaolinite	Migration of fines during completion
Illite	Can trap migrating fines. Generally non-reactive to fluids
Smectites	Swelling in the presence of water-based muds. High bound-water
Chlorite	Log resistivity suppression, high bound water; iron gel precipitates
Ankerite (Ca-Mg carbonate)	Precipitates ferric hydroxide if treated with HCl
Siderite	Precipitation of iron with some completion fluids
Pyrite	Log suppression if above 7 %
Glauconite	Log suppression if high percentages present

author had an experience in Egypt where a well flowing 5000 BOPD with rates climbing, suddenly went to 0 BOPD. The culprit was an unauthorized acid-frac job that, instead of boosting the rate under natural flow, caused the mud system in the well to turn into a substance that resembled peanut butter in viscosity. Despite proving the cause with lab tests that duplicated the result, plus the clear coincidence of the unauthorized acid treatment with the drop in production, the well was never redrilled. Nobody wanted to accept responsibility.

But in great teams and companies, the wells get retested and completion techniques get revised until great well performance is achieved.

6.8 A Note on Calculating Reserves

Once porosity and Sw values have been agreed upon, the last step in any log analysis project is to estimate reserves. An excellent summary is provided by (Sustakoski and Morton-Thompson 1992). An additional source is that of (Hartmann and Beaumont 1999). The basic equations are summarized in Fig. 6.21.

It is important to remember that reserve estimates are in volumes of economically recoverable reserves. These equations return oil and gas in place. The Boi and Bgi values, when needed for accuracy, are derived from detailed pressure, temperature and fluid properties. These numbers convert volumes that are present under subsurface conditions to conditions at the surface, in the volumes that will be sold and produced. Conversion of the in-place volumes needs adjustment for recovery factors. These vary by the type of reservoir, fluids and pressures, and are often difficult to accurately predict.

Hence, estimates of reserves are usually risk-weighted in probability buckets, or min, max and most likely cases. A list of suggested ranges for recovery factors is given in Table 6.3 (Hartmann and Beaumont 1999). Gas recoveries listed in this tables are probably more toward the low end, as many operators assume gas recoveries approaching 90–100 %.

6.9 Summary

In many cases, recognition of hydrocarbons on logs is fairly straightforward. However, when conductive minerals are involved or high clay content, either in pores or as laminae in the reservoirs, oil and gas pay may be difficult to recognize. In these cases, the use of FMI, NMR and other tools designed to deal with these situations is warranted. Every geoscientists should understand the basics of well log analysis at least enough to ask the right questions of expert log analysts that may be helping with an evaluation.

In addition, formations are sometimes damaged during drilling or completion and care must be taken not to walk away from a potentially productive reservoir just

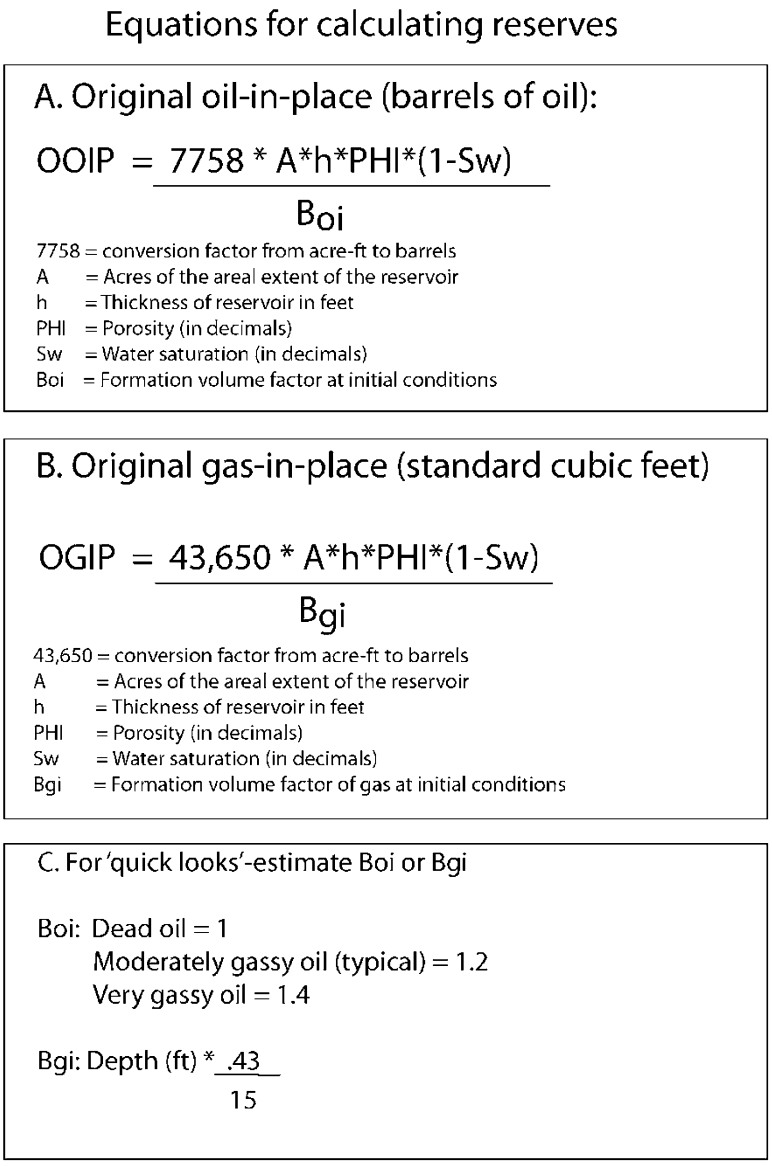

Fig. 6.21 Original oil and gas-in-place equations for reserve estimation. Equation shown in (**c**) is from Hartmann and Beaumont (1999)

because of a production failure. Discussions with team members, using all the available rock and petrophysical data will usually lead to recognition of formation damage and appropriate remediation. There are times however, when personalities may get in the way of doing the right thing. When that happens, wells are occasionally abandoned that are within a field waiting to be developed.

Table 6.3 Suggested recovery factor ranges. Modified from Hartmann and Beaumont (1999)

Drive mechanism	Gas ultimate recover (%)	Oil ultimate recover (%)	Comments
Strong water	30–40	45–60	Example: Nubia sandstone, Egypt
Partial water	40–50	30–45	
Gas expansion	50–70	15–60	
Solution gas	N/A	10–25	
Rock	60–80	10–60	Relatively rare
Gravity drainage	N/A	50–70	Relatively rare

For the creative interpreter who is carefully evaluating the shows, logs and completions, these are potentially lucrative exploration opportunities.

References

Ahmed U, Crary SF, Coates GR (1991) Permeability estimation: the various sources and their interrelationships. J Pet Geol 43:578–587

Akkurt R, Guillory AJ, Tutunjian PN, Vinegar HJ (1996a) NMR logging of naturation gas reservoirs. Log Anal 37:10

Akkurt R, Prammer MG, Moore MA (1996) Selection of optimal acquisition parameters for Mril logs. SPWLA 37th annual logging symposium, Society of Petrophysicists and Well-Log Analysts, New Orleans, Louisiana, p 13

Allen D (1988) Probing for permeability: an introduction to measurements. Tech Rev 36:6–20

Archie GE (1942) The electrical resistivity log as an aid in determining some reservoir characteristics. J Pet Technol 5:54–62

Asquith G, Krygowski D (eds) (2004) Basic well log analysis, 2nd edn, AAPG methods in exploration series. American Association of Petroleum Geologists, Tulsa, OK, 244 p

Asquith GB (ed) (1985) Handbook of log evaluation techniques for carbonate reservoirs, AAPG methods in exploration series No. 5. American Association of Petroleum Geologists, Tulsa, OK, 47 p

Asquith GB (2006) Quick guide to carbonate well log analysis with flow chart, case studies and problems, Midwest PTTC workshop. PTTC Technology Connections, Grayville, IL, p 280

Bennion DB, Thomas FB (1994) Underbalanced drilling of horizontal wells: does it really eliminate formation damage. Society of Petroleum Engineers, SPE 27352, pp 153–162

Bennion DB, Thomas FB, Bietz RF (1996) Formation damage and horizontal wells--a productivity killer? Society of Petroleum Engineers, pp 1–12

Boyd A, Darling H, Tabanou J (1995) The lowdown on low-resistivity pay. Oil Field Review, Schlumberger, p 15

Chai SN, Carney S, Leal L, Boardman D, Shepstone K (2008) Low resistivity low contrast pay in complex Miocene reservoirs of the Malaysia Thailand Joint Development Area (MTJDA). Thirty-Second annual convention & exhibition, Indonesia Petroleum Association, May 2008, p 18

Claverie M, Allen DF, Heaton NJ, Bordakov GA (2010) A new look at low resistivity and low-contrast (LRLC) pay in clastic reservoirs. Annual technical conference and exhibition, Society of Petroleum Engineers, Florence, Italy, p 12

Coates GR, Xiao L, Prammer MG (1999) NMR logging principles and applications. Halliburton Energy Services, Houston, TX, p 232

Coates GR, Marschall D, Mardon D, Galford J (1997) A new characterization of bulk-volume irreducible using magnetic resonance. SPWLA 38th annual logging symposium, Society of Petrophysicists and Well-Log Analysts, Houston, TX

Cook PL, Schneeflock RD, Bush JD, Marble JC (1990) Trimble field, Smith county, MS: 100 BCF of by-passed pay at -7000'. Gulf Coast Assoc Geol Soc XL:135–145

Cowan B (1997) Nuclear magnetic resonance and relaxation. Cambridge University Press, Cambridge, 434 p

Dolly ED, Mullarkey JC (1996) French #2-Goldengate North Field, Aux Vases Sandstone, Wayne County, Illinois. In: Dolly ED, Mullarkey JC (eds) Producing low contrast, low resistivity reservoirs, Guidebook. Rocky Mountain Association of Geologists, Denver, CO, pp 122–123

Dolson J, Burley SD, Sunder VR, Kothari V, Naidu B, Whiteley NP, Farrimond P, Taylor A, Direen N, Ananthakrishnan B (2015) The discovery of the Barmer Basin, Rajasthan, India, and its petroleum Geology. Am Assoc Pet Geol Bull 99:433–465

Doveton JH (1994) Geologic log analysis using computer methods, vol 2, AAPG computer applications in geology, No. 2. American Association of Petroleum Geologists, Tulsa, OK, 169 p

Fukushima E, Roeder SBW (1981) Experimental pulse NMR: a nuts and bolts approach. Addison-Wesley, London, 539 p

Halliburton (2015) Oil based mud imaging (OMRI) log service. Halliburton. http://www.halliburton.com/en-US/ps/wireline-perforating/wireline-and-perforating/open-hole-logging/borehole-imaging/oil-based-mud-imaging-omri-log-service.page

Hartmann DJ, Beaumont EA (1999) Predicting reservoir system quality and performance. In: Beaumont EA, Foster NH (eds) Exploring for oil and gas traps: treatise of petroleum geology, handbook of petroleum geology, vol 1. American Association of Petroleum Geologists, Tulsa, OK, pp 9.3–9.154

Henderson S (2004) Nuclear magnetic resonance logging, AAPG methods in exploration series. American Association of Petroleum Geologists, Tulsa, OK, pp 103–113

Hurley N (2004) Borehole images, basic well log analysis, AAPG methods in exploration series, v. Methods in exploration series No. 16. American Association of Petroleum Geologists, Tulsa, OK, pp 151–163

Joshi SD (1991) Formation damage. Pennwell Publishing Company, Tulsa, OK, p 8

Kasino RE, Davies DK (1979) Environments and diagensis, Morrow Sands, Cimarron country (Oklahoma), and significance to regional exploration, production and well completion practices, Pennsylvanian Sandstones of the Mid-Continent. Tulsa Geological Society, Tulsa, OK, pp 169–194

Kennedy MC (2004) Gold fool's: detecting, quantifying and accounting for the effects of pyrite on modern logs. 45th Annual logging symposium, Society of Professional Well Log Analysts, p 12

Kenyon WE, Day PI, Straley C, Willemsen JF (1986) Compact and consistent representation of rock NMR data for permeability estimation. SPE annual technical conference and exhibition, Society of Petroleum Engineers, New Orleans, Louisiana, USA, p 22

King GE (2009) Formation damage--effects and overview (online powerpoint). In Engineering GEK (ed). George E. King, p 61Engineeringhttp://gekengineering.com/Downloads/Free_Downloads/Formation_Damage.pdf

Kleinberg RL, Vinegar HJ (1996) NMR properties of reservoir fluids. Log Anal 37:20–32

Krygowski DA (2003) Guide to petrophysical interpretation, online report. Wyoming University, Austin, TX, Daniel A. Krygowski, p 147

Krygowski DA, Cluff RM (2012) Pattern recognition in a digital age: a gameboard approach to determining petrophysical parameters. AAPG annual convention and exhibition, Long Beach, CA, USA, AAPG Search and Discovery Article #40929, p 6

Lovell M, Parkinson N (eds) (2002) Geological Applications of Well Logs, AAPG methods in exploration series, No. 13. American Association of Petroleum Geologists, Tulsa, OK, 292 p

Mardon D, Gardner JS, Coates GR, Vinegar HJ (1996a) Experimental study of diffusion and relaxation of oil water mixtures in model porous media. SPWLA 37th Annual logging symposium, Society of Petrophysicists and Well-Log Analysts, New Orleans, Louisiana, p 14

Mardon D, Miller D, Howard A, Coates G, Jackson J, Spaeth R, Nankervis J (1996b) Characterization of light hydrocarbon-bearing reservoirs by gradient NMR well logging: a Gulf of Mexico case study. SPE annual technical conference and exhibition, Society of Petroleum Engineers, Denver, Colorado, p 10

Minh CC, Jaffuel F, Poirier Y, Haq SA, Baig MH, Jacob C (2011), Quantitative estimation of formation damage from multi-depth of investigation NMR logs. SPWLA 52nd annual logging symposium, Colorado Springs, Co, USA, p 11

Moore MA, Akkurt R (1996) Nuclear magnetic resonance applied to gas detection in a highly laminated Gulf of Mexico turbidite invaded with synthetic oil filtrate. SPE annual technical conference and exhibition, Society of Petroleum Engineers, Denver, Colorado, p 5

Murphy DP (1995) NMR logging and core analysis-simplified. World Oil 216:65–70

Naidu BS, Burley SD, Dolson J, Farrimond P, Sunder VR, Kothari V, Mohapatra P, Whiteley N (2016) Hydrocarbon generation and migration modelling in the Barmer Basin of western Rajasthan, India: lessons for exploration in rift basins with late stage inversion, uplit and tilting. Petroleum System Case Studies, v. Memoir 112. American Association of Petroleum Geologists, Tulsa, OK

Passey QR, Dahlberg KE, Sullivan KB, Yin H, Brackett RA, Xiao YH, Guzman-Garcia AG (2006a) The clastic thin-bed problem, AAPG archie series No. 1. American Association of Petroleum Geologist, Tulsa, OK, p 210

Passey QR, Dahlberg KE, Sullivan KB, Yin H, Brackett RA, Xiao YH, Guzman-Garcia AG (2006b) Digital core imaging in thinly bedded reservoirs, AAPG archie series, No. 1. American Association of Petroleum Geologist, Tulsa, OK, pp 91–107

Passey QR, Dahlberg KE, Sullivan KB, Yin H, Brackett RA, Xiao YH, Guzman-Garcia AG (2006c) Petrophysical evaluation of hydrocarbon pore-thickness in thinly bedded clastic reservoirs, AAPG archie series, No. 1. American Association of Petroleum Geologist, Tulsa, OK, 210 p

Passey QR, Dahlberg KE, Sullivan KB, Yin H, Brackett RA, Xiao YH, Guzman-Garcia AG (2006d) A roadmap for evaluating thin-bedded clastic reservoirs, AAPG archie series, No. 1. American Association of Petroleum Geologist, Tulsa, OK, pp 17–25

PetroWiki (2015) Nuclear magnetic resonance (NMR) logging. SPE. http://petrowiki.org/Nuclear_magnetic_resonance_(NMR)_logging

Pittman ED, King GE (1986) Petrology and formation damage control, upper cretaceous sandstone, offshore gabon. Clay Miner 21:781–790

Prammer MG, Mardon D, Coates GR, Miller MN (1995) Lithology-independent gas detection by gradient-NMR logging. SPE annual technical conference and exhibition, Society of Petroleum Engineers, Dallas, TX, p 12

Shepherd M (2009) Where hydrocarbons can be left behind. In: Shepherd M (ed) Oil field production geology. American Association of Petroleum Geologists, Tulsa, OK, pp 211–215

Sneider RM (2003) Worldwide examples of low resistivity pay. Houston Geological Society, Houston, TX, pp 47–59

Sneider RMB, Kulha JT (1995) Low-resistivity, low-contrast productive sands. AAPG annual convention, p 205

Sustakoski RJ, Morton-Thompson D (1992) Reserves Estimation. In: Morton-Thompson D, Woods AM (eds) Development geology reference manual. American Association of Petroleum Geologists, Tulsa, OK, pp 513–517

Tabarovsky L, Georgi D (2000) Effect of pyrites on HDIL measurements. 41st Annual logging symposium, Society of Professional Well Log Analysts, p 13

Thomas JBJ (2001) The importance of using geologic information to complete wells, Tulsa Geological Society monthly luncheon presentation. Tulsa Geological Society and AAPG Search and Discovery, Tulsa, OK, p 39

Timur A (1968) Effective porosity and permeability of sandstones investigated through Nuclear Magnetic Resonance principles. SPWLA 9th annual logging symposium, Society of Petrophysicists and Well-Log Analysts, New Orleans, Louisiana, p 18

Timur A (1969) Pulsed nuclear magnetic resonance studies of porosity, movable fluid and permeability in sandstones. J Petrol Geol 21 SPE-2045-PA:775–786

Trueblood S (2013) Finding big oil fields in East Africa: Inhassoro: the southernmost oil field in the East African rift system?, SASOL Petroleum International. http://64be6584f535e2968ea8-7b17ad3adbc87099ad3f7b89f2b60a7a.r38.cf2.rackcdn.com/EA%20Oil%20Forum%20-%20Sasol%20Presentation.pdf

Turner JR (1997) Recognition of low resistivity, high permeability reservoir beds in the Travis Peak and Cotton Valley of East Texas. Gulf Coast Assoc Geol Soc XLVII:10

Worthington PF (2000) Recognition and evaluation of low-resistivity pay. Pet Geosci 6:77–92

Zhang Q, Lo SW, Huang C, Hirasaki GJ, Kobayashi R, House WV (1998) Some exceptions to default NMR rock and fluid properties. SPWLA 39th Annual Logging Symposium, Society of Petrophysicists and Well-Log Analysts, Keystone, Colorado, p 14

Chapter 7
Using Fluid Inclusion Data in Exploration

Contents

Abstract Fluid inclusions are micron-scale fluid filled cavities in rocks, generally in cements. They frequently contain both water and hydrocarbons which can give valuable information on the temperature of emplacement, hydrocarbon quality and type and water salinity. Classic fluid inclusion studies utilize thin sections over limited intervals of section. Fluid Inclusion Stratigraphy (FIS), in contrast, analyzes bulk samples over an entire well bore from many samples to extract large amounts of data on hydrocarbon distributions in a well.

Plots of hydrocarbon abundance and type from FIS data can help identify pay zones, seals, near-misses (proximity to pay) and migration pathways. When coupled with burial history modeling, fluid inclusion microthermometry data can be used to

J. Dolson, *Understanding Oil and Gas Shows and Seals in the Search for Hydrocarbons*, DOI 10.1007/978-3-319-29710-1_7

infer timing of emplacement of hydrocarbons. In many dry holes, FIS data provides a much more detail look at oil shows than will be captured on logs or well reports.

7.1 Introduction and Overview of Fluid Inclusions

One of the most exciting things that has happened in the last several decades for oil show analysis are techniques designed to utilize geochemical information contained in trapped oil and gas in fluid inclusions, particularly those that can be applied economically to large sample sets. Fluid inclusions are micron-scale, fluid filled cavities in or between crystals in rock material (Fig. 7.1).

They form during diagenetic modifications when cement is added to pore space and micro-fractures, and various studies have verified that they generally contain representative samples of the pore fluid from whence they were trapped, barring some rather unusual circumstances (Sterner and Bodnar 1984). Their presence and composition can be used to track migration of aqueous and petroleum fluids. In unconventional reservoirs that are organic rich, partial conversion of kerogen or bitumen to oil and gas results in a spongy network of nanopores with restricted interconnectivity that function as loci for fluid entrapment. As will be shown, in these specific reservoirs the fluid that is extracted from these nanopores often corresponds in a general way to current production, in terms of both distribution and composition.

A short introduction to fluid inclusions in oil exploration is provided through AAPG's 2008 Getting Started Series (Hall 2008). Key papers cited in this collection are those of (Alpin et al. 1999; Burley et al. 1988, 2000; Burruss et al. 1983; Karlsen et al. 1993; McLimans 1987; Munz 2001; Oxtoby et al. 1995; Prezbindowski and Larese 1987;

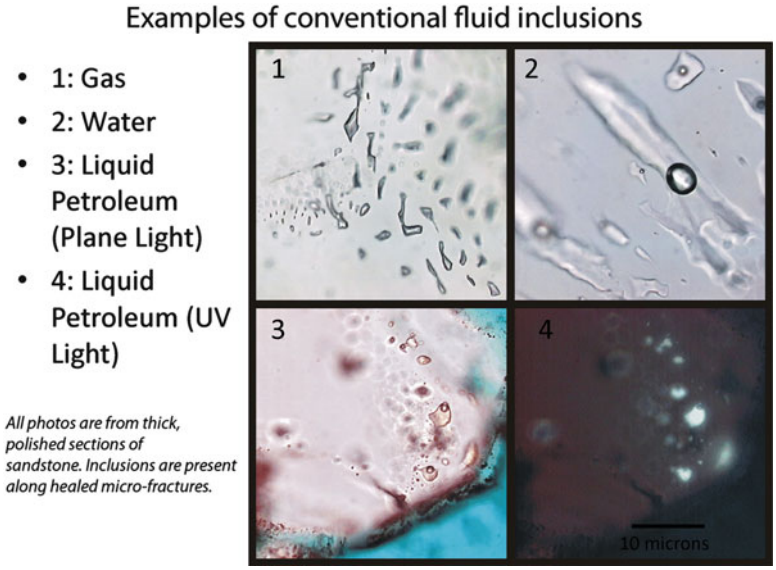

Fig. 7.1 Examples of fluid inclusions

Sterner and Bodnar 1984; Wilkinson et al. 1998). Some good practical applications are those of Arouri et al. (2010), Bhullar et al. (2003) and Brewster and Hall (2001).

For many years, this information was treated by many explorers as somewhat academic, of dubious value and tedious and time-consuming to obtain. Good case histories, however, have already been shown in Chap. 5 with the light oil discovery downdip of heavy oil (GS 160-5, Gulf of Suez) and the opening of the deep Oligocene play in the Nile Delta (Habbar-1 fluid inclusion information). The authors of this section have a long history of using fluid inclusion data successfully in exploration, as have many others. The use of fluid inclusion data is now a fairly standard practice in many companies, as it often provides that 'new idea from new data' required to break paradigms and deliver new plays.

Perhaps the most exciting development, however, has been using mass processing of cuttings to obtain a geochemical signature down an entire wellbore from archived, unpreserved samples. This process is called Fluid Inclusion Stratigraphy (FIS). It was developed and patented in 1990 by Amoco Production Company and was subsequently released in 1997 through a spin-off company: Fluid Inclusion Technologies, which remains the only commercial organization to offer this service. The information obtained provides a reasonably cheap and robust data set. In can be done quickly, with turn-around time in a few days or weeks. Much of this chapter is focused on the FIS approach. The geochemical information extracted can be done on any old dry hole, regardless of age of the samples.

The basic results provide information that is conceptually similar to head space gas analysis (Kolb and Ettre 2006) with some important differences. Head space gas analysis is discussed in the next chapter, but can only be run on cuttings captured at the rig site on a new well. Hence, unless you are within a company that has these data, it is not generally available to other geoscientists, and is almost never available on old dry holes. As access to cuttings is possible decades after a well is drilled, and are accessible through other companies or government repositories, being able to run any analysis on these legacy cuttings is a huge advantage. In addition, Head space and mud gas information is only going to give you information regarding fluids that are between the grains of the rock now, not what was trapped or migrated through in the past. Additionally, FIS provides information on species that are not typically analyzed via head space gas analyses, such as the aromatics, organic acids and inorganics such as H, He and sulfur species. These other compounds provide important information with regard to source and process.

There are some limitations and things to be aware of, however. Firstly, the effectiveness of fluid entrapment can be influenced by lithology, residence time and opportunities for encapsulation created by diagenetic processes. Consequently, in certain, shallow, diagenetically quiescent siliciclastic systems inclusions are not formed at levels above detection. Secondly, contamination by drilling fluid can mask or modify the signal and hinder interpretation of the natural fluid distribution and composition. This is essentially restricted to wells drilled with oil-base mud, in which residual drilling fluid is retained within certain lithologies, such as highly unconsolidated "gummy" claystones and salt. Drilling-synthesized fluid inclusions can often be found within healed fractures in salt drilled with OBM, although they have not been recognized by the authors in any other lithology or mineral. Finally,

drill bit metamorphism can reconstitute rock material and encapsulate natural pore fluid, drilling mud and bit-generated volatiles within closed pores. This last process will be explained further below.

Taken as a whole, however, there is great benefit to being able to capture FIS data on old wells and thus being able to detect and interpret things others have never seen. Additionally, use of FIS as a geochemical screening tool aids in selection of samples for other geochemical analyses, including conventional fluid inclusion microthermometry, and extract GCMS or GC-CSIA. More examples follow.

7.1.1 The Reality of Migration: It Is Complicated!

Any tools from shows data you have not only help in understanding the trapped reservoirs, but in the case of geochemical information and FIS, help to understand and perhaps even predict migration from source to trap. A favorite term many of my colleagues use in understanding migration is the need to 'think like a molecule'. Oil and gas molecules go where the physical conditions force them to go. The schematic in Fig. 7.1 illustrates a point, and is based conceptually on a number of cases in the Gulf of Mexico and elsewhere where oils at shallow Tertiary levels have been typed to deeper Cretaceous or Jurassic source rocks. The source rocks, in these cases, are often kilometers below the trapped hydrocarbons. Setting up 3D migration models to simulate vertical migration is covered in Chap. 9, but conceptually shown here (Fig. 7.2).

Deep source rocks fill and spill along reservoir carrier beds until the seal capacity of a trap is reached and they can migrate vertically. This can occur by capillary leakage, excess fluid pressure or cross-fault juxtaposition of carrier beds. The result is a complex

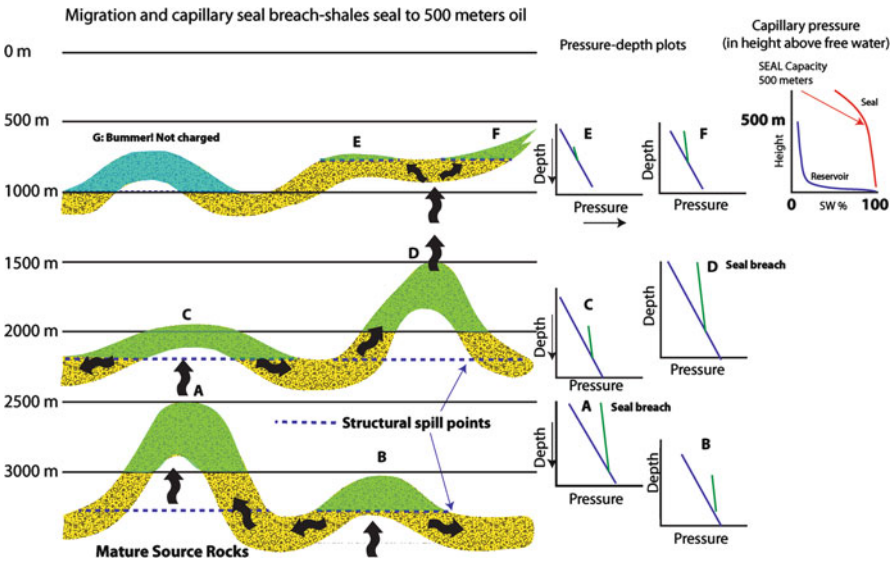

Fig. 7.2 The reality of migration. It's complicated

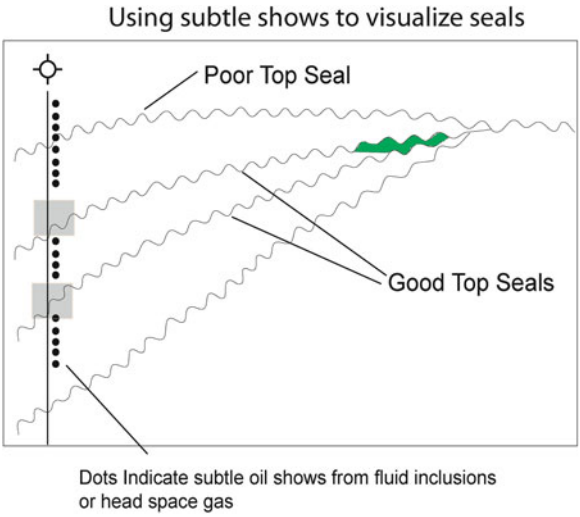

Fig. 7.3 Recognition of seals from fluid inclusions

layering of oils from those source rocks leaving some deeper structures full, but overlying structures barren and stratigraphic traps (F) filled in positions not easily predicted.

What is needed, then, is a more comprehensive look at migration from tools like FIS to try to see where seals are in the system and where hydrocarbons have been in the past or are still there at present. Picture the settings in a dry hole where fluid inclusion or head space data, or even perhaps mud or shows indicate vertical breaks which are seals. This information can be used to track the seals laterally and updip to find potential traps along migration pathways (Fig. 7.3).

In addition, it is nice to have information others won't have! In Fig. 7.4 a cemented sandstone only has oil shows as inclusions in the cement. These will not show up on a mud log or cuttings description, but can be key to a new pool. In the Habbar-1 example shown in Chap. 5 for the play opening analysis of the deep Oligocene, the mud log data only indicated possible residual gas in the dry hole. The fluid inclusion data showed oil, good gravities and even a temperature of emplacement of the oil. That information was used to help predict that the deeper play would not only work, but it would have condensate as well as gas. No one else had that data, so they could not begin to visualize that play in the same way.

7.2 Conventional Fluid Inclusion Analysis

Despite their small size (Fig. 7.5), fluid inclusions contain a wealth of useful information. One of the many advantages of fluid inclusion analysis is that the trapped volatiles are compositionally very similar to the original composition of the bulk fluid. So, a great deal of information can be obtained from them, including the API gravity, composition, source, temperature of oil emplacement, and salinity of the water at time of oil emplacement. All of this information can be input into petroleum system migration models and potentially simulated as migration through time.

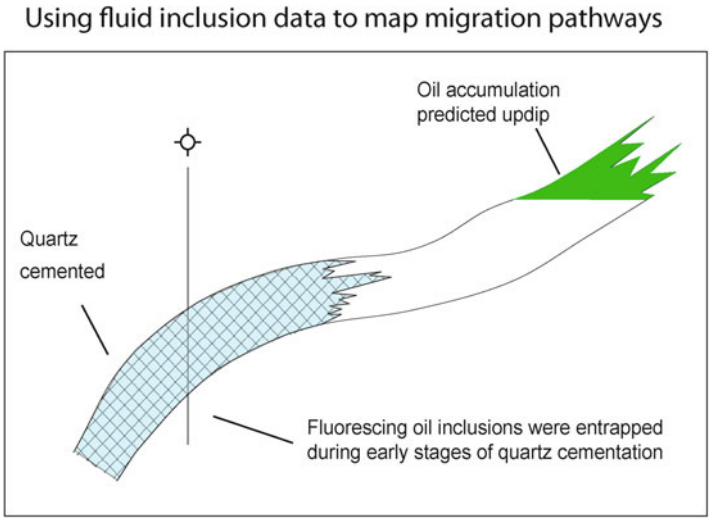

Fig. 7.4 Fluid inclusions trapped in early cements indicating a migration pathway updip. Modified from Dolson et al. (1999). Reprinted by permission of the AAPG, whose further permission is required for further use

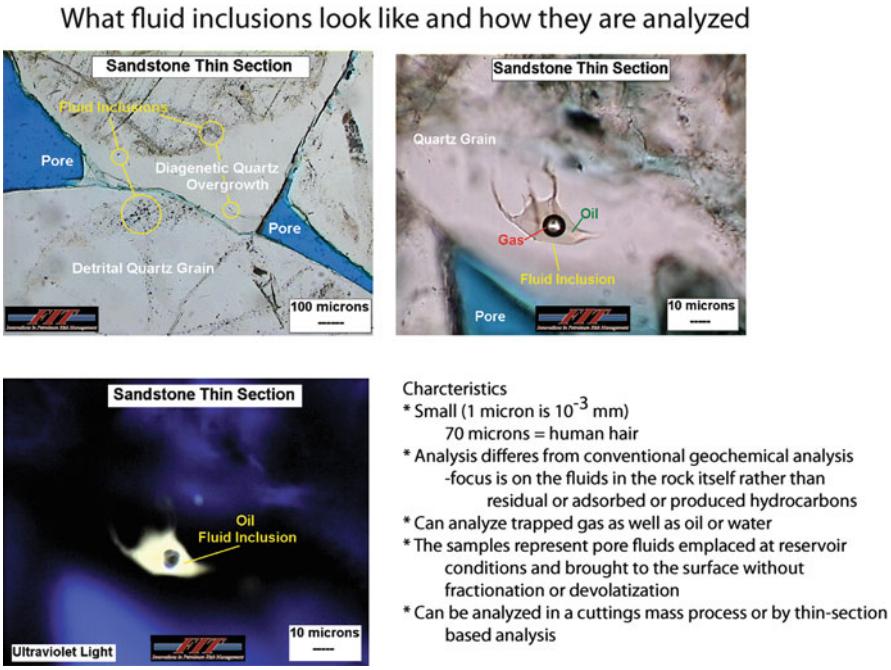

Fig. 7.5 Fluid inclusion information readily obtained

The classic approach to fluid inclusion studies is based on thin-section evaluation as shown in Figs. 7.1 and 7.5. Optical work is carried out using thick, polished sections of rock material under transmitted plane-polarized light and under episcopic illumination with a high-intensity UV source. The latter allows oil and condensate inclusions to be identified by their fluorescence. Inclusion populations are identified, along with relevant variables, such as fluorescence color, distribution and abundance. Optically-determined inclusion abundance in conventional reservoirs has been shown to be related to a combination of reservoir quality, hydrocarbon saturation and residence time. Thus, migration paths can often be distinguished from paleo-accumulations based on the visual abundance of liquid petroleum inclusions (Fig. 7.6). Gas inclusions, which do not typically fluoresce, are more difficult to identify and quantify, and relative abundance must be judged by destructive techniques, such as FIS.

7.2.1 Using Microthermometry Data and Identifying Hydrocarbon Types and Salinities

Once appropriate inclusions are mapped quantitative data can be collected with a fluid inclusion microthermometry stage (Fig. 7.7). This is a specially designed controllable temperature chamber that is placed on an XY stage of a petrographic microscope. The sample containing the inclusions of interest is placed inside the chamber and phase changes within individual fluid inclusions are manually recorded by an operator that is viewing the sample down the microscope through the glass windows of the chamber. Phase changes are compared to appropriate chemical systems to derive the desired data such as temperature, salinity and API gravity. The theory and details of fluid inclusion microthermometry are beyond the scope of this chapter and the reader is referred to classic works by (Roedder 1984)) and (Goldstein

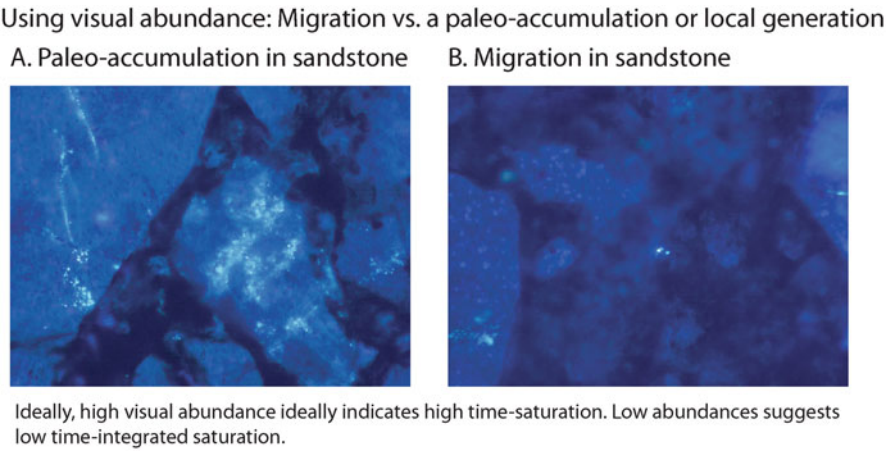

Fig. 7.6 Using visual abundance to recognize paleo-accumulations and migration pathways

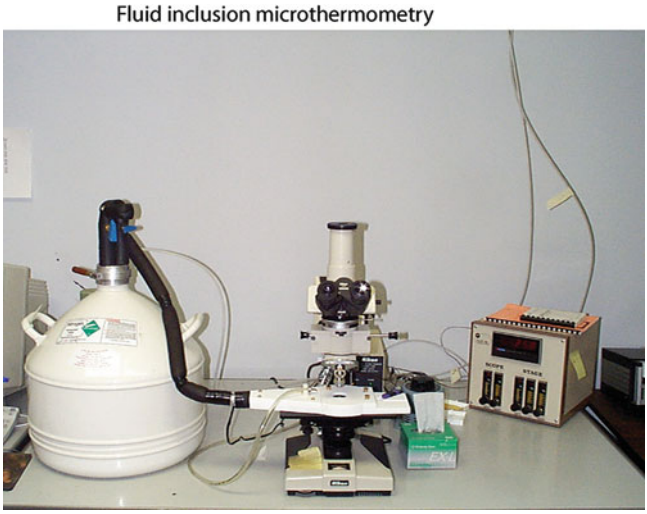

Fig. 7.7 Microthermometry equipment

and Reynolds 1994) for further information. Following is a brief discussion of the main uses of classical fluid inclusion data with some examples.

The most common piece of quantitative information provided by fluid inclusion microthermometry is temperature. There is generally a particular population of aqueous fluid inclusions in both carbonate and siliciclastic rocks that track maximum burial temperature. The mechanisms and reasoning involved are debatable and incompletely understood. However, it is an empirical observation that, given adequate data, the maximum thermal exposure of a given sample can often be estimated to within approximately 5 °C (Fig. 7.8).

Other inclusions are more likely to record actual cementation temperatures, and the trained microthermometrist can distinguish the various populations and what type of data they are likely to yield. It has also been shown by various studies that there is a relationship between maximum Th and vitrinite reflectance (Ro) (e.g., Barker and Pawlewicz 1986). We have found that a simple application of equation for basins subsiding at a rate of 1 °C/10 million years provides a reasonable correlation to measured Ro when the maximum interpreted burial temperature via inclusion Th is used (Burnham and Sweeney 1989). Often this calculated Ro is within 0.1–0.2 of independently determined reflectance.

It should be noted that diagenetic studies, although possible with fluid inclusions, usually depend on the presence of primary inclusions in the cement of interest that have not been modified by post-entrapment processes such as stretching or leakage. While these may be present, they are often quite difficult to find, and in any case, one will generally obtain a fragmentary diagenetic history.

Homogenization temperatures derived from petroleum inclusions are more a function of saturation state of the fluid (e.g., proximity to bubble point or dew point) than actual temperatures of formation. Consequently, it is inaccurate to quote Th of liquid petroleum inclusions as formation temperatures without evidence of near-

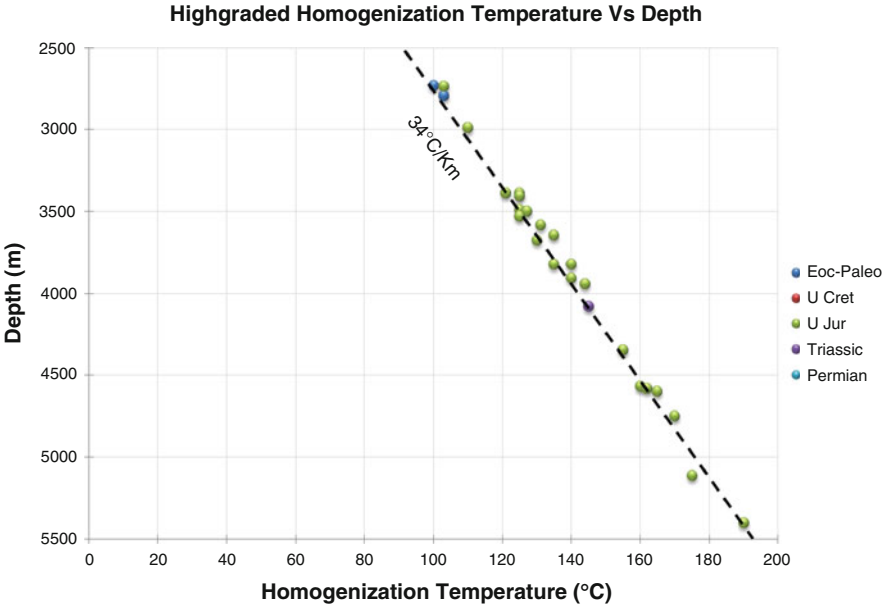

Fig. 7.8 Tracking maximum burial temperature with microthermometry data

gas-saturated conditions. Combined temperatures from coexisting aqueous and petroleum inclusions can be used to evaluate both trapping temperature of the petroleum phase (the Th of the aqueous inclusions) and proximity to bubble point or dew point of the petroleum phase (difference in Th between coexisting aqueous and petroleum inclusions).

Salinity is determined by freezing the inclusion with liquid nitrogen, and then heating the frozen inclusion until the last solid phase melts. The so-called freezing point depression is a function of total dissolved constituents (generally salts such as NaCl and CaCl), and salinity can be estimated by reference to the appropriate phase diagram. Salinity can often be used to imply the source of aqueous fluids in a reservoir, which can help define plumbing systems and fluid migration routes. Additionally, aqueous inclusions that are co-entrapped with petroleum inclusions may contain pore fluid that approximates the irreducible water within the reservoir and can help with water saturation calculations where reliable water data are unavailable (Fig. 7.9).

API gravity can be estimated from quantitative fluorescence techniques. A number of researchers have independently established correlation schemes, which are based on the fact that lower gravity inclusions tend to fluoresce toward the red wavelengths, while high gravity inclusions tend to fluoresce toward the blue wavelengths (Fig. 7.10). This relationship can be quantified fairly accurately, although certain oils give unusual fluoresce.

In a broader sense, petroleum inclusion data (and paired aqueous and petroleum inclusions) can be used to constrain models that include aspects of expulsion, migration and trap formation (Figs. 7.11 and 7.12). Temperatures derived from paired aqueous and petroleum inclusions and estimated or measured API gravities

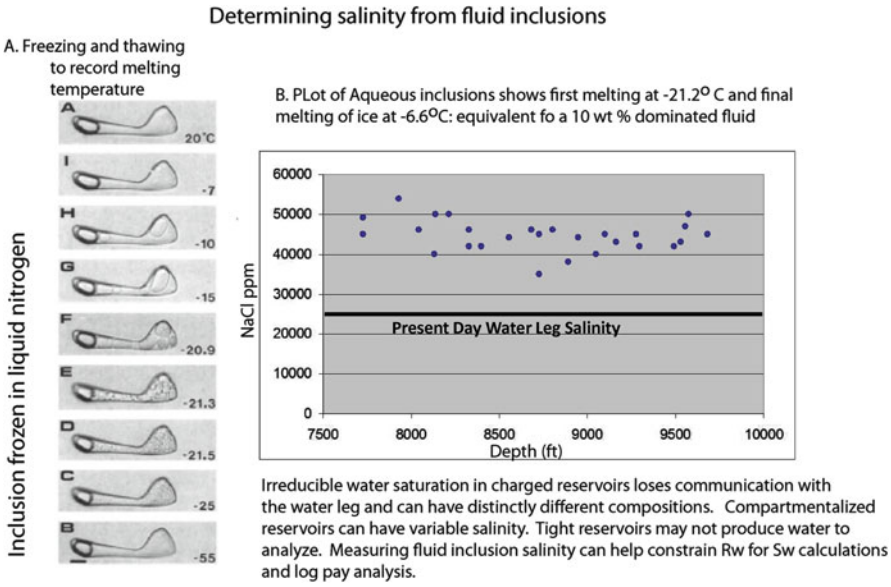

Fig. 7.9 Salinity technique for fluid inclusions. Modified from Goldstein and Reynolds 1994

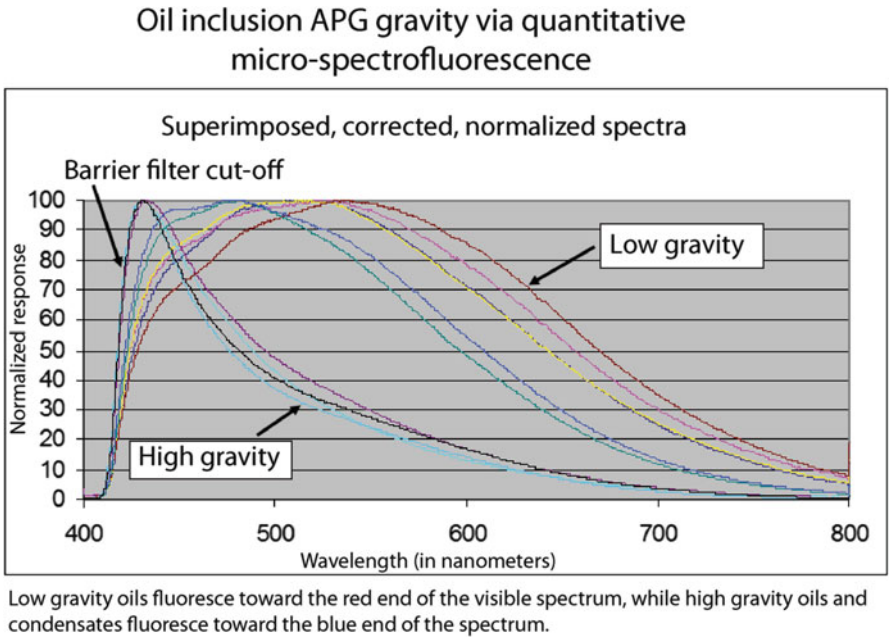

Fig. 7.10 Determining API gravity

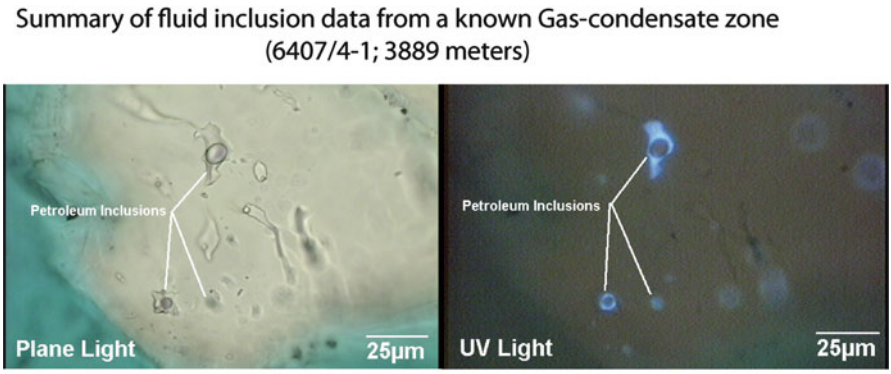

Fig. 7.11 Gas-condensate example

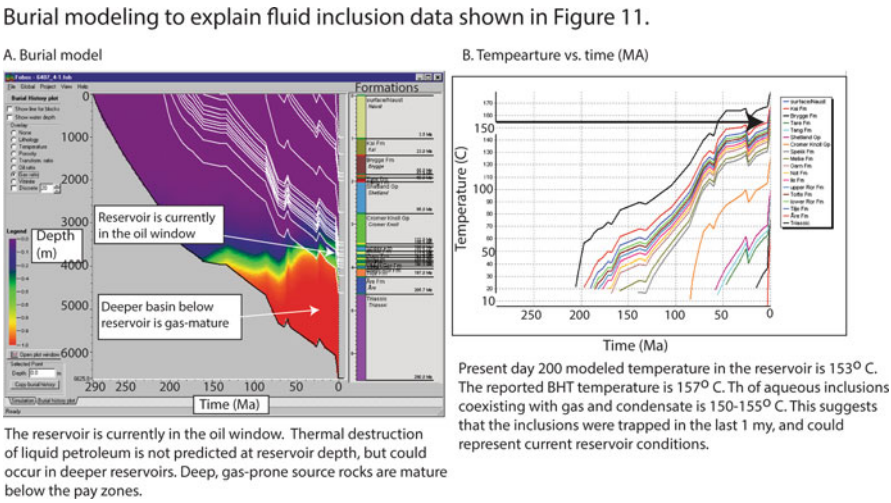

Fig. 7.12 Basin modeling to explain the microthermometry (Th) shown in Fig. 7.11

can be considered in the context of the implied or known distribution of source rock and source rock maturity through time. The age of the hydrocarbon migration or charge event can be evaluated in light of trap formation. Even the presence or absence of migration indications via petrography or FIS can provide calibration for migration vectors, as well as basic answers regarding the presence of an active petroleum system at some time.

Using the Th data from Fig. 7.11, and combining it with a basin model (Fig. 7.12) a reasonable conclusions is that the inclusions sampled were emplaced within the last one million years, and may represent the actual fluids currently in the reservoir, and not a prior migration event.

If present in sufficient abundance, hydrocarbon inclusion liquids and gases can be extracted and analyzed via GC/GCMS (Karlsen et al. 1993) and compound specific isotope analysis (Wavrek et al. 2004) In this context, the extracts become essentially equivalent to unfractionated whole oils and DST gases and can be treated accordingly to evaluate source, maturity and process. Obviously, connecting migration pathways or paleo-accumulations determined from FIS or petrography to a specific source rock can be quite useful where multiple source rocks are present (Fig. 7.13).

Occasionally, as is often also the case in biostratigraphic analysis, there are recycled inclusions from older formations. A geological knowledge of the provenance of the reservoirs being examined is useful in this case. It is not sufficient to simply exclude from consideration all petroleum fluid inclusions that occur within detrital portions of clastics (although this is a good idea for aqueous inclusions). Physical compaction and microfracturing occur through a large portion of a basin's history, even within the zone of chemical compaction. This results in a high percentage of oil inclusions that occur within detrital grains, but are not recycled. Our observations are that reworked oil inclusions are generally present only in low abundance, if at all, because resedimentation is generally a dissipative and winnowing process rather than a concentrating process in this respect. Thus, inclusion abundance above a spec-

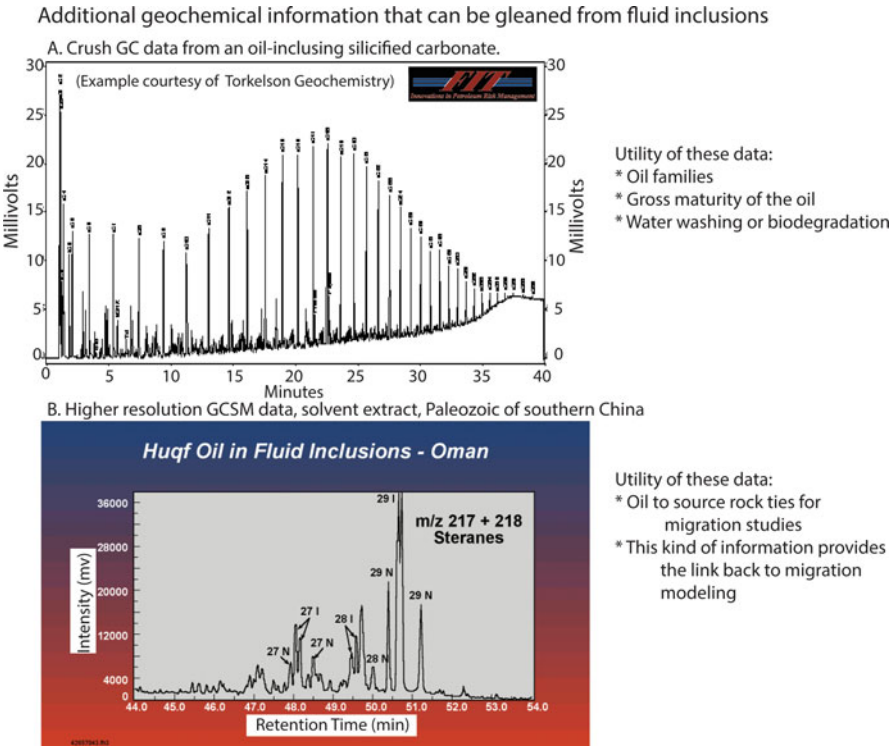

Fig. 7.13 Extracting geochemical signatures from fluid inclusions

ified level almost always indicates migrated petroleum. FIS signals that cut across stratigraphic or provenance boundaries are also evidence of migrated rather than recycled signals. We have rarely observed FIS signals that are attributable to reworked inclusions, in part because the abundance of such inclusions is generally below detection, and the effect on FIS data is simply to produce a slight increase in baseline without significant compartmentalization of chemistry.

7.3 Bulk Fluid Inclusion Analysis with FIS

As in the case of any exploration program, where the regional geological setting should be known before diving into detail, the FIS approach offers a broader and quicker view. The thin section approach can be used to derive a lot of very good information but has limitations:

1. The analysis assumes the most relevant samples have been picked (which may not be the case).
2. Petroleum compositions (except API gravity) are typically crudely constrained, or inferred by local production.
3. It is difficult to apply to dry gas problems, owing to lack of fluorescence and general difficulty in identifying these inclusions.
4. If regional work is desired, it is time intensive and expensive.

The FIS approach is different, and while having its own limitations, is a much better place to start to visualize hydrocarbons trapped in inclusions. The process is shown in Fig. 7.14. Approximately 0.5 g of rock material is cleaned of surface contamination, placed in a vacuum system and crushed to liberate the trapped volatiles. The molecular species are simultaneously analyzed via direct quadrupole mass spectrometry using multiple residual gas analyzers. The released signal is fleeting and must be analyzed quite rapidly; consequently, the entire analytical cycle is less than a minute. Instruments are automated to allow throughput of over 600 samples in a 24 h period. Such capacity allows every sample from a wellbore to easily be analyzed in a single analytical run under substantially similar conditions. Instruments are calibrated with internal standards so that data are comparable from day to day.

When processed, mass spectra from individual samples can be used much like a gas chromatogram to fingerprint the fluid type. More importantly, individual ions that are related to specific organic compound families or inorganic species can be displayed in depth with colors set to record various associations (Fig. 7.15).

Summary diagrams are provided which show major species of hydrocarbons in the samples (Fig. 7.16). In both cases, seals can be spotted by an abrupt decrease in the amount and type of inclusions.

Data can be plotted at a common scale for inter-comparison, or at a scale that accentuates the variation within the given wellbore The data are categorized with respect to strength and presence or absence of key indicator species by statistical comparison to a global database containing several million analyses from all over the world (Fig. 7.17).

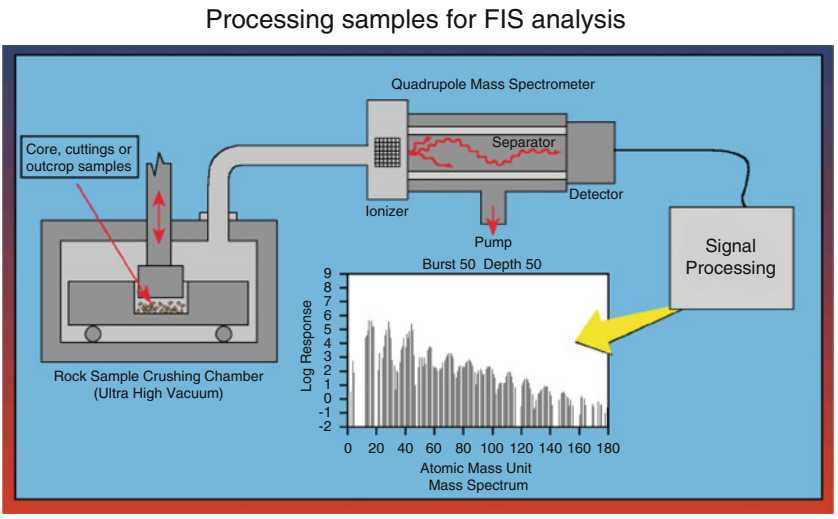

Fig. 7.14 Mass sample processing for fluid inclusion stratigraphy (FIS). Figure courtesy of Fluid Inclusion Technologies, Inc

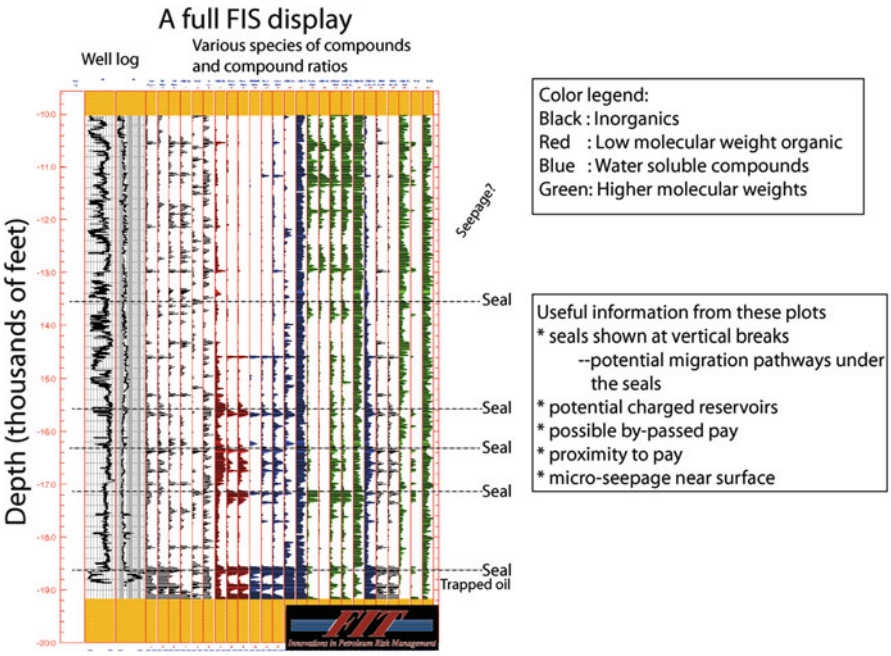

Fig. 7.15 Fluid inclusions stratigraphy-all tracks and compounds

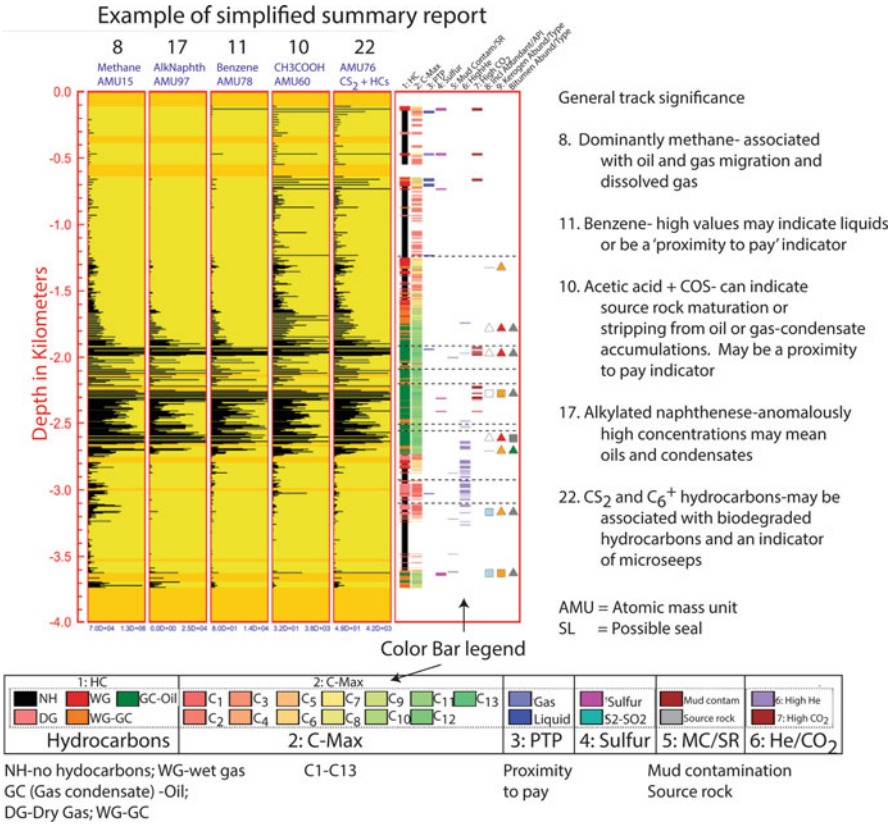

Fig. 7.16 Typical summary data and tracks

In any case, there is no reason to discount a clear anomaly within a well that appears to be sub-anomalous on a global concentration scale but has a clear positive concentration deviation from baseline within the wellbore.

One of the fundamental questions that can be answered from a dry hole FIS analysis is whether or not there is any evidence of migration (or paleo-accumulations). If so, then what hydrocarbon type is suggested and over what stratigraphic intervals (Fig. 7.18).

Secondarily it is important to assess the geometry of the anomalies, for instance how focused they are within the stratigraphic sections: are they diffuse without abrupt tops and bases or do they jump out at you from the depth plot. The difference between these two end-members can be a measure of migration or charge volume and effectiveness of seals. Seals are essentially defined as boundaries between low and high FIS responses, and/or chemically distinct intervals (Fig. 7.19).

Comparison to offset wells, can help identify regional seals and migration pathways. Structural mapping on those seals is the first step toward prospecting, as the migration pathways are now confirmed under the seals. Abrupt bases of features may represent paleo-petroleum-water contacts (Fig. 7.19), but only if high visual oil inclusion abundance is indicated by petrographic work, and if the base of the anomaly is not controlled by porosity. For instance, the abrupt decrease in hydrocarbon

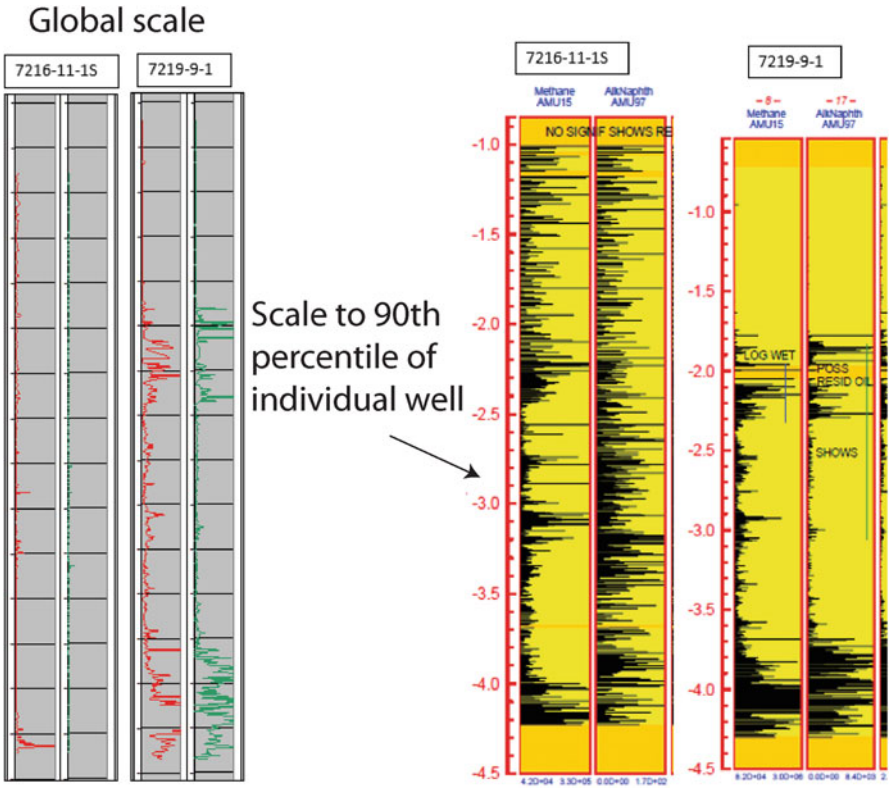

Fig. 7.17 FIS plots are calibrated at a global scale

response within a clean sandstone with porosity suggests a fluid contact, whereas, a decrease at the base of effective porosity (e.g., a sand-shale contact) suggests that the paleo-petroleum-water contact is located off-structure.

A progressive increase in hydrocarbon response with depth (especially methane) often indicates diffusion through tight rock, in some cases from below, and in others from progressive maturation of intercalated kerogen, or even increased pore pressure (Fig. 7.20).

Shallow dry gas features that begin at first returns and decrease abruptly below about 65 °C current temperature can indicate active microseepage of light thermogenic hydrocarbons from depth followed by bacterial alteration by thermophilic anaerobes (Fig. 7.20). This process produces a characteristic set of volatile species in FIS data, including biogenic methane, CO_2, H_2S, SO_2, COS, and CS_2. Macroseepage can involve higher hydrocarbons, particularly where oil seeps are known at the surface. Although appearing in FIS "paleo-fluid" data, these microseeps or macroseeps appear to be related to present-day processes. Obviously, the presence in essentially recent marine sediments implicates a recent process, but additionally, there is a good statistical correlation with deep accumulations (particularly liquid petroleum accumulations) where FIS microseeps are found. For instance, an FIS evaluation of

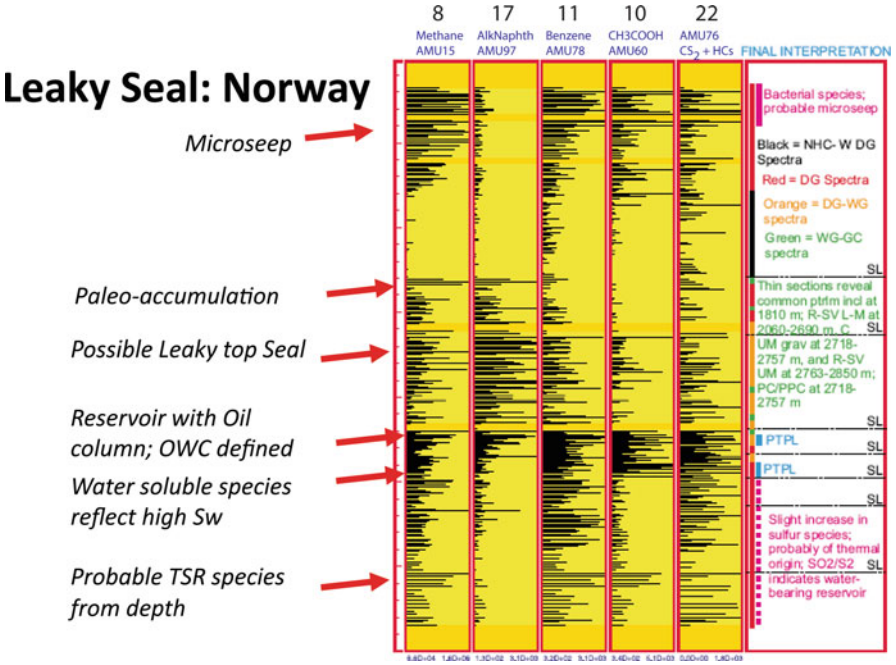

Fig. 7.18 Hydrocarbon types and leaky seal interpretations, Norway

approximately 180 wells drilled on the Texas shelf indicated that FIS microseeps were present in 90 % of wells that had deep production. 75 % of deep dry holes did not have this feature, and our current understanding would suggest that the remaining 25 % may have bypassed pay, or may represent near misses.

7.3.1 Proximity to Pay

The water-soluble hydrocarbons (chiefly aromatics and organic acids) have long been used to look for proximity to hydrocarbons or surface seeps (Burtell and Jones 1996; Matusevich and Shvets 1973). The principle is the same as for groundwater contamination plumes or elemental geochemical anomalies associated with mineral deposits (Grimes et al. 1986). Mobile species will tend to be transported or diffuse away from the anomaly (within the water leg or across a bounding fault, for instance, Figs. 7.21 and 7.22) creating a larger target than the anomaly itself.

By recognizing the anomaly, one can infer that the accumulation of interest is within a prescribed distance. In FIS data, the two key indicator species are benzene and acetic acid. The downdip leg of an oil accumulation and acetic acid anomaly is clear on Fig. 7.22, for example.

Absolute concentrations are generally not as important as the ratio of one of these compounds to a less soluble species, particularly for benzene which is almost always present in greater absolute abundance in the oil than the water in contact

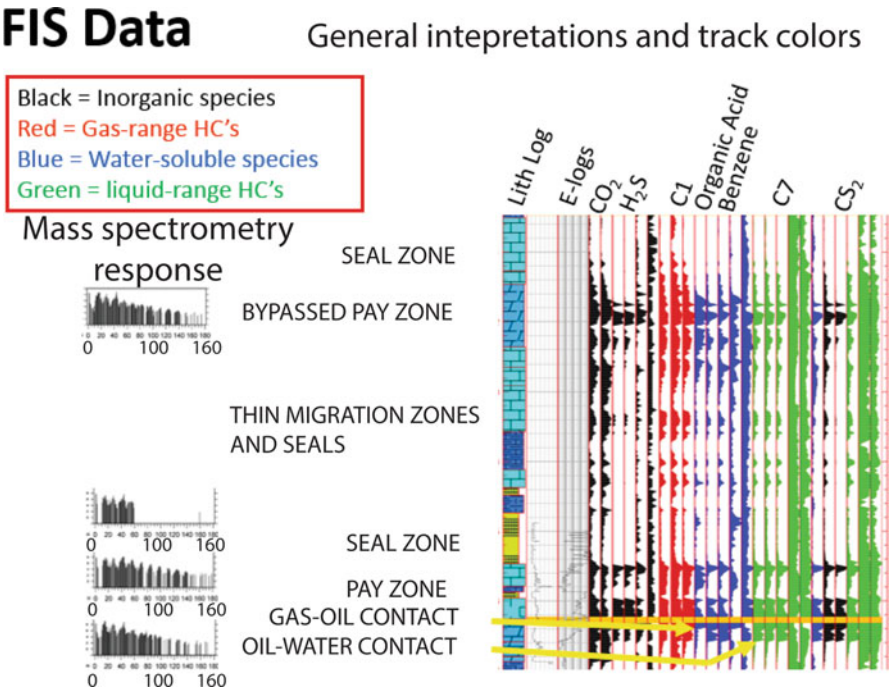

Fig. 7.19 General interpretations of tracks

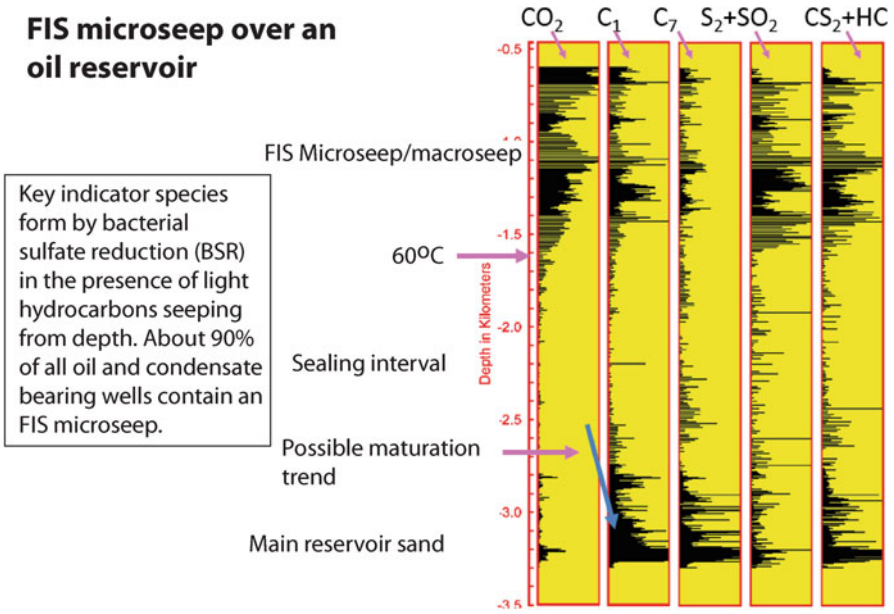

Fig. 7.20 Microseeps and maturation trends from FIS

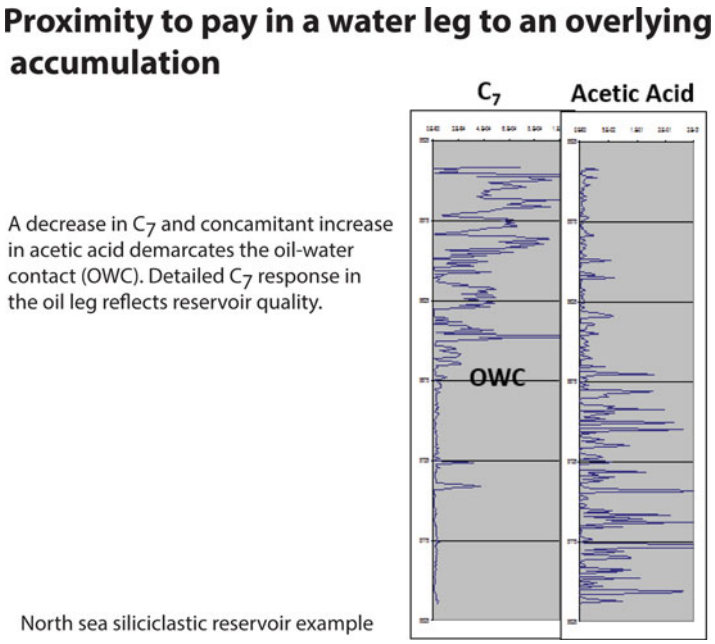

Fig. 7.21 FIS identification of proximity to pay and an oil-water contact

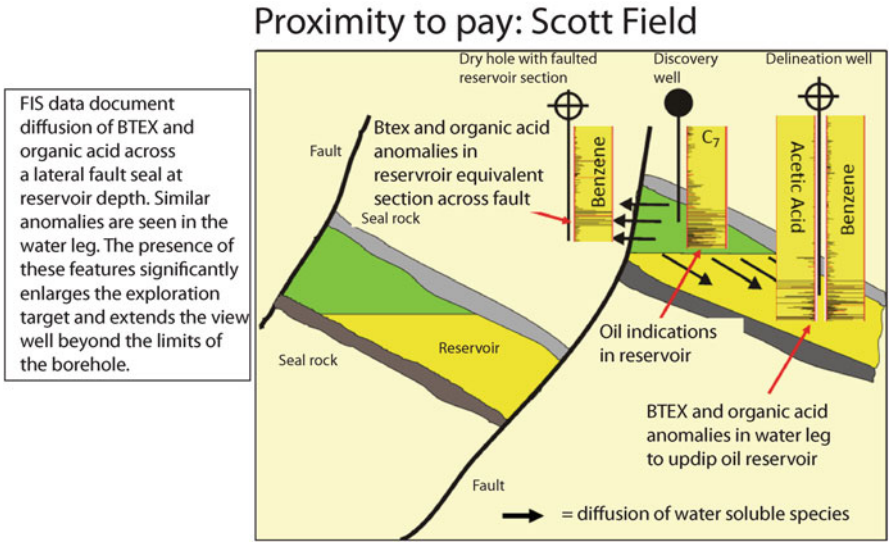

Fig. 7.22 Acetic acid and benzene (BTEX) anomalies indicating proximity to pay, Scott Field, North Sea

with it. For a given carbon number, the aromatics are most soluble, the alkanes are least soluble, and the cycloalkanes have intermediate solubility in water. Thus ratios of benzene to n-hexane or cyclohexane, and acetic acid to n-butane are often used. As with shallow microseeps, empirical data from thousands of wells suggest that FIS proximity-to-pay (PTP) anomalies are present-day features that are at least partially facilitated by the drilling process. It is also suggested that FIS PTP anomalies suggest that they can be detected as far as about 8 km from the petroleum-water contact. Finally, the presence of benzene only without acetic acid suggests proximity to a wet gas accumulation, whereas acetic acid anomalies (with or without benzene) suggest proximity to an oil or condensate accumulation. This is because acetic acid in this instance is produced by in-reservoir alteration of liquid-range alkanes. Similar observations have been made by Russian researchers based on analysis of basin brines.

Because there are a number of processes that affect the strength of the PTP signal (effectiveness of encapsulation, oil composition, salinity of the pore fluid, hydrodynamics) anomalies are generally interpreted in terms of presence rather than concentration. Likewise, absence of an anomaly does not necessarily indicate that there is no charge nearby. The anomalies can only be used in the positive sense. As with other FIS interpretations, logic and context is important. If an anomaly occurs within a potential reservoir section that is wet at the wellbore location but contains visible liquid petroleum inclusions, then lateral prospectivity is suggested. If it occurs in an irrelevant section with no reasonable nearby potential, then perhaps it is not significant or is produced by other processes (bacterial alteration of organic matter, thermal maturation of organic matter, etc.).

7.3.2 Bacterial and Thermal Alteration

Finally, bacterial or thermal alteration is indicated in FIS data by presence of CO2 and sulfur species. The association of these volatiles with microseeps has already been discussed, and similar chemistries are identified in bacterially altered petroleum accumulations. It is often important to distinguish biodegraded low gravity fluid inclusions (e.g., identified optically) from low maturity inclusions. Usually, biodegraded oils have FIS responses that contain sulfur species, CO2 and perhaps other chemical indications of biodegradation (e.g., low ratios of n-alkanes to cycloalkanes). A number of other observations can be helpful here, including Th of petroleum inclusions, and biomarker analysis of extracted oil (Fig. 7.23).

Thermal alteration often produces similar species via thermochemical sulfate reduction. This generally occurs at temperatures above about 140 °C (Worden et al. 1995). The distinction between bacterial sulfate reduction (BSR) and themochemical sulfate reduction (TSR) is usually obvious from a number of lines of evidence, including burial history, induration of host rocks, coarseness of mineral cements, Th of fluid inclusions, presence or absence of pyrobitumen, and methane isotopic data from extracted volatiles (Fig. 7.24).

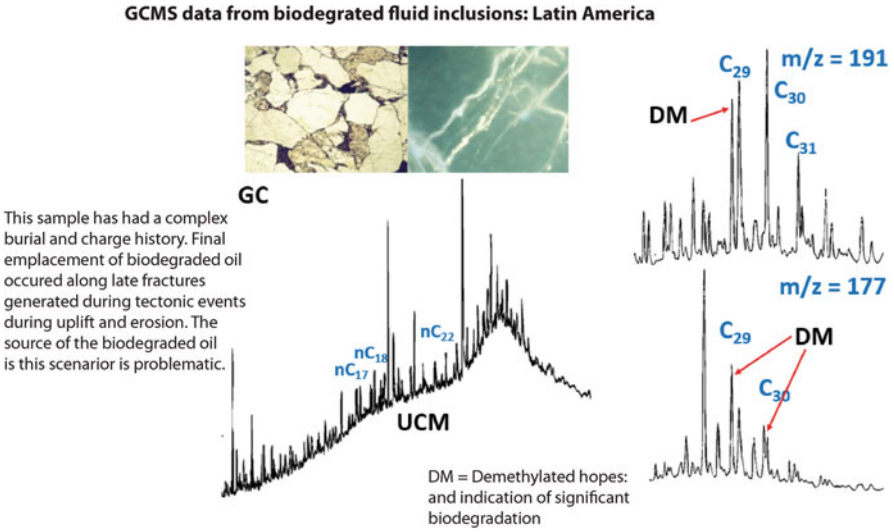

Fig. 7.23 Recognition of biodegraded fluids from FIS

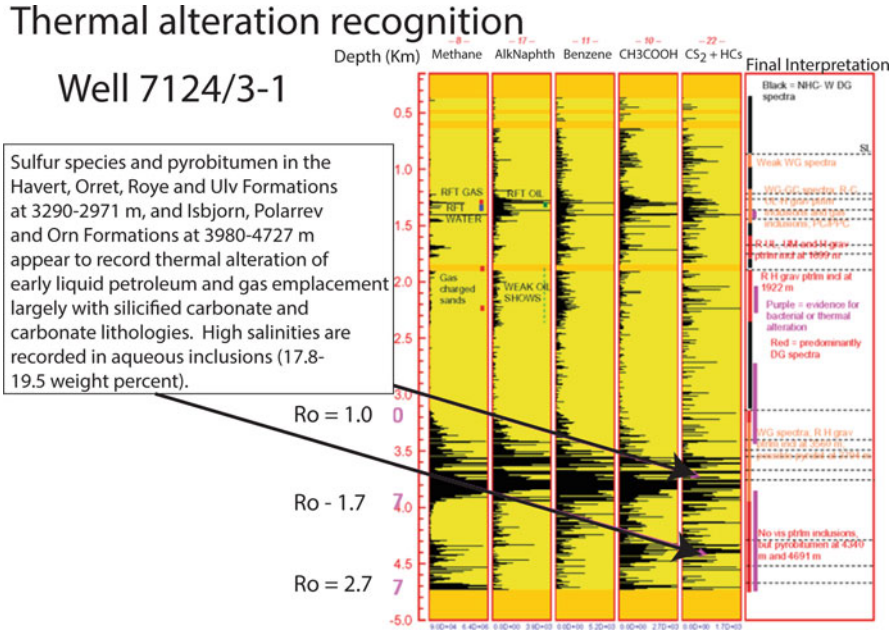

Fig. 7.24 Thermal alteration recognition from sulfate reduction

7.3.3 A Note on Drill Bit Metamorphism (DBM)

Although recognized for many years (Graves 1986; Taylor 1983; Wegner et al. 2009), prominent instances of drill bit metamorphism (DBM) is a relatively recent phenomenon that has arisen due to changes in drilling practices designed to increase penetration rates, reduce drill bit changes and facilitate directional steering in challenging drilling environments. It results in numerous artifacts in mud gas data, and irreparably compromises evaluation of rock cuttings by geochemical, petrophysical or petrological means. DBM is most commonly observed where polycrystalline-diamond compact (PDC) or diamond-impregnated bits are used with a downhole mud motor (or turbo drill) in place of the more conventional roller-cone bits and top-drive configuration. The changes to the gas chemistry are almost universally restricted to situations in which OBM is being used as the drilling fluid. Examination of drill bit records (Fig. 7.25) will usually show a confirmation of hard drilling and multiple bit changes which could be related to anomalous FIS signatures.

High temperatures at the drill bit degrade the mud, creating some unique species not found in natural systems, as well as some that are typically associated with thermochemical sulfate reduction and/or cracking of oil to gas in natural systems. The former include alkenes (a.k.a. olefins) and CO (carbon monoxide). Natural species include hydrogen, CO2, benzene, COS and CS2. Carbon isotopic characteristics of bit-generated gas are also distinct (typically shifted to higher, more mature

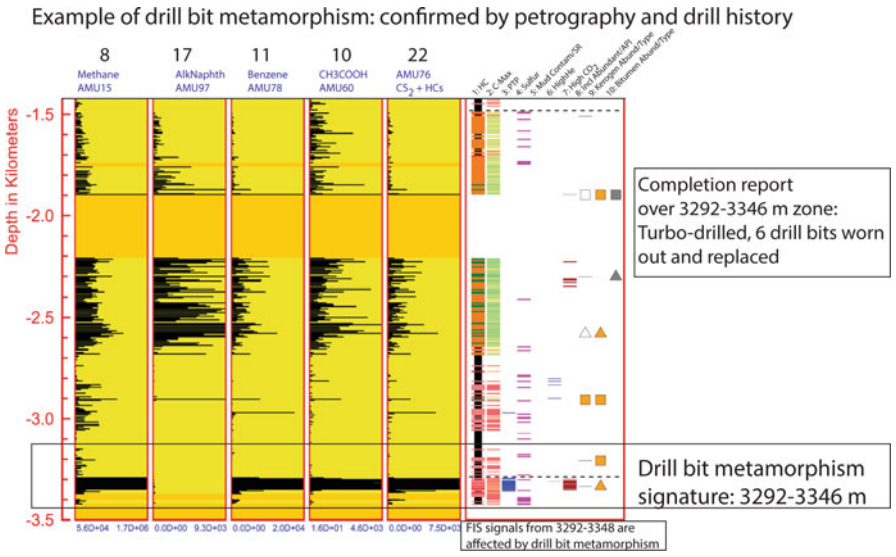

Fig. 7.25 An example of anomalous FIS signatures related to drill bit metamorphism (DBM). A quick check is to look at bit records indicating very difficult drilling. This example has 6 drill bits worn out over a short interval

values). DBM gases can be auto-encapsulated as "drilling induced" fluid inclusions in reconstituted rock material, thus affecting FIS data.

What effects does this process have on FIS data? We first recognized the effect in the early 1990s when investigating proximity to pay relationships in the North Sea (Fig. 7.26), and were able to make the connection between the present-day nature of PTP and the drilling-enhanced encapsulation of recent pore fluids. So, in essence, the PTP application owes at least some of its utility to the same process that is problematic when extreme, as does the shallow microseep application.

The first and most important fact is that DBM is not particularly common in the context of global cuttings databases. As an example, of the 300+ wells that we have analyzed via FIS in the Norwegian and Barents Seas, less than 10 % display ANY evidence of DBM, and less than 2 % (i.e., 6 in 300) display what would be considered major DBM effects (i.e., those that would prevent any useful data from being obtained from the main reservoir sections). Secondly, DBM is more common in recently drilled wells, being essentially nonexistent in pre-1990 boreholes (e.g., less than 5 % of the total drilled footage of pre-1990 wells used diamond bits, where DBM is most pronounced).

Thirdly, DBM produces characteristic and definitive FIS responses that are not currently misinterpreted, although they may not have been fully recognized or appreciated in the past. Petrographic evaluation of these intervals provides unequivocal visual confirmation (Fig. 7.26).

Analysis of these "drilling induced" fluid inclusions via gas-chromatography and isotopic techniques provide further evidence for the process (Fig. 7.27). Finally, DBM is only of practical interpretive consequence when it occurs within reservoir sections. Even here, however, the data should not be automatically discounted, as natural species are encapsulated along with DBM gas (e.g., helium), and petrographic study can be completed on unaltered cuttings from these intervals.

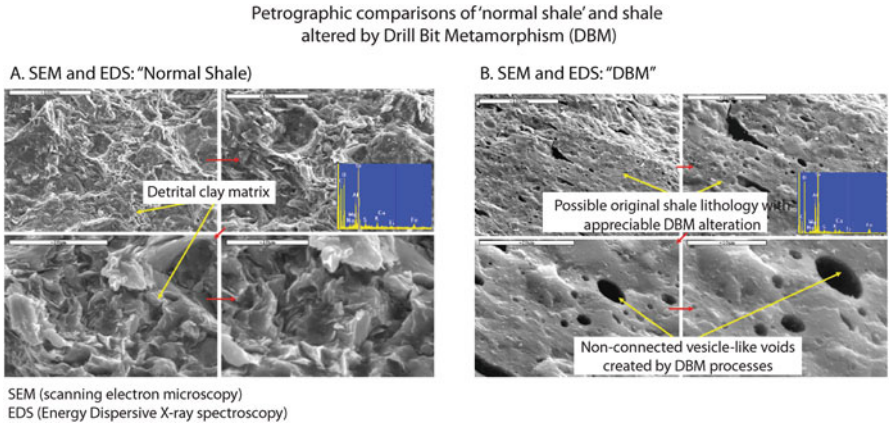

Fig. 7.26 Petrographic recognition of DBM fluid inclusion anomalies

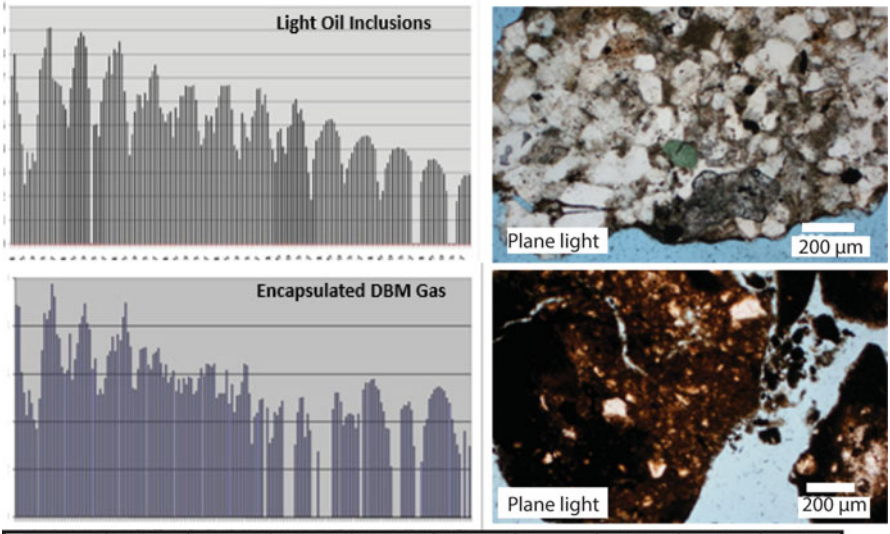

	CO	Methane	Ethane	Ethene	Propane	Propene	dC1	dC2	dC3
NATURAL	0	262400	42700	0	23900	0	N/A	-36	-31
DBM	124200	279400	1710	2670	3450	1260	-33	-27	-25

Natural light oil FIS spectrum and sandstone cutting (top) compared to DBM spectrum and sandstone/shale cuttings (bottom). Selected gas-chromatograph and isotope data from natural and DBM cuttings. Note alkenes and CO in the latter.

Fig. 7.27 Additional petrographic evidence for DBM

7.4 FIS Interpretation Examples

Recently, applications of FIS to unconventional plays have been investigated. Because many of these resource plays are self-sourced (or proximally sourced) and self-sealed, the fluid that is extracted from fluid inclusions (including nanopores) is often compositionally and volumetrically similar to the hydrocarbon that will eventually be produced. This provides great potential for establishing production fairways using archived cuttings from wells drilled for conventional targets in the region, and thus building significant fluid databases without drilling additional wells. This is particularly useful at the early development stage, as acreage positions will not have been fully established, and land lease costs may be lower. Of these unconventional applications, the most practical are ultimately aimed at predicting fluid type, composition and volume within tight rock, as well as identifying variability along horizontal wells that can be exploited for more effective completions.

A series of examples serves to illustrate the foregoing discussion of the basic applications of FIS to exploration for conventional and unconventional reservoirs.

7.4.1 *Northwest Coast of Australia*

The first is a classic example from the Northwest Shelf of Australia (Fig. 7.28), and is illustrative of using FIS to lower risk associated with drilling a prospect based on response in an adjoining dry hole.

The dry hole, called Madeleine, was drilled 20 years prior to discovery of Wanaea field. There were no conventional shows in spite of being drilled quite close to the oil-water contact and the area was gas prone, hence, was not attractive to operators at the time. FIS and petrographic analysis of Madeleine provide evidence of the updip accumulation. The depth plots show FIS methane response in red and C7 response (an oil indicator) in green. First, the shallow feature in the dry hole represents an FIS bacterial microseep suggesting the presence of deeper oil or condensate bearing reservoirs in the area. Second, the FIS response in the reservoir section indicates migration of liquid-range hydrocarbons, which are of economic interest in the area. Third, petrographic and microthermometric study of thin sections from the reservoir reveals undersaturated light oil inclusions in sandstone with measured API gravies near 46 (consistent with 47 gravity oil produced from Wanaea). Finally, presence of anomalous benzene and acetic acid within the wet reservoir at Madeleine indicate nearby presence of reservoired oil or condensate. Cumulatively, these data significantly lower the risk associated with drilling the updip structure.

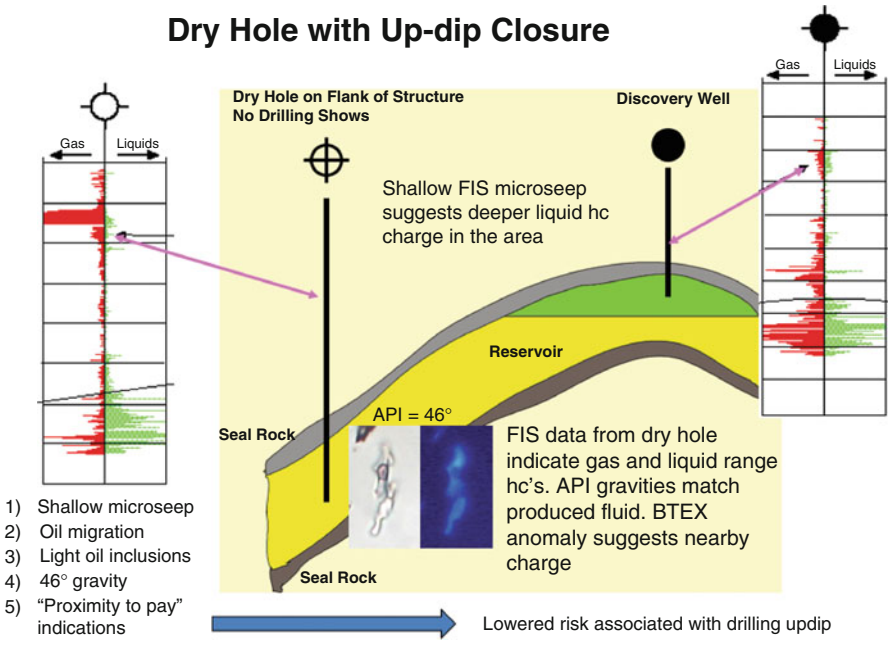

Fig. 7.28 NW coast of Australia example

7.4.2 Prospect Ranking

A second example illustrates the prospect ranking utility of FIS (Fig. 7.29). Three dry holes are shown in three fault-separated blocks within a geographically restricted area. Only the middle wells document evidence of migration, in this case gas-condensate below a very effective regional seal. The strength of the response suggests that the zone may have penetrated a paleo-accumulation. Petrography documents the presence of gas-condensate inclusions with high API gravities. Exploration should logically be focused within the fault block that received migration.

7.4.3 Barents Sea

Another example (Fig. 7.30) shows several gas and oil/condensate discoveries located west of the Polheim Sub-platform and Loppa High in the Barents Sea that were made between 2011 and 2014. Before any of these fields were penetrated, FIS was conducted on a nearby dry hole with shows (well 7219/9-1) and was found to contain a 300 m gross thickness paleo-column of oil in the Jurassic that was probably sourced from the overlying Hekkingen Formation.

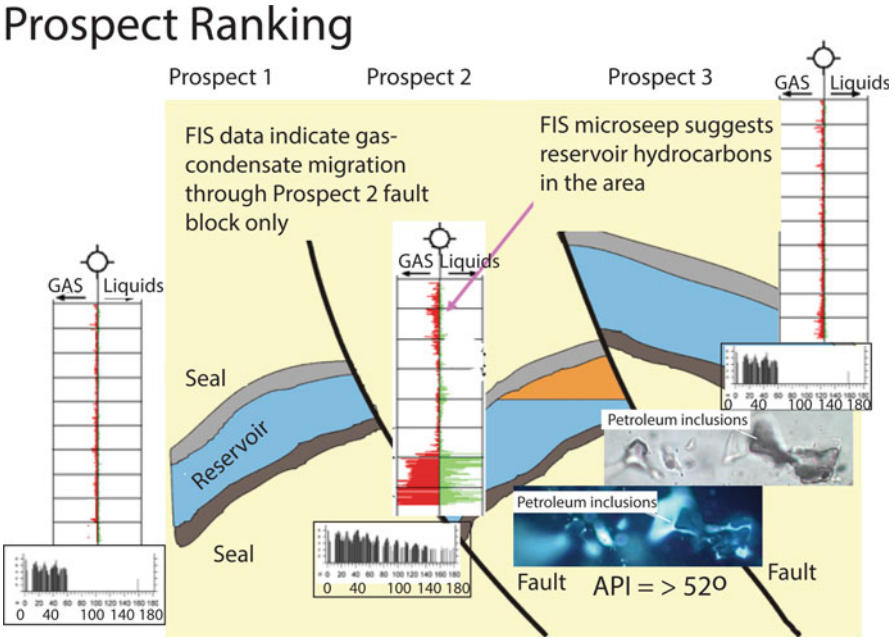

Fig. 7.29 Prospect ranking example

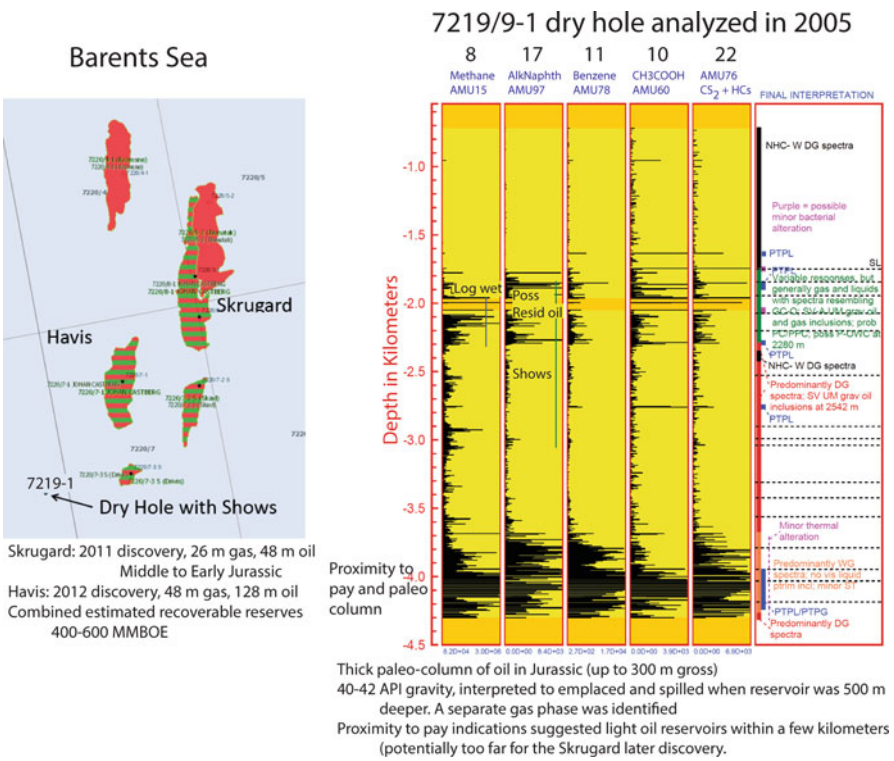

Fig. 7.30 Barents Sea dry hole example

Measured gravities were light, in the 40-42° range, and the fluid was interpreted to have been emplaced and spilled when the reservoir was about 500 m deeper based on microthermometric data. A separate gas phase was identified and was also interpreted to have been emplaced at depth. Proximity to pay indications suggested that liquid petroleum is still reservoired within a few kilometers distance. Interestingly, the initial discovery was the most eastward and is too far away to account for the anomalies identified in the well, based on the suggested 8 Km limit for FIS PTP anomalies. The more recent discoveries Havis (renamed as part of the Johan Castberg complex) or Drivis are implicated. Note that the dry hole also indicates a separate petroleum system within the Triassic (Snadd Fm) that is dominated by wet gas (the BHT is 145 °C and maximum burial temperature may have been near 160 °C or so). A separate source rock is implicated (probably Triassic or older), and this gas is probably the fluid that has invaded the overlying Jurassic reservoir.

7.4.4 Sogn Graben

The last example is in the Sogn Graben area, which contains a number of oil and gas fields that are largely Jurassic in age. A complex fill and spill history related to progressive maturation and westward downward tilting (eastward uplift) results in

lighter fluids displacing heavier fluids, and general movement to the east. The gas and condensate field Gjoa is shown in Fig. 7.31.

The dry hole 36/7–3 encountered no significant shows, but FIS and petrographic data indicate the presence of a 100 m paleo-column of 31–35° undegraded oil in the Cretaceous. Proximity to oil/condensate anomalies are identified in this and deeper sections, suggesting that they may be sensing nearby liquid petroleum charge. The shallower zone also contains well developed sulfur species anomalies (mainly sulfate) which generally indicates high Sw, and also suggests a source of sour gas components (bacterial or thermal). No evidence of significant biodegradation is implied by measured oil gravities, thus perhaps it indicates influx of mature gas from depth.

Microthermometry data suggest that oil was trapped at about 75–85 °C. Oil appears to have been near gas saturation and thus may have spilled from a reservoir that contained a gas cap, or the paleo-column may have had a gas cap updip. Interestingly, the Gjoa Field well 35/9-1 appears to have spilled moderate gravity oil below a gas cap, and may have contributed gas-saturated oil to this paleo-column. Since maximum burial temperature at this depth appears to have been near 100–105 °C, the oil was probably emplaced during uplift, and may be a more recent event than implied for fields to the east. The ultimate sink for this lost oil column is unknown. The top seal appears to have been relatively competent, as for most wells in the area (Fig. 7.31). Thus, lateral leakage or remigration during tilting are favored hypotheses to explain the paleo-accumulation. Depending on structures in the area,

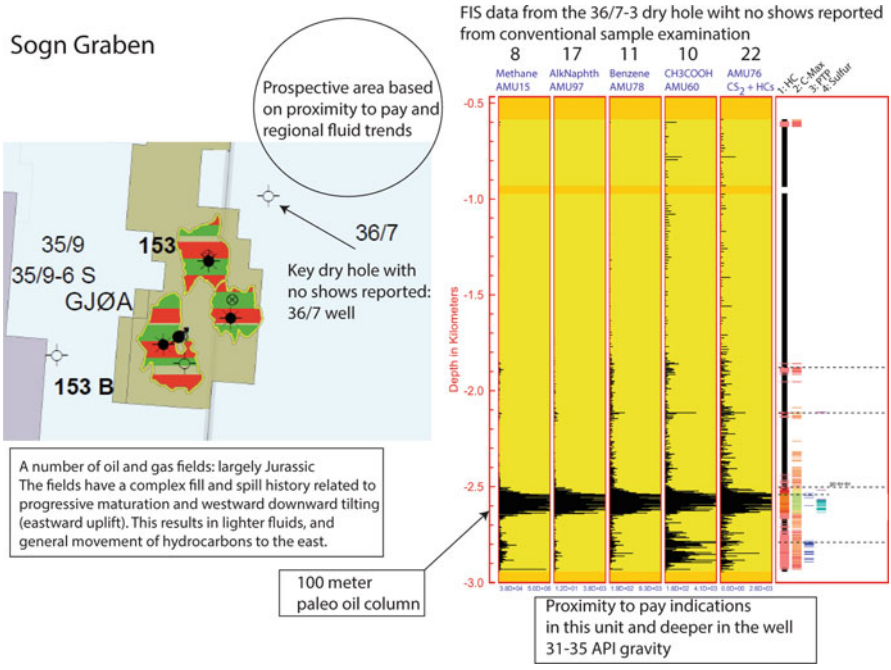

Fig. 7.31 Sogn graben

and considering the likely distance of proximity to pay indicators and the regional direction of fill and spill, this circled are in Fig. 7.30 is a likely exploration target for the moderate gravity oil that was remigrated from well 36/7-3.

7.4.5 *Unconventional Well Performance-Mancos Shale, Utah*

A practical and simple application of using FIS data in an unconventional play to qualitatively predict eventual relative well performance during production is diagramed in Fig. 7.32.

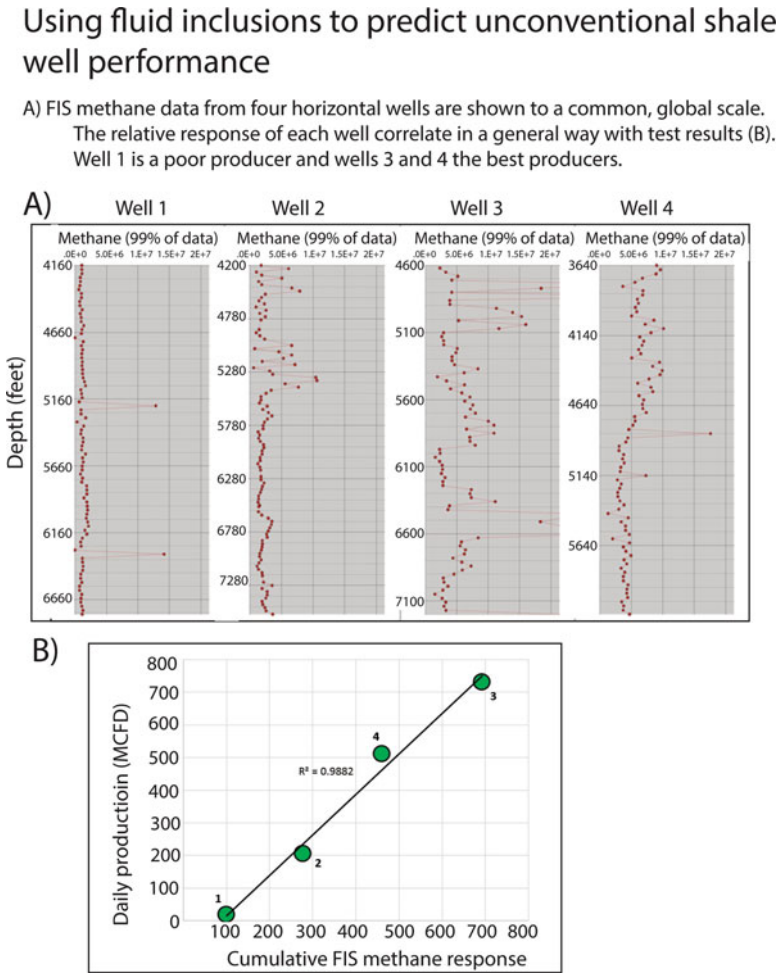

Fig. 7.32 Predicting well performance in unconventional shale gas wells

Shown are methane responses from four horizontal wells in a geographically restricted area (Fig. 7.32a). The curves are plotted to the same response scale with measured depth on the vertical axis. It is obvious that the four wells are quite different, both in terms of strength of response, and consistency of response through the lateral. Experience tells us that this variability often correlates with producibility (possibly related to fracture or intergranular porosity). The well on the left is the worse, and the two on the right are the best. If one sums the area under the curves and does some normalizing to account for difference in scales, an astonishingly strong correlation with production is produced (32B). Here, one can easily distinguish a good well from a poor well. Because these FIS responses are intrinsic to the rock before drilling and are thus not affected by drilling parameters or completion, they can help distinguish a poor producer that arises from completion issues from one that arises from drilling the wrong section of rock. These data can be used to help plan completions, including deciding where to stage boundaries for hydraulic fracturing. Fracturing across a porosity or fracture density boundary generally results in poor fracturing efficiency, and thus should be avoided.

The second unconventional example is from the Mancos Formation, a thick, heterolithic unconventional oil and gas target in the Western United States (Fig. 7.33).

Six cores were analyzed over a broad depth range (Birgenheier et al. 2011 and Ressetar 2012). As is typically the case with emerging plays, maturity windows and fluid type boundaries are incompletely understood. Additionally, there is the

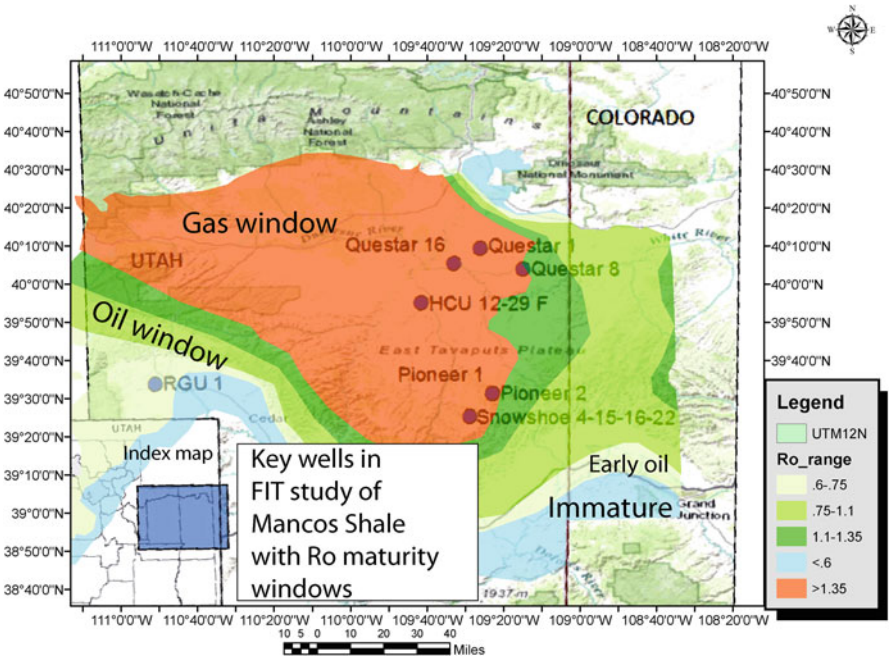

Fig. 7.33 Mancos core study base map and vitrinite reflectance map, base Mancos Shale. Vitrinite oil and gas windows are from Ressetar (2012)

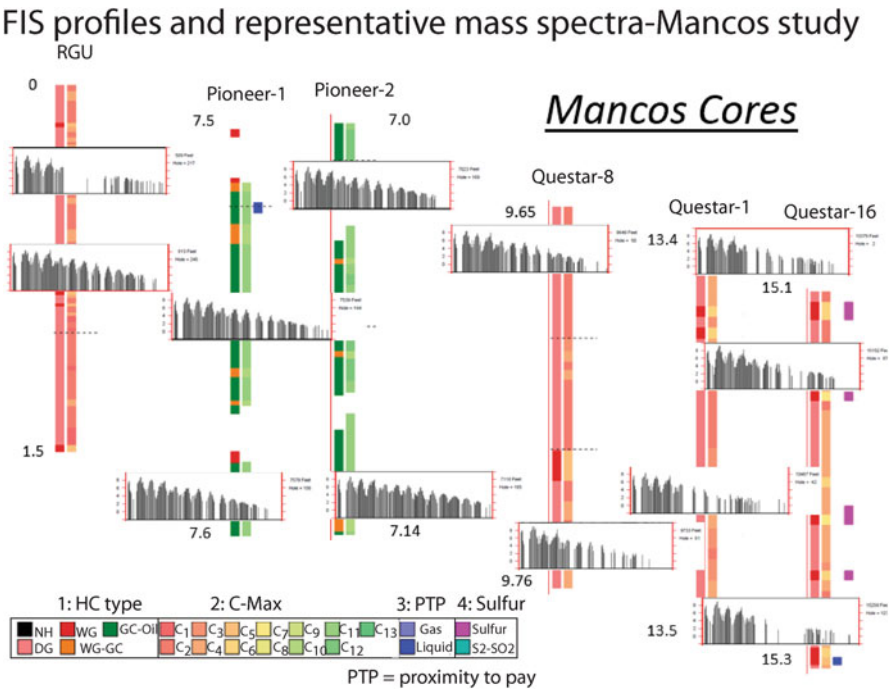

Fig. 7.34 FIS responses, Mancos area. See Fig. 7.33 for location

interplay of migrated and locally generated hydrocarbons, and some stratigraphic sections of the Mancos are quite sandy or silty and rather organic lean.

Interpreted FIS hydrocarbon profiles are shown in Fig. 7.34. The shallow RGU core is immature, and yet gives gas FIS gas and liquids anomalies, and contains migrated oil (moderate and upper-moderate gravity oil inclusions verified optically). An oily sweet spot is identified in the Pioneer cores and optical data indicate high abundance of light oil inclusions. Finally, the deeper Questar cores indicate progressively drier hydrocarbons with some evidence of secondary cracking of oil to gas in Questar 16 (FIS sulfur species and pyrobitumen in thin section). By analyzing historical wells from the area, a better picture of the vertical and lateral distribution of fluid chemistry and volumes can be obtained.

7.4.6 Example of Detecting Oil Shows Missed on Mud Logs: Barmer Basin, India

The Barmer Basin of India is a recently discovered Tertiary rift (Dolson et al. 2015; Farrimond et al. 2015; Naidu et al. in press). Shows databases built by staff at Cairn Energy India have been collected from over 150 wells and integrated into maturation

and modeling of the basin evolution. The geochemical database is extensive and a number of key dry holes were analyzed for FIS.

An example is shown in Fig. 7.35.

One of the more important exploration wells (well A in Fig. 7.35) tested a large down-thrown 3-way fault trap up against basement. This well is one of only a handful of wells with no shows on logs or mud logs in the entire basin, which has kilometers of mature source rock over wide areas. To explain the total lack of shows, not only was fault seal initially deemed a culprit, due to juxtaposition to potential fractures in basement strata, but migration failure was also assumed.

The FIS data, however, clearly shows that this area had abundant migration. However, maturation models at multiple levels as well as migration vectors suggested there had to have been migration and charge to this trap. The FIS data confirmed that, showing strong evidence not only of hydrocarbons throughout the section, but micro-seepage at the shallow levels. As the trap geometry seems relatively robust, the failure now has to be attributed to fault seal failure.

Significantly, this is a good example of how the lack of shows in a well does not mean a lack of migration and charge. Even wells proximal to giant oil fields can be totally barren of shows immediately downdip of the FWL, especially if the carrier beds are thick and highly porous. FIS data is a good way to detect those more subtle migration pathways.

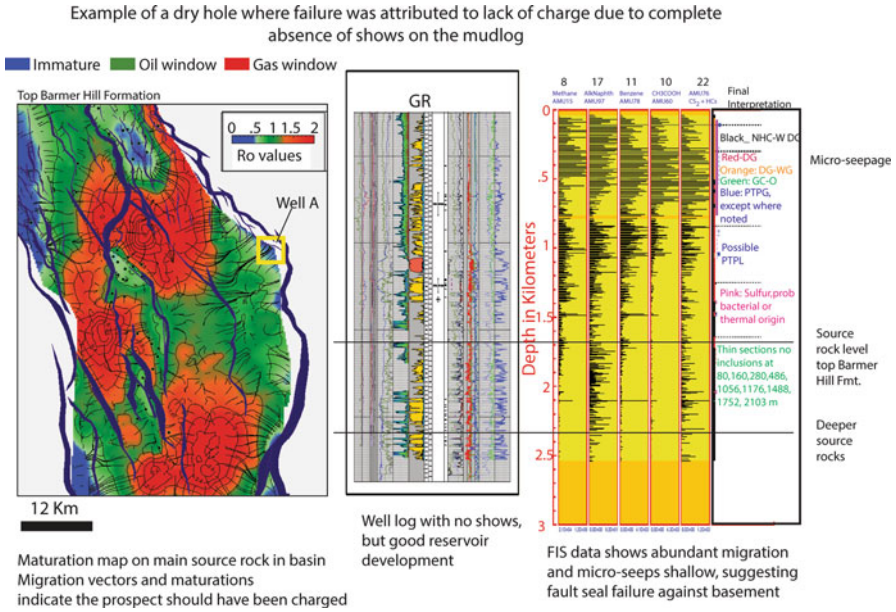

Fig. 7.35 Dry hole with no shows re-corded misinterpreted as not having received charge. Figure and example contributed by Cairn India, with permission

7.5 Summary

Once the FIS screening is done, a great deal of additional information can be gleaned from a detailed, and more traditional look at the samples. GC and GCMS analysis of the oils in the inclusions themselves can help determine general oil type and a source to oil correlation.

This kind of information can allow a migration model to be built with a higher degree of confidence. In Chap. 8, we cover the basic principles of oil to source correlations and some fundamental geochemical principles. Recognition of fluid and migration anomalies is one of the best ways to generate new ideas and plays in any basin. In some cases, FIS and geochemical data may indicate oil and gas shows that cannot be typed to any known hydrocarbon system. That kind of information can help open new play opportunities, even in old, mature exploration areas.

For many companies, fluid inclusions stratigraphy has become a standard part of exploration programs, helping to glean information on migration, trap and charge that cannot be detected by other methods.

References

Alpin AC, Macleod G, Larter SR, Pedersen KS, Sorensen H, Booth T (1999) Combined use of confocal laser scanning microscopy and PVT simulation for estimating the composition and physical properties of pertroleum in fluid inclusions. Mar Pet Geol 16:97–110

Arouri KR, Laer PJV, Prudden MH, Jenden PD, Carrigan WJ, Al-Hajji AA (2010) Controls on hydrocarbon properties in a Paleozoic petroleum system in Saudi Arabia: exploration and development implications. Am Assoc Pet Geol Bull 94:163–188

Barclay SA, Worden RH, Parnell J, Hall DL, Sterner SM (2000) Assessment of fluid contacts and compartmentalization in sandstone reservoirs using fluid inclusions: an example from the Magnus oil field, North Sea. Am Assoc Pet Geol Bull 84:489–504

Barker CE, Pawlewicz MJ (1986) The correlation of vitrinite reflectance with maximum temperature in humic organic matter. In: Stegena L, Buntebarth G (eds) Paleogeothermic. Springer-Verlag, Berlin, pp 79–83

Bhullar AG, Primio RD, Karlsen DA, Gustin D-P (2003) Determination of the timing of petroleum system events using petroleum geochemical, fluid inclusion, and PVT data: an example from the Rind discovery and Troy Field, Norwegian North Sea. In: Duppenbecker S, Marzi R (eds) Multidimensional basin modeling. American Association of Petroleum Geology, Tulsa, Oklahoma, pp 123–135

Birgenheier LP, Johnson C, Kennedy AD, Horton B, McLennan J (2011) Integrated Sedimentary, Geochemical, and Geomechanical Evaluation of the Mancos Shale. Uinta Basin, Utah, AAPG Annual Convention and Exposition, Houston, Texas, American Association of Petroleum Geologists Search and Discovery Article #90124

Brewster C, Hall D (2001) Deep, geopressured gas accumulations and fluid inclusion stratigraphy (FIS) signatures: exploration implications from the lower Miocene trend. Houston Geological Society, Gulf of Mexico, pp 27–33

Burley SD, Mullis J, Matter A (1988) Timing diagenesis in the Tartan Reservoir (UK North Sea): constraints from combined cathodoluminescence microscopy and fluid inclusions studies. Mar Pet Geol 6:98–120

Burnham AK, Sweeney JJ (1989) A chemical kinetic model of vitrinite reflectance maturation. Geochim et Cosmochim Acta 53:2649–2657

Burruss RC, Cercone KR, Harris PM (1983) Fluid inclusion petrography and tectonic-burial history of the Al Ali No. 2 well: evidence for the timing of diagenesis and oil migration, northern Oman foredeep. Geology 11:567–570

Burtell SG, Jones VT (1996) Benzene content of subsurface brines can indicate proximity of oil, gas. Oil Gas J 93:59–64

Dolson JC, Bahorich MS, Tobin RC, Beaumont EA, Terlikoski LJ, Hendricks ML (1999) Exploring for stratigraphic traps. In Beaumont EA, Foster NH (eds) Exploring for oil and gas traps: treatise of petroleum geology. Handbook of petroleum geology, vol 1. American Association of Petroleum Geologists, Tulsa, Oklahoma. pp 21.2–21.68

Dolson J, Burley SD, Sunder VR, Kothari V, Naidu B, Whiteley NP, Farrimond P, Taylor A, Direen N, Ananthakrishnan B (2015) The discovery of the Barmer Basin, Rajasthan, India, and its petroleum Geology. Am Assoc Pet Geol Bull 99:433–465

Farrimond P, Naidu BS, Burley SD, Dolson J, Whiteley N, Kothari V (2015) Geochemical characterization of oils and their source rocks in the Barmer Basin. Petroleum Geoscience, Rajasthan, p 22

Goldstein RH, Reynolds TJ (1994) Systematics of fluid inclusions in diagenetic minerals: SEPM v. Short Course 31, p. 198 pp

Graves W (1986) Bit-generated rock textures and their effect on evaluation of lithology, porosity and shows in drill-cutting samples. Am Assoc Pet Geol Bull 70:1129–1135

Grimes DJ, Ficklin WH, Allen WH, McHugh JB (1986) Anomalous Gold, antimony, arsenic, and tungsten in ground water and alluvium around disseminated gold deposits along the Getchell Trend, Humboldt, County, Nevada. J Geochem Explor 7052:351–371

Hall D (2008) Fluid inclusions in petroleum systems. In Hall D (ed) AAPG getting started series no. 15. American Association of Petroleum Geologists

Karlsen DA, Nedkvitne T, Larter SR, Bjorkykke K (1993) Hydrocarbon composition of authigenic inclusions: application to elucidation of petroleum reservoir filling history. Geochim Cosmochim Acta 57:3641–3659

Kolb B, Ettre LS (2006) Static headspace-Gas chromatography: theory and practice. Wiley-Interscience, Hoboken, NJ, p 335

Matusevich VM, Shvets VM (1973) Significance of organic acids of subsurface waters for oil-gas exploration in West Siberia. Pet Geol 11:459–464

McLimans RK (1987) The application of fluid inclusions to migration of oil and diagenesis in petroleum reservoirs. Appl Geochem 2:585–603

Munz IA (2001) Petroleum inclusions in sedimentary basins: systematic, analytical methods and applications. Lithos 55:195–212

Naidu BS, Burley SD Dolson J Farrimond P, Sunder VR, Kothari V, Mohapatra P, Whiteley N (in press) Hydrocarbon generation and migration modelling in the Barmer Basin of western Rajasthan, India: lessons for exploration in rift basins with late stage inversion, uplit and tilting, Petroleum System Case Studies, v. Memoir 112. Tulsa, Oklahoma: American Association of Petroleum Geologists

Oxtoby NH, Mitchell AW, Gluyas JG (1995) The filling and emptying of the Ula Oilfield: fluid inclusion constraints. In: Cubitt JM, England WA (eds) The geochemistry of reservoirs, v. Special publication No. 86. Geological Society of London, London, pp 141–157

Prezbindowski DR, Larese RE (1987) Experimental stretching of fluid inclusions in calcite-implications for diagenetic studies. Geology 15:333–336

Ressetar R (2012) Mancos Geology and Project Overview, Uinta Basin Oil and Gas Collaborative Group Meeting, Vernal, Utah, Utah Geological Survey; http://geology.utah.gov/resources/energy/oil-gas/shale-gas/cret-shale-gas/, p. 26

Roedder E (1984) Fluid inclusions: mineralogical society of America. Rev Minera 12:644

Sterner SM, Bodnar RJ (1984) Synthetic fluid inclusions in natural quarts 1. Compositional types synthesized and applications to experimental geochemistry. Geochim Cosmochim Acta 48:2659–2668

Taylor JCM (1983) Bit metamorphism can change character of cuttings. Oil Gas J 81:107–112
Wavrek DA, Coleman D, Pelphrey S, Hall S, Tobey M, Jarvie DM (2004) Got gas? Innovative technologies for evaluating complex reservoir zones (abstr.). American Association of Petroleum Geologists, Dallas, Texas
Wegner LM, Pottorf RJ, Macleod G, Wood EW, Otten G, Dreyfus S, Justawan H (2009) Drill bit metamorphism: Recognition and impact on show evaluation, SPE Annual Technical Conference and Exhibition, New Orleans, Louisiana, Society of Petroleum Engineers, p. 9
Wilkinson JJ, Lonergan L, Fairs T, Herrington RJ (1998) Fluid inclusion constraints on conditions and timing of hydrocarbon migration and quartz cementation in Brent Group reservoir sandstone, Columbia Terrace, northern North Sea. In: Parnell J (ed) Dating and duration of fluid flow and fluid-rock interaction, v. Special Publications, vol 144. Geological Society of London, London
Worden RH, Smalley PC, Oxtoby NH (1995) Gas souring by thermochemical sulfate reduction at 140 °C. Am Assoc Pet Geol Bull 79:854–863

Chapter 8
Shows and Geochemistry: Extracting More Information from Source Rocks and Hydrocarbons

Contents

Abstract An understanding of petroleum geochemistry has become an essential part of shows and seals analysis. With the emergence of unconventional source rock plays, prospect selection and play fairway screening now requires a full understand of Rock Eval, source rock characteristics, maturation, migration and rock mechanics. A wide variety of analytical tools such as mud isotubes and head space gas analysis supplement traditional mud log analysis and provide a wealth of interpretive information.

Geochemical signatures from oil and gas analysis can be used to understand oil to source rock correlations and to map migration pathways, both vertically and laterally from the kitchen. Evaluating how robust a petroleum systems maturation and migration model is requires a full understanding of the limits of the model, as well

J. Dolson, *Understanding Oil and Gas Shows and Seals in the Search for Hydrocarbons*, DOI 10.1007/978-3-319-29710-1_8

as calibrating the results by comparison to high quality shows databases. Where possible, fluid analysis from the fields or shows should be done to try to determine the source of the fluids and thus the possible migration routes to the trap.

8.1 Introduction

This is a very big topic condensed into a short summary. The focus is on understanding the basic language of geochemistry as it relates to understanding source rocks, maturation and migration. The emphasis remains on show evaluation techniques to help find both conventional and unconventional traps. Emphasis is thus placed on common and practical ways to validate migration models and also assess potential mature source rock fairways for unconventional plays.

The topic of source rock evaluation has advanced substantially in the last decade, and continues to evolve at a rapid pace. This has been driven primarily by the increased production and drilling boom involving unconventional shale oil and gas, where geochemical knowledge is essential to understand the play. Only the very basic components of this topic can be covered in this book. Likewise, matching oils to their original source rocks is a complex topic unto itself, but the basic principles and common techniques are important to be aware of.

Ultimately, some of the best tools for recognizing a new play may come from an astute look at the oil geochemistry from shows, tests or fluid inclusions. Anomalous oils, for instance, may indicate a completely untapped and new petroleum system. Mud isotubes or headspace gas may show increased wetness with depth, indicating deeper liquid accumulations or migration pathways. Too often, wells are abandoned at shallow levels without finding trapped oil in the deeper petroleum system. Many times a new play has been generated simply by deciding to explore deeper in the section, viewing the shallow plays as mere 'seepage' from deeper source rocks. Examples of this have already been shown in the Nile Delta in Chap. 5 and are a major driver for deep sub-salt exploration in the Gulf of Mexico.

Shortened overviews of petroleum geochemistry are in AAPG's 1999 Treatise of Petroleum Geology (Beaumont and Foster 1999). Some of the key papers dealing with the basics of source rocks and oil analyses are those of (Law 1999; Waples and Curiale 1999). An additional excellent overview book is that of (Magoon and Dow 1994).

Technical background and global resource potential of shale oil and gas plays is best treated by (EIA 2007, 2010, 2011). Some excellent references dealing with evaluation methods in shale plays are illustrated by recent publications by (EIA 2009; Engelder et al. 2009; Wrightstone 2009, 2010; Harper and Kostelnik 2013a, b, c; DCNR 2014). The Barnett Shale is another well studied shale gas play and covered by (Jarvie 2003; Montgomery et al. 2005; Hill et al. 2007; Jarvie et al. 2007; Pollastro 2007; Zhao et al. 2007; EIA 2008; Kinley et al. 2008; Loucks et al. 2009).

8.2 Source Rock Quality and Maturation

8.2.1 The Language of Source Rocks

For decades, source rock shows were considered of interest but no commercial value. Although fractured shales had been found and developed for centuries, the focus was on secondary migration and conventional traps. Source rocks themselves were deemed important, but more from a migration and maturation analysis. With the advent of horizontal drilling and multi-stage hydraulic fracturing, however, a revolution in production has occurred and many basins now have the bulk of their drilling activity in the mature source rock fairways.

Source rocks fall in four categories (Law 1999):

1. Potential source rocks
   - Have enough organic matter to generate and expel hydrocarbons if thermally matured elsewhere.
2. Effective source rocks
   - Contain organic matter presently generating and/or expelling hydrocarbons in commercial quantities.
3. Relic effective source rocks
   - Effective source rocks which have ceased generating and expelling hydrocarbons before exhausting its organic matter.
4. Spent source rocks
   - Source rocks that no longer are capable of expelling hydrocarbons, usually after reaching an overly mature state or starting with low initial carbon content

Interestingly, the world is replete with proven hydrocarbon systems working with relic effective source rocks. As shown in previous chapters, many basins have undergone multi-phase tectonic histories involving burial and repeated uplift and perhaps reburial. These kinds of basins may have multiple periods of hydrocarbon generation and expulsion. Most onshore Tertiary basins have had some degree (often kilometers) of erosion and uplift, with source rocks having gone through the oil and gas windows millions of years before present, and yet these basins still contain prolific hydrocarbon resources. The reasons for this involve the quality of seals, geometry of the traps at time of formation and the ability upon uplift and tilting, of hydrocarbons to spill and fill into new traps from older accumulations, as shown in the Hugoton and West Siberia case studies in Chap. 5.

From an exploration standpoint, however, it is important to recognize which kind of source systems you are dealing with, and then properly model the timing of maturation and generation. Many outcrop studies are dealing largely with thermally immature source rocks and thus would be classed as potential source rocks where found. Basinward, these same source rocks may be generating significant hydrocarbons today or in the past. Exploring in basins of spent source rocks is a reasonably difficult endeavor unless some traps remain on the migration path, and most or all of these traps would be filled with dry gas.

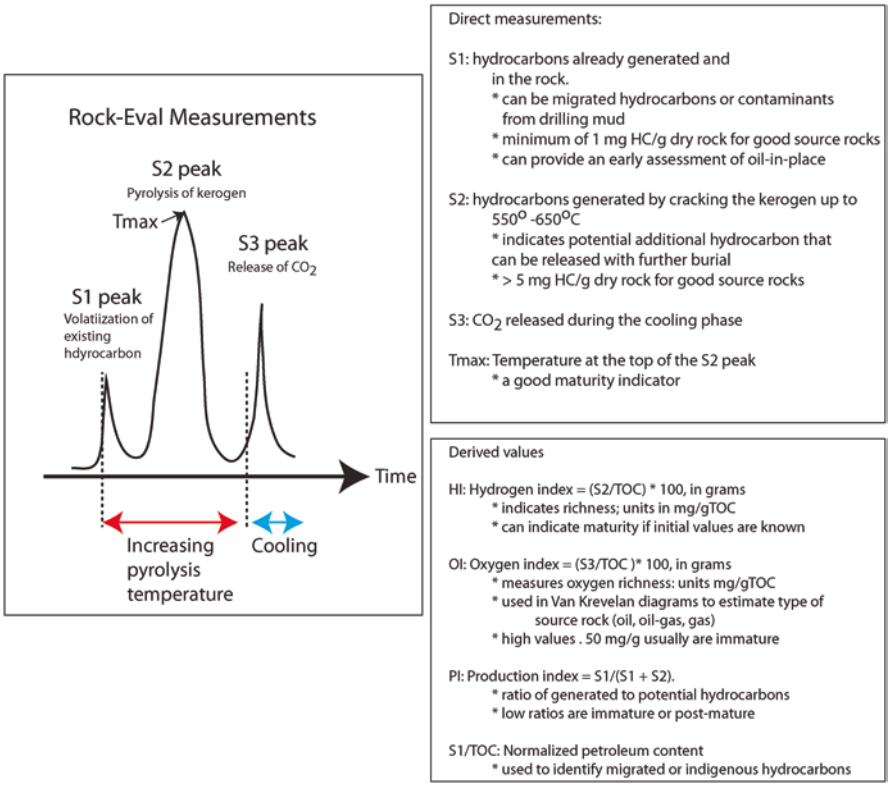

Fig. 8.1 Rock Eval pyrolysis and measured and derived values. Modified from (DCNR 2014)

8.2.2 Rock Eval Pyrolysis

Source rock quality varies by original depositional environment and subsequent burial and maturation. Source rock quality parameters are measured directly in a lab by a process called Rock Eval Pyrolysis (Fig. 8.1). No serious explorer today can function without a thorough understanding of Rock Eval measurements and how to use them to find unconventional resource or assess remaining exploration potential in a basin or a new play in any basin. The critical thing to remember about Rock Eval pyrolysis is that is measures the content of the source rock at present, not what it started out at. Many prolific oil and gas basins exist where current Rock Eval measurements would classify the source rocks as having poor gas or oil generation potential simply because the source rocks that have charged all those known traps have themselves matured enough to convert most of the original kerogen to free hydrocarbons (bitumen).

Rock Eval measurements can be done on cores or cuttings, but involves heating a sample to 550–650 °C, depending on the vintage of the instrument, and driving off hydrocarbons. Three major peaks are produced as hydrocarbons and CO_2 are driven

from the rock over the time of the test. The most important of the measured values are S1, S2, Tmax and S3 as shown on Fig. 8.1. Derived values of HI and OI are in mg/gTOC and are used for source rock classification. HI, in some cases, can indicate levels of maturation, and is a key parameter entered into petroleum systems models to model volumes generated and expelled.

When oil is generated in a source rock, free hydrocarbons are generated and these are what is measured by the S1 peaks. So S1 measures the free hydrocarbons in the pore systems. As such, it may also contain some migrated hydrocarbons. S1 peaks, if large, can also mean the samples were contaminated with drilling mud or pipe dope. The size of the peak and value in mgHC/g of rock is also a good indicator of oil shale potential for unconventional plays (Downey et al. 2011), as it is directly measuring the volume of oil in the source rock itself.

The S2 peak measures the source potential of the sample at its current level of maturation. S2 values are highest in thermally immature samples and degrade substantially as source rocks are matured. So low S2 values may not mean low potential in the past. Tmax values can also be used to estimate maturity of the sample. Low S2 peaks will show low source potential in highly mature source rocks or very lean source rocks. The S3 peak occurs during the cooling phase and measures the amount of oxygen in the kerogen, but is converted to CO_2 in the pyrolysis procedure.

There are a number of derived values from these direct measurements (see Fig. 8.1 for terms and equations). The hydrogen index (HI) should never exceed 1200 (and rarely exceeds 1000), and is, when coupled with TOC and OI, an excellent indicator of the type of source rock (oil, oil-gas or gas-prone). High HI source rocks are generally oil prone. The oxygen index (OI) can help determine if the source rock is gas or oil prone. High OI values are associated with source rocks that generate gas. The production index (PI) is a measurement of hydrocarbon generation (and hence maturity). The normalized petroleum content can be used to identify migrated or indigenous hydrocarbons, something that is important in screening shale oil and gas plays.

8.2.3 Source Rock Quality

Figure 8.2 (Farrimond et al. 2015) shows a good way to screen source rock quality with Rock Eval HI, OI and TOC data. The diagram is a pseudo Van Krevelen diagram with a TOC histogram summarizing Rock Eval data in the Barmer Basin of India by formation. The sizes of the symbols vary by the TOC content.

Lines on the pseudo Van Krevelen diagram break out four types of source rocks:

1. Type I-these are oil prone kerogens common in algal-rich source rocks, typical in lacustrine environments
2. Type II- oil and gas prone kerogens typical of many marine source rocks, both carbonate and clastic

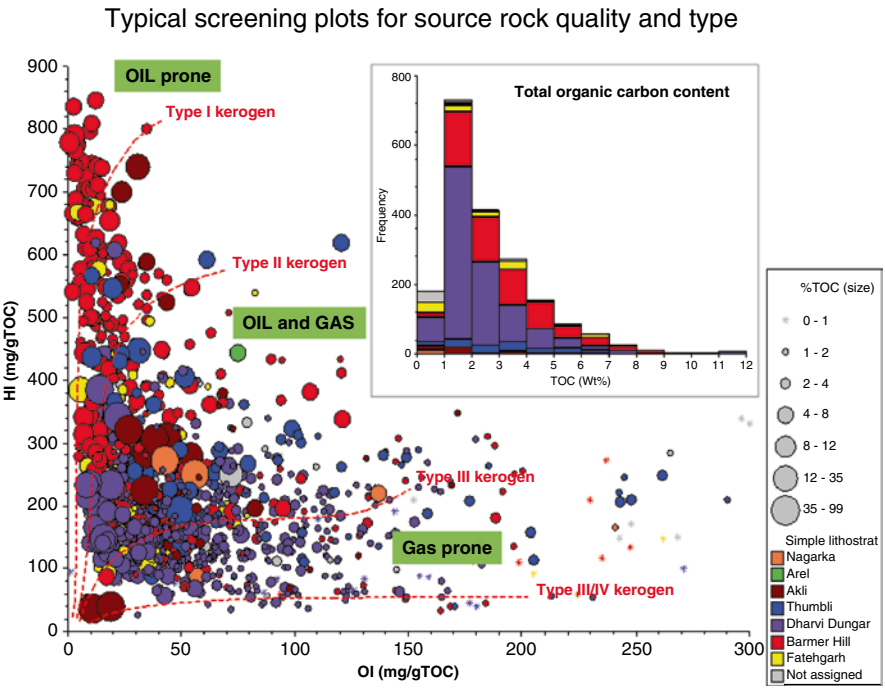

Fig. 8.2 Pseudo Van Krevelen diagram and TOC histogram with classes of source rock type. From Farrimond et al. (1993). Reprinted by permission of the Geological Society of London

3. Type III-gas prone source rocks with low HI and high OI. These are typical of many continental shales or deltaic source rocks
4. Type IV- inert source rocks incapable of generating hydrocarbons

General rules of thumb are that fair source rocks have TOC values of 1–2 %, good source rocks have 2–5 % TOC, with excellent source rocks >5 %. Low TOC and HI rocks can still generate hydrocarbons, but will be highly gas prone and volumetrically significant only if scattered through the section over thick intervals. This is the case in many deltaic reservoirs, where land plant material is mixed with lean marine source rocks. Oil-prone source rocks generally require HI values in excess of about 200 HI. Some very algal-prone source rocks generate very little gas. Conversely, low HI and TOC source rocks in many continental sediments (Type III kerogens) may generate no oil at all.

Most reports also provide a geochemical log (Fig. 8.3) which summarizes all the information on the well graphically (Fig. 8.3). These plots make it easy to see which formations and lithologies are likely source rocks, at least at present levels of maturation.

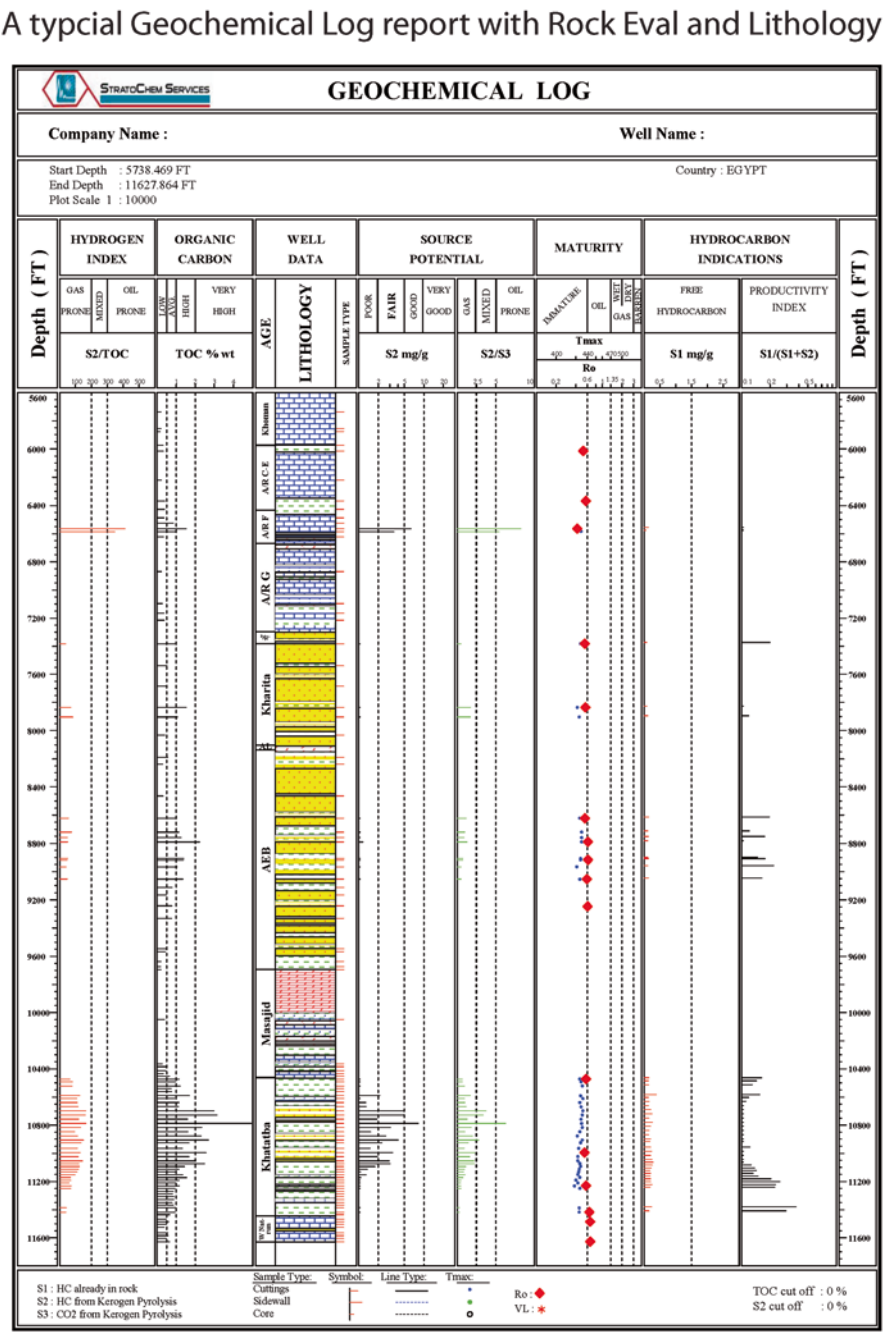

Fig. 8.3 Typical geochemical log. Figure courtesy of Stratochem Services

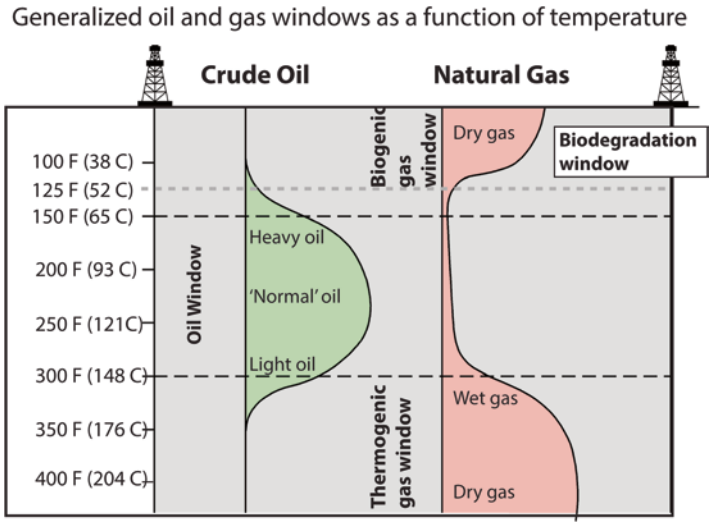

Fig. 8.4 Typical oil and gas window summaries. Figure adapted from BP/Chevron Drilling Consortium course notes, used with permission

8.2.4 Maturation and Source Rock Type

It is good to remember some 'rules of thumb' on oil and gas windows, but also to recognize that those windows vary by the type of source rock. Figure 8.4 shows a typical summary with temperature that is useful to remember in a general sense. One of the more important parts of the diagram is the shallow biogenic gas window, which also coincides with temperatures that allow bacteria to live in the pores and biodegrade the oil quality. At these low temperatures, biogenic gas is also created from bacterial degradation of sedimentary organic matter. Predicting dry gas vs. oil or wet gas, then also requires understanding vertical and lateral migration. Biogenic dry gas, for instance, is sometimes found in deeper reservoirs mixed with thermogenic gas or oil. This can happen if traps are old enough to preserve the biogenic gas during further burial and later migration.

One of the other things that can confuse a beginning interpreter is the difference between the temperatures shown on Fig. 8.4 and that which is obtained from a Tmax pyrolysis result. Tmax is an instantaneous measure in a lab at ambient pressures of the oil driven from a source rock and is not directly comparable to subsurface temperatures and maturation.

This is because source rocks mature as a function of time and temperature. Hydrocarbons volatized (S1) and pyrolysized (S2) by Rock Eval are produced essentially instantaneously and the maturation is not directly comparable to maturation and expulsion in the subsurface.

Time is also a variable. One of the really landmark papers on maturation as a function of time and temperature is that of (Waples 1980), who brought to the west

a key paper by Nikolai Lopatin (Lopatin 1971). The Lopatin method involves a 'time-temperature-index' that is the foundation of all modern petroleum systems modeling software.

An analogy of the effect of time and temperature is cooking a chicken. You can cook a chicken over a long period in an oven at a low temperature over many hours or quickly in a micro-wave oven. In the geological record, time and temperature work together and low temperatures, applied to rocks over a very long period of time, can mature hydrocarbons. Thus Tmax values will not be the same as those temperature values in a mature source rock in the subsurface. For instance, a Tmax of 435 °C may equate to a subsurface maturation temperature of 100–110 °C, again, depending on source rock type and its burial history.

There are several common ways to assess maturity of a source rock (Tables 8.1 and 8.2):

1. Vitrinite reflectance
2. Spore coloration index
3. Thermal alteration index
4. Tmax

Table 8.1 General source rock quality assessment

Generation Potential	Wt. % TOC, Shales	Wt % TOC, Carbonates	Comments
Poor	0.0–0.5	0.0–0.2	In disseminated deltaic shales over long intervals, significant volumes of gas can be generated from TOC's at 0.5 % or less
Fair	0.5–1	0.2–0.5	
Good	1.0–2.0	0.5–1.0	
Very Good	2.0–5.0	1.0–2.0	
Excellent	>5.0	>2.0	

After Law (1999). Note that measured current TOC is not indicative of past TOC. Low current TOC can occur in rocks that are thermally mature and have generated large amounts of hydrocarbons in the past

Table 8.2 General comparison of maturity values by maturation range. Modified from Law (1999)

Vitrinite (Ro%)	Spore coloration Index (SCI)	Thermal alteration index	Tmax (°C)	General maturity	Comments
0.2–0.6	4–6	2–2.6	415–430	Immature	Can be lower depending on kinetics
0.6–0.8	6–7.4	2.6–2.8	430–440	Early oil	
0.8–1.2	.4–8.3	2.8–3.2	440–465	Oil	
1.2–1.35	8.3–8.7	3.2–3.4	465–470	Oil and wet gas	
1.35–1.5	8.5–8.7	3.4–3.5	470–480	Wet gas	
1.5–2.0	8.7–9.2	3.5–3.8	480–500	Dry gas	
2.0–3.0	9.2–10	3.8–4.0	500–500+	Dry gas	
•3.0	10+	4.0	500+	Over mature	

Vitrinite reflectance (Ro) was developed over a century ago to measure the rank of coals. Highly mature coals like anthracite, for example, have shiny surfaces reflecting light. Low maturity lignites do not have reflectivity. The process involves making polished thin sections of woody material and measuring the amount of reflected light on the sample under a microscope. Subjectivity in deciding which samples are actual vitrinite can cause errors in measurement, typically values that are too low if the samples are algal rich and mistaken for vitrinite. Spore Coloration Index (SCI) and Thermal Alteration Index are other measurements, both measuring the color of palynomorphs, chitin, solid bitumen, conodonts or other components that respond to changes during maturation. Since woody plants necessary to derive Ro data did not evolve until the Devonian, in older rocks, the SCI or TAI approach may be the only visual way to assess maturity. SCI and TAI measurements, being simple color scales, are more prone to variability from the interpreter.

Tmax values have been qualitatively compared to vitrinite and spore coloration index and a rough comparison made. Tmax is often the least susceptible to opinion, as it is a direct measurement from the rock itself. SCI and Ro values can vary substantially by the interpreter or lab. As a result, maturation is best viewed and calibrated by multiple approaches. The best answer in any trend is given by the fluids recovered themselves (assuming only very short-range migration), and that comes back to maintaining a good shows database and being aware of production.

Another variable on maturation values is the kinetics of the source rock itself. Many workers follow a BP model (Pepper and Corvi 1995a) to classify source rocks. The values in Table 8.1 are a good guide, but the source rocks themselves may mature at greatly different temperatures and maturation levels. A Type III coaly source for instance, may not expel significant hydrocarbons until Ro values up to 1.0 have been reached, where Type II source rocks would be well in the oil window at that point.

The models developed by Pepper and Corvi have been built into many commercial software packages, one of which is Kinex (www.zetaware.com). Plots from Kinex for the five basic BP classes of source rocks are shown on Fig. 8.5.

It is common to use not just the Type I, II and III classifications on pseudo Van Krevelen diagrams, but also the BP classes in Fig. 8.5. Aquatic source rocks, for instance, are roughly equivalent to Type I and II source rocks and their kinetics are not substantially different from one another. In the northern part of the Barmer Basin in India (Dolson et al. 2015) algal-rich lacustrine source rocks have TOC's in excess of 10 % and HI's reaching 1000. These source rocks mature at even lower temperatures than those shown in Fig. 8.5a and c, entering the oil window as low as 85 °C. This reinforces the need, where possible, to obtain actual kinetic data on a source sample so as to be able to model it properly.

Note in Fig. 8.5f that the terrestrial lignin-rich source rocks are not only incapable of generating oil, they don't begin to expel any hydrocarbons until about 160 °C.

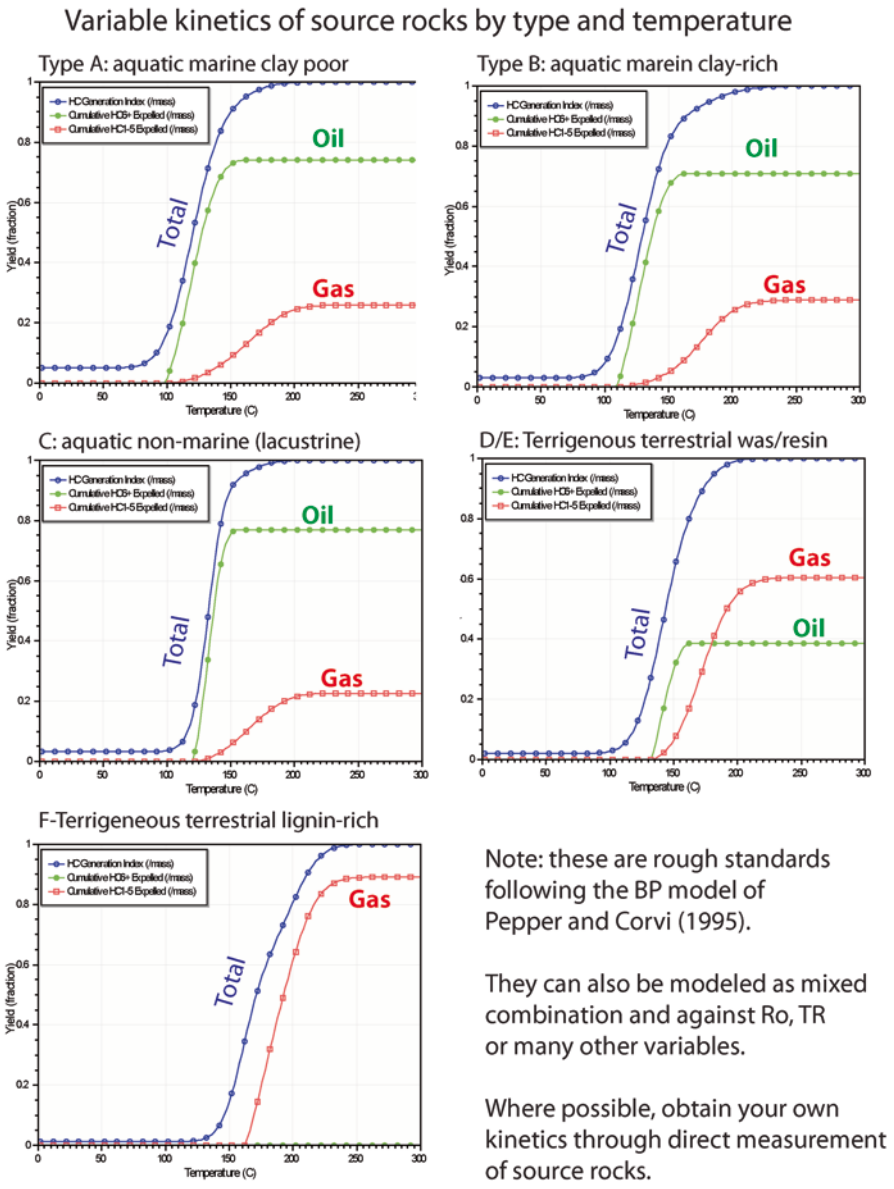

Fig. 8.5 BP models of source rock fluid expulsion by temperature (form Kinex software default values)

8.2.4.1 Maturation and Rock Eval Numbers: What you see is not What you Had

Perhaps the most important point about source rock quality is that Rock Eval data only measures what is currently in the source rock. It does not assess what the source rock was originally. In screening source rock plays, this makes a difference. Plays where the current source rocks may have TOC of 1.5 % and HI's as low as 25 may look like poor gas prone source rocks, but have initially started out as world-class oil-prone source rocks. This, for example, is the case for the prolific Marcellus Shale play of Pennsylvania, where the best gas wells are located in trends of low current HI and TOC.

The difference between the initial and current TOC is due to maturation. Hence, understanding initial values quantitatively is a key to understanding the volume of oil and gas generated and thus available for migration. Petroleum systems modeling packages utilize initial TOC and HI maps, along with thickness, to estimate volumes of hydrocarbons generated and retained. This information comprises one of many screening techniques for shale plays and is essential for estimating potential in new conventional plays.

Figure 8.6 shows a good example of HI reduction with maturation. The values are from an algal-rich, oil prone kerogen (plotted from multiple wells and depth) with very low OI values and HI values that approach 750, but are as low as 50.

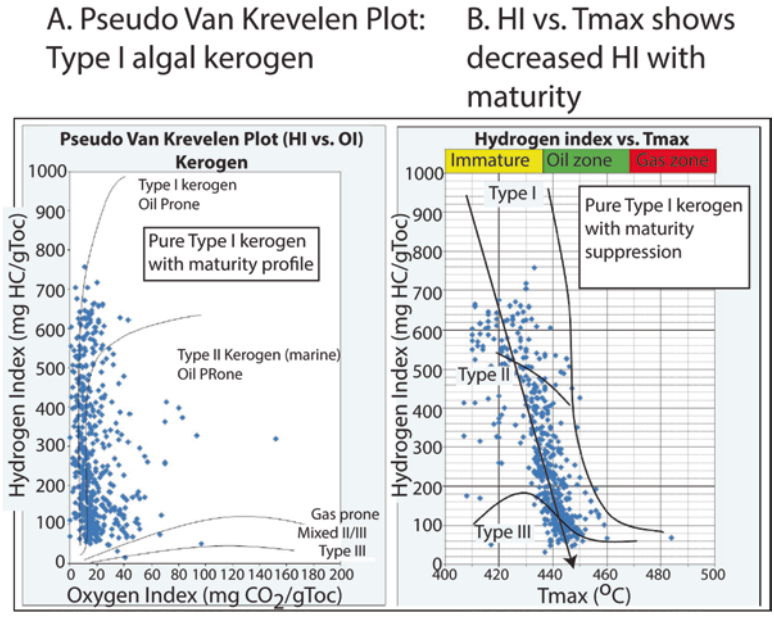

Fig. 8.6 HI reduction as a function of maturation

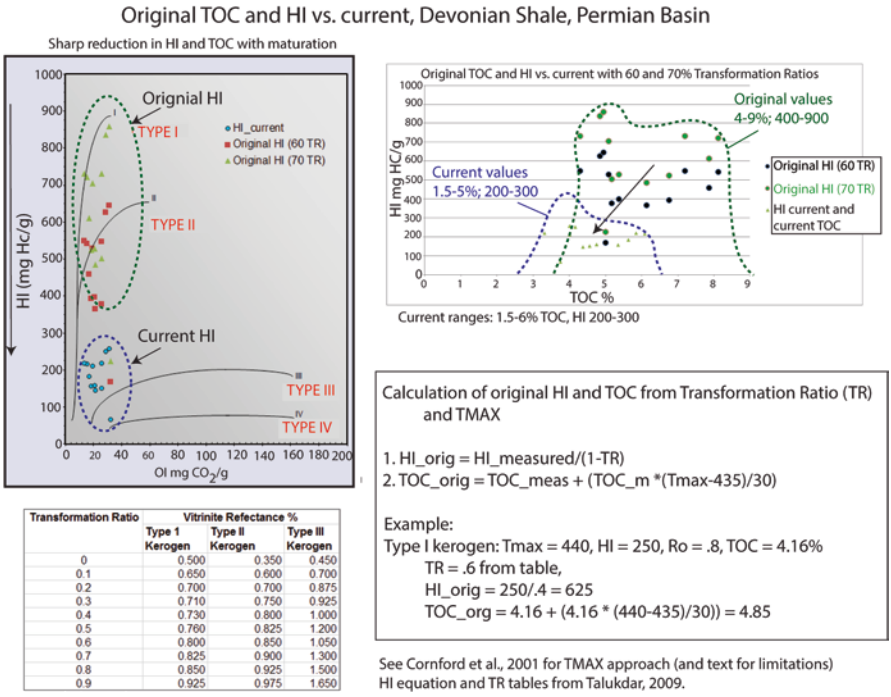

Transformation Ratio	Vitrinite Refectance %		
	Type 1 Kerogen	Type II Kerogen	Type III Kerogen
0	0.500	0.350	0.450
0.1	0.650	0.600	0.700
0.2	0.700	0.700	0.875
0.3	0.710	0.750	0.925
0.4	0.730	0.800	1.000
0.5	0.760	0.825	1.200
0.6	0.800	0.850	1.050
0.7	0.825	0.900	1.300
0.8	0.850	0.925	1.500
0.9	0.925	0.975	1.650

Fig. 8.7 Original HI and TOC vs. maturation using Tmax or transformation ratios

Plotted against Tmax, however, a clear reduction in values is shown, indicating that the lower HI values are not the initial values, but what is left after maturation. Where the Tmax values are 420 or lower, the HI values are probably showing the initial HI, which would be between 600 and 750 HI.

The degree to which source rocks have expelled or 'transformed' their hydrocarbons is called the Transformation Ratio (TR). Figure 8.7 has a table used commonly (Talukdar 2009) to relate vitrinite reflectance values to TR for various types of kerogens. The higher the TR, the more the source rock has expelled hydrocarbons and the more diluted it becomes in its HI and TOC. It is too easy to view low TOC and HI values as indicative of poor source rocks when in fact, they were initially excellent but have gone through the oil or gas window, greatly reducing the values.

The difference between what is in a rock now and what was there initially is actually the volume of kerogen converted to hydrocarbons. Therefore, knowing initial conditions vs. current gives a way to quantify what has been expelled.

In order to evaluate source rock potential and volumes generated, then, maps of initial HI and TOC have to be generated, along with thickness maps of the source rock. There are a number of industry algorithms and approaches, but most derive their methodologies from equations provided in (Pepper and Corvi 1995a, b, 1995). For the typical interpreter, however, some good screening tools are available to make those estimates.

For single point estimates using Rock Eval inputs, an online calculator is available (He 2015). Two other equations are shown in Fig. 8.7. Original HI is the easiest to calculate as it is simply by Eq. 8.1:

$$\text{Original HI} = HImeas \div \left(1 - TR\right) \tag{8.1}$$

Where HImeas = value calculated from Rock Eval and TR = estimated transformation ratio

For lack of a better resource, the values for TR can be input from the tables shown in Fig. 8.7 for the various kerogen types. Original TOC takes into account S1 values in the Zetaware web calculator mentioned. An alternative method useful for screening large sample sets is from a method developed by (Cornford et al. 2001) and available online (Cornford 2015). This technique uses Tmax as a measure of maturity and the equations and results on a sample data set are shown in Fig. 8.7.

Figure 8.7 has data from a set of Devonian shale samples from the Permian Basin, captured as part of a shale oil play evaluation. The operator was alarmed when the TOC and HI values derived from Rock Eval came back from the vendor marked as 'low to poor generative capability'. Regionally, and across North America, Devonian shales are known for their rich source rocks and this initially looked like an exception. The problem was the low HI values. However, when correcting back to initial HI and TOC using a variety of approaches, the original HI and TOC was much higher. The initial source rock conditions were a world-class algal-rich marine source rock which had expelled a lot of its hydrocarbons, explaining the low numbers. The shifts from original to current TOC and HI are clear in Fig. 8.7, shown with downward sloping arrows.

One additional calculation for original TOC is that of (Talukdar 2009), shown in Eq. 8.2:

$$\text{Toc\_original} = \text{TOC\_measured} / (1 \ \left(\text{TR} * \text{dV}_{\text{toc}}\right) \tag{8.2}$$

Where dV_{toc} values are given by kerogen type as:

1. Type I (62.5 %)
2. Type II (48.2 %
3. Type III (25.2 %)

For example, for a sample Type I algal kerogen with TOC-measured 4 at a TR of 0.7, TOC_original = 4/(1-(0.7*0.625)) = 7.1 % Original TOC.

So how is this used? Calculating the volumes of oil and gas generated or remaining in the source itself is key to understanding not just potential in traditional conventional traps, but in assessing the source rock potential itself as an unconventional play. Single point calculations are not as useful as looking at histograms of ranges of values over an interval and then doing a conversion on the mean or other numbers that appear to represent the overall interval best. This is somewhat analogous to choosing porosity-perm pairs for pseudo-capillary pressure. Generalizations have to be made. Frequently, online databases provided by state or Federal government

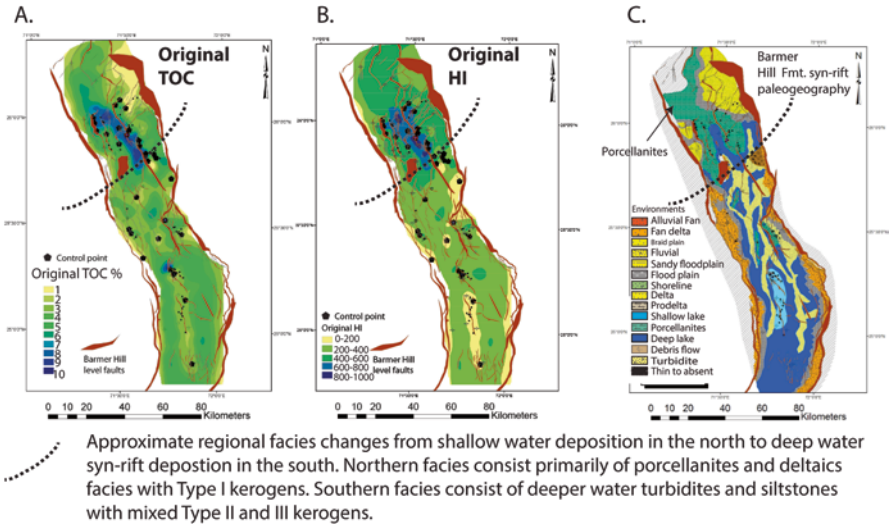

Fig. 8.8 Original TOC and HI maps, Barmer Basin. Figure from Naidu et al. (in press)

divisions in the USA provide Rock Eval and Ro data as single points per formation, where the data has already been treated as an average of many more samples.

In the example shown in Fig. 8.8 (Naidu et al. in press) and Naidu et al. (2012), original TOC and HI values have been generalized per well from multiple data sets at the major source rock intervals. Initial TOC and HI values have been hand contoured around the basin to match the depositional environment, rather than simply contoured by a computer. In the northern basin, the Barmer Hill Formation shales are a nearly pure Type I algal kerogen, but in the south, they are diluted with clastics from turbidites entering the deep basin and a more Type II-III kerogen. Those geographic changes are reflected in the maps. It can be difficult at times to separate low HI and TOC values as due to maturation or original facies. In the maps shown in Fig. 8.8, there was enough geochemical data to suggest that much of the lower HI was not just a function of deeper and hotter burial, but lower initial values.

Separating out the effects of burial vs. the depositional controls boils down to doing good geological work with facies maps of the source rocks themselves.

These maps indicate that the northern basin should be more oil prone and the southern portion, dominated by Type II-III kerogens, more gas prone at any level during the maturation process. That conclusion matches well with production, as there is very little gas to the north, except where the basin has been uplifted. In uplifted areas, residual oil legs are common and almost all the gas appears to have come out of solution to form small gas caps (analogous to the Hugoton and West Siberia residual migration cases discussed in Chap. 5).

Ultimately, different kerogen kinetics were used in this study based on different facies, using local kinetic data available by facies and a full basin model. The results are shown in Fig. 8.9. Maps like these offer better prediction of fluid phase and the potential of the source rocks themselves.

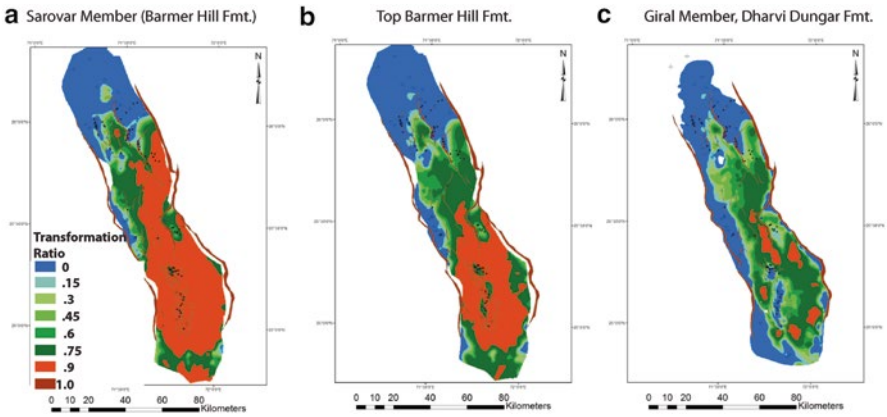

Fig. 8.9 Barmer Basin transformation ratio maps at three levels, using variable kinetics. Figure from Naidu et al. (in press)

Simply gridding key Rock Eval and Ro data without converting back to original TOC and HI can, however, give excellent predictability in any basin. While petroleum systems software offers the ability to generate maturation maps and volumetrics quickly, simply mapping the data available and looking at production and shows can often provide the answer needed to explore.

An example is shown in Fig. 8.10. All of the data used in this example is available by download either from the United States Geological Survey, or the state geological surveys of Ohio and Pennsylvania. The well data consists not just of location and status, but has information on initial flow rate, operators and other data. All of the wells historically drilled can be taken from free websites and then production records also pulled. The producing wells in Pennsylvania (red circles and pies) are from production in the Devonian Marcellus Formation as of 2012. Note that the Marcellus shale producers are confined almost solely to the Ro window of 1.2 or above.

Prior screening of the Marcellus Rock Eval showed a strong relationship between Tmax, Ro and HI, with HI values decreasing abruptly with maturity. Thus, gridding HI data from the online database does an excellent job of defining the Marcellus play (Fig. 8.11).

A sharp ramp or 'HI wall' of decreased HI values is apparent on the map. The Marcellus play can be seen to be largely confined to current HI values of 25–100. Most workers in this area believe the widespread Devonian shales, had initial HI values of about 600. The difference on the map can be almost certainly attributed to maturation, not changes in depositional environment. A similar ramp or 'HI wall' has been documented in the Devonian Bakken Formation as marking the eastern limits of that play in the Williston Basin (Nordeng and LeFever 2009).

One of the lessons in these maps is that you don't need to have a lot of software to understand what data sets like these mean. Simply gridding or contouring maturation data and visually inspecting HI and other data for possible facies overprint on low values can be done with simple tools and good geological insight.

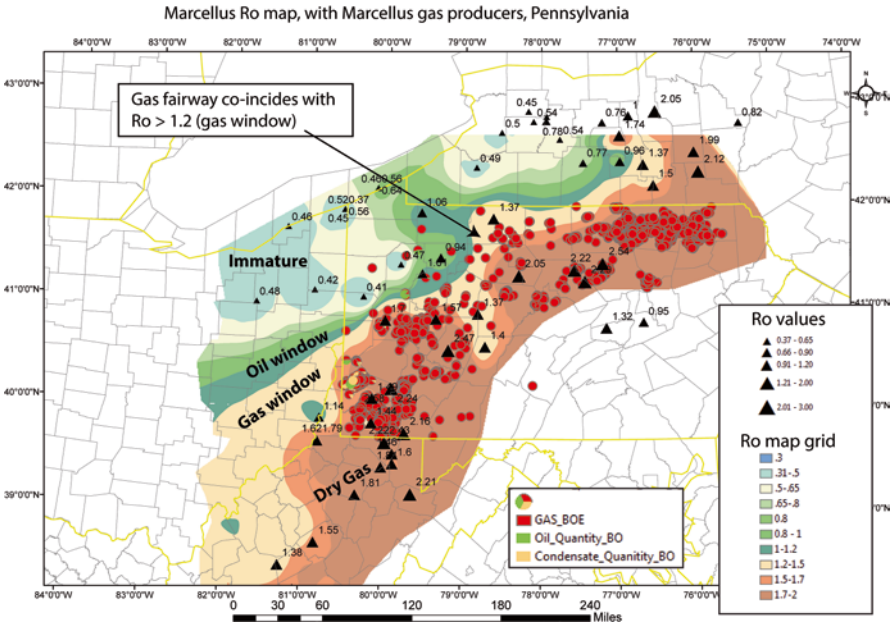

Fig. 8.10 Marcellus Ro data and production ratios by phase, Pennsylvania and Eastern USA

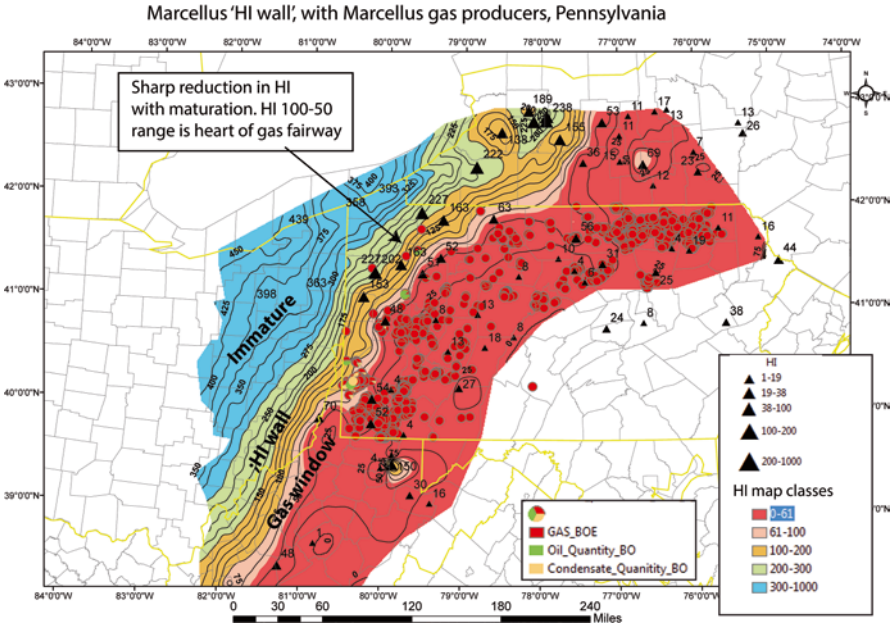

Fig. 8.11 Marcellus 'HI wall' and limits to the gas play

8.2.4.2 Delta LogR and Resistivity Mapping

One of the landmark papers dealing with logs and source rocks was that of Meissner (1978). Meissner noted that the Bakken Shales in North Dakota had high resistivity wherever they were thermally mature. He not only quantified this from wells and related it to the presence of hydrocarbons, but built maps of Bakken Shale resistivity that showed clearly where the Bakken Shales were thermally mature. He also mapped overpressure in the Bakken and gave a number of example of fields producing from the Bakken Shales and suggesting a broader pay might exist. Ironically the maps he published in 1978 effectively outlined what 25 years later would become the heart of the Bakken oil play, one of the biggest oil plays in the USA history. Update maps of Bakken resistivity (Nordeng and LeFever 2009) have refined the edges, but not significantly altered the 1978 publication.

Some ideas take a while to mature and sink in when they are novel! By the late 1980s operators were trying to test thermally mature Bakken shales with horizontal wells, but tried completing in the wrong zones (soft and pliable shales). High initial well rates cratered to zero or sub-economic within days or weeks and the shales collapsed after the hydraulic fracturing and closed the artificially induced fractures. Over time, a middle siltstone layer encased above and below with good source rocks, but brittle enough to work with horizontal drilling and hydraulic fracturing was eventually targeted. At that point, the play worked and by the later 1990s a drilling boom began which is still ongoing.

Resistivity mapping is still a primary tool used to screen all shale unconventional plays, but more advanced log techniques were developed. The first and most important log based procedure is that of the Delta LogR technique (Passey et al. 1990). Delta LogR is now an industry standard approach to recognizing source rocks. It can also be used to map maturity windows by tracking changes in resistivity, as in increasingly mature source rocks, the amount of TOC is reduced as well as the amount of free hydrocarbon remaining in the pore system.

The Delta LogR principle works on some basic and fairly simple logic (Fig. 8.12). Thermally immature source rocks have not expelled hydrocarbons, so the shales have low resistivity values. As they mature, hydrocarbons are given off, and just as in the case of a conventional trap, have high resistivity measureable by deep resistivity tools. Organic rich zones have higher shale porosities, furthermore, so there is increased porosity in the shales which can be detected by the sonic log if high TOC values are present.

Sonic velocity curves are overlain on the resistivity curve and where they track one another, the source rocks are organically lean. When the curves separate but the resistivity remains low, then high TOC source rock with porosity is present, but not expelled hydrocarbons. If the resistivity increases in the high porosity shales, then hydrocarbons are present and the separation can be noted and quantified against

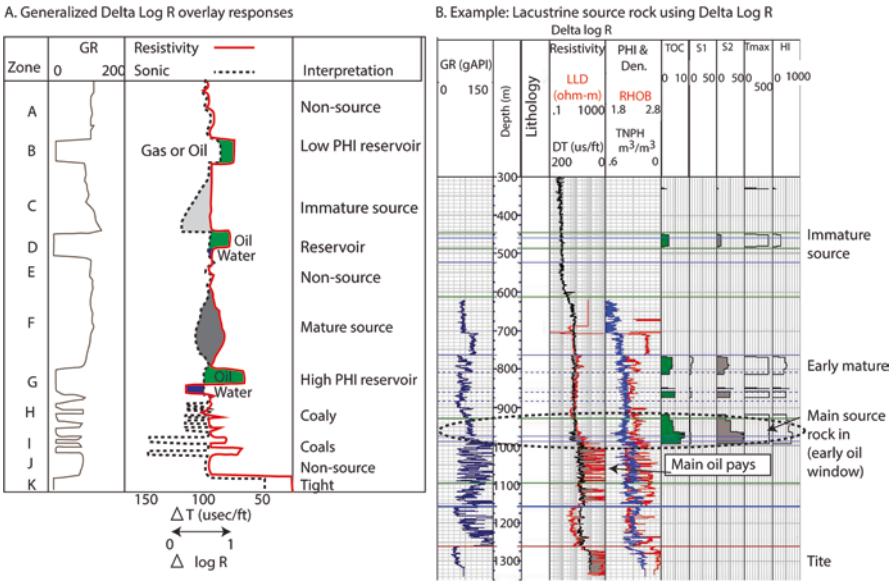

Fig. 8.12 Delta logR patterns and example. (**a**) modified from Passey et al. (1990). (**b**) courtesy of M. S. Srinivas, Cairn India. High resistivity in B below the zone circled as mature source rock (*green*) is from conventional oil pays

measured TOC and maturation in those zones. Interestingly, when the samples reach high enough maturity that the source rock is spent, the resistivity drops back to low values and the tracks overlay one another again.

Figure 8.12b shows an example from the Mangala field in India. There is good separation and high resistivity in the main source rock interval, which can be readily spotted by the high GR readings. Below the main source rock are a number of layers of highly porous sandstone with oil pay zones. These pay zones also show separation, but in this case, the high resistivity is with oil saturation reservoirs that are easily identified by the GR and other logs as sandstones.

Resistivity mapping as a screening tool is here to stay. The patterns to recognize on a map going into a basin basically changes from low resistivity where thermally mature and then high resistivity in the oil gas window. If the basin is deep enough that the same zone is spent and over mature, then the resistivity drops back to low values again downdip of the play. This phenomenon was initially described by (Meissner 1978). A good example of resistivity mapping to define mature source rock limits is that of (Nordeng and LeFever 2009).

More screening criteria for source rock plays are discussed later.

8.2.5 *Building Maturation Models and Understanding Heat Flow*

Understanding source rock play fairways, as well as migration and charge in the context of shows and production is best done in concert with mapping of hard data and development of predictive petroleum systems models. Burial and maturation models rely on four major components:

1. Geothermal gradient or heat flow through time
2. Conductivity of the sediments themselves
3. Restoring periods of uplift and erosion to account for total burial history
4. The kinetics of the source rock itself

The practical purpose of basin modeling is to derive some kind of predictive model for fluid phase and type in the context of current and paleo-traps and migration. Models can be as complicated as you want, or simple and predictable. The simpler the model, the more likely it is to violate all the controls in past geothermal heat flow, burial history, source kinetics and a host of other factors. But the more complicated the model gets, the more often too many assumptions are made and the modeled answer is fundamentally flawed.

At times, particularly in older rocks and basins which have undergone multiple periods of uplift and erosion, building accurate burial models is difficult at best. In the case of the Marcellus Formation, for example, the source rocks are Devonian in age, but have undergone at least five periods of uplift and re-burial. Pennsylvanian age anthracite coal mines are at the surface in Pennsylvania (testifying to deeper burial), and total erosion and uplift in some areas exceeds 3–4 km. Some of that erosion was in the Permian or Mesozoic, other events in the Tertiary. The data needed to unravel all of those episodes and account for changes in surface temperature over time and variable heat flow with time requires datasets which simply don't readily exist. In this case, maps have to be made that give predictive answers.

This example is not an exception, but pretty normal for onshore plays. In some of these trends, mapping the source rock fairways is best done simply by gridding data and generating resistivity or other maps, rather than try to accurately reconstruct burial history through time. Complicating maturation modeling further is crustal thickness and composition, which can exert considerable influence on lateral variability in maturation.

It is good to remember in the following sections, a quote largely attributed to George Box, a British mathematician:

> "All models are wrong, but some are useful"

As in the case with capillary pressure data, where the IFT and wettability numbers may have to be estimated to derive seal capacity, basin models can have an enormous number of options to model burial history and migration/maturation through time. Unfortunately, the data required to substantiate many of the assumptions that can be put to a model are often not available. It is best when faced with limited

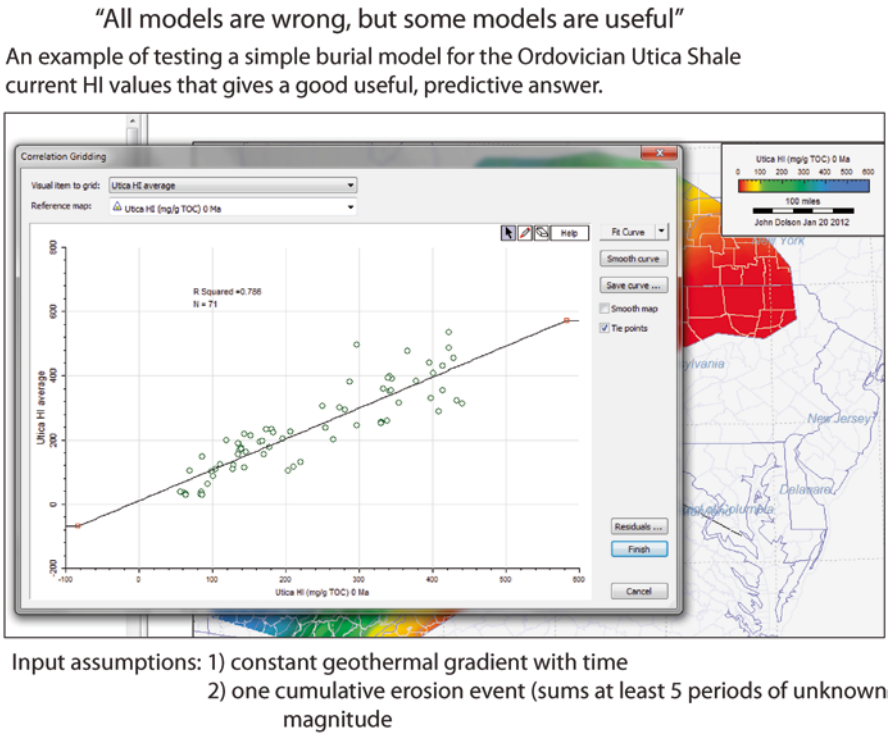

Fig. 8.13 The exploration goal is a model that is to be predictive. Keeping models simple within constraints of the data is preferable to assuming too much and guessing about too many input parameters

calibration points to keep a model simple and recognize it is probably wrong, but if it is predictive, go ahead and use it.

An example is shown in Fig. 8.13 for the Ordovician Utica Shale, where a maturation model has been built assuming one constant geothermal gradient through time over a 400 + MA period, with no lateral variations due to crustal thicknesses, and one major erosion map restoring total burial thickness over the entire Eastern United States. The erosion map encompasses at least five periods of uplift and erosion. As the Utica Shale is at the surface in many locations, it is impossible to completely understand the complexities of heat flow changes spatially and through time, as well as to restore all the Cretaceous and Tertiary burial history accurately.

What is important about the model that was built, however, is that it has a high degree of predictability. The HI values shown on Fig. 8.13 are the actual values from public domain databases plotted against a predicted HI map built with Trinity software assuming initial HI values of around 600. The correlation is excellent and allows for better gridding of the measured data by using a regional trend line. It also allows extrapolation away from the well control, something that all basin models are designed to do.

Is this model wrong? Of course it is. Is it useful? The only way to find out is to run other aspects of the model like predicted GOR, API gravity, predicted vitrinite or other parameters and compare directly to what is produced in wells and measured by other data. In this case, the predictability was very high for fluid production, so the model was used to purchase a substantial amount of exploration acreage. Good wells have now been drilled based on this work and the clients were happy with the results.

8.2.5.1 Geothermal Gradient and Heat Flow

The first step in any maturation modeling is determining appropriate geothermal gradients to use and what models to apply. Especially in frontier basin exploration, good temperature data can be very difficult to find and many assumptions then need to be made. A good summary of thermal modeling issues is covered by (He 2014).

Usually, the first step is to gather as much temperature data from wells or other sources and calibration points like vitrinite reflectance, Tmax, SCI, TAI and other data as discussed earlier. A model cannot be built or run without geothermal gradient inputs. Unfortunately, there are a lot of problems with most temperature or heat flow data sets. These are summarized in Table 8.3 (modified from www.zetaware.com website by Zhiyong He). The Zetaware website also comes with some built in calculators. An additional paper summarizing temperature calibration and correction is that of (Peters and Nelson 2009).

Calculating geothermal gradient requires a reliable average surface temperature and a reliable, adjusted for wellbore mud system cooling, temperature profile in a well. If offshore, the temperature of the sea floor is used. When projects span onshore and offshore, temperature maps of the lateral changes from sea floor to surface elevations are needed.

The basic calculation for geothermal gradient is from Eq. 8.3:

$$Geothermal\ gradient = \frac{Temperature\ in\ well - Surface\ temperature}{Depth} \tag{8.3}$$

Example: Surface temp is 21 °C, Temperature 115 °C at 2460 m. Gradient is (115–21)/2460 = 0.0382 C/m or 38.82 C/Km.

The reality of exploration remains that there is seldom any ideal data set. Abundant well header information, even if available, usually reports BHT as an uncorrected number, which almost always is notoriously low. As in pressure data, where the final pressure is not reached, extrapolations and corrections have to be made. Appendix B illustrates how to use Horner plots to correct temperature data for cooling effects of the mud, but the necessary information is, again, often missing. Production test data is best, but also commonly missing.

For the most part, calibrating geothermal gradient usually ends up having to rely on BHT temperature data from wells. If BHT is used, it is wise to check two gradients and then match to observed maturation data in models to see which fits.

Table 8.3 Sources of temperature data (in order of reliability)

Sources of data	Reliability	Comments
Continuous equilibrium temperature logs	Highest	Seldom available
Modern, electronic gauge DST data	High	Best taken where there are high flow rates. Corrections may be needed for gas tests.
Production test from shut-in wells.	High	There may also be published temperature records by formation and depth for producing fields
Bottom Hole Temperature (BHT)	Low, but easier to come by—it is seldom clear if the data is corrected for circulation time and cooling by the mud systems or simple the number measured. Corrected numbers are desired.	The most commonly available data
		May only have local control and not regional representation
		May need a Horner correction (Appendix B)
		May need correction for time of circulation of the mud system
		May need to try scenarios by adding + 33 F or +18 C to the BHT value recorded

Error bars can also be assigned. A quick method developed by Jeff Corrigan (He 2014) is simply to add 33 °F or 18 °C to the BHT temperature record. This is a 'last resort' attempt that has proven useful.

As thermal gradient is also dependent on surface temperature, inputs need to be made based on mean annual temperature data (Fig. 8.14). In the simplest models the gradient is set as constant through time (Fig. 8.14a), with the curve intercept at surface temperature. Mean annual values can be estimated from published data, web searches or estimated by latitude (Fig. 8.14b). For those wishing to complicate things further, estimates of paleo temperatures can be made in basin models using charts such as those shown in Fig. 8.14c and d.

One of the most basic corrections that needs to be made in areas with any significant topography or water depths is adjustment for elevation, particularly water depth. Water depth corrections are critical in deep water settings, as the temperature at sea floor is the input to the geothermal gradient calculation. Figure 8.15 provides an example.

The example from the northeast coastline of Brazil shows a rapid reduction in surface temperature from a mean annual onshore of 28 °C to 2–4 °C at the sea bed offshore. Failure to make a correction for water depth and temperature will result in much too low a geothermal gradient offshore.

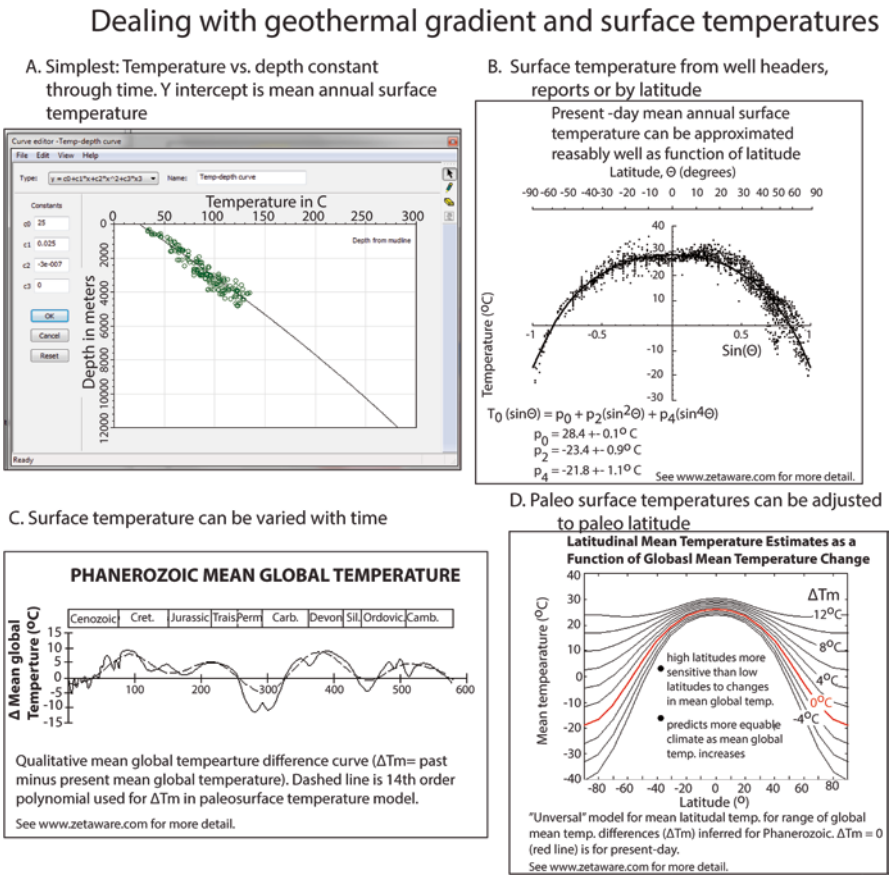

Fig. 8.14 Surface temperatures through time and latitude. (**a**) is a typical temperature-depth curve used in Trinity software to calculate present day geothermal gradients. (**b–d**) are from the Zetaware website (www.zetaware.com), and can be used to estimate paleo surface temperatures. Figures used with permission of Zetaware

8.2.5.2 Heat Flow Modelling

Basin models will also rely on thermal conductivity of the sediment and crustal heat flow. Global databases are available for heat flow, both onshore and offshore (Pollack et al. 1993; Gosnold 2011a, b), some of which is also posted on Fig. 8.15, for example. An excellent online reference to heat flow is that of (Railsback 2015), and short summaries include (He et al. 2007; He 2014), some of which is summarized in this section.

Heat flow (Q) is a measure of the rate of heat transfer. Sources of heat flow include mantle heat, radiogenic heat production from the upper crust as well as

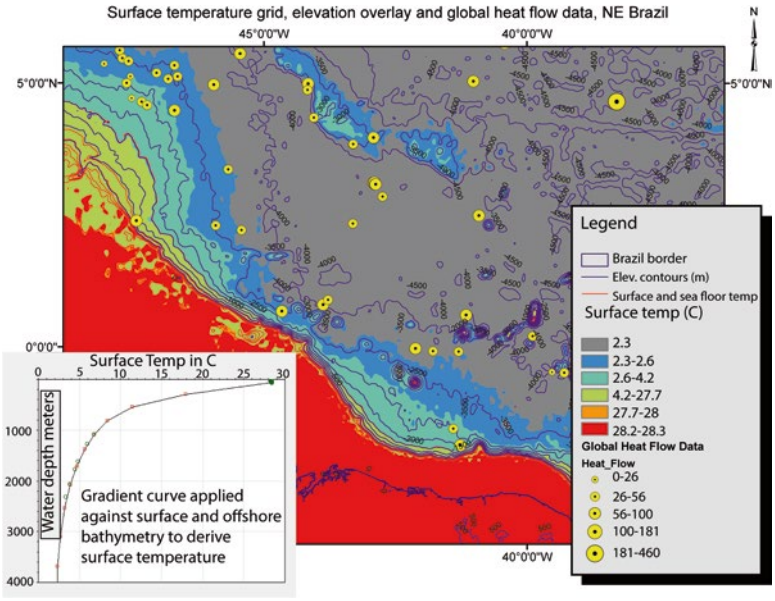

Fig. 8.15 Deep water temperate map offshore Brazil. The contours are water depth in meters. The temperatures are shown in color bands. The curve in the lower left was used to convert a digital elevation model and bathymetry grid (ETOPO1) to a surface temperature grid for input into thermal modeling

sediments. Crustal composition and heat flow (Fig. 8.16) has a major control on heat flow.

Heat flow is expressed as power per unit area and measured in milli-watt/m^2 (mw/m^2) or heat flow units (HFU, in calories/cm^2/s). Thermal conductivity (K) is a measure of power per length-degree, expressed as W/m-K or calories/cm/s.

Heat flow can be related to geothermal gradient by Eq. 8.4:

$$Q = K \times \frac{dT}{dz} \tag{8.4}$$

Where:

Q = heat flow (mW/m^2)

K = thermal conductivity

dT/dz = geothermal gradient

Or, re-written in terms of geothermal gradient as Eq. 8.5:

$$\frac{dT}{dz} = \frac{Q}{K} \tag{8.5}$$

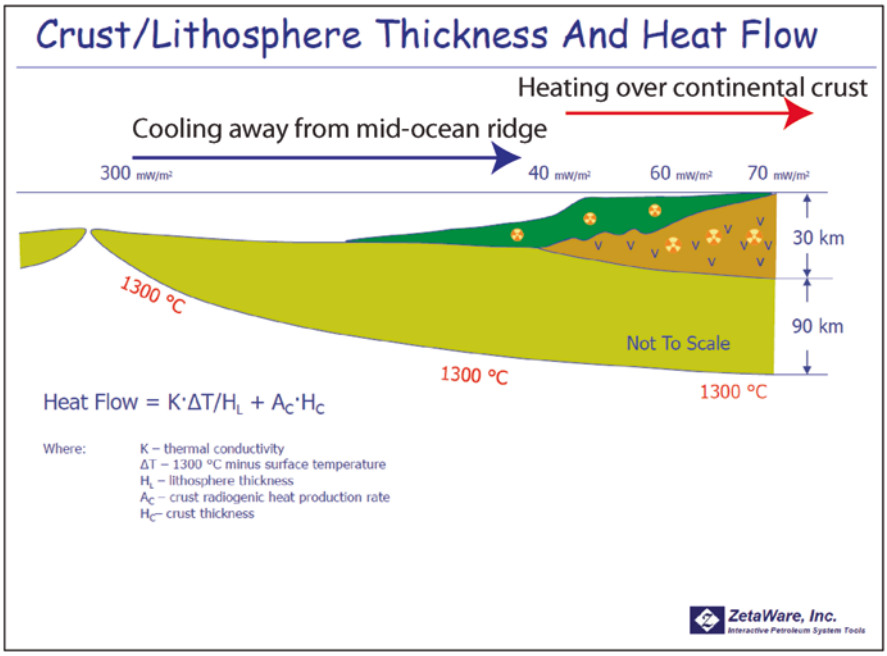

Fig. 8.16 Crustal heat flow. Continental crust is hotter than oceanic crust at the boundaries. Figure courtesy of Zhiyong He and available at www.zetaware.com

Hence, high heat flow translates to high conductivity, but highly conductive rocks are poor insulators and contribute to low geothermal gradient.

Figure 8.16 show that very high heat flow rates are found offshore along the mid-ocean ridges, but as the heavy, basaltic lavas move away from the ridges, they consolidate, cool and sink, forming oceanic crust. Very little oil and gas production exists anywhere globally over oceanic crust. One of the paradigms is that the thermal gradients are too low over cooled oceanic crust to thermally mature sediment. Thicker and more radiogenic continental crust, however, has a higher gradient.

Many seismic companies shoot long record-length seismic designed to see as deep as possible into the crust along continental boundaries. They do this because the ability to pick Moho and derive a crustal thickness can be a valuable input into a petroleum systems heat flow model.

Heat flow data, however, is usually derived from very shallow boreholes and thus may not actually represent deep crustal heat flow. In addition, heat flow is affected by the conductivity of sediments. This could easily be termed the ‘thermos effect’, as sediments act as insulators where conductivity is low (as in shales) and as conductors where it is high (as in salts). A thermos works the same way, in that insulating material is used to keep liquids hot through time. In maturation modeling, as time is a factor, good insulators like thick shales will have the effect of allowing more heating to take place with time than will layers under salt. The economic

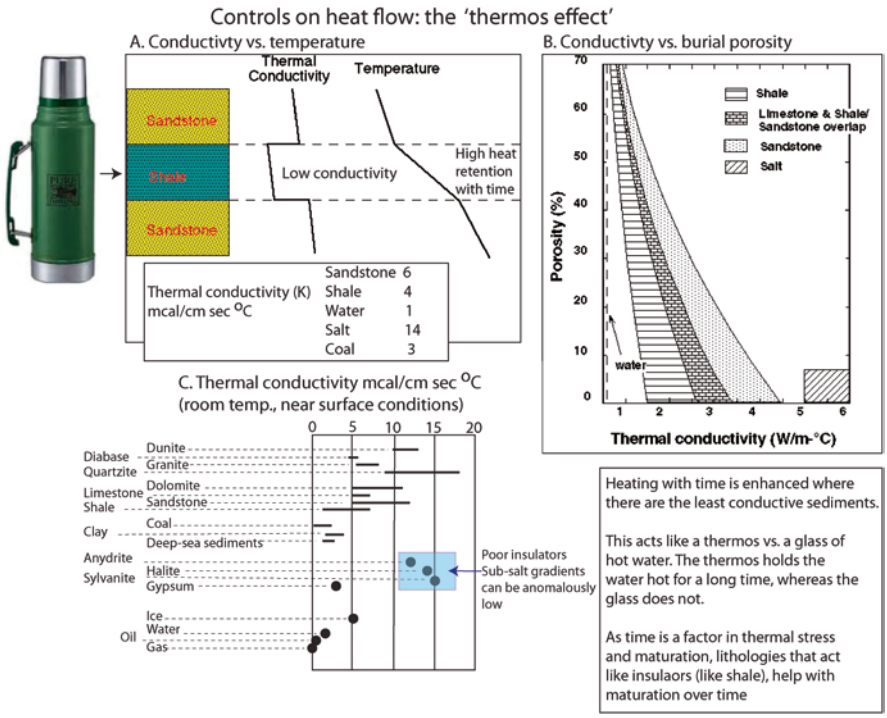

Fig. 8.17 Sedimentary heat flow controls in various lithologies and burial compaction. Images courtesy of Zhiyong He and available at www.zetaware.com. Chart C modified from Gretener (1981)

impact of this is fairly simple, in that many sub-salt plays still have oil at great depths that have not been cracked to gas due to the high conductivity of salt. Porosity reduction due to compaction is another factor. In building 1-D burial models, all of this information can be modeled and calibrated to known data (Fig. 8.17).

8.2.5.3 An Example of Basement Control on Heat Flow and Maturation-Bakken Formation, Williston Basin

One of the best examples of basement control on heat flow is that of the North American Central Plains (NACP) anomaly (Jones and Craven 1990). The NACP is a pronounced magnetic anomaly that represents a Precambrian rift event designated 'juvenile crust' by Jones and Craven. Despite the age of this rift, which has long since be re-deformed by later tectonic events, it exerts a strong influence not just on subsequent fault patterns with time, but current heat flow. Throughout Saskatchewan, higher heat flow is documented associated with the anomaly.

Publically available databases on gravity and magnetics are available (BGI 2013; UTEP 2015) and data like these should always be examined to see if crustal compo-

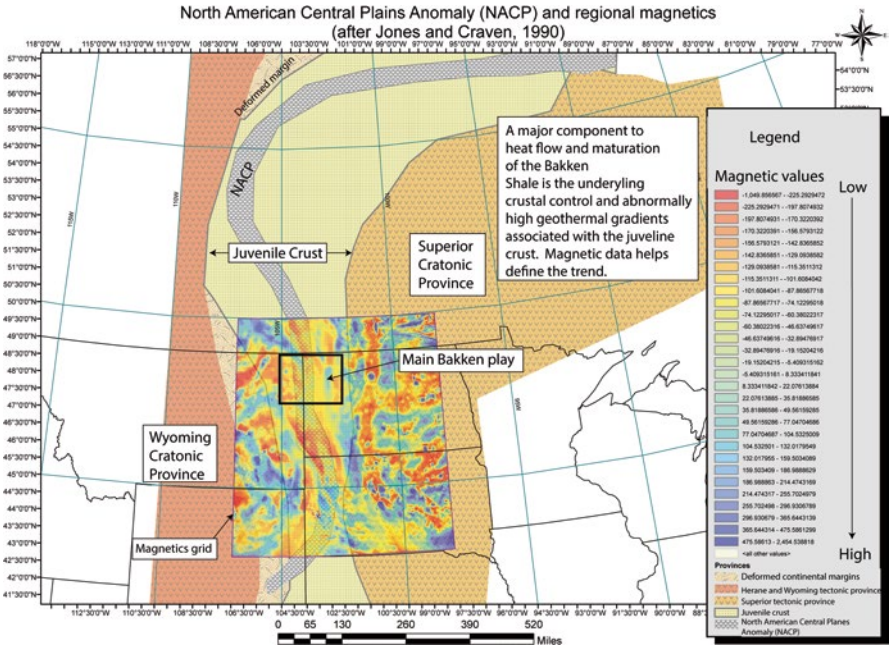

Fig. 8.18 NACP anomaly and regional magnetics. Bakken play, North Dakota

sition might be a controlling factor on maturation. A subset of the magnetic data is shown overlain on the regional interpretation of Precambrian terrains (Fig. 8.18). The heart of the Bakken oil shale play lies within the juvenile crust trend in North Dakota (Fig. 8.19).

Detailed geothermal gradient work (Meissner 1978; Price et al. 1986) documented elevated thermal gradients in the Williston basin and updated maps of this, compared to magnetic anomalies have been shown by Nordeng and LeFever (2009).

Modeling the Bakken Shale play with petroleum systems software can be difficult due to thermal variation related not just to basement, but later erosional events. In addition, the maturation trends do not closely follow current day structure, but have strong north-south overprints.

Figure 8.20 shows the 'HI wall' documented by Nordeng and LeFever (2009) but also initially identified as far back as 1978 (Meissner 1978). The close alignment with the HI wall and the edge of the Superior cratonic terrain and the juvenile crust, along with published heat flow maps, shows the importance of using the magnetic data to help model heat flow across this area.

Further confirmation of the strong north-south trend of higher maturation levels is from a grid of Upper Bakken Tmax data (Fig. 8.21).

Burial history models utilizing current structural girds (which follow the circular shape of the Williston Basin), without accounting for the strong deep crustal heat flow, would produce circular patterns of maturation. These patterns will show no correlation with actual measured maturation data and have low predictability.

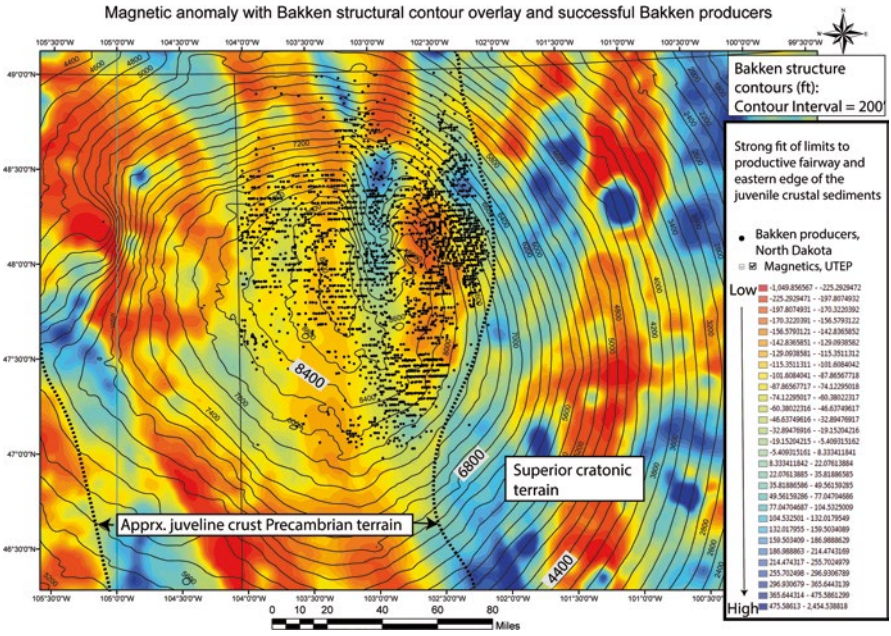

Fig. 8.19 Aeromagnetic map with Bakken horizontal shale wells in North Dakota. The juvenile crust limit roughly coincides with eastward edge of the Bakken fairway. The north-south alignment of the deeper crustal magnetic trend is associated with elevated geothermal gradient and exerts an influence on the overall maturation of Bakken source rocks

8.2.5.4 1-D Burial Models

Burial models for wells are an excellent way to understand maturation and confirm calibration of a full basin model to individual points of control. The following examples use Genesis software (www.zetaware.com) as examples.

Inputs to the models include:

1. Lithology and age of major formations
   - Includes potential source rock kerogens and kinetics
   - Builds in thermal conductivity based on lithology and compaction
2. Erosional and hiatal events with estimates of deposition and erosion at each event
3. Crustal heat flow or geothermal gradient
   - Can be fixed to a single gradient
   - Geothermal gradient can be varied through time
   - Heat flow can be varied by crustal thickness or type
   - Surface temperatures can be varied through time

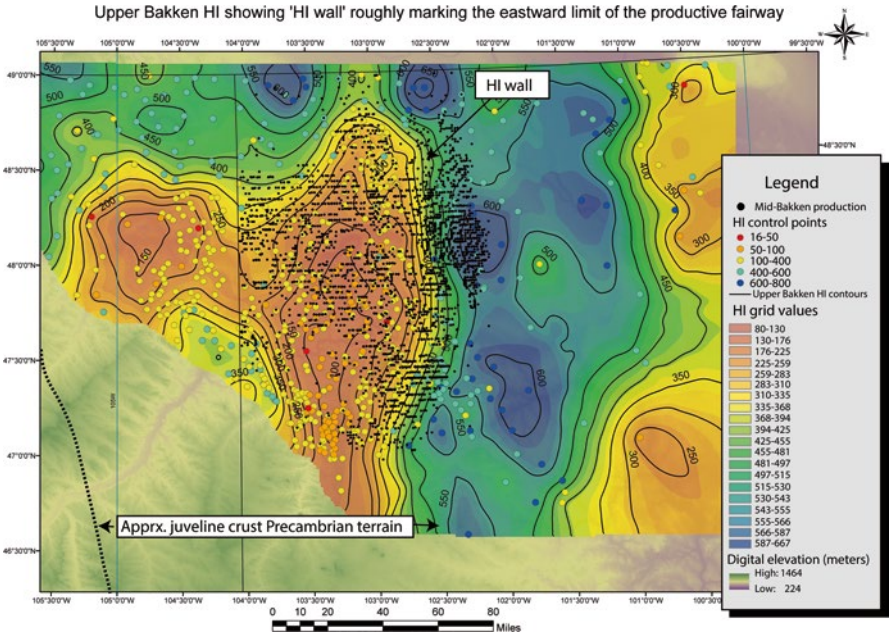

Fig. 8.20 Gridded Upper Bakken HI data. Low values to the east are most likely due to clastic input into the Devonian basins. The sharp reduction in HI is the 'HI wall' attributed to reduction in HI due to maturation

Varying geothermal gradients through time requires some calibration data like Apatite Fission track analysis (AFTA) (Green et al. 1980, 1986, 1988; Green 1988). Corrigan (1991, 1993) provides additional examples of how to work with AFTA data. Some good examples of changing thermal regime and impact of uplift are given by Beek et al. (1998), Belton and Raab (2010), Luft et al. (2005), Raab et al. (2002). Rifts, in particular, commonly undergo an early high heat pulse as they open up (McKenzie 1978; He et al. 2007).

An example from the Barmer Basin of India (Dolson et al. 2015; Farrimond et al. 2015; Naidu et al. in press) is shown in Fig. 8.22. Both vitrinite and AFTA data show different regional gradients through time in the Barmer Basin from north to south. In the south, a pronounced higher heat flow is apparent from both data sets from Paleocene through early Eocene time (Fatehgarh, Barmer Hill and lower Dharvi Dungar formations). In the north, this early heat pulse was not developed. These spatial and temporal changes have to be modeled not only at each 1-D model, but over the entire basin, using different geothermal scalers for different intervals of time.

Erosion amounts are also important to restore where the amounts may be significant enough to alter maturation timing. Techniques on how to do this were summarized in (Corcoran and Dore 2005). As was covered in part in Chap. 7, sonic, density and resistivity logs can be used to establish normal compaction curves and then be

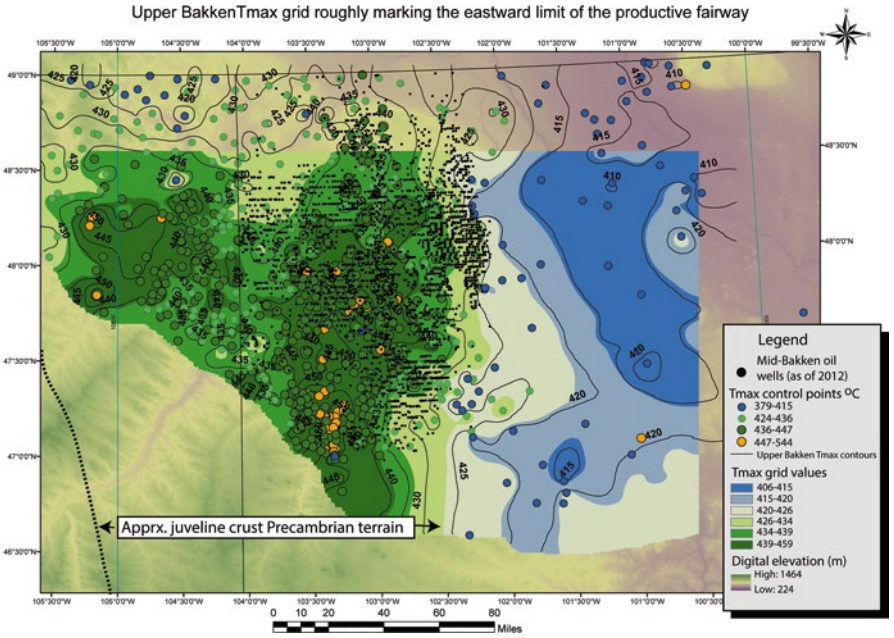

Fig. 8.21 Bakken Tmax grid showing strong north-south trend aligned with NACP magnetic anomaly and interpreted Precambrian juvenile crust

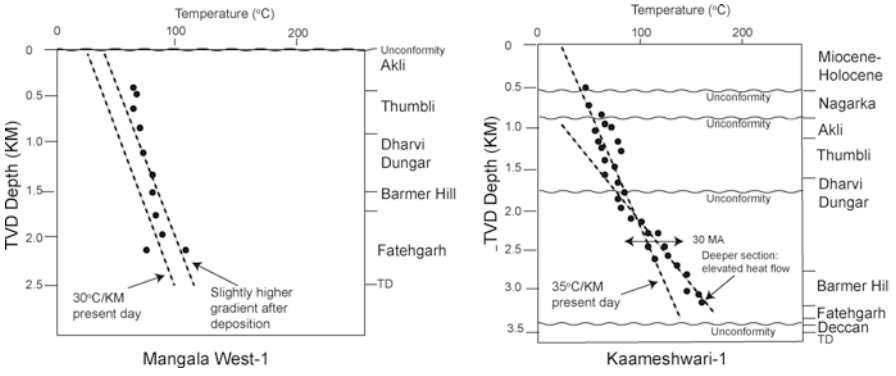

Fig. 8.22 Variation in heat flow spatially and with time. Barmer Basin, India. The northern part of the basin (Mangala West-1 example) has had a more or less constant geothermal gradient through time of 30 °C/Km. In contrast, the southern portion of the basin (Kaameshwari-1 example) had a highly elevated heat flow associated with early rifting. Cooling to a regional gradient of 35 °C/Km occurred after deposition of the lower part of the Dharvi Dungar Formation. From Dolson et al. (2015). Reprinted by permission of the AAPG, whose further permission is required for further use

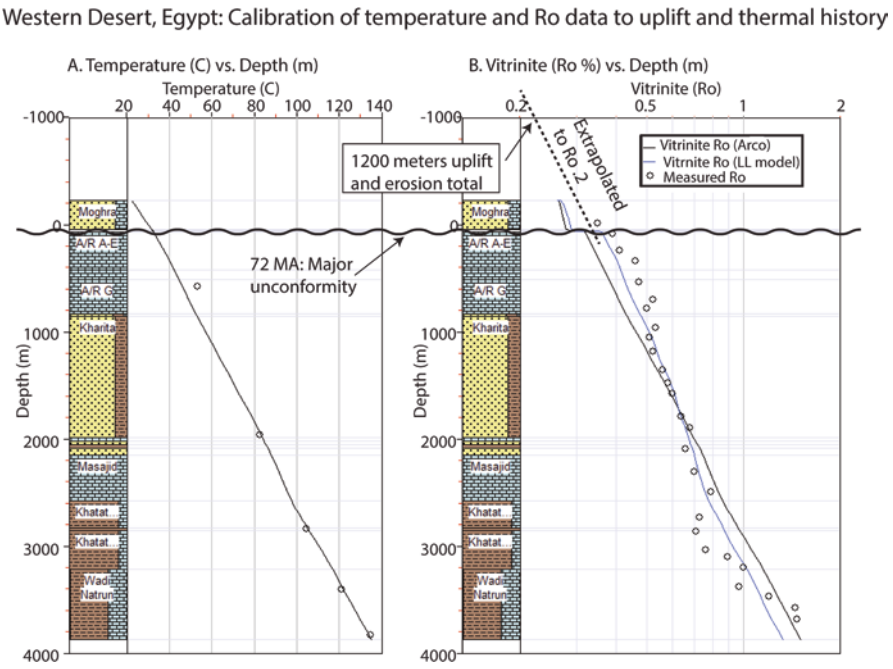

Fig. 8.23 Egypt 1-D model example of Ro and temperature calibration with restored erosion

compared to wells with uplifted and eroded section to determine missing section. Where vitrinite data is available, simple Ro vs. Depth plots can help constrain erosion amounts. Plots of Ro vs. depth, extrapolated to the 0.2 Ro value, can show erosion amounts.

By example, the Western Desert of Egypt (Wescott et al. 2011; Dolson et al. 2014) has undergone at least 11 major tectono-stratigraphic re-organizations. Figure 8.23 is a 1D burial model of a well in located in a strongly inverted rift. Ro vs. Depth plots show cumulative erosion of about 1200 m of uplift by missing section and jumps in Ro values near the base of the Miocene Mogra Formation. This surface is a major unconformity surface formed as Jurassic and Cretaceous rifts were inverted by compressional strike-slip faulting.

From a migration timing standpoint, older structures formed during periods of maximum burial and uplift would be the best targets for exploration. However, peak maturation in this and other parts of the basin, occurred in the Late Cretaceous.

Late Cretaceous closures filled first, but then as inversion occurred, had their structural geometries rotated or destroyed and hydrocarbons released, leaving residual accumulations behind. One of the things that makes exploration challenging in this area is that, once, the basin reaches peak burial, it stops to generate hydrocarbons. Even though there were at least two other periods of post-inversion subsidence (Fig. 8.24), the source rocks never again go through a second maturation

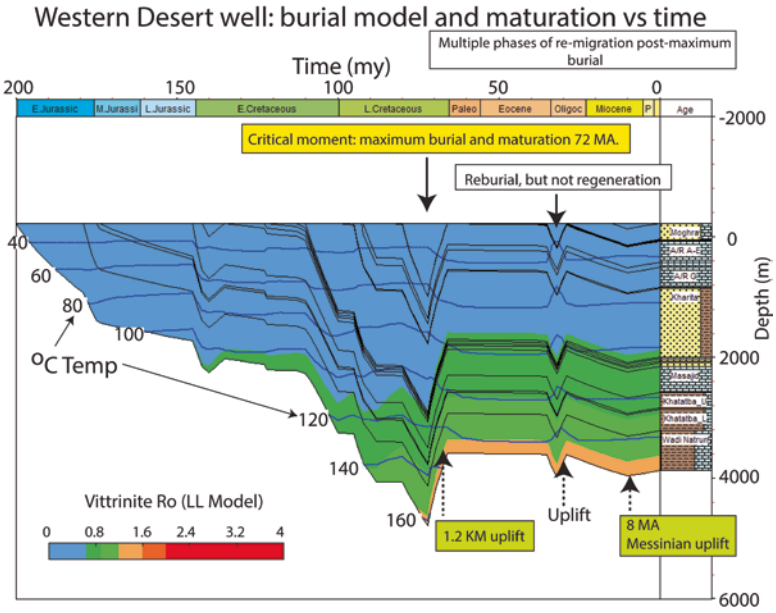

Fig. 8.24 Critical points in the Western Desert model well for expulsion and uplift

stage unless the burial or heating is more than the earlier event. Many very large inversion structure closures in Egypt have only residual shows, with smaller traps, formed later or along the re-migration paths. An example is the Qarun Oil Field (Nemec 1996; Geizery et al. 1998; Farris 2001). This field was found by drilling for a smaller, and older, non-inverted structural feature in the Gindi Basin. The Qarun field is located to close to a giant 4-way, but commercially barren, inversion structure.

Another example in the Barmer Basin is illustrated by comparison of a restored burial model line (Fig. 8.25). The northern end of the basin was buried 400–1200 m deeper during the mid to late Tertiary, but is currently being inverted as India collides northward with Asia, forming the Himalayas (Dolson et al. 2015).

The erosion model is based on sonic log velocities, Ro vs. depth and AFTA data. By adding the eroded amount back to current structure, migration at peak timing can be simulated. The northern part of the basin, in particular, has abundant residual oil shows. While it is difficult to get completely accurate paleo-structural maps at a detailed scale, and paleo-fault seal had to be taken into account in the migration and trap modeling, the blue areas in Fig. 8.26a are predicted paleo-accumulations and migration vectors from source to kitchen. These areas coincide well with known residual oils from wells (black triangles and squares). Current field outlines are superimposed on the paleo-accumulations in Fig. 8.26b. More details on the residual oils of this basin area in Naidu et al. (in press)

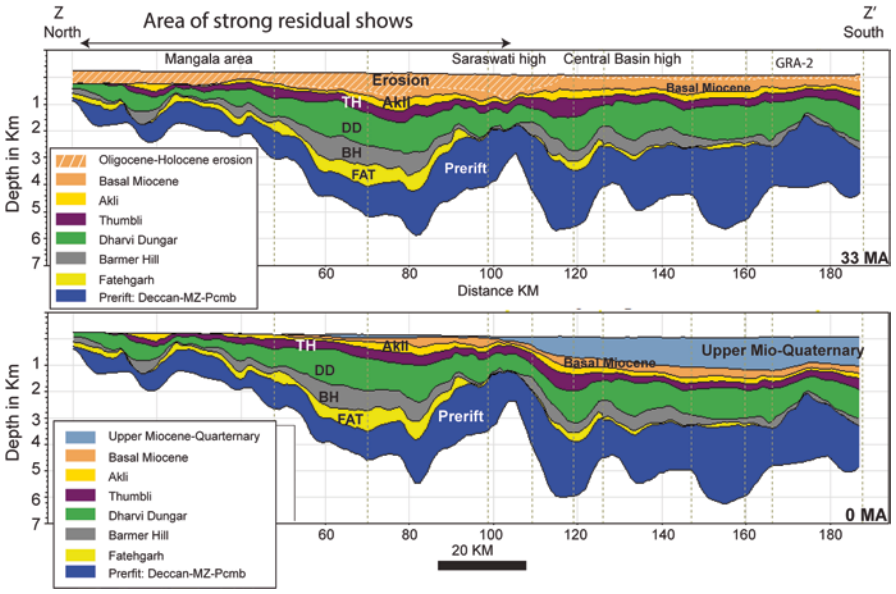

Fig. 8.25 Restored burial pre-uplift (*top*) vs. current structural configuration. The northern part of the basin is an area with abundant residual oil shows, due to hydrocarbons lost by inversion and spill. From Dolson et al. (2015). From Dolson et al. (2015). Reprinted by permission of the AAPG, whose further permission is required for further use

8.2.6 Summary: Source Rock Quality and Maturation

Understanding source rock quality, Rock Eval and maturation modeling is an essential tool for today's explorers. Kinetics of source rocks vary in terms of timing of maturation, fluid volumes and type expelled. Early screening and data collection should be a routine part of any basin evaluation. Basin models, like any model, are inherently full of uncertainties.

Lithology, kinetics, conductivity and crustal makeup and heat flow all combine to underpin robust models. However, there is seldom the quantity or type of data available to constrain heat flow and maturation through time and space well. The key to a successful model is its predictability. Simple models that are predictive, even if they over simplify what is undoubtedly a more complicated picture, have great utility.

Time is well spent building the models and remaining flexible to test alternatives when new data comes in. When a model can't be built with satisfaction or in the timeframe needed, working with existing data sets with trends in mind from geological insight may be the best (or only) approach.

The following sections look at more critical data collection with mud isotubes and headspace gas and unconventional screening tips. Lastly, we look at oil to source rock correlations as an additional tool to think about migration and calibrate migration models.

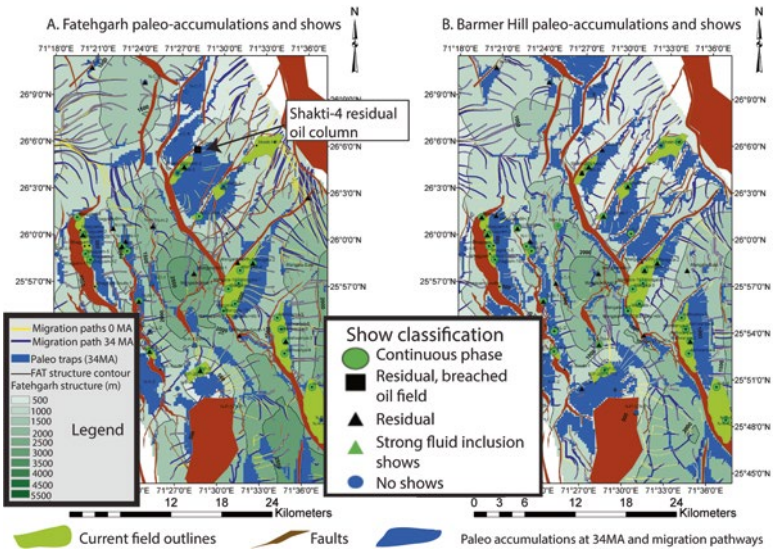

Fig. 8.26 Residual oil shows and paleo-structural accumulations vs. present accumulations. Modified from Naidu et al. (in press). From Naidu et al. (in press). Reprinted by permission of the AAPG, whose further permission is required for further use

8.3 Rig Data Collection: Headspace gas and mud Isotubes

Two of the more important types of shows information collected on a rig are analysis of the mud gas and headspace gas compositions. Gas analysis can be a powerful predictor of deeper hydrocarbons, pay zones, seepage, migration pathways and inferences on source rocks and maturity. Excellent references cover the basics (James 1983, 1990; Schoell 1983; James and Burns 1984; Clayton 1991; Coleman 1992; Schoell et al. 1993; Whiticar 1994; Prinzhofer and Huc 1995; Rooney et al. 1995). Headspace gas is most thoroughly covered in (Kolb and Ettre 2006). Overviews highlighting common uses of mud isotube and headspace in shale plays are Curtis (2010) and Ferworn et al. 2008).

Two distinct processes produce hydrocarbon gas. These are biogenic and thermogenic degradation of organic matter. Biogenic gas is formed at shallow depths and low temperatures by anaerobic bacterial decomposition of sedimentary organic matter. In contrast, thermogenic gas is formed at deeper depths by thermal cracking of sedimentary organic matter into hydrocarbon liquids and gas, and thermal cracking of oil at high temperatures into gas.

Biogenic gas consists almost entirely of methane, while in contrast, thermogenic gas can be dry, or may contain wet gas components (ethane, propane, butanes) and even heavier hydrocarbons (C5+ hydrocarbons). Biogenic methane, on average,

contains isotopically lighter carbon than thermogenic methane. Biogenic gas is also drier than many thermogenic gases.

Thermogenic gas components (methane, ethane, and propane) generated at a given thermal maturity contain, on average, isotopically heavier carbon than do the corresponding gas components generated at a lower thermal maturity. Relationships between gas isotopic compositions and source maturity have been calibrated, allowing the vitrinite reflectance equivalent Ro_{equiv} of the gas source to be estimated from the gas composition (Faber 1987; Berner and Faber 1988, 1996)

To differentiate between these various types of gases, as well as the potential kind of source rock they were generated from are a multitude of cross-plots of isotopes and other compositional information, only some of which are touched upon in this section. Some commercial software packages contain built-in algorithms for hundreds of cross-plots of geochemical data to assist with interpretation. Wells are expensive, but collection of these types of data is much less so and assures that a maximum amount of information is extracted from a well for post-appraisal.

Gas sampling (Fig. 8.27) is first done with sampling manifolds tied to the mud system, yielding mud gas data. Secondly, rock samples themselves are taken, added to jars of distilled water with some bactericide and the gas allowed to come into solution into the water for analysis. This latter technique is termed headspace gas. When both types of analyses are run on a well, a great deal of information is captured.

The techniques provide the best analysis not only of gas already in solution in the pore systems, but in gas adhered and adsorbed onto the surface of the rocks themselves (Fig. 8.28).

Figure 8.28 generalizes the differences and collection techniques. Mud gas in solution in the mud system is from gas liberated from rocks while drilling, either as background gas or over a prospective pay zone. Older techniques involved rather clumsy vacutainers and gas bags, both of which had not only sample collection but storage problems. Isotubes, on the other hand are small tubes that are placed directly into the manifold of the mudline, sample gas directly and then can be taken out and put in containers for shipping. On many drilling rigs, these IsoTubes are immediately analyzed and interpretations generated in real time. For the most part, the gas being analyzed is free gas from within the pore systems.

Headspace gas data (both compositional and isotopic) are subject to alteration effects, especially when stored for long times. Such alteration of the headspace gases may include some biogenic methane generation within the IsoJars. Some other effects include preferential loss of the lightest hydrocarbons, oxidation, and bacterial degradation. These processes tend to result in heavier (less negative) carbon and hydrogen isotopic values and higher gas wetness. To obtain more accurate gas data, it is recommended to collect mud gases in IsoTubes in addition to headspace gases. If there is no mud gas data, we have no way to assess the validity of the headspace gas data. Usually, headspace gases are much wetter than mud gases at the same or nearly the same depth due to preferential loss of the lightest gases as the cuttings are being circulated to surface. In addition, the headspace gases are usually isotopically heavier (less negative) than the mud gases due to possible bacterial oxidation in the IsoJars, dissolution effects, and fractionation on desorp-

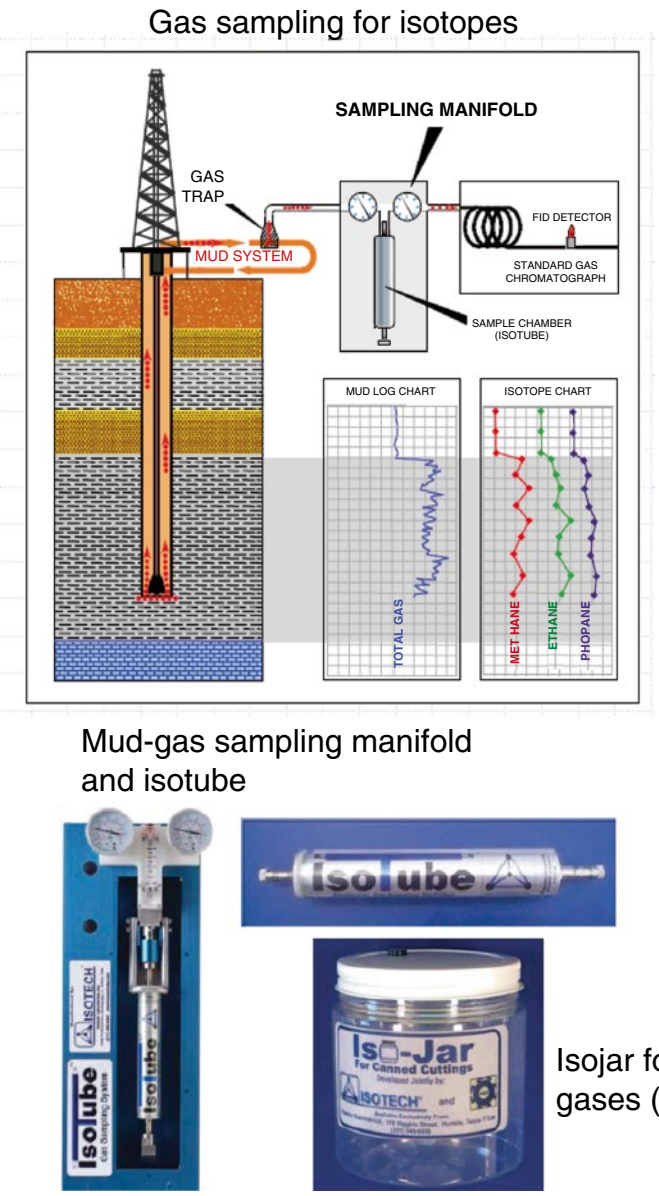

Fig. 8.27 Mud gas sampling methods. From Ferworn et al. (2008). Reprinted with permission

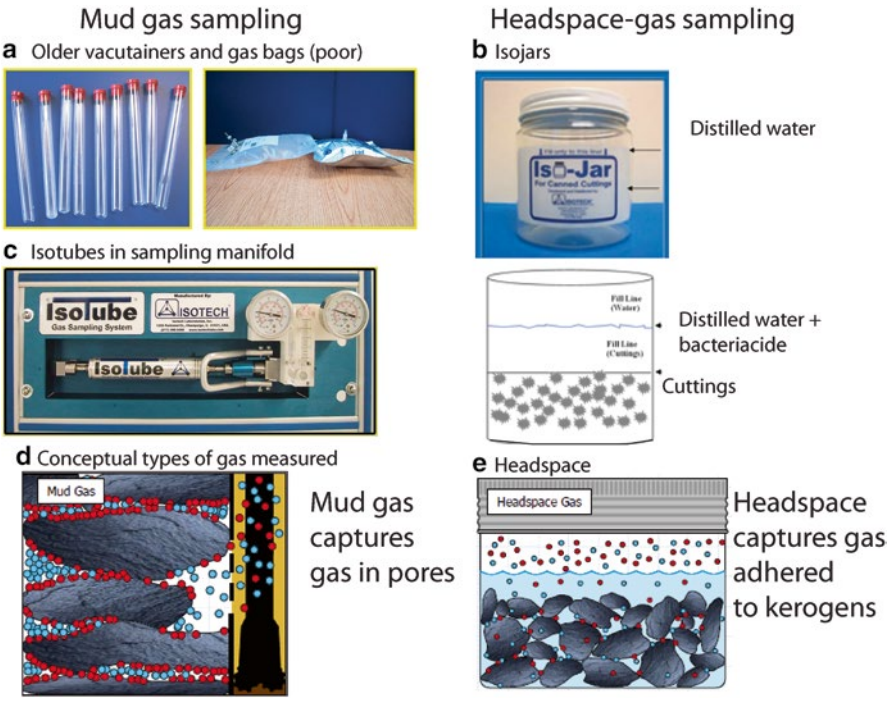

Fig. 8.28 Differences between sampling techniques and analysis, isotubes vs. headspace. (**a**) courtesy of Stratochem Services. (**b**–**e**) from Curtis (2010). Reprinted with permission

tion either within the well bore, at the surface, or in the IsoJars. For these reasons, we generally rely on mud gas data much more heavily when interpreting well gases.

In some case studies the gas results display that the gases being sampled by the IsoTubes and IsoJars are somewhat compositionally and chemically different. The difference in the gas composition is best illustrated by the dryness of the IsoTubes mud gases relative to the IsoJars headspace gases. This is primarily due to the differing rates at which the different hydrocarbon gases escape from the mud and rock chips. Specifically, because methane escapes at a faster rate from the mud than do the other hydrocarbon gases. The resulting IsoTubes mud gases are therefore slightly enriched in methane. Conversely, IsoJars headspace gases are wetter than the IsoTubes mud gases because methane can escape faster from the rock chips than do the other hydrocarbon gases and by the time the rock chips are canned they are slightly depleted in methane. In addition, the headspace gases are isotopically slightly heavier relative to the IsoTubes mud gases (up to 4 % for Methane, 2 % for Ethane and 1 % for Propane). This could be attributed to fractionation of the gases in the IsoJars.

Kerogen-rich rocks, in particular, have much of the gas adsorbed to the organic matter surfaces. Combination of isotube and head space gas can help identify permeable zones due to the differing ways that each collection technique samples data. An example is shown on Fig. 8.29, where comparison of mud isotube and head space gas is used to identify permeable zones in shales.

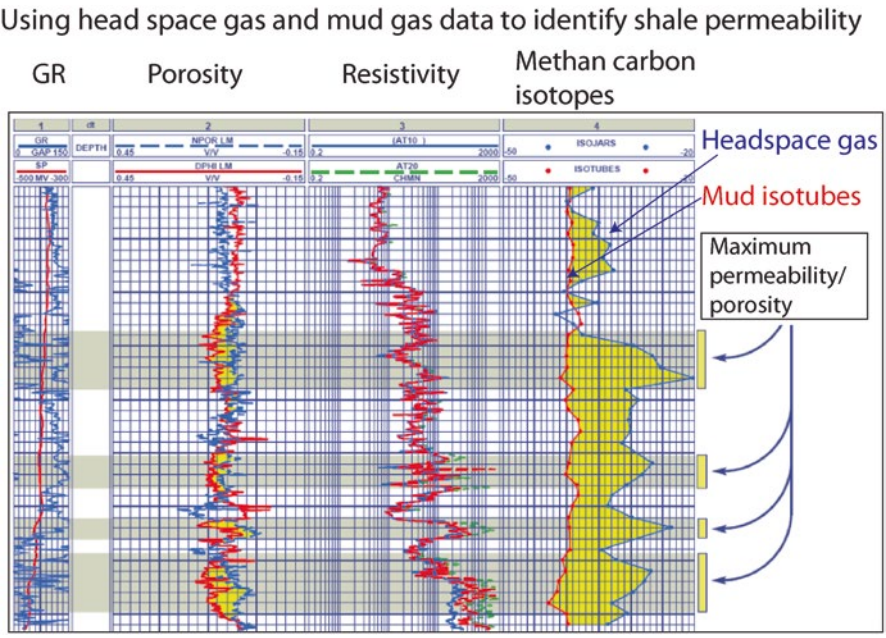

Fig. 8.29 Permeability detection in shales with isotubes and head space gas. From Curtis (2010). Reprinted with permission

Standard core data in shales and simple visual inspection often gives a poor to qualitative guide to shale permeabilities. As the permeabilities are at best micro Darcy levels, and more normally at nano-darcies, plots like this can help an oil company decide where to drill and hydraulically fracture a shale that at first glance appears to be only a good seal.

For conventional analysis, there are a number of displays as discussed in Chap. 3, but also shown on Fig. 8.30.

The example shown is typical of many wells in the Western Desert of Egypt, where multi-phase tectonics and Cretaceous age maturation has left a mixture of residual and trapped hydrocarbons. Many of the continuous phase shows are simply remigrated hydrocarbons from older, lost traps, or simply in older structures that have retained an accumulation. The theory behind these plots is covered in Chap. 3 and in Haworth et al. (1985).

Carbon isotope data is one of the best ways to type gas, not only from a maturity standpoint, but families of gases that might have come from a common source rock (Fig. 8.31).

This kind of analysis is crucial to understand migration. For instance, isotopic analysis might find that two gas fields located close to one another have wildly different isotopic compositions. One accumulation might show high gas maturity, indicating a much deeper source, while the other is biogenic or a different maturity gas. Basin modeling may help determine likely source rocks for the different gases.

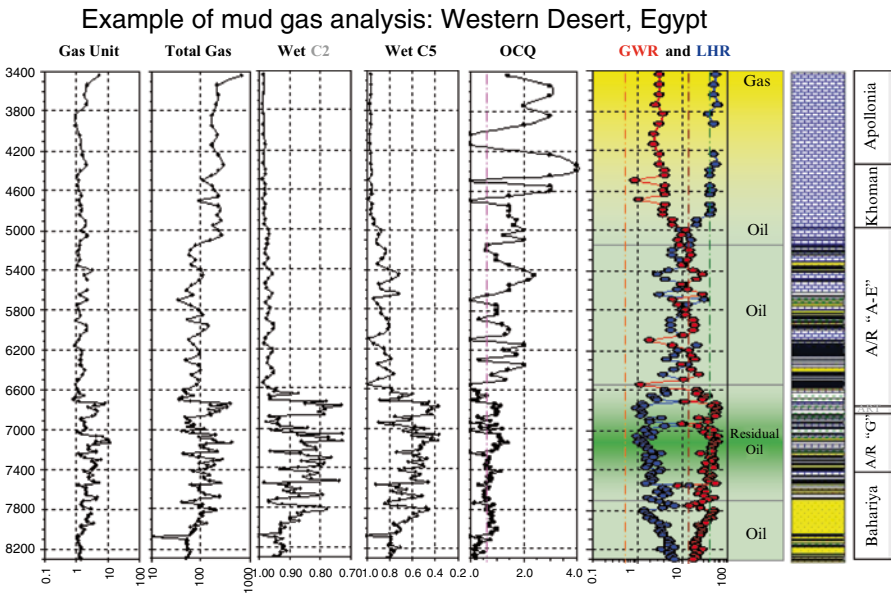

Fig. 8.30 Wetness ratio plots from mud gas to identify pays, shows and residual hydrocarbons. See Haworth et al. (1985) for wetness ratio plot calculations and Chap. 3 for further discussion. Figure courtesy of Stratochem Services, Egypt

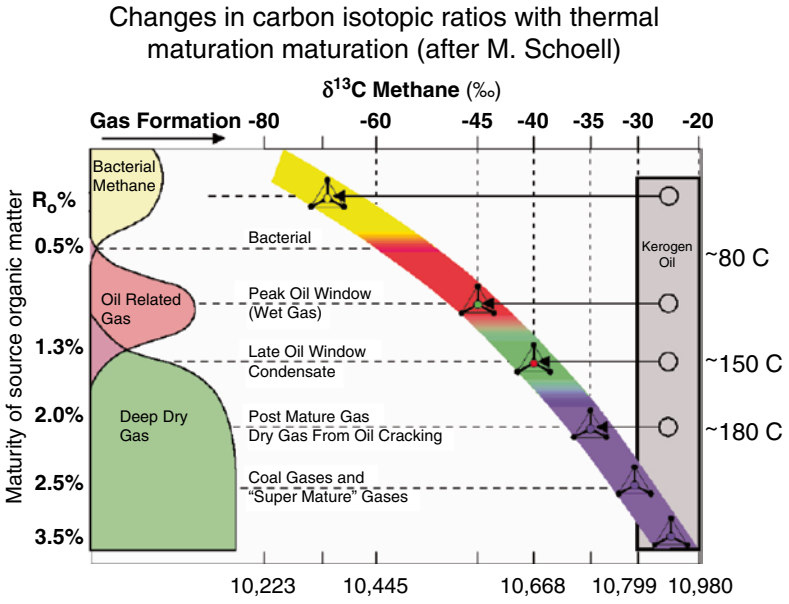

Fig. 8.31 Carbon isotopes and maturity levels. From Ferworn et al. (2008). Used with permission

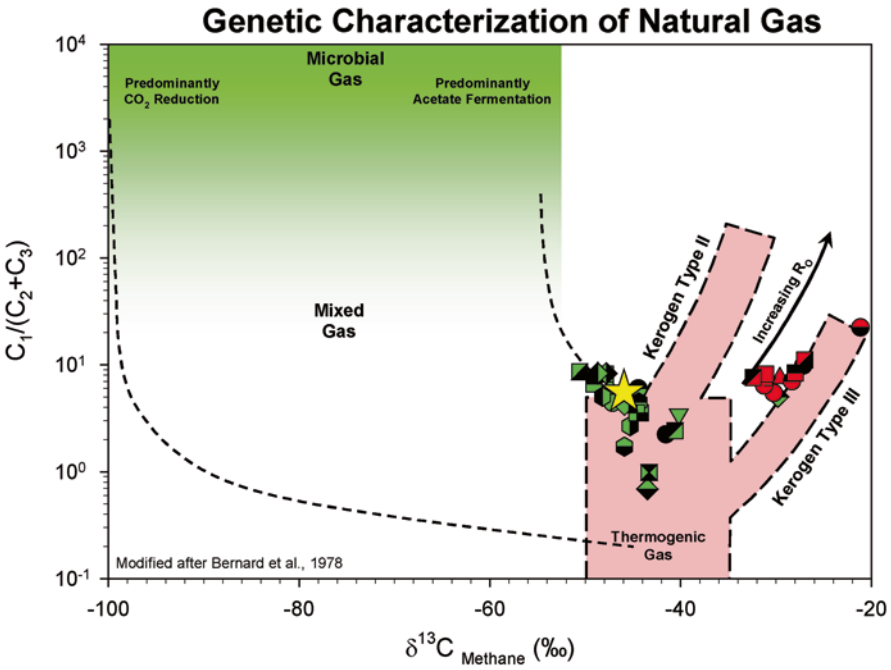

Fig. 8.32 Different kerogen types and maturation interpreted from gas data. Figure courtesy of Stratochem Services, Egypt

Understanding how these different traps, located at or near the same structural level received their charge, could provide a breakthrough to understand where other traps might exist.

An example of a plot that might yield such interpretations is shown on Fig. 8.32. Not only are two possible kerogen source rock types identified but the gases are highly mature and thermogenic in origin. The trick now is to figure out which source rocks they might have come from based on the basin models and maturation. In some cases, the analysis, along with other techniques discussed in Sect. 8.4, may indicates that the gas compositions must be coming from an unidentified source rock, perhaps information that would be key to a new play.

Differing gas maturities and families can also be seen in cross-plots if methane isotopes and gas wetness (Fig. 8.33).

The same data can be viewed in a number of different ways to assess maturity, as shown on Fig. 8.34.

Vertical patterns of hydrocarbon distributions not only help identify seals and migration pathways, but may point to deeper potential as yet untapped in a basin. Simple depth plots like those shown on Fig. 8.35 can be used to speculate on vertical seepage or lateral migration. When plots are compared well to well, they can help indicate compartmentalization in the reservoirs (Milkov et al. 2007; Dzou and Milkov 2011).

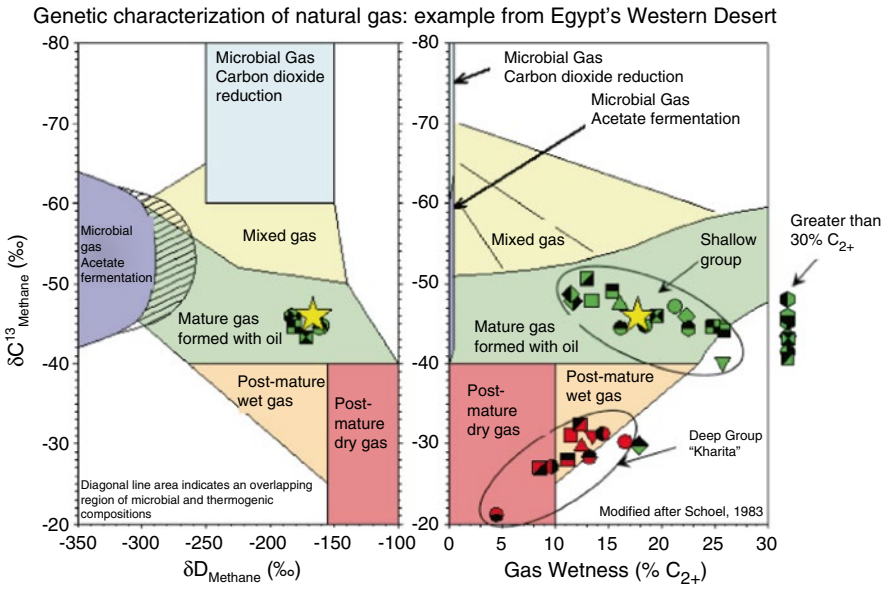

Fig. 8.33 Western Desert gas classifications, Egypt. Figure courtesy of Stratochem Services, Egypt

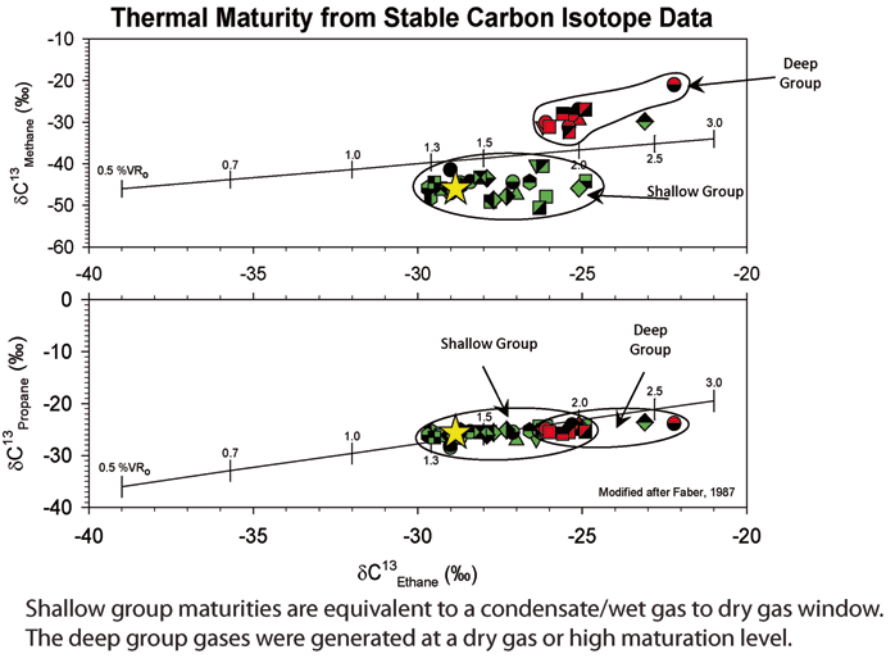

Fig. 8.34 Gas maturities, Egypt example. Figure courtesy of Stratochem Services, Egypt

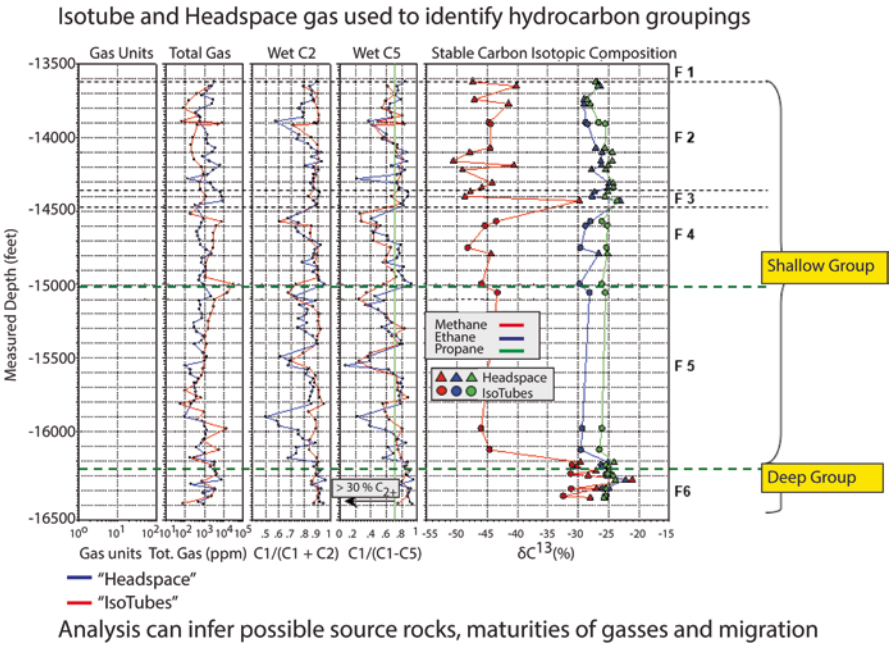

Fig. 8.35 Vertical distribution of gas families by depth. Figure courtesy of Stratochem Services, Egypt

Lastly, there are many novel uses for exploration in source rock plays, many of which are summarized in Breyer (2012) and Hill et al. (2008). One of the novel approaches (Fig. 8.36) is recognition of overpressure in shales (Ferworn et al. 2008).

8.3.1 Summary

This short discussion shows just a few of many examples of the use of mud and headspace gas in exploration. Source rock plays (Sect. 8.3) rely heavily on geochemical assessment of the kerogen itself, but also the pressures, fluid phases and a host of other criteria. No geoscientists working in the petroleum industry today can survive without some basic understandings of this important topic. The reader is encouraged to delve much more thoroughly into this topic with literature already cited.

The tools and technologies being developed for understanding source rock plays are creating true paradigm shifts in how we explore and produce oil and gas. In a book such as this, only the very basic topics can be covered and the reader made aware of the wealth of information that can be gleaned from petroleum geochemistry.

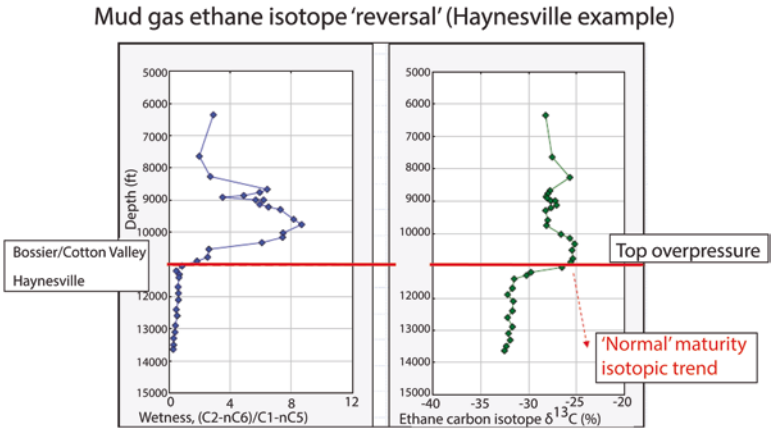

Fig. 8.36 Carbon isotopes used to find overpressure in shale. From Ferworn et al. (2008). Used with permission

8.4 Some Source Rock Play Screening Criteria

Every source rock play has its own characteristics, but all share some things in common:

1. High quality source rocks with hydrocarbons remaining to be produced
2. Thermally mature source rocks, but not overly mature to where hydrocarbons are lost or immature to where moveable hydrocarbons are not present
3. Enough brittleness to allow hydraulic fracturing to work

The easiest way to screen a basin for a source rock play is to be in a basin where production is already established and prolific. Those reservoired oils and gases came from source rocks, so that is a good place to start. Resource potentials in source rock plays are staggering (EIA 2010, 2011; Breyer 2012). For years, it has been noted that only a small percentage (<10 %) of conventional resources have generally been discovered vs. what has been generated. The remaining 90 % is either lost through migration and seepage at the surface or remains to be found. Much of that still remains locked in the source rock itself.

Figure 8.37 shows a conceptual basis for understanding shale gas (Cornford 2010). As hydrocarbons are produced and either reside adsorbed onto the kerogen grains themselves or in the pore systems, a process called diffusion flow (Javadpour 2008) and desorption of methane liberates some of these hydrocarbons. The generation of hydrocarbons creates higher pore pressure and micro-fractures which further allow oil and gas to move through the nanno-darcy pore networks. If larger natural fractures exist, then the gas or oil may be produced without horizontal wells.

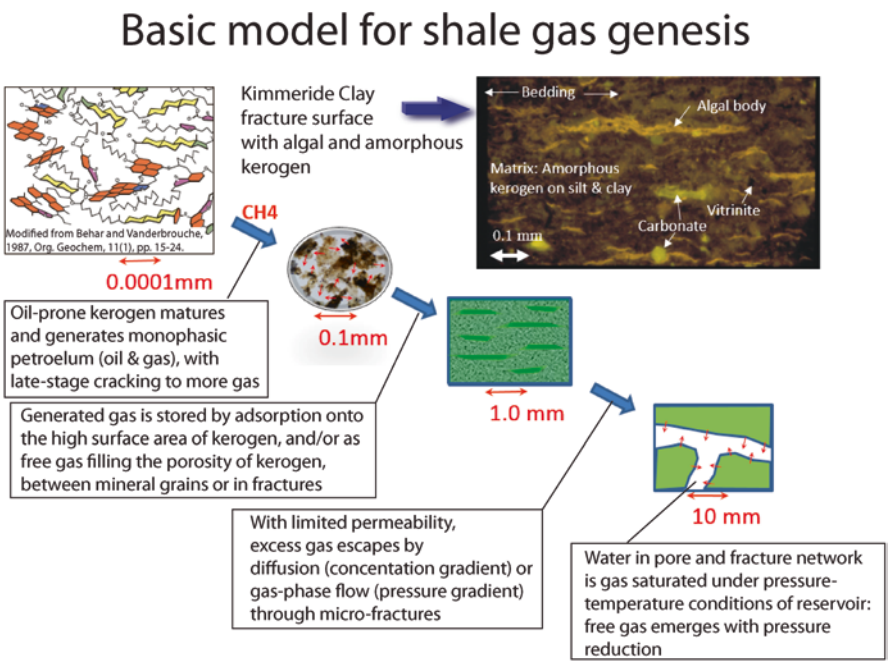

Fig. 8.37 Shale gas genesis. *Upper left* figure modified from Behar and Vandenbroucke 1987. Slide courtesy of IGI Ltd, UK, used with permission

Some of the oldest fields in the USA, for instance, are from fractured shale formations in Colorado and the Eastern US. But it has taken horizontal drilling technology to unlock these very tight shale formations where the larger fracture systems are not present.

Source rock plays can be difficult in detail, however. Every source rock play shares some common elements, but they vary by facies and age. A number of papers illustrate subtle differences (Breyer 2012; Curtis 2002; Curtis et al. 2008, 2010; Hill et al. 2008). Figure 8.38 illustrates key differences in many of the source rock plays Too often, particularly in companies driven by engineers who oversimplify or underappreciate geological insight in shales, these plays are viewed as 'turn-key drilling'. When this happens, a trend is identified, leases locked up and drilling commences. Often, that drilling ends up with a lot of disappointing wells. Just some of the screening criteria needed to understand source rock plays are listed in Fig. 8.37. The plots of thickness, maturity, adsorbed gas, TOC and GIP shown on Fig. 8.37 clearly illustrate that every play is a bit different.

One of the most important screening criteria are the mechanical properties of the shales themselves. Analysis of successful plays in the USA generally requires not just organically rich source rocks, a significant amount of silica, carbonate or rock fragments to provide brittleness (Ottman and Bohacs 2014). An excellent review of

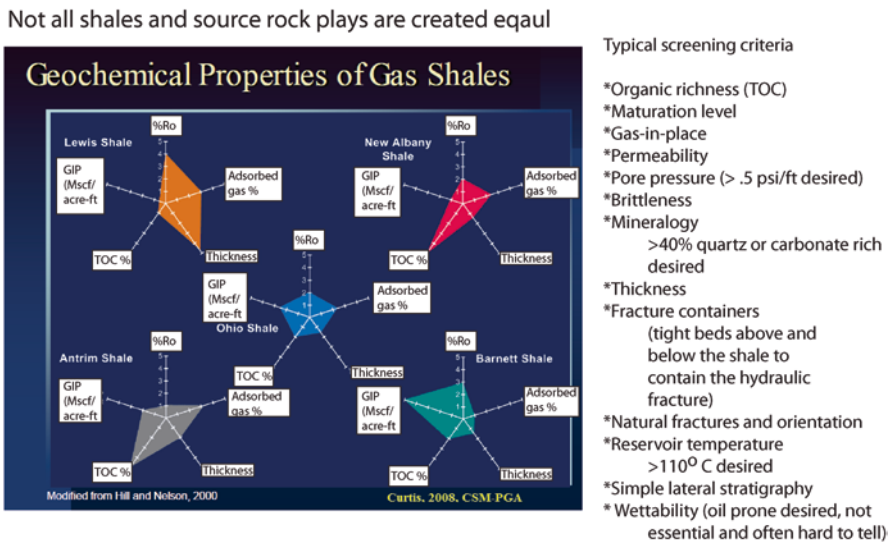

Fig. 8.38 Variation in just some of the parameters used to screen shale plays. Modified from Curtis (2010) and Schamel (2008). Reprinted by permission of the RMAG and AAPG

the mechanical challenges of hydraulic fracturing as it relates to rock type and regional stress fields is that of King (2010).

The earliest efforts to produce from the Bakken Shale, for instance, failed because the source rocks themselves were very elastic and hydraulic fractures closed quickly as the oil was produced. It took years to figure out than the Middle Bakken Siltstone, which is not a source rock, but contains the oil from the surrounding shales, should be the target. Likewise, the Union Springs member of the Marcellus Formation (Harper and Kostelnik 2013b; Lash and Engelder 2011) (Drozd and Cole 1994; Hardage et al. 2013; Lash and Blood 2010; Smith and Leone 2010) or the Point Pleasant member of the Utica Shale are the primary targets for horizontal drilling. One of the best summaries of screening criteria is that of (Sondergeld et al. 2010).

As in the case with conventional reservoirs, shale porosity is also needed. There is no point pursuing a play where the porosity in the shales is too low to provide sufficient storage and volumes for hydrocarbons.

Some of the most thorough studies for understanding how to screen and evaluate shale plays are those of the Mississippian Barnett Shale in Texas. An excellent summary is that of Montgomery et al. (2005), which outlines the heart of the play from the standpoint of presence or absence of porosity and brittle layers, maturity, hydraulic fracture containers above and below the source rocks. Additional key papers illustrate other screening criteria (EIA 2008; Hill et al. 2007; Jarvie 2003; Jarvie et al. 2007; Kinley et al. 2008; Loucks et al. 2009; Montgomery et al. 2005; Pollastro 2007; Zhao et al. 2007).

8.4.1 Sweet Spots

Sweet spots are basically areas within unconventional plays where geological conditions make for the highest rate wells and best long-term production. Finding the right place to drill in an unconventional shale play, however, remains an evolving art. Several papers cover the key technical screening criteria (Brittenham 2010; Hoeve et al. 2010; Ottman and Bohacs 2014; Sondergeld et al. 2010; Wang and Gale 2009). While there are many attributes than can be mapped and quantified to screen some common characteristics seem to be present in most of the current productive trends (Ottman and Bohacs 2014):

1. Higher remaining organic content and maturation generally >1 % Ro.
2. Brittle rock that can hold fractures, ideally with hardness percentage >50 %.
3. Porosity remaining in the source rock and brittle zones
4. Elevated pore pressure to help drive recovery (usually coincides with higher maturation window).

A more comprehensive listing of key shale screening criteria is given in Table 8.4 (modified from (Sondergeld et al. 2010).

In a typical technical screening, maps of the criteria listed above are built and overlain upon one another to determine the area where most of the favorable criteria are met. When done well, these kinds of risk maps have a high probability of identifying the 'sweet spots' and the best acreage to pursue. An example (modified from (EIA 2008) is shown in Fig. 8.39. The sweet spot shown is high-graded from maturation >1.4 Ro and north of the southern limit of the Upper Barnett hydraulic fracture barrier (Marble Falls Limestone). Additional criteria such as brittleness and OGIP could be added to these screening criteria for further refinement.

Additional screening criteria, as in conventional plays includes:

1. Is there existing infrastructure and large leases available? Remote basins, while prospective, require drilling and pipeline infrastructure to initiate a shale play.
2. Is the tax regime favorable?
3. Sources of water or other frac fluids.
4. Is there local community support for drilling?

8.4.1.1 A Note on Calculating Volumes of Oil or Gas in Shale

Volumetric calculations of gas or oil remaining in place in shales remains an evolving subject, as traditional Archie saturation equations were developed for permeable sandstones, not shales and tight siltstones. Although this topic is beyond the scope of this section, there are a number of good papers and tools online to help determine reserves in shales. These techniques, however, are continually being modified and improved as more data is collected on shale cores globally and new techniques developed.

Table 8.4 Some key screening criteria for shale plays

Parameter	Desired result	Sources of data and comments
Water saturation (Sw)	<40 %	Log analysis or unconventional shale core. Often difficult to obtain early on. Reliance on resistivity mapping in shales is often a good proxy for low water saturation, and can be mapped regionally.
Depth	Shallowest depth to dry gas window or to the mature oil window for shale oil plays.	Petroleum systems modeling and mapping.
Fractures	Vertical vs. horizontal orientation and open, not closed.	Regional mapping, borehole breakout, FMI logs.
Gas composition and type	Low CO_2 and H_2S; thermogenic gas; gas filled porosity > 2 %; High API gravity for oil plays.	Mud logs, PVT reports; petroleum systems models, log analysis.
Shale heterogeneity	The less the better.	Log correlations.
Structural complexity	Simple ramp dip preferred with limited faulting.	Mapping, seismic, dipmeters.
Mineralogy (for brittleness)	>40 % silica or carbonate, low clay content.	XRD, SEM, cores, logs.
OGIP (free and sorbed)	>100 BCF/mi^2 (or other economic criteria). For oil plays a suitable economic cutoff (frequently in the 30–100 MMBOIP/mi^2.	Log analysis or production profiles or petroleum systems modeling.
Permeability	>100 Nano Darcy.	Capillary pressure, NMR logs (calculated). Often difficult to obtain.
Poisson's ratio (measures how a rock deforms under stress) and Young's Modulus (measures elasticity and brittleness)	<0.25 for Poisson's ratio; > 3.0 MMPSIA for Young's modulus.	Core based compressional studies. Often difficult to acquire the data until well into a play or prospect.
Pressure	>0.5 psi/ft.	Mud isotubes, log-based pressures from resistivity or sonic, possibly mud-weights. Can be difficult to estimate from only mud-weights.
Reservoir temperature	>230 °F (110 °C).	DST reports, well logs, petroleum systems modeling.
Seals	Fracture barriers above and below the target interval.	Logs or core studies.
Shows	High gas readings or production on trend.	Mud logs and well tests.
Thermal maturity	>1.4 Ro for dry gas; > 1.0 for oil plays.	Vitrinite, TAI, SCI or petroleum systems modeling; resistivity mapping.

(continued)

Table 8.4 (continued)

Parameter	Desired result	Sources of data and comments
Thickness	>30 m (can vary with economics). Some shale plays target 3–10 m thick brittle zones.	
Total Organic Carbon (TOC)	>2 % (desired); plays can still work with current Rock Eval much lower if original TOC was high and hydrocarbons remain trapped in pores.	Rock Eval.
Wettability	Preferred oil-prone kerogen.	Special core analysis; often difficult to determine.

Screening criteria that is the most difficult to assess early are listed in orange colors. All other criteria are routinely used in play screening. Table modified from Sondergeld et al. (2010)

The DeltaLogR technique discussed earlier remains a key step in reserve analysis, identifying zones of higher porosity and TOC in organic-rich shales. The best analyses are iterative, attempting matches of predicted remaining oil or gas in shales using petroleum system modeling software and comparing those values with calculations from well logs and production data. When attempting calculations of gas or oil generated and retained in petroleum systems modeling software, inputs remain:

1. A good isopach of the source rock interval
2. An isopach of the original TOC and HI
3. A good thermal maturation model
4. A knowledge of the source rock kinetics

Once these data are in a model, the model can be run to test volumes generated and retained. Calibration of these models with log-derived techniques is an additional step.

A good approach to using conventional logs in combination with the DeltaLogR techniques is covered by Holmes et al. (2012) and Holmes et al. (2009, 2011). A similar technique is advocated by Bowman (2010). An excellent historical overview of shale gas calculations is that of Cluff (2010). For quick looks using Rock Eval data and an idea of initial TOC and HI values and current level of maturation is an online resource calculator (http://www.zetaware.com/utilities/srp/index.html). Using Rock Eval data to estimate oil in place in shales from S1 Rock Eval data is covered by Downey et al. (2011). The technique is relatively simple and works under the assumption that the S1 values provide an approximation of the oil currently remaining in the shale pore systems. New tools (such as NMR logs) are constantly being modified and developed to try to quantify hydrocarbons in shales more accurately.

In the end, production profiles provide the final answer of recoverable reserves, but are often difficult to come by in an opening play.

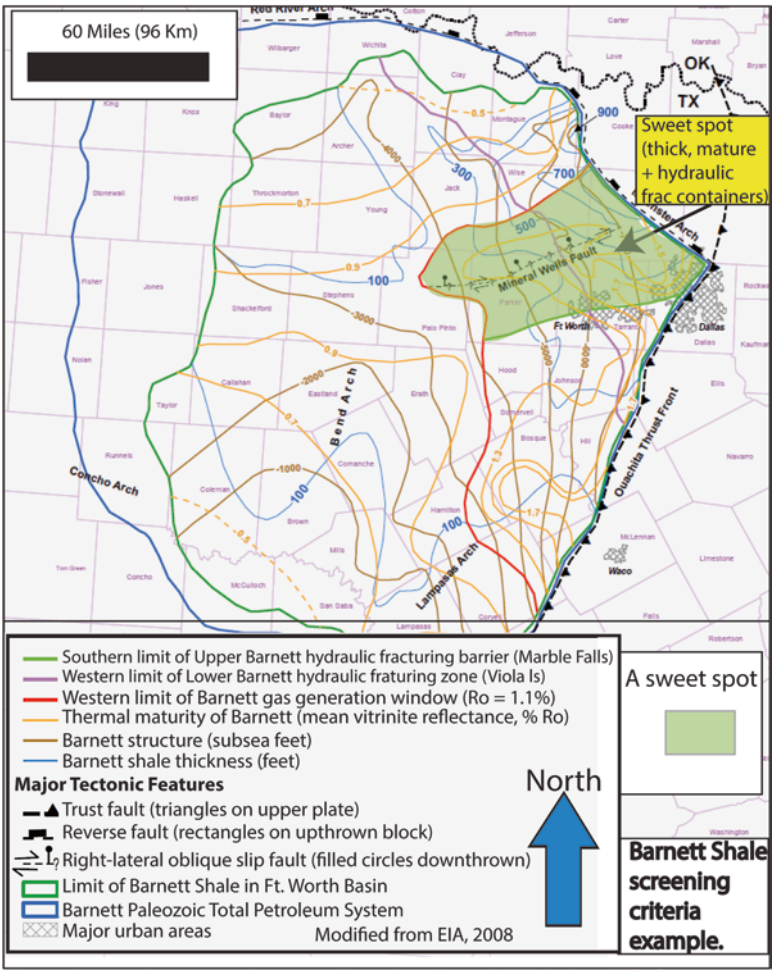

Fig. 8.39 An example of overlay map of key screening criteria, Barnett Shale, Texas. Source: EIA 2008

8.5 Oil to Source Correlations

A key test to understanding your shows database in the context of migration and entrapment remains correlation of oil or gas characteristics by thermal maturity and molecular composition. In an ideal world, geochemical analysis of a reservoired oil can yield data which definitively ties it to a known source rock. Along with maturation and seal maps, it is then possible to test models of vertical and lateral migration from source to trap.

Table 8.5 Basic types of data used in oil to source rock correlations. Summarized from Waples and Curiale (1999)

Data Type	Examples	Comments and utility
Elemental parameters (bulk composition)	Sulfur, nitrogen, nickel, vanadium and trace elements; API gravity, wax content, pour point, viscosity	Used to compare similar oil families. Maturity should be taken into account as Sulfur, API gravity, wax content and other parameters are susceptible to changes in thermal maturity.
Isotopic (stable isotope comparisons)	Carbon isotopes on whole oils, extracts (bitumen), bulk fractions or kerogens. Compound specific isotopes. Sulfur and hydrogen isotopes. Compound-specific isotope analysis (CSIA) of n-alkanes and other compounds.	Can be used to do source to oil correlations and recognition of similar families of oils or source rocks. Hydrogen isotopes are largely used for gas differentiation. In some cases, can be typed to specific ages or environments of source rocks.
Molecular (relative abundance of specific molecules in an oil or source rock extract)	Gas chromatography (GC) Gas chromatography/mass spectrometry (GCMS or GCMS-MS) Pyrolysis-Gas Chromatography (Py-GC) High-performance liquid chromatography (HPLC)	Provides the best chemical correlation between source rocks and oils, focusing on characteristics (often ratios) that are diagnostic for particular source rocks.

A good summary of source to oil correlations for a novice remains that of (Waples and Curiale 1999). Rather than provide a comprehensive overview of this topic, we provide some examples of basic principles and practical applications in a number of basins and plays. Some additional examples and theory are covered in Curiale (1994), Dzou and Milkov (2011), Mello et al. (1988), Milkov et al. (2007), Schoell (1983) and Schoell et al. (1993) (Table 8.5).

8.5.1 Examples of Utility of Understanding Basic Oil and Rock Geochemistry Correlations

The simplest screening criterion is usually elemental analysis available in published data on fields or wells. Screening of API gravity, wax content, GOR, Sulfur content and other parameters should be done in map view, cross-plots and visualized in cross-sections.

Trinity software, for example, has a tool termed ‘hot spot’ which allow any spatial data with location and depth to be visualized and cross-plotted quickly. Figure 8.40 shows an example from offshore Brazil which displays API gravities

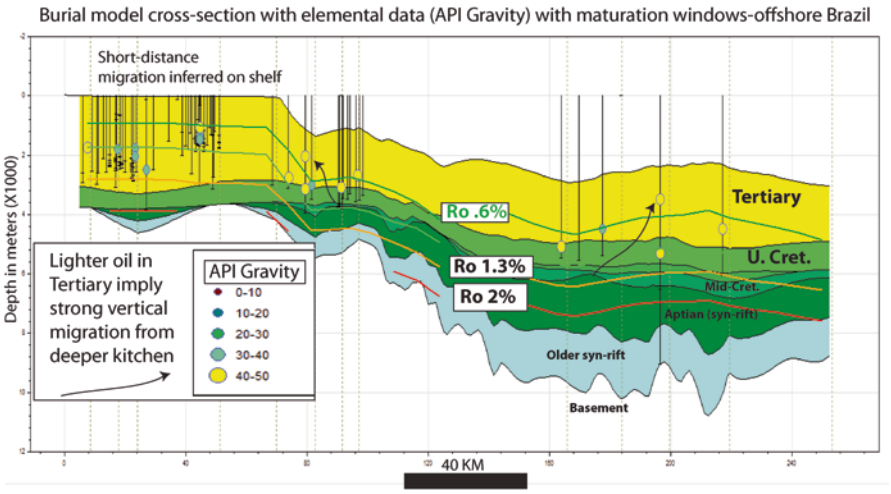

Fig. 8.40 API gravity from a commercial database of oil and gas fields reserves and characteristics. Vertical lines are wells. Symbol sizes and colors vary by the range of API gravity

at various depths from a commercial oil and gas field database. In this case, some higher API oils in the Tertiary section must have migrated significant vertical distances based on the oil and gas maturation windows (although API gravity changes markedly by biodegradation and phase fractionation). Further work with seal maps and other shows databases may eventually be able to predict that migration pathway. This kind of bulk compositional data can also be helpful in validating a maturation mode. In Fig. 8.40, the oil and gas windows on the shelf agree well with the API gravities recovered in fields, suggesting a local source and short-range migration.

The use of isotopic data is commonly done to understand maturation and depositional environment. In Fig. 8.41, data from source rock extracts and oils from the Ogaden Basin in Ethiopia are shown. Despite the maturity differences, depositionally, the Sterane plot shows that the source rocks are dominantly estuarine or of mixed marine sources. This information is very useful for modifying paleogeographic maps and assessing source rock presence, type and maturity.

8.5.1.1 Nile Delta, Egypt

Another of using GC-MS data to tie source to oils is shown on Fig. 8.42 (Dolson et al. 2014). For many decades, the source of the oil and gas in the Nile Delta was assumed to originate from Miocene shales of the Qantara Formation. However, deeper oil and gas shows, indicated additional, untapped source rocks might occur in Oligocene and older strata. Despite thousands of onshore wells penetrating the Oligocene, no source rocks were found.

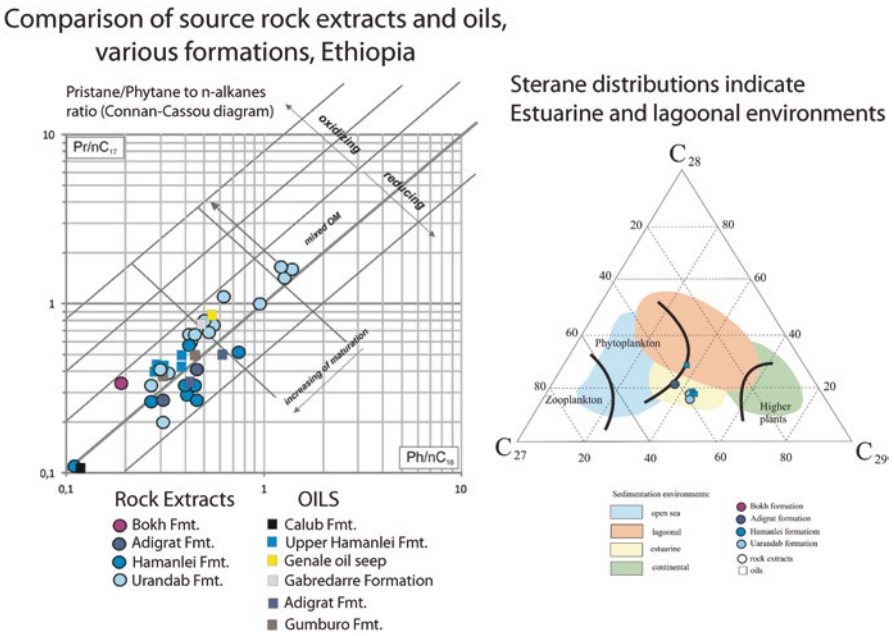

Fig. 8.41 Use of alkane and sterane data to determine level of maturation of both oils and extracts, and source rock depositional environment. The left hand plot uses data from GC analysis and the right-hand plot from GC-MS

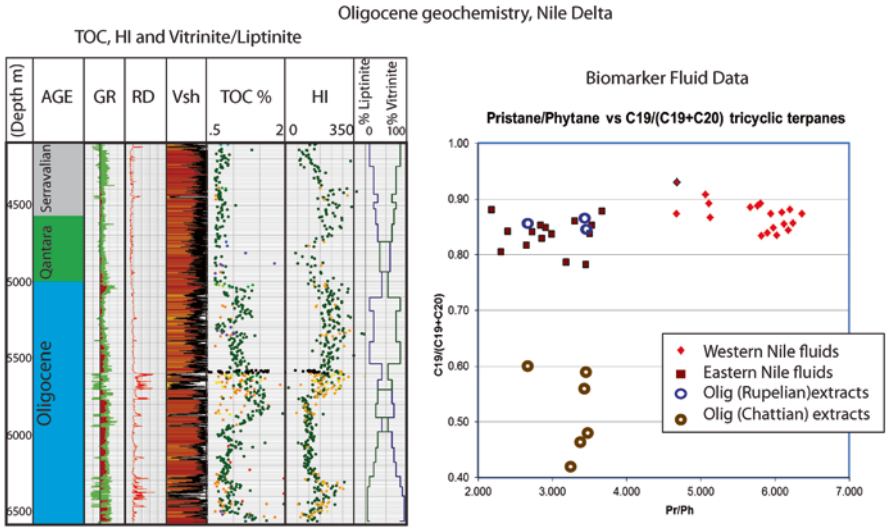

Fig. 8.42 Oil-source proving at least some Oligocene source rock potential, Nile Delta. From Dolson et al. (2014). Reprinted by permission of the AAPG, whose further permissions is required for further use

However, with the discovery of the deep Oligocene reservoirs at the giant Satis Field in 2008, confirmation finally came of an Oligocene source rock contribution to many oil and gas fields in the Nile Delta. Pristane-Phytane vs. tricyclic terpane data shown in Fig. 8.42 indicate an excellent match of fluids in the eastern Nile Delta with Rupelian (Oligocene) extracts from a core in the Satis Field. Interestingly, the source of fluids in the Western Nile delta cannot be explained by this plot and although the Chattian age extracts are viable source rocks, fluids that can be typed to them have not yet been found. This information is very useful to exploration for deeper pay zones and petroleum systems in the region.

8.5.1.2 Barmer Basin, India

A significant amount of rock and oil data has been systematically collected by Cairn India, Pty. in the Barmer Basin of India. Thorough reviews of this basin and its petroleum geochemistry are given by Dolson et al. (2015) and Farrimond et al. (2015). A summary of oil grouping based on the stable carbon isotope composition of the saturated and aromatic hydrocarbon fractions is shown in Fig. 8.43. While the precise source to oil correlations are difficult to make, inferences as to origin of each

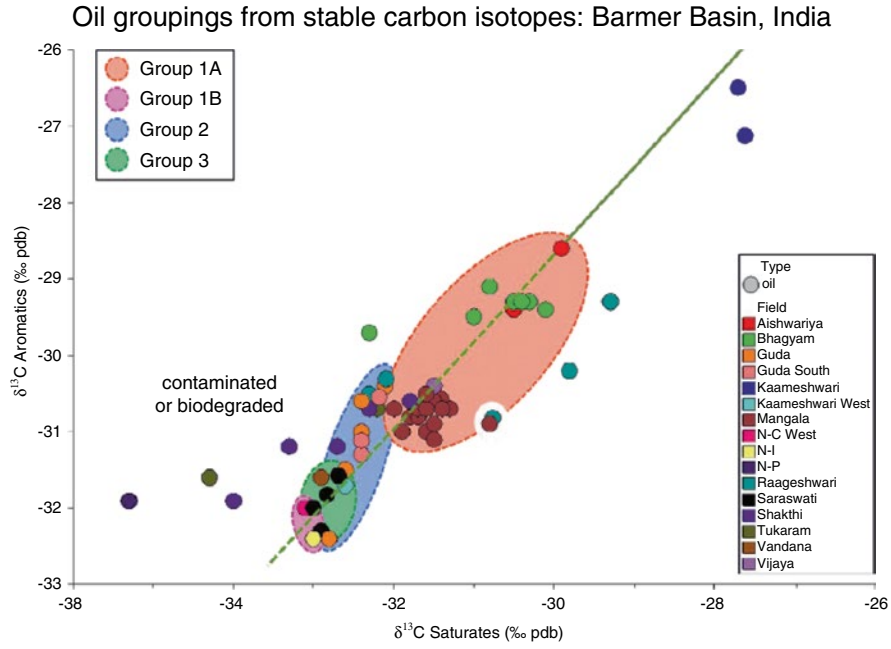

Fig. 8.43 Oil groups, Barmer Basin, India. Additional molecular data was used to define these oil groupings. From Farrimond et al. (2015). Reprinted by permission of the Geological Society of London

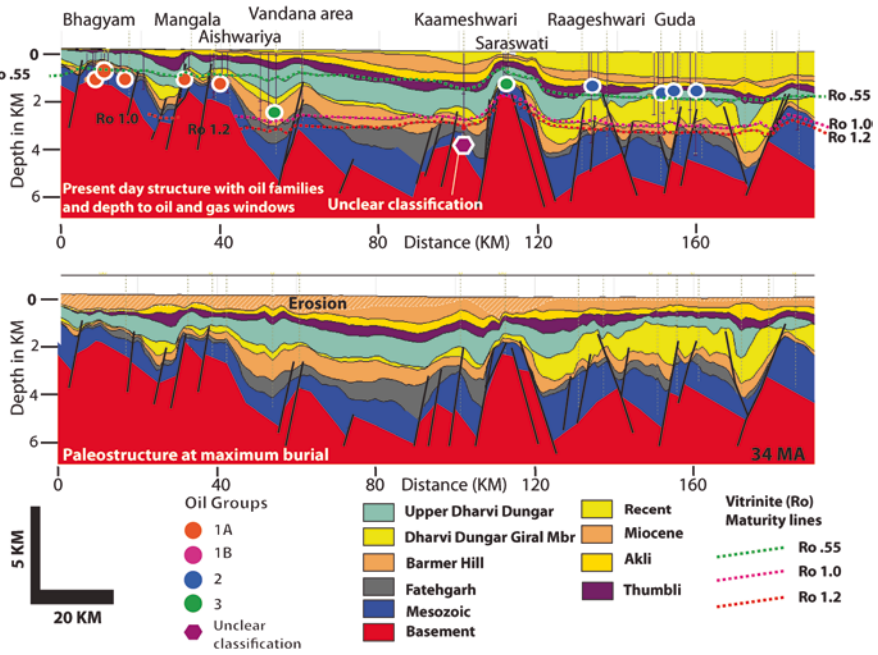

Fig. 8.44 Burial model cross-section, Barmer Basin, with oil groupings from Fig. 8.43 posted. The bottom diagram is paleo-structure at 34 MA and the top diagram current structural shape (Farrimond et al. 2015). Group III oils are locally sourced in the southern part of the basin by the Dharvi Dungar Formation. Groups IA and 1B oil in the northern basin as sourced from the Barmer Hill Formation. Group 3 oil sources are unknown, but may be from Mesozoic sources. Reprinted with permission of EAGE

oil group can be made from spatial distribution of the oil relative to known source rocks at maturation levels matching those of the oils themselves.

A regional cross-section in the basin, with the oil groupings plotted on a burial model line (Fig. 8.44) helps speculate on migration pathways, seals and unknown deeper potential. Group 1A and 1B oils are closely associated with the organic rich Barmer Hill source rocks (Eocene), and occur dominantly in the northern part of the basin. Group 2 oils are from the upper Eocene Thumbli and Dharvi Dungar formations and are located to the south, where the Dharvi Dungar shales are thermally mature and oil prone. Group 3 oils have not been definitively typed to any known source and may well be coming from deeper Mesozoic source rocks only recently confirmed to be present in the basin.

Simply visualizing the oil types on a structural and stratigraphic section is enough to allow key questions to be asked about migration and entrapment. There may be significant deeper potential if the anomalous oils in the deep basin can be typed to a new source rock and petroleum system.

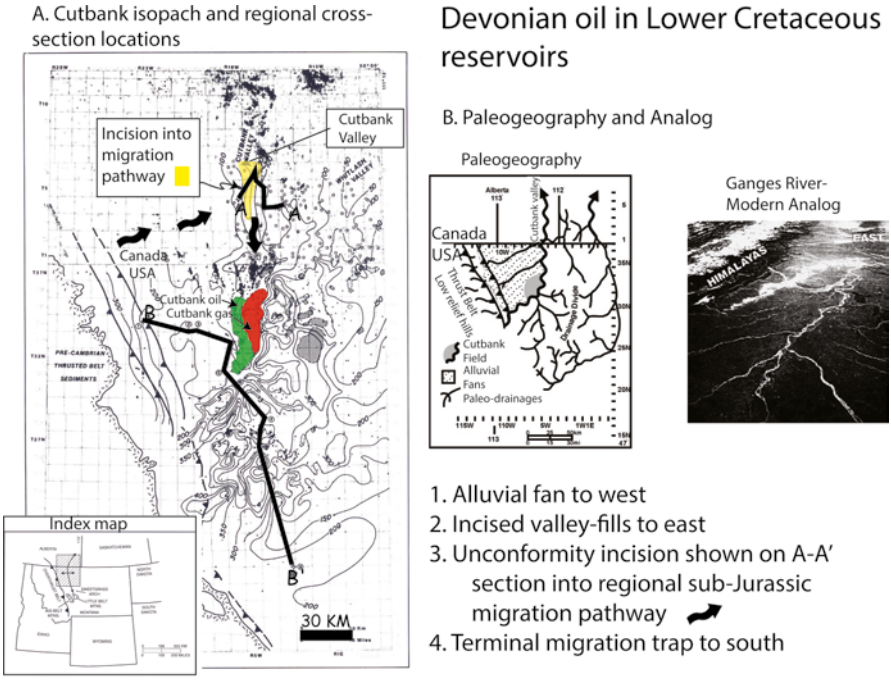

Fig. 8.45 Location of Cutbank Field and key cross-sections with migration pathways noted. Modified from Dolson et al. (1993) and Dolson and Piombino (1994). Reprinted by permission of the RMAG

8.5.2 A Case History of Migration Modeling from Oil to Source Correlations: Cutbank Field, Montana

A good example of using GCMS data to type oils to source rocks is that of Dolson et al. (1993). In this study, GCMS data from cores and oils led to the recognition of the Devonian as the source for oil in the giant Cutbank Field (Fig. 8.45).

The field is a giant incised valley fill trap in Lower Cretaceous fluvial reservoirs developed on the flank of the Sweetgrass Arch. Cross-section A-A′ (Fig. 8.46) shows that the incision on the valley network in Canada cuts through Jurassic shale and into the regional dolomitized limestone of the Mississippian Sun River Dolomite. Oil staining and residual shows are ubiquitous in virtually every well that penetrates the upper portion of the Sun River Dolomite beneath the seals of the Jurassic shales, indicating it is a major migration pathway (Fig 8.47).

The origin of these oil shows in the Sun River Dolomite was initially attributed to the black shales of the overlying Jurassic Rierdon Formation, but source rock analysis indicated none of these shales were viable source rocks anywhere in the area. While looking at oil and gas potential in the deeper Devonian Bakken/Exshaw Shales, however, a key core was identified and extracts from the core taken, along

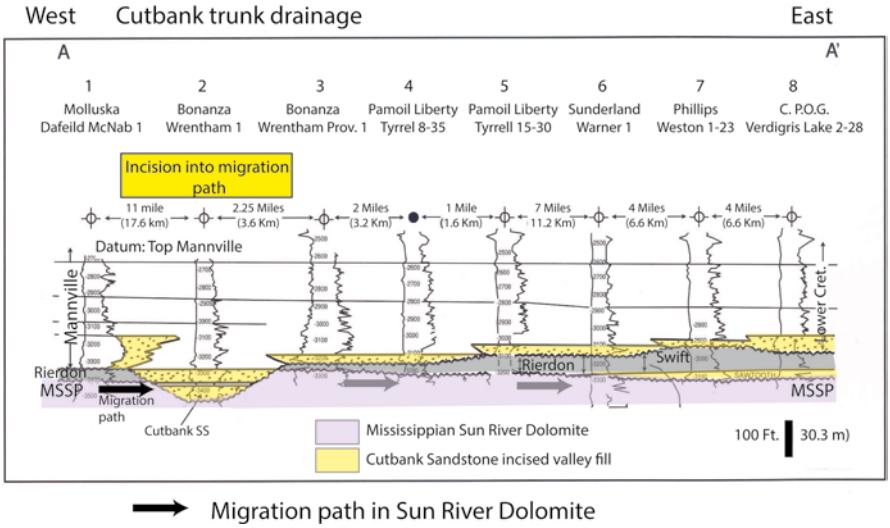

Fig. 8.46 Cross-section A-A′ with migration pathway noted in the Mississippian Sun River Dolomite. Modified from Dolson et al. (1993). Reprinted by permission of the RMAG. In the south, cross-section B-B′ (Fig. 8.47) shows that incision on the unconformity is less deep and does not bevel into the migration pathway of the Sun River Dolomite

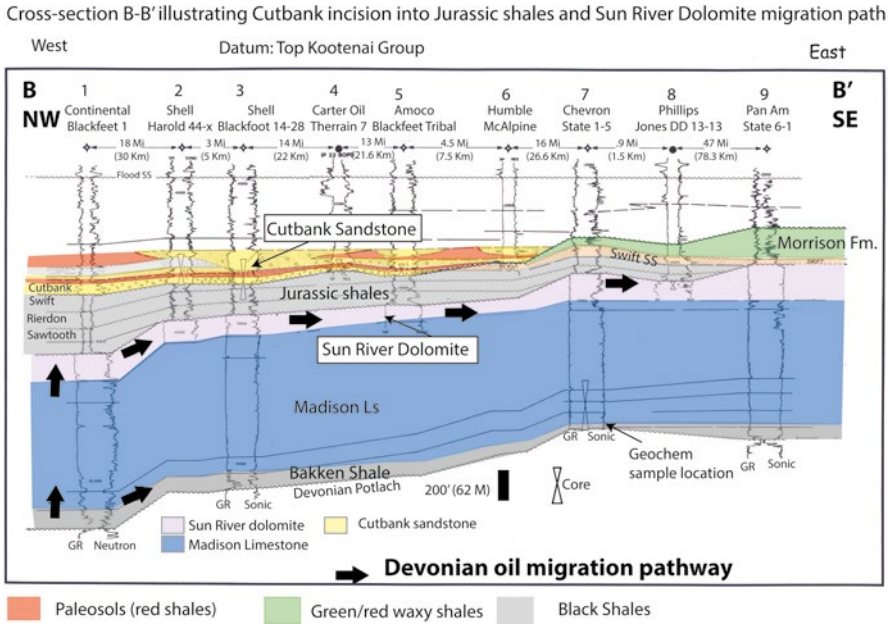

Fig. 8.47 Cross-section B-B′. Modified from Dolson et al. (1993). Reprinted by permission of the RMAG

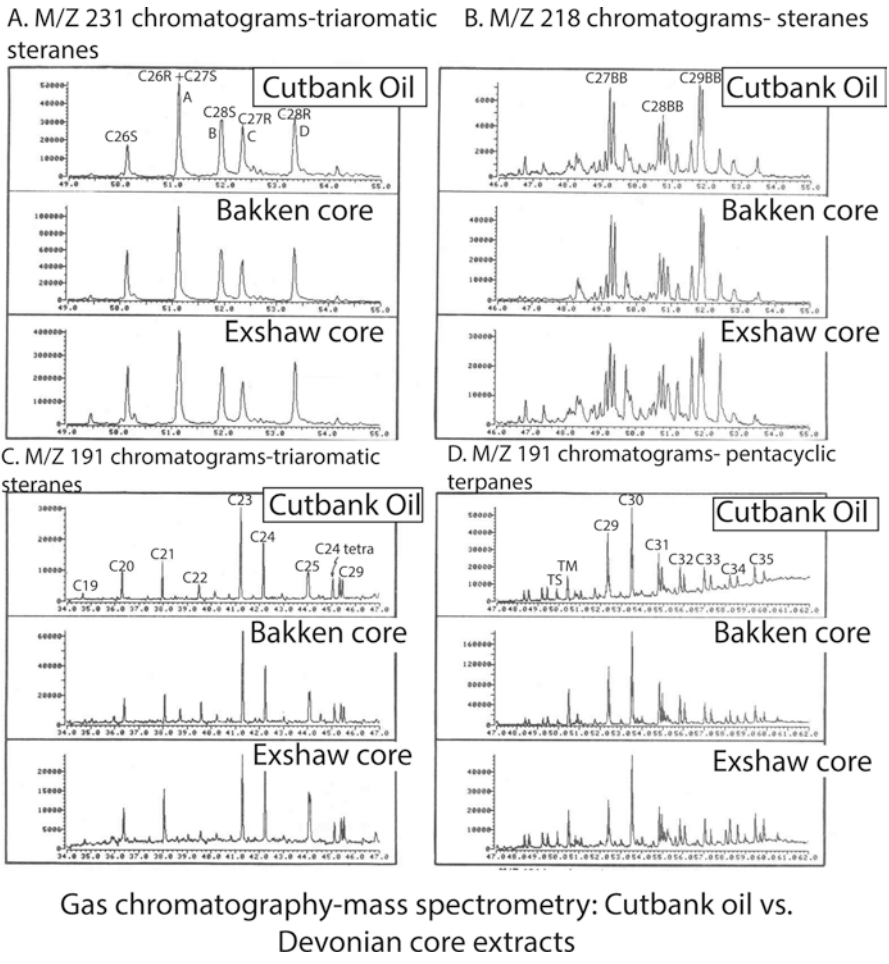

Fig. 8.48 GCMS mass chromatograms of Devonian shale extracts vs. oils in the Cutbank Lower Cretaceous reservoirs (from Dolson et al. 1993). Reprinted by permission of the RMAG

with extracts of a number of oils at various levels from other wells spanning Devonian through Lower Cretaceous reservoirs.

The results are shown in Fig. 8.48. There is little doubt from these data that the Bakken Shale has generated oil and gas to the west of the area in the vicinity of the overthrust belt. These oils have migrated vertically to the Sun River Dolomite and then laterally beneath the Jurassic Shales. Traps along that Sun River Formation migration pathway also yielded Devonian oil signatures. The migration path eventually stopped at a terminal migration trap in the Mississippian of the Kevin-Sunburst dome to the east of the Cutbank Field.

The only point where the Cutbank valley network intersects the Sun River migration pathway is to the north in Canada as shown in Fig. 8.45, over 50 km north of

the field. In addition, thermally mature Bakken Shales are only present about 50 km west near the edge of the thrust belt. Consequently, migration and charge in the Cutbank Field required extensive vertical, as well as lateral migration.

In a frontier area with a similar 'plumbing system', it would be very difficult to predict this kind of trap and charge scenario. This field was found with the drill bit in 1926, looking for a downdip extension of the Kevin-Sunburst dome. It was a surprise then, and would almost certainly be a surprise today.

8.6 Summary

Petroleum geochemistry is now an essential skill set for any explorer or development geologist. The tools of the geochemist provide powerful additional clues about migration and entrapment. It is virtually impossible to evaluate or participate successfully in unconventional shale plays without a firm grasp of the fundamental principles covered in this chapter. The technology of unconventional shale exploration, and geochemical, log, and rock properties that make each play work is a rapidly evolving science. Even with conventional exploration insight gained from incorporating geochemical data into prospects and plays can significantly reduce risk and highlight new play potential.

No effective explorer working today can ignore the important contribution that a knowledge of source rocks, oils and gas geochemistry can provide. The tools to quantify and visualize these data are increasingly sophisticated and have become a routine part of any exploration program.

References

Beaumont EA, Foster NH (eds) (1999) Exploring for oil and gas traps: treatise of petroleum geology, handbook of petroleum geology. American Association of Petroleum Geologists, Tulsa, Oklahoma, p 1162

Beek PVD, Mbede E, Andriessen P (1998) Denudation history of the Malawi and Rukwa Rift flanks (East African Rift System) from apatite fission track thermochronology. J Afr Earth Sci 26:363–385

Behar F, Vandenbroucke M (1987) Chemical modelling of kerogens. Org Geochem 11:15–24

Belton DX, Raab MJ (2010) Cretaceous reactivation and intensified erosion in the Archean–Proterozoic Limpopo Belt, demonstrated by apatite fission track thermochronology. Tectonophysics 480:99–108

Berner U, Faber E (1988) Maturity related mixing model for methane, ethane and propane, based on carbon isotopes. Org Geochem 13:67–72

Berner U, Faber E (1996) Empirical carbon isotope/maturity relationships for gases from algal kerogens and terrigenous organic matter, based on dry, open-system pyrolysis. Org Geochem 24:947–955

BGI (2013) Toolbox, Bureau Gravimetrique International, EGM2008 maps, Observatoire Midi-Pyrénées 14, Avenue Edouard Belin 31401 Toulouse Cedex 9, France, Bureau Gravimétrique International/International Gravimetric Bureau

Bowman T (2010) Direct method for determining organic shale potential from porosity and resistivity logs to identify possible resource plays, AAPG Annual Convention, New Orleans, Louisiana, AAPG Search and Discovery Article #110128, p. 34
Breyer JA (ed) (2012) Shale reservoirs: giant resources for the 21st century, v. Memoir 97. American Association of Petroleum Geologists, Oklhamona, p 451
Brittenham MD (2010) Unconventional discovery thinking in resource plays: Haynesville trend, North Louisiana, AAPG Annual Convention, New Orleans, Louisiana, AAPG Search and Discovery Article #110136
Clayton C (1991) Carbon isotope fractionzatin during natural gas generation from kerogen. Mar Pet Geol 8:232–240
Cluff B (2010) Log evaluation of gas shales: a 35-year perspective, Monthly meeting, The Denver Well Logging Society, Denver, Colorado, Society of Petrophysicists and Well Log Analysts
Coleman DD (1992) The use of geochemical fingerprinting to identify migrated gas at the Epps Underground Gas Storage Field: Society of Petroleum Engineers, v. Paper No. 24926, p. 725–734
Corcoran DV, Dore AG (2005) A review of techniques for the estimation of magnitude and timing of exhumation in offshore basins. Earth Sci Rev 72:129–168
Cornford C (2010) Petroleum geochemical aspects of shale gas exploration. Integrated Geochemical Interpretation (IGI), Bideford
Cornford C (2015) Correcting TOC using an empirical calculations. In: http://www.igiltd.com/ig.NET%20Sample%20Pages/254.html, ed., United Kingdom, Integrated Geochemical Interpretation (IGI Ltd.)
Cornford C, Burgess C, Gliddon T, Kelly R (2001) Geochemical truths in large data sets—II: Risking petroleum systems. 20th International Meeting on Organic Geochemistry, p. 322–323
Corrigan JD (1991) Inversion of apatite fission track data for thermal history information. J Geophys Res 96:10,347–10,260
Corrigan JD (1993) Apatite fission-track analysis of Oligocene strata in South Texas, U.S.A.: Testing annealing models. Chem Geol 104:227–249
Curiale JA (1994) Correlation of oils and source rocks-a conceptual and historical perspective. In: Dow WG, Magoon LB (eds) The petroleum system-from source to trap, v. Memoir 60. American Association of Petroleum Geologists, Tulsa, Oklahoma, pp 251–260
Curtis JB (2002) Fractured shale-gas systems. Am Assoc Pet Geol Bull 86:1921–1938
Curtis JB (2010) U.S. Shale Gas: from resources and reserves to carbon isotope anomalies. In: Agency PG (ed) Energy seminar, Stanford University, golden. Colorado School of Mines, Colorado, p 41
Curtis JB, Hill DG, Lillis PG (2008) Realities of shale gas resources: yesterday, today and tomorrow: NAPE
DCNR (2014) Thermal maturation and petroleum generation, Pennsylvania Department of conservation and Natural Resources (DCNR). http://www.dcnr.state.pa.us/topogeo/econresource/oilandgas/marcellus/sourcerock_index/sourcerock_maturation/index.htm, p. 1.
Dolson JC, Piombino JT (1994) Giant proximal foreland basin non-marine wedge trap: Lower Cretaceous Cutbank Sandstone, Montana. In: Dolson JC, Hendricks ML, Wescott WA (eds) Unconformity-Related Hydrocarbons in Sedimentary Sequences. The Rocky Mountain Association of Geologists, Denver, Colorado, pp 135–148
Dolson JC, Piombino J, Franklin M, Harwood R (1993) Devonian oil in Mississippian and Mesozoic reservoirs--unconformity controls on migration and accumulation, Sweetgrass Arch, Montana. Mountain Geol 30:125–146
Dolson JC, Atta M, Blanchard D, Sehim A, Villinski J, Loutit T, Romine K (2014) Egypt's future petroleum resources: A revised look in the 21st Century. In: Marlow L, Kendall C, Yose L (eds) Petroleum Systems of the tethyan region, v. Memoir 106. American Association of Petroleum Geologists, Tulsa, Oklahoma, pp 143–178
Dolson J, Burley SD, Sunder VR, Kothari V, Naidu B, Whiteley NP, Farrimond P, Taylor A, Direen N, Ananthakrishnan B (2015) The discovery of the Barmer Basin, Rajasthan, India, and its petroleum Geology. Am Assoc Pet Geol Bull 99:433–465

Downey MW, Garvin J, Lagomarsina RC, Nicklin DF (2011) Quick look determination of oil-in-place oil shale resource plays, AAPG Annual Convention and Exhibition, Houston, Texas, AAPG Search and Discovery Article #40764

Drozd RJ, Cole GA (1994) Point Pleasant-Brassfield (!) petroleum system, Appalachian Basin, USA. In: Magoon LG, Dows WG (eds) The petroleum system-from source to trap: Tulsa. American Association of Petroleum Geologists, Oklahoma, pp 387–398

Dzou L, Milkov AV (2011) Advanced interpretations of stable isotopic composition of gases in working petroleum systems, AAPG Hedberg Conference. Natural gas geochemistry: Recent developments, applications, and technologies, Beijing, China, AAPG Search and Discovery Article #90134, p. 2

EIA (2007) US Coalbed methane: past, present and future. Energy Information Administration Office of Oil and Gas, Washington, p 1

EIA (2008) Barnett Shale, Ft. Worth Basin, Texas. Wells by year of first production and orientation. Energy Information Administration Office of Oil and Gas, Washington, p 1

EIA (2009) Marcellus shale gas play, Appalachian Basin Washington, USA. Energy Information Administration Office of Oil and Gas, p. 1

EIA (2010) Shale gas plays, Lower 48 states. Energy Information Administration Office of Oil and Gas, Washington, p 1

EIA (2011) World shale gas resources: An initial assessment of 14 regions outside the United States Washington, USA. Energy Information Administration Office of Oil and Gas, p. 365

Engelder T, Lash GG, Uzcategui RS (2009) Joint sets that enhance production from Middle and Upper Devonian gas shale of the Appalachian Basin. Am Assoc Pet Geol Bull 93:857–889

Faber E (1987) Zur isotopengeochemie gasformiger Kohlen wasserstoffe. Erdol Erdgas Kohle 103:210–218

Farrimond P, Naidu BS, Burley SD, Dolson J, Whiteley N, Kothari V (2015) Geochemical characterization of oils and their source rocks in the Barmer Basin. Petroleum Geoscience, Rajasthan, India, p 22

Farris M (2001) Sedimentological and reservoir quality correlations of the Cretaceous Lower Bahariya, Qarun Field:, Proprietary project 99177 for Apache Corporation, Badley Ashton and Associates Ltd.

Ferworn K, Zumberge J, Reed J, Brown S (2008) Gas character anomalies found in highly productive shale gas wells, http://www.papgrocks.org/ferworn_p.pdf, p. 26

Geizery ME, Moula IA, Aziz SA, Helmy M (1998) Qarun field geological model and reservoir characterization: a successful case from the Western Desert. In: Eloui M (ed) Proceedings of the 14th Petroleum Conference, 1. The Egyptian General Petroleum Corporation, Cairo, Egypt, pp 279–297

Gosnold W (2011a) Global heat flow database. International Union of Geodesy and Geophysics, p. 77

Gosnold W (2011b) Heat flow and radioactivity. Geoneutrino Workshop, Deadwood, South Dakota. University of North Dakota, p. 68

Green PF (1988) The relationship between track shortening and fission track age reduction in apatite: combined influences of inherent instability, annealing anisotropy, length bias and system calibration. Earth Planet Sci Lett 89:335–352

Green PF, Duddy IR, Laslett GM, Hegarty KA, Gleadow AJW, Lovering JF (1980) Thermal annealing of fission tracks in apatitie: 4. Quantitative modelling techniques and extension to geological timescales. Chem Geol (Isotope Geoscience Section) 79:155–182

Green PF, Duddy IR, Gleadow AJW, Tintgate PR, Laslett GM (1986) Thermal annealing of fission tracks in apatite: 1. A qualitative description. Chem Geol (Isotope Geoscience Section) 59:237–253

Green PF, Duddy IR, Gleadow AJW, Laslett GM (1988) Can fission track annealing in apatite be described by first-order kinetics? Earth Planet Sci Lett 87:216–228

Gretener PE (1981) 2: Fundamental terms and concepts, CN17: geothermics: using temperature in hydrocarbon exploration (course notes), v. CN17. American Association of Petroleum Geologists, Tulsa, Oklahoma, pp 2–14

Hardage BA, Alkin E, Backus MM, DeAngelo MV, Sava D, Wagner D, Graebner RJ (2013) Evaluation of fracture systems and stress fields within the Marcellus Shale and Utica Shale and characterization of associated water-disposal reservoirs: Appalachian Basin, Research Partnership to Secure Energy for America. Bureau of Economic Geology, Austin Texas, p 261

Harper JA, Kostelnik J (2013a) The Marcellus shale play in Pennsylvania part 4: drilling and completion, geological survey. Department of Conservation and Natural Resources, Middletown, Pennsylvania, p 18

Harper JA, Kostelnik J (2013a) The Marcellus shale play in Pennsylvania, geological survey. Middletown, Pennsylvania: Pennsylvania Department of Conservation and Natural Resources

Harper JA, Kostelnik J (2013b) The Marcellus Shale Play in Pennsylvania part 2: Basic Geology Geological Survey. Middletown, Pennsylvania, Pennsylvania Department of Conservation and Natural Resources, p. 21

Haworth JH, Sellens M, Whittaker A (1985) Interpretation of hydrocarbon shows using light (C_1-C_5) hydrocarbon gases from mud-log data. Am Assoc Pet Geol Bull 69:1305–1310

He Z (2014) Practical thermal history modeling, *in* Zetaware, ed. Tutorial-Genesis and Trinity modeling software, Houston, Texas, p 36

He Z (2015) ZetaWare, Inc.—Source Rock Potential Calculator. http://www.zetaware.com/utilities/srp/index.html, Houston, Texas, Zetaware, Inc

He Z, Crews SG, Corrigan J (2007) Rifting and heat flow: why the McKenzie model is only part of the story. AAPG Hedberg Conference, The Hague, The Netherlands, p. 16

Hill RJ, Zhang E, Katz BJ, Tang Y (2007) Modeling of gas generation from the Barnett Shale, Fort Worth Basin, Texas. Am Assoc Pet Geol Bull 91:501–521

Hill DG, Lillis PG, Curtis JB (eds) (2008) Gas shale in the rocky mountains and beyond: 2008 guidebook: Denver. Rocky Mountain Association of Geologists, Colorado, 373 p

Hoeve MV, Meyer SC, Preusser J, Makowitz A (2010) Basin-wide delineation of gas shale 'sweet spots' using density and neutron logs: Implications for qualitative and quantitative assessment of gas shale resources, AAPG/SEC/SPE/SPWLA Hedbert conference "critical assessment of shale resource plays". American Association of Petroleum Geologists, Austin, Texas, p 3

Holmes M, Holmes D, Holmes A (2009) Relationship between porosity and water saturation: Methodology to distinguish mobile from capillary bound water. AAPG Annual Convention, Denver, Colorado, AAPG Search and Discovery Article #110108, p. 27

Holmes M, Holmes D, Holmes A (2011) A petrophysical model to estimate free gas in organic shales. Annual Conference and Exhibition, Houston, Texas, AAPG Search and Discovery Article #40781

Holmes M, Holmes A, Holmes D (2012) A petrophysical model for shale reservoirs to distinguish macro porosity, mirco porosity and TOC. Annual Conference and Exhibition, Long Beach, California, AAPG and Digital Formation Analysis

James AT (1983) Correlation of natural gas by use of carbon isotopic distribution between hydrocarbon components. Am Assoc Pet Geol Bull 67:1176–1191

James AT (1990) Correlation of reservoired gases using the carbon isotopic compositions of wet gas components. Am Assoc Pet Geol Bull 74:1441–1458

James AT, Burns BJ (1984) Microbial alteration of subsurfce natural gas accumulations. Am Assoc Pet Geol Bull 68:957–960

Jarvie D (2003) The Barnett Shale as a model for unconventional shale gas exploration, Humble Geochemical Service. Humble Instruments and Services, Inc., p. 91.

Jarvie DM, Hill RJ, Ruble TE, Pollastro RM (2007) Unconventional shale-gas systems: The Mississippian Barnett Shale of north-central Texas as one model for thermogenic shale-gas assessment. Am Assoc Pet Geol Bull 91:475–499

Javadpour F (2008) Nanopores and apparent permeability of gas flow in mudrocks (shales and siltstones). J Can Petrol Geol 48:1–21

Jones AG, Craven JA (1990) The North American central plains conductivity anomaly and its correlation with gravity, magnetic, seismic, and heat flow data in Saskatchewan, Canada. Phys Earth Planet In 60:169–194

King GE (2010) Thirty years of gas shale fracturing: what have we learned? SPE Annual Technical Conference and Exhibition, Florence, Italy, Society of Petroleum Engineers, p. 50
Kinley TJ, Cook LW, Breyer JA, Jarvie DM, Busbey AB (2008) Hydrocarbon potential of the Barnett Shale (Mississippian), Delaware Basin, west Texas and southeastern New Mexico. Am Assoc Pet Geol Bull 92:967–991
Kolb B, Ettre LS (2006) Static headspace-Gas chromatography: theory and practice. Wiley-Interscience, Hoboken, p 335
Lash GG, Blood R (2010) Sequence stratigraphy and its bearing on reservoir characteristics of shale successions-examples from the Appalachian Basin, AAPG Eastern Section Meeting, Kalamazoo, Michigan, AAPG Search and Discovery Article #50289, p. 66
Lash GG, Engelder T (2011) Thickness trends and sequence stratigraphy of the Middle Devonian Marcellus Formation, Appalachian Basin: Implications for Acadian foreland basin evolution. Am Assoc Pet Geol Bull 95:61–103
Law C (1999) Evaluating source rocks. In: Foster N, Beaumont EA (eds) Treatise of the handbook of petroleum geology. American Association of Petroleum Geologists, Tulsa, Oklahoma, pp 6-1–6-41
Lopatin NV (1971) Temperature and geologic time as factors in coalification. Akad Nauk SSSR IzvSerGeol (in Russian) 3:95–106
Loucks RG, Reed RM, Ruppel SC, Jarvie DM (2009) Morphology, genesis and distribution of nanometer-scale pores in siliceous mudstones of the Mississippian Barnett Shale. J Sediment Res 79:848–861
Luft FF, Luft JL, Chemale F Jr, Lelarge MLMV, Avila JN (2005) Post-Gondwana break-up record constraints from apatite fission track thermochronology inNWNamibia. Radiat Meas 39:116
Magoon LB, Dow WG (eds) (1994) The Petroleum system--from source to trap: AAPG memoir 60. American Association of Petroleum Geologists, Tulsa, Oklahoma, p 655
McKenzie D (1978) Some remarks on the development of sedimentary basins. Earth Planet Sci Lett 40:25–32
Meissner FF (1978) Petroleum Geology of the Bakken Formation, Williston basin, North Dakota and Montana: The economic geology of the Williston basin. Proceedings of the Montana Geological Society, 24th Annual Conference, p. 207–227
Mello MR, Gaglianone PC, Brassell SC, Maxwell JR (1988) Geochemical and biological marker assessment of depositional environments using Brazilian offshore oils. Mar Pet Geol 5:205–223
Milkov AV, Goebel E, Dzou L, Fisher DA, Kutch A, McCaslin N, Bergman DF (2007) Compartmentalization and time-lapse geochemical reservoir surveillance of the Horn Mountain oil field, deep water Gulf of Mexico. Am Assoc Pet Geol Bull 91:847–876
Montgomery SL, Jarview DM, Bowker KA, Pollastro RM (2005) Mississippian Barnett shale, Fort Worth Basin, north-central Texas: Gas shale play with multi-trillion cubic foot potential. Am Assoc Pet Geol Bull 89:155–175
Naidu BN, Kothari V, Whiteley NJ, Guttormsen J, Burley S (2012) Calibrated basin modelling to understand hydrocarbon distribution in Barmer Basin, India. AAPG International Conference and Exhibition, Singapore, AAPG Search and Discovery Article #10448
Naidu BS, Burley SD, Dolson J, Farrimond P, Sunder VR, Kothari V, Mohapatra P, Whiteley N (in press) Hydrocarbon generation and migration modelling in the Barmer Basin of western Rajasthan, India: lessons for exploration in rift basins with late stage inversion, uplift and tilting, Petroleum System Case Studies, v. Memoir 112. Tulsa, Oklahoma: American Association of Petroleum Geologists
Nemec MC (1996) Qarun Oil Field, Western Desert, Egypt. In: Youssef M (ed) Proceedings of the 13th Petroleum Conference. v. 1. Cairo, Egypt: The Egyptian General Petroleum Corporation, p. 193–202
Nordeng SH, LeFever JA (2009) Organic geochemical patterns in the Bakken source system (poster), North Dakota. North Dakota Geological Survey, p. 1 poster
Ottman J, Bohacs K (2014) Conventional reservoirs hold keys to the 'Un's': AAPG Explorer, p. 2

Passey QR, Creaney S, Kulla JB, Moretti FJ, Stroud JD (1990) A practical model for organic richness from porosity and resistivity logs. Am Assoc Pet Geol Bull 74:1777–1794
Pepper AS, Corvi PJ (1995a) Simple kinetic models of petroleum formation—Part I, Oil and gas generation from kerogen. Mar Pet Geol 12:477–496
Pepper AS, Corvi PJ (1995b) Simple kinetic models of petroleum formation—Part III: Modeling an open system. Mar Pet Geol 12:417–452
Pepper AS, Dodd TA (1995) Simple kinetic models of petroleum formation—Part II, oil-gas cracking. Mar Pet Geol 12:321–340
Peters KE, Nelson PH (2009) Criteria to determine borehole formation temperatures for calibration of basin and petroleum systems models. AAPG Annual Conference and Exhibition, Denver, Colorado, AAPG Search and Discovery Article #40463 (2009), p. 27
Pollack HN, Hurter SJ, Johnson JR (1993) Heat flow from the Earth's interior: analysis of the global data set. Rev Geophys 31:231–245
Pollastro RM (2007) Total petroleum system assessment of undiscovered resources in the giant Barnett Shale continuous (unconventional) gas accumulation, Fort Worth Basin, Texas. Am Assoc Pet Geol Bull 91:551–578
Price LC, Dawas T, Pawlewics M (1986) Organic metamorphism in the lower missippian-upper Devonian bakken shales: part 1: rock eval pyrolysis and vitrinite reflectance. J Pet Geol 9:125–162
Prinzhofer AA, Huc AY (1995) Genetic and post-genetic molecular and isotopic fractionations in natural gases. Chem Geol 126:281–290
Raab MJ, Brown RW, Gallagher K, Carter A, Weber K (2002) Late Cretaceous reactivation of major crustal shear zones in northern Namibia: constraints from apatite fission track analysis. Tectonophysics 349:75–92
Railsback LB (2015) Petroleum Geoscience and Subsurface Geology: heat flow chart. http://www.gly.uga.edu/railsback/PGSG/ThermalCond&Geothermal01.pdf, Athens, Georgia, University of Georgia
Rooney MA, Claypool GE, Chung HM (1995) Modeling thermogenic gas generation using carbon isotope ratios of natural gas hydrocarbons. Chem Geol 126:219–232
Schamel SC (2008) Potential shale gas resources in Utah. In: Hill DG, Lillis PG, Curtis JB (eds) 2008 Guidebook. Rocky Mountain Association of Geologists, Denver, Colorado, pp 119–161
Schoell M (1983) Genetic characterization of natural gases. Am Assoc Pet Geol Bull 67:2225–2238
Schoell M, Jenden PD, Beeunas MA, Coleman DD (1993) Isotope analysis of gases in the gas field and gas storage operations. Society of Petroleum Engineers, v. SPE Paper No. 26171, p. 337–344
Smith LB, Leone J (2010) Integrated characterization of Utica and Marcellus Black Shale gas plays, New York State. AAPG Annual Convention and Exhibition, New Orleans, Louisiana, AAPG Search and Discovery Article #50289, p. 36
Sondergeld CH, Newsham KE, Comisky JT, Rice MC, Rai CS (2010) Petrophysical considerations in evaluating and producing shale gas resources. Soc Petrol Eng SPE 131768:1–34
Talukdar SC (2009) Application of geochemistry for shale gas assessment. Baseline Resolution, Weatherford Labs
UTEP (2015) Gravity and magnetic extract utility, pan American center for earth and environmental studies (PACES). http://irpsrvgis08.utep.edu/viewers/Flex/GravityMagnetic/GravityMagnetic_CyberShare/, University of Texas at El Paso
Wang FP, Gale JFW (2009) Screening criteria for shale-gas systems. Gulf Coast Assoc Geol Soc 59:779–793
Waples DW (1980) Time and temperature in petroleum formation: Application of Lopatin's method to petroleum exploration. Am Assoc Pet Geol Bull 64:916–926
Waples DW, Curiale JA (1999) Oil-oil and oi-source rock correlation. In: Foster N, Beaumont EA (eds) Treatise of the handbook of petroleum geology. American Association of Petroleum Geologists, Tulsa, Oklahoma, pp 8-1–8-71

Wescott WA, Atta M, Blanchard DC, Cole RM, Georgeson ST, Miller DA, O'Hayer WW, Wilson AD, Dolson JC, Sehim A (2011) Jurassic rift architecture in the northeastern Western Desert, Egypt, AAPG International Conference and Exhibition, Milan, Italy, AAPG Search and Discovery Article No. 10379

Whiticar MJ (1994) Correlation of natural gases with their sources. In: Magoon LB, Dow WG (eds) The Petroleum system, from source to trap, v. AAPG memoir 60. American Association of Petroleum Geologists, Tulsa, Oklahoma, pp 261–283

Wrightstone G (2009) Marcellus Shale-geologic controls on production. AAPG Annual Convention, Denver, Colorado, AAPG Search and Discovery Article #10206, p. 10

Wrightstone G (2010) A shale tale: Marcellus odds and ends, 2010 winter meeting of the independent oil and gas association of West Virginia. p. 32

Zhao H, Givens NB, Curtis B (2007) Thermal maturity of the Barnett shale determined from well-log analysis. Am Assoc Pet Geol Bull 91:535–549

Chapter 9
Building and Testing Migration Models

Contents

Abstract One of the ultimate goals of shows and seal analysis is construction of migration and trap models that integrate with petroleum systems models to predict the migration and entrapment of hydrocarbons through time in three dimensions. Because migration takes place at a molecular scale, it is impossible to fully model migration correctly. However, simulations on the major carrier beds and seals can be done which provide useful predictive models, even if the scale is fairly crudely generalized.

As our ability to visualize depositional systems with seismic and other tools becomes more sophisticated, so will the migration simulations. While recognizing the limitations on any model, it is still important to generate scenarios that honor the shows data. Multiple combinations of facies, seal and hydrodynamic flow maps may produce the similar results. Risk maps, however, can be built which combine the best results into risk index maps which can then be used to determine the most likely areas of hydrocarbon accumulations, despite which model is used.

This short chapter provides an overview of both the potential and ways to address the pitfalls in migration modelling.

J. Dolson, *Understanding Oil and Gas Shows and Seals in the Search for Hydrocarbons*, DOI 10.1007/978-3-319-29710-1_9

9.1 The Scale Challenge in Migration Modelling

Migration of petroleum is a complex process. Despite substantial advances in a knowledge of this topic in the last several decades, it begins at a molecular level that can be modeled, but not directly observed. Modeling and visualizing hydrocarbon migration from the best available seismically and well-constrained 3D models is somewhat analogous to understanding how the human body works from a CT scan. Despite the high resolution of the scan, and ability to slice and analyze in three dimensions, for instance, a human brain, the complexity of how the brain works ultimately is at a molecular scale impossible to visualize directly at present.

Shows data remains the only way to validate any migration model or trap map. Take, for instance, a simulated model using a good 3D seismic depth converted image using Trinity software (Fig. 9.1).

The upper figure is a depth converted seismic section in a transpressional rift basin. Basement strata is highlighted in red. Modeling migration quantitatively using this seismic line could require a great deal of work to convert each change in amplitude to reasonable seal and reservoir pairs—but the solution would still be limited to the resolution of the seismic. Doing this accurately requires well control, velocity information as it varies with depth and laterally along the section, and the ability to model each impedance contrast accurately in values of meters or psi of seal capacity. Some petroleum systems modelers will spend weeks or months trying to simulate a line like this and in the end, only get an approximate answer over hundreds of meters of section, and with many assumptions built into the model. Also, remember that vertical seismic resolution on a line like this is, at best, about 30 m for each reflective

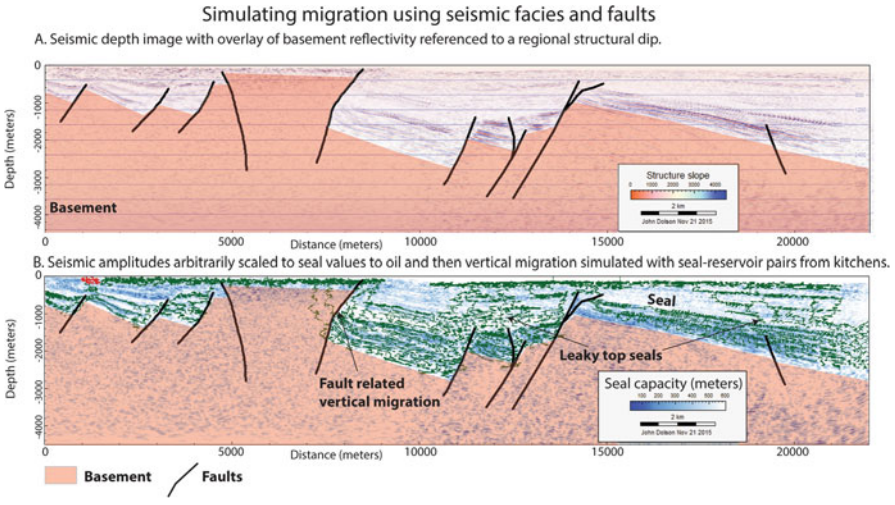

Fig. 9.1 A seismic section modeled in depth with amplitude variations converted to reservoir and seal pairs. *Green lines* are predicted migration pathways to oil out of the source rock kitchens

horizon. Thus, the model is still not going to completely satisfy migration in nature, as even beds a few centimeters thick can be migration conduits. It is a good idea, then, to always remember that scale makes a difference and migration and trap models are, at best, crude approximations of actual migration in the subsurface.

Another approach is to simply take the color variations from the amplitude changes and scale them to relative seal and reservoir pairs (Fig. 9.2b), in values of meters of seal capacity to oil or gas. In this case, the seal capacity assumes an oil-water system with maximum seal capacity to 600 m. The lightest colored transparent amplitudes generally identified as shales, and are given the maximum value. The darkest amplitudes are assumed to represent reservoirs and (are) given a seal capacity of 0. Ranges between the darkest and lightest values are simply scaled arithmetically. While certainly wrong in absolute values, a resulting migration simulation (bottom) shows that the migration that occurs is not simple, but has many vertical leak points around faults or in areas where top-seals might leak due to internal facies variations.

The real modelling problem is compounded tremendously with a knowledge that this process, illustrated somewhat schematically on Fig. 9.1, must be done in a full 3D volume in order to get accurate answers. In the end, many scenarios are possible and only a good shows and seals database remains to validate the model and test its accuracy.

9.2 Some Migration Concepts

A number of basic papers deal with migration modeling and these include (England 1994; England et al. 1987, 1991; Gussow 1953, 1954; MacKenzie and Quigley 1988; Matthews 1999; Schowalter 1979; Tissot and Welte 1984). Rather than focus on the details of theory of migration losses, volumetrics, differential entrapment and migration, this chapter deals with understanding and trying to quantify migration models with oil shows visualized in 2 and 3D space.

Take for instance, a schematic representation of migration with simple pairs of reservoir and seal (Fig. 9.2). As demonstrated in Chap. 5 and discussed throughout this book, traps fill to the seal capacity of the weakest seal and then leak updip to the next trap, assuming an adequate volume of oil remains to migrate. If the column height is sufficient for buoyancy to overcome topseal, then the traps also leak vertically into the overlying reservoir systems. If insufficient volume is available for long range migration, some traps (as in traps H and D in Fig. 9.2) remain uncharged. It is quite common, however, to have extensive vertical and lateral migration and the only way to really detect this is with shows data already illustrated at length in this book.

It is also common to have gas trapped differentially updip of oil, through leaky seals that allow gas migration but differentially entrap oil (Schowalter 1979). In addition, phase changes occur during migration, as fluids reach lower temperatures and pressures. England et al. (1991) and Matthews (1999) summarize a number of important changes that occur during and after migration (Table 9.1).

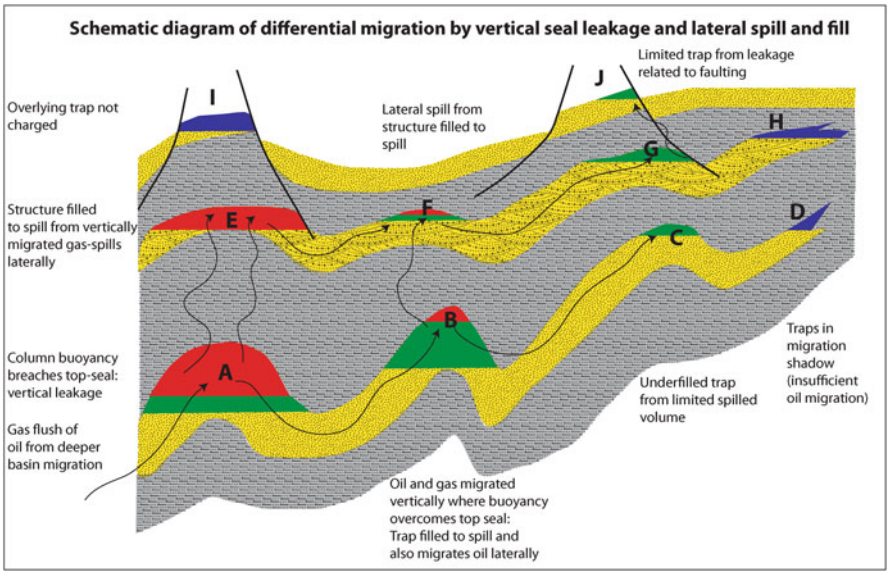

Fig. 9.2 Differential entrapment and migration. Traps (A–C) are from migration in the deepest carrier bed. Trap A was originally oil but has been flushed by later gas, spilling both oil and gas updip to B and C. Trap D is barren, as it is beyond the limits of lateral hydrocarbon migration. Vertical migration occurs from the deep carrier bed from traps A and B, which are sealed to the limit of the seal capacity of the structures for the fluid buoyancy at both levels. The traps are filled to spill, but also leak vertically to traps E–G. Trap J is filled from vertical migration along a fault. Traps H and I remain barren, in vertical and lateral migration shadows

Table 9.1 Some changes that can occur during and after migration. Summarized from England et al. (1991) and Matthews (1999)

Process	Comment
Biodegradation	Typically at temperatures <70 °C; asphaltenes rise and API gravity falls.
Water washing	Can occur where water is still flowing past oil (as in hydrodynamic conditions), even at higher temperatures. Removal of more soluble light ends occurs.
Gas deasphalting	Occurs when co-mixing certain oil and gas products resulting in precipitation of asphaltenes.
Mixing	Migration of hydrocarbons from different source facies into the same carrier beds and traps, producing mixed oils that might be difficult to distinguish from which source rock they were derived.
Gravity segregation	Occurs in static columns, resulting in higher API gravities at the top of the column gradually becoming lower API at the bottom.
Oil to gas cracking	Occurs at very high temperatures and pressures as traps are buried deeper.
Phase partitioning	Changes due to decreased temperature and pressure. Good examples are discussed in the Hugoton and West Siberia case histories in Chap. 5, where gas caps and remigration are associated with reduced temperature and pressure related to regional uplift.

Migration losses also occur along any migration pathway, as reservoirs intercept the migration front and divert oil to other traps. These losses can be significant and difficult to quantify, and in some cases, may need to be modeled to test the viability of traps updip of the kitchens. Estimates of migration loss of 10 % or higher are assumed in many cases (England et al. 1987). Modelling software allows setting migration losses and values of 6 MMBO/km^2 that are often assumed as a starting point, but values as high as 30 MMBO/km^2 are also documented (www.zetaware.com). Estimates can also be made by looking at the known in-place hydrocarbon volumes in an existing trap, and then calculating the volume of oil and gas expelled from the available fetch area downdip. The volumetric differences divided by the fetch area can serve as an estimate of migration loss.

Regardless of changes made during migration, careful analysis of shows and geochemistry can help explain the migration routes and/or identify key questions that need to be resolved to explain anomalous shows and traps.

9.3 Long Range Migration

Long range migration is common in many sedimentary basins, particularly in areas of ramp structural dip and extensive carrier beds like aeolian sandstones or regionally porous dolomites and limestones. Long range migration in good carrier beds should not be overlooked in any basin. Many risk assessments use the area of the mature kitchen as the primary focus of exploration, dismissing lateral migration. An example was shown in Chap. 5 with the Buzzard Field in the North Sea. Many other examples exist. Risk maps should incorporate the possibility of long range migration and utilize all available data external to the mapped kitchens to assess if lateral migration out of the kitchen has occurred.

One of the best documented examples of long range migration is that of the Athabascan Tar Sands (Creaney et al. 2012) for the Western Canadian Basin. Long range migration in excess of 100 km has been documented. As this is one of the world's largest petroleum traps, dismissing lateral migration is areas like this could lead to a real undervaluation of exploration potential.

In the western USA, long range migration through extensive Permo-Pennsylvanian aeolian dune reservoirs is well documented (Claypool et al. 1978; Gorenc and Chan 2015; Hansley 1995; Huntoon et al. 1994, 1999; Maughan 1984, 1994). Figure 9.3 summarizes the distribution of source rocks that could potentially charge the Permo-Pennsylvanian reservoirs and locations of major traps in Wyoming and Utah.

The Elaterite Tar trap is particularly interesting in that the trap is entirely encased in red shales and sandstones with no trace of any source rock vertically or laterally near the accumulations. It has, however, received 16 BBO charge in a giant stratigraphic pinchout-trap (Fig. 9.4). If this were a viable light oil accumulation, it would be the biggest conventional trap in the United States, dwarfing Prudhoe Bay and East Texas fields. The migration pathway is well understood by direct observation of lithology color, but how the oil and gas got into those sandstone still remains a mystery.

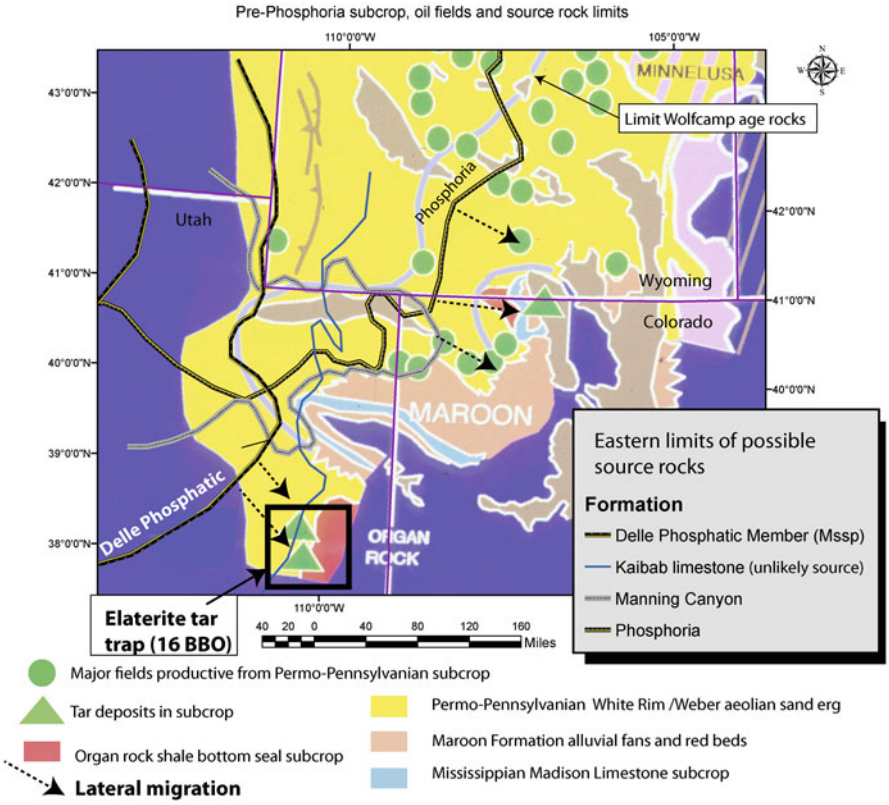

Fig. 9.3 Example of long range migration through a regionally extensive aeolian sand belt: Permo-Pennsylvanian White Rim and Tensleep Sandstones, Wyoming and Utah. The Mississippian Delle Phosphatic member of the Desert Creek Formation is the most likely source rock for the 16 BBO Elaterite tar trap, and is located over 40 miles (64 km) from the terminal trap. Likewise, Permian Phosphoria source rocks charge many reservoir east of their physical limits, in excess of 100 miles (160 km) to the east

Normally, sandstones in Permo-Triassic strata in western Wyoming and Utah are an orange color, due to extensive iron minerals and hematite cements common to the arid depositional system. However, where hydrocarbon migration has occurred, the reducing front from the migrating oils has altered the minerals to a white color. Thus, the migration pathways can be observed and mapped, even from cars or helicopters, where the white colorations stand out against the red shales. A similar process has recently be documented in red beds in the Neuquen Basin of Argentina (Pons et al. 2015).

Huntoon et al. (1999) use burial history reconstructions, fluid inclusion microthermometry and oil typing to suggest that the Delle Phosphate Member of the Mississippian Desert Creek Limestone is the most likely source for these oils. If so, significant vertical, as well as lateral, migration has occurred to the trap (Fig. 9.5).

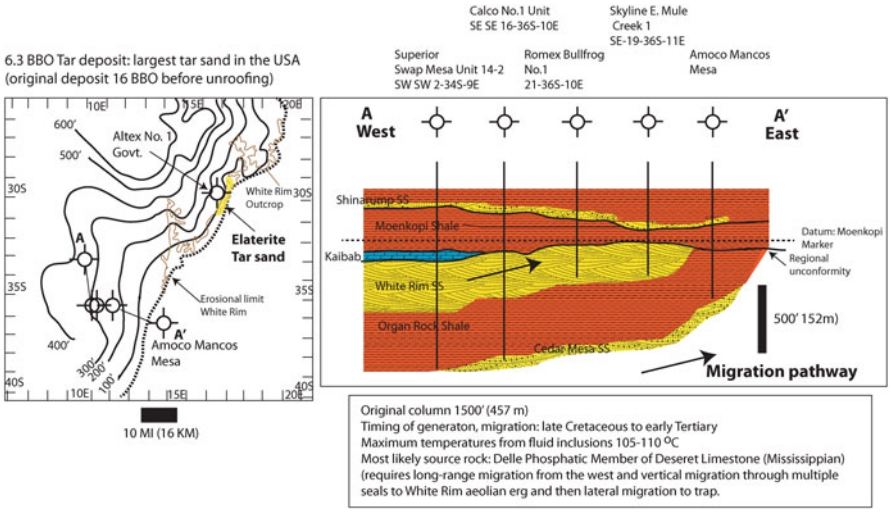

Fig. 9.4 The White Rim trap. Modified from Huntoon et al. (1994). Contours on map are the isopach of the White Rim Sandstone

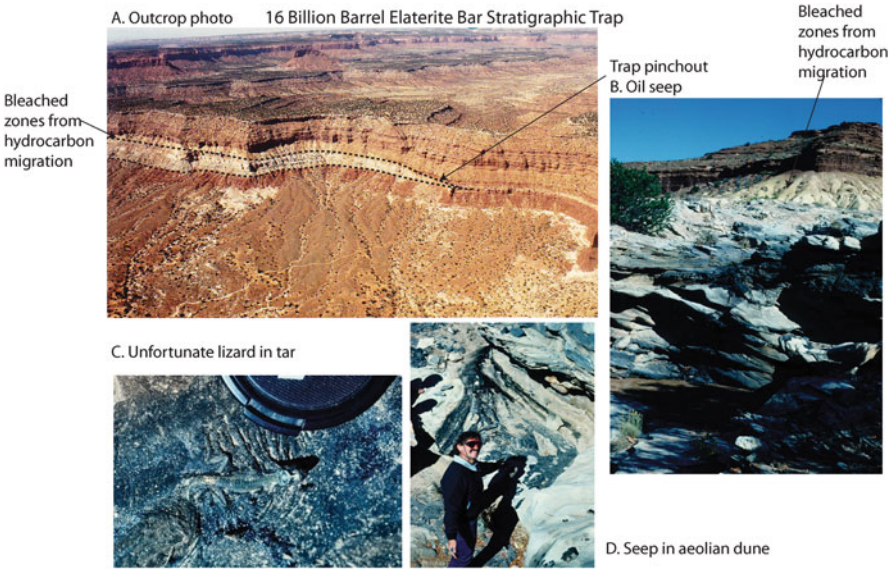

Fig. 9.5 Outcrop exposures of the 16 BBO Elaterite Tar sand trap and oil seeps. Long distance migration, marked visibly by a change from red sandstone to white sandstone along the migration pathway, is required to charge this trap

Regardless of how the oil got there, this is a very good example, as in the case of the Cutbank Sandstone discussed in Chap. 8, of a giant oil accumulation occurring in strata that would easily be written off as not possible to charge based on their stratigraphic and structural setting.

9.4 Building Migration Models and Recognizing Limits with Risk Maps

Despite the limitations to our ability to build fully accurate migration models, it is important to attempt to understand oil and gas shows from a migration standpoint and develop predictive models. Figure 9.6 shows the components that go into a good migration model.

In any petroleum systems modeling package, seal capacity in meters of column height or psi of displacement pressure must be set for faults as well as the facies involved in migration. As shown throughout this book, this can be made complicated or simple, but reality is always more complicated than any model. Fault seal capacity, for example, varies by throw, lithology offset, the character of the fault gouge itself, stress orientation and a combination of all of these components. Likewise, lateral and top seals will vary by depositional system and even subtle capillary changes within a given facies of the top seal. It is simply virtually impossible to model all of these variables exactly. Often, however, models are developed which still manage to explain most of the oil and gas shows data, giving the work

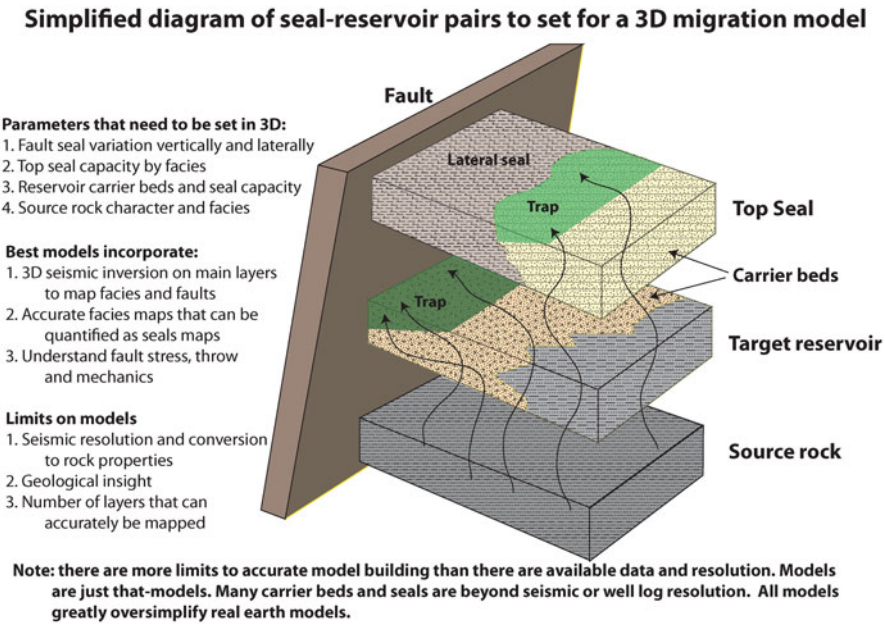

Fig. 9.6 For each reservoir layer, seals must be set up that incorporate fault, lateral and top seals. If hydrodynamic flow is present, that must also be factored in. Models are more robust in areas of good 3D seismic where high confidence can be placed on fault geometries in 3D space, as well as facies associated with the reservoirs and seals. It is functionally impossible however, to model all potential carrier beds and seals. At best, the major carriers and faults need to be looked at and calibrated to known oil and gas shows

some serious usefulness. The simple migration model in the Desert Creek Formation of Utah and Colorado (Chap. 5), using seal capacity from pseudo-capillary pressure plots from permeability and porosity data, coupled with a DST shows map, is a good example. The Desert Creek Formation migration model with seals explained 90 % of the oil and gas found in that trend, even without rigorous core and log-based paleogeographic maps.

In addition, seal capacity may need to be varied and tested against fluid phase, as seals to gas may be quite different from seals to oil. This gets even more complicated and difficult to do when modeling migration through time, where initial traps might effectively seal long columns of oil, but as later gas flushing occurs, and the oil displaced, seal change capacity may be reduced as the gas columns develop. At some point, however, trying to solve all problems in time and space begins to simply compound assumptions upon assumptions, reducing the predictability of the models. The more complicated the model gets, ironically, the less likely it may be to actually be useful if one or more of the assumptions turns out to be grossly in error.

Seismic data can provide substantial improvement in fault and facies seal mapping, especially where high quality 3D data is available. Conversion of seismic facies to seal maps can be done with seismic inversion using rock property modeling or tested with end member judgements on seal capacity from known traps or local experience.

In the example shown in Fig. 9.7, seismic amplitudes were converted to potential seal capacity in meters of column height to oil by a simple algorithm based on amplitude strength. The model shown is just one of many used in this area and faults seals have also been varied in capacity based on throw, top seal thickness and other factors. Several different models produced different results that could also explain the

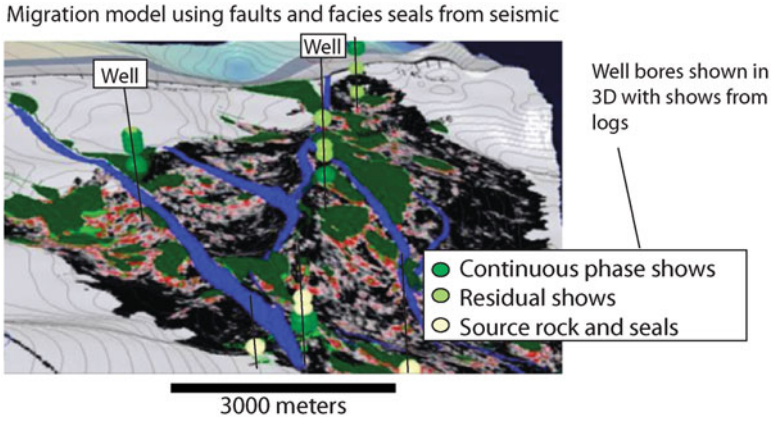

Fig. 9.7 Seismic amplitudes converted to seals and used in a migration model, along with fault seals. Shows data are shown in 3D as *circles* around well bores. *Dark green colors* are continuous phase shows, *light green* residual shows and *white circles* source rocks and seals. This is the only way to effectively validate a migration model and multiple scenarios should be tried

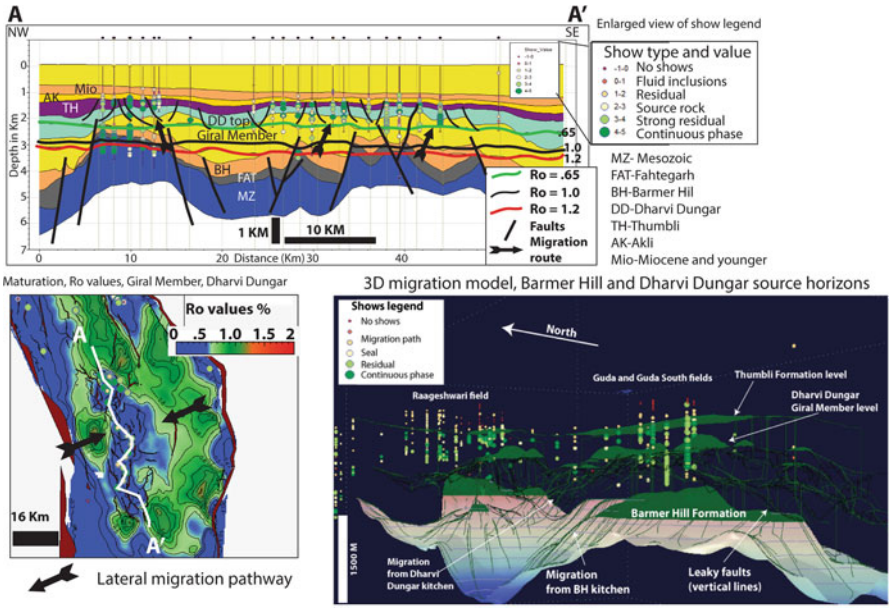

Fig. 9.8 3D vertical and lateral migration models, Barmer Basin, India. The crest of this structure is thermally immature (*bottom left figure*), but oil has migrated nearly a kilometer vertically to terminal traps in the Eocene Thumbli Sandstones (*top figure*). Mixing of oil families from deeper source rocks may have occurred through vertical migration along faults, as shown in the *bottom left figure*. From Naidu et al. (2016). Reproduced by permission of the AAPG, whose further permission is required for further use

observed shows in the wells. Ultimately, regardless of the inputs, the examination of those models that explain the shows data is the best way to determine a location to drill based on a migration model. Simply by picking an area that most of the models indicate should work may be the best way to screen a prospective location.

In another example from the Barmer Basin of India, quite a bit of geochemical oil and source rock data (Farrimond et al. 2015) was used to build a 3D migration model. This model is shown in Fig. 9.8 (Naidu et al. 2016). The Central Basin High in the Barmer Basin has large structural closures with pay zones at multiple levels over 1–2 km of section. The uppermost oil pays are located in the Eocene Thumbli Formation, which is thermally immature throughout the basin (oil pays are noted on the cross-section of the figure). The nearest thermally mature source rock is the Giral Member of the Dharvi Dungar Formation, which is only mature on the flanks of the uplift, as shown in the lower left map in Fig. 9.8. The Thumbli oils are unique in the basin and believed to have been derived from the Giral Member shales or from a mixture of oils from the Giral Member and deeper source rocks like the Barmer Hill Formation.

The 3D migration model shown in the lower right image models charge from both the Barmer Hill and Giral Member source rocks. Faults present at multiple levels in the model have been given variable, but low seal capacity. These faults are

thus set to leak after small columns are trapped, as the thick intervening shales are effective seals to vertical migration. The shows and accumulations cannot be explained by simple vertical leakage through the shales, and fault leakage is a key part of the migration story. The results agree fairly well with the observed shows and also confirm that highly faulted areas in the Thumbli Formation are the easiest areas to charge from vertical migration. Exploration risk increases significantly down-flank where no faults are present to tap the deeper source rocks.

Risk assessment in any given migration model is best done by testing multiple models and then building risk maps which incorporate the results of multiple scenarios. Over-reliance on one answer, even from a model that looks like a work of art from the software package, is a recipe for failure.

9.5 Making Migration Risk Index Maps

Given the uncertainty in any model, it is a good idea to test a variety of combinations of reservoirs and seals and then match the model results to the shows. One way to handle migration risk maps is to generate values for migration pathways and traps and then sum the results into a final risk map-. If using software like Trinity, these kinds of maps are termed 'risk index maps'.

In the example in Fig. 9.9, three migration scenarios are used from the Temsah Field area in Egypt, as discussed in much more detail in Chap. 4. Model A uses

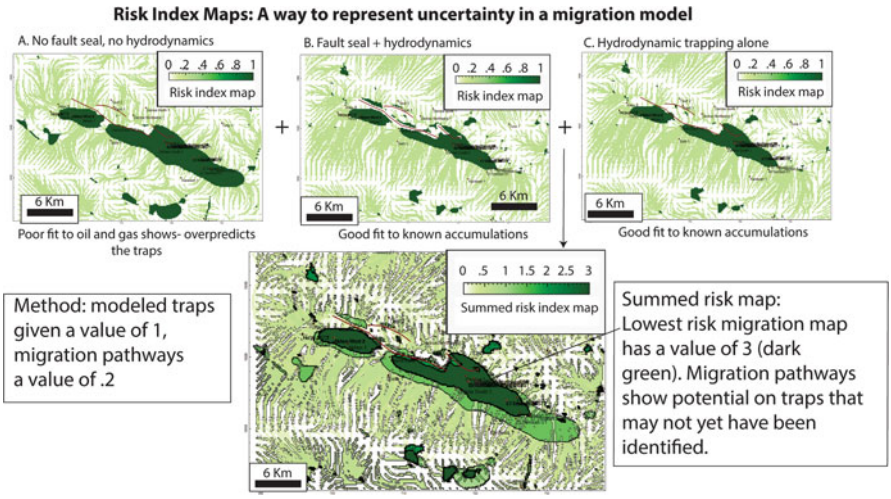

Fig. 9.9 A migration risk index map. This example utilizes scenarios for the Temsah Field area discussed in Chap. 4. Migration pathways are given a value of 0.2 and accumulations a 1. The summed risk map (*bottom*) is lowest risk where every model, regardless of parameters, appears to have predicted an accumulation. The summed risk model is an excellent fit to known oil and gas accumulations at this level

structural four-way closures only, and over-predicts the size of the trap. It does, however, manage to contain all the wells with production from this horizon. Model B uses a combination of fault seals plus hydrodynamics, and is a better fit to the oil and gas shows. Model C uses hydrodynamic flow only.

In each model, migration pathways are assigned a value of 0.2 and traps are assigned a value of 1. All three scenarios are summed together to produce the final risk map (bottom figure). The dark green areas are where all models predicted an accumulation. This map fits very well with the established production. Additional maps using seismic facies of the deep water slope channel reservoirs could be made and used as an additional layer of prediction of where reservoirs and seals exist. More variations on fault seal capacity could also be run. Risking the migration pathway itself is useful, as not all structural or stratigraphic traps may have been identified or quantified in the migration model, giving an idea of additional exploration potential.

In the end, generating these kinds of risks maps is the best way to show uncertainty in a migration model. For further rigorous assessment, the thickness and kinetics of the source rocks could be added, as well as migration losses, to make sure enough hydrocarbon is available along the migration pathway to actually give an accumulation.

9.6 Summary

A strong case can be made that reliance on a complicated migration model with one solution that takes many months to derive probably serves academic curiosity more than it does practical oil and gas exploration. All interpreters need to keep in mind just how wrong their maps might be. Oil and gas molecules go where the physical rules governing migration and entrapment force them to go. It is virtually impossible to ensure that all structural maps, fault patterns, facies belts, and hydrodynamic interpretations are perfect. Any maps will always approximate reality at various scales. However, no geoscientist today can ignore the importance of thinking about, and attempting to model, migration with seals and hydrodynamic flow.

On the positive side, models are routinely run which help understand risk and predict the location of new pools. Remaining flexible with the inputs is a key to learning to de-risk entrapment. The science of modeling and quantifying migration is steadily improving, as are the tools required to build seal and reservoir maps necessary to run the models. In the end, the best results are obtained from maps that are generated by interpreters or teams that can acknowledge the limits of their maps and continually seek new data and ideas on how to make the maps more predictive.

Those who can quantify the risks and uncertainties, while doing it quicker and better than others, will reap the benefits in the real world of exploration.

References

Claypool GE, Love AH, Maughan EK (1978) Organic geochemistry, incipient metamorphism, and oil generation in the Black Shale Members of Phosphoria Formation, Western Interior, United States. Am Assoc Pet Geol Bull 62:98–120

Creaney S, Allan J, Cole KS, Fowler MG, Brooks PW, Osadetz KG, Macqueen RW, Snowdon LR, Riediger CL (2012) Petroleum generation and migration in Western Canada Sedimentary Basin, Geological Atlas of the Western Canada Sedimentary Basin. Alberta Geological Survey. http://www.ags.gov.ab.ca/publications/wcsb_atlas/a_ch31/ch_31.html

England WA (1994) Secondary migration and accumulation of hydrocarbons. In: Magoon LB, Dow WG (eds) The Petroleum System—from source to trap. The American Association of Petroleum Geologists, Tulsa, OK, pp 211–217

England WA, Mackenzie AW, Mann DM, Quigley TM (1987) The movement and entrapment of petroleum fluids in the subsurface. J Geol Soc Lond 144:327–347

England WA, Mann AL, Mann DM (1991) Migration from source to trap. In: Merrill RK (ed) Source and migration processes and evaluation techniques, AAPG treatise of petroleum geology, handbook of petroleum geology. The American Association of Petroleum Geologists, Tulsa, OK, pp 23–46

Farrimond P, Naidu BS, Burley SD, Dolson J, Whiteley N, Kothari V (2015) Geochemical characterization of oils and their source rocks in the Barmer Basin, Rajasthan, India. Pet Geosci 21:301–321

Gorenc MA, Chan MA (2015) Hydrocarbon induced diagenetic alteration of the Permian White Rim Sandstone, Elaterite Basin, Southeast Utah. Am Assoc Pet Geol Bull 99:807–829

Gussow WC (1953) Differential trapping of hydrocarbons. Alberta Soc Pet Geol News Bull 1:4–5

Gussow WC (1954) Differential entrapment of oil and gas: a fundamental principle. Am Assoc Pet Geol Bull 38:816–853

Hansley PL (1995) Diagenetic and burial history of the Lower Permian White Rim Sandstone in the Tar Sand Triangle, Paradox Basin, Southeastern Utah: Evolution of Sedimentary Basins-Paradox Basin. United States Geological Survey, Washington, DC

Huntoon JE, Dolson JC, Henry BM (1994) Seals and migration pathways in paleogeomorphically trapped petroleum occurrences: Permian White Rim Sandstone, Tar-Sand Triangle area, Utah. In: Dolson JC, Hendricks ML, Wescott WA (eds) Unconformity-related hydrocarbons in sedimentary sequence. The Rocky Mountain Association of Geologists, Denver, Colorado, pp 99–118

Huntoon JE, Hansley PL, Naeser ND (1999) The search for a source rock for the giant Tar Sand Triangle accumulation, southeast Utah. Am Assoc Pet Geol Bull 83:467–496

MacKenzie AS, Quigley TM (1988) Principle of geochemical prospect appraisal. Am Assoc Pet Geol Bull 72:399–415

Matthews MD (1999) Migration of Petroelum. In: Beaumont EA, Foster NH (eds) Exploring for oil and gas traps: treatise of petroleum geology, handbook of petroleum geology, vol 1. American Association of Petroleum Geologists, Tulsa, OK, pp 8.3–7.38

Maughan EK (1984) Geological setting and some geochemistry of petroleum source rocks in the Permian phosphoria formation, hydrocarbon source rocks of the greater rocky mountain region. Rocky Mountain Association of Geologists, Denver, CO, pp 479–495

Maughan EK (1994) Phosphoria formation (Permian) and its resource significance in the Western Interior, USA, PANGEA: Global Environments and Resources, v. Memoir 17, Canadian Society of Petroleum Geologists, pp 479–495

Naidu BS, Burley SD, Dolson J, Farrimond P, Sunder VR, Kothari V, Mohapatra P, Whiteley N (2016) Hydrocarbon generation and migration modelling in the Barmer Basin of western Rajasthan, India: lessons for exploration in rift basins with late stage inversion, uplift and tilt-

ing. Petroleum System Case Studies, v. Memoir 112. American Association of Petroleum Geologists, Tulsa, OK

Pons MJ, Rainoldi AL, Franchini M, Giusiano A, Cesaretti N, Beaufort D, Patriere P, Impiccini A (2015) Mineralogical signature of hydrocarbon circulation in Cretaceous red beds of the Barda Gonzalez area, Neuquen Basin, Argentina. American Association of Petroleum Geologists Bulletin 99:525–554

Schowalter TT (1979) Mechanics of secondary hydrocarbon migration and entrapment. Am Assoc Pet Geol Bull 63:723–760

Tissot BP, Welte DH (1984) Petroleum formation and occurrence. Springer, Berlin

Appendix A
Common Conversion Equations and Fluid Classifications

Working with shows data requires constant analysis between various units of measurement. Some of the most common units and conversions are given in these tables (Figs. A1, A2, A3).

J. Dolson, *Understanding Oil and Gas Shows and Seals in the Search for Hydrocarbons*, DOI 10.1007/978-3-319-29710-1

Common conversion factors: area and volume

	FROM	Input	Output		TO	Multiplier
Linear Units						
feet	(ft)	3.3	1.007	meters	(m)	0.3050
meters	(m)	1	3.281	feet	(ft)	3.2808
miles	(m)	1	0.621	kilometers	(km)	0.6214
Area Units						
square feet	(ft2)	1	0.093	sq. meters	(m2)	0.0930
square miles	(mi2)	1	2.590	sq. kilometers	(km2)	2.5900
acres	(ac)	1	0.405	hectares	(ha)	0.4050
acres	(ac)	640	2.590	sq. kilometers	(km2)	0.0040
square meters	(m2)	1	10.764	sq. feet	(ft2)	10.7640
square kilometers	(km2)	1	0.386	sq. miles	(mi2)	0.3860
hectares	(ha)	1	2.471	acres	(ac)	2.4710
acres	(ac)	320	1.295	sq. kilometers	(km2)	0.0040
sq. kilometers	(km2)	5	1235.527	acres	(ac)	247.1054
sq. miles		1	2.590	sq. kilometers		2.5900
Volume	**units**					
cubic feet	(ft3)	1	0.028	cubic meters	(m3)	0.0283
cubic feet (oil)	(ft3)	100	23.748	barrels	(bbl)	0.2375
cubic feet (gas)	(ft3)	1000000	172.400	barrels oil equivalent	(boe)	0.0002
cubic meters	(m3)	1000	35315.000	cubic feet	(ft3)	35.3150
cubic meters	(m3)	100	629.000	barrels	(bbl)	6.2900
metric tons	(T)	1000	7330.000	barrels	(bbl)	7.3300
Thousand tons	(thousT)	1	0.007	million barrels	(mmbo)	0.0073
metric tons	(T)	1000000	7.330	million barrels	(mmbo)	0.0000
thousand cubic feet	(mcf)	1	28.317	cubic meters	(m3)	28.3170
million cubic feet	(mmcf)	1	28.317	thousand cubic meters	(thousand m3	28.3170
billion cubic feet	(bcf)	1	28.317	million cubic meters	(million m3)	28.3170
trillion cubic feet	(tcf)	1	28.317	billion cubic meters	(billion m3)	28.3170
cubic meters	(m3)	1000	35.314	thousand cubic feet	(mcf)	0.0353
thousand cubic meters	(thousand m3)	1000	35.314	million cubic feet	(mmcf)	0.0353
thousand cubic meters	(thousand m3)	1000	0.035	billion cubic feet	(bcf)	0.0000
thousand cubic meters	(thousand m3)	1000	0.000	trillion cubic feet	(tcf)	0.0000
million cubic meters	(million m3)	1	35.315	million cubic feet	(mmcf)	35.3150
million cubic meters	(million m3)	1	0.035	billion cubic feet	(bcf)	0.0353
billion cubic meters	(billion m3)	1000	35.314	trillion cubic feet	(tcf)	0.0353
thousand cubic meters	(thousand m3)	1000	1.000	million cubic meters	(million m3)	0.0010
thousand cubic meters	(thousand m3)	100,000	0.100	billion cubic meters	(billion m3)	0.0000
million cubic meters	(million m3)	1000	1.000	billion cubic meters	(billion m3)	0.0010
gallons	(gal)	1	3.785	liters	(L)	3.7850
liters	(L)	1	0.264	gallons	(gal)	0.2640
liters	(L)	1	0.006	barrels	(bbl)	0.0063
barrels	(bbl)	1	0.159	cubic	meters (m3)	0.1590
barrels	(bbl)	1	0.140	metric	tons (MT)	0.1400
barrels	(bbl)	1	158.987	liters	(L)	158.9870

Fig. A1 Common areas and volumes conversions

Common conversions: Mass, Pressure and Energy

	FROM	Input	Output		TO	Multiplier
Mass	**units**					
pounds	(lb)	1	0.454	kilograms	(kg)	0.4540
kilograms	(kg)	1	2.205	pounds	(lb)	2.2050
short tons	(ton)	1	0.907	metric tons	(MT)	0.9070
metric tons	(MT)	1	1.102	short tons	(ton)	1.1020
Pressure	**units**					
pound-force per square in	(psi)	1	6.895	kilopascals	(kPa)	6.8950
pound-force per square in	(psi)	1	0.069	bars	(bar)	0.0690
pounds per sq. inch per foot	psi/ft	1	19.250	pounds per gallon	(ppg)	19.2500
pounds per gallon	ppg	9	0.468	psi/ft		0.0519
kilopascals	(kPa)	1	0.145	pound-force per square in.	(psi)	0.1450
kilopascals	(kPa)	1	0.010	bars	(bar)	0.0100
megapascals	(Mpa)	1	145.000	pounds per square in.	(psi)	145.0000
kilpascals/m	(kPa/m)	10	0.442	pounds per square in/ft	(psi/ft)	0.0442
bars	(bar)	5	72.520	pound-force per square in.	(psi)	14.5040
bars	(bar)	1	100.000	kilopascals	(kPa)	100.0000
grams per cubic centimeter	(g/cc)	0.35	0.152	pounds per square in/ft	(psi/ft)	0.4335
grams per cubic centimeter	(g/cc)	1	8.345	pounds per gallon	(ppg)	8.3450
grams per cubic centimeter	(g/cc)	1	9.806	kilopascals	(kPa)	9.8060
Energy	**units**					
British thermal units	(Btu)	1	1.055	kilojoules	(kJ)	1.0550
kilojoules	(kJ)	1	0.948	British thermal units	(Btu)	0.9480

Degree API gravity = (141.5/ Specific Gravity at 60°F) - 131.5

API gravity	Specific Gravity at 60F	kg/m3	g/cc	psi/ft
8	1.0143	1012	1.01	0.4382
9	1.0071	1005	1.01	0.43517
10	1.0000	998	1	0.43213
15	0.9659	964	0.96	0.41741
20	0.9340	932	0.93	0.40356
25	0.9042	902	0.9	0.39057
30	0.8762	874	0.87	0.37844
35	0.8498	848	0.85	0.36718
40	0.8251	823	0.82	0.35636
45	0.8017	800	0.8	0.3464
50	0.7796	778	0.78	0.33687
55	0.7587	757	0.76	0.32778
58	0.7467	745	0.75	0.32259

Equations in excel.

API gravity	Specific Gravity at 60F	kg/m3	g/cc	psi/ft
8	=141.5/(F85+131.5)	1012	=H85*1000/(100*100*100)	=I85*0.433
9	=141.5/(F86+131.5)	1005	=H86*1000/(100*100*100)	=I86*0.433
10	=141.5/(F87+131.5)	998	=H87*1000/(100*100*100)	=I87*0.433
15	=141.5/(F88+131.5)	964	=H88*1000/(100*100*100)	=I88*0.433
20	=141.5/(F89+131.5)	932	=H89*1000/(100*100*100)	=I89*0.433
25	=141.5/(F90+131.5)	902	=H90*1000/(100*100*100)	=I90*0.433
30	=141.5/(F91+131.5)	874	=H91*1000/(100*100*100)	=I91*0.433
35	=141.5/(F92+131.5)	848	=H92*1000/(100*100*100)	=I92*0.433
40	=141.5/(F93+131.5)	823	=H93*1000/(100*100*100)	=I93*0.433
45	=141.5/(F94+131.5)	800	=H94*1000/(100*100*100)	=I94*0.433
50	=141.5/(F95+131.5)	778	=H95*1000/(100*100*100)	=I95*0.433
55	=141.5/(F96+131.5)	757	=H96*1000/(100*100*100)	=I96*0.433
58	=141.5/(F97+131.5)	745	=H97*1000/(100*100*100)	=I97*0.433

Fig. A2 Pressure, mass, energy and API gravity conversions

Commun fluid classifications

A. Water and hydrocarbon densities.

Fluid	API	Specific Gravity at 60F	kg/m3	g/cc	psi/ft	Solids (ppm)	Comments
Highly saline water						330,000	Dead Sea example
Salt water			1030	1.03	0.4460	> 100,000	
Fresh water			1000	1	0.4330	< 100,000	Very fresh formation water < 10,000 ppm
Bitumen	8	1.014	1012	1.012	0.4382		
Bitumen	9	1.007	1005	1.005	0.4352		
Bitumen	10	1.000	998	0.998	0.4321		
Heavy oil	15	0.966	964	0.964	0.4174		
Heavy oil	20	0.934	932	0.932	0.4036		
Normal oil	25	0.904	902	0.902	0.3906		
Normal oil	30	0.876	874	0.874	0.3784		
Normal oil	35	0.850	848	0.848	0.3672		
Normal oil	40	0.825	823	0.823	0.3564		
Light oil	45	0.802	800	0.8	0.3464		
Light oil	50	0.780	778	0.778	0.3369		
Condensate/gas	55	0.759	757	0.757	0.3278		
Condensate/gas	58	0.747	745	0.745	0.3226		
Wet gas			400	0.4	0.1732		Gas gradients vary substantially with pressure and temperature
Wet gas			200	0.2	0.0866		
Dry Gas			100	0.1	0.0433		
Dry Gas			7	0.007	0.0030		

B. Mud gas classification and components.

Component	Description	Dry gas Mol %	Wet gas Mol %	Gas condensate Mol %	Volatile oil Mol %	Black oil Mol %	Comments
CO_2	Carbon dioxide	0.1	1.41	2.37	1.82	0.02	
N_2		2.07	0.25	0.31	0.24	0.34	
C_1	Methane	86.12	92.46	73.19	57.6	34.62	
C_2	Ethane	5.91	3.18	7.8	7.35	4.11	
C_3	Propane	3.58	1.01	3.55	4.21	1.01	
iC_4	Isobutane	1.72	0.8	0.71	0.74	0.76	
nC_4	Normal butane		0.24	1.45	2.07	0.49	
iC_5	Isopentane	0.5	0.13	0.64	0.53	0.43	C_5 and higher are important possible oil show indicators
nC_5	Normal pentane		0.08	0.68	0.95	0.21	
C_{6s}	Hexane		0.14	1.09	1.92	1.16	
C_{7+}	Heptane		0.82	8.21	22.57	56.4	
Density measures							
GOR (SCF/STB)	Gas oil ratio (standard ft^3/stock tank barrel)		69000	5965	1465	320	
OGR (STB/MMSCF)	Oil gas ratio (stock tank barrels/million standard ft^3	0	15	165	680	3125	
API gravity	API gravity		65	48.5	36.7	23.6	

Fig. A3 Common fluid classifications. Figure 8 modified from Whitson, 1992

References

Whitson CH (1992) Petroleum reservoir fluid properties. In: Morton-Thompson D, Woods AM (eds) Development Geology Reference Manual. Tulsa, Oklahoma: American Association of Petroleum Geologists, p. 504–507

Appendix B
Constructing Winland Pore Throat Graphs in Excel

Porosity and permeability is best initially viewed with overlays of predicted pore throat radii. The plots not only show potential seals and baffles by facies or pore throat distribution, but can be used to estimate inputs to pseudo-capillary pressure spreadsheets (Appendix D) by choosing representative porosity and permeability pairs by pore size. The equations are discussed at length in the book, but are also in (Pittman, 1992).

The overlay lines are calculated by giving standard ranges of porosity on the x axis and then solving for permeability using the Winland R35 equation, for each port size. Examples follow (Figs. A4, A5, A6).

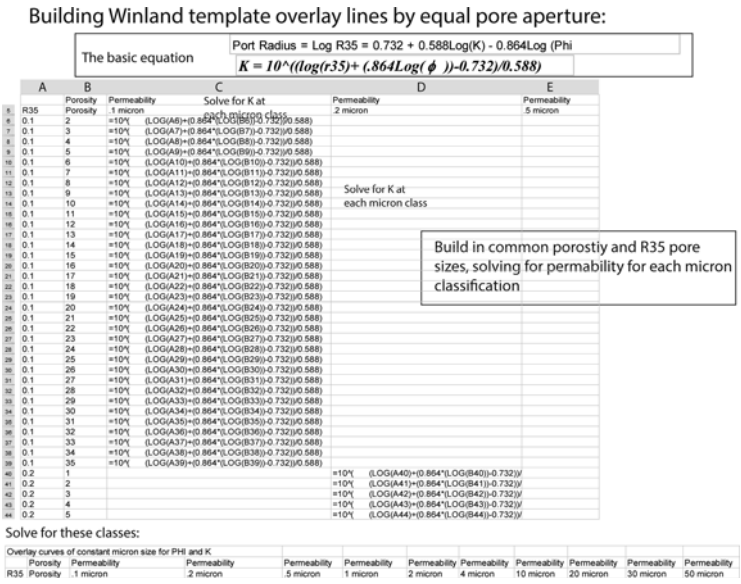

Fig. A4 This is the basic way to set up the overlay lines. Porosity must be entered as whole percent, not decimal

J. Dolson, *Understanding Oil and Gas Shows and Seals in the Search for Hydrocarbons*, DOI 10.1007/978-3-319-29710-1

Building Winland template overlay lines by equal pore aperture:

The basic equation	Port Radius = Log R35 = 0.732 + 0.588Log(K) - 0.864Log (Phi
	$K = 10^{((\log(r35)+ (.864\log(\phi))-0.732)/0.588)}$

An answer example

		Porosity	Permeability	Permeability	Permeability	Permeability
R35		Porosity	.1 micron	.2 micron	.5 micron	1 micron
0.1	2		0.0031			
0.1	3		0.0057			
0.1	4		0.0087			
0.1	5		0.0121			
0.1	6		0.0158			
0.1	7		0.0198			
0.1	8		0.0241			
0.1	9		0.0286			
0.1	10		0.0334			
0.1	11		0.0384			
0.1	12		0.0437			
0.1	13		0.0491			
0.1	14		0.0548			
0.1	15		0.0606			
0.1	16		0.0666			
0.1	17		0.0728			
0.1	18		0.0792			
0.1	19		0.0858			
0.1	20		0.0925			
0.1	21		0.0994			
0.1	22		0.1064			
0.1	23		0.1136			
0.1	24		0.1209			
0.1	25		0.1284			
0.1	26		0.1360			
0.1	27		0.1438			
0.1	28		0.1517			
0.1	29		0.1597			
0.1	30		0.1678			
0.1	31		0.1761			
0.1	32		0.1845			
0.1	33		0.1931			
0.1	34		0.2017			
0.1	35		0.2105			
0.2	1			0.0037		
0.2	2			0.0102		
0.2	3			0.0185		
0.2	4			0.0283		
0.2	5			0.0392		
0.2	6			0.0513		
0.2	7			0.0643		
0.2	8			0.0782		

Fig. A5 If you did it right, you should get numbers like these. Note that porosity is in whole percent, not decimal

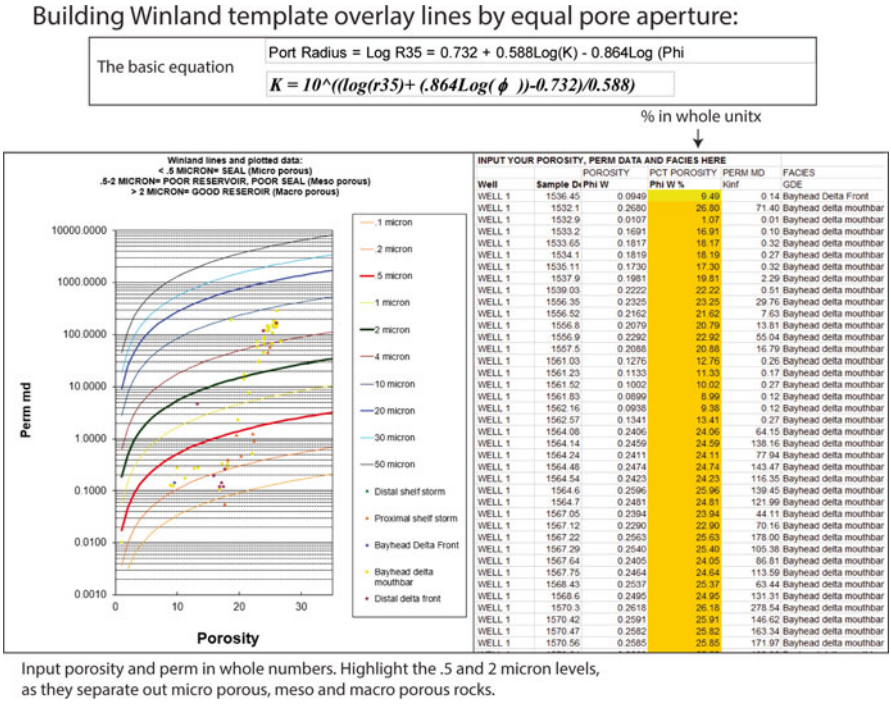

Well	Sample Dv	POROSITY Phi W	PCT POROSITY Phi W %	PERM MD Kinf	FACIES GDE
WELL 1	1536.45	0.0949	9.49	0.14	Bayhead Delta Front
WELL 1	1532.1	0.2680	26.80	71.40	Bayhead delta mouthbar
WELL 1	1532.9	0.0107	1.07	0.01	Bayhead delta mouthbar
WELL 1	1533.2	0.1691	16.91	0.10	Bayhead delta mouthbar
WELL 1	1533.65	0.1817	18.17	0.32	Bayhead delta mouthbar
WELL 1	1534.1	0.1819	18.19	0.27	Bayhead delta mouthbar
WELL 1	1535.11	0.1730	17.30	0.32	Bayhead delta mouthbar
WELL 1	1537.9	0.1981	19.81	2.29	Bayhead delta mouthbar
WELL 1	1539.03	0.2222	22.22	0.51	Bayhead delta mouthbar
WELL 1	1556.35	0.2325	23.25	29.76	Bayhead delta mouthbar
WELL 1	1556.52	0.2162	21.62	7.63	Bayhead delta mouthbar
WELL 1	1556.8	0.2079	20.79	13.81	Bayhead delta mouthbar
WELL 1	1556.9	0.2292	22.92	55.04	Bayhead delta mouthbar
WELL 1	1557.5	0.2088	20.88	16.79	Bayhead delta mouthbar
WELL 1	1561.03	0.1276	12.76	0.26	Bayhead delta mouthbar
WELL 1	1561.23	0.1133	11.33	0.17	Bayhead delta mouthbar
WELL 1	1561.52	0.1002	10.02	0.27	Bayhead delta mouthbar
WELL 1	1561.83	0.0899	8.99	0.12	Bayhead delta mouthbar
WELL 1	1562.16	0.0938	9.38	0.12	Bayhead delta mouthbar
WELL 1	1562.57	0.1341	13.41	0.27	Bayhead delta mouthbar
WELL 1	1564.08	0.2406	24.06	64.15	Bayhead delta mouthbar
WELL 1	1564.14	0.2459	24.59	138.16	Bayhead delta mouthbar
WELL 1	1564.24	0.2411	24.11	77.94	Bayhead delta mouthbar
WELL 1	1564.48	0.2474	24.74	143.47	Bayhead delta mouthbar
WELL 1	1564.54	0.2423	24.23	116.35	Bayhead delta mouthbar
WELL 1	1564.6	0.2596	25.96	139.45	Bayhead delta mouthbar
WELL 1	1564.7	0.2481	24.81	121.99	Bayhead delta mouthbar
WELL 1	1567.05	0.2394	23.94	44.11	Bayhead delta mouthbar
WELL 1	1567.12	0.2290	22.90	70.16	Bayhead delta mouthbar
WELL 1	1567.22	0.2563	25.63	178.00	Bayhead delta mouthbar
WELL 1	1567.29	0.2540	25.40	105.38	Bayhead delta mouthbar
WELL 1	1567.64	0.2405	24.05	86.81	Bayhead delta mouthbar
WELL 1	1567.75	0.2464	24.64	113.59	Bayhead delta mouthbar
WELL 1	1568.43	0.2537	25.37	63.44	Bayhead delta mouthbar
WELL 1	1568.6	0.2495	24.95	131.31	Bayhead delta mouthbar
WELL 1	1570.3	0.2618	26.18	278.54	Bayhead delta mouthbar
WELL 1	1570.42	0.2591	25.91	146.62	Bayhead delta mouthbar
WELL 1	1570.47	0.2582	25.82	163.34	Bayhead delta mouthbar
WELL 1	1570.56	0.2585	25.85	171.97	Bayhead delta mouthbar

Fig. A6 Final graphs will readily show flow units by facies. Remember that porosity is entered as whole percent, not decimal. This is an example broken out by facies

References

Pittman E (1992) Relationship of porosity and permeability to various parameters derived from mercury injection-capillary pressure curves for sandstone. Am Assoc Pet Geol Bull 76: 191–198

Appendix C
Equations in Excel to Convert Mercury-Injection Capillary Pressure Data to Height Above Free Water

The conversion of mercury injection data takes two steps (Fig. A7):

The methodology and equations are further detailed in numerous papers (Glover, 2015; Hartmann and Beaumont, 1999; Pittman, 1992; Schowalter, 1979; Vavra et al., 1992; Washburn, 1921). The reader is also referred to Appendix A, which

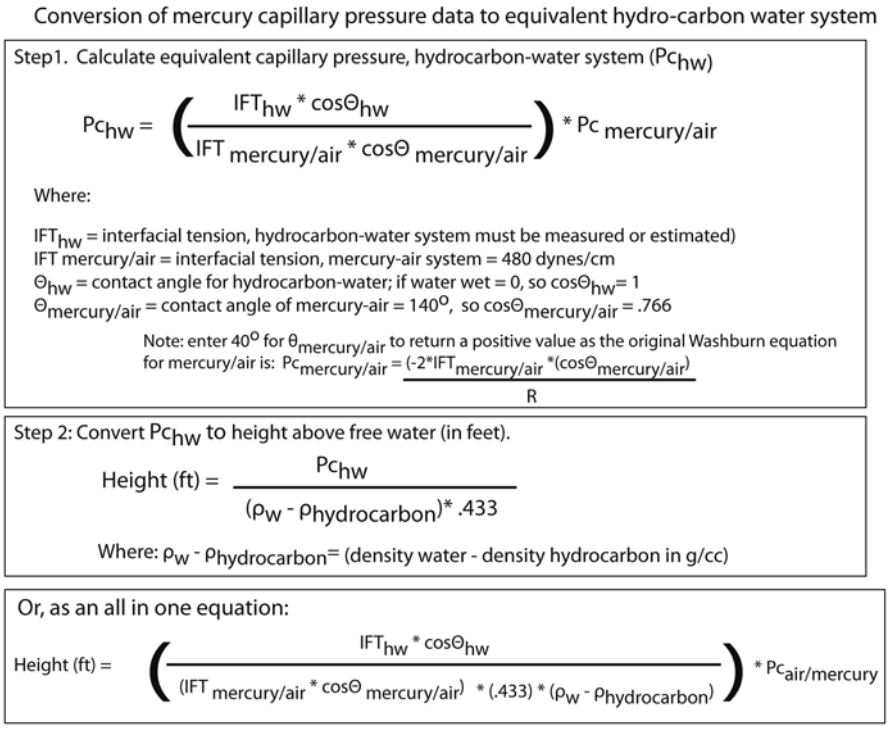

Fig. A7 Equations for conversion to height above free water using mercury-air data

J. Dolson, *Understanding Oil and Gas Shows and Seals in the Search for Hydrocarbons*, DOI 10.1007/978-3-319-29710-1

contains conversion formulas and tables useful. It is particularly useful to remember that 1 g/cc density = .433 psi/ft. It is also useful to remember or calculate density in g/cc based on API gravity from equations shown earlier and in Appendix A. Inputs to all of the capillary pressure spreadsheets will be in metric units, with output in both feet and meters. Also note that in Excel, converting the cosine of a number first requires conversion of the angle to radians. This is built into the spreadsheets shown. With a hand-held calculator, this is not necessary.

The Excel equations are shown in Fig. A8 and an example plot using the input parameters shown on Fig. A8 is shown in Fig. A9.

A. Inputs to convert to height above free water

Input		
Interfacial tension (dynes/cm)	$IFT_{w/hc}$	30
Wettability (degrees)	Θ w/hc (water to hydrocarbon)	30
Density (g/cc)	$\rho_{hydrocarbon}$ (Density, g/cc)	0.7
Density (g/cc)	ρ_{w} (Density water, g/cc)	1
Interfacial tension (dynes/cm)	$IFT_{mercury/air}$	480
Wettability (degrees)	Θ (mercury/)air	140

Depth	2856
Wellname	Well 1
Depth	2856
Porosity	15.86 por
Permeability	0.87 md
Facies	tidal flat
Core SW	
Degree of Stain	mod stain

This kind of information is useful to enter for legends with details or the rocks being analyzed (they are not used in equations)

Key input parameters

B. Equations used to convert values in A to height above free water.

	Step 1 numerator	Step 1 denominator	Capillary Pressure, Lab (psi)	Hg saturation (whole %)	Pc hw	Sw	Height ,m	Height, ft.	Pore Throat Radius (microns)	Pore radius calculation formula in psi mercury
11	IFThw * cos(Θ) hw	IFT merc/air * cos(Θ)merc/air	1	0.2	=($C$12/$D$12) *E11	=100-F11	=J11/3.281	=(G11/((($C$5-$C$4)*0.433))	=$L$11/E11	=(2*$C$7)*(ABS(COS(RADIANS($C$8)))*0.145))
12	=C2*(ABS(COS(RADIANS($C$3))))	=C7*(ABS(COS(RADIANS($C$8))))	3	0.5	=($C$12/$D$12) *E12	=100-F12	=J12/3.281	=(G12/((($C$5-$C$4)*0.433))	=$L$11/E12	
13			5	0.6	=($C$12/$D$12) *E13	=100-F13	=J13/3.281	=(G13/((($C$5-$C$4)*0.433))	=$L$11/E13	
14			7	0.7	=($C$12/$D$12) *E14	=100-F14	=J14/3.281	=(G14/((($C$5-$C$4)*0.433))	=$L$11/E14	
15			10	0.8	=($C$12/$D$12) *E15	=100-F15	=J15/3.281	=(G15/((($C$5-$C$4)*0.433))	=$L$11/E15	
16			15	1	=($C$12/$D$12) *E16	=100-F16	=J16/3.281	=(G16/((($C$5-$C$4)*0.433))	=$L$11/E16	
17			20	1.5	=($C$12/$D$12) *E17	=100-F17	=J17/3.281	=(G17/((($C$5-$C$4)*0.433))	=$L$11/E17	
18			40	30	=($C$12/$D$12) *E18	=100-F18	=J18/3.281	=(G18/((($C$5-$C$4)*0.433))	=$L$11/E18	
19			60	39.7	=($C$12/$D$12) *E19	=100-F19	=J19/3.281	=(G19/((($C$5-$C$4)*0.433))	=$L$11/E19	
20			80	44.9	=($C$12/$D$12) *E20	=100-F20	=J20/3.281	=(G20/((($C$5-$C$4)*0.433))	=$L$11/E20	
21			100	48.4	=($C$12/$D$12) *E21	=100-F21	=J21/3.281	=(G21/((($C$5-$C$4)*0.433))	=$L$11/E21	
22			150	53.8	=($C$12/$D$12) *E22	=100-F22	=J22/3.281	=(G22/((($C$5-$C$4)*0.433))	=$L$11/E22	
23			200	57.3	=($C$12/$D$12) *E23	=100-F23	=J23/3.281	=(G23/((($C$5-$C$4)*0.433))	=$L$11/E23	
24			300	61.7	=($C$12/$D$12) *E24	=100-F24	=J24/3.281	=(G24/((($C$5-$C$4)*0.433))	=$L$11/E24	
25			500	67.2	=($C$12/$D$12) *E25	=100-F25	=J25/3.281	=(G25/((($C$5-$C$4)*0.433))	=$L$11/E25	
26			750	73.8	=($C$12/$D$12) *E26	=100-F26	=J26/3.281	=(G26/((($C$5-$C$4)*0.433))	=$L$11/E26	
27			1000	78.3	=($C$12/$D$12) *E27	=100-F27	=J27/3.281	=(G27/((($C$5-$C$4)*0.433))	=$L$11/E27	
28			1250	80.9	=($C$12/$D$12) *E28	=100-F28	=J28/3.281	=(G28/((($C$5-$C$4)*0.433))	=$L$11/E28	
29			1500	83.2	=($C$12/$D$12) *E29	=100-F29	=J29/3.281	=(G29/((($C$5-$C$4)*0.433))	=$L$11/E29	
30			1750	85	=($C$12/$D$12) *E30	=100-F30	=J30/3.281	=(G30/((($C$5-$C$4)*0.433))	=$L$11/E30	
31			2000	86.6	=($C$12/$D$12) *E31	=100-F31	=J31/3.281	=(G31/((($C$5-$C$4)*0.433))	=$L$11/E31	

$$R = \frac{2\gamma cos\theta}{Pc}$$

Notes:
1. IFT and wettability need to be estimated if no direct measurements are available
2. Densities are in g/cc and should represent subsurface temperatures and pressures. Appendix A2 has many equivalencies for input.

Fig. A8 Input equations in Excel for mercury-air capillary pressure conversions to height above free water

Output answer:

Input		
Interfacial tension (d	$IFT_{w/hc}$	30
Wettability (degrees	Θ w/hc (water to hyd	30
Density (g/cc)	$\rho_{hydrocarbon}$ (Density, g/cc	0.7
Density (g/cc)	ρ_{w} (Density water, g/cc)	1
Interfacial tension (d	$IFT_{mercury/air}$	480
Wettability (degrees	Θ (mercury/)air	140

Depth	2856
Wellname	Well 1
Depth	2856
Porosity	15.86 por
Permeability	0.87 md
Facies	tidal flat
Core SW	
Degree of Stain	mod stain

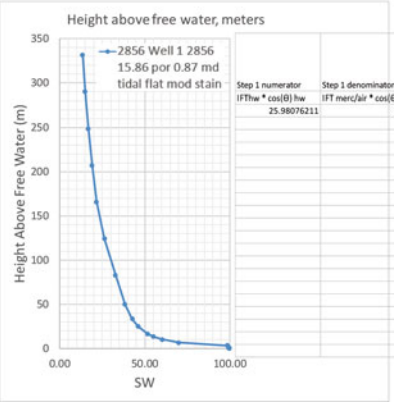

Step 1 numerator IFThw * cos(Θ) hw	Step 1 denominator IFT merc/air * cos(Θ)merc/air	
25.98076211		367.7013327

Capillary Pressure, Lab (psi)	Hg saturation (whole %)	Pc hw	Sw	Height ,m	Height, ft	Pore Throat Radius (microns)	Pore radius calculation formula in psi mercury
1.00	0.20	0.07065724	99.80	0.16578	0.5439356	106.633386	106.6333865
3.00	0.50	0.21197173	99.50	0.49735	1.631806979	35.544462	
5.00	0.60	0.35328621	99.40	0.82892	2.719678298	21.326677	
7.00	0.70	0.4946007	99.30	1.16048	3.807549617	15.233341	
10.00	0.80	0.70657242	99.20	1.65783	5.439356596	10.663339	
15.00	1.00	1.05985863	99.00	2.48675	8.159034894	7.108892	
20.00	1.50	1.41314484	98.50	3.31567	10.87871319	5.331669	
40.00	30.00	2.82628969	70.00	6.63134	21.75742638	2.665835	
60.00	39.70	4.23943453	60.30	9.94701	32.63613957	1.777223	
80.00	44.90	5.65257937	55.10	13.2627	43.51485277	1.332917	
100.00	48.40	7.06572422	51.60	16.5783	54.39356596	1.066334	
150.00	53.80	10.5985863	46.20	24.8675	81.59034894	0.710889	
200.00	57.30	14.1314484	42.70	33.1567	108.7871319	0.533167	
300.00	61.70	21.1971727	38.30	49.735	163.1806979	0.355445	
500.00	67.20	35.3286211	32.80	82.8917	271.9678298	0.213267	
750.00	73.80	52.9929316	26.20	124.338	407.9517447	0.142178	
1000.00	78.30	70.6572422	21.70	165.783	543.9356596	0.106633	
1250.00	80.90	88.3215527	19.10	207.229	679.9195745	0.085307	
1500.00	83.20	105.985863	16.80	248.675	815.9034894	0.071089	
1750.00	85.00	123.650174	15.00	290.121	951.8874042	0.060933	
2000.00	86.60	141.314484	13.40	331.567	1087.871319	0.053317	

Fig. A9 Graphical and numeric solution for equations shown in Fig. A8

References, Capillary Pressure Conversion, Appendix B

Glover P (2015) Chapter 8: capillary pressure, formation evaluation msc course notes. United Kingdom: Leeds University

Hartmann DJ, Beaumont EA (1999) Predicting reservoir system quality and performance. In: Beaumont EA, Foster NH (eds) Exploring for oil and gas traps: treatise of petroleum geology. Handbook of Petroleum Geology, v. 1: Tulsa, Oklahoma, American Association of Petroleum Geologists, p. 9.3–9.154

Pittman E (1992) Relationship of porosity and permeability to various parameters derived from mercury injection-capillary pressure curves for sandstone. Am Assoc Pet Geol Bull 76:191–198

Schowalter TT (1979) Mechanics of secondary hydrocarbon migration and entrapment. Am Assoc Pet Geol Bull 63:723–760

Vavra CL, Kaldi JG, Sneider RM (1992) Geological applications of capillary pressure: a review. Am Assoc Pet Geol Bull 76:840–850

Washburn EW (1921) Note on a method of determining the distribution of pore seizes in a porous material. Proc Nat Acad Sci 7:115–116

Appendix D
Equations in Excel to Make Pseudo-Capillary Pressure Curves

The following examples show 3 different equations and approaches to understanding height above free water. All three approaches yield identical answers. There are other approaches, but these are good enough to provide a practical look at potential reservoir performance and seal capacity. Building up these spreadsheets to contain more than one rock type on a plot or spreadsheet is advisable to get a feel for the ranges of variations in solutions, not just due to uncertainty in IFT, wettability or subsurface densities, but due to the fact that rocks are complex and one solution will seldom provide the only answer.

Three separate approaches are used to reinforce the mathematical concepts behind capillarity. In the even the reader has a different way to calculate pore throat radii, these equations form a basis for substituting in other solutions to pore throat sizes, and thus facilitate personalizing new spreadsheets with other solutions.

The reader is also referred to Appendix A, which contains conversion formulas and useful tables. It is particularly useful to remember that 1 g/cc density = 0.433 psi/ft. It is also useful to remember or calculate density in g/cc based on API gravity from equations shown earlier and in Appendix A. Inputs to all of the capillary pressure spreadsheets will be in metric units, with output in both feet and meters. The conversion equations used convert to height above free water in feet, and then a second column converts to meters.

Also note that in Excel, converting the cosine of a number first requires conversion of the angle to radians. This is built into the spreadsheets shown. With a handheld calculator, this is not necessary.

Conversion using (Hartmann and Beaumont, 1999) equations with (Pittman, 1992) pore throat estimates from porosity and permeability (Figs. A10, A11, A12, A13, A14, A15).

J. Dolson, *Understanding Oil and Gas Shows and Seals in the Search for Hydrocarbons*, DOI 10.1007/978-3-319-29710-1

Pseudo-capillary pressure using Pittman (1992) pore throat equations

1. Step 1- Calculate R values from equations
2. Step 2- Convert to height above free water (ft)

Inputs to equations from your area

Sample	Porosity (whole pct)	Perm (md)
Rock 1	15	2
IFT (γ)	30.000000	
Theta (θ)	0.000000	
Density water (g/cc)	1.000000	
Density hydrocarbon (g/cc)	0.800000	

Hartmann and Beaumont equation

H (ft) = (0.670 * IFT (Cos θ))/(R * (Dw-Dh))

Where IFT = Interfacial tension of hydrocarbon-water in dynes/cm

θ = Wettability

Dw = Density of water in g/cc

Dh = Density of hydrocarbon in g/cc

R = Pore throat radius at R_{10} from above

Mercury Percentile	Pittman equations R in micron	Equiv SW %	.670*ycosθ	R*(Dw-Dh	Equiv H ft	Equiv H m
r10	=10^((0.459+0.5*LOG(C2)-0.385*LOG(B2)))	90	=0.67*(($B$4)*(COS(RADIANS($B$5))))	=B11*($B$6-$B$7)	=D11/E11	=F11/3.281
r15	=10^((0.333+0.509*LOG(C2)-0.344*LOG(B2)))	85	=0.67*(($B$4)*(COS(RADIANS($B$5))))	=B12*($B$6-$B$7)	=D12/E12	=F12/3.281
r20	=10^((0.218+0.519*LOG(C2)-0.303*LOG(B2)))	80	=0.67*(($B$4)*(COS(RADIANS($B$5))))	=B13*($B$6-$B$7)	=D13/E13	=F13/3.281
r25	=10^((0.204+0.531*LOG(C2)-0.35*LOG(B2)))	75	=0.67*(($B$4)*(COS(RADIANS($B$5))))	=B14*($B$6-$B$7)	=D14/E14	=F14/3.281
r30	=10^((0.215+0.547*LOG(C2)-0.42*LOG(B2)))	70	=0.67*(($B$4)*(COS(RADIANS($B$5))))	=B15*($B$6-$B$7)	=D15/E15	=F15/3.281
r35	=10^((0.255+0.565*LOG(C2)-0.523*LOG(B2)))	65	=0.67*(($B$4)*(COS(RADIANS($B$5))))	=B16*($B$6-$B$7)	=D16/E16	=F16/3.281
r40	=10^((0.36+0.582*LOG(C2)-0.68*LOG(B2)))	60	=0.67*(($B$4)*(COS(RADIANS($B$5))))	=B17*($B$6-$B$7)	=D17/E17	=F17/3.281
r45	=10^((0.609+0.608*LOG(C2)-0.974*LOG(B2)))	55	=0.67*(($B$4)*(COS(RADIANS($B$5))))	=B18*($B$6-$B$7)	=D18/E18	=F18/3.281
r50	=10^((0.778+0.626*LOG(C2)-1.205*LOG(B2)))	50	=0.67*(($B$4)*(COS(RADIANS($B$5))))	=B19*($B$6-$B$7)	=D19/E19	=F19/3.281
r55	=10^((0.948+0.632*LOG(C2)-1.426*LOG(B2)))	45	=0.67*(($B$4)*(COS(RADIANS($B$5))))	=B20*($B$6-$B$7)	=D20/E20	=F20/3.281
r60	=10^((1.096+0.648*LOG(C2)-1.666*LOG(B2)))	40	=0.67*(($B$4)*(COS(RADIANS($B$5))))	=B21*($B$6-$B$7)	=D21/E21	=F21/3.281
r65	=10^((1.372+0.643*LOG(C2)-1.979*LOG(B2)))	35	=0.67*(($B$4)*(COS(RADIANS($B$5))))	=B22*($B$6-$B$7)	=D22/E22	=F22/3.281
r70	=10^((1.664+0.627*LOG(C2)-2.314*LOG(B2)))	30	=0.67*(($B$4)*(COS(RADIANS($B$5))))	=B23*($B$6-$B$7)	=D23/E23	=F23/3.281
r75	=10^((1.88+0.609*LOG(C2)-2.626*LOG(B2)))	25	=0.67*(($B$4)*(COS(RADIANS($B$5))))	=B24*($B$6-$B$7)	=D24/E24	=F24/3.281
rApex	=10^((0.459+0.5*LOG(C2)-0.385*LOG(B2)))		=0.67*(($B$4)*(COS(RADIANS($B$5))))	=B25*($B$6-$B$7)	=D25/E25	=F25/3.281
rpd (showalter)	=10^((0.459+0.5*LOG(C2)-0.385*LOG(B2)))		=0.67*(($B$4)*(COS(RADIANS($B$5))))	=B26*($B$6-$B$7)	=D26/E26	=F26/3.281
rAPEX	=10^((-0.117+0.475*LOG(C2)-0.099*LOG(B2)))		=0.67*(($B$4)*(COS(RADIANS($B$5))))	=B27*($B$6-$B$7)	=D27/E27	=F27/3.281

Pittman equations Equiv Sw is1-R precentile; r10 = 90% Sw Converts numerator Converts denominator

Fig. A10 Pittman equations (Pittman, 1992) in excel and conversion to height above free water from Hartmann and Beaumont, 1999

Answer using inputs given and conversion equation from Hartmann and Beaumont, 1999

Sample	Porosity (whole pct)	Perm (md)
Rock 1	15	2
IFT (γ)	30.000000	
Theta (θ)	0.000000	
Density water (g/cc)	1.000000	
(g/cc)	0.800000	

Mercury Percentile	Pittman equations R in micron	Equiv SW %	.670*ycosθ	R*(Dw-Dh	Equiv H ft	Equiv H m
r10	1.434564	90		20.10	0.2869	70.06	21.35
r15	1.206838	85		20.10	0.2414	83.28	25.38
r20	1.042027	80		20.10	0.2084	96.45	29.40
r25	0.895808	75		20.10	0.1792	112.19	34.19
r30	0.768608	70		20.10	0.1537	130.76	39.85
r35	0.645634	65		20.10	0.1291	155.66	47.44
r40	0.543823	60		20.10	0.1088	184.80	56.33
r45	0.443112	55		20.10	0.0886	226.81	69.13
r50	0.354205	50		20.10	0.0708	283.73	86.48
r55	0.289164	45		20.10	0.0578	347.55	105.93
r60	0.214634	40		20.10	0.0429	468.24	142.71
r65	0.173013	35		20.10	0.0346	580.88	177.04
r70	0.135292	30		20.10	0.0271	742.84	226.41
r75	0.094387	25		20.10	0.0189	1064.77	324.53
rApex	1.434564			20.10	0.2869	70.06	21.35
rpd (showalter)	1.434564			20.10	0.2869	70.06	21.35
rAPEX	0.812000			20.10	0.1624	123.77	37.72

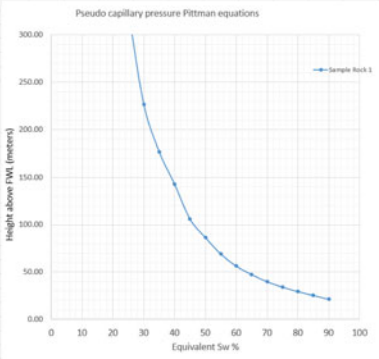

Fig. A11 Answer for the inputs given in Fig. A10. The r10 value approximates both seal capacity and position of the oil-water contact above free water. In this example, the rock is a highly effective seal and the oil-water contact would be 21.35 m (70.06') meters above free water

Inputs to equations from your area

	A	B	C
1	Sample	Porosity (whole pct)	Perm
2	Rock 1	15.000000	1.00
3			
4	IFT	30.00000	
5	Theta	30.00000	
6	Density water (g/cc)	1.00000	
7	Density hydrocarbon (g/cc)	0.84000	

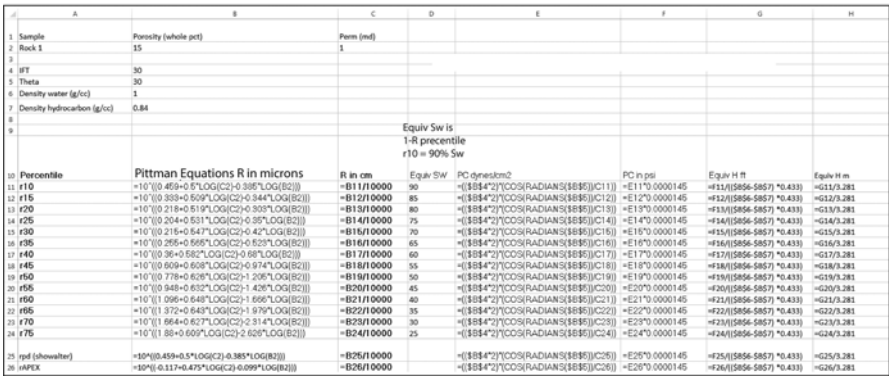

	A	B	C	D	E	F	G	H
1	Sample	Porosity (whole pct)	Perm (md)					
2	Rock 1	15	1					
3								
4	IFT	30						
5	Theta	30						
6	Density water (g/cc)	1						
7	Density hydrocarbon (g/cc)	0.84						
8								
9				Equiv Sw is 1-R precentile r10 = 90% Sw				
10	Percentile	Pittman Equations R in microns	R in cm	Equiv SW	PC dynes/cm2	PC in psi	Equiv H ft	Equiv H m
11	r10	=10^((0.459+0.5*LOG(C2)-0.395*LOG(B2)))	=B11/10000	90	=((($B$4*2)*(COS(RADIANS($B$5)))C11))	=E11*0.0000145	=F11/($B$6-$B$7) *0.433)	=G11/3.281
12	r15	=10^((0.333+0.509*LOG(C2)-0.344*LOG(B2)))	=B12/10000	85	=((($B$4*2)*(COS(RADIANS($B$5)))C12))	=E12*0.0000145	=F12/($B$6-$B$7) *0.433)	=G12/3.281
13	r20	=10^((0.218+0.519*LOG(C2)-0.303*LOG(B2)))	=B13/10000	80	=((($B$4*2)*(COS(RADIANS($B$5)))C13))	=E13*0.0000145	=F13/($B$6-$B$7) *0.433)	=G13/3.281
14	r25	=10^((0.204+0.531*LOG(C2)-0.35*LOG(B2)))	=B14/10000	75	=((($B$4*2)*(COS(RADIANS($B$5)))C14))	=E14*0.0000145	=F14/($B$6-$B$7) *0.433)	=G14/3.281
15	r30	=10^((0.216+0.647*LOG(C2)-0.42*LOG(B2)))	=B15/10000	70	=((($B$4*2)*(COS(RADIANS($B$5)))C15))	=E15*0.0000145	=F15/($B$6-$B$7) *0.433)	=G15/3.281
16	r35	=10^((0.255+0.665*LOG(C2)-0.523*LOG(B2)))	=B16/10000	65	=((($B$4*2)*(COS(RADIANS($B$5)))C16))	=E16*0.0000145	=F16/($B$6-$B$7) *0.433)	=G16/3.281
17	r40	=10^((0.36+0.582*LOG(C2)-0.68*LOG(B2)))	=B17/10000	60	=((($B$4*2)*(COS(RADIANS($B$5)))C17))	=E17*0.0000145	=F17/($B$6-$B$7) *0.433)	=G17/3.281
18	r45	=10^((0.609+0.608*LOG(C2)-0.974*LOG(B2)))	=B18/10000	55	=((($B$4*2)*(COS(RADIANS($B$5)))C18))	=E18*0.0000145	=F18/($B$6-$B$7) *0.433)	=G18/3.281
19	r50	=10^((0.778+0.626*LOG(C2)-1.206*LOG(B2)))	=B19/10000	50	=((($B$4*2)*(COS(RADIANS($B$5)))C19))	=E19*0.0000145	=F19/($B$6-$B$7) *0.433)	=G19/3.281
20	r55	=10^((0.948+0.632*LOG(C2)-1.426*LOG(B2)))	=B20/10000	45	=((($B$4*2)*(COS(RADIANS($B$5)))C20))	=E20*0.0000145	=F20/($B$6-$B$7) *0.433)	=G20/3.281
21	r60	=10^((1.096+0.648*LOG(C2)-1.666*LOG(B2)))	=B21/10000	40	=((($B$4*2)*(COS(RADIANS($B$5)))C21))	=E21*0.0000145	=F21/($B$6-$B$7) *0.433)	=G21/3.281
22	r65	=10^((1.372+0.643*LOG(C2)-1.979*LOG(B2)))	=B22/10000	35	=((($B$4*2)*(COS(RADIANS($B$5)))C22))	=E22*0.0000145	=F22/($B$6-$B$7) *0.433)	=G22/3.281
23	r70	=10^((1.664+0.627*LOG(C2)-2.314*LOG(B2)))	=B23/10000	30	=((($B$4*2)*(COS(RADIANS($B$5)))C23))	=E23*0.0000145	=F23/($B$6-$B$7) *0.433)	=G23/3.281
24	r75	=10^((1.88+0.609*LOG(C2)-2.626*LOG(B2)))	=B24/10000	25	=((($B$4*2)*(COS(RADIANS($B$5)))C24))	=E24*0.0000145	=F24/($B$6-$B$7) *0.433)	=G24/3.281
25	rpd (showalter)	=10^((0.459+0.5*LOG(C2)-0.385*LOG(B2)))	=B25/10000		=((($B$4*2)*(COS(RADIANS($B$5)))C25))	=E25*0.0000145	=F25/($B$6-$B$7) *0.433)	=G25/3.281
26	rAPEX	=10^((-0.117+0.475*LOG(C2)-0.099*LOG(B2)))	=B26/10000		=((($B$4*2)*(COS(RADIANS($B$5)))C26))	=E26*0.0000145	=F26/($B$6-$B$7) *0.433)	=G26/3.281

Fig. A12 Classic equations treat R in cm. Here are the conversions

Answer using inputs given and conversion equation from Hartmann and Beaumont, 1999
These are the answers for equations using R in cm, which is the classic way of displaying the equation for capillarity.
Winland equations return a value of R in microns, and 10,000 microns = 1 cm
The example is a meso-porous rock layer, partially oil-wet and an IFT of 30 and density of .84 g/cc (oil) in a fresh water system, where Dw = 1 g/cc.

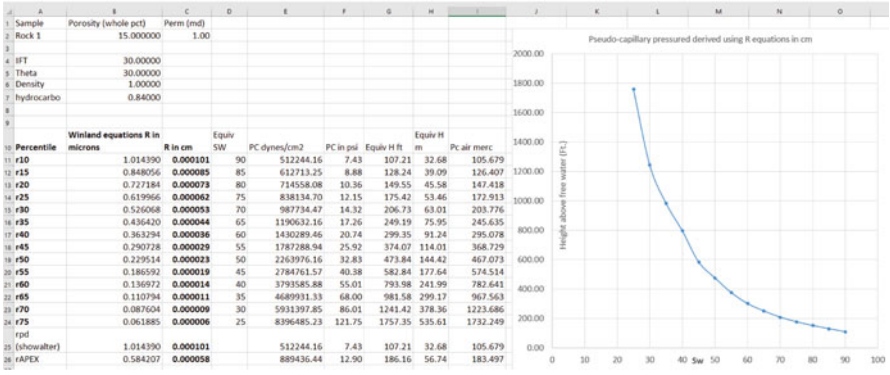

	A	B	C	D	E	F	G	H	I
1	Sample	Porosity (whole pct)	Perm (md)						
2	Rock 1	15.000000	1.00						
3									
4	IFT	30.00000							
5	Theta	30.00000							
6	Density	1.00000							
7	hydrocarbo	0.84000							
8									
9									
10	Percentile	Winland equations R in microns	R in cm	Equiv SW	PC dynes/cm2	PC in psi	Equiv H ft	Equiv H m	Pc air merc
11	r10	1.014390	0.000101	90	512244.16	7.43	107.21	32.68	105.679
12	r15	0.848056	0.000085	85	612713.25	8.88	128.24	39.09	126.407
13	r20	0.727184	0.000073	80	714558.08	10.36	149.55	45.58	147.418
14	r25	0.619966	0.000062	75	838134.70	12.15	175.42	53.46	172.913
15	r30	0.526068	0.000053	70	98734.47	14.32	206.73	63.01	203.776
16	r35	0.436420	0.000044	65	1190632.16	17.26	249.19	75.95	245.635
17	r40	0.363294	0.000036	60	1430289.46	20.74	299.35	91.24	295.078
18	r45	0.290728	0.000029	55	1787288.94	25.92	374.07	114.01	368.729
19	r50	0.229514	0.000023	50	2263976.16	32.83	473.84	144.42	467.073
20	r55	0.186592	0.000019	45	2784761.57	40.38	582.84	177.64	574.514
21	r60	0.136972	0.000014	40	3793585.88	55.01	793.98	241.99	782.641
22	r65	0.110794	0.000011	35	4689931.33	68.00	981.58	299.17	967.563
23	r70	0.087604	0.000009	30	5931397.85	86.01	1241.42	378.36	1223.686
24	r75	0.061885	0.000006	25	8396485.23	121.75	1757.35	535.61	1732.249
25	rpd (showalter)	1.014390	0.000101		512244.16	7.43	107.21	32.68	105.679
26	rAPEX	0.584207	0.000058		889436.44	12.90	186.16	56.74	183.497

The R10 value yields a height of 105.6′ above free water (32.68 m). This rock is capable of holding a 107′ column and would also have the oil-water contact 107′ above the free water level. If it had a 70 % Sw, it would already be 206′ into the trap, but would look wet and non-commercial on logs.

Fig. A13 Answers for the case in Fig. A12. If I saw this rock on a trap, I'd be looking nearby for rock with a better quality reservoir in order to get better saturations. Alternatively, I'd continue to drill updip to lower saturations, if possible

Conversions using solutions from Glover (2015)

Inputs to equations from your area

	A	B	C
1	Sample	Porosity (whole pct)	Perm (md)
2	Rock 1	12	1
3			
4	IFT (γ)	30.000000	
5	Theta (θ)	0.000000	
6	Density water (g/cc)	1.000000	
7	Density hydrocarbon (g/cc)	0.800000	

Pittman equations

Conversion to Pc psi

	A	B	C	D	E	F	G
9	Mercury Percentile	Pittman equations R in micron	Equiv SW %	2ycosθ/R	PC in psi	Equiv H ft	Equiv H m
10	r10	=10^((0.459+0.5*LOG(C2)-0.385*LOG(B2)))	90	=(($B$4*2)*(COS(RADIANS($B$5)))/B10))	=D10*0.145	=E10/(($B$6-$B$7) *0.433)	=F10/3.281
11	r15	=10^((0.333+0.509*LOG(C2)-0.344*LOG(B2)))	85	=(($B$4*2)*(COS(RADIANS($B$5)))/B11))	=D11*0.145	=E11/(($B$6-$B$7) *0.433)	=F11/3.281
12	r20	=10^((0.218+0.519*LOG(C2)-0.303*LOG(B2)))	80	=(($B$4*2)*(COS(RADIANS($B$5)))/B12))	=D12*0.145	=E12/(($B$6-$B$7) *0.433)	=F12/3.281
13	r25	=10^((0.204+0.531*LOG(C2)-0.35*LOG(B2)))	75	=(($B$4*2)*(COS(RADIANS($B$5)))/B13))	=D13*0.145	=E13/(($B$6-$B$7) *0.433)	=F13/3.281
14	r30	=10^((0.215+0.547*LOG(C2)-0.42*LOG(B2)))	70	=(($B$4*2)*(COS(RADIANS($B$5)))/B14))	=D14*0.145	=E14/(($B$6-$B$7) *0.433)	=F14/3.281
15	r35	=10^((0.255+0.565*LOG(C2)-0.523*LOG(B2)))	65	=(($B$4*2)*(COS(RADIANS($B$5)))/B15))	=D15*0.145	=E15/(($B$6-$B$7) *0.433)	=F15/3.281
16	r40	=10^((0.36+0.582*LOG(C2)-0.68*LOG(B2)))	60	=(($B$4*2)*(COS(RADIANS($B$5)))/B16))	=D16*0.145	=E16/(($B$6-$B$7) *0.433)	=F16/3.281
17	r45	=10^((0.609+0.608*LOG(C2)-0.974*LOG(B2)))	55	=(($B$4*2)*(COS(RADIANS($B$5)))/B17))	=D17*0.145	=E17/(($B$6-$B$7) *0.433)	=F17/3.281
18	r50	=10^((0.778+0.626*LOG(C2)-1.205*LOG(B2)))	50	=(($B$4*2)*(COS(RADIANS($B$5)))/B18))	=D18*0.145	=E18/(($B$6-$B$7) *0.433)	=F18/3.281
19	r55	=10^((0.948+0.632*LOG(C2)-1.426*LOG(B2)))	45	=(($B$4*2)*(COS(RADIANS($B$5)))/B19))	=D19*0.145	=E19/(($B$6-$B$7) *0.433)	=F19/3.281
20	r60	=10^((1.096+0.648*LOG(C2)-1.666*LOG(B2)))	40	=(($B$4*2)*(COS(RADIANS($B$5)))/B20))	=D20*0.145	=E20/(($B$6-$B$7) *0.433)	=F20/3.281
21	r65	=10^((1.372+0.643*LOG(C2)-1.979*LOG(B2)))	35	=(($B$4*2)*(COS(RADIANS($B$5)))/B21))	=D21*0.145	=E21/(($B$6-$B$7) *0.433)	=F21/3.281
22	r70	=10^((1.664+0.627*LOG(C2)-2.314*LOG(B2)))	30	=(($B$4*2)*(COS(RADIANS($B$5)))/B22))	=D22*0.145	=E22/(($B$6-$B$7) *0.433)	=F22/3.281
23	r75	=10^((1.88+0.609*LOG(C2)-2.626*LOG(B2)))	25	=(($B$4*2)*(COS(RADIANS($B$5)))/B23))	=D23*0.145	=E23/(($B$6-$B$7) *0.433)	=F23/3.281
24	rpd (showalter)	=10^((0.459+0.5*LOG(C2)-0.385*LOG(B2)))		=(($B$4*2)*(COS(RADIANS($B$5)))/B24))	=D24*0.145	=E24/(($B$6-$B$7) *0.433)	=F24/3.281
25	rAPEX	=10^((-0.117+0.475*LOG(C2)-0.099*LOG(B2)))		=(($B$4*2)*(COS(RADIANS($B$5)))/B25))	=D25*0.145	=E25/(($B$6-$B$7) *0.433)	=F25/3.281

Equiv Sw is 1-R precentile r10 = 90% Sw

Fig. A14 An example of a moderate porosity, low permeability meso-porous rock solved by height conversions given by Glover (2015) after calculating Pc and converting to Psi

These are the answers for equations using R in microns, as calculated by Pittman (1992).

This is a meso-porous reservoir, water wet with an IFT of 30 and density of .80 g/cc (oil) in a fresh water system, where Dw = 1 g/cc.

	A	B	C	D	E	F	G
1	Sample	Porosity (whole pct)	Perm (md)				
2	Rock 1	12	1				
3							
4	IFT (γ)	30.000000					
5	Theta (θ)	0.000000					
6	Density water (g/cc)	1.000000					
7	Density hydrocarbon (g/cc)	0.800000					
8							
9	Mercury Percentile	Pittman equations R in micron	Equiv SW %	2ycosθ/R	PC in psi	Equiv H ft	Equiv H m
10	r10	1.105389	90	54.28	7.87	90.88	27.70
11	r15	0.915718	85	65.52	9.50	109.71	33.44
12	r20	0.778051	80	77.12	11.18	129.12	39.35
13	r25	0.670327	75	89.51	12.98	149.87	45.68
14	r30	0.577755	70	103.85	15.06	173.88	53.00
15	r35	0.490443	65	122.34	17.74	204.84	62.43
16	r40	0.422821	60	141.90	20.58	237.60	72.42
17	r45	0.361308	55	166.06	24.08	278.05	84.75
18	r50	0.300322	50	199.79	28.97	334.51	101.96
19	r55	0.256500	45	233.92	33.92	391.66	119.37
20	r60	0.198648	40	302.04	43.80	505.73	154.14
21	r65	0.172306	35	348.22	50.49	583.04	177.70
22	r70	0.146816	30	408.67	59.26	684.27	208.55
23	r75	0.111191	25	539.61	78.24	903.51	275.38
24	rpd (showalter)	1.105389		54.28	7.87	90.88	27.70
25	rAPEX	0.597257		100.46	14.57	168.21	51.27

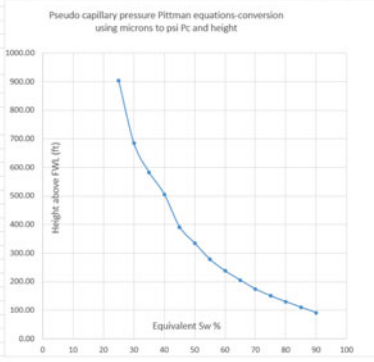

The R10 value yields a height of 90.88′ above free water (27.7 m). This rock is capable of holding only a 91′ column and would also have the oil-water contact 91′ (24m) above the free water level. The low porosity might be puzzling. A 65% Sw would place this example 200′ (52 m) into the trap.

Fig. A15 Solution for example in Fig. A14. Dw = water density

Example 2: Using R in Centimeters Instead of Mu

Case 3: Simple conversions use R as mu, but with a different solution for height above free water. Solution from (Glover, 2015).

These example show not only different mathematical solutions for capillary pressure, but the problem of relying on porosity alone to assess rock quality. The best rock has the lowest porosity (Figs. A14 and A15). The worst rock the best porosity (Figs. A10 and A11). Learning to run sensitivities from different porosity and permeability combinations, and fluid phases is an essential part of understanding Sw and oil and gas shows. All three of these rock types could exist within a short interval of one another, both vertically in a well and laterally on a map. Understanding where each facies is with respect to saturations will lead to much better ideas on how to develop a discovery, interpret an old dry hole or use the data to build a migration model with seals.

References

Glover P (2015) Chapter 8: capillary pressure, formation evaluation MSc course notes. United Kingdom: Leeds University

Hartmann DJ, Beaumont EA (1999) Predicting reservoir system quality and performance. In: Beaumont EA, Foster NH (eds) Exploring for oil and gas traps: treatise of petroleum geology, Handbook of Petroleum Geology, v. 1: Tulsa, Oklahoma: American Association of Petroleum Geologists, p. 9.3–9.154

Pittman E (1992) Relationship of porosity and permeability to various parameters derived from mercury injection-capillary pressure curves for sandstone. Am Assoc Pet Geol Bull 76:191–198.

Appendix E
Converting Paleogeographic Maps or Shapefiles in ARCGIS to Grids

As covered in Chap. 5, migration modeling with seals is essential to see traps that are not pure 4-way structural closures. Software packages like Trinity have built-in tools to create polygons and then convert them to grids for use in migration. These grids can contain seals from faults or facies, but start with polygons that then must be converted to a seal value in feet or meters of seal capacity to a given hydrocarbon-water system.

Good paleogeographic maps often contain both facies and critical fault polygons. They should be built carefully with as much geological insight as possible. When done, the faults and facies polygons can be converted very quickly to grids that can then be used in a migration model. Building the input map should be done with this end point in mind, making sure that the facies belts are consistent with reasonable seal capacities based on experience, pseudo-capillary pressure or capillary pressure data.

The first step is to create the shapefile, making it as consistent as possible with known production, shows or rock property data. The example in Fig. A16 is from the Desert Creek Formation example used in Chap. 5 to model migration using both Trinity and simple grid manipulation in other software. The seal data should be entered as a data type of 'double', which means numbers with decimals can be put in the field. Enter the numbers you wish to use in the appropriate field (in this case, Seal_max).

Step 2. Use Arc Toolbox to convert the seals data to a grid. Instructions are in Fig. A17. The term 'feature' in ARCGIS can refer to a shapefile or a Feature Class in a Geodatabase. This step will create the grid you need to run migration with.

Step 3: Look at your results and make sure they are correct. In the example in Fig. A18, there are small white gaps noted as 'a potential problem: some gaps in the gird'. This is due to the polygons not having been completely clipped to one another properly. In a case like this, it is good to go back and edit the original polygons to eliminate the gap, as the gap will act as a null along the migration pathway.

J. Dolson, *Understanding Oil and Gas Shows and Seals in the Search for Hydrocarbons*, DOI 10.1007/978-3-319-29710-1

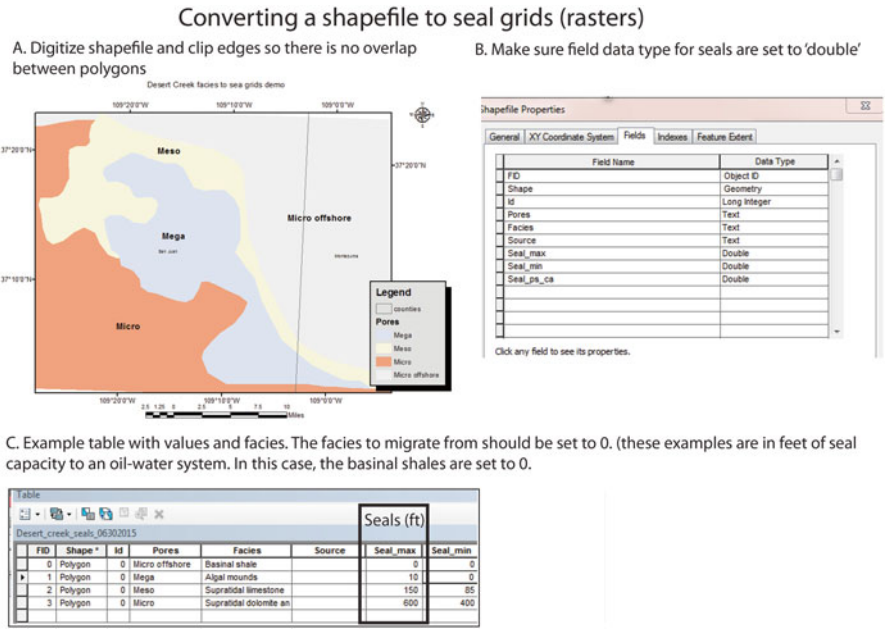

Fig. A16 Step 1. Create a shapefile that contains fields with a 'data type' of 'double'. This allows numbers to be entered instead of text. The numbers will be converted to grids that match the shapefile polygons

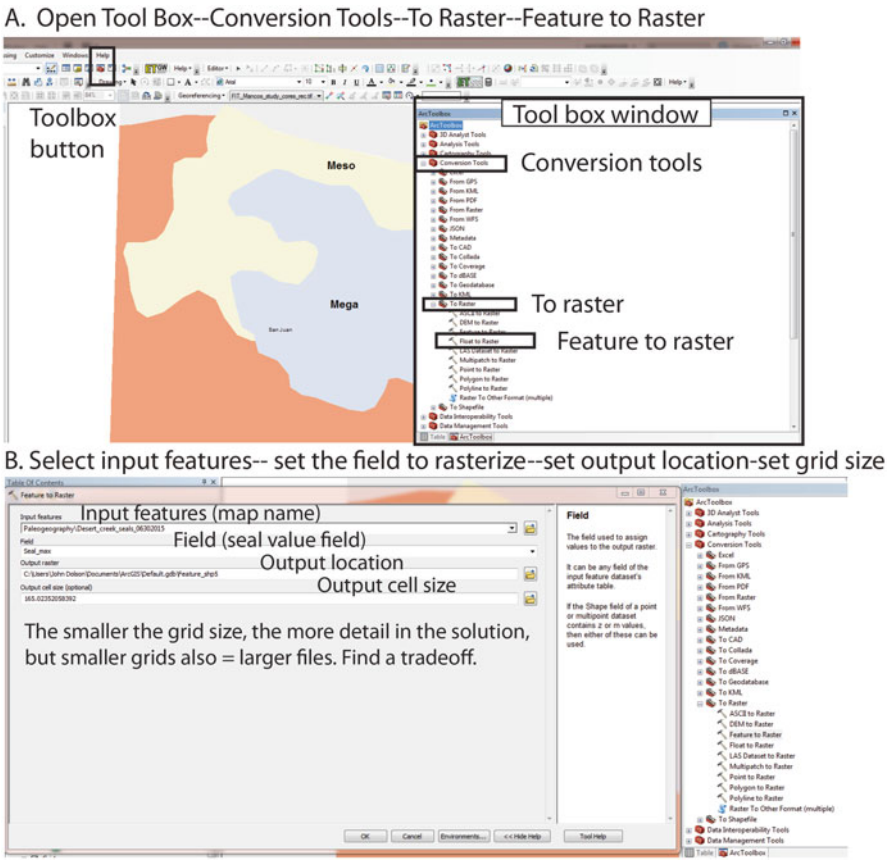

Fig. A17 Using Tool Box, open the conversion tools window, then 'to raster', then 'feature to raster'. Identify your shapefile or feature class (if in a Geodatabase), select the field, output location and grid cell size. Run the program

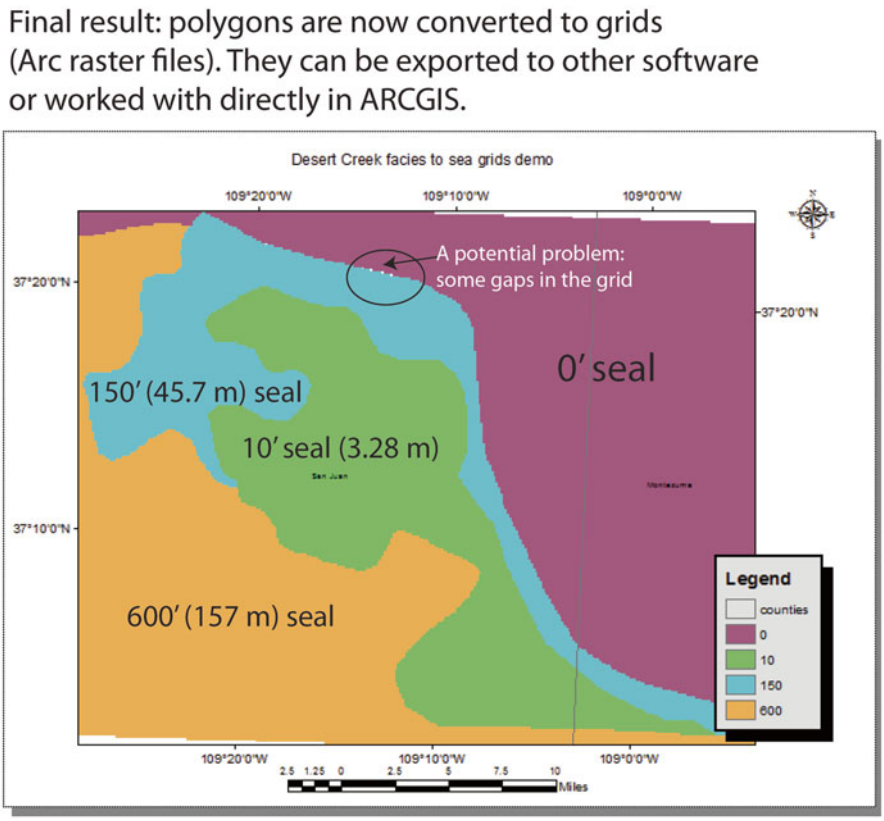

Fig. A18 The final result. This grid, while close, has a problem area identified which should be corrected by editing the original polygons and clipping them so that the edges are seamless with no gap. The grid map be fixable in other software also, depending on the editing capability of each program

The result in Fig. A18 is a good example. If hydrodynamics is not involved, this grid can be added directly to the structure map (if the map is in positive TVD numbers) and then closures looked for (as shown in Chap. 5). If the structure map is in subsea numbers (like -1500 ft), then take this grid and subtract the structure map. The results will be the same and where there are closures, there are traps.

The quantitative theory behind this is covered in Chap. 5 using capillary pressure theory. But as the results are in feet or meters, when you make this map, you are effectively solving the capillary pressure part of the migration algorithms using your knowledge of the area or other tools that make you comfortable the seal values are reasonable.